SYNTHESIS OF NOVEL SPIRO HETEROCYCLIC COMPOUNDS AND BIOLOGICAL EVALUATION

A THESIS SUBMITTED TO

NATIONAL INSTITUTE OF TECHNOLOGY
WARANGAL

FOR THE DEGREE OF

DOCTOR OF PHILOSOPHY
IN
CHEMISTRY

BY

VENKATA BHARAT NISHTALA
(Roll No. 701448)

DEPARTMENT OF CHEMISTRY
NATIONAL INSTITUTE OF TECHNOLOGY
WARANGAL-506 004, TELANGANA, INDIA

NOVEMBER, 2018

Dedicated to

…..My parents and guide

Dr. B. Srinivas
Assistant Professor
Department of Chemistry
National Institute of Technology
Warangal - 506 004
Telangana, India

Mobile : +91-9703351571
Email : basavojusrinivas@nitw.ac.in

CERTIFICATE

This is to certify that the research work presented in this thesis entitled **"Synthesis of Novel Spiro Heterocyclic Compounds and Biological Evaluation"** submitted by **Mr. Venkata Bharat Nishtala** for the degree of Doctor of Philosophy in Chemistry, National Institute of Technology, Warangal (Telangana), under my supervision and that the same has not been submitted elsewhere for a degree.

Date:

Place:

Dr. B. Srinivas

Thesis Supervisor

DECLARATION

I hereby declare that the research work presented in this thesis entitled **"Synthesis of Novel Spiro Heterocyclic Compounds and Biological Evaluation"** has been carried out by me under the supervision of **Dr. B. Srinivas**, Assistant Professor, Department of Chemistry, National Institute of Technology Warangal. I declare that this work is original and has not been submitted in part or full, for any degree or diploma to this or any other university.

Date:

Place: **(Venkata Bharat Nishtala)**

ACKNOWLEDGEMENTS

The work presented in this thesis would not have been possible without my close association with many people. I take this opportunity to extend my sincere gratitude and appreciation to all those who made this Ph. D., thesis possible.

It gives me immense pleasure and delight to express my deep sense of gratitude to my teacher and research guide ***Dr. B. Srinivas***, Assistant Professor, Department of Chemistry, National Institute of Technology, Warangal for his inspiring and valuable guidance. His unfailing attention, unmitigated encouragement and co-operation have helped me in attaining my goal. It would have been impossible to achieve this goal without his able support and valuable advice. I consider myself fortunate that he has given me a decisive tune, a significant acceleration to my career. I will be thankful to him throughout my lifetime.

I am greatly indebted to ***Prof. N. V. Ramana Rao***, Director, National Institute of Technology, Warangal allowing me to submit my research work in the form of a thesis. I express my gratitude to ***Prof. T. Srinivasa Rao*** and ***Prof. G. R. C. Reddy***, former Directors, National Institute of Technology, Warangal for giving me the opportunity to carry out the research work.

My special words of thanks to ***Prof. P. V. Srilakshmi,*** Head, Department of Chemistry and ***Prof. K. V. Gobi, Prof. V. Rajeswar Rao, Prof. B. Rajitha,*** former Heads, Department of Chemistry, National Institute of Technology, Warangal for their valuable advices, help and support.

I express my sincere thanks to the Doctoral Scrutiny Committee (DSC) members, ***Prof. P. Nageswara Rao, Prof. V. Rajeswar Rao***, Department of Chemistry and ***Prof. N. Narasaiah***, Department of Materials & Metallurgical Engineering for their support and encouragement.

I take this opportunity to express thanks to ***Prof. B. Venkata Appa Rao***, ***Prof. G. V. P. Chandramouli***, ***Prof. I. Ajit Kumar Reddy***, ***Prof. A. Ramachandraiah***, ***Prof. K. Laxma Reddy, Dr. Vishnu Shanker***, ***Dr. Venkatathri Narayanan***, ***Dr. D. Kashinath***, ***Dr. K. Hari Prasad, Dr. Raghu Chitta, Dr. S. Nagarajan, Dr. M. Raghasudha, Dr. C. Jugun Prakash, Dr. Ravinder Pawar*** for their suggestions and encouragement.

Financial assistance from the Government of India, Ministry of Human Resource Development ***(MHRD)*** in the form of fellowship is gratefully acknowledged.

My sincere thanks to ***Dr. K. Suresh Babu*** (Senior Scientist), ***Dr. N. Jagadeesh Babu*** (Senior Scientist), CSIR-IICT Hyderabad, and ***Dr. G. Bhargavi*** (Post Doctoral Fellow), University of Hyderabad for their valuable suggestions.

I express my sincere thanks to ***Dr. Y. Narsimha Reddy***, Professor, Department of Pharmacology & Toxicology, Pharmaceutical Sciences, Kakatiya University for evaluating anticancer and antioxidant activity and ***Dr. Vijay Kumar Pasala***, Associate Professor, Natural Products Division, Osmania University, Hyderabad for evaluating the antimicrobial activity.

I am thankful to ***G. Durgayya***, Department of Pharmacology & Toxicology, Pharmaceutical Sciences, Kakatiya University for evaluating anticancer and antioxidant activity and ***Ch. Mahesh***, Natural Product Division, Osmania University, Hyderabad for evaluating the antimicrobial activity.

It gives me great pleasure to express my gratitude to my colleagues and friends ***Dr. G. Ramesh, P. Vinay, A. Bhargava Sai, B. Sowmya, T. Sanjay, K. Ramaiah, M. Venkanna, M. Saikumar, A. Naveen Reddy, T. Dhanunjay Rao, Dr. V. Krishnaiah, Dr. V. Ravi Babu, Dr. L. Suresh, Dr. P. Sagar Vijay Kumar, Dr. K. Vimal Kumar, Dr. B. Janardhan, M. Srikanth, N. Satyanarayana, K. Sujatha, A. Rajini, B. Mayuri, J. Parameswara chary, Ch. Raju, K. Vijendar reddy, P. Babji, V. Sunil Kumar, P. Mahendranath, Dr. B. Rajitha, Dr. S. Kanaka Raju, Dr. M. Satyanarayana, Ch. Suman, Dr. M. Narsimha Reddy, Dr. P. Sreenu, Dr. K. Koteshwara Reddy, Dr. T. Surender, Dr. T. Ramesh, Dr. G. Srinivasa Rao, Dr. A. Ajay Kumar, Dr. R. Rajkumar, Dr. Tewodros Birhanu, Dr. T. Surendar, Dr. B. Thirupaiah, Dr. B. Santosh Kumar, R. Venkatesh, S. Suresh, K. Shekar, G. Ambedhkar, K. Satish, G. Sivaparvathi, G. Srinath, G. Sripal Reddy, M. Sirisha, P. Venkatesham*** for their good compensation and creating a nice atmosphere in and outside the laboratory and their encouragement and help during my research period.

Words are short to express my deep sense of gratitude to my family members: Parents: ***Vara Prasada Rao*** and ***Padmavati***; Spouse: ***Devi***; Son: ***Vara Prasad***; Brothers: ***Satyanarayana*** and ***Giri***; Sisters in Law: ***Deepa*** and ***Priya;*** Nephews: ***Maithra Varun and Sameer***; Niece: ***Gayatri*** for their constant support, cooperation, encouragement, inspiration, love and affection whose blessings made the journey worth effort. I owe everything to them.

(Venkata Bharat Nishtala)

ABBREVIATIONS

5-HT7	:	5-Hydroxytryptamine 7
5-HT1AR	:	5-Hydroxytryptamine receptor 1A
5-HT2AR	:	5-Hydroxytryptamine receptor 2A
5-HT6R	:	5-Hydroxytryptamine receptor 6
17β-HSD3	:	17β-Hydroxysteroid dehydrogenase type 3
ABTS	:	2,2'-Azino-bis(3-ethylbenzothiazoline-6-sulphonic acid)
ACC	:	Acetyl-CoA carboxylase
AchE	:	Acetylcholinesterase
ADME	:	Absorption, distribution, metabolism and excretion
ALA	:	Alanine
Anti-AD	:	Antiaggregation and disaggregation
ARG	:	Arginine
ASN	:	Asparagine
ASP	:	Aspartate
ATP	:	Adenosine triphosphate
Brr2	:	Bad response to refrigeration 2
CB2R	:	Cannabinoid type 2 receptor
CCR2	:	Chemokine receptor 2
$CDCl_3$	:	Deuterated chloroform
CH_3CN	:	Acetonitrile
CoMFA	:	Comparative Molecular Field Analysis
Conc	:	Concentration
CYS	:	Cysteine
DES	:	Deep eutectic solvent
DMSO-d_6	:	Deuterated Dimethyl sulfoxide
DMF	:	*N*, *N*-Dimethylformamide
DMSO	:	Dimethyl sulfoxide
DNA	:	Deoxyribonucleic acid
DPPH	:	2,2-diphenyl-1-picrylhydrazyl/1,1-diphenyl-2-picrylhydrazyl

EtOH	:	Ethanol
FITC	:	Fluorescein Isothiocyanate
FTIR	:	Fourier transform infrared
GABAA-a1	:	Gamma-aminobutyric acid A receptor with subunit alpha-1
GLN	:	Glutamine
GLU	:	Glutamate
GLY	:	Glycine
GPR119	:	G-protein-coupled receptor 119
HIS	:	Histidine
HIV	:	Human immunodeficiency virus
hSGLT1	:	Human Sodium-Glucose Cotransporter 1
hSGLT2	:	Human Sodium-Glucose Cotransporter 2
human NK-112	:	Human natural killer 112
Hz	:	Hertz
IC_{50}	:	Half maximal inhibitory concentration
LACP	:	Link aggregation control protocol
LEU	:	Leucine
ILE	:	Isoleucine
LNCaP	:	Lymph Node Carcinoma of the Prostate
LYS	:	Lysine
MAO	:	Monoamine oxidase
M11/cc-pVDZ	:	Farallons Mac recorder format (Sampling rate 11)/correlation-consistent polarized double zeta
MDM2	:	Mouse double minute 2 homolog
MeOH	:	Methanol
c-MET	:	Mesenchymal to Epithelial Transition
MET	:	Methionine
MIC	:	Minimum Inhibitory Concentration
mmol	:	milli mole
MP	:	Melting point
MTT	:	3-(4,5-dimethylthiazol-2-yl)-2,5-diphenyltetrazolium Bromide
MTB	:	Mycobacterium tuberculosis

NADP	:	Nicotinamide adenine dinucleotide phosphate
NADPH	:	Reduced form of nicotinamide adenine dinucleotide phosphate
ND	:	Not determined
NMR	:	Nuclear Magnetic Resonance
NO	:	Nitric oxide
NPY Y5	:	Neuropepetide Y Y5 receptor
ORTEP	:	Oak Ridge Thermal Ellipsoid Plot
p53	:	Posphoprotein p53 (tumor protein)
PDB	:	Protein Data Bank
PDE5	:	Phosphodiesterase type 5
PEG	:	Polyethylene glycol
PHE	:	Phenylalanine
ppm	:	Parts per million
PRO	:	Proline
p-TSA	:	*Para*-toluene sulphonic acid
QSAR	:	Quantitative Structure Activity Relationship
RNA	:	Ribonucleic acid
rt	:	Room temperature
SAR	:	Structure–activity relationship
SD	:	Standard deviation
SER	:	Serine
SOI	:	Secondary orbital interaction
SXRD	:	Single Crystal X-ray Diffraction
THR	:	Threonine
TLC	:	Thin Layer Chromatography
TMS	:	Tetramethylsilane
TRPV1 subfamily	:	Transient receptor potential cation channel V member 1
US	:	Ultra-sonication
µg/mL	:	microgram/milli litre
µM	:	micro molar

GENERAL REMARKS

1. Nuclear Magnetic Resonance (NMR) spectra were recorded on Bruker-400 MHz spectrometer (Bruker Corporation Ltd., Germany) using Tetramethylsilane (TMS) as the internal standard. Chemical shifts (δ) have been expressed in ppm units downfield from TMS. Selected data are reported as follows. Chemical shifts, multiplicity, (s = singlet, d = doublet, t = triplet, q = quartet, dd = doublet of doublet and m = multiplet), coupling constants (J in Hz) as assignments.

2. Mass spectra were recorded on Jeol JMSD-300 spectrometer (Jeol Ltd., Tokyo, Japan).

3. Infrared (IR) spectra were recorded on Perkin-Elmer 100S (Perkin-Elmer Ltd. United Kingdom)/Thermo Nicolet Nexus 670 spectrometer (Thermo Electron Corporation Ltd., Waltham Massachusetts, US) using KBr pellets. Values have been expressed in cm^{-1}.

4. Elemental analyses (C, H, N) were performed on a Carlo-Erba model EA1108 analytical unit (Triad Scientific Ltd., New Jersey, USA).

5. All the melting points were recorded in open capillaries using Stuart SMP30 apparatus (Bibby Scientific Ltd. United Kingdom) and are uncorrected.

6. All evaporations were carried out under reduced pressure on Büchi/Heidolph rotary evaporator below 50 ^{o}C.

7. All the reactions were monitored by thin layer chromatography (TLC) with F_{254} silica-gel precoated sheets (Merck, Darmstadt, Germany). The visualization was accomplished with UV light and iodine vapours.

8. All the reagents and solvents were purchased from Aldrich/Spectrochem and used without further purification.

CONTENTS

CHAPTER-I

INTRODUCTION

1.1. Introduction

Heterocyclic chemistry is a branch of organic chemistry in which the compounds contain atleast one hetero atom (N, O, S etc.,). Heterocyclic compounds are present in various drugs, agrochemicals, nucleic acids, vitamins, heme and chlorophyll, etc. The heterocyclic compounds exhibit various biological activities like antimicrobial, antiinflammatory, analgesic, antiepileptic, antiviral, antineoplastic, antihypertensive, antimalarial, antianxiety, antioxidant, antidepressant, antihistaminic, antitubercular, antiparkinson's, antidiabetic, antiobesity etc., [1-3]. Among the heterocyclic compounds, spiro compounds are the unique class of heterocyclic compounds.

In 1900, Adolf von Baeyer first discussed the nomenclature of the spiran. Spiro compounds are the compounds in which the two rings are joined by a single atom. The construction of spiro cyclic framework has always been a challenging task for the chemists because it often requires synthetic design based on specific targets [4]. For the past few decades the synthesis of spiro compounds plays a vital role in organic synthesis because of their unique structural features (conformational features) and their biological and industrial implications. Many spiro compounds possess promising biological activities such as anticancer, antibacterial, anticonvulsant, antituberculosis, anti-Alzheimer’s, pain-relief, antidermatitis, antimicrobial and antioxidant. These compounds were also used as pesticides, laser dyes, electroluminescent devices etc., [5, 6].

The biological activity of the spiro compounds is evidenced by the retention of neurotoxic properties of perhydrohistrionicotoxin (Figure 1.1), an analogue of natural product histrionicotoxin (Figure 1.1) [7]. It was well known that the spiro functionality is present in phytochemicals, either in alkaloids, lactones or terpenoids. The histrionicotoxin is isolated from the skin extracts of dendrobats histrionius (poison dart frog). Histrionicotoxin is acting as a potent nicotinic receptor antagonist [8].

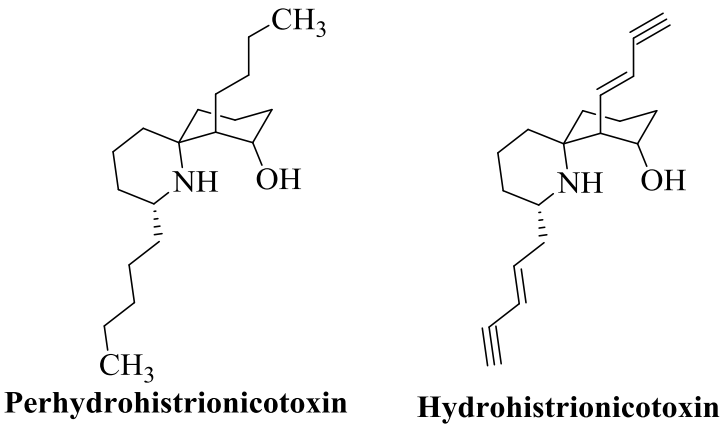

Perhydrohistrionicotoxin **Hydrohistrionicotoxin**

Figure 1.1

Some spiro ketals (Figure 1.2) were isolated from *Chrysanthemum coronanium*, a common vegetable of southern China. Some of these compounds were found to have antifeeding activity towards silkworm, spasmolytic and antiphlogistic activity [7, 9].

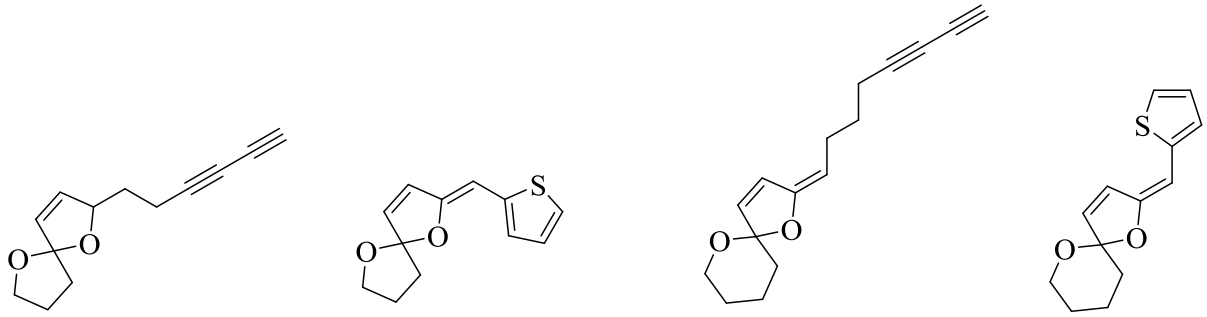

Figure 1.2

Hu et al. reported the isolation of spirobisnapthalene derivatives i.e., Decaspirones F-H (Figure 1.3), the bioactive secondary metabolites from the saprophytic fungus, *Helicoma Wirid.* These compounds were exhibited the modest activity against the multiple antibiotic resistant strain, *Pseudomonas aeruginosa* [10].

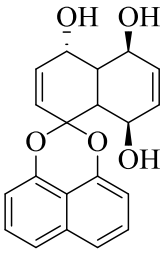

Decaspirone-F

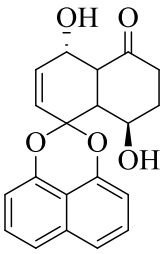

Decaspirone-G

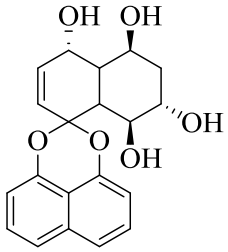

Decaspirone-H

Figure 1.3

Li et al. researched on the spiro compounds (Figure 1.4) containing macrolactum and thiadiazoline rings and their fungicidal activity [11].

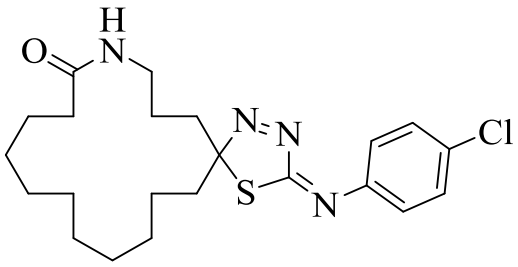

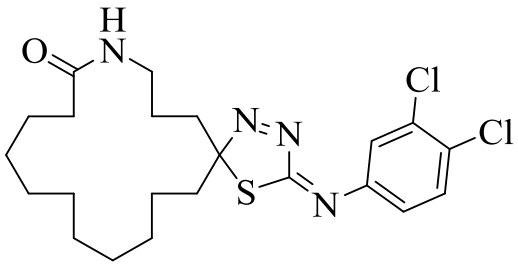

Figure 1.4

Apart from above mentioned comounds, the spiro[pyrrolidin-3,3'-indole] ring system is a prominent structural motif in a number of natural products like vinblastine and vincristine that function as cytostatics and are of prime importance in cancer chemotherapy [12]. The alkaloids containing a spiro-[indole-pyrrolidine] nucleus are cell-cycle-specific cytostatic agents that arrest mitosis and metaphase by acting as spindle poisons. They are also found to be useful in cancer chemotherapy [13]. Some of the biological active spiro compounds were shown in figure 1.5 [14-19].

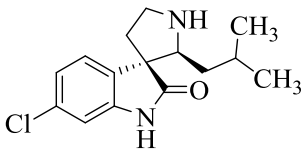

Elacomine

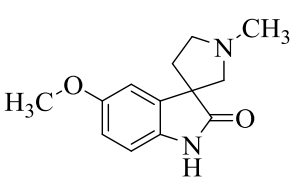

Horsfiline

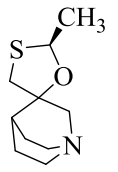

Cevimeline

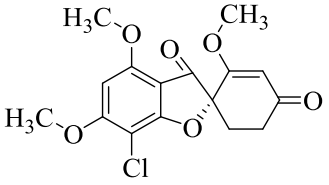

Griseofulvin

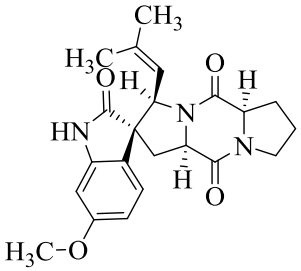

Spirotryptostatin A

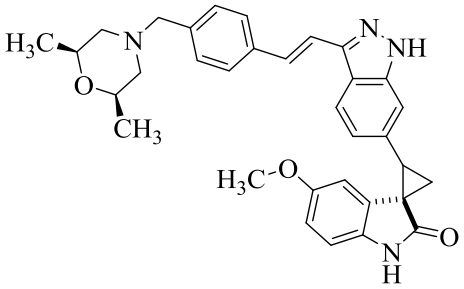

CFI-400945

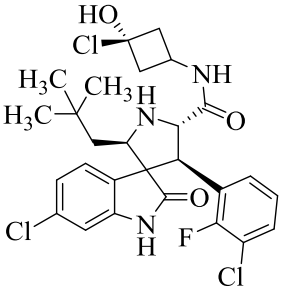

MI-888

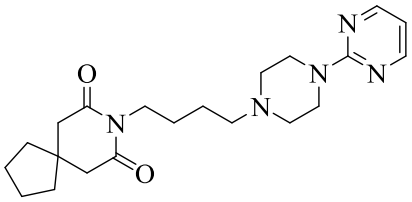

Buspirone

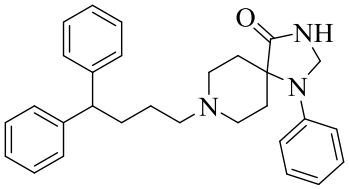

Fluspirilene

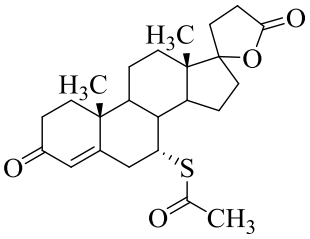

Spironolactone

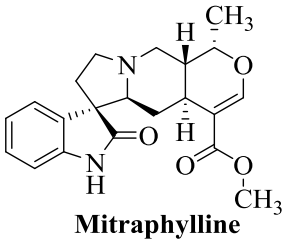

Mitraphylline

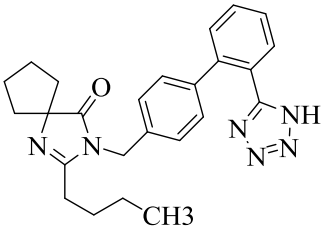

Irbesartan

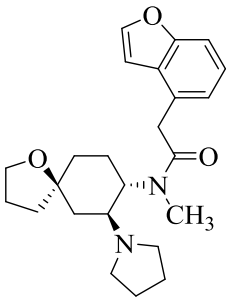

Enadoline

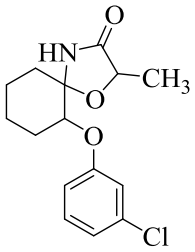

Enilospirone

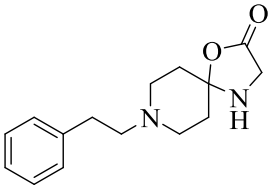

Fenspiride

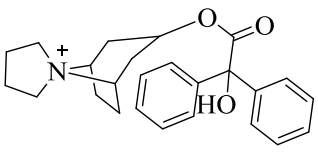

Trospium

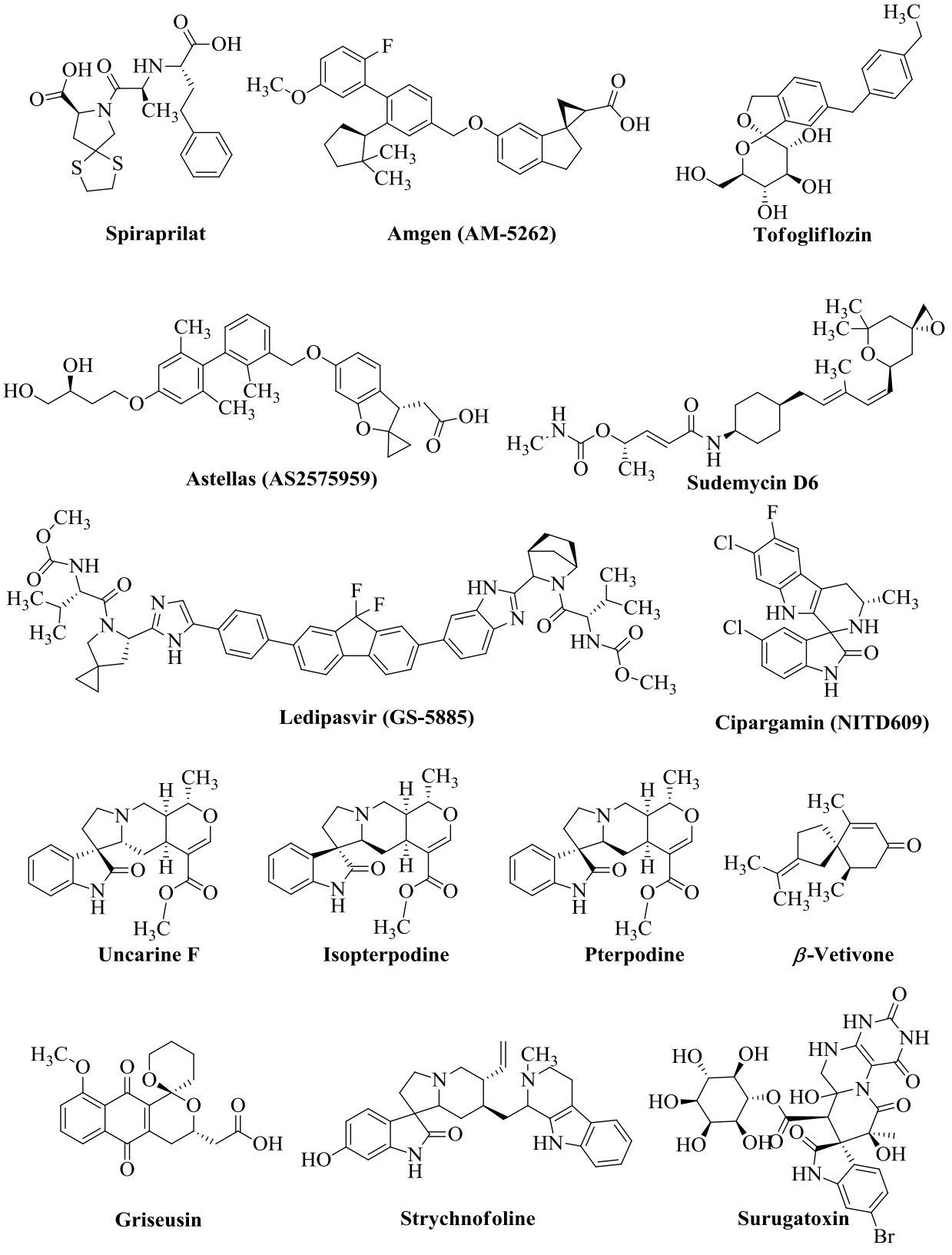
Spiraprilat
Amgen (AM-5262)
Tofogliflozin
Astellas (AS2575959)
Sudemycin D6
Ledipasvir (GS-5885)
Cipargamin (NITD609)
Uncarine F
Isopterpodine
Pterpodine
β-Vetivone
Griseusin
Strychnofoline
Surugatoxin

Figure 1.5

Gollner et al. described the scaffold modification based on Wang's pioneering MDM2−p53 inhibitors led to novel, chemically stable spirooxindole compounds bearing a spiro[3*H*-indole-3,2'-pyrrolidin]-2(1*H*)-one scaffold that are not prone to epimerization as observed for the initial spiro[3*H*-indole-3,3'-pyrrolidin]-2(1*H*)-one scaffold (Figure 1.6). The *in vitro* results were supported the *in silico* molecular docking studies [20].

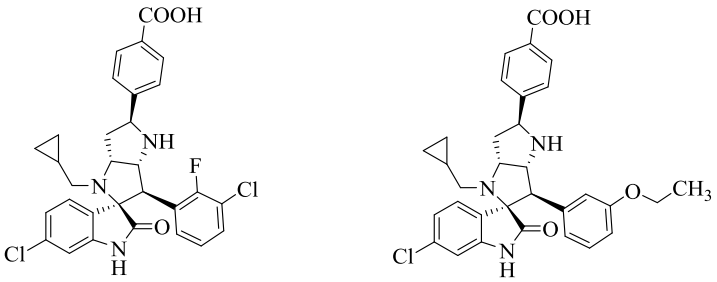

Figure 1.6

Manojit pal and coworkers reported the synthesis of the spiro-2,3-dihydroquinazolin-4(1*H*)-one derivatives under ultrasonication method at room temperature (Figure 1.7). In this report, the amberlyst-15 was used as a green and reusable catalyst. The synthesized compounds were tested for their potential against mycobacterium tuberculosis H37Rv chorismate mutase [21].

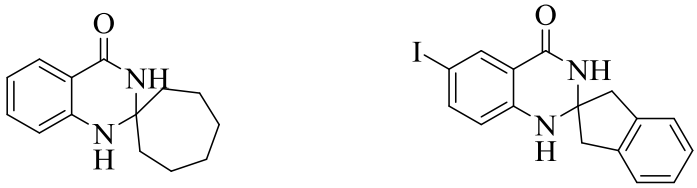

Figure 1.7

Koshizawa and coworkers described the discovery, synthesis and evaluation of the series of spiro[chromane-2,4'-piperidine] derivatives (Figure 1.8). The synthesized compounds were found to be potent and orally bioavailable GPR119 agonists. The SAR studies on head and tail moieties in the target compounds were also studied [22].

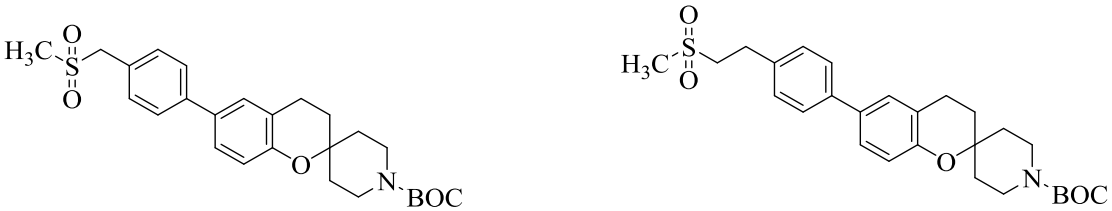

Figure 1.8

Kamata and coworkers reported the design and synthesis of spiro-piperidines (Figure 1.9). These compounds exhibit potent ACC inhibitory activity and favorable pharmacokinetic profiles in rats. The SAR studies were also evaluated for the target compounds [23]. They also synthesized spiro-pyrazolidinedione derivatives without quaternary chiral center by structure based drug design (Figure 1.9). The compounds displayed high ACC inhibitory activities [24].

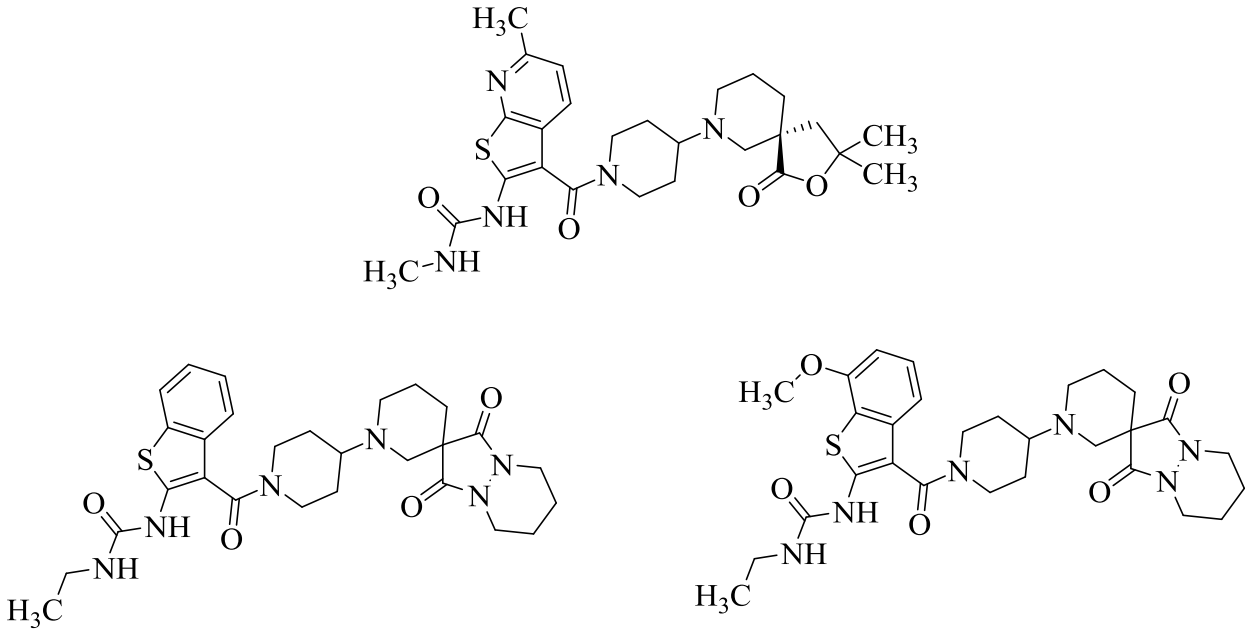

Figure 1.9

Bharkavi et al. synthesized the novel dispiroindenopyrrolidine/pyrrolothiazole–thiochroman hybrids, which has been achieved by one-pot multicomponent 1,3-dipolar cycloaddition of azomethine ylide (Figure 1.10). All the synthesized compounds were evaluated for their *in vitro* antimycobacterial, anticancer and AchE inhibitory activities [25]. The authors also reported an efficient one-pot microwave assisted stereoselective synthesis of novel dihydro-2'*H*-spiro[indene-2,1'-pyrrolo-[3,4-*c*]pyrrole]tetraones through three-component 1,3-dipolar cycloaddition and evaluation of their antimycobacterial activity and inhibition of AChE (Figure 1.10) [26].

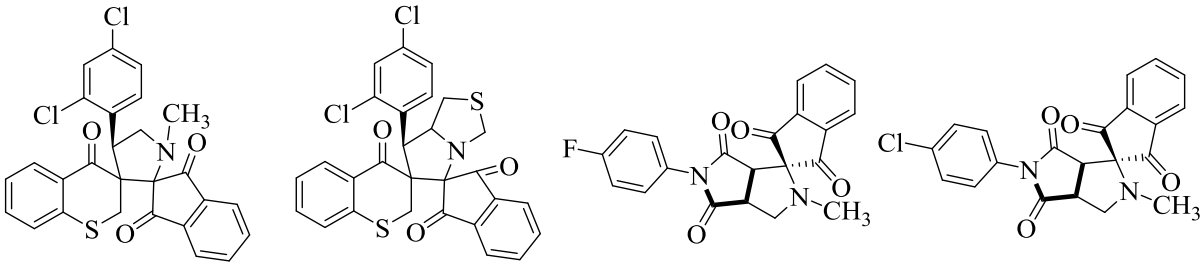

Figure 1.10

Sriram and coworkers described the synthesis and evaluation of 4',5'-dihydrospiro[piperidine-4,7'-thieno[2,3-*c*]pyran] analogues against both active and dormant mycobacterium tuberculosis (Figure 1.11). The structure activity profile was also illustrated for the target compounds [27].

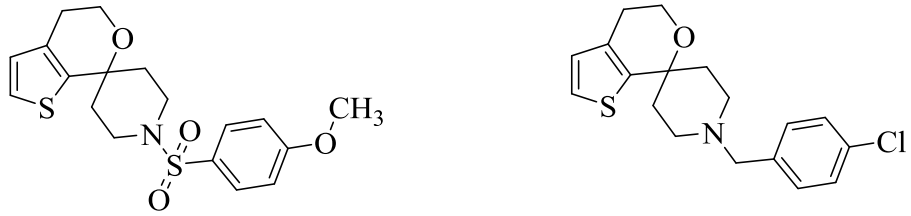

Figure 1.11

Cheng et al. reported (±)-Juglanaloid A and B, two pairs of naturally occurring alkaloid enantiomers bearing an unprecedented spiro[benzofuranone-benzazepine] skeleton, were isolated from the bark of juglans mandshurica maxim (Figure 1.12). The potential anti-AD properties were evaluated by the thioflavin T-assay [28].

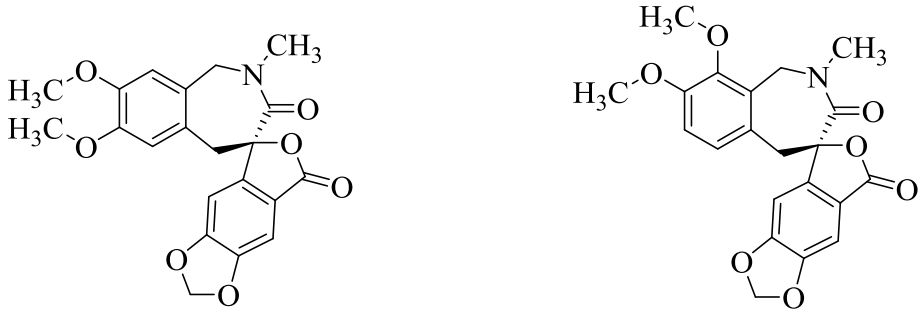

Figure 1.12

Perumal and coworkers reported the synthesis of a regio- and stereo-selective spiro-pyrrolothiazolyloxindoles *via* a one-pot multicomponent 1,3-dipolar cycloaddition (Figure

1.13). The target compounds were evaluated for their *in vitro* antitubercular activity against MTB [29].

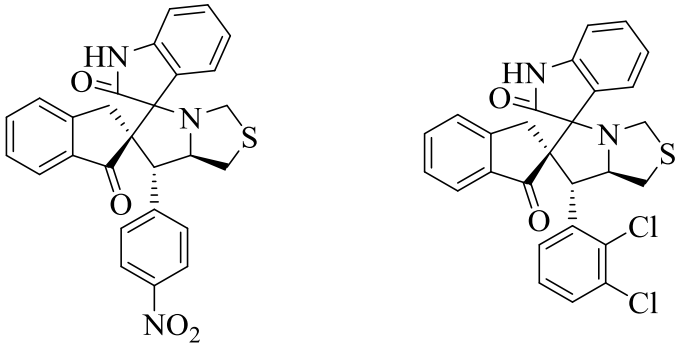

Figure 1.13

Maryamabadi et al. reported a simple, efficient, catalyst free and one-pot multicomponent green approach for the synthesis of spiro-dihydropyridine derivatives by the application of PEG-400 as a green biodegradable polymeric medium (Figure 1.14). The ability of synthesized compounds in the inhibition of acetyl and butyryl cholinesterase was investigated *in vitro*. *In silico* molecular docking studies were also carried out for the target compounds [30].

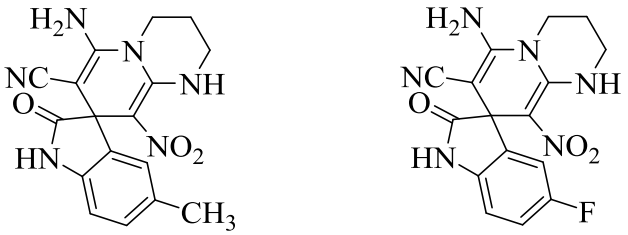

Figure 1.14

Dandia and coworkers developed a simple, green and catalyst-free novel protocol for the synthesis of medicinally important spiro[indole-3,2'[1,3]-thiazine]-2,4'-dione and spiro[acenaphthylene-1,2'[1,3]thiazine]dione libraries by the tandem reaction of readily available reagents in 1-butyl-3-methylimidazolium hexafluorophosphate [bmim][PF_6] (Figure 1.15). The ionic liquid has been used as a solvent as well as catalyst for this reaction. The synthesized compounds were subjected to antimycobacterial efficacy against mycobacterium tuberculosis H37Rv strain and DNA cleavage activity [31]. They also reported the ultrasound promoted, cerium ammonium nitrate catalyzed sustainable synthesis of spiro[indoline-3,4'-pyrano[2,3-*c*]pyrazole] derivatives (Figure 1.15). The synthesized

compounds were evaluated for their *in vitro* antioxidant activity by employing DPPH, NO and ABTS essays [32].

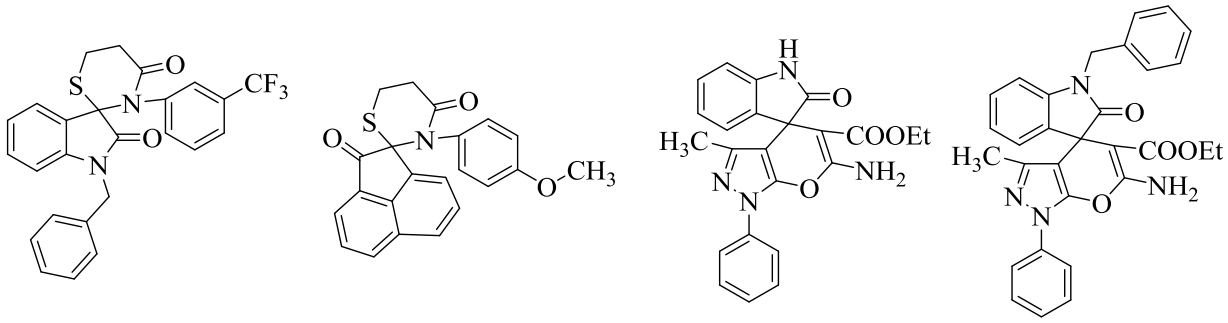

Figure 1.15

Xiao et al. were synthesized a series of spiro-piperidine azetidinone derivatives and evaluated as potential TRPV1 antagonists (Figure 1.16). The plasma stability was investigated and the problems included in their stability were resolved. Further, SAR study lead to the discovery of a potent antagonist with good oral pharmacokinetic profile in rat [33].

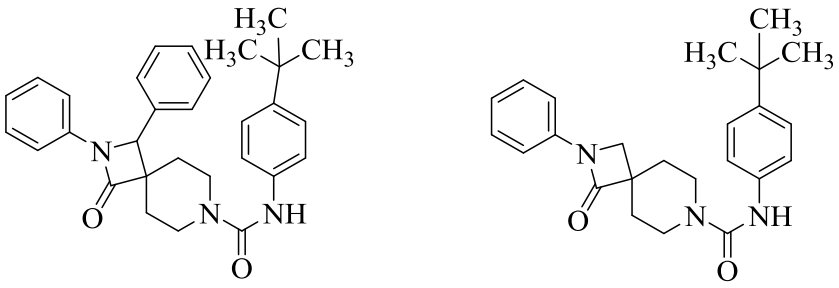

Figure 1.16

Bonacorso and coworkers reported the synthesis of the 2,5-substituted 4-(trifluoromethyl)-spirochromeno[4,3-*d*]pyrimidines (Figure 1.17). The synthesized compounds were evaluated for their analgesic effect in a mouse pain model [34].

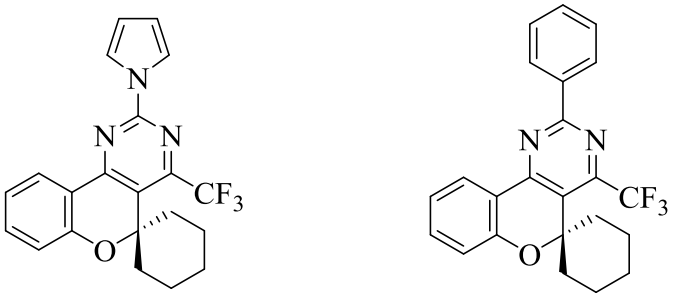

Figure1.17

Sampath kumar and coworkers reported the design and synthesis of the spiro derivatives of parthenin by the dipolar cycloaddition. The majority of the synthesized compounds were exhibited significant anticancer activity (Figure 1.18). The SAR studies were illustrated for the synthesized compounds. A mechanistic correlation of anticancer activity along with *in vivo* and western blotting experiments was also described [35].

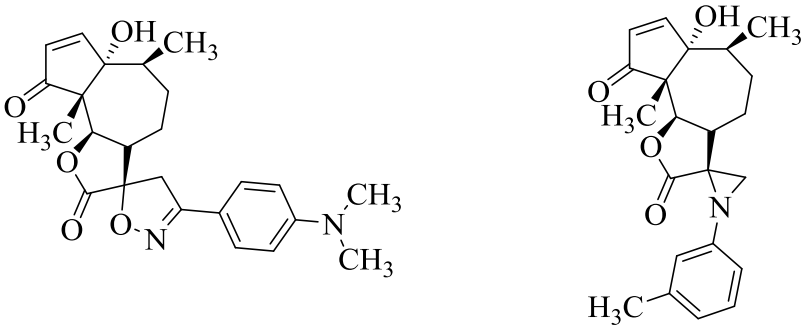

Figure 1.18

Yang et al. reported the design, synthesis of hydrazide-based peptidomimetics. The target compounds were exhibited potential antiHIV-1 as selective gelatinase inhibitors (Figure 1.19) [36].

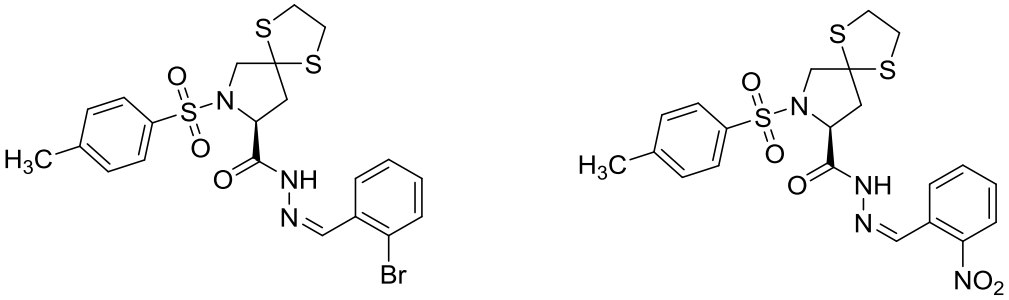

Figure 1.19

Kusanur et al. described the synthesis of the spiro[indolo-1,5-benzodiazepines] from 3-acetyl coumarins (Figure 1.20). The synthesized compounds were tested for their antimicrobial and antianxiety activity [37].

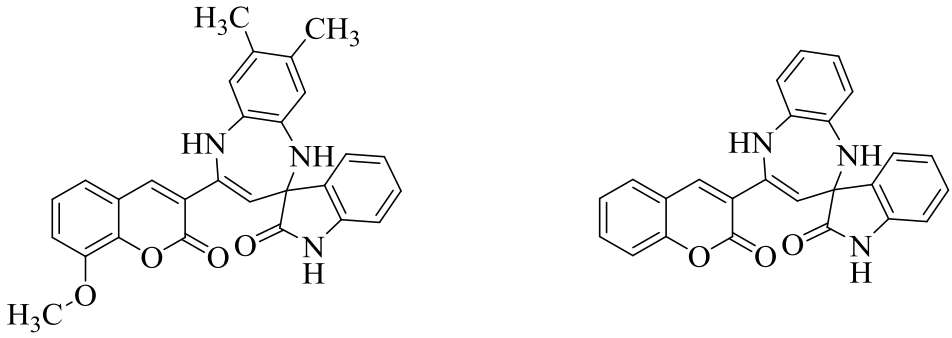

Figure 1.20

Kamal and coworkers reported a library of spiro[cyclopropane-1,3'-indolin]-2'-ones. The synthesized compounds were exhibited promising anticancer activity (Figure 1.21). Based on the screening results, SAR of the pharmacophore was proposed. Further, measurement of mitochondrial membrane potential and Annexin V-FITC assay was performed [38].

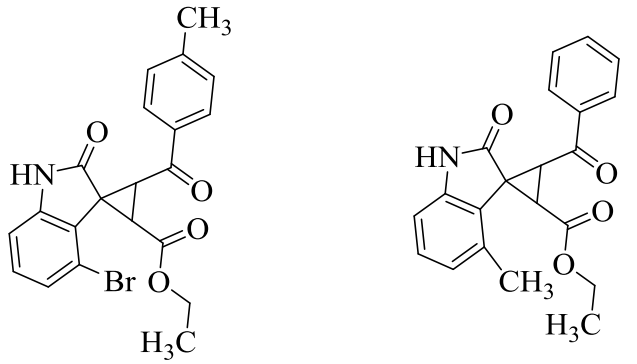

Figure 1.21

Ameen et al. reported a series of spiro-substituted 2,3-dihydroquinazolin-4(1*H*)-ones and quaternary piperidinium salt of quinazoline with two acetylenic groups and their azides (Figure 1.22). The synthesized compounds were screened for their anticancer activity and PDE5 inhibitory activity [39].

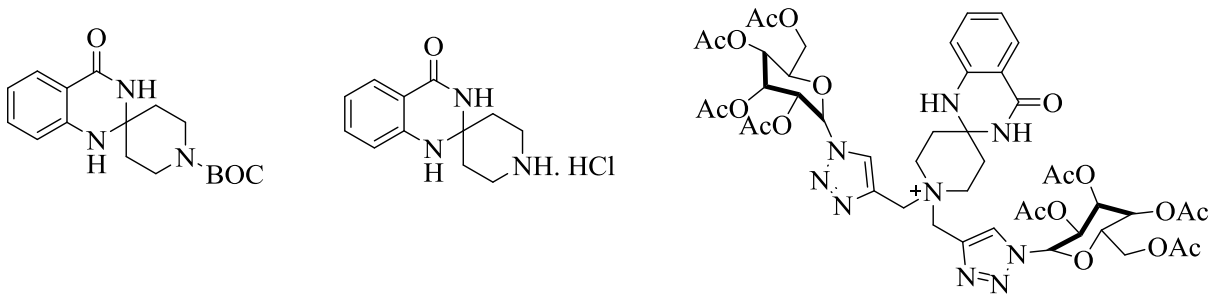

Figure 1.22

Matsuda and coworkers described the design and synthesis of 7-azaspiro[3,5]nonane derivatives. The synthesized compounds were found to be poential GPR119 agonists (Figure 1.23). These compounds were further evaluated for the pharmacokinetics profile in Sprague-Dawley (SD) rats and a favorable glucose lowering effect in diabetic rats [40].

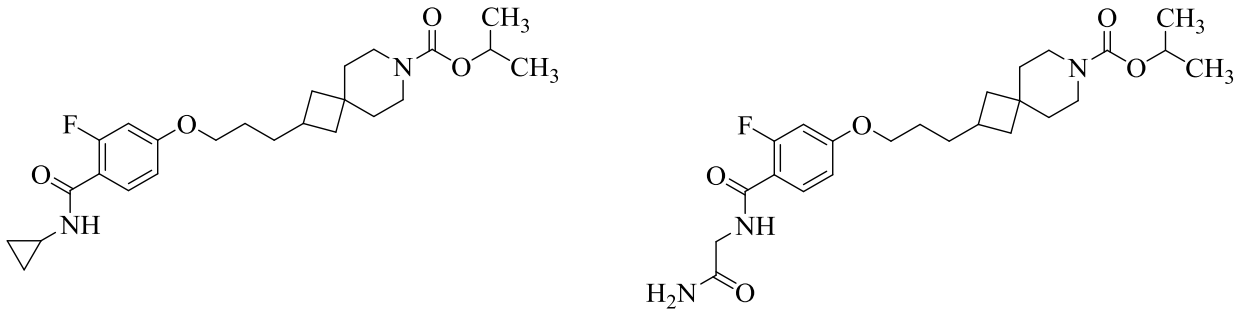

Figure 1.23

Fatahala and coworkers reported the efficient synthesis of the spiro derivatives for pyrrolopyrimidines (Figure 1.24). All the synthesized compounds evaluated for their *in vitro* antihyperglycemic activity. The SAR studies were also explored for these compounds [41].

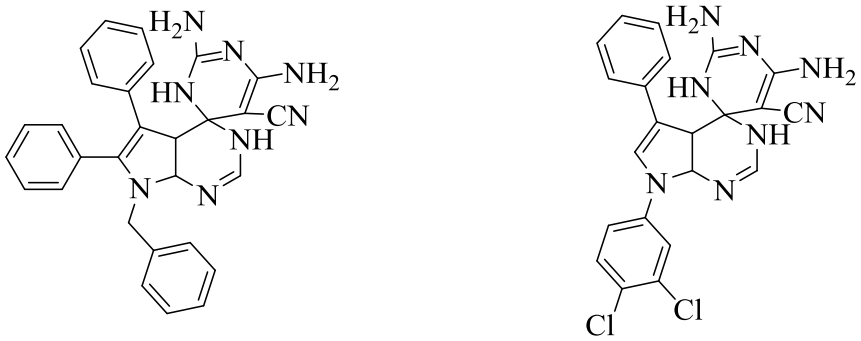

Figure 1.24

Zhang et al. described the discovery and synthesis of a series of polycyclic spiro-fused carbocyclicoxindoles (Figure 1.25). The synthesized compounds were investigated for their *in vitro* antiproliferative activity. They were effectively increased the protein levels of cleaved caspase-3, p53, and MDM2. The antiproliferative activity was well correlated with the molecular docking studies [42].

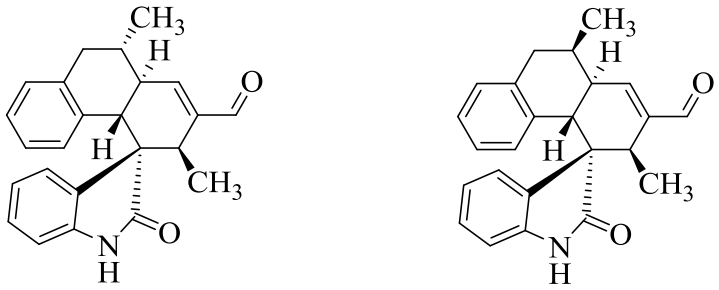

Figure 1.25

Kelemen et al. reported the design and synthesis of spiro[pyrrolidine-3,3′-oxindole] derivatives representing a novel scaffold of 5-HT7 receptor ligands (Figure 1.26). The synthesized analogues were validated as low nanomolar ligands showing selectivity in a panel of related serotonin receptor subtypes including 5-HT1AR, 5-HT2AR and 5-HT6R [43].

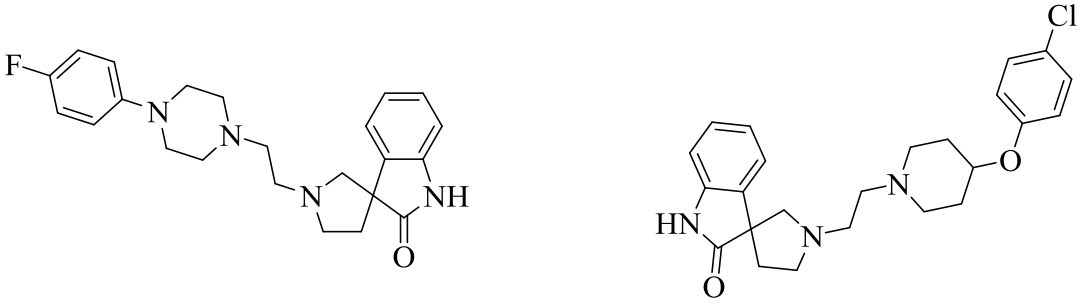

Figure 1.26

Stathakis et al. described a synthetic protocol for the construction of second generation analogs of rigid 6,7-spiro scaffolds (Figure 1.27). The synthesized compounds were subjected to RNA fluorescence assay, coupled transcription-translation assay (for bacterial *in vitro* transcription/translation) and TNT quick coupled transcription/translation assay (for eukaryotic *in vitro* transcription/translation) [44].

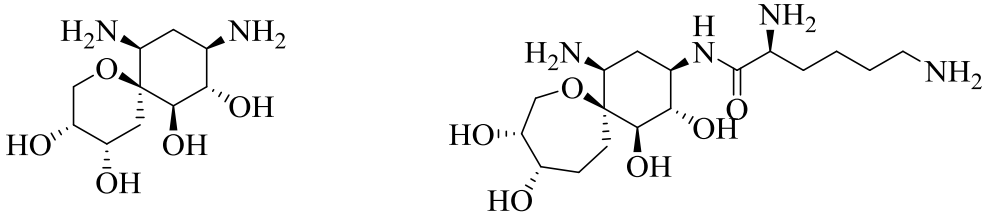

Figure 1.27

Abdou and coworkers descried the synthesis of spiro triazaphosphones and phosphoramides compounds. These compounds exhibit potent antineoplastic activity (Figure 1.28). The SAR studies were discussed for the target compounds [45].

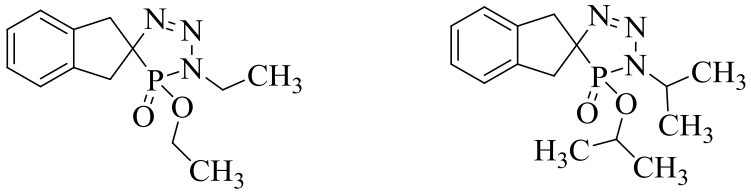

Figure 1.28

Wei et al. reported the design and synthesis of spiro-pentacylamides (Figure 1.29). The biological evaluation of synthesized compounds unveiled that these compounds were potent acetyl-CoA carboxylase inhibitors and antiproliferative agents. The *in silico* molecular docking studies supports the *in vitro* ACC activity [46].

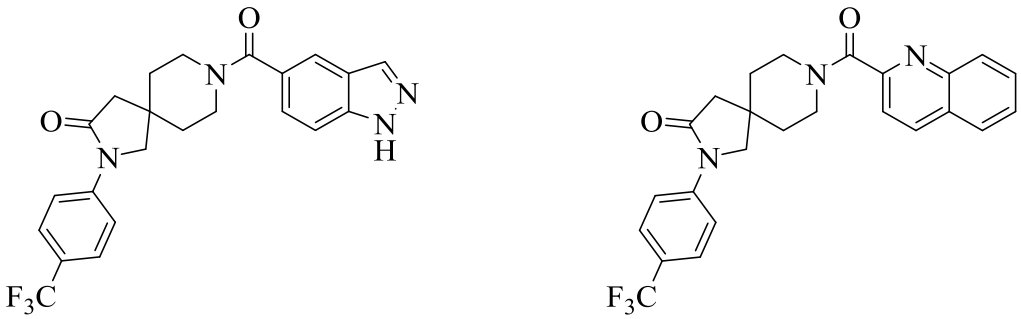

Figure 1.29

Mondal and coworkers reported the chemo, regio and stereoselective synthesis of novel spiro-pyrrolizidino-oxindole adducts of withaferin-A *via* one-pot three-component [3+2] azomethine ylide cycloaddition and their cytotoxicity evaluation (Figure 1.30) [47].

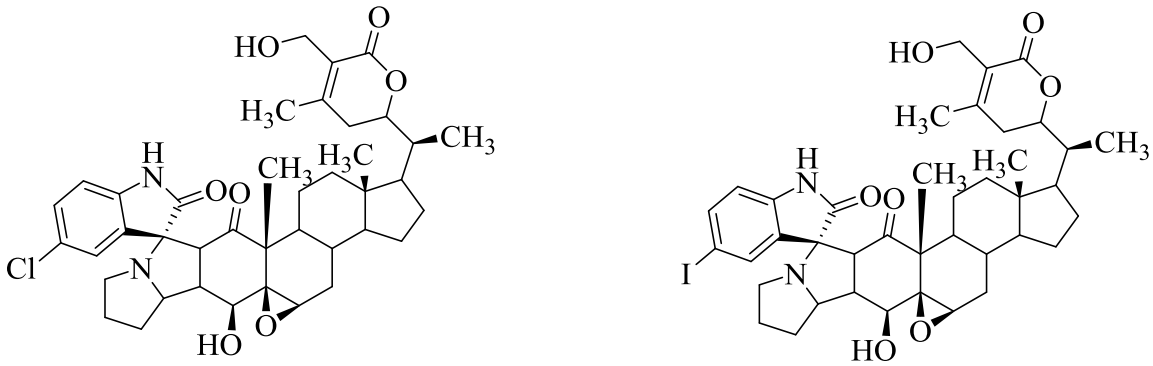

Figure 1.30

Ismail et al. reported the efficient method for the synthesis of the spiro[pyrazolo[4,3-]pyrimidinones and spiro[benzo[4,5]thieno[2,3-*d*]pyrimidine-2,3'-indoline]-2',4(3*H*)-diones under mild conditions using catalytic $InCl_3$ and their evaluation for anticancer activity (Figure 1.31) [48].

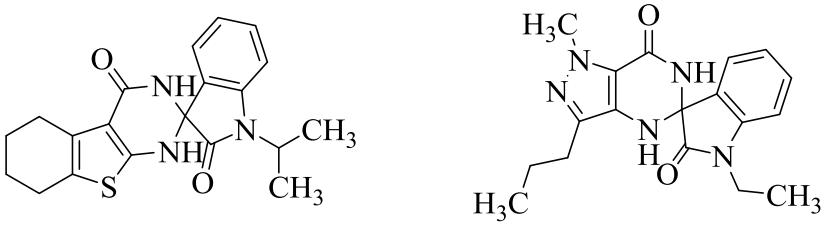

Figure 1.31

Qin et al. described the discovery and synthesis of 6,7,8,9-tetrahydro-5*H*-pyrido[4,3-*c*]azepin-5-ones (Figure 1.32). These compounds were tested for the chemo type CCR2 antagonist activity by employing a cut-and-sew scaffold hopping strategy. The systematic SAR study was illustrated for the target compounds [49].

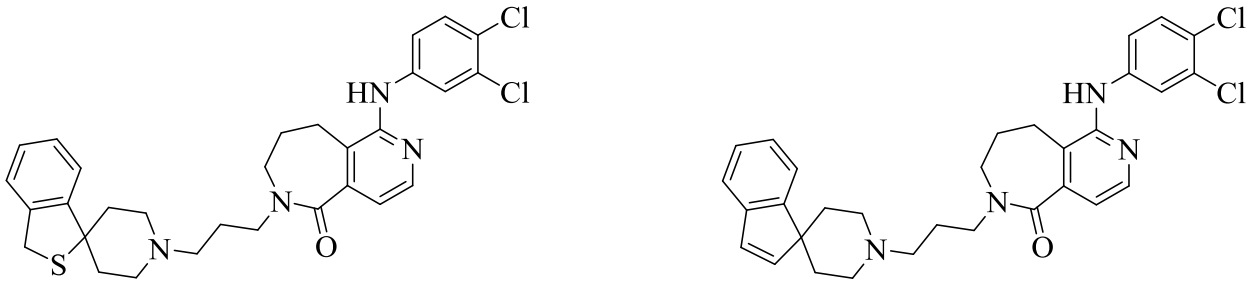

Figure 1.32

Gill et al. reported the one-pot, four-component synthesis and SAR studies of spiro[pyrimido[5,4-*b*]quinoline-1',5'-pyrrolo[2,3-*d*]pyrimidine] derivatives catalyzed by *β*-cyclodextrin in water as potential anticancer agents (Figure 1.33) [50].

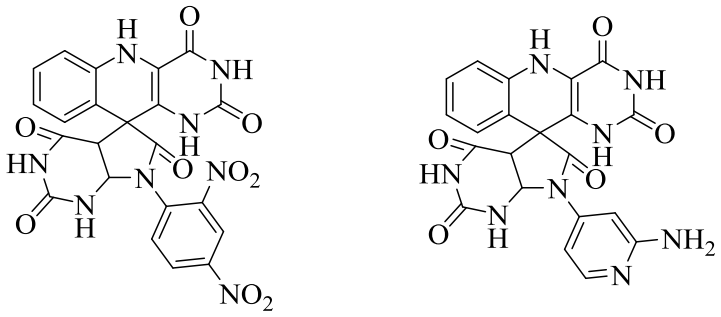

Figure 1.33

Bhaskarachar et al. described the design and synthesis of functionalized spiro-quinolines with barbituric and thiobarbituric acids (Figure 1.34). The synthesized compounds were evaluated for their anticancer and apoptosis activity [51].

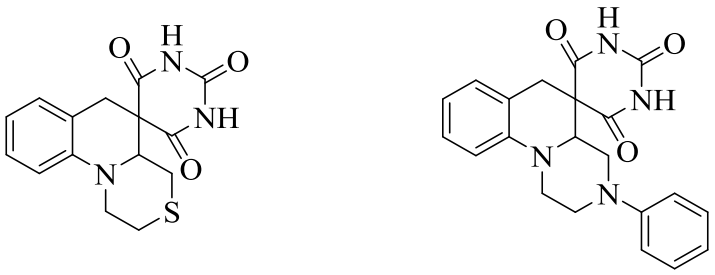

Figure 1.34

Ito and coworkers described the synthesis of a structurally distinct spiro[indole-3,2'-pyrrolidin]-2(1*H*)-one based Brr2 inhibitors. Using an RNA dependent ATPase assay as a guide, high-throughput screening, hit validation by SAR study and subsequent chemical optimization to increase the ATPase inhibitory activity were explored (Figure 1.35). Thereafter, selectivity and helicase inhibitory activity of optimized compounds were studied [52].

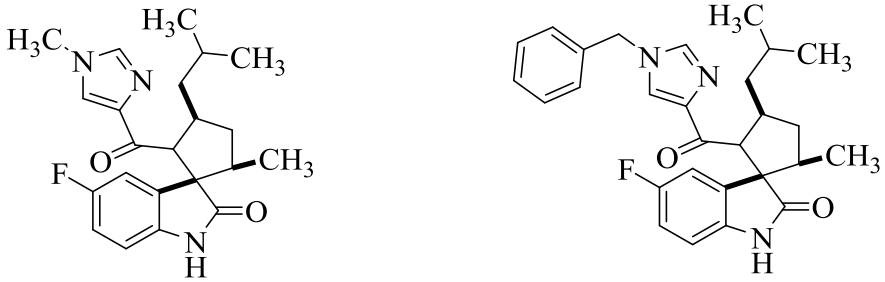

Figure 1.35

Lee and coworkers described a green and efficient protocol for the construction of spirooxindole derivatives bearing pyrano[2,3-*c*]pyrazole in presence of CeO_2 nano particles by a multicomponent coupling reaction (Figure 1.36). The synthesized spirooxindole derivatives showed potent antioxidant and antibacterial activities [53].

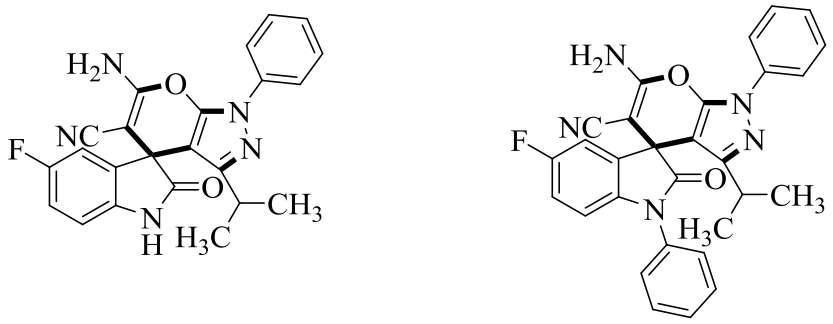

Figure 1.36

Thanusu et al. reported the synthesis and spectral analysis of ethyl 7,9-diaryl-1,4-diazaspiro[4,5]dec-9-ene-6-carboxylates (Figure 1.37). The synthesized compounds were evaluated as a new class of antibacterial and antifungal agents [54].

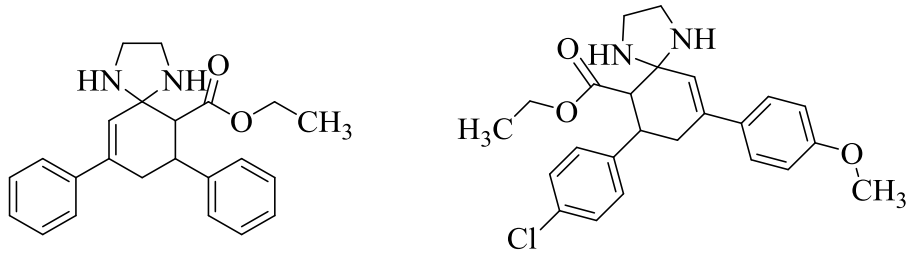

Figure 1.37

Xu et al. reported the synthesis of O-spiro C-aryl glucosides and tested for the inhibition of hSGLT1 and hSGLT2 (Figure 1.38). The target compounds were found that sodium-dependent glucose co-transporter 2 (SGLT2) inhibitors [55].

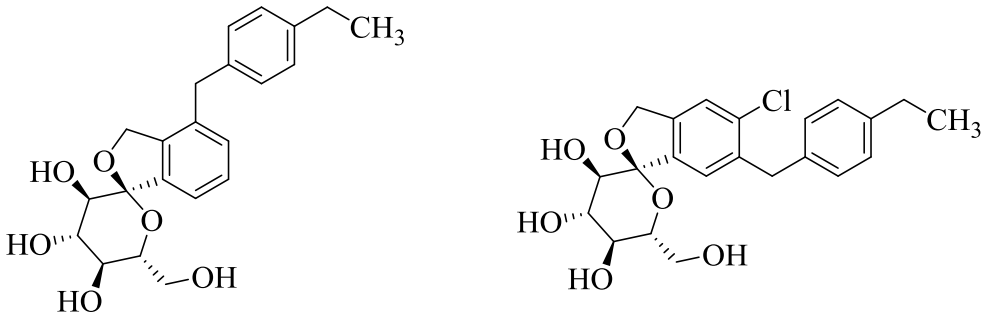

Figure 1.38

Thaler et al. reported the discovery and synthesis of a new class of spiro[2*H*-(1,3)-benzoxazine-2,4'-piperidine] derivatives (Figure 1.39). The target compounds were exhibited the histone deacetylase inhibition activity. The *in vivo* studies were also carried out for the target compounds to confirm the *in vitro* ADME data. The microsomial stability studies were carried out for selected compounds [56].

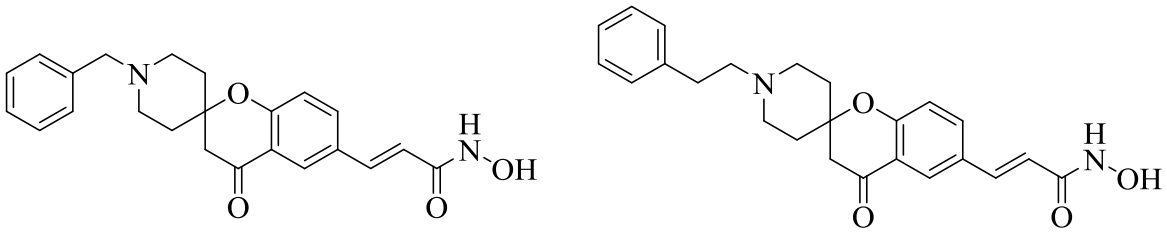

Figure 1.39

Gazzar and coworkers described a facile, regioselective synthesis of the spiro-thioxanthene and spiro-xanthene-9',2-[1,3,4]thiadiazole derivatives *via* 1,3-dipolar cycloaddition (Figure 1.40). The target compounds exhibited potential analgesic and antiinflammatory activities. The toxicology studies were also carried out on the synthesized compounds [57].

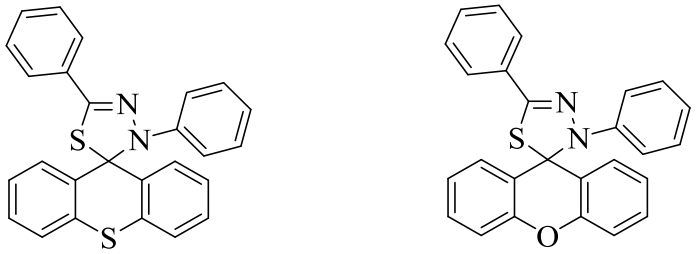

Figure 1.40

Imaeda et al. reported the discovery, synthesis and SAR study of 3,4-dihydro-1*H*-spiro(naphthalene-2,2'-piperidin)-1-ones as potassium-competitive acid blockers (Figure 1.41). The *in vivo* studies on rats were carried out for the synthesized compounds. The molecular docking studies were also carried out for the target compounds [58].

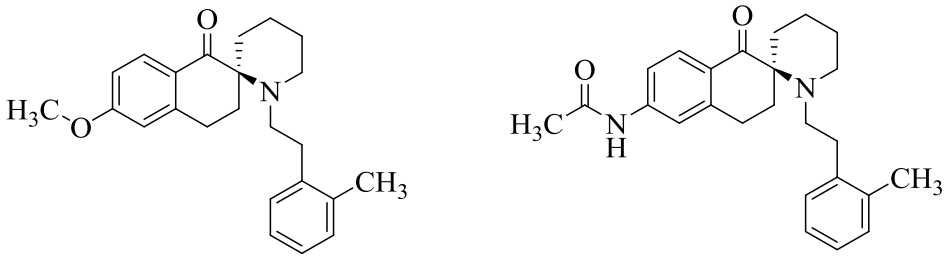

Figure 1.41

Shah and coworkers reported the design and synthesis of a series of spiro[azetidine-2,3'-indole]-2,4(1'*H*)-dione derivatives (Figure 1.42). The synthesized compounds were evaluated for their *in vitro* antibacterial and antifungal activities [59].

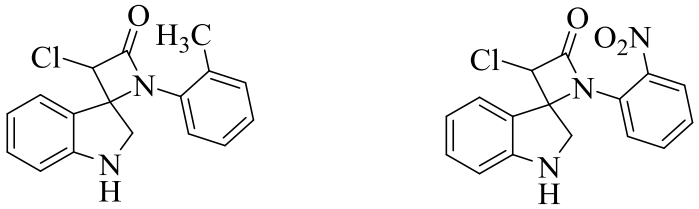

Figure 1.42

Girgis et al. reported the 1,3-dipolar cycloaddition reaction to afforded 7,9-dimethyl-1,3,4-triaryl-1,2,7,9-tetraaza-spiro[4,5]dec-2-ene-6,8,10-triones in a highly regioselective manner (Figure 1.43). The potentiating effects of the synthesized compounds on hypnotic action of sodium thiopental were investigated *in vivo* using Albino mice. A hypothesis of molecular modeling study, including fitting of the synthesized compounds into 3D-pharmacophore and their docking into optimized homology model of GABAA-a1 were consistent with the observed pharmacological properties [60].

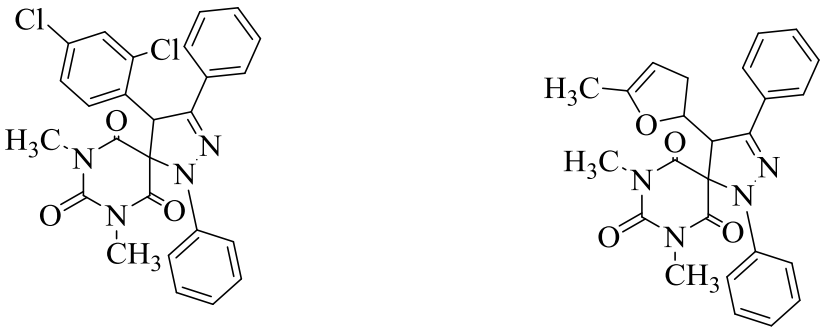

Figure 1.43

The incorporation of several biologically active molecules into a single molecule is the new strategy for the modern drug discovery [61]. Basing on this view, several biologically active heterocyclic moieties like quinoline, tetrazole, furan, thiophene, pyridine and coumarin were incorporated along with the target spiro compounds. Most of the synthesized compounds were evaluated for their *in vitro* anticancer, antibacterial, antifungal,

antioxidant activities and *in silico* molecular docking studies. A brief review on biological importance of the above mentioned heterocyclic scaffolds were also discussed in this chapter.

1.2. Quinolines

Quinoline is one of the prominent scaffolds for the construction of several heterocyclic motifs. Because of their wide occurrence in natural products and a broad spectrum of biological activities, they play a vital role in medicinal chemistry [62]. The incorporation of quinoline or its derivatives with other molecule may increase their biological activity or create new medicinal properties like antitumor activity, cytotoxic toward the leukemia P388 cells, etc., [63]. Quinoline containing molecules exhibit anticancer activity through different mechanisms like apoptosis, inhibition of angiogenesis, disruption of cell migration, growth inhibitors by cell cycle arrest and modulation of nuclear receptor responsiveness etc., [64]. Among quinolines, 2-chloro-3-formyl quinoline plays a prominent role in medicinal chemistry because it is a key intermediate for the synthesis of several alkaloids and biologically active molecules through various functional group interconversions [65]. On the other hand, 2-oxoquinoline is an alkaloid and possess broad spectrum of biological activities like anticancer, antioxidant, antiinflammation etc., [66, 67]. The chalcones derived from quinolines were also found to possessed the cytotoxic properties [68]. Some of the biologically active quinoline based molecules were shown in figure 1.44 [64-69].

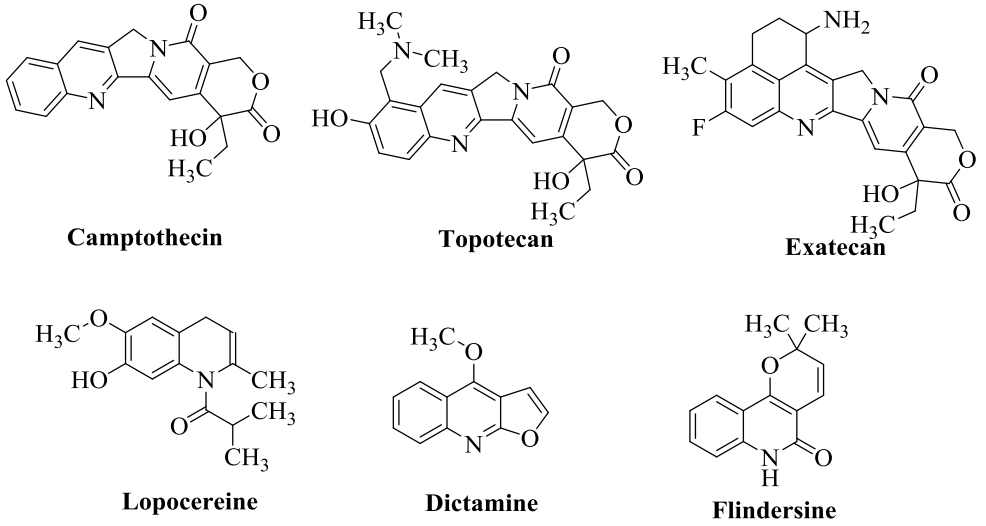

Figure 1.44

1.3. Tetrazoles

Tetrazole derivatives are well known compounds with highly pronounced biological activities like antiviral, antibacterial, antifungal, antiallergic, anticonvulsant and anti-inflammatory properties [70, 71]. In drug design, tetrazoles are regarded as an isostere for the carboxylate group [72]. Tetrazoles have wide range of applications as specialty explosives, in photography and information recording systems [73]. The tetrazole fused quinolines were known to increase the biological activities of individual precursors [70b, 74, 75]. Some of the drugs containing the tetrazole ring in their core moiety were shown in figure 1.45 [74-77].

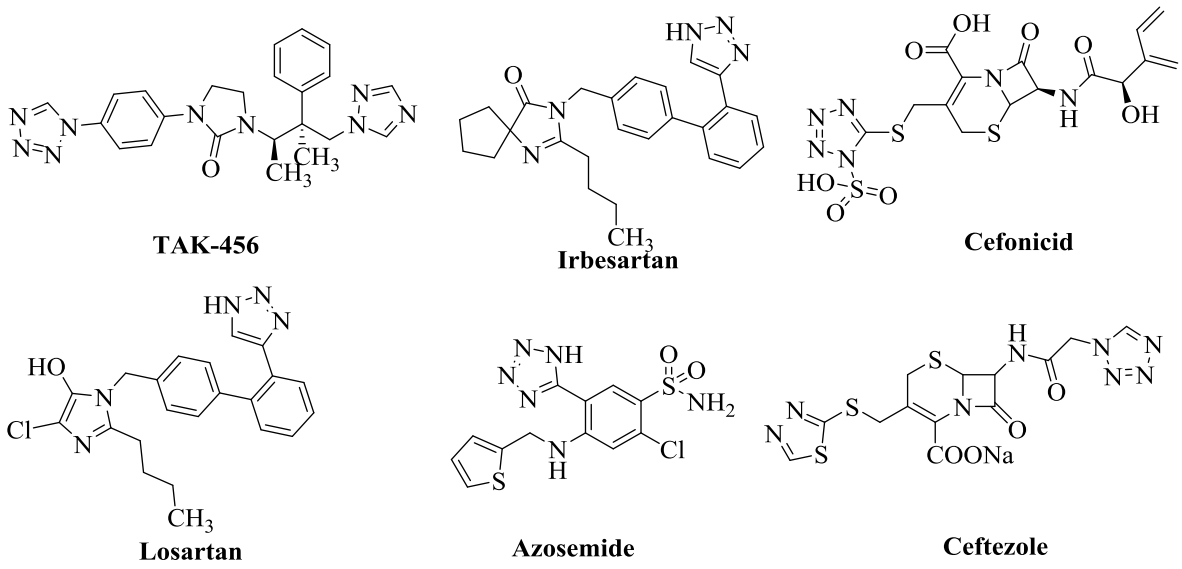

Figure 1.45

1.4. Furan, Thiophene and Pyridines

Furan, thiophene and pyridine plays a vital role in the biological activity of the several drugs. Furan based compounds exhibited various biological activities like antihyperglycemic, analgesic, antiinflammatory, antibacterial, antifungal, and antitumor activities [78]. The thiophene ring is present in numerous pharmacologically important compounds and natural products [79]. Thiophene based molecules exhibited anticancer, antiallergic, anticonvulsant etc., [79, 80]. Pyridine is a core moiety in many important natural compounds like vitamins (niacin and pyridoxine), the ubiquitous redox system NADP/NADPH and alkaloids (nicotine). Hence it is known for a wide range of biological

activities [81]. Some of the representative compounds having furan, thiophene and pyridine in their core structures were shown in figure 1.46 [79, 81-83].

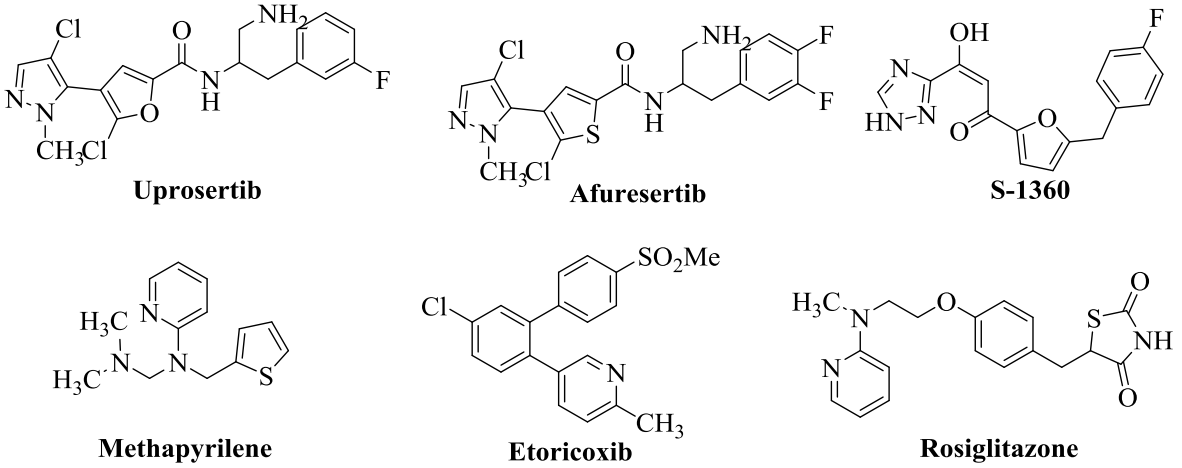

Figure 1.46

1.5. Coumarins

Coumarins (2*H*-chromen-2-one) are the polyphenolic plant-derived compounds pertained to the benzopyrones chemical class, mainly found in plants of the family of *Umbelliferae, Rutaceae, Guttiferae, Clusiaceae, Oleaceae*, *Caprifoliaceae, Apiaceae* and *Nyctaginaceae* [84]. Coumarin is also known as 1,2-benzopyrone or *o*-hydroxycinnamic acid-8-lactone, which were consisting the fused benzene and α-pyrone rings and gained much more attention due to their presence as a core moiety in many natural [85] and synthetic [86] biologically active products and also due to their variety of biological applications that includes anticancer, antimicrobial, antioxidant, antiallergic, antithrombotic, antiinflammatory, antituberculosis, anticoagulant, vasorelaxant, antiHIV, cyclooxygenase and lipoxygenase inhibitors, antifertillity, antipsychotic, MAO inhibitory activity and also as antiviral agents [87-94]. Some of the pharmacologically potent compounds contain the coumarin ring in their core structures were shown in figure 1.47 [84, 95].

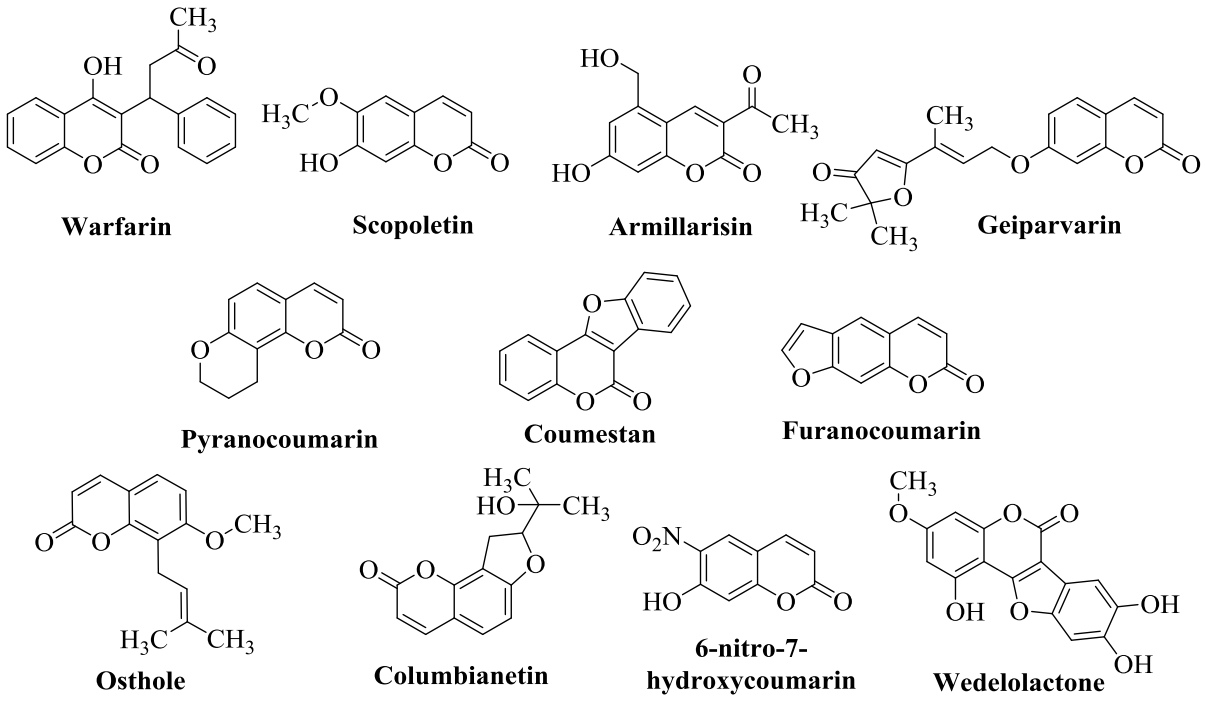

Figure 1.47

The rapid development of privileged diversity oriented syntheses (pDOS) to obtain biologically active molecules in a minimum number of steps is a new strategy for the modern drug discovery program. Even though these approaches are useful, they are not suitable for the library generation because of the limitations like the longer reaction times, multisteps for the synthesis, low yields, tedious isolation/purification of the resulting products, etc. Hence, synthesis of the biologically active molecules *via* the incorporation of one or more biological active molecules into a single hybrid framework is tedious in multistep approach. In this regard, multicomponent reactions are considered as an ideal synthetic tool for the generation of diverse drug-like molecules [96-99].

1.10. Multicomponent reaction (MCR)

MCRs are the prominent synthetic tool by allowing minimum of three components in one-pot to obtain the diverse polyfunctional drug-like scaffolds through the formation of several covalent bonds between carbon-carbon and carbon-hetero atoms. In these reactions most of the starting materials are retained and the isolation of intermediate is not required. The significant advantages of MCRs are high atom economy, efficiency, mild conditions,

high convergence or divergence, library generation, the easier progress of the reaction, decreased reaction times, high selectivity, etc., [96, 100-115]. Because of the variation of substituents, skeleton and stereochemistry, the diversity was achieved in MCR approach [116]. Based on the reactivity concept, MCRs can be divided into three different categories. In domino-type MCRs, all reagents have to be present from the very beginning of the process. The subsequent addition of components in a well-defined order without changing the reaction conditions is known as sequential MCR. Finally, the consecutive MCR implements the subsequent addition of reagents by changing the conditions from step to step [117]. The formation of cyanohydrins imines, first described by Gerhard and Laurent in 1838, can be considered as the first multicomponent reaction. After that, several methodologies like Strecker synthesis, Hantzsch reaction, Biginelli reaction, Mannich reaction, Passerini reaction, Ugi reaction, etc., were developed [118]. The multicomponent 1,3-dipolar cycloaddition is an efficient method for the synthesis of five membered heterocyclic compounds in a highly regio- and stereo-selective manner. The nitrogen containing spiro compounds like spiropyrrolizidines with stereogenic centers were synthesized *via* multicomponent 1,3-dipolar cycloaddition reaction because these reactions are concerted [119, 120].

1.11. Molecular docking studies

The major application of the molecular docking studies is to design the compounds *in silico* and targeted against proteins (macromolecules), the binding modes of these compounds (ligands) with active site of a target protein. Thus the compounds which are strongly bound to a protein were treated as lead molecules. In *in vitro* experiments, drugs are discovered by a chance in a trial-and-error method by using high-throughput screening of a large number of compounds against a given target. This process is time consuming and highly expensive. Whereas, if the 3D structure of the compound is known, then the molecular docking is a useful tool in the identification of drug candidates by a virtual screening of compound databases. The energetically more favorable ligand conformation is suitable for the docking. In general, low energy scores represent the better protein-ligand bindings [121]. The most commonly used heuristic search algorithms that have been applied to molecular docking are simulated annealing, tabu search and evolutionary algorithms [122-126]. The molecular

docking studies in the thesis work were carried out by using AutoDock Tools (ADT) version 1.5.6 and AutoDock version 4.2.5.1 docking program.

AutoDock is a suite of free open–source software (http://autodock.scripps.edu) for the computational docking and virtual screening of designed molecules to macromolecular receptors and has been widely used in research and drug discovery [127]. AutoDock is a computational docking program based on an empirical free energy force field and rapid Lamarckian genetic algorithm search method [124, 127]. AutoDock Tools is an interactive graphical tool for coordinate preparation, docking and analysis [128].

References

1) R. Dua, S. Shrivastava, S. K. Sonwane, S. K. Srivastava, *Adv. Bio. Res.* **2011**, *5*, 120.
2) J. A. Joule, K. Mills. *Heterocyclic Chem.* John Wiley & Sons, **2010**.
3) J. Clayden, N. Geeves, S. Warren, *Organic Chemistry*, Oxford University Press, 2nd ed., **2012**.
4) G. S. Singh, Z. Y. Desta, *Chem. Rev.* **2012**, *112*, 6104.
5) H. Foks, D. P. Ksepko, M. Janowiec, Z. Zwolska, E. A. W. Kopec, *Acta Pol. Pharm.* **2004**, *61*, 473.
6) K. Bethge, H. H. Pertz, K. Rehse, *Arch. Pharm. (Weinheim)* **2005**, *338*, 78.
7) R. Pradhan, M. Patra, A. K. Behera, B. K. Mishra, R. K. Behera, *Tetrahedron.* **2006**, *62*, 779.
8) P. Saraswat, G. Jeyabalan, M. Z. Hassan, M. U. Rahman, N. K. Nyola, *Syn. Commun.* **2016**, *46*, 1643.
9) E. Palaska, M. Aytemir, I. T. Uzbay, D. Erol, *Eur. J. Med. Chem.* **2001**, *36*, 539.
10) H. Hu, H. Guo, E. Li, X. Liu, Y. Zhou, Y. Che, *J. Nat. Prod.* **2006**, *69*, 1672.
11) J. J. Li, X. M. Liang, S. H. Jin, J. J. Zhang, H. Z. Yuan, S. H. Qi, F. H. Chen, D. Q. Wang, *J. Agric. Food Chem.* **2010**, *58*, 2659.
12) G. T. Zitouni, O. Ozdemir, K. Guven, *Arch. Pharm. (Weinheim),* **2005**, *338*, 96.
13) T. S. Jeong, K. S. Kim, S. J. An, K. H. Cho, S. Lee, W. S. Lee, *Bioorg. Med. Chem. Lett.* **2004**, *14*, 2715.
14) B. Yu, D. Q. Yu, H. M. Liu, *Eur. J. Med. Chem.* **2015**, *97*, 673.
15) Y. Zheng, C. M. Tice, S. B. Singh, *Bioorg. Med. Chem. Lett.* **2014**, *24*, 3673.

16) L. K. Smith, I. R. Baxendale, *Org. Biomol. Chem*. **2015**, *13*, 9907.

17) G. Lotfy, M. M. Said, E. S. H. E. Ashry, E. S. H. E. Tamany, A. A. Dhfyan, Y. M. A. Aziz, A. Barakat, *Bioorg. Med. Chem.***2017**, *25*, 1514.

18) P. R. Mali, P. K. Shirsat, N. Khomane, L. Nayak, J. B. Nanubolu, H. M. Meshram, *ACS Comb. Sci*., **2017**, *19*, 633.

19) O. A. Attanasi, L. A. Campisi, L. D. Crescentini, G. Favi, F. Mantellini, *Org. Biomol. Chem*. **2015**, *13*, 277.

20) A. Gollner, D. Rudolph, H. Arnhof, et al. *J. Med. Chem*. **2016**, *59*, 10147.

21) D. Rambabu, S. K. Kumar, B. Y. Sreenivas, S. Sandra, A. Kandale, P. Misra, M. V. B. Rao, M. Pal, *Tetrahedron Lett.* **2013**, *54*, 495.

22) T. Koshizawa, T. Morimoto, G. Watanabe, T. Fukuda, N. Yamasaki, S. Hagita, Y. Sawada, A. Okuda, K. Shibuya, T. Ohgiya, *Bioorg. Med. Chem. Lett.* **2018**, 28, 3236.

23) M. Kamata, T. Yamashita, A. Kina, M. Funata, A. Mizukami, M. Sasaki, A. Tani, M. Funami, N. Amano, K. Fukatsu, *Bioorg. Med. Chem. Lett.* **2012**, *22*, 3643.

24) M. Kamata, T. Yamashita, A. Kina, M. Tawada, S. Endo, A. Mizukami, M. Sasaki, A. Tani, Y. Nakano, Y. Watanabe, N. Furuyama, M. Funami, N. Amano, K. Fukatsu, *Bioorg. Med. Chem. Lett.* **2012**, *22*, 4769.

25) C. Bharkavi, S. V. Kumar, M. A. Ali, H. Osman, S. Muthusubramanian, S. Perumal, *Bioorg. Med. Chem*. **2016**, *24*, 5873.

26) C. Bharkavi, S. V. Kumar, M. A. Ali, H. Osman, S. Muthusubramanian, S. Perumal, *Bioorg. Med. Chem. Lett.* **2017**, *27*, 3071.

27) K. K. Alluri, R. S. Reshma, R. Suraparaju, S. Gottapu, D. Sriram, *Bioorg. Med. Chem*. **2018**, *26*, 1462.

28) Z. Y. Cheng, Y. Q. Du, Q. Zhang, B. Lin, P. Y. Gao, X. X. Huang, S. J. Song, *Tetrahedron Lett.* **2018**, *59*, 2050.

29) P. Prasanna, K. Balamurugan, S. Perumal, P. Yogeeswari, D. Sriram, *Eur. J. Med. Chem.* **2010**, *45*, 5653.

30) A. Maryamabadi, A. Hasaninejad, N. Nowrouzi, G. Mohebbi, B. Asghari, *Bioorg. Med. Chem.* **2016**, *24*, 1408.

31) A. Dandia, R. Singh, D. Saini, *J. Chem. Sci.* **2013**, *125*, 1045.

32) A. Dandia, D. Saini, S. Bhaskaran, D. K. Saini, *Med. Chem. Res*. **2014**, *23*, 725.

33) D. Xiao, A. Palani, R. Aslanian, B. A. McKittrick, A. T. McPhail, C. C. Correll, P. T. Phelps, J. C. Anthes, D. Rindgen, *Bioorg. Med. Chem. Lett.* **2009**, *19*, 783.

34) H. G. Bonacorso, W. C. Rosa, S. M. Oliveira, I. Brusco, E. S. Brum, M. B. Rodrigues, C. P. Frizzo, N. Zanatta, *Bioorg. Med. Chem. Lett.* **2017**, *27*, 1551.

35) D. M. Reddy, N. A. Qazi, S. D. Sawant, A. H. Bandey, J. Srinivas, M. Shankar, S. K. Singh, M. Verma, G. Chashoo, A. Saxena, D. Mondhe, A. K. Saxena, V. K. Sethi, S. C. Taneja, G. N. Qazi, H. M. S. Kumar, *Eur. J. Med. Chem.* **2011**, *46*, 3210.

36) L. Yang, P. Wang, J. F. Wu, L. M. Yang, R. R. Wang, W. Pang, Y. G. Li,Y. M. Shen, Y. T. Zheng, X. Li, *Bioorg. Med. Chem.* **2016**, *24*, 2125.

37) R. A. Kusanur, M. Ghate, M. V. Kulkarni, *J. Chem. Sci.* **2004**, *116*, 265.

38) C. N. Reddy, V. L. Nayak, G. S. Mani, J. S. Kapure, P. R. Adiyala, R. A. Maurya, A. Kamal, *Bioorg. Med. Chem. Lett.* **2015**, *25*, 4580.

39) M. A. Ameen, E. Kh. Ahmed, M. Ramadan, H. A. A. E. Naby, A. A. A. Haseeb, *Monatsh. Chem.* **2017**, *148*, 1513.

40) D. Matsuda, M. Kawamura, Y. Kobashi, F. Shiozawa, Y. Suga, K. Fusegi, S. Nishimoto, K. Kimura, M. Miyoshi, N. Takayama, H. Kakinuma, N. Ohtake, *Bioorg. Med. Chem.* **2018**, *26*, 1832.

41) S. S. Fatahala, S. Mahgub, H. Taha, R. H. A. E. Hameed, *J. Enzyme Inhib. Med. Chem*. **2018**, *33*, 809.

42) L. Zhang, W. Ren, X. Wang, J. Zhang, J. Liu, L. Zhao, *Eur. J. Med. Chem.* **2017**, *126*, 1071.

43) Á. A. Kelemen, G. Satała, A. J. Bojarski, G. M. Keserű, *Bioorg. Med. Chem. Lett.* **2018**, *28*, 2418.

44) C. I. Stathakis, I. Mavridis, G. Kythreoti, A. Papakyriakou, I. A. Katsoulis, T. Cottin, P. Anastasopoulou, D. Vourloumis, *Bioorg. Med. Chem. Lett.* **2010**, *20*, 7488.

45) W. M. Abdou, N. A. Ganoub, E. Sabry, *Monatsh. Chem*. **2016**, *147*, 619.

46) Q. Wei, L. Mei, Y. Yang, H. Ma, H. Chen, H. Zhang, J. Zhou, *Bioorg. Med. Chem.* **2018**, *26*, 3866.

47) Y. P. Bharitkar, S. Kanhar, N. Suneel, S. K. Mondal, A. Hazra, N. B. Mondal, *Mol. Divers*. **2015**, *19*, 251.

48) Ismail, B. Kuthati, G. Thalari, V. Bommarapu, C. Mulakayala, S. K. Chitta, N. Mulakayala, *Bioorg. Med. Chem. Lett.* **2017**, *27*, 1446.

49) L. H. Qina, Z. L. Wang, X. Xiea, Y. Q. Long, *Bioorg. Med. Chem.* **2018**, *26*, 3559.

50) C. H. Gill, A. V. Chate, G. Y. Shinde, A. P. Sarkate, S. V. Tiwari, *Res. Chem. Intermed.* **2018**, *44*, 4029.

51) R. K. Bhaskarachar, V. G. Revanasiddappa, S. Hegde, J. P. Balakrishna, S. Y. Reddy, *Med. Chem. Res.* **2015**, *24*, 3516.

52) M. Ito, M. Iwatani, T. Yamamoto, T. Tanaka, T. Kawamoto, D. Morishita, A. Nakanishi, H. Maezaki, *Bioorg. Med. Chem.* **2017**, *25*, 4753.

53) R. Shrestha, K. Sharma, Y. R. Lee, Y. J. Wee, *Mol. Divers*. **2016**, *20*, 847.

54) J. Thanusu, V. Kanagarajan, M. Gopalakrishnan, *Chem. Heterocycl. Comp.* **2011**, *47*, 60.

55) B. Xu, B. Lv, Y. Feng, G. Xu, J. Du, A. Welihinda, Z. Sheng, B. Seed, Y. Chen, *Bioorg. Med. Chem. Lett.* **2009**, *19*, 5632.

56) F. Thaler, M. Varasi, A. Abate, G. Carenzi, A. Colombo, C. Bigogno, R. Boggio, R. D. Zuffo, D. Rapetti, A. Resconi, N. Regalia, S. Vultaggio, G. Dondio, S. Gagliardi, S. Minucci, C. Mercurio, *Eur. J. Med. Chem.* **2013**, *64*, 273.

57) H. N. Hafez, M. I. Hegab, I. S. Ahmed-Farag, A. B. A. El-Gazzar, *Bioorg. Med. Chem. Lett*. **2008**, *18*, 4538.

58) T. Imaeda, K. Ono, K. Nakai, Y. Hori, J. Matsukawa, T. Takagi, Y. Fujioka, N. Tarui, M. Kondo, A. Imanishi, N. Inatomi, M. Kajino, F. Itoh, H. Nishida, *Bioorg. Med. Chem.* **2017**, *25*, 3719.

59) R. J. Shah, N. R. Modi, M. J. Patel, L. J. Patel, B. F. Chauhan, M. M. Patel, *Med. Chem. Res.* **2011**, *20*, 587.

60) A. S. Girgis, H. Farag, N. S. M. Ismail, R. F. George, *Eur. J. Med. Chem.* **2011**, *46*, 4964.

61) N. Sudhapriya, P. T. Perumal, C. Balachandran, S. Ignacimuthu, M. Sangeetha, M. Doble, *Eur. J. Med. Chem*. **2014**, *83*, 190.

62) S. Jain, V. Chandra, P. K. Jain, K. Pathak, D. Pathak, A. Vaidya, *Arab. J. Chem.* **2016**, DOI: 10.1016/j.arabjc.2016.10.009.

63) (a) Z. Z. Ma, Y. Hano, T. Nomura, Y. J. Chen, *Heterocycles.* **1997**, *46,* 541; (b) P. G. Mandhane, R. S. Joshi, P. S. Mahajan, M. D. Nikam, D. R. Nagargoje, C. H. Gill, *Arab. J. Chem.* **2015**, *8*, 474.

64) O. Afzal, S. Kumar, M. R. Haider, M. R. Ali, R. Kumar, M. Jaggi, S. Bawa, *Eur. J. Med. Chem.* **2015**, *97*, 871.

65) (a) M. Nyerges, A. Pinter, A. Viranyi, G. B. L. Token. *Tetrahedron.* **2005**, *61*, 8199; (b) M. M. Maluleka, M. J. Mphahlele, *Tetrahedron.* **2013**, *69*, 699.

66) B. Yu, Z. Yu, P. P. Qi, D. Q. Yu, H. M. Liu, *Eur. J. Med. Chem.* **2015**, *95*, 35.

67) B. Yu, X. N. Sun, X. J. Shi, P. P. Qi, Y. C. Zheng, D. Q. Yu, H. M. Liu, *Steroids.* **2015**, *102*, 92.

68) M. M. Ghora, F. A. Raga, H. I. Heiba, W. M. Ghora, *J. Heterocyclic Chem.* **2011**, *48*, 1269.

69) F. Hayat, E. Moseley, A. Salahuddin, R. L. V. Zyl, A. Azam, *Eur. J. Med. Chem.* **2011**, *46,* 1897.

70) (a) B. Schmidt, B. Schieffcr, *J. Med. Chem.* **2003**, *46,* 2261; (b) A. A. Bekhit, O. A. El-Sayed, E. Aboulmagd, J. Y. Park, *Eur. J. Med. Chem.* **2004**, *39,* 249.

71) (a) V. V. Zarubaev, E. L. Golod, P. M. Anfimov, A. A. Shtro,V. V. Saraev, A. S. Gavrilov, A. V. Logvinov, O. I. Kiselev, *Bioorg. Med. Chem.* **2010**, *18,* 839; (b) T. D. Connor, A. P. Young and M. V. Strandtmann, *US Patent*, **1980**, *4*, 225; (c) C. L. Mitchell, *Toxicol. Appl. Pharmacol.* **1964**, *6,* 23; (d) K. Raman, S. S. Parmar, S. P. Singh, *J. Heterocycl. Chem.* **1980**, *17*, 1137.

72) (a) L. V. Myznikov, A. Hrabalek, G. I. Koldobskii, *Chem. Heterocycl. Compd.* **2007**, *43*, 1; (b) H. R. Meier, H. Heimgartner, *In Methoden der Organischen Chemie (Houben-Weyl); Schumann, E., Ed.; Georg Thieme: Stuttgart*, **1994**, *E8d,* 664; (c) R. N. Butler, *Comprehensive Heterocyclic Chemistry;* A. R. Katritzky, C. W. Rees, Pergamon, *Oxford,* **1984**, *5,* 791.

73) R. S. Upadhayaya, S. Jain, N. Sinha, N. Kishore, R. Chandra, S. K. Arora, *Eur. J. Med. Chem.* **2004**, *39,* 579.

74) A. H. Kategaonkar, R. U. Pokalwar, S. S. Sonar, V. U. Gawali, B. B. Shingate,M. S. Shingare, *Eur. J. Med. Chem.* **2010**, *45,* 1128.

75) S. S. Sonar, S. A. Sadaphal, R. U. Pokalwar, B. B. Shingate, M. S. Shingare, *J. Heterocyclic Chem.* **2010**, *47*, 441.

76) V. A. Ostrovskii, R. E. Trifonov, E. A. Popova, *Russ. Chem. Bull. Int. Ed.* **2012**, *61*, 768.

77) C. N. S. S. P. Kumar, D. K. Parida, A. Santhoshi, A. K. Kota, B. Sridhar, V. J. Rao, *Med. Chem. Commun.* **2011**, *2*, 486.

78) K. Manna, Y. K. Agrawal, *Bioorg. Med. Chem. Lett.* **2009**, *19*, 2688.

79) Y. N. Mabkhot, F. Alatibi, E. N. Nasser, E. Sayed, S. A. Showiman,N. A. Kheder, A. Wadood, A. Rauf, S. Bawazeer, T. B. Hadda, *Molecules.* **2016**, *21*, 222.

80) V. K. Patel, A. Singh, D. K. Jain, P. Patel, R. Veerasamy, P. C. Sharma, H. Rajak, *Future J. Pharm. Sci.* **2017**, *3*, 71.

81) M. Baumann, I. R. Baxendale, *Beilstein. J. Org. Chem.* **2013**, *9*, 2265.

82) S. Radi, S. Tighadouini, O. Feron, O. Riant, M. Bouakka, R. Benabbes, Y. N. Mabkhot, *Molecules.* **2015**, *20*, 20186.

83) D. R. Boyd, N. D. Sharma, N. Gunaratne, S. A. Haughey, M. A. Kennedy, J. F. Malone, C. C. R. Allen, H. Dalton, *Org. Biomol. Chem.* **2003**, *1*, 984.

84) (a) S. Emami, S. Dadashpour, *Eur. J. Med. Chem*. **2015**, *102*, 611; (b) M. Z. Hassan, H. Osman, M. A. Ali, M. J. Ahsan, *Eur. J. Med. Chem*. **2016**, *123*, 236.

85) F. Borges, F. Roleira, N. Milhazes, L. Santana, E. Uriarte, *Curr. Med. Chem*. **2005**, *12*, 887.

86) (a) S. S. Sahoo, S. Shukla, S. Nandy, H. B. Sahoo, *Eur. J. Expt. Biol*. **2012**, *2*, 899; (b) C. A. Kontogiorgis, D. J. H. Litina, *Bioorg. Med. Chem. Lett*. **2004**, *14*, 611.

87) A. Lacy, R. O'Kennedy, *Curr. Pharm. Des*. **2004**, *10*, 3797.

88) (a) D. A. Ostrov, J. A. H. Prada, P. E. Corsino, K. A. Finton, N. Le, T. C. Rowe, *Antimicrob. Agents. Chemother*. **2007**, *51*, 3688; (b) F. Chimenti, B. Bizzarri, A. Bolasco, D. Secci, P. Chimenti, A. Granese, S. Carradori, D. Rivanera, A. Zicari, M. M. Scaltrito, F. Sisto, *Bioorg. Med. Chem. Lett*. **2010**, *20*, 4922.

89) (a) I. Kostova, S. Bhatia, P. Grigorov, S. Balkansky, V. S. Parmar, A. K. Prasad, L. Saso, *Curr. Med. Chem*. **2011**, *18*, 3929; (b) G. L. Xi, Z. Q. J. Liu, *Agric. Food Chem*. **2015**, *63*, 3516.

90) X. M. Peng, G. L. Damu, C. Zhou, *Curr. Pharm. Des*. **2013**, *19*, 3884.

91) (a) Y. Bansal, P. Sethi, G. Bansal, *Med. Chem. Res*. **2013**, *22*, 3049; (b) K. C. Fylaktakidou, D. J. H. Litina, K. E. Litinas, D. N. Nicolaides, *Curr. Pharm. Des*. **2004**, *10*, 3813.

92) A. Manvar, A. Bavishi, A. Radadiya, J. Patel, V. Vora, N. Dodia, K. Rawal, A. Shah, *Bioorg. Med. Chem. Lett*. **2011**, *21*, 4728.

93) (a) J. R. Hwu, S. Y. Lin, S. C. Tsay, E. De Clercq, P. Leyssen, J. Neyts, *J. Med. Chem*. **2011**, *54*, 2114; (b) E. B. Ong, N. Watanabe, A. Saito, Y. Futamura, K. H. Abd El Galil, A. Koito, N. Najimudin, H. Osada, *J. Biol. Chem*. **2011**, *286*, 14049;

94) M. Curini, F. Epifano, F. Maltese, M. C. Marcotullio, S. P. Gonzales, J. C. Rodriguez, *Aust. J. Chem.* **2003**, *56*, 59.

95) C. Kontogiorgis, A. Detsi, D. H. Litina, *Expert. Opin. Ther. Pat*. **2012**, *22*, 437

96) P. Vincetti, A. Brianza, N. Scalacci, G. Costantino, D. Castagnolo, M. Radi, *Tetrahedron Lett.* **2016**, *57*, 1464.

97) H. Liu, G. Dou, D. Shi, *J. Comb. Chem.* **2010**, *12*, 633.

98) Y. Arun, K. Saranraj, C. Balachandran, P. T. Perumal, *Eur. J. Med. Chem.* **2014**, *74*, 50.

99) A. Hazra, Y. P. Bharitkar, D. Chakraborty, S. K. Mondal, N. Singal, S. Mondal, A. Maity, R. Paira, S. Banerjee, N. B. Mondal, *ACS Comb. Sci.*, **2013**, *15*, 41.

100) (a) M. R. Nabid, S. J. T Rezaei, R. Ghahremanzadeh, A. Bazgir, *Ultrason. Sonochem.* **2010**, *17*, 159; (b) V. Sridharan, K. Karthikeyan, S. Muthusubramanian, *Tetrahedron Lett*. **2006**, *47*, 4221. c) V. B. Nishtala, J. B. Nanubolu, S. Basavoju, *Res. Chem. Intermed.* **2017**, *43*, 1365.

101) B. H. Rotstein, S. Zaretsky, V. Rai, A. K. Yudin, *Chem. Rev.* **2014**, *114*, 8323.

102) A. Dömling, *Chem. Rev.* **2006**, *106*, 17.

103) W. Chen, X. Peng, L. Zhong,Y. Li, R. Sun, *ACS Sustainable Chem. Eng.* **2015**, *3*, 1366.

104) C. Liu, M. Shen, B. Lai, A. Taheri, Y. Gu, *ACS Comb. Sci.* **2014**, *16*, 652.

105) A. N. Muller, I. R. Correa, Jr. H. Prinz, C. Rosenbaum, K. Saxena, H. J. Schwalbe, D. Vestweber, G. Cagna, S. Schunk, O. Schwarz, H. Schiewe, H. Waldmann. *Proc. Natl. Acad. Sci.* **2006**, *103*, 10607.

106) (a) J. Andraos, *ACS Sustainable Chem. Eng.* **2013**, *1,* 496; (b) J. Andraos, *Org. Process Res. Dev.* **2005**, *9,* 404; (c) P. Slobbe, E. Ruijter, R. V. A. Orru, *Med. Chem. Commun.* **2012**, *3,* 1189; (d) S. Periyaraja, P. Shanmugam, A. B. Mandal, T. S. Kumar, P. Ramamurthy, *Tetrahedron.* **2013**, *69,* 2891; (e) S. L. Zhu, S. J. Ji, X. M. Su, C. Sun, Y. Liu, *Tetrahedron Lett.* **2008**, *49,* 1777; (f) U. Kusebauch, B. Beck, K. Messer, E. Herdtweck, A. Dömling, *Org. Lett*. **2003**, *5,* 4021.

107) (a) A. Dömling, W. Wang, K. Wang, *Chem. Rev.* **2012**, *112,* 3083; (b) I. V. Magedov, A. Kornienko, *Chem. Heterocycl. Compd.* **2012**, *48,* 33; (c) R. C. Cioc, E. Ruijter, R. V. A. Orru, *Green Chem.* **2014**, *16,* 2958; (d) C. Kalinski, M. Umkehrer, L. Weber, J. Kolb, C. Burdack, G. Ross, *Mol. Diversity* **2010**, *14,* 513; (e) I. A. Zanze, *Curr. Opin. Chem. Biol.* **2008**, *12,* 324. (f) W. H. Moos, C. R. Hurt, G. A. Morales, *Mol. Diversity* **2009**, *13,* 241; (g) B. B. Touré, D. G. Hall, *Chem. Rev.* **2009**, *109,* 4439; (h) C. Lamberth, A. Jeanguenat, F. Cederbaum, A. D. Mesmaeker, M. Zeller, H. J. Kempf, R. Zeun, *Bioorg. Med. Chem.* **2008**, *16,* 1531; (i) R. Kakuchi, *Angew. Chem. Int. Ed.* **2014**, *53,* 46.

108) L. Hai, G. Dou, D. Shi, *J. Comb. Chem.* **2010**, *12,* 633.

109) A. S. Girli, Y. Deureust, B. Kariuki, D. W. Knight, *Tetrahedron.* **2013**, *69,* 69.

110) J. F. A. Filho, B. C. Lemos, A. S. D. Souza, S. Pinheiro, S. J. Greco, *Tetrahedron.* **2017**, *73,* 6977.

111) T. N. Trinh, A. M. Cluskey, *Tetrahedron Lett.* **2016**, *57,* 3256.

112) M. S. Reddy, L. R. Chowhan, N. S. Kumar, P. Ramesh, S. B. Mukkamala, *Tetrahedron Lett.* **2018**, *59,* 1366.

113) Y. H. He, J. F. Cao, R. Li, Y. Xiang, D. C. Yang, Z. Guan, *Tetrahedron.* **2015**, *71,* 9299.

114) M. C. Bellucci, A. Sganappa, M. Sani, A. Volonterio, *Tetrahedron.* **2015**, *71,* 7630.

115) P. Pattnaik, S. Nayak, D. R. Mishra, P. Panda, B. P. Raiguru, N. P. Mishra, S. Mohapatra, N. A. Mallampudi, C. S. Purohit. *Tetrahedron Lett.* **2018**, *59,* 2688.

116) A. D. Morozova, E. A. Muravyova, V. S. Shishkina, V. Elena, Y. V. Senko, V. A. Chebanova, *J. Heterocyclic Chem.* **2017**, *54,* 932.

117) L. Levi, T. J. J. Muller, *Chem. Soc. Rev.* **2016**, *45,* 2825.

118) S. Brauch, S. S. V. Berkela, B. Westermann, *Chem. Soc. Rev.* **2013**, *42,* 4948.

119) (a) J. A. Xiao, H. G. Zhang, S. Liang, J. W. Ren, H. Yang, X. Q. Chen, *J. Org. Chem.* **2013**, *78*, 11577; (b) A. Kumar, G. Gupta, S. Srivastava, A. K. Bishnoi, R. Saxena, R. Kant, R. S. Khanna, P. R. Maulikc, A. Dwivedib, *RSC Adv.* **2013**, *3*, 4731; (c) G. R. Sarker, M. A. B, *Tetrahedron.* **2006**, *62*, 10332. (d) P. J. S. Gomes, C. M. Nunes, A. A. C. C. Pais, T. M. V. D. P. Melo, L. G. Arnaut, *Tetrahedron Lett.* **2006**, *47*, 5475.

120) (a) S. Haddad, S. Boudriga, F. Porzio, A. Soldera, M. Askri, M. Knorr, Y. Rousselin, M. M. Kubicki, C. Golz, C. Strohmann, *J. Org. Chem.* **2015**, *80*, 9064; (b) A. Thangamani, *Eur. J. Med. Chem.* **2010**, *45*, 6120.

121) R. Thomsen, M. H. Christensen. *J. Med. Chem.* **2006**, *49*, 3315.

122) S. Kirkpatrick, C. D. Gelatt, M. P. Vecchi, *Science.* **1983**, *220*, 671.

123) D. S. Goodsell, A. J. Olson, *Proteins: Struct. Funct. Genet.* **1990**, *8*,195.

124) D. R. Westhead, D. E. Clark, C. W. Murray, *J. Comput. Aided Mol. Des.* **1997**, *11*, 209.

125) G. Jones, P. Willett, R. C. Glen, A. R. Leach, R. Taylor, *J. Mol. Biol.* **1997**, *267*, 727.

126) G. M. Morris, D. S. Goodsell, R. S. Halliday, R. Huey, W. E. Hart, R. K. Belew, A. J. Olson, *J. Comput. Chem.* **1998**, *19*, 1639.

127) S. Forli, R. Huey, M. E. Pique, M. Sanner, D. S. Goodsell, A. J. Olson, *Nat. Protoc.* **2016**, *11*, 905.

128) G. M. Morris, *J. Comput. Chem.* **2009**, *30*, 2785.

CHAPTER-II (SECTION-A)

Multicomponent regioselective synthesis of quinolinyl spiropyrrolizidines *via* 1,3-dipolar cycloaddition and biological evaluation

2A.1. Introduction

Nowadays, cancer became a cautious widespread disease in the world. It induces the rapid deregulation of the pathological proliferation of abnormal cells through a highly complex multi-step process [1, 2]. The anticancer drugs have various drawbacks like several side effects, difficult in isolation, complex in synthesis, low availability and high cost etc., [3, 4]. Hence there is a need to design and develop new, safe, suitable therapeutic agents with high proficiency and efficacy to suppress the morbidity and mortality rate in human beings. For this concern, the diverse multifunctional quinoline based compounds and spiro compounds were used as one of the potent anticancer agents [1, 2, 4-7].

Quinoline is one of the eminent scaffolds for the synthesis of several heterocyclic compounds. Because of their wide occurrence in natural products and a broad spectrum of biological activities, these moieties play a vital role in medicinal chemistry [8]. The anticancer activity of the quinoline containing molecules follows different mechanisms such as apoptosis, inhibition of angiogenesis, disruption of cell migration, growth inhibitors by cell cycle arrest and modulation of nuclear receptor responsiveness etc., [9].

The spiro heterocyclic compounds are considered as a growing field of interest due to their miscellaneous biological and pharmacological activities [10, 11]. These compounds are important structural motifs, present in numerous alkaloids and pharmaceuticals [12]. They have various biological activities like antiviral, antitumor, antibiotic, local anesthetics, antimicrobial, inhibitors of human NK-112 receptor, etc., [13-16].

Ali and coworkers reported a facile synthesis of the highly functionalized indanone substituted dispiropyrrolidines regio-selectively *via* three component [3+2] cycloaddition reaction under conventional heating and microwave irradiation methods (Figure 2A.1). These compounds were evaluated for their *in vitro* antimycobacterial activity and cytotoxic activities [17].

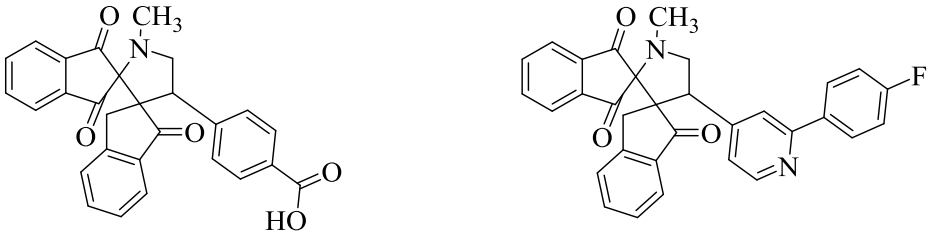

Figure 2A.1

Perumal and coworkers described the synthesis of various spirooxindole derivatives *via* one-pot multicomponent 1,3-dipolar cycloaddition reaction (Figure 2A.2). All the synthesized compounds were biologically screened for their potential antibacterial and antifungal activities [18].

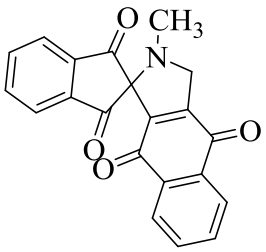

Figure 2A.2

Kathiravan et al. developed an efficient method for the synthesis of ferrocenyl dispiropyrrolidine and pyrrolizidine derivatives by [3+2] cycloaddition methodology (Figure 2A.3). The ferrocenyl Baylis-Hillman adduct was used as a dipolarophile in this reaction. All the synthesized compounds were evaluated for their antimicrobial activity [19].

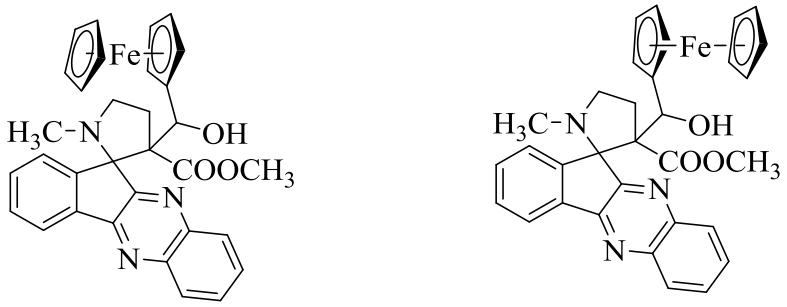

Figure 2A.3

Filatov et al. reported a simple and efficient method for the synthesis of spiro compounds *via* a highly diastereoselective one-pot three-component 1,3-dipolar cycloaddition of

cyclopropenes with azomethine ylide generated from 11*H*-indeno[1,2-*b*]quinoxalin-11-one (Figure 2A.4). The mechanism and stereochemistry of the reaction were studied computationally at M11/cc-pVDZ level. All the synthesized molecules were tested for their *in vitro* cytotoxic activity [20].

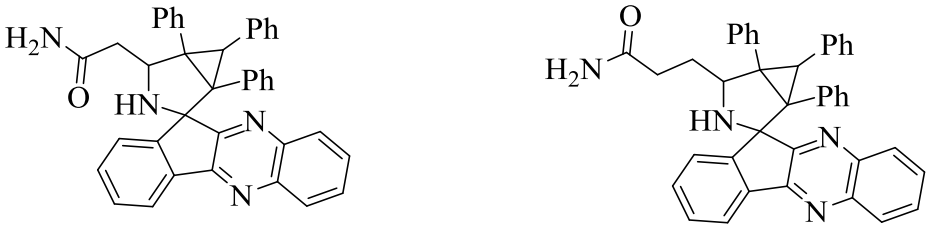

Figure 2A.4

2A.1.1. Various approaches for the synthesis of spiroindene and spiroindenoquinoxailino pyrrolizidines

Dandia and coworkers reported the green synthesis of a high degree chemo-, regio- and stereo-selective dispiro heterocycles by assembling different pharmacophoric moieties like piperidinone, 1,3-indanedione and pyrrolidine *via* an efficient and highly selective one-pot multicomponent 1,3-dipolar cycloaddition approach by using guanidine based task-specific ionic liquid, 1,1,3,3-tetramethylguanidine acetate ([TMG][Ac]) (Scheme 2A.1) [21].

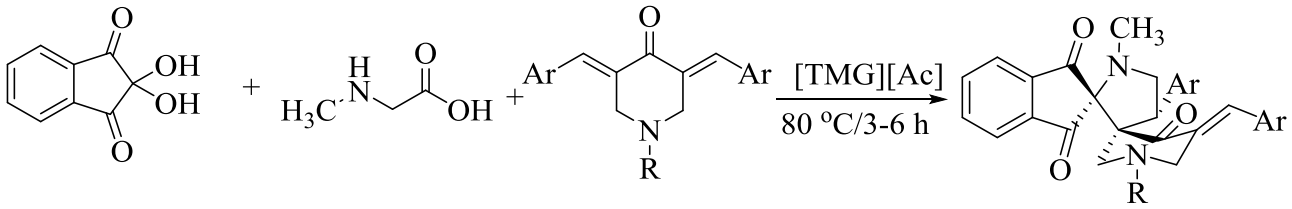

Scheme 2A.1

Moghaddam and coworkers reported the synthesis of regiospecific dispiropyrrolidines containing thiophenone ring *via* one-pot three-component 1,3-dipolar cycloaddition reactions of azomethine ylide (Scheme 2A.2). The reaction proceeds in highly regio- and stereo-controlled manner [22].

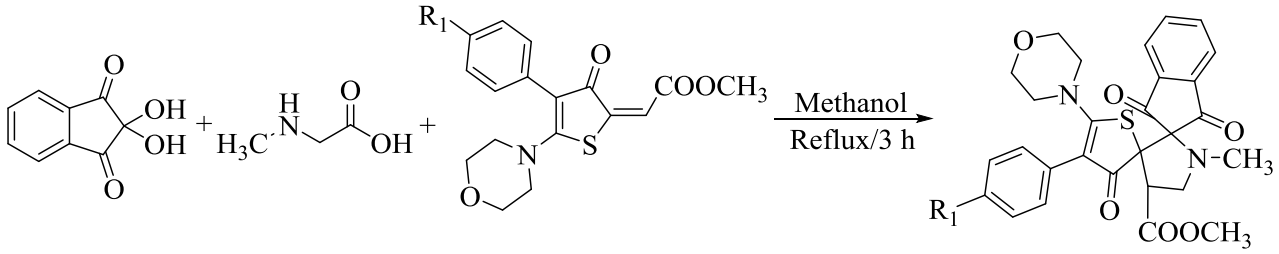

Scheme 2A.2

Rajesh et al. described the efficient, eco-compatible, chemo-, regio- and stereo-selective synthesis of a library of spiro compounds *via* multicomponent 1,3-dipolar cycloaddition reaction in the presence of recyclable ionic liquid, [Bmim]Br (Scheme 2A.3) [23].

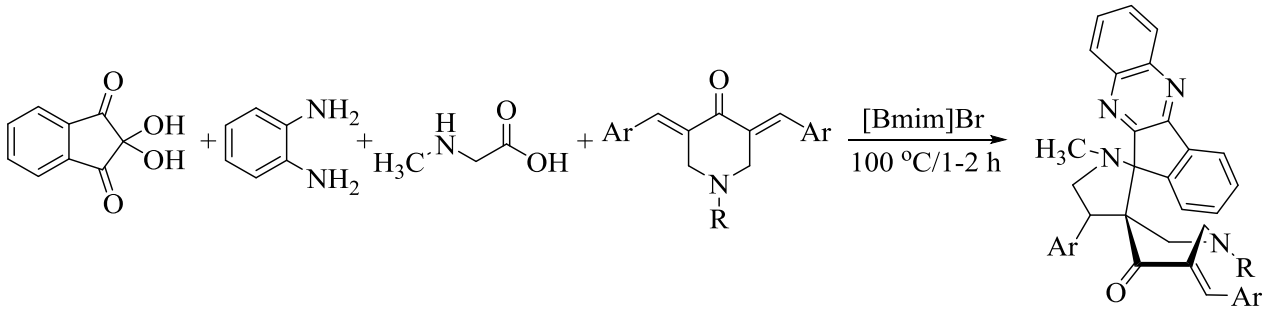

Scheme 2A.3

Babu et al. reported an efficient regioselective synthesis of dispiroindenoquinoxalino pyrrolizidine compounds *via* one-pot four-component [3+2] cycloaddition of azomethine ylide by using heteropolyacid $H_4[Si(W_3O_{10})_3]$–silica as a catalyst (Scheme 2A.4) [24].

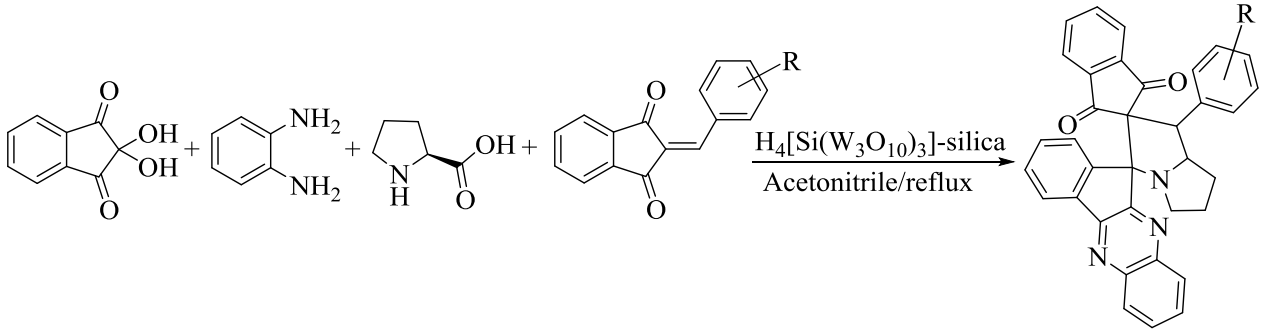

Scheme 2A.4

2A.2. Present work

The new approach of the drug discovery is the incorporation of various organic molecules in a single hybrid framework [25]. Such modifications may improve the biological properties of the hybrid molecule when compared to the parent molecule. It is somewhat

difficult to carry out such modifications in a multistep process in terms of separation, purification, the selectivity of the target product over to the side product etc., in each step, when compared to multicomponent approach [26-29]. The multi-component 1,3-dipolar cycloaddition reaction is one of the prominent methods to produce nitrogen containing five-membered heterocyclic compounds in regio- and stereo-selective manner. So many spiropyrrolizidines with stereogenic centers were synthesized *via* multicomponent 1,3-dipolar cycloaddition reaction because these reactions follow the concerted mechanism. These reactions were carried out under different methods like microwave, ultrasonication etc., [30-36].

Based on the view of biological applications of the quinoline containing moieties, herewith, we are reporting the synthesis of the quinolinyl spiropyrrolizidines by incorporating the quinolinyl chalcones, L-proline, ninhydrin/quinoxaline in a single framework *via* multicomponent 1,3-dipolar cycloaddition reaction and evaluation of their *in vitro* anticancer, antioxidant activities and *in silico* molecular docking studies.

2A.2.1. Synthesis of quinolinyl spiropyrrolizidines 4a-g

An equimolar mixture of ninhydrin **1**, L-proline **2** and dipolarophiles **3a-g** in methanol at room temperature produce the quinolinyl spiropyrrolizidines **4a-g** for 30-90min. All the reactions were monitored by TLC. The crude products were filtered and washed with methanol. The pure products were obtained from recrystallization in methanol (Scheme 2A.5).

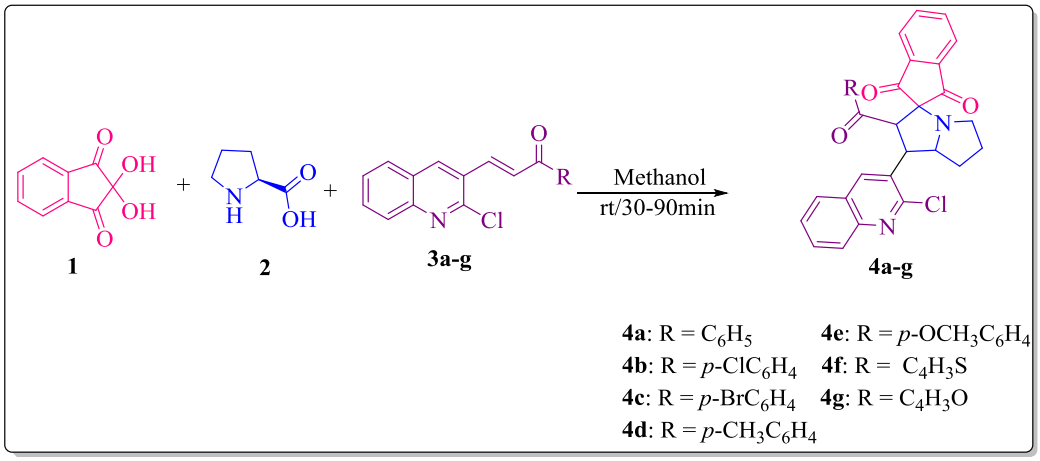

Scheme 2A.5

2A.2.2. Synthesis of quinolinyl spiropyrrolizidines 6a-g

An equimolar mixture of 11*H*-indeno[1,2-*b*]quinoxalin-11-one **5**, L-proline **2** and dipolarophiles **3a-g** in methanol under reflux condition produce the quinolinyl spiropyrrolizidines **6a-g** in 3-5h. All the reactions were monitored by TLC. The crude products were filtered and washed with methanol. The pure products were obtained from recrystallization in methanol (Scheme 2A.6).

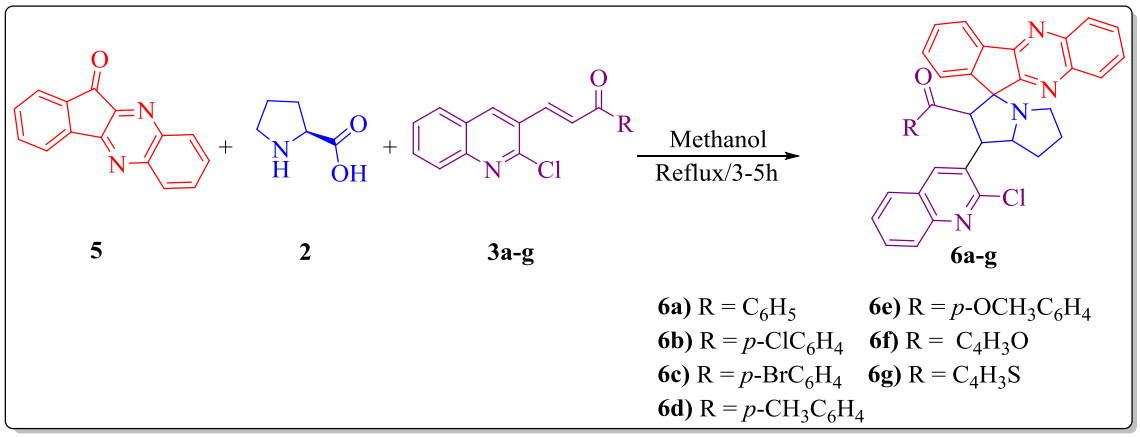

Scheme 2A.6

2A.2.3. The plausible reaction mechanism for the synthesis of quinolinyl spiropyrrolizidines 4a-g and 6a-g

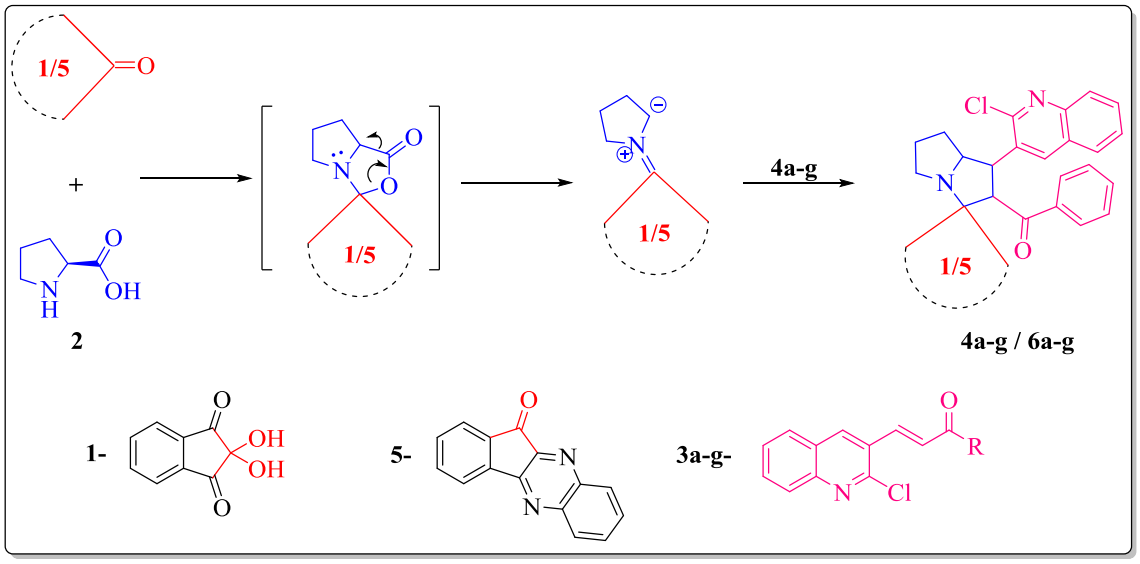

Scheme 2A.7

2A.2.4. The plausible approach of the azomethine ylide and dipolarophile for the formation of regio-selective quinolinyl spiropyrrolizidines

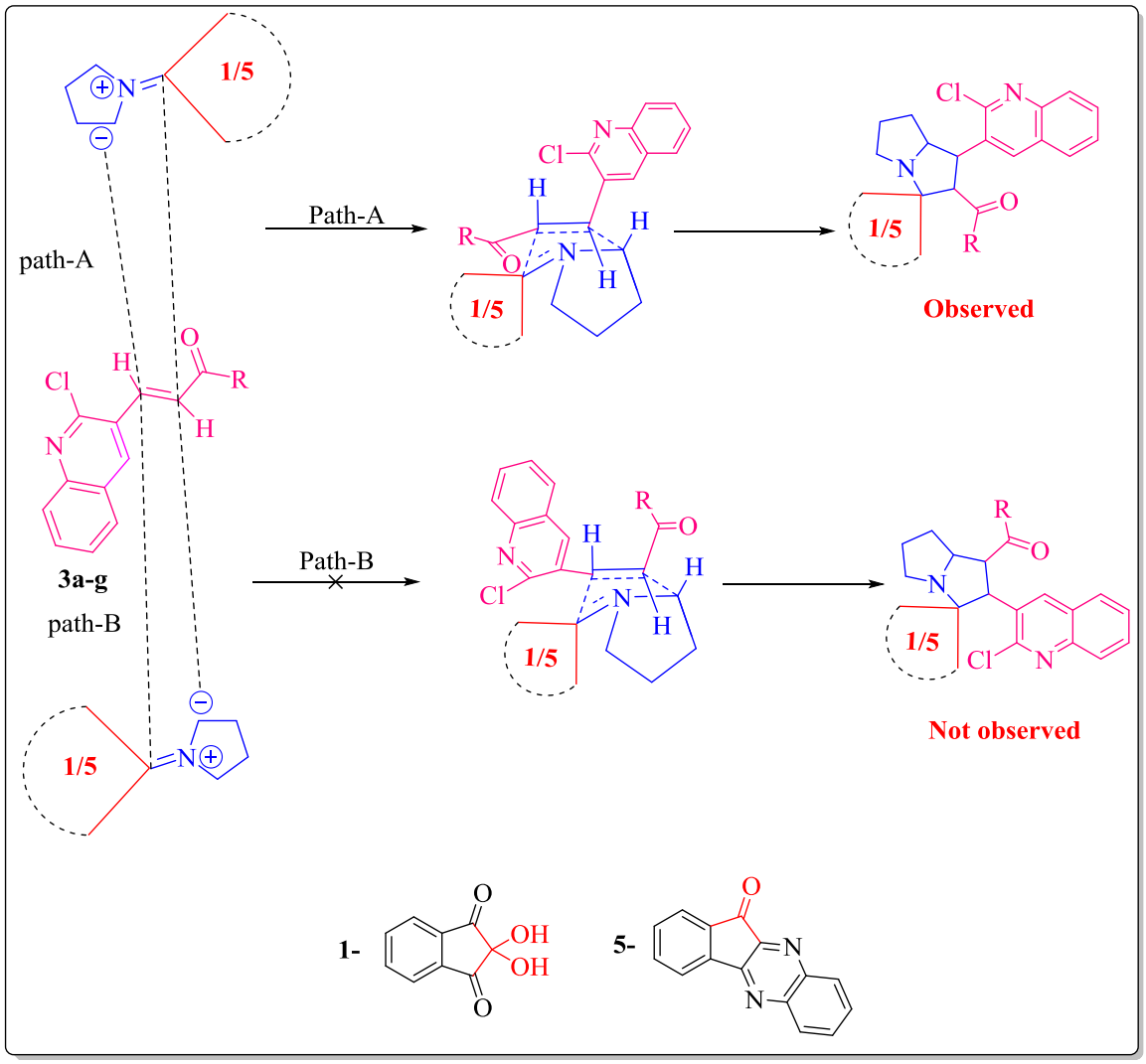

Scheme 2A.8

2A.3. Results and discussion

2A.3.1. Chemistry

Initially, the reaction was carried out by taking equimolar amounts of ninhydrin **1**, L-proline **2**, and dipolarophile **3a**, which were reacted in methanol at room temperature to produce **4a**. The reaction was completed in 90 min with 76% yield. Then, a model reaction was carried out at room temperature in acetonitrile, ethanol, dioxane to study the effect of

solvent on the reaction in terms of yield and reaction time. Among these solvents, high yield with short time was observed in methanol and hence methanol was considered as an opted solvent to carry out the reaction. Further, the reaction was carried out under reflux condition. But the yields were decreased with increasing the temperature. The obtained product was filtered and purified by recrystallization in methanol. On the other hand, another reaction was carried out by choosing 11*H*-indeno[1,2-*b*]quinoxalin-11-one **5**, L-proline **2** and dipolarophile **3a** to obtain the compound **6a**. However, there was no progress in the reaction at room temperature in the above mentioned solvents for 24h. Then, the screening of the model reaction was carried out in above mentioned solvents under reflux condition. Here also, it was noticed that the increase of yield with short time was observed in methanol. Further, the reaction was carried out in methanol at different temperatures. The precipitated product was filtered and purified by recrystallization in methanol. The optimization reaction conditions to synthesize the compounds **4a** and **6a** were summarized in table 1.

In order to delineate this approach the remaining quinolinyl spiropyrrolizidines, **4b-g** and **6b-g** were synthesized under similar optimized conditions (Scheme 2A.5 and Scheme 2A.6). The times and yields of the reaction were shown in table 2. The quinolinyl spiroindenepyrrolizidines **4a-g** was obtained at room temperature for 30-90min and quinolinyl spiroquinoxalinopyrrolizidines **6a-g** were obtained at reflux condition for 3-5h in methanol. The plausible reaction mechanism for the formation of the target compounds **4a-g** and **6a-g** were shown in Scheme 2A.7. The *in situ* generated azomethine ylide may attack the dipolarophile *via* Path-A or Path-B. Due to the electron withdrawing nature of the carbonyl group of the dipolarophiles **4a-g**, the electron density on the *β*-carbon atom decreases. Hence azomethine ylide attacks on the dipolarophile regioselectively by following the Path-A, but not the Path-B. The mechanism of regioselectivity of the reaction was shown in Scheme 2A.8.

Table 1. Optimization of the 1,3-dipolar cycloaddition reaction to form quinolinyl spiropyrrolizidines **4a** and **6a**.

S. No.	Solvent	Temperature	Compound 4a[a,c,d]		Compound 6a[b,c,d]	
			Yield (%)	Time (Min)	Yield (%)	Time (h)
1	Methanol	rt	76	90	---	12
2	Ethanol	rt	72	90	---	12
3	Acetonitrile	rt	69	74	---	12
4	1,4-Dioxane	rt	64	120	---	12
5	Methanol	rt	76	120	---	---
6	Methanol	Reflux	65	60	73	3
7	Ethanol	Reflux	68	40	70	3
8	Acetonitrile	Reflux	65	35	65	2.5
9	1,4-Dioxane	Reflux	67	45	62	4
10	Methanol	40 °C	69	60	trace	3

[a]All the reactions were carried out by using ninhydrin **1** (1 mmol), L-proline **2** (1 mmol) and dipolarophile **3a** (1 mmol) as starting materials**.** [b]All the reactions were carried out by using 11*H*-indeno[1,2-*b*]quinoxalin-11-one **5** (1 mmol), L-proline **2** (1 mmol) and dipolarophile **3a** (1 mmol) as starting materials**.** [c]The reaction progress was monitored by TLC. [d]Isolated yields.

Table 2: The regioselectively synthesized quinolinyl spiropyrrolizidines **4a-g** and **6a-g**[a,b,c,d].

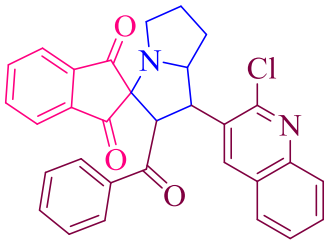

4a
(60min / 76%)

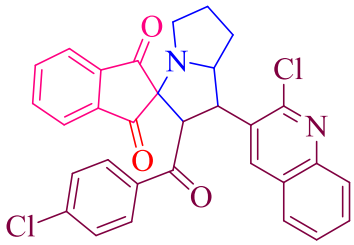

4b
(60min / 71%)

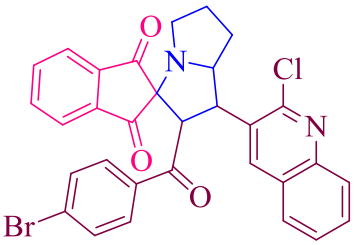

4c
(90min / 74%)

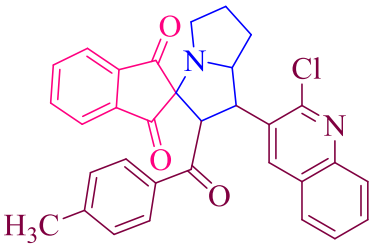

4d
(45min / 76%)

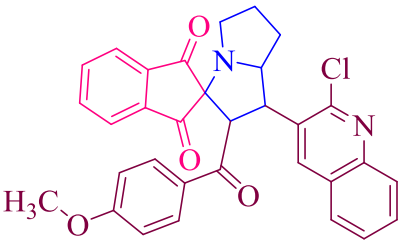

4e
(30min / 78%)

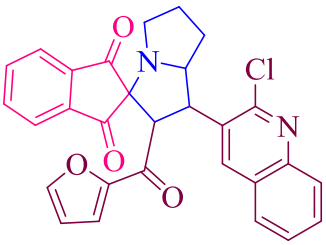

4f
(50min / 74%)

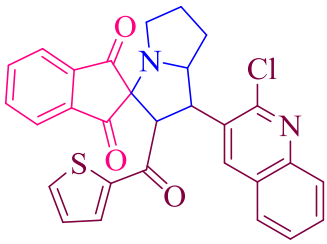

4g
(60min / 75%)

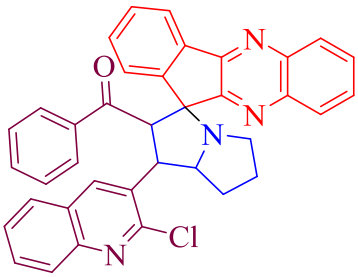

6a
(3h / 74%)

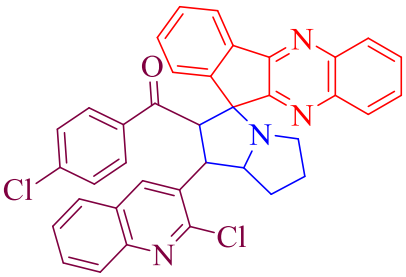

6b
(5h / 77 %)

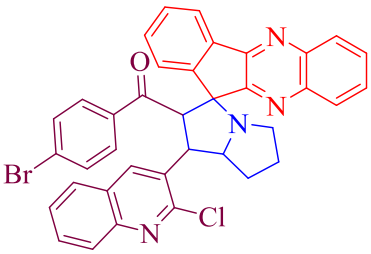

6c
(5h / 76 %)

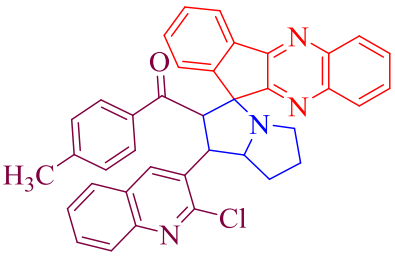

6d
(4h / 73 %)

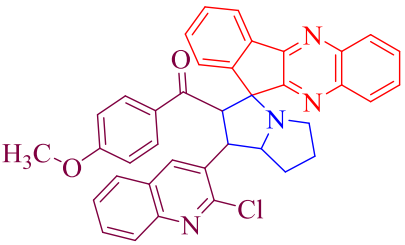

6e
(4h / 74%)

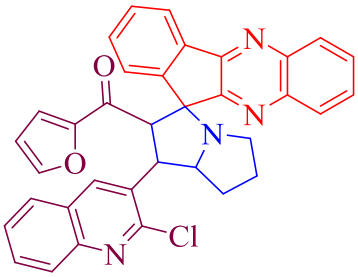

6f
(3h / 76%)

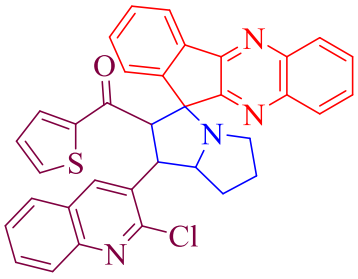

6g
(3h / 74%)

[a]The products **4a-g** were formed from the equimolar mixture ninhydrin **1** (1 mmol), L-proline **2** (1 mmol) and dipolarophile **3a** (1 mmol) in methanol at room temperature. [b]The products **6a-g** were

obtained from 11*H*-indeno[1,2-*b*]quinoxalin-11-one **5** (1 mmol), L-proline **2** (1 mmol) and dipolarophile **3a** (1 mmol) in methanol under reflux condition**.** [c]The reaction progress was monitored by TLC. [d]Isolated yields.

All the synthesized compounds **4a-g** and **6a-g** were well characterized by the spectral data (IR, ^{1}H NMR, ^{13}C NMR and mass) as well as elemental analyses (CHN). For instance, The IR spectrum of the compound **4e** (Figure 2A.5) showed stretching frequencies at 1741, 1705 cm^{-1} and 1670 cm^{-1}, which correspond to the two carbonyl groups of indene ring and benzoyl carbonyl group respectively. In the ^{1}H NMR spectrum, the peaks at δ 5.34 (d, 1H, J = 12.0 Hz), 4.69 (t, 1H, J = 10.0Hz) and 4.01-3.93 (m, 1H) represents the protons at C-15, C-14 and C-10 positions respectively. The peak at δ 3.64 corresponds to the three protons of the methoxy (-OCH_3) group. In ^{13}C NMR spectrum, the peaks at δ 47.13, 65.03 and 73.27 correspond to the carbon atoms at C-15, C-14, C-10 positions. The peak at δ 55.89 corresponds to the methoxy carbon atom. The peak at δ 79.64 corresponds to the spiro carbon at the C-16 position. Further, in the ^{13}C NMR spectrum, the peaks at δ 201.33, 200.98 and 194.83 confirms the presence of these three carbonyl groups. Moreover, the appearance of the peak at *m/z* 537.01 in mass spectrum evidenced the formation of the compound **4e.** Further, the structure of the compound was confirmed by the crystal structure of **4e** (Figure 2A.6).

The FTIR spectrum of the compound **6a** (Figure 2A.5) was showing the stretching frequency at 1683 cm^{-1} corresponds to the benzoyl carbonyl group. The ^{1}H NMR spectrum of the compound **6a** showed peaks at δ 5.79 (d, 1H, J = 12.0 Hz), 4.83 (t, 1H, J = 10.8 Hz) and 4.23-4.17 (m, 1H) represent the protons at C-27, C-28 and C-16 positions respectively. In ^{13}C NMR spectrum, the peaks at δ 47.83, 65.38 and 73.48 represent the carbon atom at C-27, C-28 and C-16 positions. The peak at δ 74.88 corresponds to the spiro carbon at the C-9 position. The peak at δ 195.82 represents the carbon atom of the benzoyl carbonyl group. In addition to this, the peak at *m/z* 579.10 in mass spectrum confirms the formation of the compound **6a**. Further, the structure of the compound was confirmed by the crystal structure of the compound **6a** (Figure 2A.7). The crystallographic data and structural refinement parameters of the compounds **4e** and **6a** were shown in table 3.

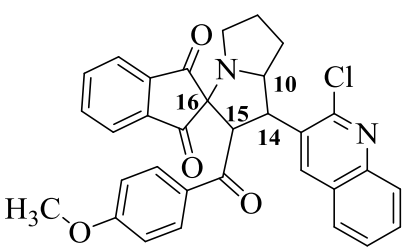

Compound **4e**

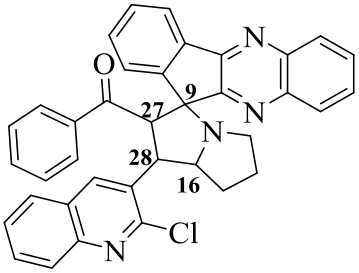

Compound **6a**

Figure 2A.5.

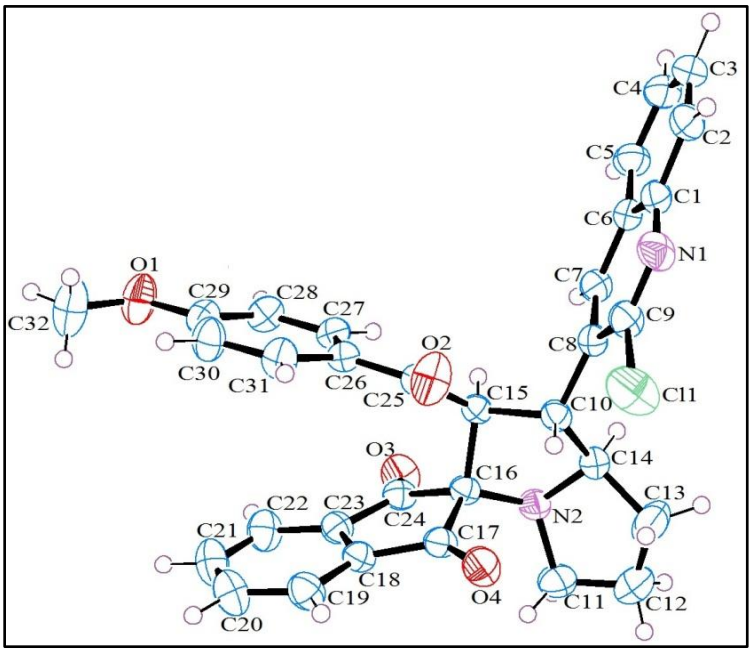

Figure 2A.6. The ORTEP representation of the compound **4e**. The thermal ellipsoids are drawn at 50% probability level. The asymmetric unit shows only one enantiomer having the configurations at the chiral centers C10 (R), C14 (R) and C15 (S).

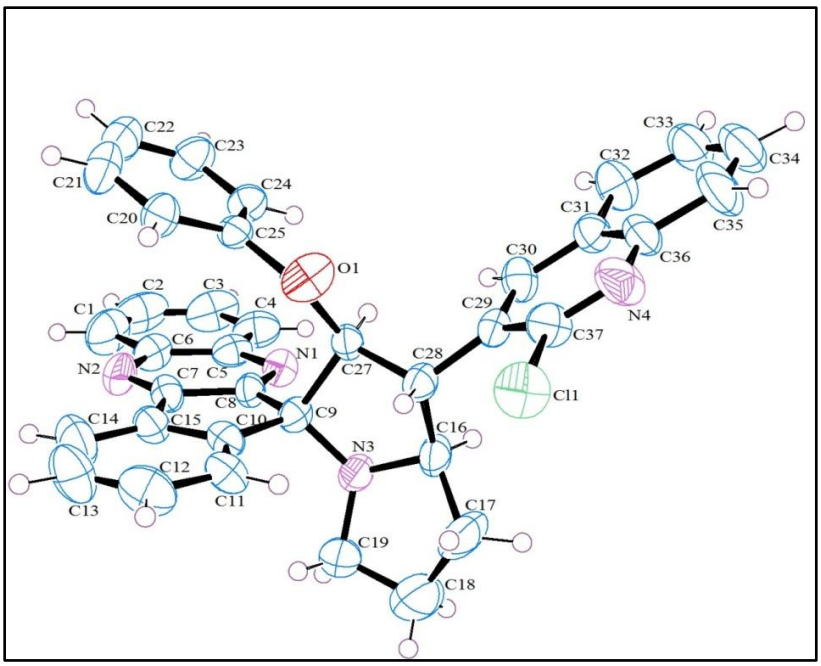

Figure 2A.7. The ORTEP representation of the compound **6a**. The thermal ellipsoids are drawn at 50% probability level. The asymmetric unit shows only one enantiomer having the configurations at the chiral centers C9 (R), C16 (R), C27 (S) and C28 (R).

Table 3. The salient crystallographic data and structure refinement parameters of the compounds **4e** and **6a**.

	4e	**6a**
Empirical formula	$C_{32}H_{25}ClN_2O_4$	$C_{37}H_{27}ClN_4O$
Formula weight	536.99	579.08
Crystal system	Triclinic	Orthorhombic
Space group	*P*-1	*Pbca*
T/K	293(2)	296(2)
a/Å	8.7167(10)	11.3126(7)
b/Å	12.1894(19)	19.3274(15)
c/Å	12.8624(17)	28.238(2)
α/°	85.845(6)	90
β/°	81.399(6)	90
γ/°	80.747(6)	90
Z	2	8
V/Å^3	1332.1(3)	6174.0(8)
D_{calc}/ g/cm^3	1.339	1.246
F(000)	560	2416
μ/mm^{-1}	0.185	0.160

θ/°	1.60 to 28.23	1.44 to 28.44
Index ranges	$-11 \leq h \leq 7$	$-15 \leq h \leq 13$
	$-14 \leq k \leq 16$	$-25 \leq k \leq 24$
	$-16 \leq l \leq 16$	$-36 \leq l \leq 37$
N-total	10800	48349
N-independent	5925	7741
N-observed	3941	4174
Parameters	353	383
R_1 ($I > 2\sigma(I)$)	0.0520	0.1751
wR_2 (all data)	0.1829	0.5229
GOF	1.075	1.889
CCDC	1830589	1830590

2A.3.2. Biological evaluation

2A.3.2.1. Anticancer activity

MTT assay was employed to all the synthesized compounds **4a-g** and **6a-g** to evaluate their potential for *in vitro* anticancer activity against neuroblastoma cell line (IMR32), alveolar carcinoma cell line (A549), breast cancer cell line (MCF7) and human embryonic kidney 293 cell line (HEK293T). The results were summarized in table 4.

Among all the target compounds **4a-g**, the compound **4e** exhibited significant activity against the IMR32 and A549 cell lines with IC_{50} values 14.64 ± 0.17 µM and 22.95 ± 0.13 µM respectively. Among the synthesized compounds **6a-g,** the compound **6f** showed potent activity against A549 cell line and significant activity against IMR32 cell line with IC_{50} values 12.18 ± 0.44 µM and 17.22 ± 0.25 µM respectively. The compound **6e** exhibited significant inhibition activity against A549 cell line with IC_{50} value 19.33 ± 0.96 µM. Further, the compounds **4d**, **4e**, **6e** and **6f** were tested against human embryonic kidney 293 (HEK293T) cell line and observed the IC_{50} values 63.54 ± 0.03 µM, 69.63 ± 0.63 µM, 78.54 ± 0.89 µM and 81.70 ± 0.32 µM respectively. The survival curves of the three cancer cell lines i.e., IMR32, A549 and MCF7 against the synthesized compounds were shown in figure 2A.8.

Table 3. The *in vitro* anticancer activity of the quinolinyl spiropyrrolizidines **4a-g** and **6a-g**.

S. No.	Compound	IC_{50} (μM)[a]			
		IMR32	**A549**	**MCF7**	**HEK293T**
1	**4a**	42.79 ± 0.73	58.25 ± 0.24	36.48 ± 0.39	ND[b]
2	**4b**	47.41 ± 0.16	46.21 ± 0.26	40.72 ± 0.75	ND
3	**4c**	44.37 ± 0.49	46.80 ± 0.93	48.52 ± 0.15	ND
4	**4d**	29.06 ± 0.75	33.43 ± 0.86	45.19 ± 0.29	63.54 ± 0.03
5	**4e**	**14.64 ± 0.17**	**22.95 ± 0.13**	26.38 ± 0.50	69.63 ± 0.63
6	**4f**	49.02 ± 0.70	50.26 ± 0.60	49.74 ± 0.93	ND
7	**4g**	38.23 ± 0.93	41.41 ± 0.45	40.54 ± 0.76	ND
8	**6a**	37.86 ± 0.49	38.76 ± 0.46	37.84 ± 0.36	ND
9	**6b**	43.31 ± 0.37	34.53 ± 0.73	38.88 ± 0.32	ND
10	**6c**	38.94 ± 0.81	34.88 ± 0.51	28.15 ± 0.75	ND
11	**6d**	39.46 ± 0.43	40.14 ± 0.22	37.29 ± 0.47	ND
12	**6e**	28.41 ± 0.74	**19.33 ± 0.96**	25.36 ± 0.18	78.54 ± 0.89
13	**6f**	**17.22 ± 0.25**	**12.18 ± 0.44**	27.38 ± 0.02	81.70 ± 0.32
14	**6g**	33.86 ± 0.49	39.76 ± 0.46	38.84 ± 0.36	ND
15	***Cis*-Platin**	6.05 ± 1.04	10.23 ± 0.45	8.01 ± 0.39	ND

[a]IC_{50}: The concentration of the compound (μM) that exhibits the 50% cell growth inhibition. [b]ND-Not determined.

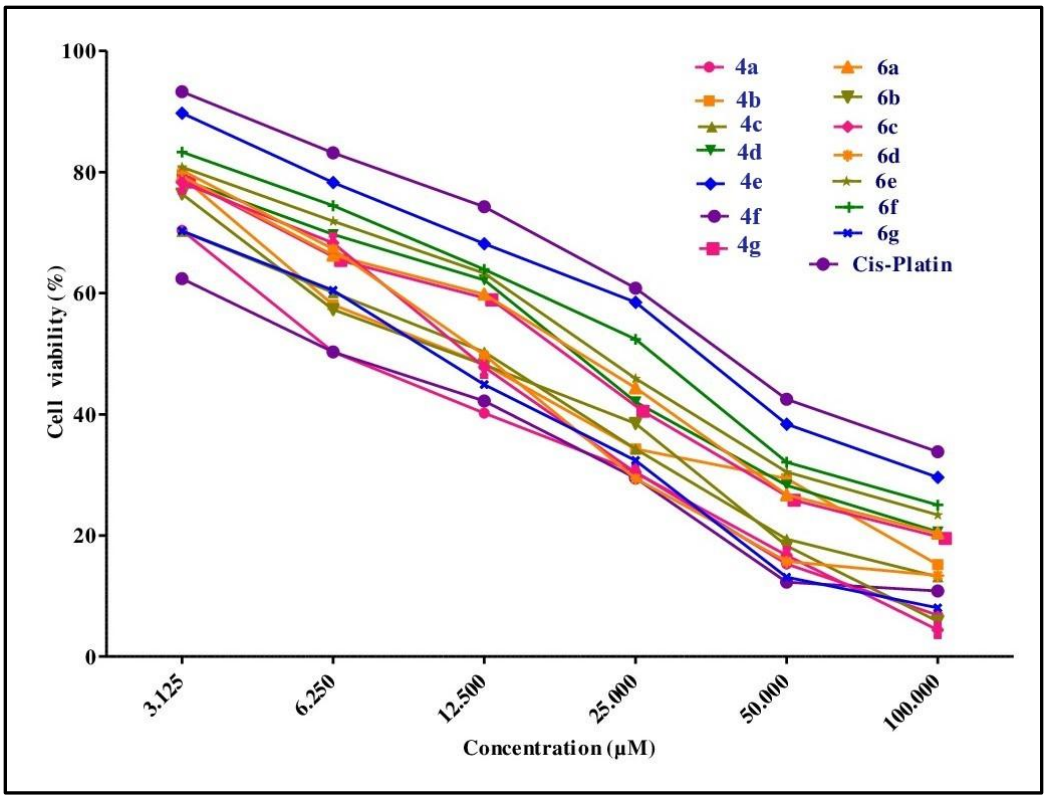
100
80
60
40
20
0
Cell viability (%)
3.125
6.250
12.500
25.000
50.000
100.000
Concentration (µM)
4a
4b
4c
4d
4e
4f
4g
6a
6b
6c
6d
6e
6f
6g
Cis-Platin

a)

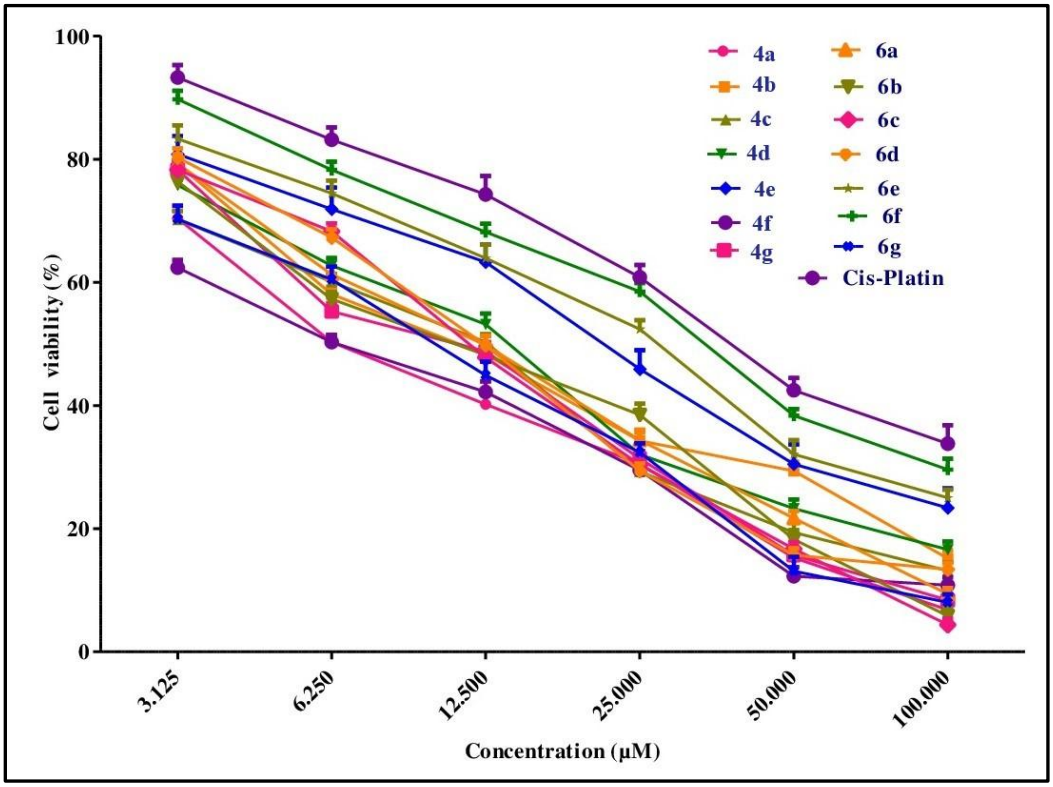
100
80
60
40
20
0
Cell viability (%)
3.125
6.250
12.500
25.000
50.000
100.000
Concentration (µM)
4a
4b
4c
4d
4e
4f
4g
6a
6b
6c
6d
6e
6f
6g
Cis-Platin

b)

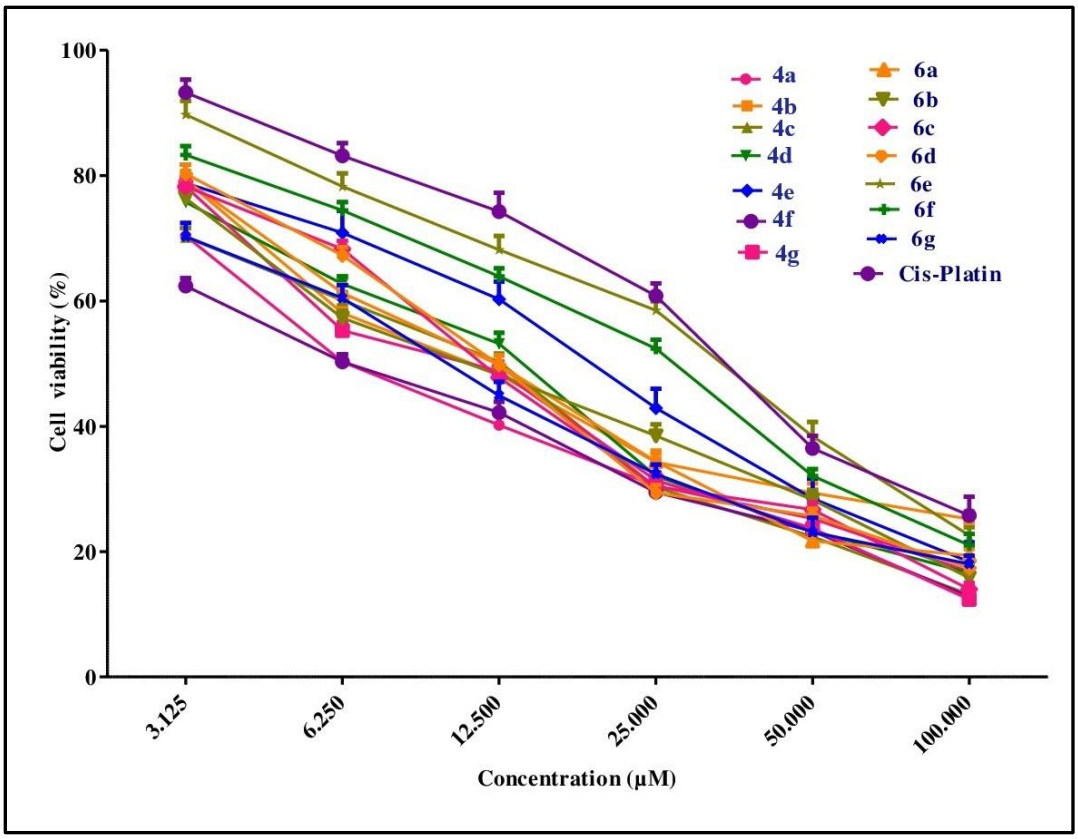

c)

Figure 2A.8. The survival curves of a) IMR32, b) A549 and c) MCF7 cell lines.

2A.3.2.2. Antioxidant activity

The synthesized compounds **4a-g** and **6a-g** were evaluated for their *in vitro* radical scavenging activity. The radical scavenging activity results are depicted in table 4. All the compounds exhibited the radical scavenging activity with IC_{50} values ranging from 8.64 ± 0.43 to 39.42 ± 0.54 µM. Among all the compounds, compound **6f** exhibiting potent antioxidant activity with IC_{50} value 8.64 ± 0.43 µM. The compound **6e (**12.33 ± 0.72 µM**)** exhibited significant antioxidant activity. The compounds **4d**, **4e** and **6d** were exhibited good radical scavenging activity with the IC_{50} values 17.23 ± 1.06 µM, 14.67 ± 1.11 µM and 16.48 ± 0.35 µM respectively.

Table 4. The antioxidant activity of the target compounds **4a-g** and **6a-g**.

S. No.	Compound	IC_{50} (µM)
1	**4a**	21.08 ± 0.38
2	**4b**	34.17 ± 0.45
3	**4c**	39.42 ± 0.54
4	**4d**	**17.23 ± 1.06**
5	**4e**	**14.67 ± 1.11**
6	**4f**	31.35 ± 1.02
7	**4g**	22.27 ± 0.55
8	**6a**	22.55 ± 0.69
9	**6b**	35.51 ± 0.87
10	**6c**	38.54 ± 0.74
11	**6d**	**16.48 ± 0.35**
12	**6e**	**12.33 ± 0.72**
13	**6f**	**8.64 ± 0.43**
14	**6g**	26.1 ± 0.98
15	**Ascorbic acid**	6.63 ± 0.68

2A.4. Molecular docking studies

The ligand-protein complex assessment is one of the bases of the modern structure-based drug design. The *in silico* molecular docking studies were carried out against proteins IDO1 (PDB ID: 2D0U), ALK (PDB ID: 2XP2) and EGFR (PDB ID: 4HJO) by using AutoDock Tools (ADT) version 1.5.6 and AutoDock version 4.2.5.1 docking program.

IDO1, Indoleamine-2,3-dioxygenase, is a foremost rate-limiting enzyme for the amino acid L-tryptophan catabolism *via* kynurenine pathway to convert the L-tryptophan to N-formylkynurenine. This step involves the depletion of tryptophan leading to cease the growth of microbes as well as T-cells. So it is useful in designing the various anticancer agents to suppress T-cell differentiation and proliferation [37, 38]. Hence it is an attractive target for the numerous anticancer agents. ALK (Anaplastic Lymphoma Kinase) is a receptor tyrosine kinase, which has been detected in non small cell lung cancer. The oncogenic

mutations of ALK were observed in familial and sporadic cases of neuroblastoma. The potent oncogenic activity was induced by the echinoderm microtubule protein-like4-Anaplastic Lymphoma Kinase (EML4-ALK) fusion variants and causes the lung adenocarcinoma. Hence ALK is considered as a suitable target for the therapeutic intervention of cancer [26, 39]. The epidermal growth factor receptor is an extracellular protein leads to cell proliferation, differentiation and survival, by inducing the tyrosine autophosphorylation and receptor dimerization [40-43]. Overexpression of EGFR leads to colon cancers and its mutations causes various cancer diseases like anal cancer, squamous-cell carcinoma of the lung, glioblastoma etc., [44-46]. Hence it is an attractive target for the several anticancer agents.

By considering the above reasons, we have chosen IDO1, ALK and EGFR proteins as the target receptors for the docking studies and compared their binding energies which were summarized in Table 5. The hydrogen bonding data for the compounds **4a-g** and **6a-g** against IDO1 was shown in Table 6. The comparative molecular docking studies of the targeted scaffolds **4a-g** and **6a-g** with the target receptors IDO1, ALK and EGFR (as shown in Table 6) unambiguously confirm the affinity of these synthesized compounds with the receptor IDO1 is better than that of receptors ALK and EGFR. Hence IDO1 was chosen as the target receptor for the detailed discussion. Among all the synthesized compounds the compound **6a**, **6e** and **6f** were found to be potential inhibitors inferred by their least binding energies −11.57, −11.82 and −11.83 kcal/mol respectively.

The docking results reveal that the compound **6a** exhibits a strong hydrogen bonding interaction in between the carbonyl group of benzoyl group and amino acid residue ALA264 with bond length 1.67 Å. The phenyl group in the quinoxaline ring interacts with the amino acid residue LEU388, the pyrrolizine ring interacts with the amino acid residues HIS346, VAL35 and ILE354, the phenyl ring in benzoyl group with amino acid residue LEU234, the phenyl ring in quinoline moiety interacts with amino acid residues PHE214, ILE217 and ALA 264, and the pyridyl ring in quinoline moiety interacts with amino acid residues PHE214 and ALA 264 through hydrophobic interactions. The compound **6e** exhibit four hydrogen bonds: one in between the carbonyl group and amino acid residue ALA264 with bond length 1.65 Å, two in between the two nitrogen atoms and amino acid residues SER263

and HIS346 separately with bond lengths 2.30 Å and 2.81 Å respectively, and one in between methyl group of methoxy group with amino acid ARG231 with bond length 2.73 Å. The phenyl ring in the quinoxaline moiety interacts with LEU388, the pyrrolizine ring interacts with the amino acid residues HIS346, VAL35 and ILE354, the phenyl ring in benzoyl group with amino acid residue LEU234, the phenyl ring in quinoline moiety interacts with amino acid residues PHE214, VAL170 and ALA 264, and the pyridyl ring in quinoline moiety interacts with amino acid residues PHE163, PHE214 and ALA 264 through hydrophobic interactions.

The compound **6f** exhibited one hydrogen bond in between the oxygen atom of the furan ring and amino acid residue HIS346. The pyrazinyl phenyl ring in the quinoxaline moiety interacts with VAL170, PHE214 and ALA264, the pyrazine ring in the quinoxaline moiety interacts with HIS346, PHE163 and ALA264, the phenyl ring in the quinoxaline moiety interacts with the amino acid PHE163, the pyrrolizine ring interacts with the amino acid residues PHE163 and ALA264, the furan ring interacts with amino acid residues ILE354, VAL350, LEU388 and LEU384, the phenyl ring and the pyridyl ring in quinoline moiety interacts with amino acid residues GLY265 and ALA 264 through hydrophobic interactions. The hydrophobic interactions were also played a vital role in increasing the affinity in between the synthesized compounds and targeted proteins [47]. The hydrogen bonding interactions and hydrophobic interactions of the compounds **6a**, **6e** and **6f** were shown in Figure 2A.9, 2A.10 and 2A.11. It was noticed that the compounds other than **6a**, **6e** and **6f** exhibited moderate binding affinities with all the three protein residues i.e., IDO1, ALK and EGFR.

Table 5. The binding energies of all the synthesized compounds against IDO1, ALK and EGFR.

S. No.	Compound	Binding Energy (kcal/ mol)		
		IDO1 (PDB ID: 2D0U)	**ALK (PDB ID: 2XP2)**	**EGFR (PDB ID: 4HJO)**
1	**4a**	−9.52	−8.45	−8.41
2	**4b**	−10.10	−8.14	−8.15
3	**4c**	−10.95	−8.16	−8.27
4	**4d**	−10.55	−7.91	−8.23
5	**4e**	−9.72	−7.84	−7.90
6	**4f**	−9.05	−7.83	−8.20
7	**4g**	−9.77	−8.34	−8.56
8	**6a**	**−11.57**	−9.84	−8.10
9	**6b**	−11.33	−9.52	−8.57
10	**6c**	−11.07	−9.54	−8.75
11	**6d**	−11.29	−9.41	−8.41
12	**6e**	**−11.82**	−9.49	−8.23
13	**6f**	**−11.83**	−10.88	−8.94
14	**6g**	−10.92	−9.82	−10.09

Table 6. The binding energies, Number of hydrogen bonds, residues involved in the hydrogen bonding and the hydrogen bond lengths of all the synthesized compounds against IDO1.

S. No.	Compound	Binding energies (kcal/mol)	IDO1 (PDB ID: 2D0U)		
			No. of hydrogen bonds	**Residues involved in the hydrogen bonding**	**Hydrogen bond length (Å)**
1	**4a**	−9.52	1	SER263	1.89
2	**4b**	−10.10	1	SER263	1.84
3	**4c**	−10.95	1	ALA264	2.96
4	**4d**	−10.55	1	ALA264	2.95

5	**4e**	−9.72	1	SER235	3.17
6	**4f**	−9.05	1	SER263	1.77
7	**4g**	−9.77	3	SER263, ALA264, HIS346	2.13, 2.35, 2.36
8	**6a**	**−11.57**	1	ALA264	1.67
9	**6b**	−11.33	3	SER263, ALA264, HIS346	1.66, 2.50, 2.75
10	**6c**	−11.07	1	ALA264	2.65
11	**6d**	−11.29	3	SER263, ALA264, HIS346	1.67, 2.63, 2.68
12	**6e**	**−11.82**	4	ALA264, SER263, HIS346, ARG231	1.65, 2.30, 2.81, 2.73
13	**6f**	**−11.83**	1	HIS346	3.10
14	**6g**	−10.92	1	ALA264	2.07

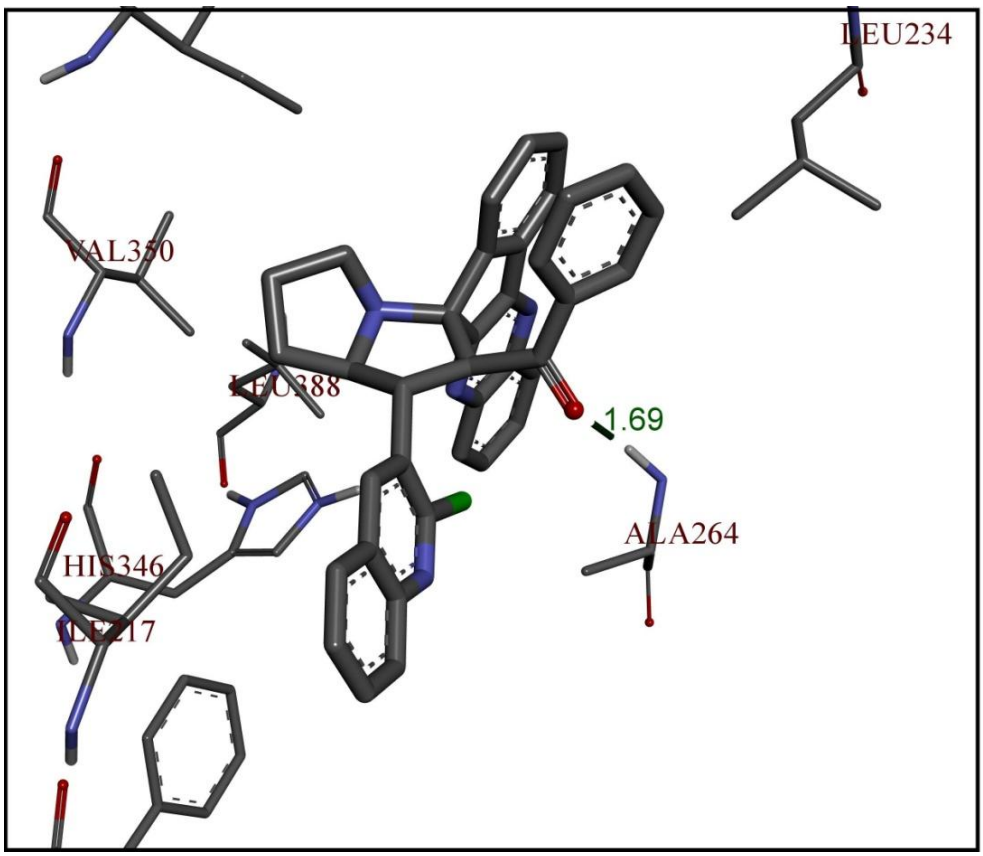

a)

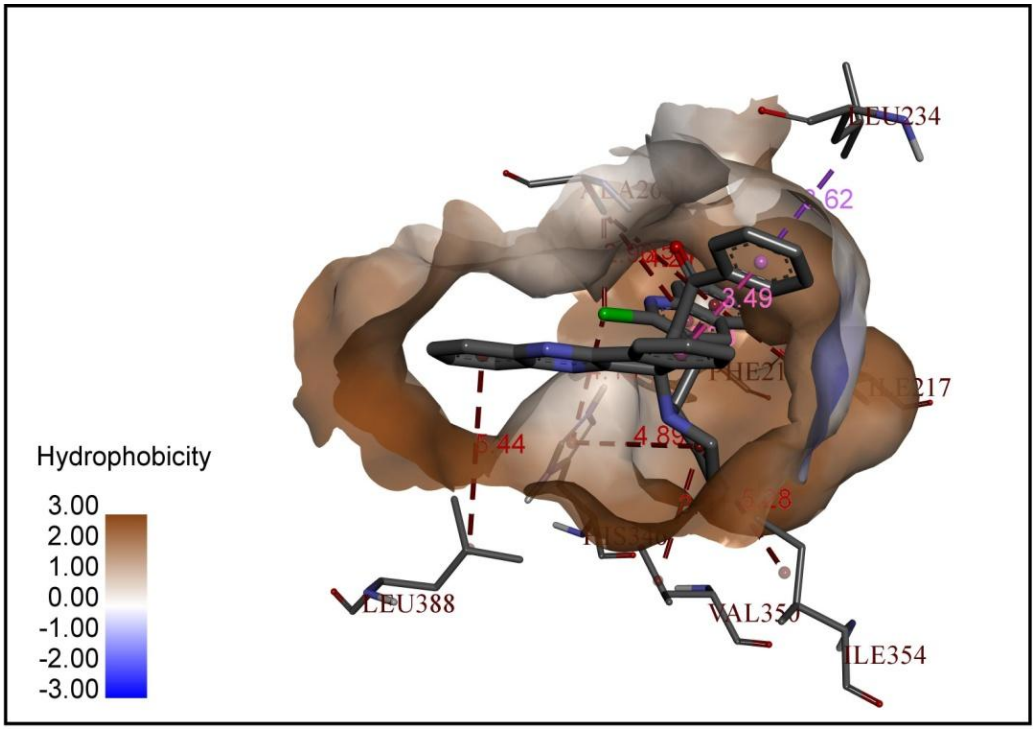

b)

Figure 2A.9. The best docking poses of the compound **6a** that shows a) The hydrogen bonding interactions, (b) The hydrophobic interactions with the protein IDO1.

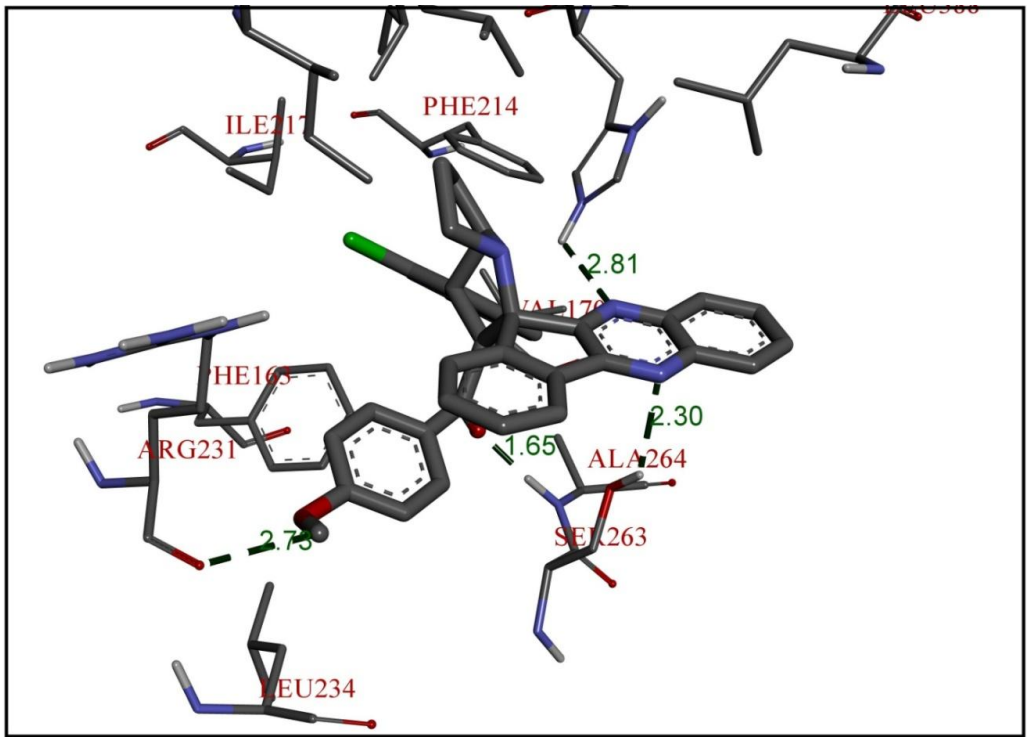

a)

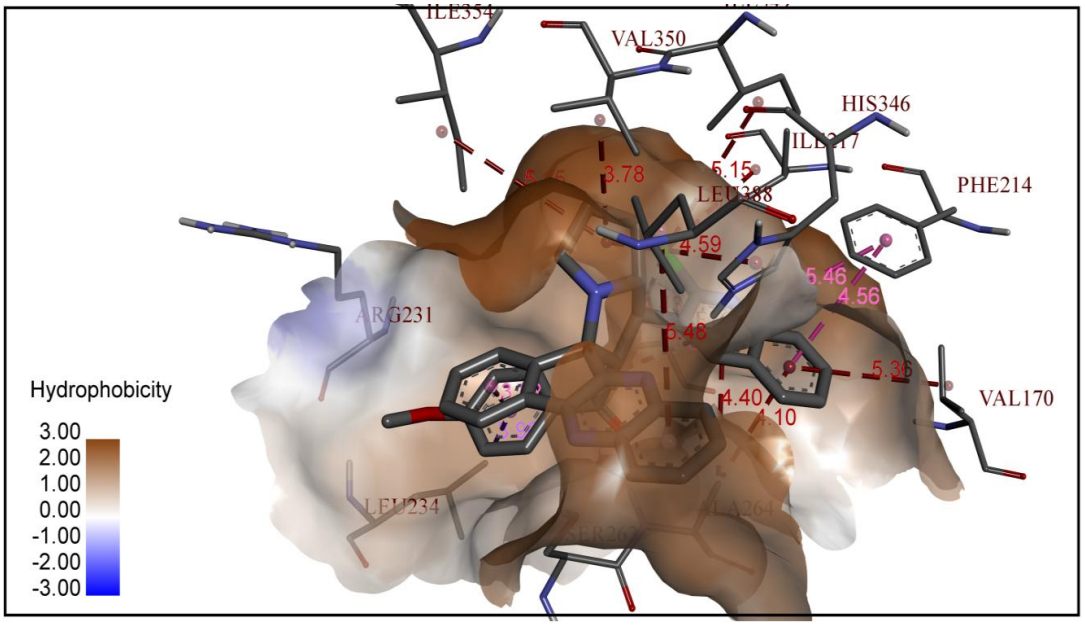

b)

Figure 2A.10. The best docking poses of the compound **6e** that shows a) The hydrogen bonding interactions, (b) The hydrophobic interactions with the protein IDO1.

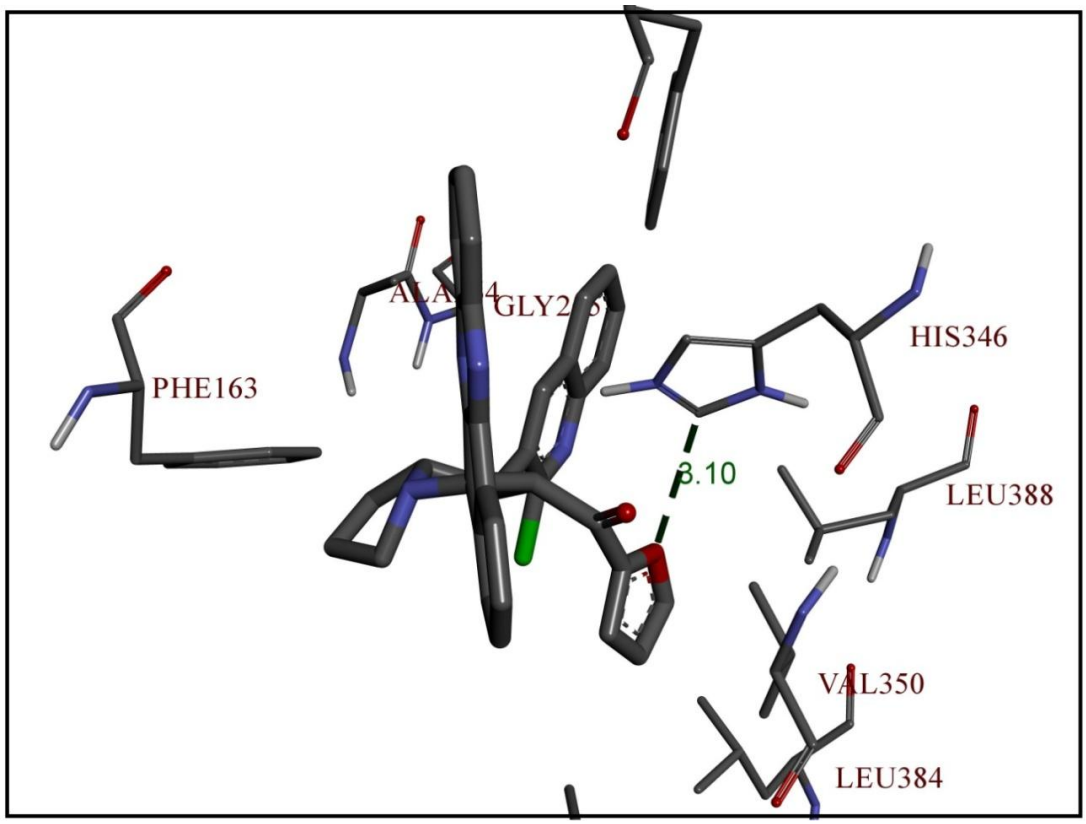

a)

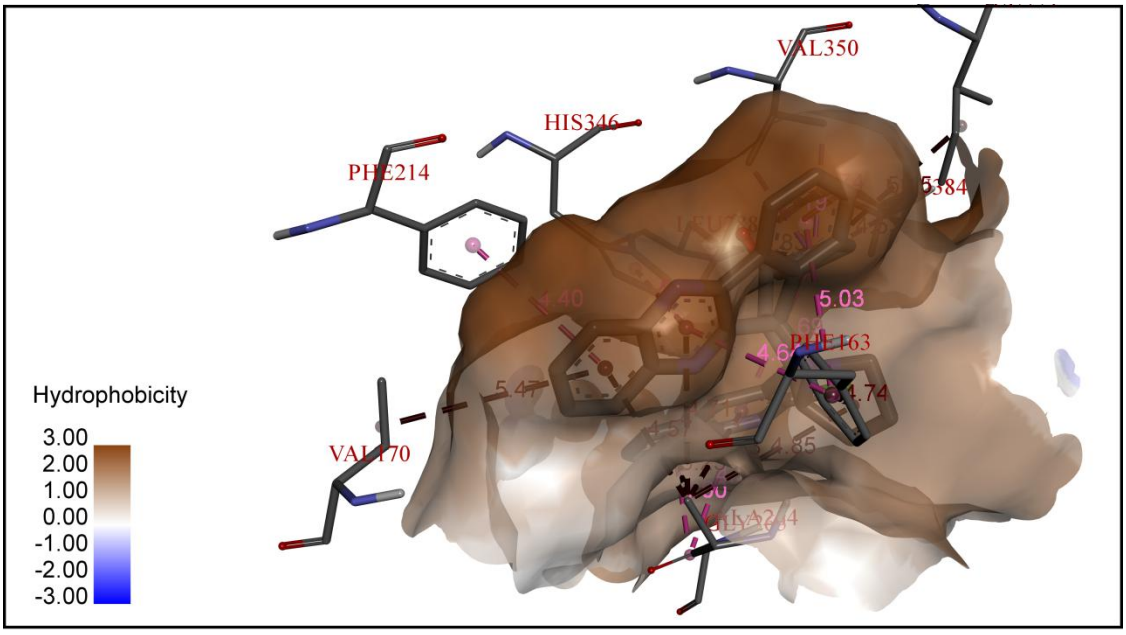

b)

Figure 2A.11. The best docking poses of the compound **6f** that shows a) The hydrogen bonding interactions, (b) The hydrophobic interactions with the protein IDO1.

2A.5. Conclusion

Various quinolinyl spiropyrrolizidines **4a-g** and **6a-g** were synthesized efficiently *via* one-pot three component 1,3-dipolar cycloaddition reaction and characterized by various spectroscopic techniques (FTIR, NMR and Mass). The structures of the compounds **4e** and **6a** were confirmed by the single crystal X-ray diffraction method. Further, all the synthesized compounds were evaluated for their *in vitro* anticancer and antioxidant activities and molecular docking studies. Especially, the compound **6f** showed significant anticancer and antioxidant activity with IC_{50} values 12.18 ± 0.44 µM and 8.64 ± 1.02 respectively**.** The compounds **4e** and **6e** exhibited moderate activity against the three tested cell lines i.e., IMR32, A549 and MCF7. The compounds **4d**, **4e** and **6e** showed moderate antioxidant activity. The *in vitro* anticancer activity (IC_{50} values) of the synthesized compounds was also supported by molecular docking studies. The IDO1 is the best protein receptor, which was unveiled from the comparative molecular docking studies on IDO1, ALK and EGFR.

2A.6. Spectral data

2'-Benzoyl-1'-(2-chloroquinolin-3-yl)-1',2',5',6',7',7a'-hexahydrospiro[indene-2,3'-pyrrolizine]-1,3-dione (4a)

Colour: Yellow. M. P. 184-186 ℃. IR (KBr, cm^{-1}): 3061, 1734, 1691, 1669, 769. ^{1}H NMR (400 MHz, DMSO-*d*6) δ: 9.04 (s, 1H), 8.33 (s, 1H), 8.03 (d, 1H, *J* = 7.6 Hz), 7.95-7.74 (m, 4H), 7.65-7.62 (m, 2H), 7.39 (d, 2H, *J* = 7.2 Hz), 7.30 (t, 1H, *J* = 7.2 Hz), 7.07 (t, 2H, *J* = 8.0 Hz), 5.41 (d, 1H, *J* = 11.6 Hz), 4.71 (t, 1H, *J* = 10.4 Hz), 4.02-3.96 (m, 1H), 2.66-2.60 (m, 2H), 2.13-1.75 (m, 4H). ^{13}C NMR (100 MHz, DMSO-*d*6) δ: 201.38, 200.97, 197.24, 151.18, 146.19, 140.46, 138.20, 137.49, 137.25, 136.70, 133.73, 131.38, 131.10, 128.55, 128.27, 128.20, 127.80, 127.75, 127.68, 123.31, 123.01, 79.64, 73.69, 63.97, 47.64, 47.36, 30.26, 28.29. ESI mass spectrum (*m/z*): 507.25 (M+). Anal. Calcd. For $C_{31}H_{23}ClN_2O_3$: C, 73.44; H, 4.57; N, 5.53; found: C, 73.72; H, 4.68; N, 5.24.

2'-(4-Chlorobenzoyl)-1'-(2-chloroquinolin-3-yl)-1',2',5',6',7',7a'-hexahydrospiro[indene-2,3'-pyrrolizine]-1,3-dione (4b)

Colour: Yellow. M. P. 189-191 ℃. IR (KBr, cm^{-1}): 3065, 2871, 1738, 1702, 1677, 753. ^{1}H NMR (400 MHz, DMSO-*d*6) δ: 9.02 (s, 1H), 8.32 (s, 1H), 8.26 (d, 1H, *J* = 8.4 Hz), 8.1-7.57 (m, 6H), 7.38 (d, 2H, *J* = 8.0 Hz), 7.11 (d, 2H, *J* = 8.0 Hz), 5.37 (d, 1H, *J* = 11.6 Hz), 4.68 (t, 1H, *J* = 10.4 Hz), 4.01-3.91 (m, 1H), 2.62-2.06 (m, 2H), 1.91-1.74 (m, 4H). ^{13}C NMR (100 MHz, DMSO-*d*6) δ: 201.32, 200.97, 196.44, 151.13, 146.21, 140.43, 138.75, 138.26, 137.62, 137.28, 135.37, 131.14, 130.41, 130.06, 129.53, 129.12, 128.65, 128.26, 127.80, 127.65, 127.41, 123.34, 123.08, 79.62, 73.57, 64.12, 49.05, 47.67, 30.24, 28.24. ESI mass spectrum (*m/z*): 542.20 (M+). Anal. Calcd. For $C_{31}H_{22}Cl_2N_2O_3$: C, 68.77; H, 4.10; N, 5.17; found: C, 68.52; H, 4.17; N, 5.45.

2'-(4-Bromobenzoyl)-1'-(2-chloroquinolin-3-yl)-1',2',5',6',7',7a'-hexahydrospiro[indene-2,3'-pyrrolizine]-1,3-dione (4c)

Colour: Yellow. M. P. 185-187 ℃. IR (KBr, cm^{-1}): 3061, 2844, 1706, 1671, 1585, 755. ^{1}H NMR (400 MHz, DMSO-*d*6) δ: 9.01 (s, 1H), 8.21-7.63 (m, 8H), 7.24-7.31 (m, 4H), 5.36 (d, 1H, *J* = 11.6Hz), 4.68 (t, 1H, *J* = 10.4 Hz), 4.01-3.96 (m, 1H), 2.61-2.06 (m, 2H), 1.92-1.76

(m, 4H). ^{13}C NMR (100 MHz, DMSO-*d*6) δ: 201.32, 200.99, 196.69, 146.22, 140.45, 138.56, 138.27, 137.63, 137.27, 135.71, 132.65, 132.49, 131.60, 131.17, 130.10, 129.13, 128.56, 128.26, 127.97, 127.81, 127.40, 126.40, 123.37, 123.10, 79.77, 73.57, 64.13, 47.67, 47.37, 30.24, 28.22. Anal. Calcd. For $C_{31}H_{22}ClBrN_2O_3$: C, 63.55; H, 3.78; N, 4.78; found: C, 63.30; H, 3.70; N, 4.52.

1'-(2-Chloroquinolin-3-yl)-2'-(4-methylbenzoyl)-1',2',5',6',7',7a'-hexahydrospiro[indene-2,3'-pyrrolizine]-1,3-dione (4d)

Colour: Yellow. M. P. 198-200 ℃. IR (KBr, cm^{-1}): 3062, 2865, 1741, 1706, 1647, 741. ^{1}H NMR (400 MHz, DMSO-*d*6) δ: 9.04 (s, 1H), 8.33 (s, 1H), 8.03 (d, 1H, *J* = 7.6 Hz), 7.95-7.74 (m, 4H), 7.65-7.62 (m, 2H), 7.39 (d, 2H, *J* = 7.2 Hz), 7.30 (t, 1H, *J* = 7.2 Hz), 7.07 (t, 2H, *J* = 8.0 Hz), 5.41 (d, 1H, *J* = 11.6 Hz), 4.71 (t, 1H, *J* = 10.4 Hz), 3.98-3.93 (m, 1H), 2.57-2.37 (m, 2H), 2.26 (s, 3H), 1.93-1.71 (m, 4H). ^{13}C NMR (100 MHz, DMSO-*d*6) δ: 201.38, 200.97, 197.24, 151.18, 146.19, 140.46, 138.20, 137.49, 137.25, 136.70, 133.73, 131.38, 131.10, 128.55, 128.27, 128.20, 127.80, 127.75, 127.68, 123.31, 123.01,79.67, 73.78, 61.38, 46.04, 45.60, 27.94, 25.26, 19.41. Anal. Calcd. For $C_{32}H_{25}ClN_2O_3$: C, 73.77; H, 4.84; N, 5.38; found: C, 73.98; H, 4.76; N, 5.54.

1'-(2-Chloroquinolin-3-yl)-2'-(4-methoxybenzoyl)-1',2',5',6',7',7a'-hexahydrospiro[indene-2,3'-pyrrolizine]-1,3-dione (4e)

Colour: Yellow. M. P. 205-207 ℃. IR (KBr, cm^{-1}): 3069, 2872, 1741, 1705, 1670, 752. ^{1}H NMR (400 MHz, DMSO-*d*6) δ: 9.02 (s, 1H), 8.32 (s, 1H), 8.01 (d, 1H, *J* = 8.0 Hz), 7.95-7.74 (m, 4H), 7.67-7.61 (m, 2H), 7.38 (d, 2H, *J* = 8.8 Hz), 6.56 (d, 2H, *J* = 8.8 Hz), 5.34 (d, 1H, *J* = 12.0 Hz), 4.69 (t, 1H, *J* = 10.0 Hz), 4.01-3.93 (m, 1H), 3.64 (s, 3H), 2.63-2.60 (m, 2H), 2.15-1.77 (m, 4H). ^{13}C NMR (100 MHz, DMSO-*d*6) δ: 201.33, 200.98, 194.83, 137.47, 137.06, 131.44, 131.08, 130.76, 128.26, 127.77, 123.24, 122.98, 113.83, 79.61, 73.59, 63.75, 55.89, 49.05, 47.48, 30.41, 28.52. ESI mass spectrum (*m/z*): 537.25 (M+). Anal. Calcd. For $C_{32}H_{25}ClN_2O_4$: C, 71.57; H, 4.69; N, 5.22; found: C, 71.38; H, 4.77; N, 5.47.

1'-(2-Chloroquinolin-3-yl)-2'-(furan-2-carbonyl)-1',2',5',6',7',7a'-hexahydrospiro[indene-2,3'-pyrrolizine]-1,3-dione (4f)

Colour: Yellow. M. P. 183-185 °C. IR (KBr, cm^{-1}): 3102, 2867, 1747, 1713, 1678, 754. ^1H NMR (400 MHz, DMSO-*d*6) δ: 8.32 (s, 1H), 7.95 (t, 2H, *J* = 7.2 Hz), 7.84-7.66 (m, 4H), 7.54 (t, 1H, *J* = 7.2 Hz), 7.37 (d, 1H, *J* = 8.8 Hz), 7.28 (d, 2H, *J* = 3.6 Hz), 6.76 (t, 1H, *J* = 4.0 Hz), 5.07 (d, 1H, *J* = 12.0 Hz), 4.87 (t, 1H, *J* = 10.8 Hz), 4.30-4.24 (m, 1H), 2.84-2.76 (m, 2H), 2.28-2.15 (m, 2H), 2.01-1.92 (m, 2H). ^{13}C NMR (100 MHz, DMSO-*d*6) δ: 201.10, 199.48, 183.48, 151.82, 151.44, 146.58, 146.43, 141.23, 140.45, 137.47, 136.47, 135.97, 131.39, 130.39, 128.21, 127.27, 127.18, 123.41, 123.17, 118.24, 112.71, 76.15, 73.47, 63.84, 48.05, 47.91, 30.03, 27.89. ESI mass spectrum (*m/z*): 495.25 (M−). Anal. Calcd. For $C_{29}H_{21}ClN_2O_4$: C, 70.09; H, 4.26; N, 5.64; found: C, 70.29; H, 4.18; N, 5.47.

1'-(2-Chloroquinolin-3-yl)-2'-(thiophene-2-carbonyl)-1',2',5',6',7',7a'-hexahydrospiro[indene-2,3'-pyrrolizine]-1,3-dione (4g)

Colour: Yellow. M. P. 173-175 °C. IR (KBr, cm^{-1}): 3074, 2867, 1741, 1707, 1659, 752. ^1H NMR (400 MHz, DMSO-*d*6) δ: 8.34 (s, 1H), 7.95 (t, 2H, *J* = 7.2 Hz), 7.84-7.66 (m, 4H), 7.54 (t, 1H, *J* = 7.2 Hz), 7.37 (d, 1H, *J* = 8.8 Hz), 7.29 (d, 2H, *J* = 3.6 Hz), 6.76 (t, 1H, *J* = 4.0 Hz), 5.07 (d, 1H, *J* = 12.0 Hz), 4.87 (t, 1H, *J* = 10.8 Hz), 4.30-4.24 (m, 1H), 2.84-2.76 (m, 2H), 2.28-2.11 (m, 2H), 2.01-1.94 (m, 2H). ^{13}C NMR (100 MHz, DMSO-*d*6) δ: 201.86, 199.86, 187.23, 151.33, 146.63, 143.46, 141.05, 140.38, 137.34, 136.65, 135.99, 135.47, 132.89, 131.03, 130.47, 128.22, 127.93, 127.23, 123.20, 77.24, 73.10, 64.90, 48.42, 47.73, 30.73, 28.68. ESI mass spectrum (*m/z*): 512.15 (M−). Anal. Calcd. For $C_{29}H_{21}ClN_2O_3S$: C, 67.90; H, 4.13; N, 5.46; found: C, 67.68; H, 4.07; N, 5.64.

(1'-(2-Chloroquinolin-3-yl)-1',2',5',6',7',7a'-hexahydrospiro[indeno[1,2-*b*]quinoxaline-11,3'-pyrrolizin]-2'yl)(phenyl)methanone (6a)

Colour: Yellow. M.P. 180-182 °C. IR (KBr, cm^{-1}): 3062, 2856, 1683, 755. ^1H NMR (400 MHz, DMSO-*d*6) δ: 9.08 (s, 1H), 8.43 (d, 1H, *J* = 7.6 Hz), 8.15 (d, 1H, *J* = 8.4 Hz), 8.04-7.86 (m,4H), 7.82-7.65 (m, 5H), 7.56 (t, 1H, *J* = 6.8 Hz), 7.04 (t, 1H, *J* = 7.2 Hz), 6.82 (d, 2H, *J* = 7.6 Hz), 6.6 (t, 2H, *J* = 7.6 Hz), 5.88 (d, 1H, *J* = 12.0 Hz), 4.84 (t, 1H, *J* = 10.8 Hz),

4.25-4.12 (m, 1H), 2.57-2.30 (m, 2H), 2.06-1.82 (m, 4H). ^{13}C NMR (100 MHz, DMSO-*d*6) *δ*: 198.00, 164.18, 152.53, 151.59, 146.24, 143.53, 142.55, 142.06, 137.63, 137.50, 136.86, 132.74, 132.31, 131.90, 131.00, 130.45, 129.84, 129.71, 129.23, 128.43, 127.87, 127.71, 127.48, 122.33, 74.55, 73.22, 65.36, 47.60, 47.15, 30.93, 28.39. ESI mass spectrum (*m/z*): 579.30 (M+). Anal. Calcd. For $C_{37}H_{27}ClN_4O$: C, 76.74; H, 4.70; N, 9.67; found: C, 76.95; H, 4.78; N, 9.41.

(4-Chlorophenyl)(1'-(2-chloroquinolin-3-yl)-1',2',5',6',7',7a'-hexahydrospiro[indeno[1,2-*b*]quinoxaline-11,3'-pyrrolizin]-2'yl)methanone (6b)

Colour: Yellow. M. P. 189-191 ℃. IR (KBr, cm^{-1}): 3003, 2867, 1679, 765. ^{1}H NMR (400 MHz, DMSO-*d*6) *δ*: 9.08 (s, 1H), 8.42 (d, 1H, *J* = 8.0 Hz), 8.32-7.55 (m, 13H), 6.77 (d, 1H, *J* = 8.4 Hz), 6.61(d, 1H, *J* = 8.0 Hz), 5.81 (d, 1H, *J* = 11.6 Hz), 4.79 (t, 1H, *J* = 10.8 Hz), 4.45-4.38 (m, 1H), 2.59-2.31 (m, 2H), 2.89-1.80 (m, 4H). ESI mass spectrum (*m/z*): 613.25 (M+). Anal. Calcd. For $C_{37}H_{26}Cl_2N_4O$: C, 72.43; H, 4.27; N, 9.13; found: C, 72.62; H, 4.35; N, 9.37.

(4-Bromophenyl)(1'-(2-chloroquinolin-3-yl)-1',2',5',6',7',7a'-hexahydrospiro[indeno[1,2-*b*]quinoxaline-11,3'-pyrrolizin]-2'yl)methanone (6c)

Colour: Yellow. M. P. 183-185 ℃. IR (KBr, cm^{-1}): 3055, 2852, 1683, 774. ^{1}H NMR (400 MHz, DMSO-*d*6) *δ*: 9.08 (s, 1H), 8.42-7.58 (m, 13H), 6.75-6.67 (m, 4H), 5.80 (d, 1H, *J* = 11.2 Hz), 4.78 (t, 1H, *J* = 9.6 Hz), 4.23-4.14 (m, 1H), 2.37-2.61 (m, 2H), 2.11-1.81 (m, 4H). Anal. Calcd. For $C_{37}H_{26}ClBrN_4O$: C, 67.54; H, 3.98; N, 8.51; found: C, 67.26; H, 3.93; N, 8.26.

(1'-(2-Chloroquinolin-3-yl)-1',2',5',6',7',7a'-hexahydrospiro[indeno[1,2-*b*]quinoxaline-11,3'-pyrrolizin]-2'yl)(*p*-tolyl)methanone (6d)

Colour: Yellow. M. P. 180-182 ℃. IR (KBr, cm^{-1}): 3059, 2801, 1704, 749. ^{1}H NMR (400 MHz, DMSO-*d*6) *δ*: 9.08 (s, 1H), 8.43 (d, 1H, *J* = 7.6Hz), 8.15 (d, 1H, *J* = 8.4 Hz), 8.03 (d, 1H, *J* = 8.0 Hz), 7.98-7.86 (m, 3H), 7.82-7.65 (m, 5H), 7.56 (t, 1H, *J* = 6.8 Hz), 7.04 (t, 1H, *J* = 7.2 Hz), 6.82 (d, 2H, *J* = 7.6 Hz), 6.60 (t, 2H, *J* = 7.6 Hz), 5.88 (d, 1H, *J* = 12.0 Hz), 4.84 (t, 1H, *J* = 10.8 Hz), 4.01-3.96 (m, 1H), 2.57-2.42 (m, 2H), 2.27 (s, 3H), 1.94-1.75 (m, 4H).

^{13}C NMR (100 MHz, DMSO-*d*6) *δ*:198.00, 164.18, 152.53, 151.59, 146.24, 143.53, 142.55, 142.06, 137.63, 137.50, 136.86, 132.74, 132.31, 131.90, 131.00, 130.45, 129.84, 129.71, 129.23, 128.43, 127.87, 127.71, 127.48, 122.33, 70.80, 70.55, 61.28, 46.19, 45.52, 27.90, 25.46, 19.43. ESI mass spectrum (*m/z*): 594.15 (M+). Anal. Calcd. For $C_{38}H_{24}ClN_4O$: C, 76.95; H, 4.93; N, 9.45; found: C, 77.17; H, 4.86; N 9.68.

(1'-(2-Chloroquinolin-3-yl)-1',2',5',6',7',7a'-hexahydrospiro[indeno[1,2-*b*]quinoxaline-11,3'-pyrrolizin]-2'yl)(4-methoxyphenyl)methanone (6e)

Colour: Yellow. M. P. 199-201 ℃. IR (KBr, cm^{-1}): 3060, 2846, 1673, 750. ^{1}H NMR (400 MHz, DMSO-*d*6) *δ*: 9.07 (s, 1H), 8.44 (d, 1H, *J* = 8.0Hz), 8.13 (d, 1H, *J* = 8.4 Hz), 8.04 (d,1H, *J* = 8.0 Hz), 7.96-7.64 (m, 8H), 7.54 (t, 1H, *J* = 7.6 Hz), 6.82 (d, 2H, *J* = 8.8 Hz), 6.07 (d, 1H, *J* = 8.8 Hz), 5.79 (d, 1H, *J* = 11.6 Hz), 4.83 (t, 1H, *J* = 10.8 Hz), 4.23-4.17 (m, 1H), 3.43 (s, 3H), 2.58-2.31 (m, 2H), 2.12-1.81 (m, 4H). ^{13}C NMR (100 MHz, DMSO-*d*6) *δ*: 195.82, 164.32, 162.63, 152.61, 151.60, 146.21, 143.61, 142.60, 142.09, 137.62, 137.36, 132.41, 131.82, 131.02, 130.44, 130.36, 130.17, 129.88, 129.74, 129.54, 129.15, 128.41, 127.99, 127.84, 127.76, 122.32, 112.74, 74.88, 73.27, 65.03, 55.54, 47.51, 47.14, 31.01, 28.52. ESI mass spectrum (*m/z*): 609.30 (M+). Anal. Calcd. For $C_{38}H_{24}ClN_4O_2$: C, 74.93; H, 4.80; N, 9.20; found: C, 74.64; H, 4.71; N, 9.47.

(1'-(2-Chloroquinolin-3-yl)-1',2',5',6',7',7a'-hexahydrospiro[indeno[1,2-*b*]quinoxaline-11,3'-pyrrolizin]-2'yl)(furan-2-yl)methanone (6f)

Colour: Yellow. M. P. 197-199 ℃. IR (KBr, cm^{-1}): 2959, 2857, 1667, 767. ^{1}H NMR (400 MHz, DMSO-*d*6) *δ*: 8.73 (s, 1H), 8.40 (d, 1H, *J* = 7.6Hz), 8.15 (d, 1H, *J* = 7.2 Hz), 8.02 (t,1H, *J* = 8.0 Hz), 7.89-7.68 (m, 5H), 7.58-7.45 (m, 3H), 6.63 (s, 1H), 6.44(s, 1H), 5.93 (s, 1H), 5.37 (d, 1H, *J* = 11.2 Hz), 5.02 (t, 1H, *J* = 10.4 Hz), 4.59-4.54 (m, 1H), 2.90-2.02 (m, 6H). ^{13}C NMR (100 MHz, DMSO-*d*6) *δ*: 184.41, 152.94, 152.14, 146.00, 143.23, 142.80, 142.13, 137.44, 137.28, 132.66, 131.32, 130.25, 129.85, 129.78, 129.68, 129.12, 128.26, 127.88, 127.55, 127.31, 127.10, 122.23, 117.45, 112.00, 74.96, 73.58, 65.88, 47.91, 47.45, 30.23, 27.42. Anal. Calcd. For $C_{35}H_{25}ClN_4O_2$: C, 73.87; H, 4.43; N, 9.85; found: C, 74.64; H, 4.51; N, 9.65.

(1'-(2-Chloroquinolin-3-yl)-1',2',5',6',7',7a'-hexahydrospiro[indeno[1,2-*b*]quinoxaline-11,3'-pyrrolizin]-2'yl)(thiophene-2-nyl)methanone (6g)

Colour: Yellow. M. P. 200-202 °C. IR (KBr, cm^{-1}): 3102, 2957, 1714, 755. ^{1}H NMR (400 MHz, DMSO-*d*6) δ: 8.68 (s, 1H), 8.45 (d, 1H, *J* = 7.6Hz), 8.11 (d, 1H, *J* = 7.6 Hz), 8.00 (d,1H, *J* = 6.8 Hz), 7.89-7.79 (m, 4H), 7.70 (t, 1H, *J* = 6.8 Hz), 7.71 (s, 1H), 7.61-7.46 (m, 3H), 6.59 (s, 1H), 6.30 (s, 1H), 5.48 (d, 1H, *J* = 11.6 Hz), 5.04 (t, 1H, *J* = 10.4 Hz), 4.53-4.37 (m, 1H), 2.84-2.56 (m, 2H), 2.17-1.92 (m, 4H). ^{13}C NMR (100 MHz, DMSO-*d*6) δ: 188.50, 164.55, 153.05, 151.66, 146.57, 143.71, 143.19, 142.85, 142.00, 137.38, 137.12, 134.29, 132.38, 131.77, 131.39, 130.30, 129.90, 129.62, 129.18, 129.11, 128.22, 128.08, 127.50, 127.31, 127.15, 127.09, 122.23, 75.30, 73.45, 66.36, 48.14, 47.90, 30.58, 27.67. Anal. Calcd. For $C_{38}H_{24}ClN_4O_2$: C, 71.84; H, 4.31; N, 9.58; found: C, 72.07; H, 4.38; N, 9.79.

2A.7. Crystallographic data of compound 4e and 6a

CCDC 1830589 and CCDC 1830590 contains the supplementary crystallographic data (.cif) of the compounds **4e** and **6a** respectively. These data can be obtained free of charge from The Cambridge Crystallographic Data Centre *via* www.ccdc.cam.ac.uk/structures.

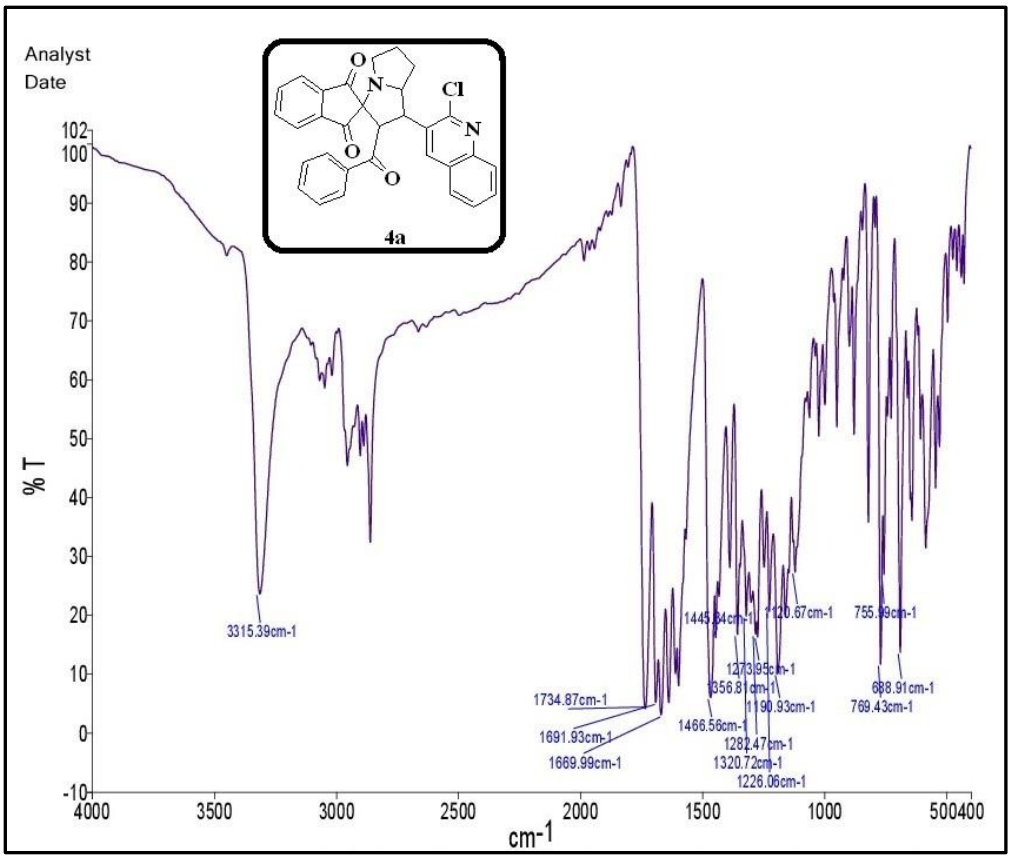

IR spectrum of the compound **4a**

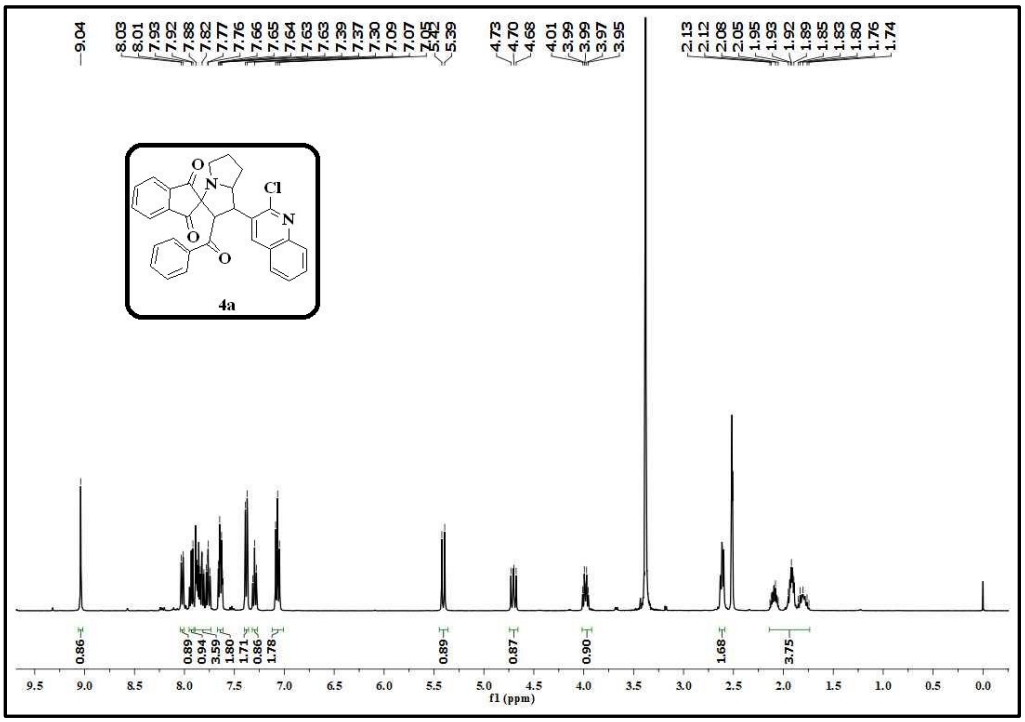

^{1}H NMR spectrum of the compound **4a**

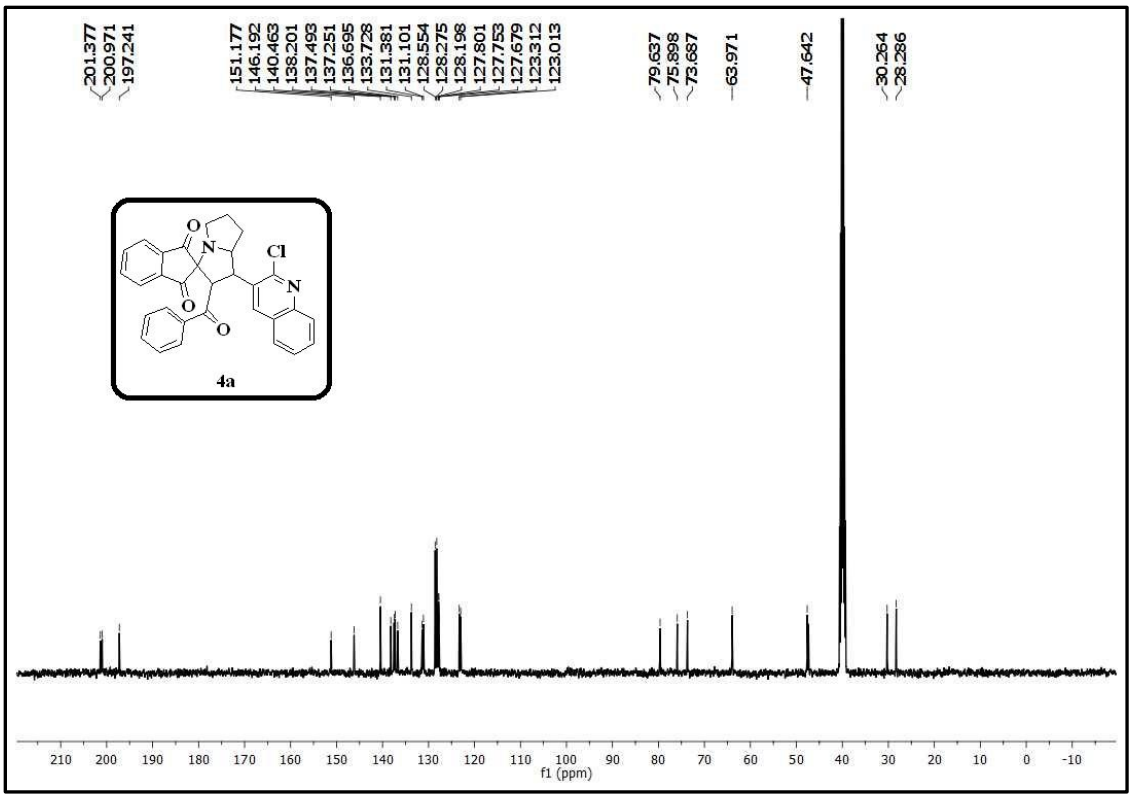

^{13}C NMR spectrum of the compound **4a**

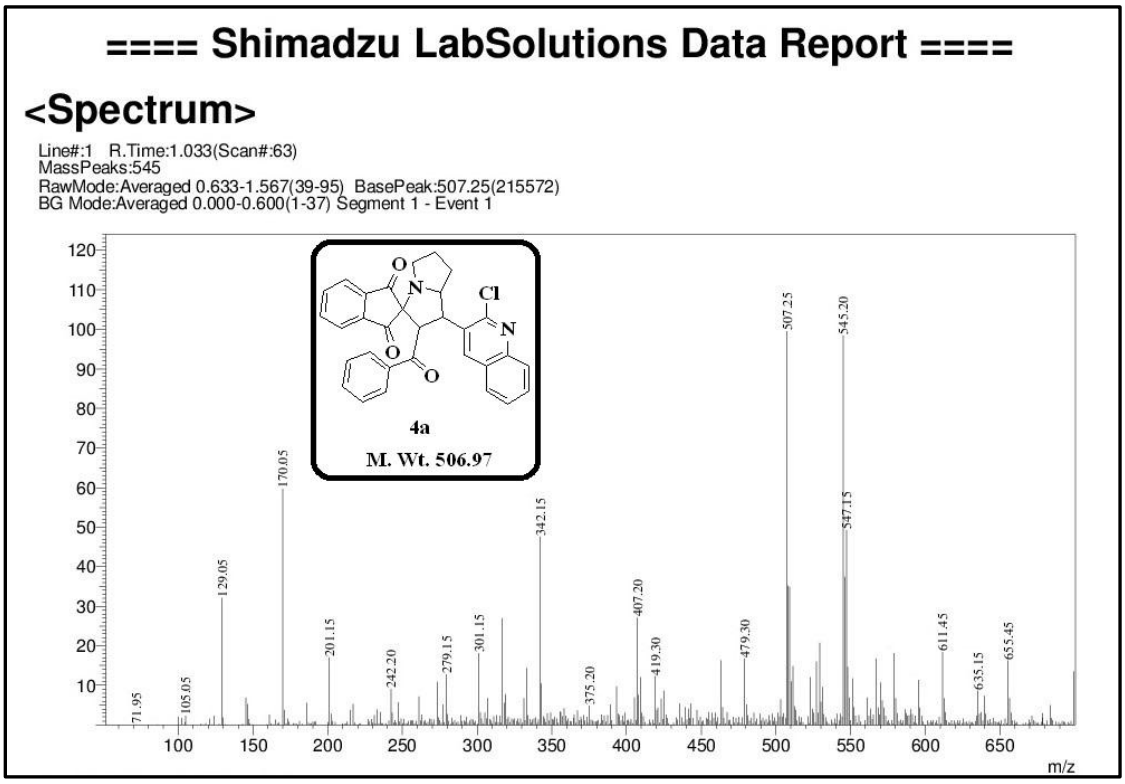

Mass spectrum of the compound **4a**

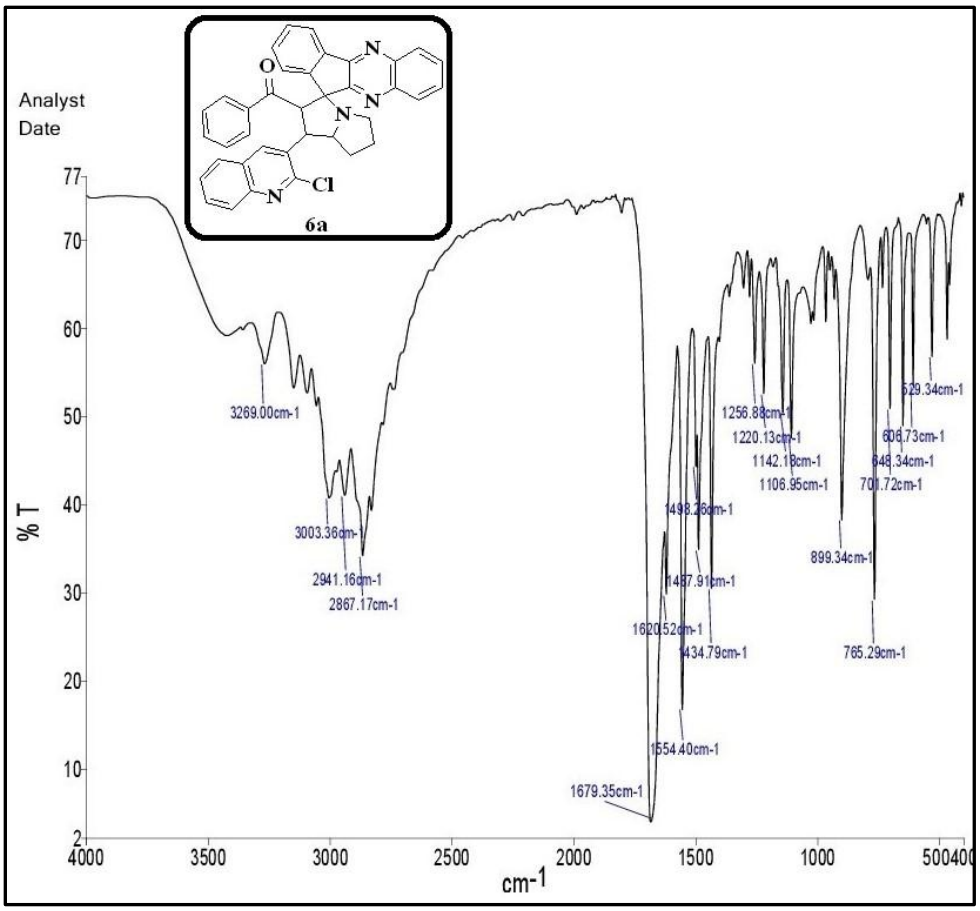

IR spectrum of the compound **6a**

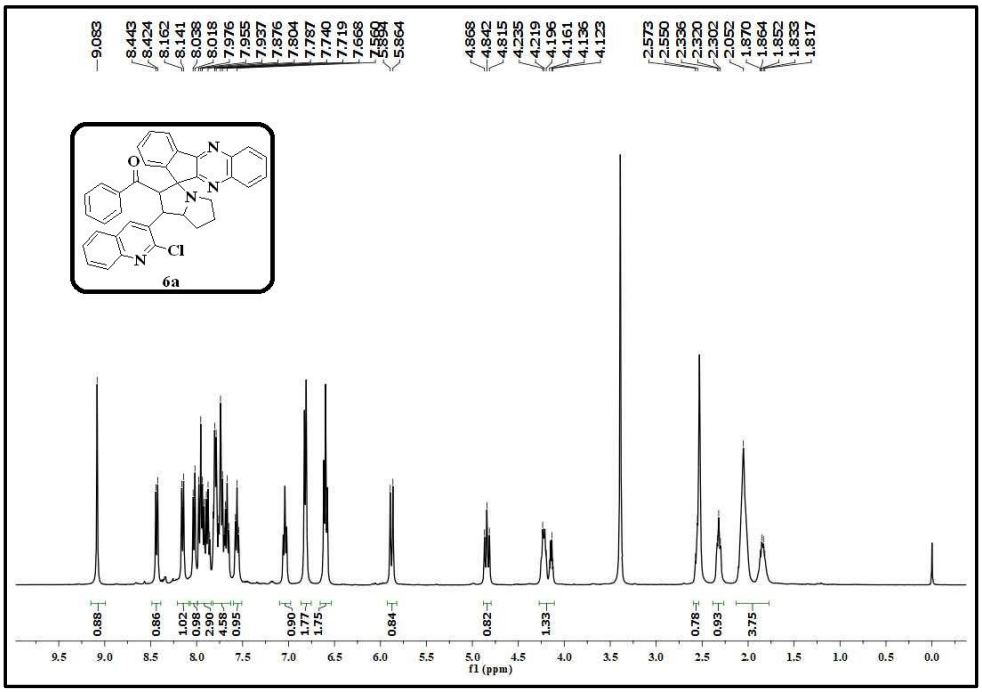

^{1}H NMR spectrum of the compound **6a**

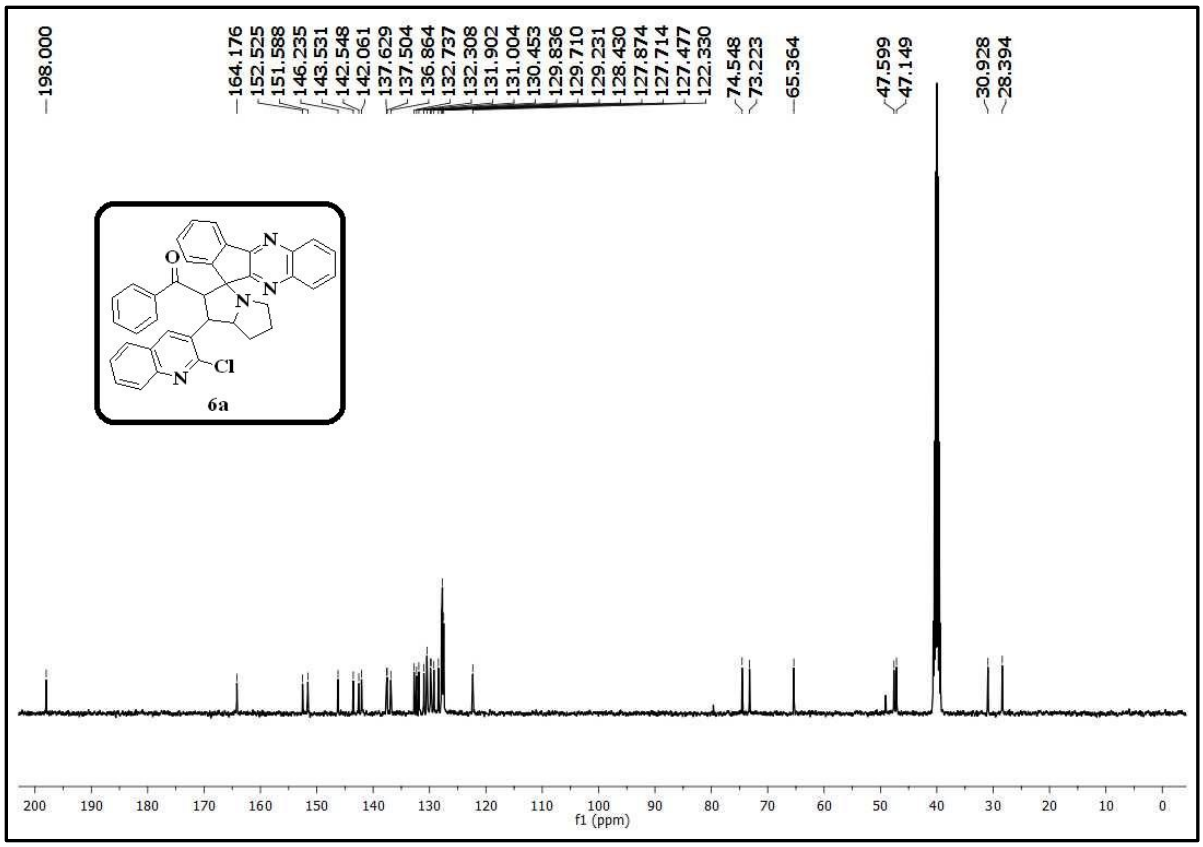

^{13}C NMR spectrum of the compound **6a**

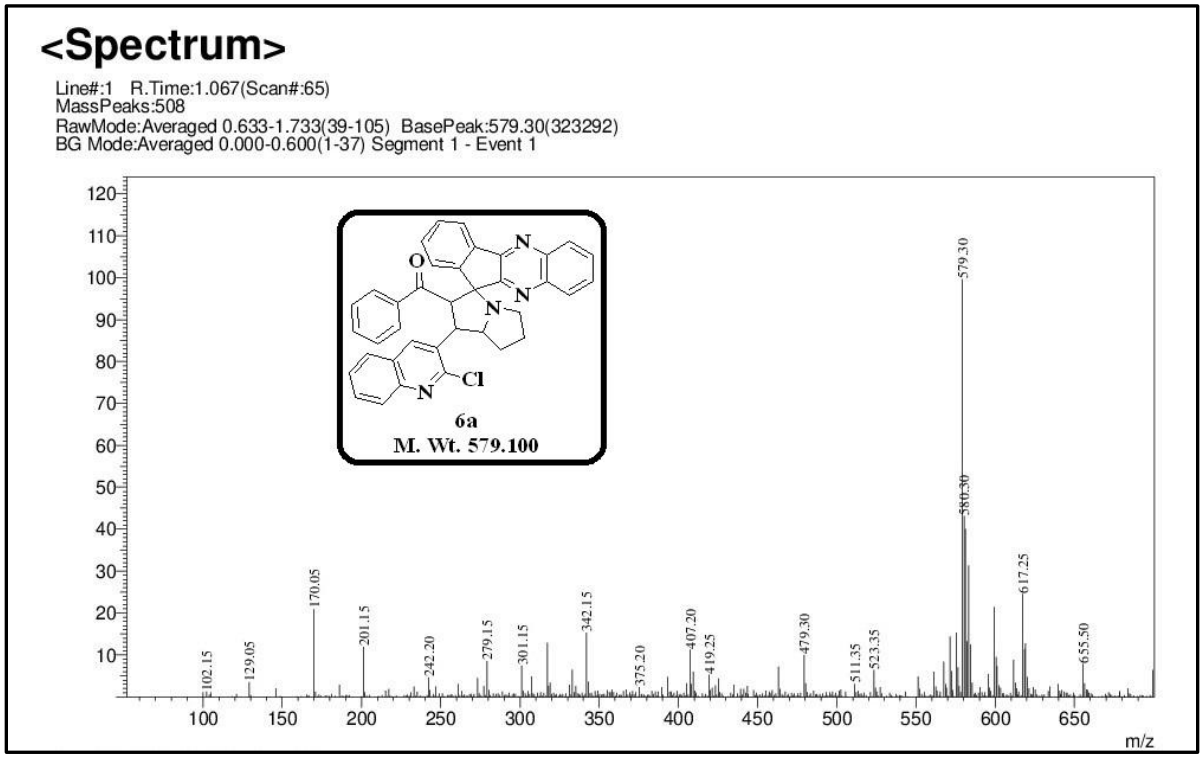

Mass spectrum of the compound **6a**

CHAPTER-II (SECTION-B)

Synthesis of regioselective quinoline grafted spirooxindolopyrrolizidines *via* 1,3-dipolar cycloaddition reaction and biological evaluation

2B.1. Introduction

Spirooxindoles plays a vital role in medicinal chemistry because of various aspects like their wide occurrence in natural products, distinctive structural feature, diverse medicinal properties etc., [48-50]. The modern strategy for the drug discovery is the rapid assembly of the structurally different compounds [50]. Hence various polyfunctional spirooxindoles were developed by incorporating the several organic molecules along with spirooxindoles into a single molecule [51, 52]. Among several natural and synthetic compounds, the compounds containing the spirooxindole ring in their core moiety are one of the compounds exhibiting potent anticancer activity [53, 54]. Synthesis of the bioactive compounds in multistep process is tedious to some extent in several reactions in terms of separation, purification, selectivity of the targeted product over to the side product etc., in each step [55, 56]. In this regard, the multicomponent reaction approach is useful when compared with multistep reaction process to synthesize the diverse chemical library of drug-like molecules [55-57].

In multicomponent reaction approach, three or more substrates react in one-pot to form a poly-functional complex molecules through the formation of several covalent bonds between carbon-carbon and carbon-heteroatoms without the isolation of highly reactive intermediate [58-61]. Waldmann et al., called the MCRs as biology-oriented synthesis (BIOS) because of their efficacy to produce the diverse biologically activity molecules [62]. The remarkable advantages of MCRs are high atom economy, efficiency, mild conditions, high convergence or divergence, library generation, the easier progress of the reaction, decreased reaction times, high selectivity, etc., [57, 63, 64]. Multicomponent 1,3-dipolar cycloaddition is an efficient method for the synthesis of various like spirooxindolopyrrolizidines with stereogenic centers regioselectively because these reactions are concerted [65-67].

Lotfy and coworkers reported the synthesis of dispiro heterocycles incorporating pyrrolothiazole and oxindole ring chemo-, regio- and stereo-selectively *via* one-pot three component [3+2] cycloaddition reaction under reflux condition in methanol (Figure 2B.1). All these molecules were evaluated for their *in vitro* anticancer activity against breast and leukemia cancer cell lines and apoptosis studies. Also, the authors have studied the molecular docking studies and they were correlated with the *in vitro* anticancer results [68].

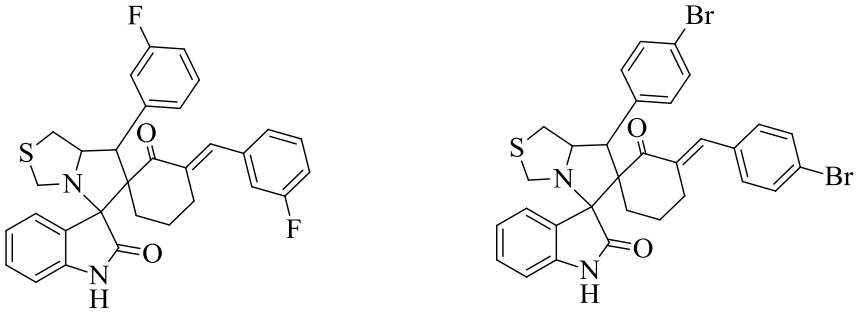

Figure 2B.1

Meshram and coworkers described the synthesis of spirooxindoles *via* one-pot multicomponent 1,3-dipolar cycloaddition reaction under microwave irradiation, catalyst free and base free conditions in an aqueous medium (Figure 2B.2). The *in vitro* anticancer activity results of these compounds exhibited moderate to potent cytotoxic activity [54].

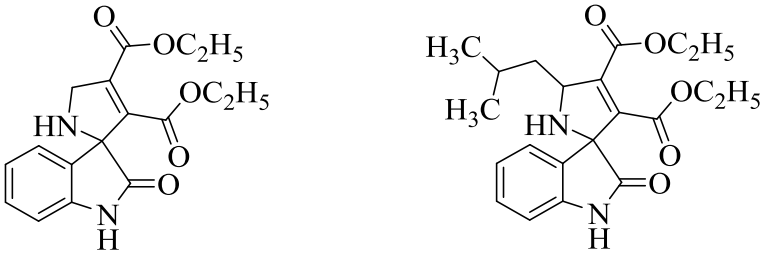

Figure 2B.2

Arun et al. reported the synthesis of spirooxindolopyrrolidine compounds *via* one-pot multicomponent 1,3-dipolar cycloaddition reaction of azomethine ylide (Figure 2B.3). These compounds were evaluated for their anticancer activity and apoptosis analysis against A549 human lung adenocarcinoma cancer cell line and DNA fragmentation studies. The *in vitro* anticancer activity was correlated with molecular docking studies [55].

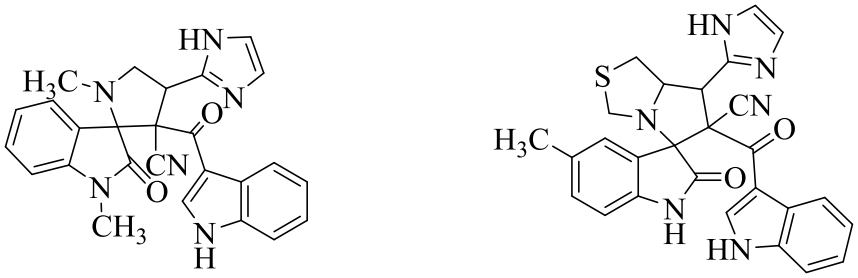

Figure 2B.3

Parthasarathy et al. reported the synthesis of structurally diverse spirooxindole derivatives *via* gold catalyzed tandem double condensation reaction under microwave irradiation method (Figure 2B.4). The synthesized molecules were evaluated for their *in vitro* antimicrobial and anticancer activities. The *in vitro* anticancer activity results were correlated with molecular docking studies [69].

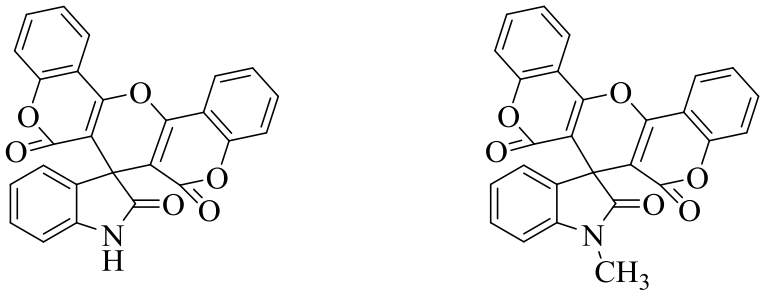

Figure 2B.4

Tiwari and coworkers described the synthesis of 2,3-dihydrooxazole-spirooxindoles *via* multi step approach (Figure 2B.5). All the synthesized compounds were evaluated for their antibacterial and antifungal activities. The minimum bactericidal concentration, minimum inhibitory concentration and minimum fungicidal concentration were determined for all the synthesized compounds [70].

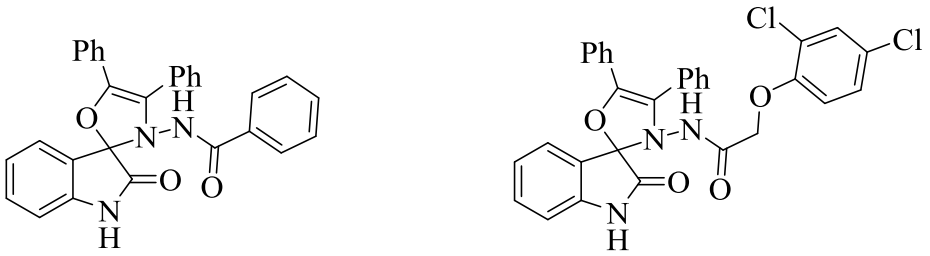

Figure 2B.5

2B.1.2. Various synthetic approaches for the synthesis of spirooxindoles

Zhang et al. reported the synthesis of the spirooxindoles *via* one-pot three-component reaction through the green reaction system of a catalytic amount of molecular iodine (Scheme 2B.1). The molecular iodine was used as an alternative catalyst for lewis acids like transition metals [71].

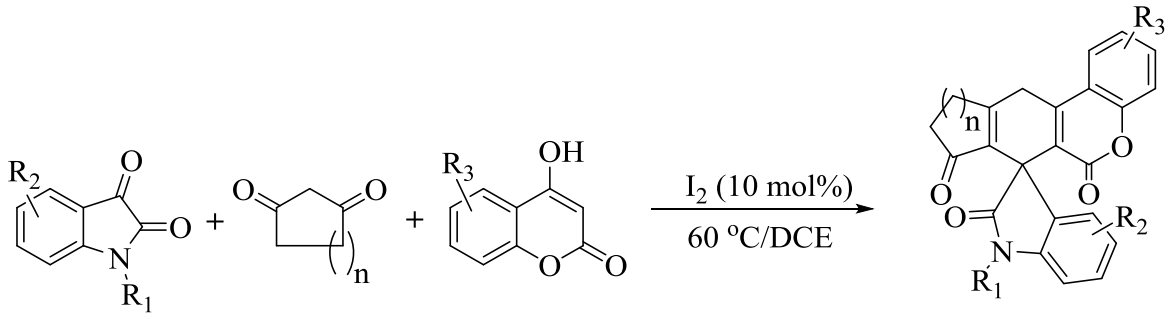

Scheme 2B.1

Roh et al. described the efficient synthesis of dihydrofuranyl spirooxindoles *via* montmorillonite K-10-catalyzed propargylation of 1,3-dicarbonyl compounds with isatin-derived propargylic alcohols and subsequent base-mediated 5-exo-dig cyclization (Scheme 2B.2) [72].

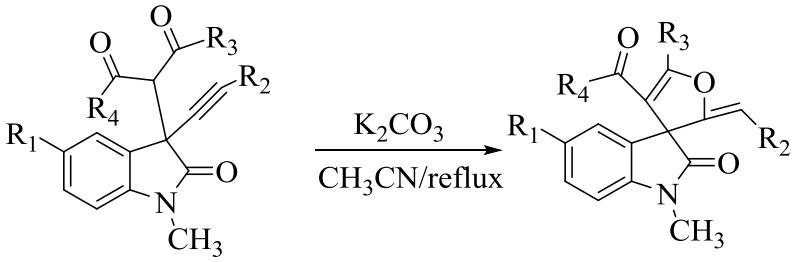

Scheme 2B.2

Lin and coworkers reported the biocatalytic domino reaction for the synthesis of spirooxindoles diastereoselectively (Scheme 2B.3). The *Aspergillus oryzae* was used as a biocatalyst. The designed chemo-enzymatic two-step process was successfully utilized for the synthesis of representative spirooxindole derivatives [73].

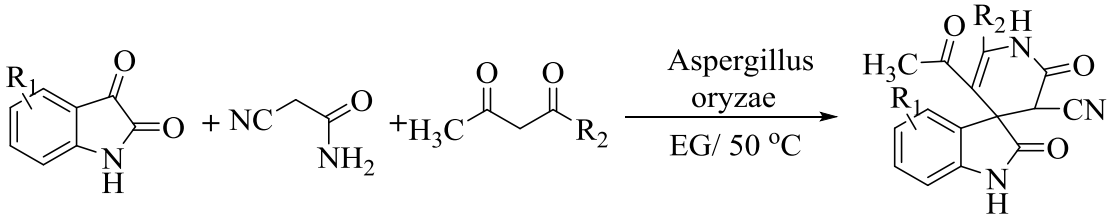

Scheme 2B.3

Zhang et al. described N-heterocyclic carbene-mediated formal [3+3] annulation of isatin derived *α,β*-unsaturated acids for the synthesis of functionalized 3,4'-spirooxindole-*δ*-

lactones (Scheme 2B.4). Isatin-derived *α,β*-unsaturated acyl azoliums, which were generated *in situ* undergo [3+3] annulation with 1,3-dicarbonyl compounds [74].

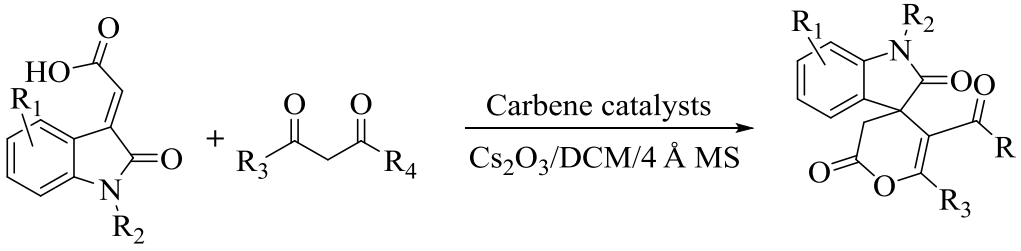

Scheme 2B.4

Ranjit Kumar and coworkers described the facile, combinatorial, regioselective synthesis of spiro-oxindole-pyrrolizine or pyrrolothiazole fused coumarin hybrid heterocycles *via* sequential multicomponent approach under ultrasound irradiation method (Scheme 2B.5). The reaction proceeds *via* aldol condensation-intramolecular cyclization-1,3-dipolar cycloaddition-decarboxylation process sequentially in one-pot without the isolation of intermediates [75].

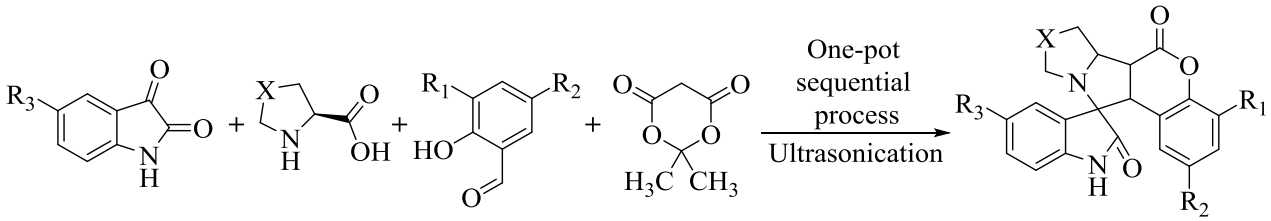

Scheme 2B.5

2B.2. Present work

The combination of quinolines or its derivatives with other molecule may increase their biological activity or create new medicinal properties like anti-tumor activity, cytotoxic toward the leukemia P388 cells, etc., [76]. Among quinolines, 2-chloro-3-formylquinoline plays a prominent role in medicinal chemistry because it is a key intermediate for the synthesis several alkaloids and biologically active molecules through various functional group interconversions [77]. The chalcones synthesized from 2-chloro-3-formylquinoline were also found that they contain cytotoxic properties [78].

Considering the need and significance in developing the new anticancer agents, herewith, we report the synthesis of novel quinolinyl spirooxindolo pyrrolizidines by incorporating the quinolinyl chalcones with isatin and L-proline *via* a bio-oriented multicomponent 1,3-dipolar cycloaddition reaction and their *in vitro* anticancer, antioxidant and molecular docking studies.

2B.2.1. Synthesis of quinolinyl spirooxindolopyrrolizidines 4a-u

An equimolar mixture of isatin derivatives **1a-c**, L-proline **2** and dipolarophiles **3a-g** were refluxed for 2-5h in ethanol. The progress of all the reactions was monitored by TLC. The crude products were filtered and purified by recrystallization in ethanol (Scheme 2B.8).

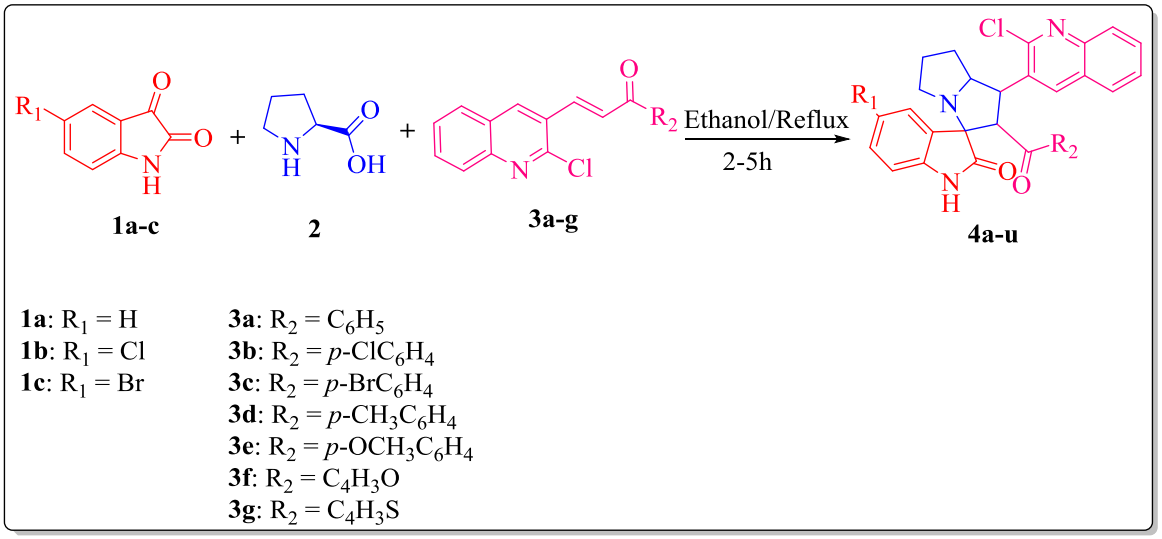

Scheme 2B.8

2B.2.2. The plausible reaction mechanism for the synthesis of the quinolinyl spirooxindolopyrrolizidines.

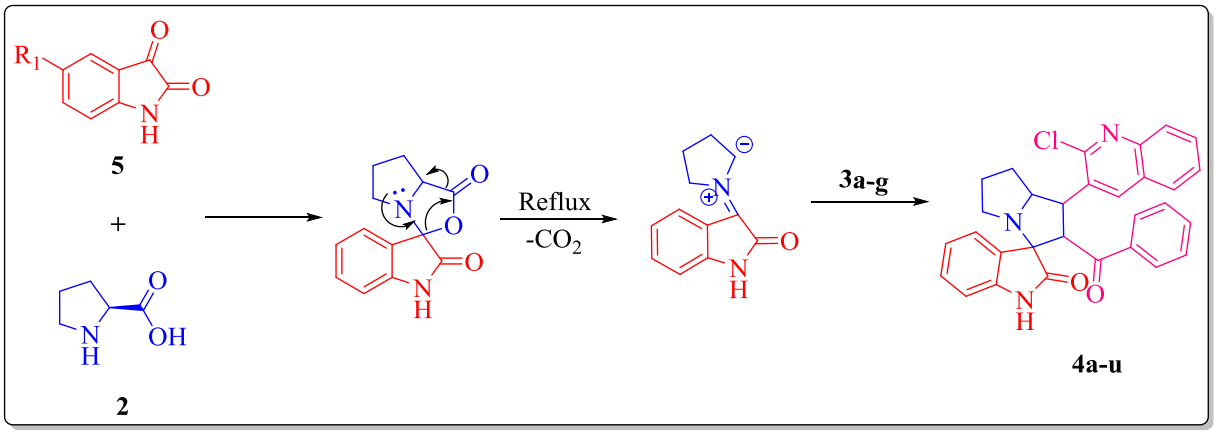

Scheme 2B.9

2B.2.3. The plausible approach of the azomethine ylide on dipolarophile for the formation of regio-selective quinolinyl spirooxindolopyrrolizidine 4d

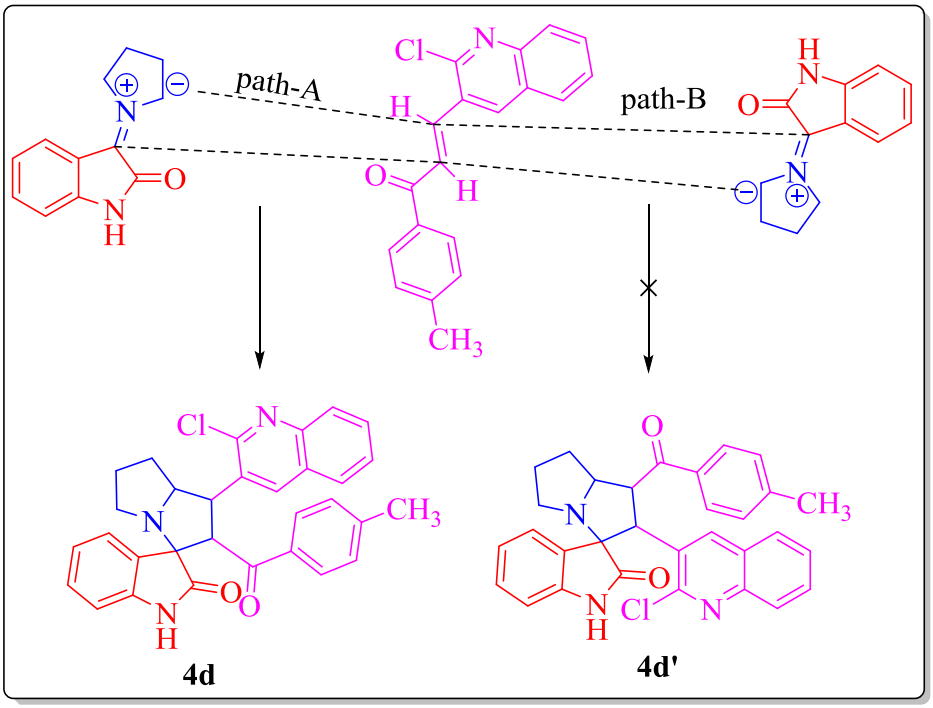

Scheme 2B.10

2B.2.4. Diastereoselective synthesis of the compound 4d *via* 1,3-dipolar cycloaddition reaction

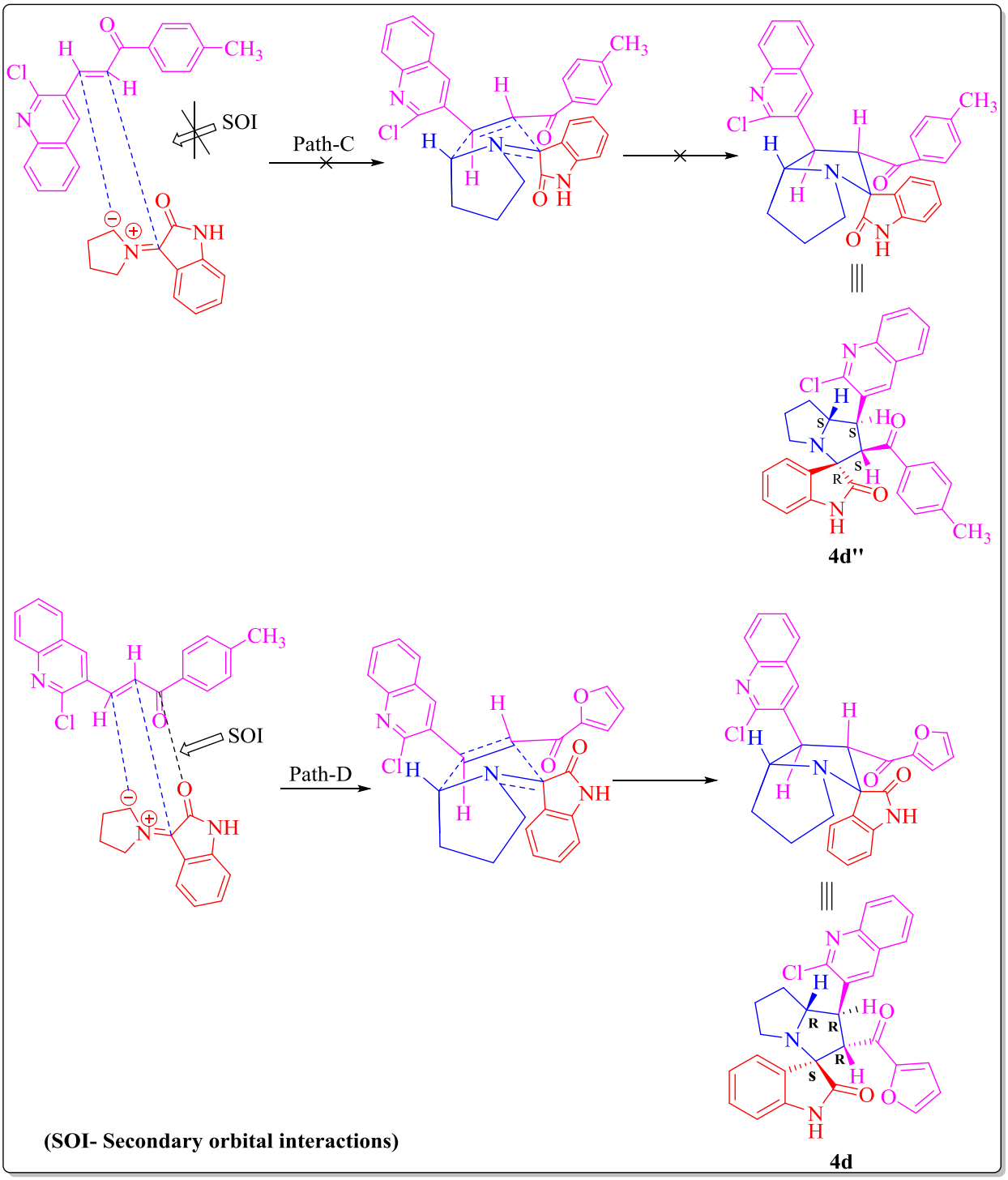

Scheme 2B.11

2B.3. Results and discussion

2B.3.1. Chemistry

Initially, a pilot reaction was carried out by choosing equimolar amounts of the isatin **1a**, L-proline **2** and dipolarophile **3a** in methanol under reflux condition. However, the corresponding spirooxindolopyrrolizidine **4a** was obtained in 5h with 68% yield. Then the screening of the reaction was carried out by using different solvents like 1,4-dioxane, ethanol and acetonitrile to study the effect of solvent on the reaction. It was observed that the quinolinyl spirooxindolopyrrolizidine **4a** was formed with a high yield at less reaction time in ethanol. Hence ethanol was taken as a solvent for further reactions. The optimized reaction conditions were summarized in table 1. The compound was purified by simple filtration and followed by recrystallization in ethanol.

Table 1. The optimized reaction conditions for the synthesis of target compound **4a**[a,b,c].

S. No.	Solvent	Method	Time(h)	Yield (%)
1	1,4-dioxane	Reflux	7	63
2	Methanol	Reflux	5	68
3	Ethanol	Reflux	4	72
4	Acetonitrile	Reflux	4	65
5	Tetrahydrofuran	Reflux	5	56

[a]All the reactions were carried out by using an equimolar mixture of isatin **1a**, L-proline **2** and dipolarophile **4a** as substrates under reflux method. [b]All the reactions were monitored by TLC. [c]Isolated yield.

Further, in order to extend the reaction method, the quinolinyl spirooxidolopyrrolizidines **4a-u** were synthesized by using an equimolar mixture of isatin derivatives **1a-c**, L-proline **2** and dipolarophiles **3a-g** under similar optimized condition (S**cheme 2B.8**). The azomethine ylide, generated *in situ* from the reaction of isatin derivatives **1a-c** with L-proline **2**, was reacted with dipolarophiles **3a-g** to form the compounds **4a-u** in 2-5h. The target compounds **4a-u** were shown in table 2.

Table 2. The quinolinyl spirooxindolopyrrolizidines **4a-u**[a,b,c,d].

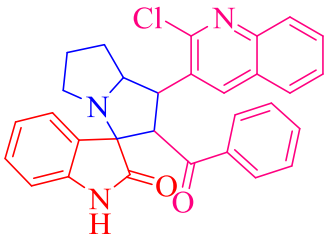 **4a** (4h / 72%)	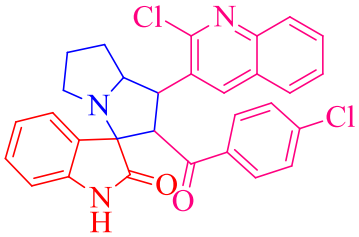 **4b** (3h / 74%)	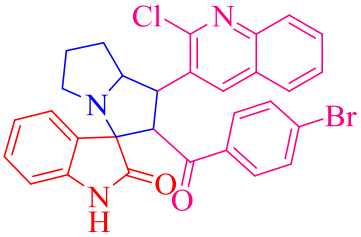 **4c** (4h / 73%)
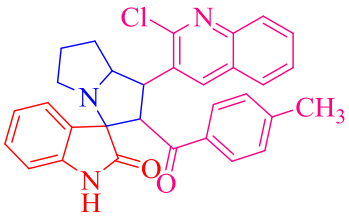 **4d** (5h / 68%)	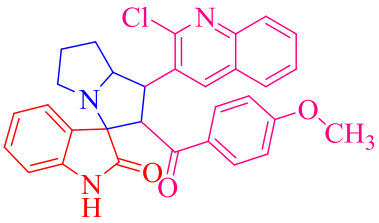 **4e** (5h / 71%)	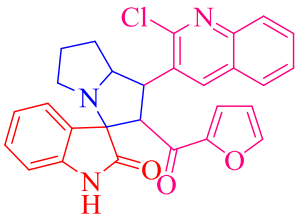 **4f** (3h / 72%)
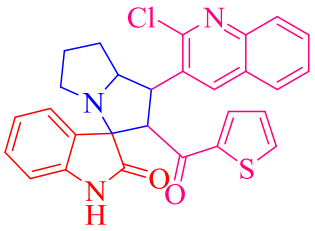 **4g** (2h / 76%)	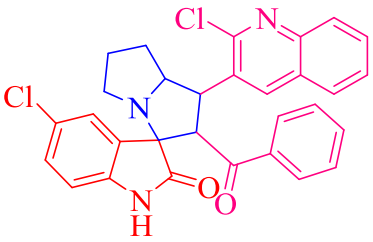 **4h** (3h / 74%)	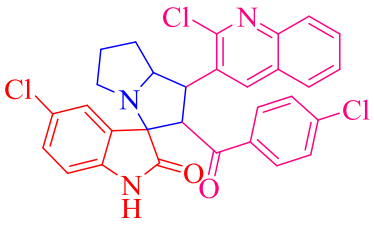 **4i** (4h / 76%)
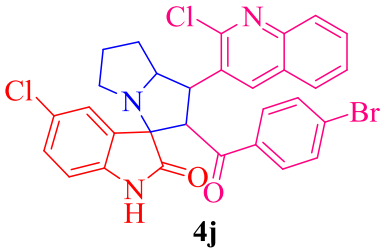 **4j** (3h / 70%)	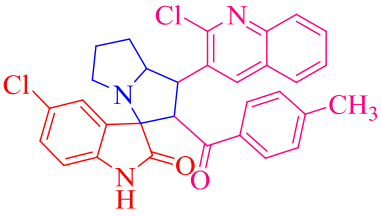 **4k** (3h / 73%)	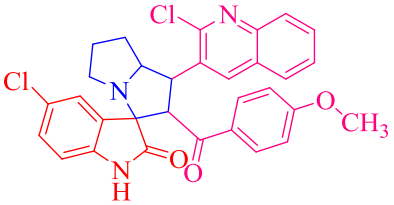 **4l** (2h / 73%)

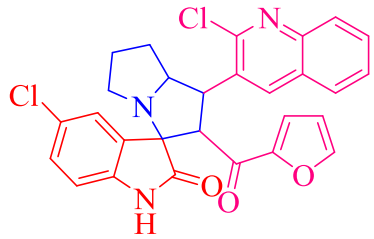

4m

(2h / 70%)

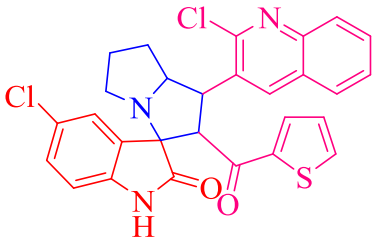

4n

(2h / 74%)

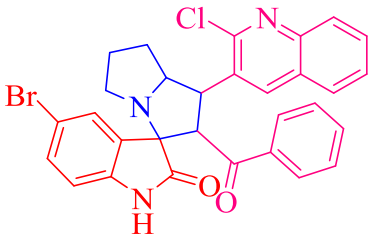

4o

(4h / 72%)

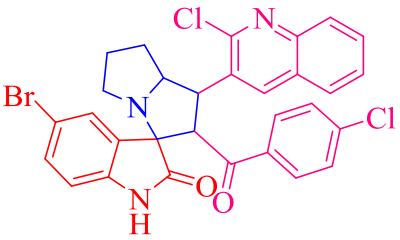

4p

(3h / 70%)

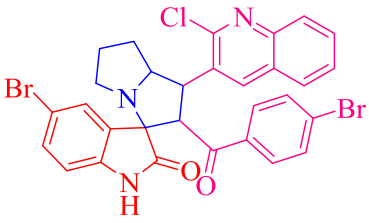

4q

(4h / 74%)

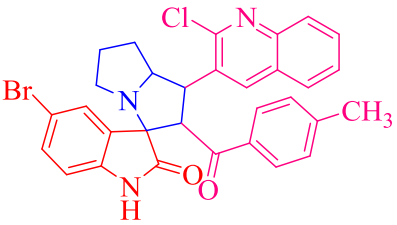

4r

(5h / 70%)

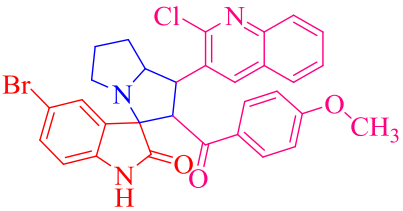

4s

(4h / 68%)

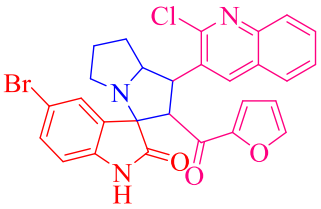

4t

(2h / 70%)

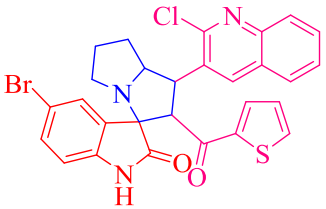

4u

(2h / 69%)

[a]All the reactions were carried out by using an equimolar mixture of isatin **1**, L-proline **2** and dipolarophile **3a** as substrates under reflux condition. [b]All the reactions were monitored by TLC. [c]Isolated yields.

The structure and regio-chemistry of compounds **4a-u** were also confirmed by their spectral data (IR, ^{1}H & ^{13}C NMR, Mass). For instance, the IR spectrum of the compound **4d** (Figure 2B.6) showed the stretching frequencies at 1727 cm^{-1} and 1675 cm^{-1}, which were due to the oxindole carbonyl group and benzoyl carbonyl group respectively. The ^{1}H NMR spectrum of the compound **4d** showed peaks at δ 5.26 (d, 1H, J = 11.6Hz), 4.55 (t, 1H, J = 10.4Hz), 3.98-3.93 (m, 1H) represents the protons at C16, C10 and C11 respectively. The peak at δ 2.26 (s, 3H) represents the methyl protons on the benzoyl ring. The peak at δ 10.24 (s, 1H) corresponds to the proton of –NH group in the oxindole ring. In ^{13}C NMR spectrum, the peaks at δ 47.72, 64.03 and 72.80 corresponds to the carbon atoms at C16, C10 and C11

positions respectively. The peak at δ 73.01 confirms the formation of spiro carbon at the C15 position. The peaks at δ 177.23, 194.61 in ^{13}C NMR spectrum further confirm the presence of the two carbonyl groups. Further, the peak at *m/z* 508.20 in mass spectrum confirms the formation of the compound **4d.** Moreover, the structure and regioselectivity of the compound **4d** were confirmed by SXRD method (Figure 2B.7). The salient crystallographic data and structure refinement parameters of the compound **4d** were shown in table 3.

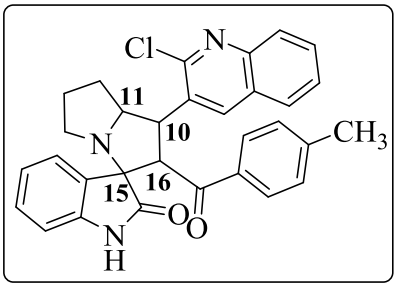

Figure 2B.6. Compound 4d

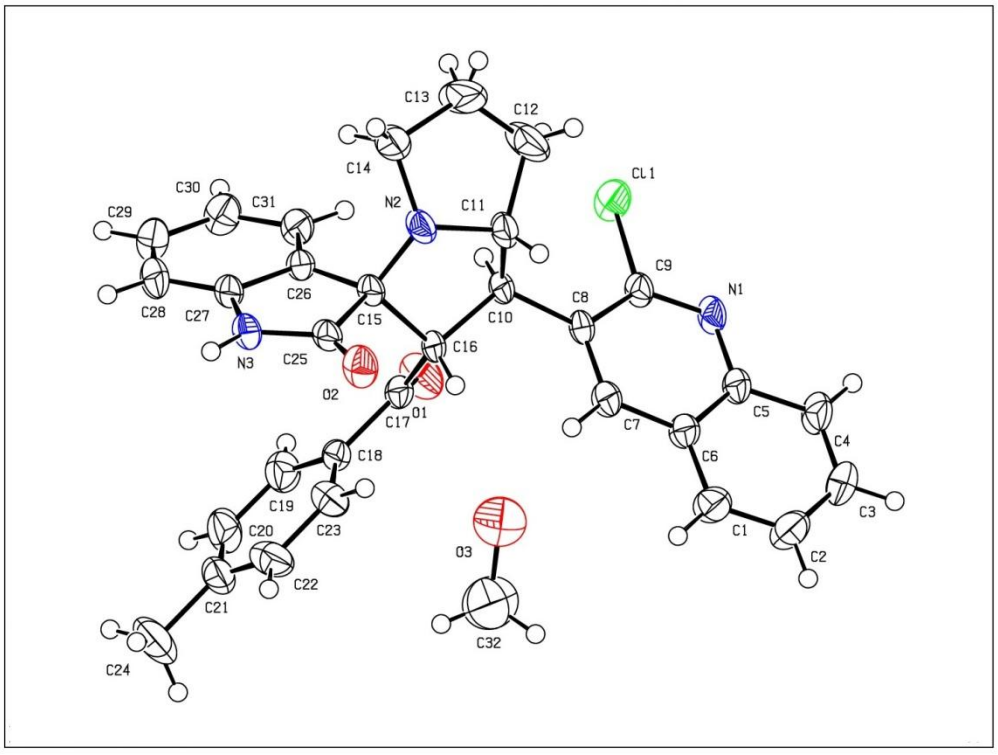

Figure 2B.7. The ORTEP representation of the compound **4d** (methanol solvate). The asymmetric units of compound **4d** shows only one enantiomer having the configurations at the chiral centers C10 (R), C11 (R), C15 (R) and C16 (S).

Table 3. The crystallographic data and structure refinement parameters of the compound **4d**.

	4d
Empirical formula	$C_{31}H_{26}ClN_3O_3.CH_3OH$
Formula weight	539.03
Crystal system	Monoclinic
Space group	$P2_1/n$
T/K	296(2)
a/Å	15.331(3)
b/Å	11.127(2)
c/Å	17.474(3)
α/°	90
β/°	114.252(9)
γ/°	90
Z	4
V/Å^3	2717.9(9)
D_{calc}/ g/cm^3	1.317
F(000)	1132
μ/mm^{-1}	0.180
θ/º	1.49 to 28.52
Index ranges	$-20 \le h \le 19$
	$-14 \le k \le 11$
	$-23 \le l \le 23$
N-total	21818
N-independent	6727
N-observed	4262
Parameters	354
R_1 ($I > 2\sigma(I)$)	0.0614
wR_2 (all data)	0.1978
GOF	1.054
CCDC	1852467

The plausible reaction mechanism for the formation of target compounds was shown scheme 2B.9. Isatin on reaction with L-proline form azomethine ylide, which was generated *in situ*. In general, the ylide containing the carbonyl group was stabilized in W-shape or in syn-confirmation [67a,79], which was shown in figure 2B.8. The ylide may attack the double bond of the dipolarophile on either side i.e., there are two different possible approaches (path-A or path-B) to form the 1,3-dipolar cycloaddition adducts **4d** and **4d'**. Since the electron density at the *β*-position to the carbonyl group of the dipolarophile was decreased by the carbonyl group, which leads to the formation of the product regio-selectively, the cyclization reaction proceeds *via* path-A but not Path-B and form the compound **4d** only. The regio selectivity of the azomethine ylide with dipolarophile **3d** was shown in scheme 2B.10.

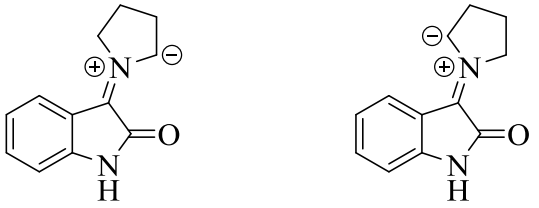

Figure 2B.8. Different geometries of azomethine ylide.

Further, the dipolarophile can exists in two orientations (faces) i.e., **a** or **b**, which were shown in figure 2B.9. The azomethine ylide may attack on either of these two orientations of dipolarophiles (**a** or **b**) i.e., *via* Path-C and Path-D to give the product diastereoselectively (Scheme 2B.11). If the azomethine ylide attacks on the dipolarophile '**a'** (Path-C)**,** then the formation of the compound **4d** would be feasible with configurations C10 (S), C11 (S), C15 (R) and C16 (S) at chiral centers. However, the crystal structure of the compound **4d** (figure 2B.7) showed that the compound **4d** was formed with C10 (R), C11 (R), C15 (S) and C16 (R) configurations at chiral centers, which confirms that the attack of azomethine ylide on dipolarophile '**b**', because there exists a secondary orbital interaction (SOI) in between the azomethine ylide and dipolarophile '**b**'. This result confirms that the dipolarophile '**b**' was the favorable orientation for the attack of azomethine ylide to form compound **4d** diastereoselectively.

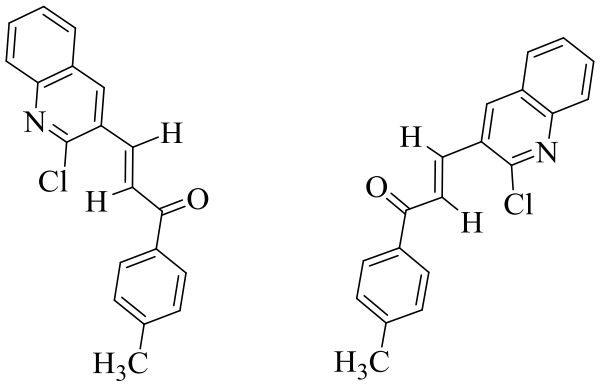

(a) **(b)**

Figure 2B.9. The possible orientations (**a** and **b**) of the dipolarophile **3d** on which the ylide can attack.

2B.3.2. Biological evaluation

2B.3.2.1. Antioxidant activity

All the synthesized compounds **4a-u** were evaluated for their *in vitro* antioxidant activity. The radical scavenging activity results were depicted in table 5. All the compounds exhibited the radical scavenging activity with the IC_{50} values ranging from 7.53 ± 0.37 µM to 49.56 ± 0.19 µM. Among all the compounds, the compounds **4p** and **4q** were exhibited potent antioxidant activity with the IC_{50} values 9.02 ± 0.42 µM and 7.53 ± 0.37 µM respectively. The compounds **4j (**11.52 ± 0.63 µM**)**, **4k (**12.89 ± 0.07 µM) and **4l (**10.29 ± 0.21 µM**)** were exhibited significant antioxidant activity. From the results, it was observed that the remarkable activity of the target compounds **4p**, **4q**, **4j**, **4k** and **4l** can be justified by looking into the mechanism of radical to quinoline nitrogen atom which stabilizes the unpaired electron in quinoline moiety that enhances the antioxidant activity [80].

Table 5. The antioxidant activity (IC_{50} values) of the target compounds **4a-u**.

S. No.	Compound	IC_{50} (µM)
1	**4a**	24.03 ± 1.02
2	**4b**	25.68 ± 0.75
3	**4c**	23.32 ± 0.56
4	**4d**	36.24 ± 0.29
5	**4e**	40.12 ± 0.28

6	**4f**	22.27 ± 0.88
7	**4g**	20.55 ± 0.74
8	**4h**	29.36 ± 0.35
9	**4i**	45.73 ± 0.42
10	**4j**	**11.52 ± 0.63**
11	**4k**	**12.89 ± 0.07**
12	**4l**	**10.29 ± 0.21**
13	**4m**	40.08 ± 0.04
14	**4n**	41.28 ± 0.11
15	**4o**	49.56 ± 0.19
16	**4p**	**9.02 ± 0.42**
17	**4q**	**7.53 ± 0.37**
18	**4r**	ND[a]
19	**4s**	ND
20	**4t**	46.58 ± 0.84
21	**4u**	48.74 ± 0.85
22	**Ascorbic acid**	6.63 ± 0.68

[a]ND- Not determined.

2B.3.2.2. Anticancer activity

All the synthesized compounds **4a-u** were evaluated for their *in vitro* anticancer activity by using MTT assay against the cell lines IMR32, A549, MCF7 and HEK293T. The MTT assay results were summarized in table 4. Among all the synthesized compounds, compound **4q** exhibited excellent activity against IMR32, A549 and MCF7 cell lines with IC_{50} values 9.60 ± 0.10 µM, 11.01 ± 0.44 µM and 10.49 ± 0.41 µM respectively. The compound **4p** exhibited good activity against MCF7 and moderate activity against IMR32 and A549 cell lines with IC_{50} values 12.51 ± 0.85 µM, 13.36 ± 0.60 µM and 15.44 ± 0.08 µM respectively. The compound **4o** exhibited significant activity against IMR32 and moderate activity against MCF7and A549 cell lines with IC_{50} values 13.89 ± 0.59 µM, 18.78 ± 0.51 µM and 20.55 ± 0.11 µM respectively. The compounds **4h** and **4j** showed moderate activity against all the three cell lines IMR32, A549 and MCF7 with IC_{50} values ranging from 16.01 ± 0.04 µM to

20.02 ± 0.29 µM respectively. The survival curves of the three cancer cell lines i.e., IMR32, A549 and MCF7 against the synthesized compounds were shown in figure 2B.8.

Structure-activity relationship (SAR) studies revealed that the substitution at the 5-position on the isatin moiety increases the biological activity. The bromo substitution on isatin derivatives at the 5-position is highly anticancer active over the other substitutions like chloro, iodo, nitro and methoxy etc., at positions 4, 5, 6 or 7 and unsubstituted isatin derivatives [81, 82]. The presence of quinoline moiety in the molecule also increases the activity [83]. The combination of the quinoline, 5-bromoisatin in a single framework might be responsible for the excellent activity of **4q**. The potent activities of the compounds **4o** and **4p** were also might be due to the presence of the bromine at 5-position on the isatin moiety and the presence of quinoline ring in these moieties.

Table 4. The anticancer activity (IC_{50} values) of the target compounds **4a-u**.

S. No.	Compound	IC_{50} (µM)[a]			
		IMR32	**A549**	**MCF7**	**HEK293T**
1	**4a**	53.00 ± 0.21	52.96 ± 0.10	48.14 ± 0.57	ND[b]
2	**4b**	49.02 ± 0.59	46.26 ± 0.60	49.74 ± 0.93	ND
3	**4c**	42.79 ± 0.73	48.25 ± 0.24	36.48 ± 0.39	ND
4	**4d**	35.21 ± 0.26	29.64 ± 0.16	36.72 ± 0.75	ND
5	**4e**	46.80 ± 0.26	25.37 ± 0.52	34.52 ± 0.15	ND
6	**4f**	38.06 ± 0.75	41.43 ± 0.86	40.19 ± 0.29	ND
7	**4g**	29.01 ± 0.23	44.05 ± 0.10	30.23 ± 0.45	ND
8	**4h**	**19.08 ± 0.35**	**17.99 ± 0.51**	**20.02 ± 0.29**	**65.64 ± 0.64**
9	**4i**	38.05 ± 0.80	30.66 ± 0.50	36.96 ± 0.25	ND
10	**4j**	**18.60 ± 0.14**	**16.01 ± 0.04**	**18.55 ± 0.38**	**61.76 ± 0.19**
11	**4k**	37.94 ± 0.81	35.68 ± 0.65	47.93 ± 0.47	ND
12	**4l**	68.43 ± 0.59	62.21 ± 0.30	62.27 ± 0.53	ND
13	**4m**	47.86 ± 0.99	44.76 ± 0.46	37.84 ± 0.36	ND
14	**4n**	43.16 ± 0.47	34.53 ± 0.77	36.65 ± 0.45	ND
15	**4o**	**13.89 ± 0.59**	**18.78 ± 0.51**	**20.55 ± 0.11**	**73.60 ± 0.80**
16	**4p**	**13.36 ± 0.60**	**15.44 ± 0.08**	**12.51 ± 0.85**	**77.20 ± 0.63**

17	**4q**	**9.60 ± 0.10**	**11.01 ± 0.44**	**10.49 ± 0.41**	**73.58 ± 0.95**
18	**4r**	ND	ND	ND	ND
19	**4s**	ND	ND	ND	ND
20	**4t**	49.02 ± 0.70	46.26 ± 0.60	49.74 ± 0.93	ND
21	**4u**	46.86 ± 0.49	44.76 ± 0.46	37.84 ± 0.36	ND
22	***Cis*-platin**	6.05 ± 1.04	10.23 ± 0.45	8.01 ± 0.39	ND

[a]IC_{50}: The concentration of the compound (µM) that exhibits the 50% cell growth inhibition.
[b]ND- Not determined.

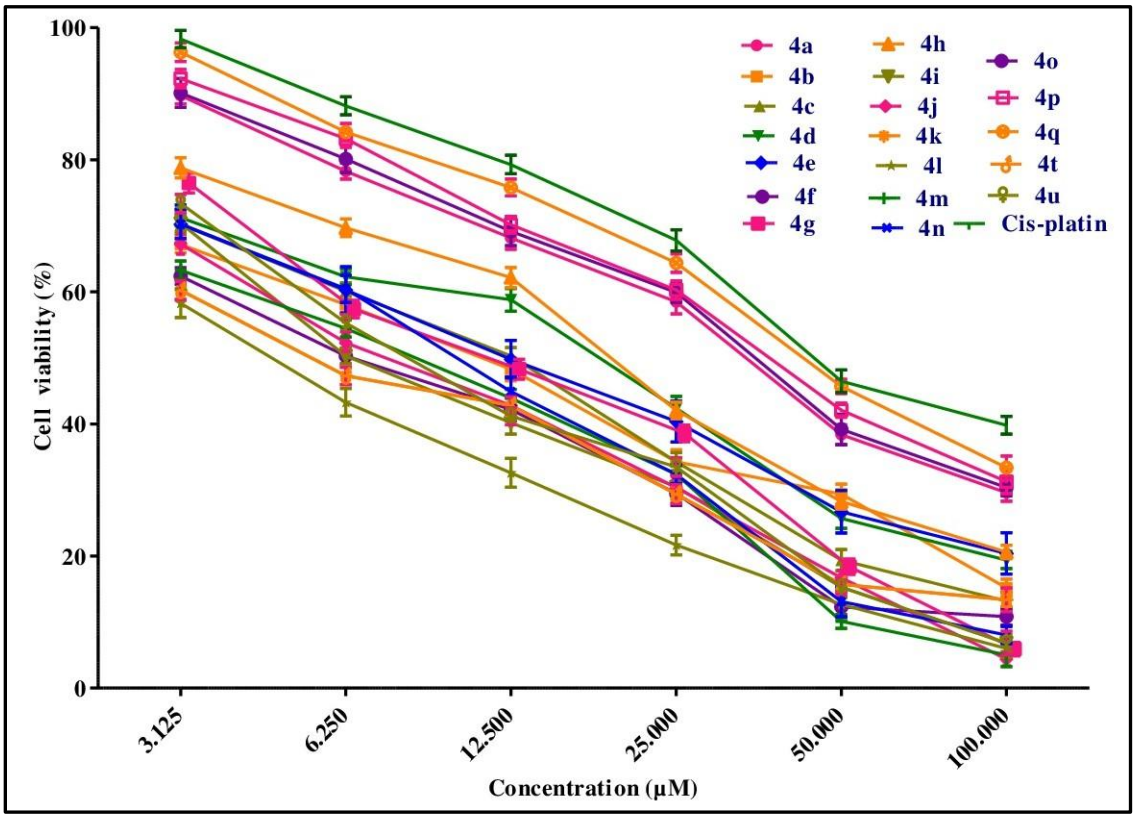

a)

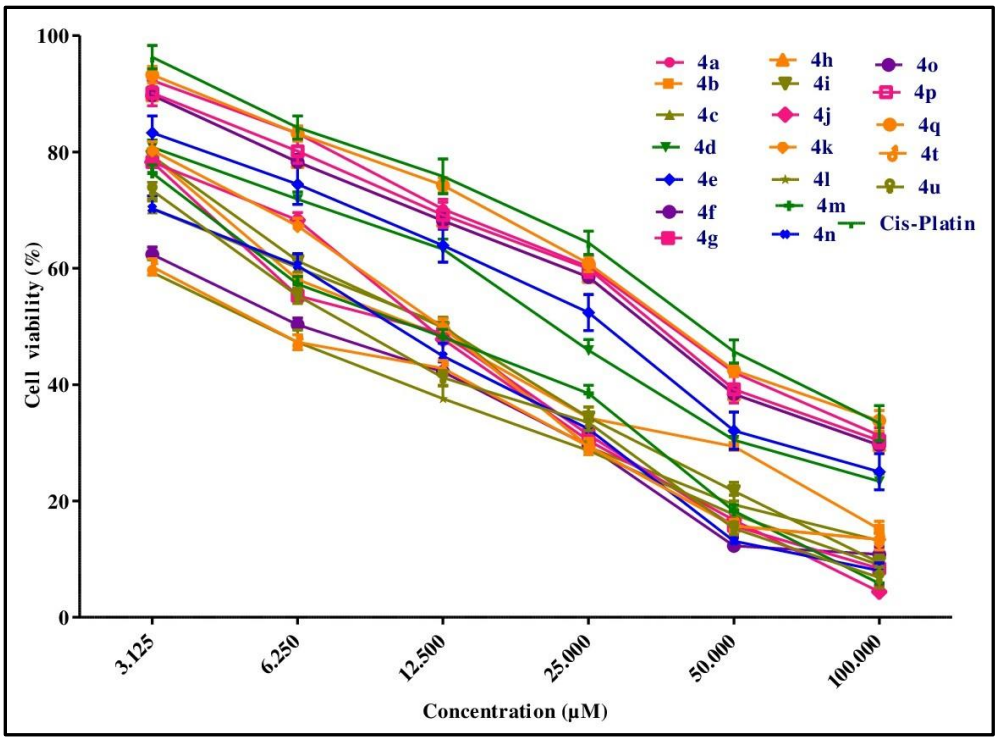

b)

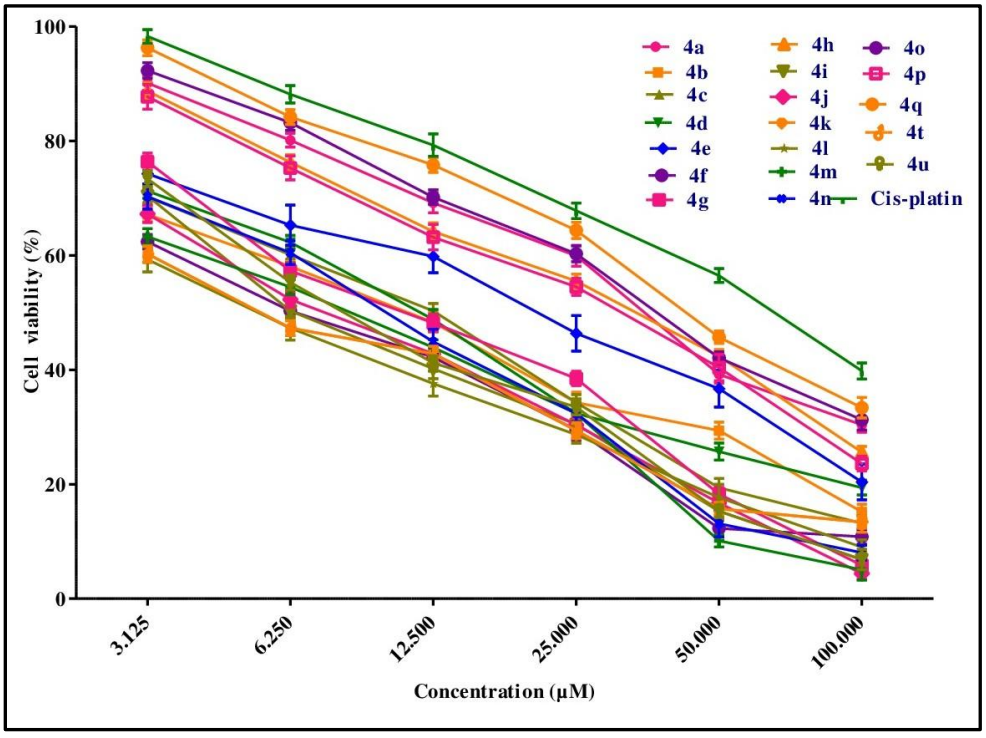

c)

Figure 2B.8. The survival curves of a) IMR32 b) A549 c) MCF7 cell lines.

2B.4. Molecular docking studies

The *in silico* molecular docking studies were carried out against proteins IDO1 (PDB ID: 2D0U), EGFR (PDB ID: 4HJO) and ALK (PDB ID: 2XP2) by using AutoDock Tools (ADT) version 1.5.6 and AutoDock version 4.2.5.1 docking program.

IDO1 (Indoleamine-2,3-dioxygenase), is the leading rate-limiting enzyme for the L-tryptophan catabolism *via* the kynurenine pathway in which L-tryptophan was converted to N-formylkynurenine. This step comprising the depletion of tryptophan that leads to arrest the growth of T-cells and microbes. So it is a useful protein in designing and developing the various anticancer agents to suppress T-cell differentiation and proliferation [37, 38]. Hence it is an attractive target for the several cytotoxic agents. Anaplastic Lymphoma Kinase (ALK), a receptor tyrosine kinase, has been found in non small cell lung cancer and its oncogenic mutations were detected in familial and sporadic cases of neuroblastoma. The EML4-ALK (echinoderm microtubule protein-like4-Anaplastic Lymphoma Kinase) fusion variant induces the oncogenic activity and causes the lung adenocarcinoma. Hence ALK is considering as a suitable target for the therapeutic intervention of cancer [8, 39]. EGFR (Epidermal dermal growth factor receptor), an extracellular protein, induces the tyrosine autophosphorylation and receptor dimerization that leads to cell proliferation, differentiation and survival [40-43]. The overexpression of the EGFR leads to colon cancer. Its mutations cause various cancer diseases like glioblastoma, anal cancer, squamous-cell carcinoma of the lung, etc., [43-46]. Hence it is an attractive target for the several anticancer agents.

By examining the aforementioned reasons, IDO1, ALK and EGFR proteins have chosen as the target receptors for the docking studies. The binding energies of the three proteins were compared and summarized in Table 6. The hydrogen bonding profile of the compounds **4a-u** with the protein IDO1 was shown in Table 7. The molecular docking studies of the targeted scaffolds **4a-u** with the target receptors IDO1, EGFR and ALK were compared (as shown in Table 6) and the results certainly confirm the affinity of all the synthesized compounds **4a-u** with the receptor IDO1 is better than that of receptors ALK and EGFR. Hence the protein receptor IDO1 was preferred as the target receptor for the elaborate discussion.

Among all the synthesized compounds **4a-u**, the compounds **4h**, **4o**, **4p** and **4q** were found to be potential inhibitors inferred by their least binding energies −11.27, −11.19, −11.10 and −11.32 kcal/mol respectively. The compound **4h** exhibit three hydrogen bonds; one in between –NH group of the oxindole ring and amino acid residue GLY262 with bond length 2.37 Å, one in between carbonyl oxygen of oxindole and amino acid residue ALA264 with bond length 1.93 Å, one in between –N– atom and amino acid residue ALA264 with bond length 2.57 Å. The pyrrolizidine ring interacts with amino acid residue ALA264 and HIS346, phenyl ring in the benzoyl group interacts with amino acid residues VAL350, ILE354 and PHE226, phenyl ring in the quinoline moiety interacts with the amino acid residues ILE217 and VAL166 and pyridyl ring in the quinoline moiety interacts with the amino acid residue ALA264 through the hydrophobic interactions. The compound **4o** exhibit three hydrogen bonds; one in between –NH group of the oxindole ring and amino acid residue GLY262 with bond length 2.36 Å, one in between carbonyl oxygen of oxindole and amino acid residue ALA264 with bond length 1.85 Å, one in between N-atom and amino acid residue ALA264 with bond length 2.64 Å. Pyrrolizidine ring interacts with amino acid residues ALA264 and HIS346, phenyl ring in the benzoyl group interacts with amino acid residues VAL350, ILE354 and PHE226, phenyl ring in the quinoline moiety interacts with the amino acid residues ILE217 and VAL166 and pyridyl ring in the quinoline moiety interacts with amino acid residue ALA264 through the hydrophobic interactions.

The compound **4p** exhibited one hydrogen bond in between carbonyl oxygen of benzoyl group and amino acid residue ALA264 with bond length 2.48 Å. The phenyl ring in the isatin moiety interacts with the amino acid residue ALA354, pyrrolizidine ring interacts with amino acid residues PHE163, PHE226, ILE349 and ILE217, phenyl ring in the benzoyl group interacts with amino acid residues ALA264 and HIS346, phenyl ring in the quinoline moiety interacts with the amino acid residues VAL170, PHE214 and ALA264, and pyridyl ring in the quinoline moiety interacts with amino acid residues PHE214 and ALA264 through the hydrophobic interactions. The compound **4q** exhibited one hydrogen bond in between carbonyl oxygen of benzoyl group and amino acid residue ALA264 with bond length 2.37Å. the pyrrolizidine ring interacts with amino acid residues PHE163, PHE226, ILE217 and ILE349, phenyl ring in the benzoyl group interacts with amino acid residues ALA264 and HIS346, phenyl ring in the quinoline moiety interacts with the amino acid

residues PHE214, ALA264 and VAL170 and pyridyl ring in the quinoline moiety interacts with amino acid residues PHE214 and ALA264 through the hydrophobic interactions. The hydrophobic interactions also played a vital role in increasing the affinity in between the synthesized compounds and target proteins [47]. The hydrogen bonding interactions and hydrophobic interactions of the compounds **4h**, **4o**, **4p** and **4q** were shown in figure 2B.9, 2B.10, 2B.11 and 2B.12. It was noticed that the compounds other than **4h**, **4o**, **4p** and **4q** exhibited moderate binding affinities with all the three protein residues i.e., IDO1, EGFR and ALK.

Table 6. The binding energies of all the synthesized compounds against IDO1, ALK and EGFR.

S. No.	Compound	Binding energy (kcal/mol)		
		IDO1 (PDB ID: 2D0U)	**EGFR (PDB ID: 4HJO)**	**ALK (PDB ID: 2XP2)**
1	**4a**	− 10.95	− 10.90	− 9.91
2	**4b**	− 10.37	− 10.30	− 9.47
3	**4c**	− 10.69	− 10.61	− 9.59
4	**4d**	− 10.35	− 10.97	− 9.40
5	**4e**	− 10.15	− 10.75	− 9.11
6	**4f**	− 10.33	− 10.21	− 8.51
7	**4g**	− 9.71	− 10.76	− 9.88
8	**4h**	**− 11.27**	− 9.65	− 9.21
9	**4i**	− 10.93	− 10.25	− 9.32
10	**4j**	− 11.09	− 10.65	− 9.29
11	**4k**	− 10.42	− 10.12	− 9.30
12	**4l**	− 10.54	− 9.95	− 8.93
13	**4m**	− 10.23	− 10.40	− 8.56
14	**4n**	− 9.00	− 10.19	− 9.17
15	**4o**	**− 11.19**	− 10.55	− 9.06
16	**4p**	**− 11.10**	− 10.84	− 9.41
17	**4q**	**− 11.32**	− 10.76	− 9.58

18	**4r**	− 11.04	− 10.64	− 9.34
19	**4s**	− 10.94	− 10.15	− 9.24
20	**4t**	− 10.58	− 10.44	− 8.47
21	**4u**	− 10.24	− 10.29	− 8.65

Table 7. The binding energies, Number of hydrogen bonds, residues involved in the hydrogen bonding and the hydrogen bond lengths of all the synthesized compounds against IDO1.

S. No.	**Compound**	**Binding energy (kcal/mol)**	**IDO1 (PDB ID: 2D0U)**		
			No. of hydrogen bonds	**Residues involved in the hydrogen bonding**	**Hydrogen bond length (Å)**
1	**4a**	− 10.95	2	ALA264, GLY262	1.92, 2.37
2	**4b**	− 10.37	1	ALA264	2.49
3	**4c**	− 10.69	1	ALA264	2.29
4	**4d**	− 10.35	1	ALA264	2.32
5	**4e**	− 10.15	1	ALA264	2.37
6	**4f**	− 10.33	2	ALA264, GLY262	1.95, 2.32
7	**4g**	− 9.71	3	ALA264, SER263	2.34, 2.68, 2.93
8	**4h**	− **11.27**	3	GLY262, ALA264	1.93, 2.37, 2.57
9	**4i**	− 10.93	1	ALA264	2.32
10	**4j**	− 11.09	1	ALA264	2.36
11	**4k**	− 10.42	2	ALA264, HIS346	1.76, 2.28
12	**4l**	− 10.54	1	ALA264	2.34
13	**4m**	− 10.23	2	ALA264, GLY262	1.90, 2.28
14	**4n**	− 9.00	1	HIS346	2.11

15	**4o**	**− 11.19**	3	ALA264, GLY262	1.85, 2.36, 2.84
16	**4p**	**− 11.10**	1	ALA264	2.48
17	**4q**	**− 11.32**	1	ALA264	2.37
18	**4r**	− 11.04	1	ALA264	2.49
19	**4s**	− 10.94	1	ALA264	2.35
20	**4t**	− 10.58	2	ALA264, GLY262	1.94, 2.33
21	**4u**	− 10.24	3	ARG231, ALA264, HIS346	2.03, 3.43, 3.49

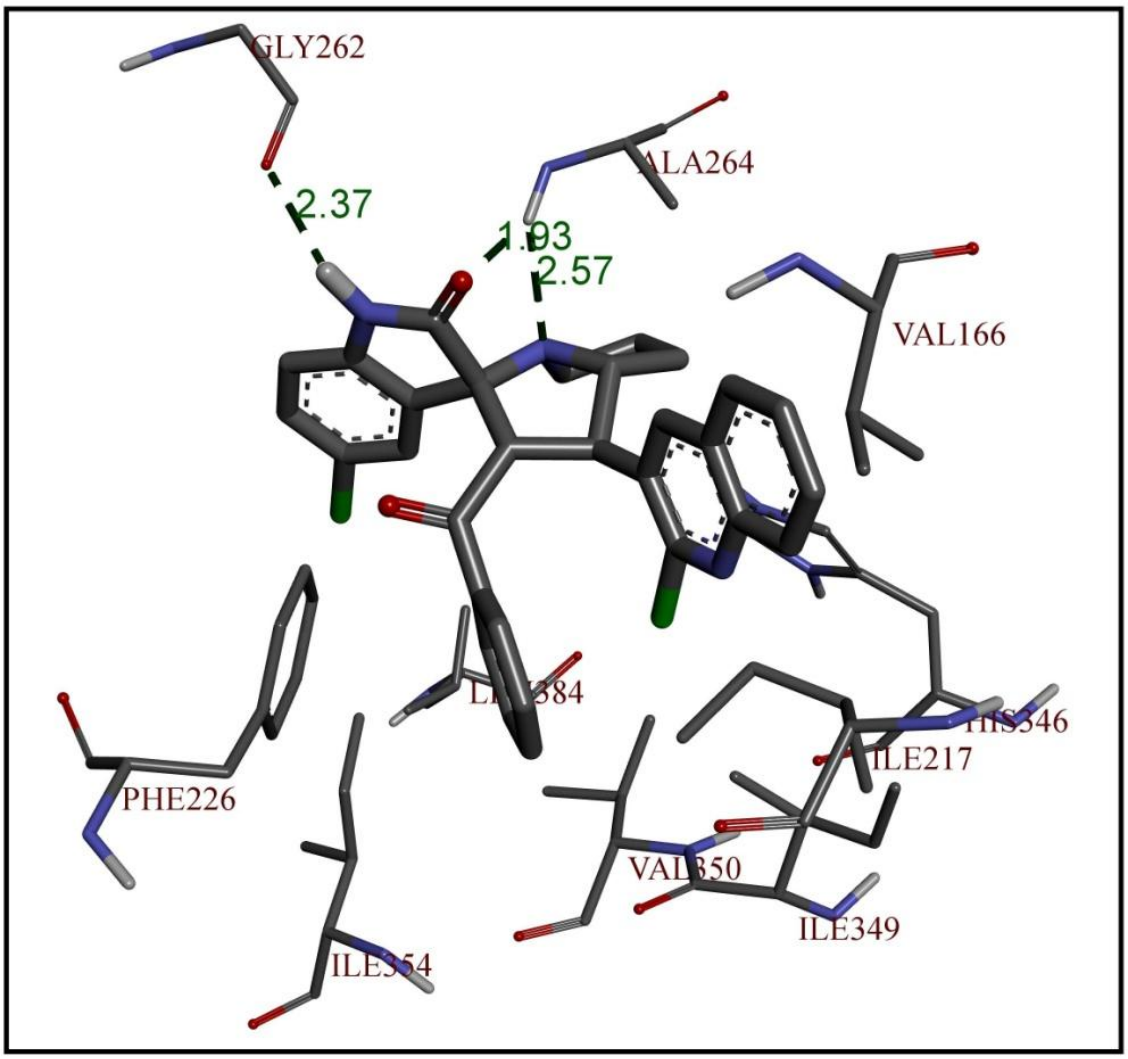

a)

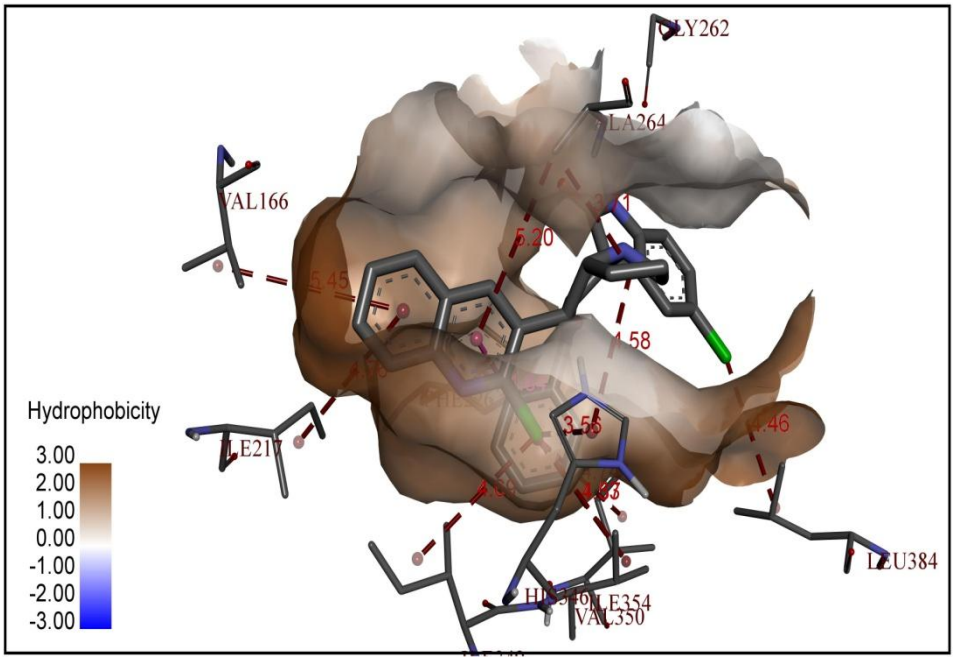

b)

Figure 2B.9. The best docking poses of the compound **4h**. a) The hydrogen bonding interactions, (b) The hydrophobic interactions.

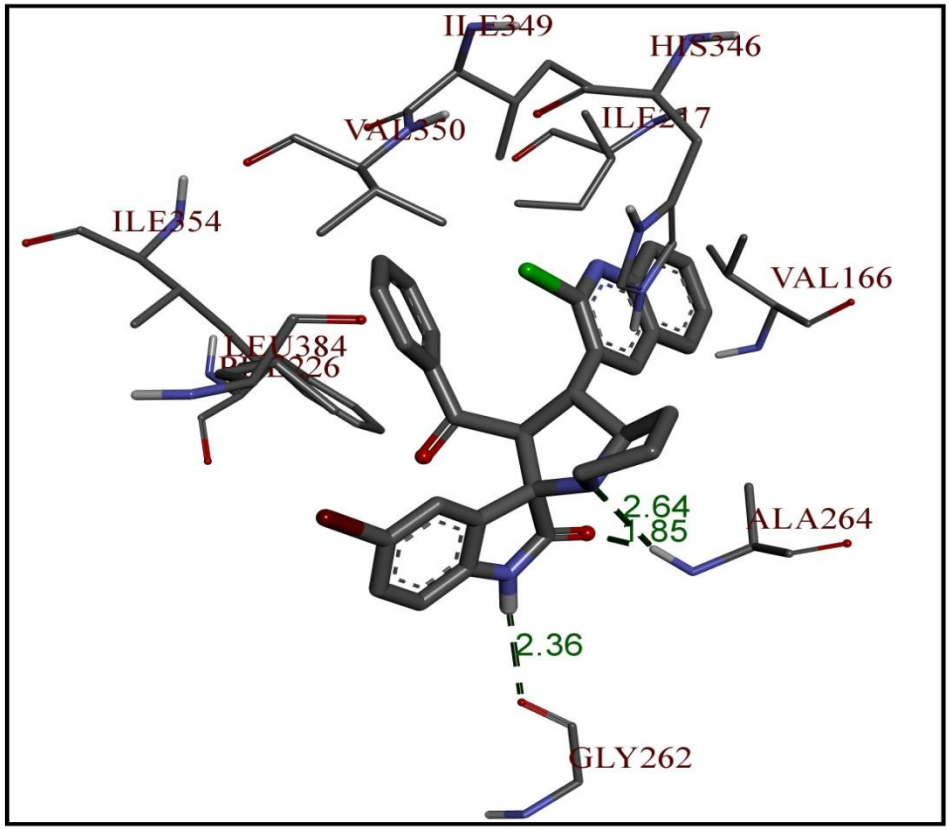

a)

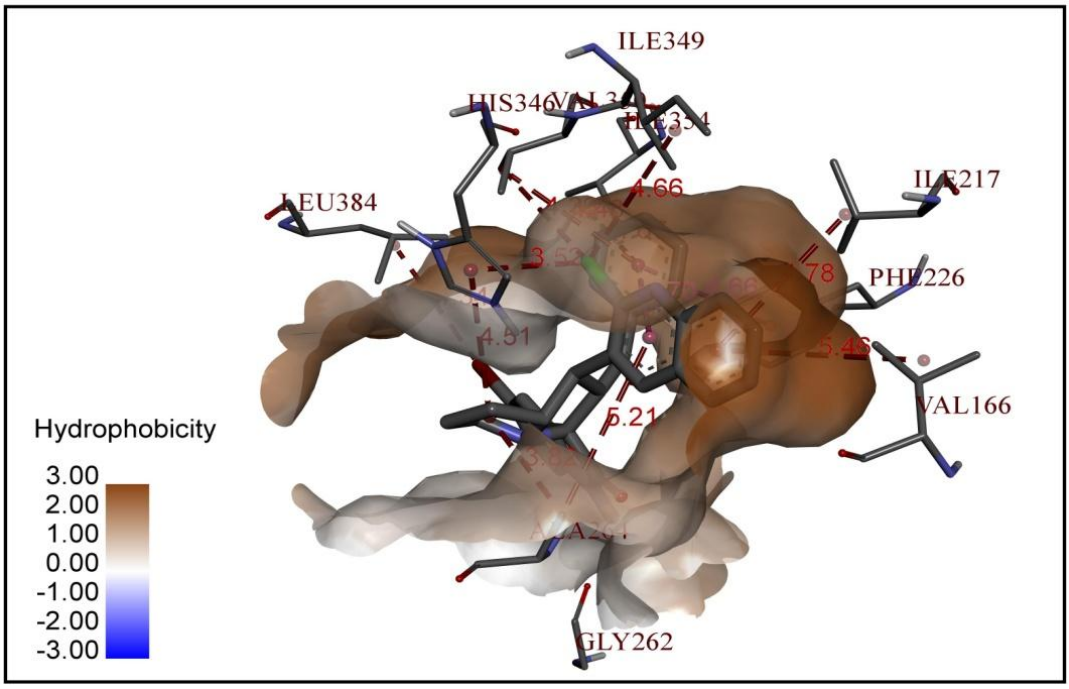

b)

Figure 2B.10. The best docking poses of the compound **4o**. a) The hydrogen bonding interactions, (b) The hydrophobic interactions.

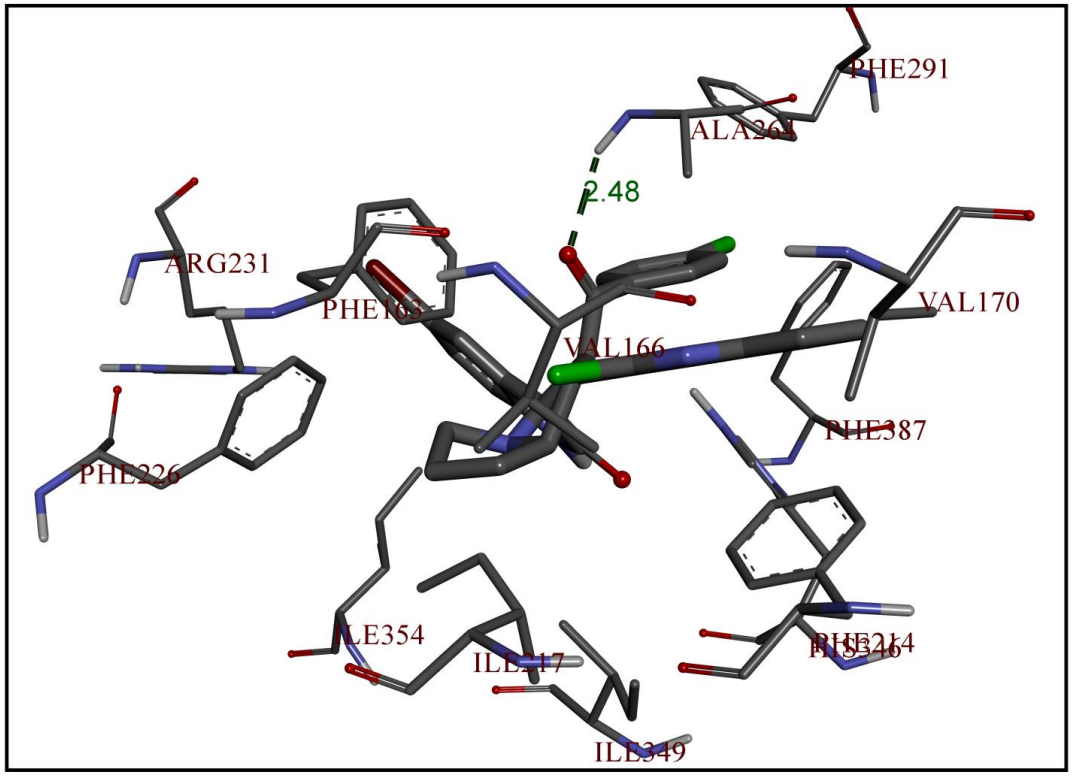

a)

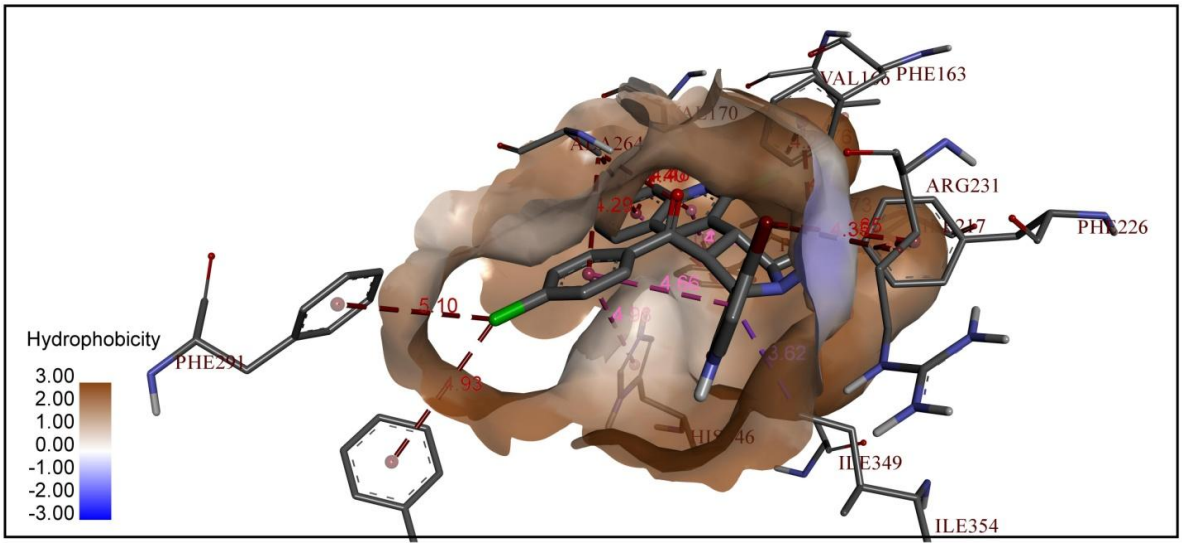

b)

Figure 2B.11. The best docking poses of the compound **4p**. a) The hydrogen bonding interactions, (b) The hydrophobic interactions.

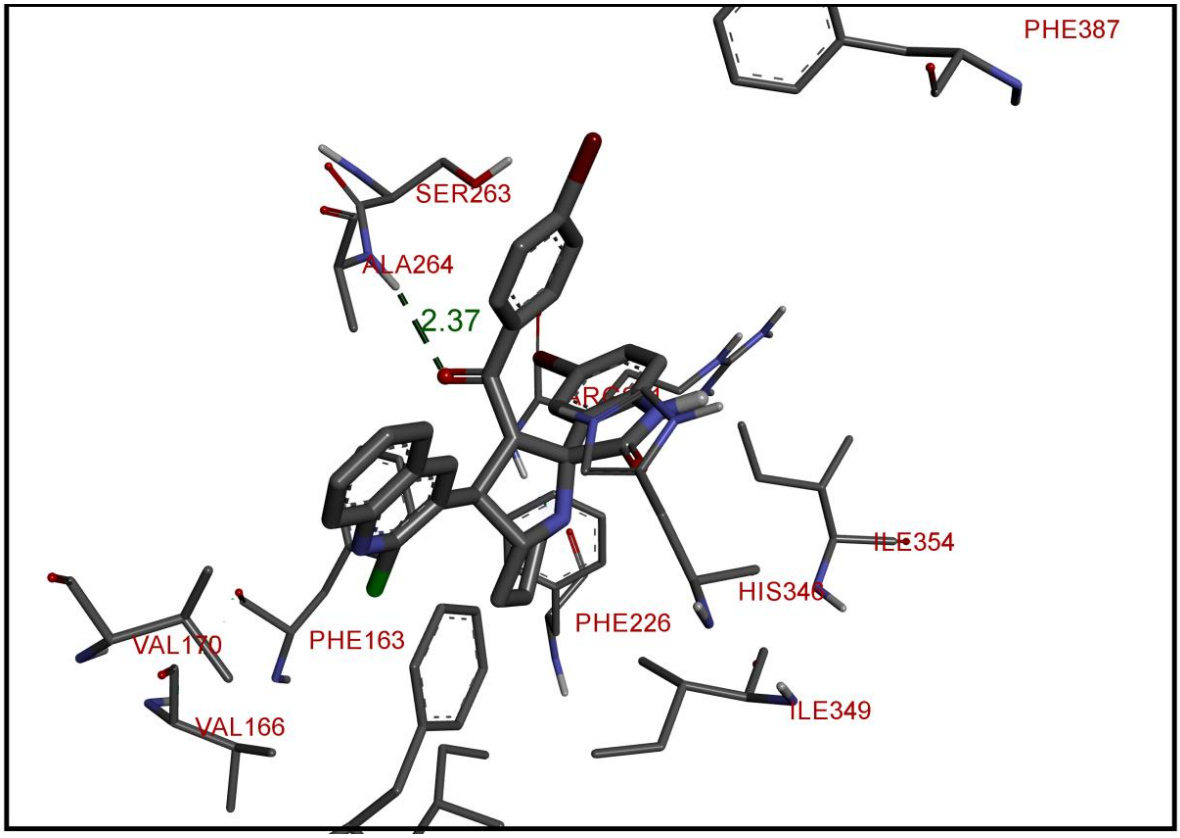

a)

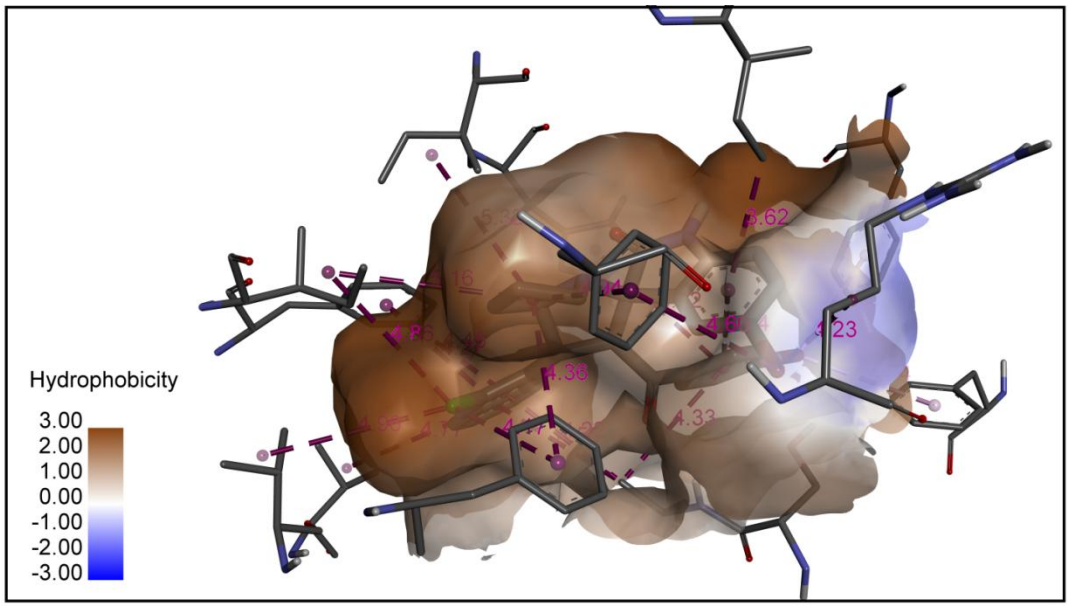

b)

Figure 2B.12. The best docking poses of the compound **4q**. a) The hydrogen bonding interactions, (b) The hydrophobic interactions.

2B.5. Conclusion

A series of novel quinolinyl spirooxindolopyrrolizidines **4a-u** were synthesized under conventional heating and characterized by various spectroscopic techniques. It was found that ultrasonication method was the prior method to synthesize the target compounds when compared with the conventional method in terms of yields and time. Further, all the target compounds screened for their *in vitro* anticancer and antioxidant activities. The compound **4q** exhibited excellent activity against the three tested cell lines i.e., IMR32, A549, MCF7. Whereas, the compounds **4h**, **4j**, **4o** and **4p** exhibited significant to moderate activity against these three cell lines. The comparative molecular docking studies showed that the IDO1 is the best target protein receptor than 4HJO and 2XP2. The compound **4q** showed the least binding energy (−11.32 kcal/mol) with IDO1. Molecular docking studies were well supported the *in vitro* anticancer activity (IC_{50} values). The compound **4p** and **4q** exhibited potent antioxidant activity.

2B.6. Spectral data

2'-Benzoyl-1'-(2-chloroquinolin-3-yl)-1',2',5',6',7',4a'-hexahydrospiro[indoline-3,3'-pyrrolizin]-2-one (4a)

Colour: White. M. P. 191-193 ℃. IR (KBr, cm^{-1}): 3441, 2840, 1728, 1672, 785. ^{1}H NMR (400 MHz, $CDCl_3$) δ: 8.44 (s, 1H), 7.99 (d, 1H, J = 8.4 Hz), 7.83 (d, 1H, J = 7.6 Hz), 7.69 (t, 1H, J = 7.2 Hz), 7.54 (t, 1H, J = 8.0 Hz), 7.42-7.32 (m, 5H), 7.22-7.12 (m, 3H), 7.055 (t, 1H, J = 7.6 Hz), 6.53 (d, 1H, J = 7.6 Hz), 5.18 (d, 1H, J = 11.6 Hz), 4.71(t, 1H, J = 10.8 Hz), 4.25-4.20 (m, 1H), 2.76-2,62 (m, 2H), 2.05-1.88 (m, 4H). ^{13}C NMR (100 MHz, DMSO-*d6*) δ: 196.72, 180.26, 146.54, 140.34, 136.83, 136.61, 132.99, 132.08, 130.30, 129.66, 128.19, 127.88, 127.40, 127.28, 127.17, 124.78, 122.73, 109.95, 73.26, 73.16, 64.72, 48.23, 30.97, 30.34, 27.22. Anal. Calcd. For $C_{30}H_{24}ClN_3O_2$: C, 72.94; H, 4.90; N, 8.51; found: C, 72.68; H, 4.98; N, 8.79.

2'-(4-Chlorobenzoyl)-1'-(2-chloroquinolin-3-yl)-1',2',5',6',7',4a'-hexahydrospiro[indoline-3,3'-pyrrolizin]-2-one (4b)

Colour: White. M. P. 180-182 ℃. IR (KBr, cm^{-1}): 3409, 2870, 1710, 1618, 752. ^{1}H NMR (400 MHz, DMSO-*d6*) δ: 10.25 (s, 1H), 8.92 (s, 1H), 8.07 (d, 1H, J = 7.6 Hz), 7.93 (d, 1H, J = 8.4 Hz), 7.78 (t, 1H, J = 8.0 Hz), 7.64 (t, 1H, J = 8.0 Hz), 7.40-7.35 (m, 4H), 7.21 (d, 1H, J = 7.6 Hz), 7.16 (t, 1H, J =7.6 Hz), 7.01 (d, 1H, J = 7.2 Hz), 6.55 (d, 1H, J = 7.6 Hz), 5.27 (d, 1H, J = 11.6 Hz), 4.52 (t, 1H, J = 10.4 Hz), 3.97-3.92 (m, 1H), 2.56-2.38 (m, 2H), 1.95-1.71 (m, 4H). ^{13}C NMR (100 MHz, DMSO-*d6*) δ: 196.80, 179.22, 151.43, 146.20, 142.44, 138.40, 137.71, 135.85, 132.07, 131.04, 130.41, 130.07, 129.99, 129.28, 128.67, 128.37, 127.86, 127.76, 126.98, 124.85, 121.84, 110.30, 73.01, 72.80, 64.10, 47.89, 47.71, 30.12, 27.43. ESI mass spectrum (*m/z*): 528.05(M+). Anal. Calcd. For $C_{30}H_{23}Cl_2N_3O_2$: C, 68.19; H, 4.39; N, 7.95; found: C, 67.92; H, 4.29; N, 7.69.

2'-(4-Bromobenzoyl)-1'-(2-chloroquinolin-3-yl)-1',2',5',6',7',4a'-hexahydrospiro[indoline-3,3'-pyrrolizin]-2-one (4c)

Colour: White. M. P. 180-182 ℃. IR (KBr, cm^{-1}): 3376, 2865, 1709, 1655, 770. ^{1}H NMR (400 MHz, DMSO-*d6*) δ: 10.27 (s, 1H), 8.92 (s, 1H), 8.06 (d, 1H, J = 8.0 Hz), 7.93 (d, 1H, J

= 8.0 Hz), 7.78 (t, 1H, *J* = 7.6 Hz), 7.65 (t, 1H, *J* = 7.6 Hz), 7.50 (d, 2H, *J* = 8.0 Hz), 7.31 (d, 2H, *J* = 8.4 Hz), 7.22-7.14 (m, 2H), 7.01 (d, 1H, *J* = 7.6 Hz), 6.56 (d, 1H, *J* = 7.6 Hz), 5.28 (d, 1H, *J* = 11.6 Hz), 4.52 (t, 1H, *J* = 10.4 Hz), 3.97-3.92 (m, 1H), 2.55-2.38 (m, 2H), 1.90-1.71 (m, 4H). ^{13}C NMR (100 MHz, DMSO-*d6*) *δ*: 196.99, 179.21, 151.42, 146.20, 142.43, 137.71, 136.15, 132.05, 131.61, 131.05, 130.08, 128.36, 127.85, 127.76, 127.64, 126.99, 124.83, 121.85, 110.31, 73.00, 72.80, 64.03, 47.88, 47.71, 30.12, 27.43. Anal. Calcd. For $C_{30}H_{23}ClBrN_3O_2$: C, 62.90; H, 4.05; N, 7.33; found: C, 62.66; H, 4.13; N, 7.06.

1'-(2-Chloroquinolin-3-yl)-2'-(4-methylbenzoyl)-1',2',5',6',7',4a'-hexahydrospiro[indoline-3,3'-pyrrolizin]-2-one (4d)

Colour: White. M. P. 234-236 °C. IR (KBr, cm^{-1}): 3436, 2843, 1727, 1675, 741. ^{1}H NMR (400 MHz, DMSO-*d6*) *δ*: 10.41 (s, 1H), 8.88 (s, 1H), 8.05 (d, 1H, *J* = 8.0 Hz), 7.90 (d, 1H, *J* = 8.4 Hz), 7.76 (t, 1H, *J* = 8.0 Hz), 7.62 (t, 1H, *J* = 7.2 Hz), 7.36 (d, 2H, *J* = 8.0 Hz), 7.23 (d, 2H, *J* = 7.6 Hz), 7.15-7.08 (m, 3H), 6.56 (t, 1H, *J* = 7.6 Hz), 5.30 (d, 1H, *J* = 11.6 Hz), 4.46 (t, 1H, *J* = 11.2 Hz), 3.99-3.94 (m, 1H), 2.55-2.39 (m, 2H), 2.25 (s, 3H), 1.92-1.71 (m, 4H). ^{13}C NMR (100 MHz, DMSO-*d6*) *δ*: 194.62, 177.23, 149.32, 144.07, 141.79, 140.33, 135.47, 132.50, 130.15, 128.89, 127.74, 127.07, 126.22, 125.72, 125.64, 125.04, 122.90, 119.56, 116.41, 108.07, 70.78, 61.38, 46.04, 45.60, 27.94, 25.26, 19.41. ESI mass spectrum (*m/z*): 502.20 (M+). Anal. Calcd. For $C_{31}H_{26}ClN_3O_2$: C, 73.29; H, 5.16; N, 8.27; found: C, 73.56; H, 5.20; N, 8.48.

1'-(2-Chloroquinolin-3-yl)-2'-(4-methoxybenzoyl)-1',2',5',6',7',4a'-hexahydrospiro[indoline-3,3'-pyrrolizin]-2-one (4e)

Colour: White. M. P. 220-222 °C. IR (KBr, cm^{-1}): 3441, 2853, 1728, 1674, 743. ^{1}H NMR (400 MHz, DMSO-*d6*) *δ*: 10.27 (s, 1H), 8.89 (s, 1H), 8.06 (d, 1H, *J* = 8.4 Hz), 7.91 (d, 1H, *J* = 8.4 Hz), 7.76 (t, 1H, *J* = 7.6 Hz), 7.62 (t, 1H, *J* = 7.2 Hz), 7.47 (d, 1H, *J* = 8.4 Hz), 7.23 (d, 1H, *J* = 7.2 Hz), 7.13 (d, 1H, *J* = 7.6 Hz), 6.99 (t, 1H, *J* = 7.2 Hz), 6.80 (d, 2H, *J* = 8.4 Hz), 6.56 (d, 2H, *J* = 7.6 Hz), 5.23 (d, 1H, *J* = 11.6 Hz), 4.56 (t, 1H, *J* = 10.8 Hz), 3.97-3.92 (m, 1H), 3.75 (s, 3H), 2.56-2.37 (m, 2H), 1.90-1.73 (m, 4H). ^{13}C NMR (100 MHz, DMSO-*d6*) *δ*: 195.23, 179.45, 163.51, 151.46, 146.17, 142.39, 137.59, 132.30, 131.03, 130.66, 129.94, 129.84, 128.35, 127.84, 127.75, 127.21, 125.06, 121.69, 113.88, 110.19, 73.06, 72.87, 63.20,

55.92, 48.20, 47.73, 30.11, 27.44. Anal. Calcd. For $C_{31}H_{26}ClN_3O_3$: C, 71.06; H, 5.00; N, 8.02; found: C, 71.25; H, 5.11; N, 8.25.

1'-(2-Chloroquinolin-3-yl)-2'-(furan-2-carbonyl)-1',2',5',6',7',4a'-hexahydrospiro[indoline-3,3'-pyrrolizin]-2-one (4f)

Colour: White. M. P. 224-226 ℃. IR (KBr, cm^{-1}): 3426, 2864, 1715, 1666, 747. ^{1}H NMR (400 MHz, DMSO-*d6*) δ: 10.49 (s, 1H), 8.82 (s, 1H), 8.05 (d, 1H, *J* = 8.0 Hz), 7.92 (d, 1H, *J* = 8.0 Hz), 7.78 (d, 2H, *J* = 10.8 Hz), 7.63 (t, 1H, *J* = 7.2 Hz), 7.23 (d, 2H, *J* = 6.4 Hz), 7.16 (d, 1H, *J* = 7.2 Hz), 6.98 (t, 1H, *J* = 7.2 Hz), 6.70 (d, 1H, *J* = 7.6 Hz), 6.56 (bs, 1H), 4.91 (d, 1H, *J* = 11.6 Hz), 4.56 (t, 1H, *J* = 10.2 Hz), 3.98-3.99 (m, 1H), 2.61-2.42 (m, 2H), 1.91-1.74 (m, 4H). ^{13}C NMR (100 MHz, DMSO-*d6*) δ: 183.58, 179.59, 151.85, 151.30, 148.91, 146.25, 142.47, 137.81, 132.04, 131.13, 129.97, 128.34, 127.85, 127.71, 127.39, 124.94, 121.78, 120.18, 112.92, 110.35, 73.28, 72.78, 63.65, 47.77, 47.68, 29.81, 27.20. Anal. Calcd. For $C_{28}H_{22}ClN_3O_3$: C, 69.49; H, 4.58; N, 8.68; found: C, 66.73; H, 4.51; N, 8.89.

1'-(2-Chloroquinolin-3-yl)-2'-(thiophene-2-carbonyl)-1',2',5',6',7',4a'-hexahydrospiro[indoline-3,3'-pyrrolizin]-2-one (4g)

Colour: White. M. P. 223-225 ℃. IR (KBr, cm^{-1}): 3449, 2965, 1714, 1653, 727. ^{1}H NMR (400 MHz, DMSO-*d6*) δ: 8.42 (s, 1H), 7.98 (t, 1H, *J* = 7.6 Hz), 7.88-7.78 (m, 1H), 7.71-7.62 (m, 2H), 7.56-7.50 (m, 2H), 7.39-7.44 (m, 2H), 7.18 (t, 1H, *J* = 7.6 Hz), 7.10 (d, 1H, *J* = 7.2 Hz), 6.92 (t, 1H, *J* = 8.0 Hz), 6.67 (d, 1H, *J* = 7.6 Hz), 5.02 (d, 1H, *J* = 11.6 Hz), 4.76 (t, 1H, *J* = 10.0 Hz), 4.25-4.20 (m, 1H), 2.80-2.65 (m, 2H), 2.05-1.89 (m, 4H). ^{13}C NMR (100 MHz, DMSO-*d6*) δ: 188.77, 179.60, 151.34, 146.25, 143.79, 142.32, 137.78, 136.38, 134.06, 131.91, 131.12, 129.96, 128.85, 128.34, 127.86, 127.82, 127.71, 127.38, 124.96, 121.89, 110.34, 73.50, 72.88, 64.24, 48.09, 47.77, 30.00, 27.38. Anal. Calcd. For $C_{28}H_{22}ClN_3O_2S$: C, 67.26; H, 4.44; N, 8.40; found: C, 67.05; H, 4.49; N, 8.68.

2'-Benzoyl-5-chloro-1'-(2-chloroquinolin-3-yl)-1',2',5',6',7',4a'-hexahydrospiro[indoline-3,3'-pyrrolizin]-2-one (4h)

Colour: White. M. P. 213-215 ℃. IR (KBr, cm^{-1}): 3417, 2843, 1710, 1674, 748. ^{1}H NMR (400 MHz, DMSO-*d6*) δ: 10.43 (s, 1H), 8.93 (s, 1H), 8.08 (d, 1H, *J* = 8.0 Hz), 7.94 (d, 1H, *J*

= 8.4 Hz), 7.78 (t, 1H, *J* = 7.6 Hz), 7.65 (t, 1H, *J* = 7.6 Hz), 7.52-7.46 (m, 3H), 7.32 (t, 2H, *J* = 7.6 Hz), 7.21 (t, 2H, *J* = 9.2 Hz), 6.56 (d, 1H, *J* = 8.4 Hz), 5.36 (d, 1H, *J* = 11.6 Hz), 4.49 (t, 1H, *J* = 11.2 Hz), 4.03-3.98 (m, 1H), 2.57-2.42 (m, 2H), 1.95-1.77 (m, 4H). ^{13}C NMR (100 MHz, DMSO-*d6*) *δ*: 197.49, 179.03, 151.25, 146.24, 141.49, 137.96, 136.92, 133.78, 131.80, 131.08, 129.96, 128.73, 128.37, 128.18, 127.86, 127.79, 127.74, 127.09, 126.83, 125.78, 111.70, 72.79, 72.70, 63.80, 48.23, 47.68, 29.97, 27.54. ESI mass spectrum (*m/z*): 528.20 (M+). Anal. Calcd. For $C_{30}H_{23}Cl_2N_3O_2$: C, 68.19; H, 4.39; N, 7.95; found: C, 68.46; H, 4.42; N, 7.70.

5-Chloro-2'-(4-chlorobenzoyl)-1'-(2-chloroquinolin-3-yl)-1',2',5',6',7',4a'-hexahydrospiro[indoline-3,3'-pyrrolizin]-2-one (4i)

Colour: White. M. P. 236-238 °C. IR (KBr, cm^{-1}): 3436, 2847, 1726, 1679, 755. ^{1}H NMR (400 MHz, DMSO-*d6*) *δ*: 10.42 (s, 1H), 8.93 (s, 1H), 8.06 (d, 1H, *J* = 8.0 Hz), 7.93 (d, 1H, *J* = 8.4 Hz), 7.78 (t, 1H, *J* = 8.0 Hz), 7.65 (t, 1H, *J* = 7.2 Hz), 7.46-7.38 (m, 4H), 7.2 (d, 1H, *J* = 10.4 Hz), 7.16 (s, 1H), 6.58 (d, 1H, J = 8.4 Hz), 5.33 (d, 1H, *J* = 11.6 Hz), 4.45 (t, 1H, *J* = 10.4 Hz), 4.00-3.95 (m, 1H), 2.55-2.41 (m, 2H), 1.96-1.77 (m, 4H). ^{13}C NMR (100 MHz, DMSO-*d6*) *δ*: 194.55, 176.74, 149.09, 144.13, 139.31, 136.59, 135.91, 133.52, 129.50, 128.97, 127.93, 127.41, 126.72, 126.23, 125.74, 125.67, 125.61, 124.84, 124.63, 123.75, 116.39, 109.67, 77.52, 70.70, 61.88, 45.93, 45.49, 27.96, 25.52. ESI mass spectrum (*m/z*): 562.15 (M-). Anal. Calcd. For $C_{30}H_{22}Cl_3N_3O_2$: C, 64.02; H, 3.94; N, 7.47; found: C, 64.22; H, 3.87; N, 7.18.

5-Chloro-2'-(4-bromobenzoyl)-1'-(2-chloroquinolin-3-yl)-1',2',5',6',7',4a'-hexahydrospiro[indoline-3,3'-pyrrolizin]-2-one (4j)

Colour: White. M. P. 236-238 °C. IR (KBr, cm^{-1}): 3435, 2845, 1726, 1679, 755. ^{1}H NMR (400 MHz, DMSO-*d6*) *δ*: 10.44 (s, 1H), 8.93 (s, 1H), 8.05 (d, 1H, *J* = 8.0 Hz), 7.92 (d, 1H, *J* = 8.4 Hz), 7.78 (t, 1H, *J* = 7.2 Hz), 7.64 (t, 1H, *J* = 7.2 Hz), 7.53 (d, 2H, *J* = 8.4 Hz), 7.36 (d, 2H, *J* = 8.4 Hz), 7.23 (d, 1H, *J* = 6.8 Hz), 7.16 (s, 1H), 6.57 (d, 1H, *J* = 8.4 Hz), 5.33 (d, 1H, *J* = 11.6 Hz), 4.40 (t, 1H, *J* = 10.4 Hz), 3.99-3.94 (m, 1H), 2.57-2.40 (m, 2H), 1.94-1.75 (m, 4H). ^{13}C NMR (100 MHz, DMSO-*d6*) *δ*: 196.87, 178.86, 151.20, 146.24, 141.42, 138.05, 135.94, 131.80, 131.60, 131.12, 130.13, 128.36, 127.97, 127.87, 127.73, 126.94, 126.74,

125.87, 111.81, 72.82, 63.93, 48.04, 47.63, 30.09, 27.66. Anal. Calcd. For $C_{30}H_{22}Cl_2BrN_3O_2$: C, 59.33; H, 3.65; N, 6.92; found: C, 59.60; H, 3.72; N, 6.67.

5-Chloro-1'-(2-chloroquinolin-3-yl)-2'-(4-methylbenzoyl)-1',2',5',6',7',4a'-hexahydrospiro[indoline-3,3'-pyrrolizin]-2-one (4k)

Colour: White. M. P. 248-250 ℃. IR (KBr, cm^{-1}): 3435, 2844, 1730, 1675, 755. ^{1}H NMR (400 MHz, DMSO-*d6*) δ: 10.42 (s, 1H), 8.90 (s, 1H), 8.07 (d, 1H, *J* = 8.0 Hz), 7.92 (d, 1H, *J* = 8.4 Hz), 7.77 (t, 1H, *J* = 8.0 Hz), 7.63 (t, 1H, *J* = 7.6 Hz), 7.40 (d, 2H, *J* = 8.0 Hz), 7.22-7.17 (m, 2H), 7.12 (d, 2H, *J* = 8.0 Hz), 6.57 (d, 1H, *J* = 8.4 Hz), 5.31 (d, 1H, *J* = 11.6 Hz), 4.48 (t, 1H, *J* = 11.2 Hz), 4.01-3.96 (m, 1H), 2.57-2.42 (m, 2H), 2.27 (s, 3H), 1.94-1.75 (m, 4H). ^{13}C NMR (100 MHz, DMSO-*d6*) δ: 176.88, 149.11, 144.11, 142.14, 139.33, 135.81, 132.32, 129.69, 128.97, 127.78, 127.23, 126.26, 125.73, 125.01, 124.81, 123.59, 116.40, 109.56, 70.80, 70.55, 61.28, 46.19, 45.52, 27.90, 25.46, 19.43. ESI mass spectrum (*m/z*): 542.20 (M+). Anal. Calcd. For $C_{31}H_{25}Cl_2N_3O_2$: C, 68.64; H, 4.65; N, 7.75; found: C, 68.40; H, 4.70; N, 7.97.

5-Chloro-1'-(2-chloroquinolin-3-yl)-2'-(4-methoxybenzoyl)-1',2',5',6',7',4a'-hexahydro[indoline-3,3'-pyrrolizin]-2-one (4l)

Colour: White. M. P. 242-244 ℃. IR (KBr, cm^{-1}): 3441, 2840, 1728, 1672, 785. ^{1}H NMR (400 MHz, DMSO-*d6*) δ: 10.45 (s, 1H), 8.91 (s, 1H), 8.06 (d, 1H, *J* = 8.0 Hz), 7.92 (d, 1H, *J* = 8.4 Hz), 7.78 (t, 1H, *J* = 7.2 Hz), 7.63 (t, 1H, *J* = 7.2 Hz), 7.52 (d, 2H, *J* = 8.8 Hz), 7.23-7.19 (m, 2H), 6.84 (d, 2H, *J* = 8.8 Hz), 6.60 (d, 1H, *J* = 8.4 Hz), 5.29 (d, 1H, *J* = 11.6 Hz), 4.48 (t, 1H, *J* = 10.8 Hz), 4.01-3.94 (m, 1H), 3.76 (s, 3H), 2.57-2.42 (m, 2H), 1.94-1.75 (m, 4H). ^{13}C NMR (100 MHz, DMSO-*d6*) δ: 195.12, 179.09, 163.72, 151.24, 146.22, 141.40, 137.93, 131.84, 131.10, 130.73, 129.88, 129.75, 128.35, 127.85, 127.73, 127.18, 126.98, 125.69, 114.04, 111.68, 73.09, 72.66, 63.08, 55.97, 48.37, 47.65, 30.10, 27.66. ESI mass spectrum (*m/z*): 558.20 (M-). Anal. Calcd. For $C_{31}H_{25}Cl_2N_3O_3$: C, 66.67; H, 4.51; N, 7.52; found: C, 66.47; H, 4.40; N, 7.25.

5-Chloro-1'-(2-chloroquinolin-3-yl)-2'-(furan-2-carbonylyl)-1',2',5',6',7',4a'-hexahydro[indoline-3,3'-pyrrolizin]-2-one (4m)

Colour: White. M. P. 237-239 ℃. IR (KBr, cm^{-1}): 3433, 2837, 1726, 1666, 769. ^{1}H NMR (400 MHz, DMSO-*d6*) *δ*: 10.66 (s, 1H), 8.40 (s, 1H), 8.05 (d, 1H, *J* = 8.0 Hz), 7.92 (d, 1H, *J* = 8.4 Hz), 7.78 (t, 2H, *J* = 7.6 Hz), 7.64 (t, 1H, *J* = 7.2 Hz), 7.29-7.20 (m, 3H), 6.73 (d, 1H, *J* = 8.0 Hz), 6.58 (bs, 1H), 4.94 (d, 1H, *J* = 11.6 Hz), 4.49 (t, 1H, *J* = 10.8 Hz), 4.03-3.98 (m, 1H), 2.63-2.44 (m, 1H), 2.27 (s, 1H), 1.94-1.79 (m, 4H). ^{13}C NMR (100 MHz, DMSO-*d6*) *δ*: 183.49, 179.21, 151.78, 151.10, 149.21, 146.29, 141.48, 138.12, 131.59, 131.20, 130.04, 128.34, 127.89, 127.68, 127.14, 127.02, 125.77, 120.45, 113.08, 111.83, 73.25, 72.58, 63.56, 47.82, 47.69, 29.79, 27.41. Anal. Calcd. For $C_{28}H_{21}Cl_2N_3O_3$: C, 64.87; H, 4.08; N, 8.11; found: C, 64.59; H, 4.17; N, 8.32.

5-Chloro-1'-(2-chloroquinolin-3-yl)-2'-(thiophene-2-carbonylyl)-1',2',5',6',7',4a'-hexahydro[indoline-3,3'-pyrrolizin]-2-one (4n)

Colour: White. M. P. 240-241 ℃. IR (KBr, cm^{-1}): 3431, 2836, 1725, 1650, 732. ^{1}H NMR (400 MHz, DMSO-*d6*) *δ*: 10.47 (s, 1H), 8.88 (s, 1H), 8.06 (d, 1H, *J* = 8.0 Hz), 7.76-7.85 (m, 3H), 7.63 (t, 1H, *J* = 7.2 Hz), 7.28 (d, 1H, *J* = 7.6 Hz), 7.18-7.12 (m, 2H), 7.02 (t, 1H, *J* = 7.2 Hz), 6.66 (d, 1H, *J* = 7.6 Hz), 5.13 (d, 1H, *J* = 11.6 Hz), 4.56 (t, 1H, *J* = 11.2 Hz), 4.04-3.92 (m, 1H), 2.58-2.43 (m, 2H), 1.92-1.77 (m, 4H). ^{13}C NMR (100 MHz, DMSO-*d6*) *δ*: 183.58, 179.59, 151.85, 151.30, 148.91, 146.25, 142.47, 137.81, 132.04, 131.13, 129.97, 128.34, 127.85, 127.71, 127.39, 124.94, 121.78, 120.18, 112.92, 110.35, 73.28, 72.78, 63.65, 47.77, 47.68, 29.81, 27.20. Anal. Calcd. For $C_{28}H_{21}Cl_2N_3O_2S$: C, 62.93; H, 3.96; N, 7.86; found: C, 62.71; H, 4.02; N, 8.11.

2'-Benzoyl-5-bromo-1'-(2-chloroquinolin-3-yl)-1',2',5',6',7',4a'-hexahydrospiro[indoline-3,3'-pyrrolizin]-2-one (4o)

Colour: White. M. P. 203-205 ℃. IR (KBr, cm^{-1}): 3437, 2886, 1726, 1679, 739. ^{1}H NMR (400 MHz, DMSO-*d6*) *δ*: 10.61 (s, 1H), 8.85 (s, 1H), 8.03-6.63 (m, 12H), 5.14 (bs, 1H), 4.52 (bs, 1H), 4.06 (bs, 1H), 2.92-1.93 (m, 6H). ^{13}C NMR (100 MHz, DMSO) δ: 197.51, 179.05, 151.27, 146.26, 141.51, 137.98, 136.94, 133.80, 131.82, 131.10, 129.98, 128.75, 128.39,

128.20, 127.88, 127.81, 127.77, 127.12, 126.85, 125.80, 111.72, 72.82, 72.72, 63.82, 48.26, 47.70, 30.00, 27.56. Anal. Calcd. For $C_{30}H_{23}BrClN_3O_2$: C, 62.90; H, 4.05; N, 7.33; found: C, 62.61; H, 4.11; N, 7.60.

5-Bromo-2'-(4-chlorobenzoyl)-1'-(2-chloroquinolin-3-yl)-1',2',5',6',7',4a'-hexahydrospiro[indoline-3,3'-pyrrolizin]-2-one (4p)

Colour: White. M. P. 217-219 °C. IR (KBr, cm^{-1}): 3417, 2840, 1707, 1676, 748. ^{1}H NMR (400 MHz, DMSO-*d6*) δ: 10.43 (s, 1H), 8.92 (s, 1H), 8.05 (d, 1H, *J* = 8.0 Hz), 7.93 (d, 1H, *J* = 8.4 Hz), 7.78 (t, 1H, *J* = 7.2 Hz), 7.65 (t, 1H, *J* = 7.2 Hz), 7.45-7.34 (m, 5H), 7.27 (s, 1H), 6.53 (d, 1H, *J* = 8.0 Hz), 5.32 (d, 1H, *J* = 11.2 Hz), 4.44 (t, 1H, *J* = 10.4 Hz), 3.98-3.96 (m, 1H), 2.43-1.79 (m, 6H). ^{13}C NMR (100 MHz, $CDCl_3$+DMSO-*d6*) δ: 195.77, 179.62, 151.24, 146.40, 141.28, 139.19, 137.09, 135.22, 132.45, 131.82, 130.43, 129.66, 129.40, 128.51, 127.93, 127.51, 127.30, 126.99, 114.14, 111.94, 73.05, 72.79, 64.38, 48.18, 47.96, 30.06, 27.17. Anal. Calcd. For $C_{30}H_{22}BrCl_2N_3O_2$: C, 59.33; H, 3.65; N, 6.92; found: C, 59.57; H, 3.75; N, 7.18.

5-Bromo-2'-(4-bromobenzoyl)-1'-(2-chloroquinolin-3-yl)-1',2',5',6',7',4a'-hexahydrospiro[indoline-3,3'-pyrrolizin]-2-one (4q)

Colour: White. M. P. 227-229 °C. IR (KBr, cm^{-1}): 3436, 2885, 1725, 1678, 770. ^{1}H NMR (400 MHz, DMSO-*d6*) δ: 10.42 (s, 1H), 8.92 (s, 1H), 8.08-7.30 (m, 10H), 6.50 (s, 1H), 5.33 (bs, 1H), 4.48 (bs, 1H), 4.00 (bs, 1H), 2.52-1.79 (m, 6H). ^{13}C NMR (100 MHz, $CDCl_3$+DMSO-*d6*) δ: 195.95, 179.61, 151.24, 146.41, 141.26, 137.06, 135.61, 132.46, 131.80, 131.48, 130.43, 129.67, 129.48, 128.05, 127.94, 127.48, 127.29, 126.97, 114.17, 111.95, 73.06, 72.80, 64.36, 48.19, 47.96, 30.07, 27.18. ESI mass spectrum (*m/z*): 651.30 (M-). Anal. Calcd. For $C_{30}H_{22}Br_2ClN_3O_2$: C, 55.28; H, 3.40; N, 6.45; found: C, 55.50; H, 3.33; N, 6.62.

5-Bromo-1'-(2-chloroquinolin-3-yl)-2'-(4-methylbenzoyl)-1',2',5',6',7',4a'-hexahydrospiro[indoline-3,3'-pyrrolizin]-2-one (4r)

Colour: White. M. P. 231-233 °C. IR (KBr, cm^{-1}): 3443, 2886, 1730, 1676, 716. ^{1}H NMR (400 MHz, DMSO-*d6*) δ: 10.43 (s, 1H), 8.90 (s, 1H), 8.07 (d, 1H, *J* = 8.0 Hz), 7.92 (d, 1H, *J*

= 8.4 Hz), 7.77 (t, 1H, *J* = 8.0 Hz), 7.63 (t, 1H, *J* = 7.6 Hz), 7.40 (d, 1H, *J* = 8.0 Hz), 7.22-7.17 (m, 2H), 7.12 (d, 2H, *J* = 8.0 Hz), 6.57 (d, 1H, *J* = 8.4 Hz), 5.31 (d, 1H, *J* = 11.6 Hz), 4.48 (t, 1H, *J* = 11.2 Hz), 4.01-3.96 (m, 1H), 2.55-2.42 (m, 3H), 2.27 (s, 3H), 1.92-1.77 (m, 4H). Anal. Calcd. For $C_{31}H_{25}BrClN_3O_2$: C, 63.44; H, 4.29; N, 7.16; found: C, 68.22; H, 4.25; N, 7.37.

5-Bromo-1'-(2-chloroquinolin-3-yl)-2'-(4-methoxybenzoyl)-1',2',5',6',7',4a'-hexahydro[indoline-3,3'-pyrrolizin]-2-one (4s)

Colour: White. M. P. 237-239 ℃. IR (KBr, cm^{-1}): 3440, 2885, 1730, 1672, 758. ^{1}H NMR (400 MHz, DMSO-*d6*) *δ*: 10.44 (s, 1H), 8.90 (s, 1H), 8.06 (d, 1H, *J* = 8.0 Hz), 7.92 (d, 1H, *J* = 8.4 Hz), 7.78 (t, 1H, *J* = 7.2 Hz), 7.63 (t, 1H, *J* = 7.2 Hz), 7.52 (d, 2H, *J* = 8.8 Hz), 7.23-7.19 (m, 2H), 6.84 (d, 2H, *J* = 8.8 Hz), 6.60 (d, 1H, *J* = 8.4 Hz), 5.29 (d, 1H, *J* = 11.6 Hz), 4.48 (t, 1H, *J* = 10.8 Hz), 4.01-3.94 (m, 1H), 3.76 (s, 3H), 2.57-2.42 (m, 2H), 1.94-1.78 (m, 4H). Anal. Calcd. For $C_{31}H_{25}BrClN_3O_3$: C, 61.76; H, 4.18; N, 6.97; found: C, 61.99; H, 4.12; N, 6.79.

5-Bromo-1'-(2-chloroquinolin-3-yl)-2'-(furan-2-carbonylyl)-1',2',5',6',7',4a'-hexahydro[indoline-3,3'-pyrrolizin]-2-one (4t)

Colour: White. M. P. 234-236 ℃. IR (KBr, cm^{-1}): 3432, 2833, 1726, 1666, 768. ^{1}H NMR (400 MHz, DMSO-*d6*) *δ*: 10.27 (s, 1H), 8.55 (s, 1H), 7.97-7.22 (m, 9H), 6.47 (d, 1H, *J* = 6.4 Hz), 5.17 (d, 1H, *J* = 10.0 Hz), 4.60 (t, 1H, *J* = 9.2 Hz), 4.20 (bs, 1H), 2.73-1.89 (m, 6H). ^{13}C NMR (100 MHz, $CDCL_3$+DMSO-*d6*) *δ*: 196.92, 179.69, 146.37, 141.41, 137.11, 136.82, 133.13, 132.30, 132.04, 130.41, 129.69, 128.73, 128.29, 128.08, 127.85, 127.56, 127.30, 127.16, 113.96, 111.82, 72.96, 72.77, 64.29, 48.26, 47.99, 29.94, 27.08. ESI mass spectrum (*m/z*): 562.15 (M-). Anal. Calcd. For $C_{28}H_{21}BrClN_3O_3$: C, 59.75; H, 3.76; N, 7.47; found: C, 59.51; H, 3.83; N, 7.70.

5-Bromo-1'-(2-chloroquinolin-3-yl)-2'-(thiophene-2-carbonylyl)-1',2',5',6',7',4a'-hexahydro[indoline-3,3'-pyrrolizin]-2-one (4u)

Colour: White. M. P. 241-242 ℃. IR (KBr, cm^{-1}): 3431, 2830, 1725, 1651, 738. ^{1}H NMR (400 MHz, DMSO-*d6*) *δ*: 10.66 (s, 1H), 8.84 (s, 1H), 8.05-7.31 (m, 8H), 6.64 (d, 2H, *J* = 4.4

Hz), 4.95 (bs, 1H), 4.49 (bs, 1H), 4.02 (bs, 1H), 2.89-1.83 (m, 6H). ^{13}C NMR (100 MHz, $CDCl_3$+DMSO-*d6*) δ: 188.29, 179.81, 151.24, 143.96, 137.17, 135.30, 132.67, 132.36, 131.77, 130.45, 130.00, 128.17, 127.92, 127.54, 127.30, 114.16, 111.91, 73.62, 72.80, 64.83, 48.19, 48.00, 29.89, 27.06. Anal. Calcd. For $C_{28}H_{21}BrClN_3O_2S$: C, 58.09; H, 3.66; N, 7.26; found: C, 58.37; H, 3.70; N, 7.01.

2B.7. Crystallographic data of compound 4d

CCDC 1852467 contains the supplementary crystallographic data (.cif) of the compounds **4d** respectively. These data can be obtained free of charge from The Cambridge Crystallographic Data Centre *via* www.ccdc.cam.ac.uk/structures.

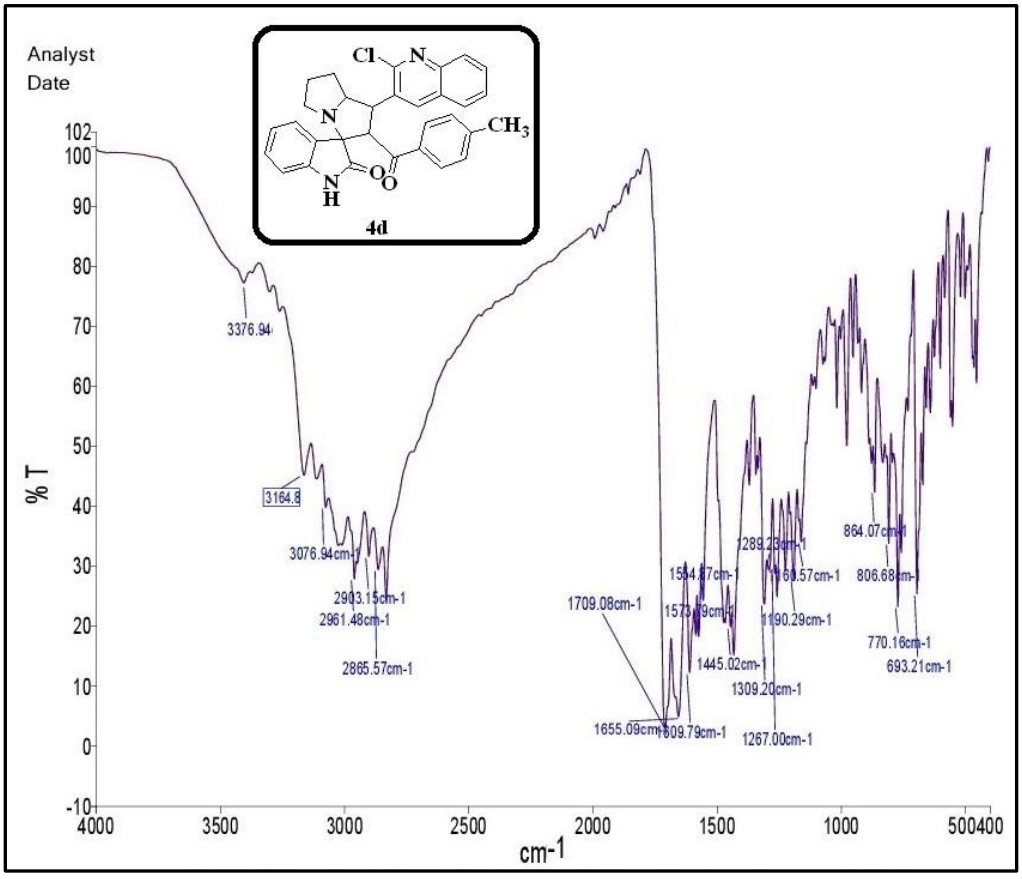

IR spectrum of the compound **4d**

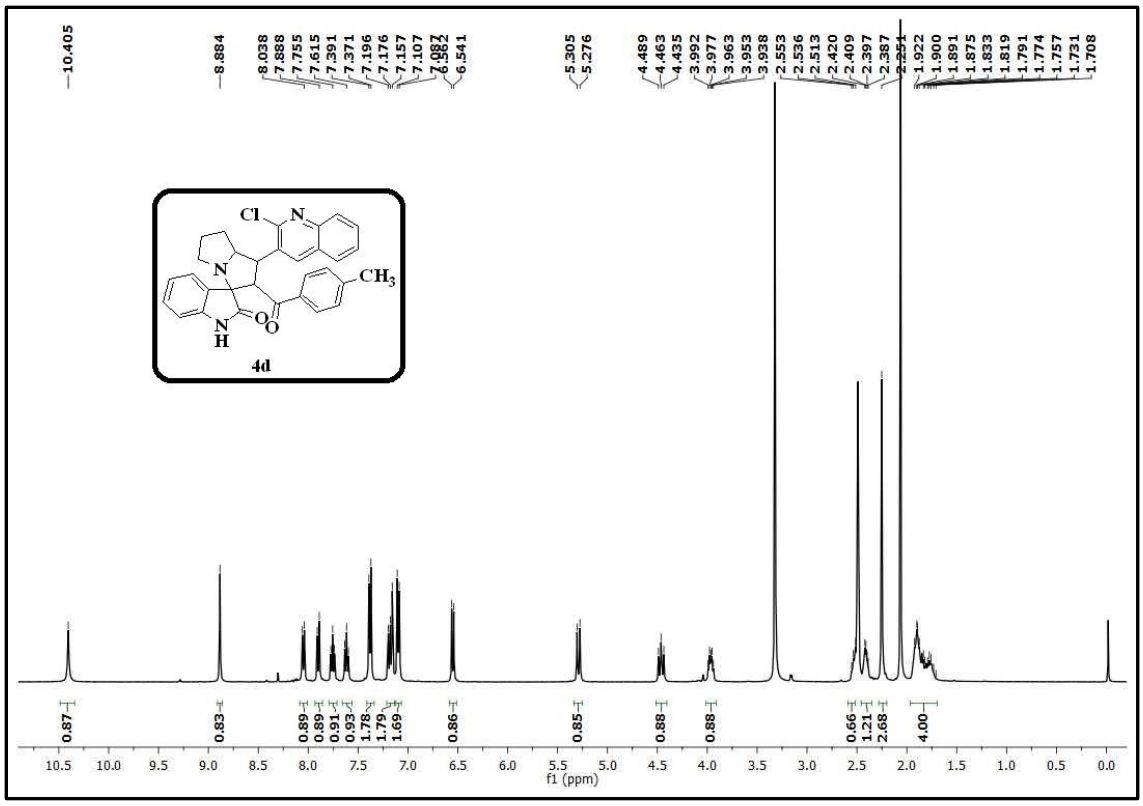

^{1}H NMR spectrum of the compound **4d**

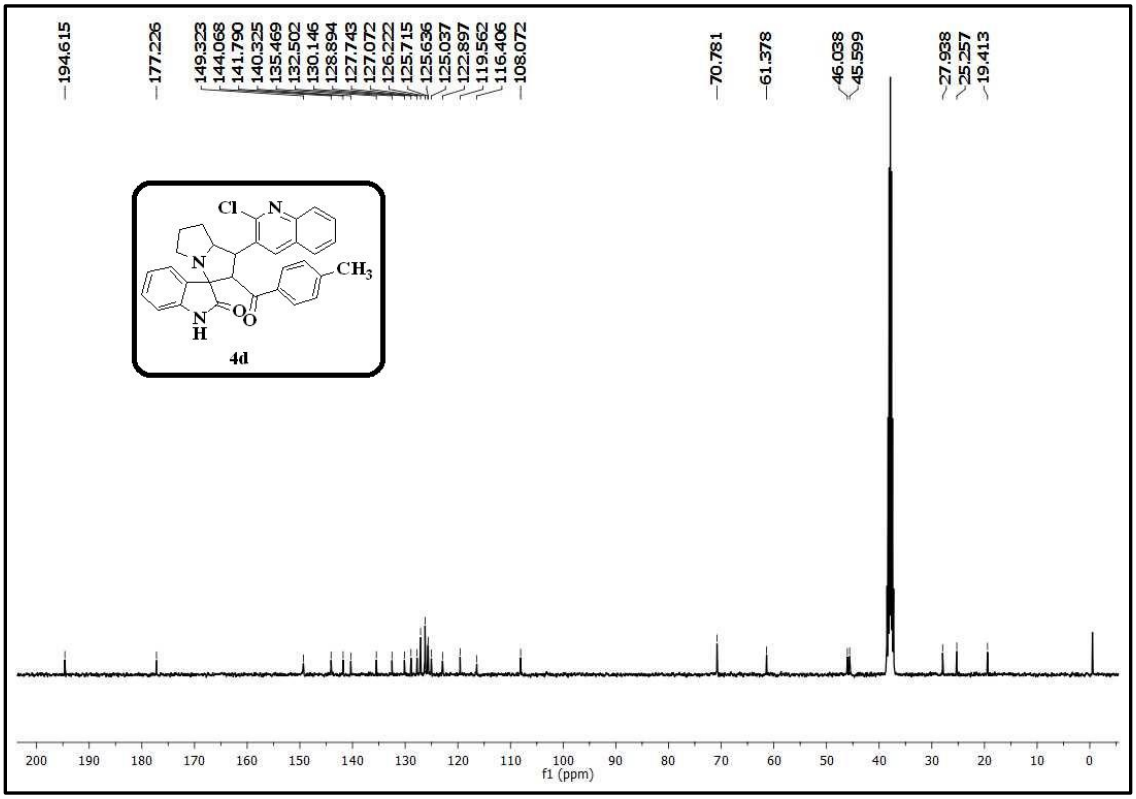

^{13}C NMR spectrum of the compound **4d**

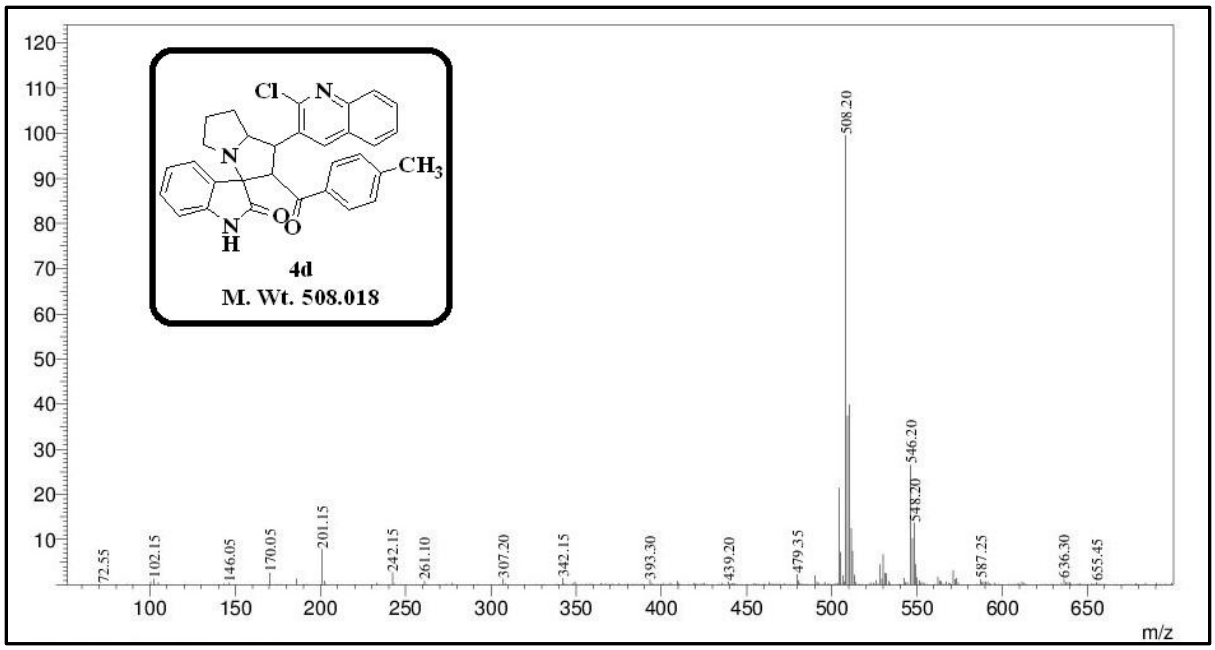

Mass spectrum of the compound **4d**

Experimental Section

Materials and methods

All the melting points were recorded by using Stuart SMP30 melting point apparatus and were uncorrected. IR spectra were recorded on Perkin-Elmer 100S series FT-IR instrument. ^{1}H NMR and ^{13}C NMR spectra were recorded in DMSO-*d*6 and $CDCl_3$ using TMS as an internal standard on a Bruker Avance III HD 400 MHz instrument and the chemical shift values were reported in ppm. Mass spectra were recorded on Joel JMSD-300 spectrometer. The progress and purity of the reactions were monitored by Thin-Layer chromatography (E. Merck, Mumbai, India) and the developed chromatogram was visualized under UV light and iodine vapors. Unless otherwise stated, all the chemicals and solvents used were of high grade and purchased from Sigma-Aldrich and spectrochem. Elemental analysis was performed on an Elementar Vario EL III analytical unit and the values were ± 0.4% of theoretical values. The dipolarophiles **3a-g** were prepared by the literature procedure [78].

Crystal structure determination of compounds

The single crystal X-ray data of the compounds were collected on a Bruker Kappa APEX-II CCD X-Ray diffractometer at 296(2)K using graphite-monochromated Mo K_α radiation (λ = 0.71073 Å). No absorption correction was carried out. The unit cell dimensions are determined by least-squares analysis and the reflection data is integrated using the SHELXTL program [84]. The crystal structures are solved by direct methods using SHELXS-97, and refinement is carried out by full-matrix least-squares technique (F^2) using SHELXL-97 [85]. Anisotropic displacement parameters are included for other than H-atoms. All the aromatic and aliphatic C−H hydrogens are positioned geometrically and treated as riding on their parent C-atoms with C−H distances of 0.93-0.97 Å. The software Mercury 2.3 (Build RC4), ORTEP-3 and X-Seed are used to prepare material for publication [86-89].

Biological assay

MTT assay

The *in vitro* anticancer activity of the synthesized compounds were determined against four different human cancer cell lines i.e., neuro blastoma cell line (IMR32), alveolar carcinoma (A549) breast cancer cell line (MCF7) and human embryonic kidney 293 cell line (HEK293T). The c*is*-platin was used as a standard drug. The cell viability in the presence of the tested samples was measured by MTT-micro cultured tetrazolium assay [90, 91]. This assay is a quantitative colorimetric method for the determination of cell viability. The assessed parameter is the metabolic activity of viable cells. Metabolically active cells reduce pale yellow tetrazolium salt (MTT) to a dark blue water-insoluble formazan, which can be directly quantified after solubilization in DMSO. The absorbance of the formazan directly correlates with the number of viable cells. IMR32, A-549, MCF7 and HEK293T cells were plated into a 96-well plate at a density 1 x 10^4 cells/well. The cells were grown overnight in the full medium and then switched to the low serum media. 1% DMSO was used as a control. After 48 h of treatment with different concentrations of test compounds, the cells were incubated with MTT (2.5 mg/mL) in the CO_2 chamber for 2h. The medium was then removed and 100 mL of DMSO was added to each well to dissolve formazan crystals. After thorough mixing, the plates were read at 570 nm for optical density, which is directly

correlated with cell quantity. The results were represented as a percentage of viability. All the experiments were carried out in triplicates. The relationship between surviving fraction and drug concentration was plotted to obtain the survival curves of IMR32, A-549, MCF7 and HEK293T. The IC_{50} values were calculated using linear regression analysis from the graph pad prism (5.02 version) (P values are significant <0.001). Data as mean ± standard deviation (S.D.) n = 4. Statistical analysis was performed using one-way ANOVA followed by Dunnett test. *$p<0.05$, $^{\#}p<0.001$, $^{\$}p<0.01$ versus Standard.The response parameter calculated was IC_{50} value, which corresponds to the concentration required for 50% inhibition of cell viability.

Antioxidant activity

The free radical scavenging capacity of the synthesized compounds was determined by using DPPH (1,1-Diphenyl-2-picrylhydrazyl) free radical method described in the literature [92-94]. Ascorbic acid was used as a standard to measure the efficiencies of the synthesized compounds. 0.2 mM solution of DPPH was prepared in 100% methanol. The required amount of ascorbic acid was dissolved in 100% methanol to prepare 1 mM solution and the test compounds were dissolved in 0.2% DMSO and methanol to prepare 1 mM stock solutions. From the stock solutions, different concentrations (3, 10, 30 and 100 µM) of solutions were prepared on diluting with methanol. 1 mL of each compound solution was added to the 3 mL of DPPH solution. After 30min, the absorbance of the solutions at 517 nm (A_1) was recorded using UV–Visible spectrophotometer. As a control, the absorbance of the blank solution of DPPH without test compound was also determined at 517 nm (A_0). The following equation was used for the calculation of the percentage (%) of scavenging activity.

Scavenging Activity (%) = $\frac{A_0 - A_1}{A_0} \times 100$

Where A_0 is the absorbance of the DPPH in the absence of antioxidant and A_1 is the absorbance of the DPPH in the presence of an antioxidant. IC_{50} values were also calculated for the compounds.

Molecular Docking protocol

In silico docking studies are useful tools to assess the binding affinity of the ligand-protein receptor. The synthesized compounds were subjected to molecular docking by using

the AutoDock Tools (ADT) version 1.5.6 and AutoDock version 4.2.5.1 docking program [95]. The 3D-structures of all the synthesized compounds were prepared by using chem3D pro 12.0 software. The optimized 3D structures were saved in .pdb format. The structure of the Anaplastic Lymphoma Kinase protein (PDB ID: 1XP2) was extracted from the protein data bank (http://www.rcsb.org/pdb), having resolution 1.90 Å. The bound ligand and water molecules in protein were removed by using Discovery Studio Visualizer version 4.0 to prepare the protein. Nonpolar hydrogens were merged and gasteiger charges were added to the protein. The grid file was saved in .gpf format. The three dimensional grid box having dimensions 60 x 60 x 60 $Å^3$ was created around the protein with spacing 0.3750 Å. The genetic algorithm was carried out with the population size and the maximum number of evaluations were 150 and 25,00,000, respectively. The docking output file was saved as Lamarckian Ga (4.2) in .dpf format. The ligand-protein complex binding sites were visualized by Discovery Studio Visualizer version 4.0.

References

1) B. Yu, D. Q. Yu, H. M. Liu, *Eur. J. Med. Chem.* **2015**, *97*, 673.
2) V. V. Kouznetsov, F. A. R. Ruíza, L. Y. V. Méndeza, M. P. Gupta, *Lett. Drug. Des. Discov.* **2012**, *9*, 680.
3) R. Guda, S. Narsimha, R. Babu, S. Muthadi, H. Lingabathula, R. Palabindela, N. R. Yellu, G. Kumar, M. Kasula, *Bioorg. Med. Chem. Lett*. **2016**, *26*, 5517.
4) P. R. Mali, P. K. Shirsat, N. B. Khomane, V. L. Nayak, J. B. Nanubolu, H. M. Meshram, *ACS comb. Sci.* **2017**, *19*, 633.
5) T. S. Latha, M. C. Reddy, S. V. Muthukonda, V. S. S. S. Srikanth, D. Lomada, *Mater. Sci. Eng. C.* **2017**, *78*, 969.
6) R. Guda, R. Korra, S. Balaji, R. Palabindela, R. Eerla, H. Lingabathula, N. R. Yellu, G. Kumar, M. Kasula, *Bioorg. Med. Chem. Lett*. **2017**, *27*, 4741.
7) M. M. Ghora, F. A. Raga, H. I. Heiba, W. M. Ghora, *J. Heterocyclic Chem.* **2011**, *48*, 1269.
8) S. Jain, V. Chandra, P. K. Jain, K. Pathak, D. Pathak, A. Vaidya, *Arab. J. Chem.* **2016**, doi: 10.1016/j.arabjc.2016.10.009.

9) O. Afzal, S. Kumar, Md. R. Haider, Md. R. Ali, R. Kumar, M. Jaggi, S. Bawa, *Eur. J. Med. Chem*. **2015**, *97*, 871.

10) A. I. Almansour, S. Ali, M. A. Ali, *Bioorg. Med. Chem. Lett.* **2012**, *22*, 7418.

11) Z. Y. Xue, X. Fang, C. J. Wang, *Org. Biomol. Chem.* **2011**, *9*, 3622.

12) S. U. Maheswari, S. Perumal, A. I. Almansour, *Tetrahedron Lett.* **2012**, *53*, 349.

13) R. R. Kumar, S. Perumal, P. Senthilkumar, P. Yogeeswari, D. Sriram, *Eur. J. Med. Chem.* **2009**, *44*, 3821.

14) (a) C. Marti, E. M. Carreira, *Eur. J. Org. Chem.* **2003**, *12*, 2209; (b) M. A. A. Gharbia, P. H. Doukas, *Heterocycle.* **1979**, *12*, 637; (c) M. J. Kornet, A. P. Thio, *J. Med. Chem.* **1976**, *19*, 892.

15) (a) P. Rosenmond, M. H. Mrerscht, C. Bub, *Eur. J. Org. Chem. Liebigs. Ann. Chem.* **1994**, *2*, 151; (b) C. H. Chou, C. L. Gong, C. C. Chao, *J. Nat. Prod.* **2009**, *72*, 830; (c) T. H. Kang, K. Matsumoto, Y. Murakami, *Eur. J. Pharmacol.* **2002**, *444*, 39; (d) C. B. Cui, H. Kakeya, G. Okada, R. Onose, H. J. Osada, *Antibiot.* **1996**, *49*, 527.

16) (a) X. M. Zhang, H. Guo, Z. S. Li, F. H.Song, W.M. Wang, H. Q. Dai, L. X. Zhang, J. G. Wang, *Eur. J. Org. Chem.* **2015**, *101*, 419; (b) S. B. Falconer, Y. A. S. Reid, A. M. King, *ACS Infect. Dis.* **2015**, *1*, 533.

17) A. C. Wei, Md. A. Ali, Y. K. Yoon, R. Ismail, T. S. Choon, R. S. Kumar, N. Arumugam, A. I. Almansour, H. Osman, *Bioorg. Med. Chem. Lett*. **2012**, *22*, 4930.

18) G. Bhaskar, Y. Arun, C. Balachandran, C. Saikumar, P. T. Perumal, *Eur. J. Med. Chem*. **2012**, *51*, 79.

19) S. Kathiravan, R. Raghunathan, G. Suresh, G. V. Siva, *Med. Chem. Res*. **2012**, *21*, 3170.

20) A. S. Filatov, N. A. Knyazev, M. N. Ryazantsev, V. V. Suslonov, A. G. Larina, A. P. Molchanov, R. R. Kostikov, V. M. Boitsov, A. V. Stepakov, *Org. Chem. Front.* **2018**, *5*, 595.

21) A. Dandia, A. K. Jain, S. Sharma, *Tetrahedron Lett*. **2012**, *53*, 5859.

22) F. M. Moghaddam, M. R. Khodabakhshi, Z. Ghahremannejad, B. K. Foroushani, S. W. Ng, *Tetrahedron Lett*. **2013**, *54*, 2520.

23) S. M. Rajesh, D. D. Bala, S. Perumal, *Tetrahedron Lett*. **2012**, *53*, 5367.

24) A. R. S. Babu, R. Raghunathan, *Tetrahedron Lett.* **2006**, *47*, 9221.

25) W. Han, H. Y. Qiu, C. Hu, W. X. Sun, R. W. Yang, J. L. Qi, X. M. Wang, G. H. Lu, Y. H. Yang, *Bioorg. Med. Chem. Lett*. **2016**, *26*, 3237.

26) Y. Arun, K. Saranraj, C. Balachandran, P. T. Perumal, *Eur. J. Med. Chem.* **2014**, *74*, 50.

27) A. Dömling, W. Wang, K. Wang, *Chem. Rev.* **2012**, *112*, 3083.

28) A. Hazra, Y. P. Bharitkar, D. Chakraborty, S. K. Mondal, N. Singal, S. Mondal, A. Maity, R. Paira, S. Banerjee, N. B. Mondal, *ACS Comb. Sci.* **2013**, *15*, 41.

29) W. A. Denn, Anticancer drug development, the contribution of synthetic organic chemistry to anticancer drug development. Chapter 1, **2002**, 187.

30) J. A. Xiao, H. G. Zhang, S. Liang, J. W. Ren, H. Yang, X. Q. Chen, *J. Org. Chem*. **2013**, *78*, 11577.

31) A. Kumar, G. Gupta, S. Srivastava, A. K. Bishnoi, R. Saxena, R. Kant, R. S. Khanna, P. R. Maulik, A. Dwivedi, *RSC Adv*. **2013**, *3*, 4731.

32) C. S. Wang, R. Y. Zhu, J. Zheng, F. Shi, S. J. Tu, *J. Org. Chem.* **2015**, *80*, 512.

33) J. Jayashankaran, R. Durga, R. S. Manian, R. Raghunathan, *Tetrahedron Lett*. **2004**, *45*, 7303.

34) S. Q. Ge, Y. Y. Hua, M. Xia, *Ultrason. Sonochem*. **2009**, *16*, 232.

35) S. Haddad, S. Boudriga, F. Porzio, A. Soldera, M. Askri, M. Knorr, Y. Rousselin, M. M. Kubicki, C. Golz, C. Strohmann, *J. Org. Chem.* **2015**, *80*, 9064.

36) A. Thangamani, *Eur. J. Med. Chem*. **2010**, *45*, 6120.

37) Entrez Gene: INDO indoleamine-pyrrole 2,3 dioxygenase.

38) H. Sugimoto, S. Oda, T. Otsuki, T. Hino, T. Yoshida, Y. Shiro, *Proc. Natl. Acad. Sci*. Usa. **2006**, *103*, 2611.

39) J. J. Cui, M. T. Dube, H. Shen, M. Nambu, P. P. Kung, M. Pairish, L. Jia, J. Meng, L. Funk, I. Botrous, M. McTigue, N. Grodsky, K. Ryan, E. Padrique, G. Alton, S. Timofeevski, S. Yamazaki, Q. Li, H. Zou, J. Christensen, B. Mroczkowski, S. Bender, R. S. Kania, M. P. Edwards, *J. Med. Chem*. **2011**, *54*, 6342.

40) R. S. Herbst, *Int. J. Rad. Onco. Biol. Phys.* **2004**, *59*, 21.

41) J. Sebastian, R. G. Richards, M. P. Walker, J. F. Wiesen, Z. Werb, R. Derynck, Y. K. Hom, G. R. Cunha, R. P. DiAugustine, *Cell Growth Differ*. **1998**, *9*, 777.

42) J. McBryan, J. Howlin, S. Napoletano, F. Martin, *J. Mam. Gland. Biol. Neopl.* **2008**, *13*, 159.

43) M. D. Sternlicht, S. W. S. borg, *J. Mam. Gland. Biol. Neopl*. **2008**, *13*, 181.

44) V. Kumar, A. Abbas, J. Aster, Robbins basic pathology, Elsevier/Saunders, Philadelphia, **2013**. pp. 179-185. ISBN 9781437717815.0.

45) T. J. Lynch, D. W. Bell, R. Sordella, S. Gurubhagavatula, R. A. Okimoto, B. W. Brannigan, P. L. Harris , S. M. Haserlat, J. G. Supko, F. G. Haluska, D. N. Louis, D. C. Christiani, J. Settleman, D. A. Haber, *N. Engl. J. Med*. **2004**, *350*, 2129.

46) F. Walker, L. Abramowitz, D. Benabderrahmane, X. Duval, V. Descatoire, D. Hénin, T. Lehy, T. Aparicio, *Hum. Pathol*. **2009**, *40*, 1517.

47) A. M. Davis, *Angew. Chem. Int. Ed*. **1999**, *38*, 736.

48) M. Fathimunnisa, H. Manikandan, K. Neelakandan, N. R. Prasad, S. Selvanayagam, B. Sridhar, *J. Mol. Struc*. **2016**, *1122*, 205.

49) F. A. Kang, Z. Sui, *Tetrahedron Lett*. **2011**, *52*, 4204.

50) N. Sudhapriya, P. T. Perumal, C. Balachandran, S. Ignacimuthu, M. Sangeetha, M. Doble, *Eur. J. Med. Chem*. **2014**, *83*, 190.

51) B. Yu, Z. Yu, P. P. Qi, D. Q. Yu, H. M. Liu, *Eur. J. Med. Chem*. **2015**, *95*, 35.

52) B. Yu, X. N. Sun, X. J. Shi, P. P. Qi, Y. C. Zheng, D. Q. Yu, H. M. Liu, *Steroids*. **2015**, *102,* 92.

53) B. Yu, D.Q. Yu, H. M. Liu, *Eur. J. Med. Chem*. **2015**, *97*, 673.

54) P. R. Mali, P. K. Shirsat, N. B. Khomane, V. L. Nayak, J. B. Nanubolu, H. M. Meshram, *ACS Comb. Sci.* **2017**, *19*, 633.

55) Y. Arun, K. Saranraj, C. Balachandran, P. T. Perumal, *Eur. J. Med. Chem*. **2014**, *74*, 50.

56) A. Hazra, Y. P. Bharitkar, D. Chakraborty, S. K. Mondal, N. Singal, S. Mondal, A. Maity, R. Paira, S. Banerjee, N. B. Mondal, *ACS Comb. Sci.* **2013**, *15*, 41.

57) A. Dömling, W. Wang, K. Wang, *Chem. Rev.* **2012**, *112*, 3083.

58) B. H. Rotstein, S. Zaretsky, V. Rai, A. K. Yudin, *Chem. Rev.* **2014**, *114*, 8323.

59) A. Dömling, *Chem. Rev*. **2006**, *106*, 17.

60) W. Chen, X. Peng, L. Zhong, Y. Li, R. Sun, *ACS Sustainable Chem. Eng*. **2015**, *3*, 1366.

61) C. Liu, M. Shen, B. Lai, A. Taheri, Y. Gu, *ACS Comb. Sci.* **2014**, *16*, 652.

62) A. N. Muller, I. R. Correa, J. H. Prinz, C. Rosenbaum, K. Saxena, H. J. Schwalbe, D. Vestweber, G. Cagna, S. Schunk, O. Schwarz, H. Schiewe, H. Waldmann, *Proc. Natl. Acad. Sci*. **2006**, *103*, 10607.

63) a) J. Andraos, *ACS Sustainable Chem. Eng*. **2013**, *1*, 496; (b) J. Andraos, *Org. Process Res. Dev*. **2005**, *9*, 404; (c) P. Slobbe, E. Ruijter, R. V. A. Orru, *Med. Chem. Commun*. **2012**, *3*, 1189; (d) S. Periyaraja, P. Shanmugam, A. B. Mandal, T. S. Kumar, P. Ramamurthy, *Tetrahedron.* **2013**, *69*, 2891; (e) V. Sridharan, K. Karthikeyan, Muthusubramanian, *Tetrahedron Lett*. **2006**, *47*, 4221; (f) S. L. Zhu, S. J. Ji, X. M. Su, C. Sun, Y. Liu, *Tetrahedron Lett*. **2008**, *49*, 1777; (g) U. Kusebauch, B. Beck, K. Messer, E. Herdtweck, A. Dömling, *Org. Lett*. **2003**, *5*, 4021.

64) (a) I. V. Magedov, A. Kornienko, *Chem. Heterocycl. Compd*. **2012**, *48*, 33; (b) R. C. Cioc, E. Ruijter, R. V. A. Orru, *Green Chem*. **2014**, *16*, 2958; (c) C. Kalinski, M. Umkehrer, L. Weber, J. Kolb, C. Burdack, G. Ross, *Mol. Diversity*, **2010**, *14*, 513; (d) I. A. Zanze, *Curr. Opin. Chem. Biol*. **2008**, *12*, 324; (e) W. H. Moos, C. R. Hurt, G. A. Morales, *Mol. Diversity*. **2009**, *13*, 241; (f) B. B. Touré, D. G. Hall, *Chem. Rev*. **2009**, *109*, 4439; (g) C. Lamberth, A. Jeanguenat, F. Cederbaum, A. D. Mesmaeker, M. Zeller, H. J. Kempf, R. Zeun, *Bioorg. Med. Chem*. **2008**, *16*, 1531; (h) R. Kakuchi, *Angew. Chem. Int. Ed*. **2014**, *53*, 46.

65) (a) J. A. Xiao, H. G. Zhang, S. Liang, J. W. Ren, H. Yang, X. Q. Chen, *J. Org. Chem*. **2013**, *78*, 11577; (b) A. Kumar, G. Gupta, S. Srivastava, A. K. Bishnoi, R. Saxena, R. Kant, R. S. Khanna, P. R. Maulik, A. Dwivedi, *RSC Adv*. **2013**, *3*, 4731;

66) (a) C. S. Wang, R. Y. Zhu, J. Zheng, F. Shi, S. J. Tu, *J. Org. Chem.* **2015**, *80*, 512; (b) J. Jayashankaran, R. Durga, R. S. Manian, R. Raghunathan, *Tetrahedron Lett*. **2004**, *45*, 7303; (c) S. Q. Ge, Y. Y. Hua, M. Xia, *Ultrason Sonochem*. **2009**, *16*, 232.

67) (a) S. Haddad, S. Boudriga, F. Porzio, A. Soldera, M. Askri, M. Knorr, Y. Rousselin, M. M. Kubicki, C. Golz, C. Strohmann, *J. Org. Chem.* **2015**, *80*, 9064; (b) A. Thangamani, *Eur. J. Med. Chem*. **2010**, *45*, 6120; (c) V. B. Nishtala, J. B. Nanubolu, S. Basavoju, *Res. Chem. Intermed*. **2016**, *43*, 1365.

68) G. Lotfy, M. M. Said, E. S. H. E. Ashry, E. S. H. E. Tamany, A. A. Dhfyan, Y. M. A. Aziz, A. Barakat, *Bioorg. Med. Chem*. **2017**, *25*, 1514.

69) K. Parthasarathy, C. Praveen, J. C. Jeyaveeran, A. A. M. Prince, *Bioorg. Med. Chem. Lett*. **2016**, *26*, 4310.

70) S. Tiwari, P. Pathak, R. Sagar, *Bioorg. Med. Chem. Lett*. **2016**, *26*, 2513.

71) M. Zhang, W. Yang, M. Qian, T. Zhao, L. Yang, C. Zhu, *Tetrahedron*, **2018**, *74*, 955.

72) H. J. Roh, S. Y. Kim, B. K. Min, J. N. Kim, *Tetrahedron Lett*. **2017**, *58*, 21.

73) Y. R. Liang, X. Y. Chen, Q. Wu, X. F. Lin, *Tetrahedron.* **2015**, *71*, 616.

74) W. Zhang, J. Xu, J. Cao, C. Fang, J. Zhu, T. Lu, D. Du, *Tetrahedron.* **2017**, *73*, 3249.

75) S. Kanchithalaivan, R. V. Sumesh, R. R. Kumar, *ACS Comb. Sci*. **2014**, *16*, 566.

76) (a) Z. Z. Ma, Y. Hano, T. Nomura, Y. J. Chen, *Heterocycles*. **1997**, *46*, 541; (b) P. G. Mandhane, R. S. Joshi, P. S. Mahajan, M. D. Nikam, D. R. Nagargoje, C. H. Gill, *Arab. J. Chem*. **2015**, *8*, 474.

77) (a) M. Nyerges, A. Pinter, A. Viranyi, G. B. L. Token, *Tetrahedron*. **2005**, *61*, 8199; (b) S. Jain, V. Chandra, P. K. Jain, K. Pathak, D. Pathak, A. Vaidya, *Arab. J. Chem*. **2016**, http://dx.doi.org/10.1016/j.arabjc.2016.10.009; (c) M. M. Maluleka, M. J. Mphahlele, *Tetrahedron.* **2013**, *69*, 699.

78) F. Hayat, E. Moseley, A. Salahuddin, R. L. V. Zyl, A. Azam, *Eur. J. Med. Chem*. **2011**, *46*, 1897.

79) P. A. Troshin, A. S. Peregudov, D. Mühlbacher, R. N. Lyubovskaya, Eur. J. Org. Chem. **2005**, 3064.

80) K. S. Mani, B. Murugesapandian, W. Kaminsky, S. P. Rajendran, *Tetrahedron Lett*. **2018**, *59*, 2921.

81) K. L. Vine, L. Matesic, J. M. Locke, M. Ranson, D. Skropeta, *Anti-Cancer Agents Med. Chem*. **2009**, *9*, 397.

82) P. Pakravan, S. Kashanian, M. M. Khodaei, F. J. Harding, *Pharmacol. Rep*. **2013**, *65*, 313.

83) (a) Z. Z. Ma, Y. Hano, T. Nomura, Y. J. Chen, *Heterocycles.* **1997**, *46*, 54; (b) P. G. Mandhane, R. S. Joshi, P. S. Mahajan, M. D. Nikam, D. R. Nagargoje, C. H. Gill, *Arab. J. Chem.* **2015**, *8*, 474.

84) SHELXTL. *Program for the Solution and Refinement of Crystal Structures*, (version 6.14); Bruker AXS Wisconsin USA, **2000**.

85) G. M. Sheldrick, SHELX-97: *Program for the Solution and refinement of Crystal Structures*, University of Göttingen, Germany, **1997**.

86) C. F. Macrae, I. J. Bruno, J. A. Chisholm, P. R. Edgington, P. McCabe, E. Pidcock, L. R. Monge, R. Taylo, J. V. D. Streek, P. A. Wood, *J. Appl. Cryst.* **2008**, *41*, 466.

87) M. N. Burnett, C. K. Johnson, 1996 ORTEPIII, Report ORNL-6895, Oak Ridge National Laboratory, Tennessee, USA.

88) L. J. Farrugia, *J. Appl. Cryst.* **1997**, *30*, 565.

89) L. J. Barbour, *J. Supramol. Chem.* **2001**, *1*, 189.

90) P. Skehan, R. Storeng, D. Scudiero, A. Monks, J. McMohan, D. Vistica, J. T. Warren, H. Bokesch, S. Kenncy, M. R. Boyd, *J. Natl. Cancer Inst*. **1990**, *82*, 1107.

91) A. Monks, D. Scudiero, P. Skehan, R. Shoemaker, K. Paull, D. Vistica, C. Hose, J. Langley, P. Cromise, *J. Natl. Cancer Inst*. **1991**, *83*, 757.

92) A. Braca, N. V. Tommasi, L. D. Bari, C. Pizza, M. Politi, I. Morelli, *J. Nat. Prod*. **2001**, *64*, 892.

93) M. R. Saha, S. M. R. Hasan, R. Akter, M. M. Hossain, M. S. Alamb, M. A. Alam, M. E. H. Mazumder, *Bangl. J. Vet. Med*. **2008**, *6*, 197.

94) M. S. Blois, *Nature*. **1958**, *181*, 1199.

95) http://autodock.scripps.edu/resources/references.

CHAPTER-III (SECTION-A)

Facile and efficient synthesis of 2-oxoquinolinyl spiropyrrolidines and pyrrolizidines *via* 1,3-dipolar cycloaddition and biological evaluation

3A.1. Introduction

Spirooxindoles are one of the prominent heterocyclic compounds have gained much importance because of their unique structural features and their wide occurrence in several natural or synthetic products. They possess a broad spectrum of medicinal properties [1-2]. Among quinolines, the synthesis of their oxo-derivatives has attracted chemists for many years because of their presence in the core moieties of a large number of bioactive compounds and natural products [3]. 2-oxoquinoline is an alkaloid, and possess remarkable biological activities like anticancer, antioxidant, antiinflammation etc. On the other hand, indenoquinoxalines also possessed a wide range of biological applications [4-12].

The rapid development of diversity-oriented syntheses to produce highly functionalized bioactive molecules through an assembly of different pharmacophoric units in a minimum number of steps is an essential tool for the modern drug discovery program. Even though these approaches are valuable, they are not suitable for the library generation because of the several drawbacks like multistep for the synthesis, longer reaction times, usage of expensive and toxic catalysts, low yields, tedious isolation/purification of the resulting products, etc. In this regard, multicomponent reactions are emerging as an ideal synthetic tool for the generation of diverse drug-like molecules [12-14].

MCR approach is an appealing ideal synthetic tool in which more than two reactants are sequentially combined to produce the combinatorial and diversity-oriented products in which the majority of atoms of the starting materials are retained [15-16]. Because of the significant benefits like high atom economy, automatable procedure, time-saving, minimization of chemical waste, wide functional group tolerance, concerted transformations, convergent one-pot process, operational simplicity and synthesis of diverse potential compounds, they play a vital role in the synthesis of pharmacophoric moieties [16-21].

The alliance of MCR approach and azomethine ylide mediated [3+2] cycloaddition reaction is one of the important strategies for the synthesis of nitrogen containing chiral spiro heterocyclic compounds [22-23]. The 1,3-dipolar cycloaddition reaction comprised with azomethine ylide and olefinic dipolarophiles produced the spiropyrrolizidines and pyrrolidines in a regio- and stereo-selective manner [13]. The principle involved in the 1,3-

dipolar cycloaddition reaction is the reaction of azomethine ylide, which was generated *in situ via* decarboxylative condensation of non-enolizable ketone and secondary amino acid, with activated dipolarophile to form the desired spiro products [21, 24-26].

Han et al. reported the design and synthesis of quinoline-2,4(1*H*,3*H*)-diones from aniline through multistep process. The synthesized compounds were evaluated for their potencies and binding energies towards the cannabinoid type 1 and type 2 (Figure 3A.1). Furthermore, the interaction modes predicted by docking simulations and the 3D-QSAR model generated with CoMFA may offer guidance for further design and modification of CB2R modulators [27].

.

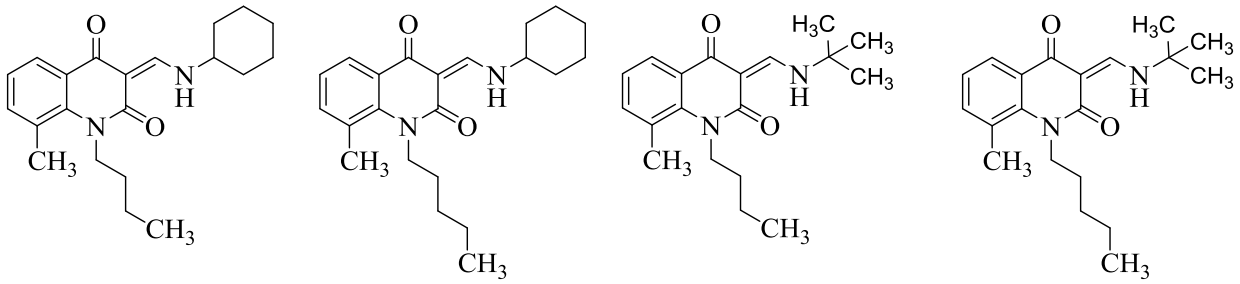

Figure 3A.1

Raitio et al. described the synthesis of 2-oxoquinoline derivatives through multistep process. The target compounds were evaluated as CB2 receptor inverse agonists (Figure 3A.2) [28].

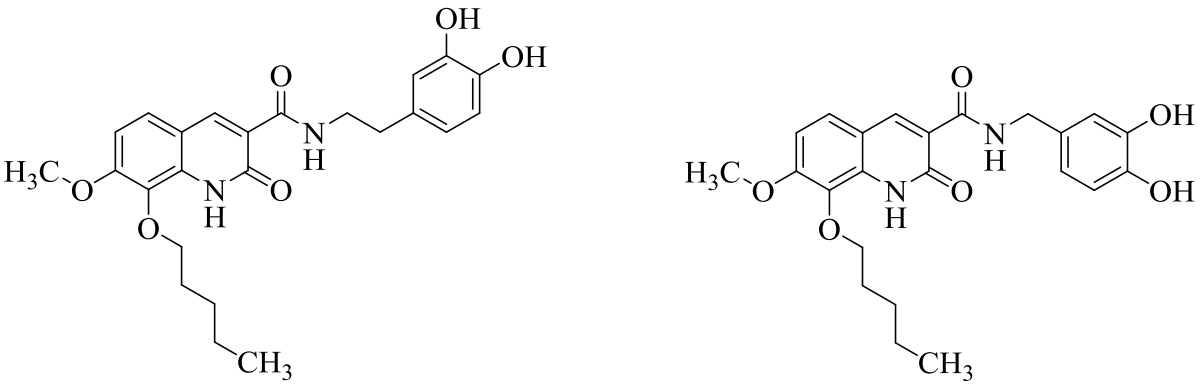

Figure 3A.2

Ruiter and coworkers explored the synthesis of 2-oxoquinoline-1-acetic acid derivatives that contain the *N*-acylglycine fragment through multistep process. All the synthesized

compounds were evaluated for their aldose reductase inhibitory activity by using rat lens assay (Figure 3A.3). The SAR studies were also carried out for the target compounds [29].

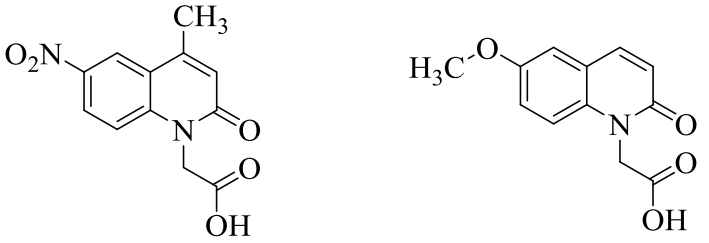

Figure 3A.3

Zhanz et al. described the synthesis of the 2-oxo-quinoline-3-carbaldehyde schiff-base derivatives through multistep process (Figure 3A.4). All the target compounds were evaluated for their antioxidant activity by using various methods i.e., DPPH, $ABTS^{+\bullet}$, $O_2^{-\bullet}$ and $H^{\bullet}$ [30].

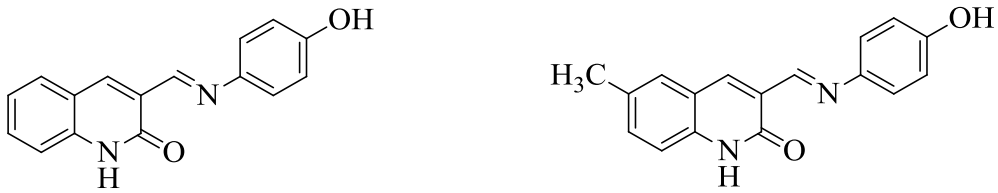

Figure 3A.4

Yan and coworkers described the facile one-pot synthesis of the library of spirooxindolopyrrolidine derivatives *via* 1,3-dipolar cycloaddition of azomethine ylide generated from sarcosine and paraformaldehyde with various 3-methyleneoxindolines (Figure 3A.5). The antimicrobial and the acetylcholinesterase inhibitory activity of the synthesized spiro compounds were also evaluated [31].

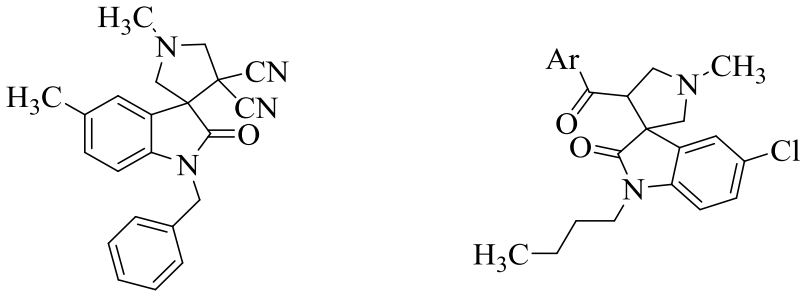

Figure 3A.5

Keseru and coworkers described the design and synthesis of spiro[pyrrolidine-3,3′-oxindole] derivatives representing a novel scaffold of 5-HT_7 receptor ligands (Figure 3A.6). The synthesized analogues were validated as low nanomolar ligands showing selectivity in a panel of related serotonin receptor subtypes including 5-HT_{1A}R, 5-HT_{2A}R and 5-HT_6R. SAR studies were also studied for the target compounds [32].

Figure 3A.6

3A.1.2. Various methods for synthesis of the spirooxindoles

Ramachary and coworkers reported the Bronsted-acid controlled, primary amine catalyzed stereoselective asymmetric synthesis of drug-like six-membered spirooxindoles from simple aliphatic substrates through a Barbas [4+2]-cycloaddition reaction by using 2-aminobuta-1,3-diene catalysis under ambient conditions (Scheme 3A.1) [33]. They also reported the highly functionalized five-membered spirooxindoles were furnished with excellent stereoselectivities by using an effective Tomita Zipper Cyclization (TZC) reaction through organophosphine catalysis (Scheme 3A.2) [34].

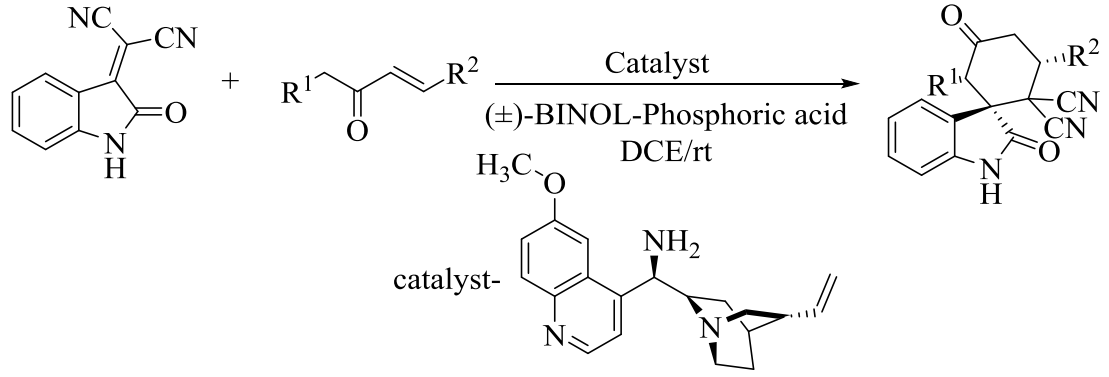

Scheme 3A.1

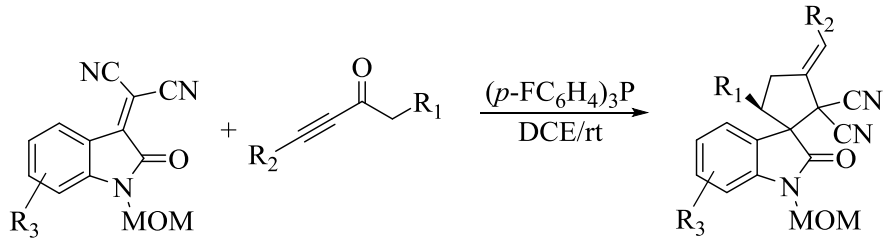

Scheme 3A.2

Babu et al. described one-pot tandem procedure for the synthesis of the functionalized spirooxindoles, which were achieved *via* vinylogous Michael addition of vinyl malononitriles on isatin–malononitrile adducts as the key step followed by a sequential intramolecular addition and isomerization reaction (Scheme 3A.3) [35].

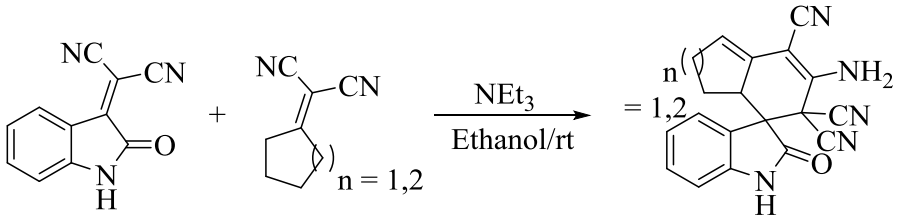

Scheme 3A.3

Lakshmi et al. described the synthesis of an expedient approach for the synthesis of dispiropyrrolidine bisoxindoles, spiropyrrolidine oxindoles and spiroindane-1,3-diones through one-pot multicomponent 1,3-dipolar cycloaddition reactions (Scheme 3A.4) [36].

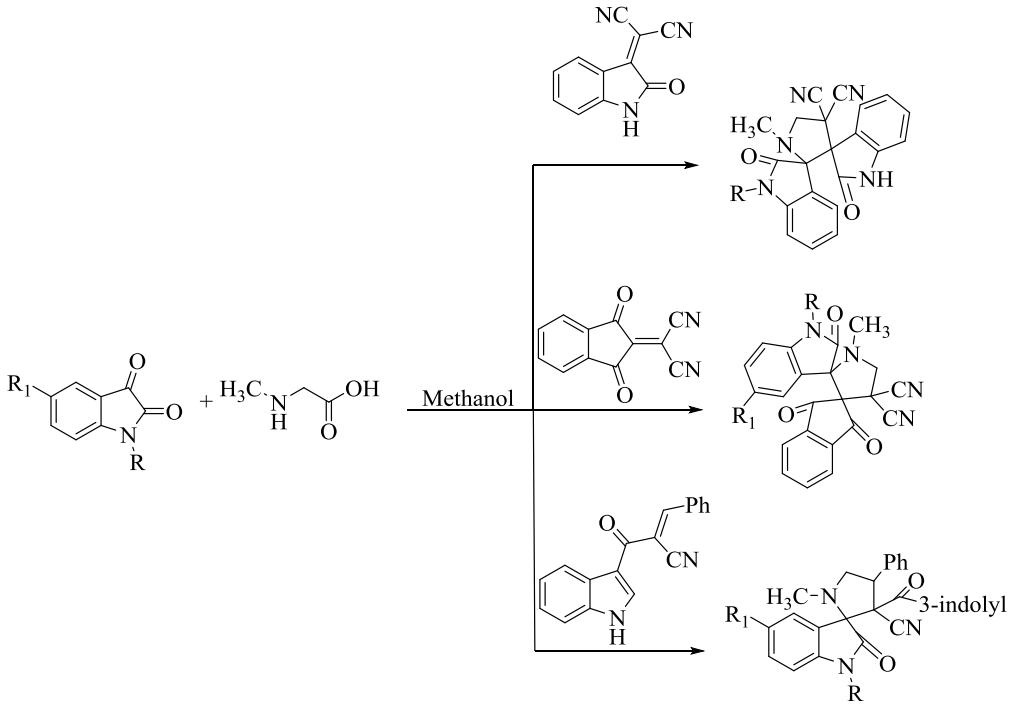

Scheme 3A.4

3A.2. Present work

By considering the aforementioned importance of the starting materials, herein, we report the facile synthesis of 2-oxoquinoline containing novel spiropyrrolidine and spiropyrrolizidine derivatives *via* a one-pot three-component 1,3-dipolar cycloaddition reaction of azomethine ylide. The target compounds were evaluated for their *in vitro* antioxidant, anticancer and antimicrobial activities. The *in silico* molecular docking studies were evaluated to find out the target cancer protein for the target compounds.

3A.2.1. Synthesis of the spirooxindolopyrrolidines and pyrrolizidines 4a-f and 6a-f

An equimolar mixture of the isatin derivatives **1a-f**, sarcosine **3**/L-proline **5** and dipolarophile **2** in ethanol under reflux condition for 3-6h produce the corresponding spirooxindolopyrrolidines and pyrrolizidines (Scheme 3A.5)**.** The progress of the reaction was checked by TLC. The obtained precipitate was filtered and purified by column chromatography.

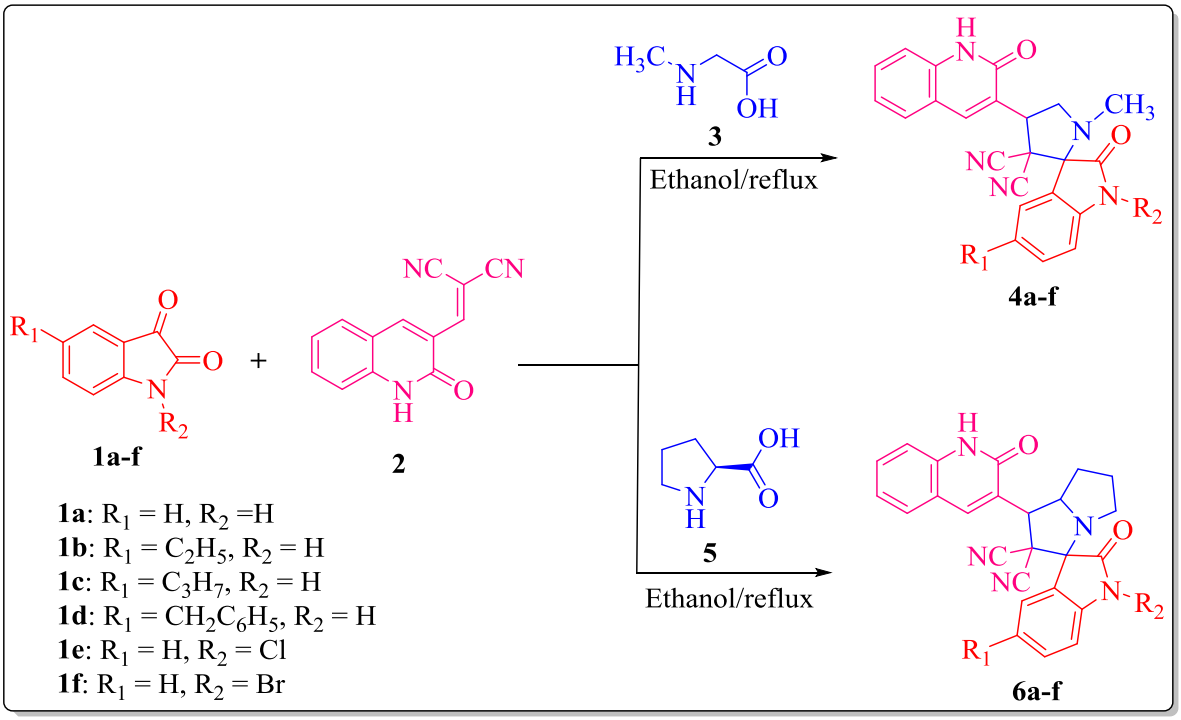

Scheme 3A.5

3A.2.2. Synthesis of the spiroquinoxalinopyrrolidines and pyrrolizidines 8a & 8b

An equimolar mixture of the quinoxaline **7**, sarcosine **3**/L-proline **5** and dipolarophile **2** in ethanol under reflux condition for 2-3h produce the corresponding spiroquinoxalinopyrrolidine and pyrrolizidine (Scheme 3A.6)**.** The progress of the reaction was checked by TLC. The obtained precipitate was filtered and purified by column chromatography.

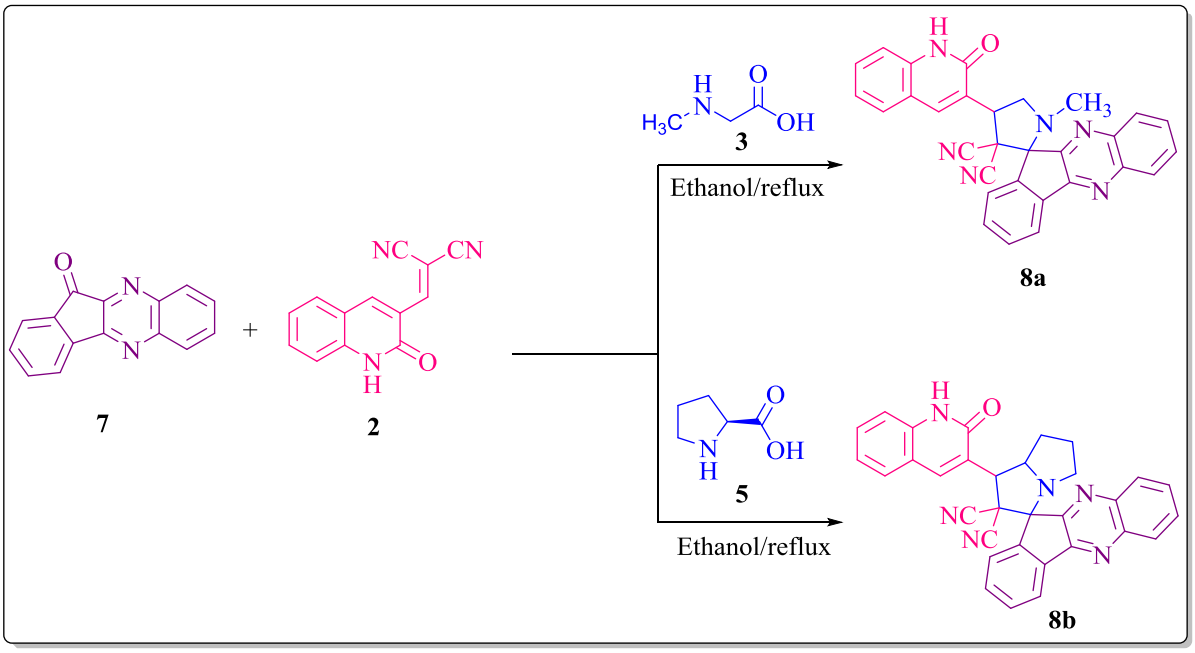

Scheme 3A.6

3A.2.3. The plausible reaction mechanism for the formation of the target compounds

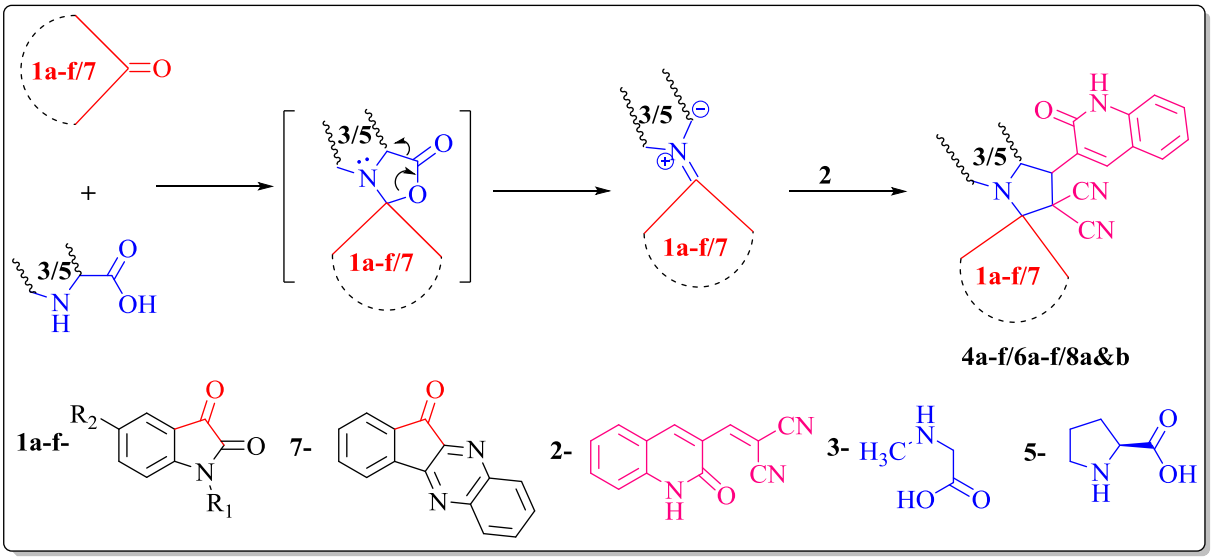

Scheme 3A.7

3A.3. Results and discussion

3A.3.1. Chemistry

Initially, to optimize the reaction condition, the pilot experiment was carried out under reflux condition in various solvents by taking isatin **1a**, L-proline **5** and dipolarophile **2** as starting materials to obtain the 2-oxoquinolinyl spirooxindolopyrrolidine **6a**. However, it was noticed that ethanol is the opted solvent to obtain the best yield at less reaction time under reflux condition. Then the model reaction was carried out at different temperatures in ethanol. The screening results were tabulated in table 1.

Table 1. The optimized reaction conditions for the synthesis of target compound **6a**[a,b,c].

S. No.	Solvent	Temperature (°C)	Time (h)	Yield (%)
1	Methanol	Reflux	4	68
2	Ethanol	Reflux	3	85
3	Acetonitrile	Reflux	3	65
4	1,4-Dioxane	Reflux	4	60
5	Tetrahydrofuran	Reflux	4	56
6	Ethanol	rt	24	--
7	Ethanol	60	9	50

[a]A mixture of the isatin **1a** (1 mmol), L-proline **5** (1 mmol) and dipolarophile **2** (1 mmol) was used as substrates in ethanol under reflux condition. [b]The progress of the reactions was monitored by TLC. [c]Isolated yields.

In order to explore the reaction approach, the target compounds **4a-f** and **6a-f** were synthesized by using similar optimized reaction condition by taking an equimolar mixture of isatin derivatives **1a-f,** sarcosine **3**/L-proline **5** and dipolarophile **2** as substrates (Scheme 3A.5). The azomethine ylide, generated *in situ* from isatin derivatives **1-f** and secondary amino acid i.e., sacrocine **3**/L-proline **5**, reacted with the dipolarophile **2** to form the target compounds **4a-f** and **6a-f** in 3-6h under reflux condition with 81-88 % yield. On the other hand, the 2-oxoquinolinyl spiroquinoxalinopyrrolidine **8a** and pyrrolizidine **8b** were synthesized by using an equimolar mixture of 11*H*-indeno[1,2-b]quinoxalin-11-one **7**, sarcosine **3**/L-proline **5** and dipolarophile **2** under reflux condition in ethanol for 2-3h with 84-86% yield (Scheme 3A.6). The crude products were filtered and purified by using column chromatography. The reaction times and yields of the reactions were shown in table 2. The

plausible reaction mechanism for the formation of the target compounds was shown in scheme 3A.7.

Table 2. 2-oxoquinolinyl spiropyrrolizidines **4a-f**, **6a-f**, **8a** and **8b**[a,b,c].

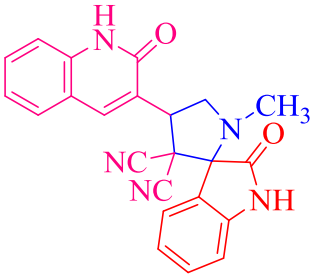 **4a** (4h / 86%)	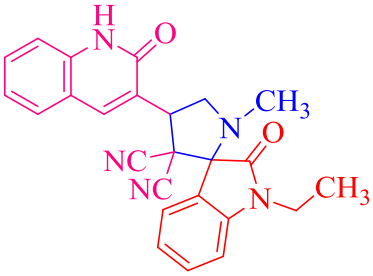 **4b** (3h / 81%)	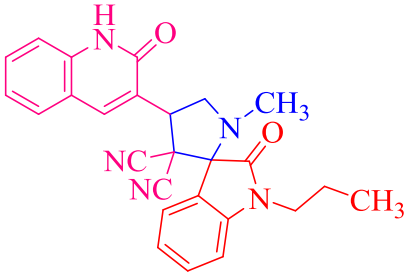 **4c** (3h / 84%)
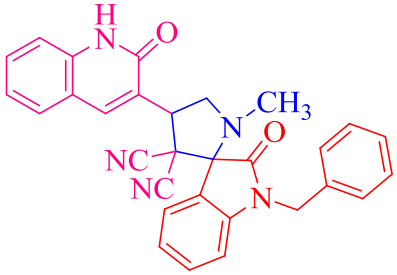 **4d** (5h / 86%)	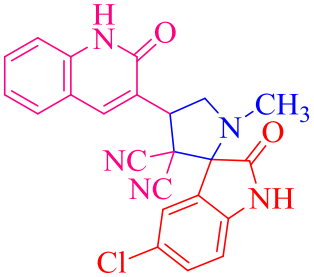 **4e** (3h / 88%)	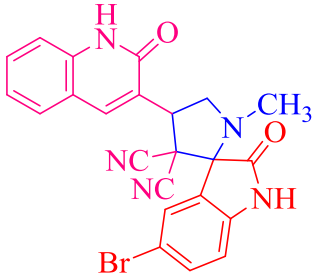 **4f** (4h / 84%)
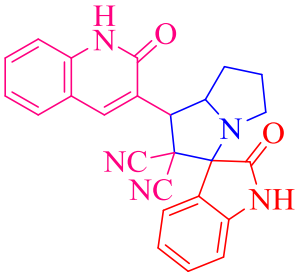 **6a** (3h / 85%)	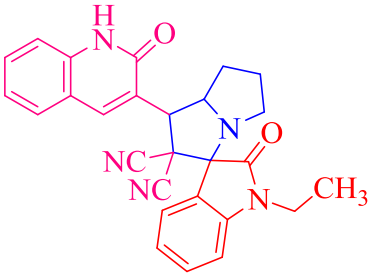 **6b** (3h / 83%)	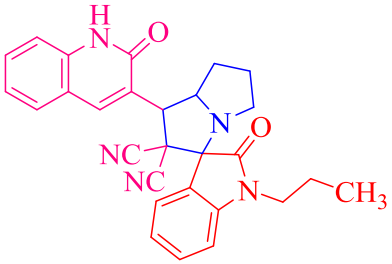 **6c** (3h / 87%)

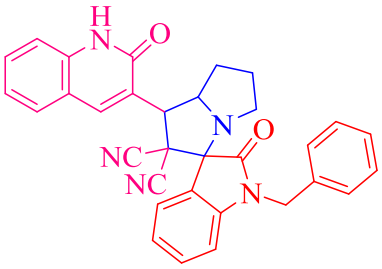

6d
(4h / 86%)

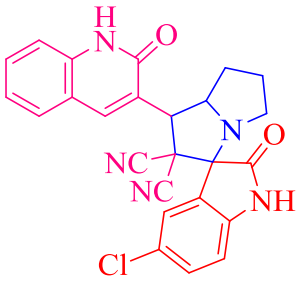

6e
(3h / 87%)

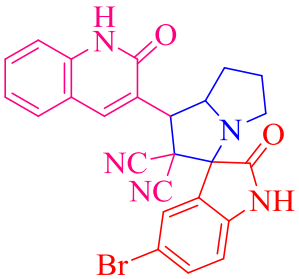

6f
(3h / 84%)

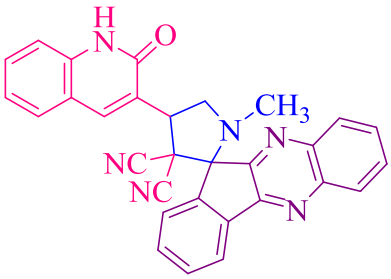

8a
(2h / 86%)

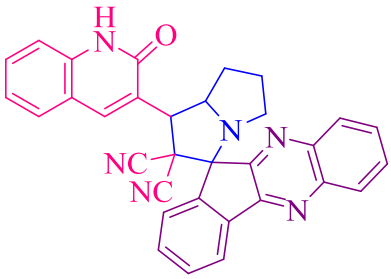

8b
(3h / 84%)

[a]All the reactions were carried out by using a mixture of the isatin derivatives **1a-f**/11*H*-indeno[1,2-b]quinoxalin-11-one **7** (1 mmol), sarcosine **3**/L-proline **5** (1 mmol) and dipolarophile **2** (1 mmol) under reflux condition in ethanol. [b]The progress of the reactions was monitored by TLC. [c]Isolated yields.

All the target compounds were well characterized by FTIR, NMR, Mass spectroscopic methods and elemental analysis. For instance, the FTIR spectrum of the compound **6a** showed the stretching frequencies at 1740 cm^{-1} and 1644 cm^{-1} corresponds to the carbonyl groups in oxindole and 2-oxoquinoline groups respectively. The stretching frequency at 2243 cm^{-1} corresponds to the nitrile (-CN) group. The ^{1}H NMR spectrum showed the peaks at δ 12.12 (s, 1H) and 11.05 (s, 1H) correspond to the proton of –NH– group in the 2-oxoquinoline and oxindole group respectively. The peak at δ 4.43 (d, 1H, J = 10.0 Hz) represents the proton of –CH group, which was directly attached to the 2-oxoquinoline ring. In ^{13}C NMR spectrum, the peaks at δ 180.13 and 164.20 correspond to the carbon atoms of the carbonyl groups of the oxindole and 2-oxoquinoline moieties respectively. The peak at δ 73.74 represents the spiro carbon atom. Further, the peak at *m/z* 422.10 (M+) in the mass spectrum confirms the formation of the compound **6a**.

3A.3.2. Biological evaluation

3A.3.2.1. Anticancer activity

The target compounds were tested for their *in vitro* anticancer activity by using MTT assay against IMR32, A549, MCF7, HeLa and HEK293T cell lines. The MTT assay results were summarized in table 3**.**

The anticancer results showed that the compound **4f** exhibited potent activity against the three cell lines IMR32, A549 and HeLa and moderate activity against MCF7 with IC_{50} values 8.12 ± 0.12 µM, 8.06 ± 0.81 µM, 10.64 ± 0.68 µM and 17.34 ± 0.12 µM respectively. The compounds **4e** and **6e** exhibited moderate activity against the four cell lines i.e., IMR32, A549, MCF7 and HeLa with IC_{50} values vary from 14.99 ± 0.91 µM to 27.13 ± 0.23 µM. The compound **6f** exhibited significant activity against the three cell lines IMR32, A549 and MCF7 and moderate activity against the HeLa cell line with IC_{50} values 13.11 ± 0.22 µM, 11.28 ± 0.16 µM, 9.36 ± 0.28 µM and 18.56 ± 0.25 µM respectively. The compound **8a** showed significant activity against three cell lines IMR32, A549 and HeLa and moderate activity against MCF7 with IC_{50} values 12.22 ± 0.21 µM, 15.18 ± 0.47 µM, 13.38 ± 0.25 µM and 15.38 ± 0.02 µM respectively. The compound **8b** showed moderate activity against the two cell lines IMR32 and MCF7 with IC_{50} values 23.08 ± 0.42 µM and 22.84 ± 0.16 µM respectively. Further, the compounds **4e**, **4f**, **6e**, **6f** and **8a** were tested against Human Embryonic Kidney 293 cell lines (HEK293T) and observed the IC_{50} values 68.72 ± 0.44 µM, 54.78 ± 0.12 µM, 60.41 ± 1.00 µM, 58.17 ± 0.96 µM and 62.72 ± 0.01 µM respectively.

The structure activity relationship studies showed that the compounds derived from isatin moiety having bromo substitution at the 5-position exhibit high activity when compared with the isatin moiety containing other substitutions (Cl, NO_2, CH_3, OCH_3) [37, 38]. The potent activity of the compound **4f** and significant activity of the compound **6f** might be due to the presence of the bromo substitution at 5-position and the presence of quinoline moiety [39].

Table 3. The anticancer activity of the synthesized compounds **4a-f**, **6a-f**, **8a** and **8b**.

S. No.	Entry	IC_{50} (μM) [a]				
		IMR32	**A549**	**MCF7**	**HeLa**	**HEK293T**
1	**4a**	38.20 ± 0.34	37.41 ± 0.22	42.86 ± 0.86	36.20 ± 1.18	ND[b]
2	**4b**	39.12 ± 0.08	45.10 ± 0.32	42.28 ± 0.68	43.34 ± 0.36	ND
3	**4c**	43.01 ± 0.21	38.48 ± 0.42	46.58 ± 0.06	45.19 ± 0.90	ND
4	**4d**	37.06 ± 1.07	38.44± 0.16	33.02 ± 0.14	39.51 ± 0.28	ND
5	**4e**	**24.64 ± 0.18**	**19.05 ± 0.19**	**14.99 ± 0.91**	**25.09 ± 0.50**	**68.72 ± 0.44**
6	**4f**	**8.12 ± 0.12**	**8.06 ± 0.81**	**17.34 ± 0.12**	**10.64 ± 0.68**	**54.78 ± 0.12**
7	**6a**	36.46 ± 0.43	34.01 ± 1.26	44.09 ± 0.07	39.19 ± 0.35	ND
8	**6b**	36.77 ± 0.74	47.38 ± 0.43	37.54 ± 0.18	32.17 ± 0.73	ND
9	**6c**	40.23 ± 0.17	38.11 ± 0.36	38.06 ± 0.61	42.37 ± 0.82	ND
10	**6d**	38.74 ± 0.12	43.88 ± 1.27	43.15 ± 0.63	37.55 ± 0.72	ND
11	**6e**	**18.23 ± 0.04**	**21.70 ± 0.43**	**27.13 ± 0.23**	**21.35 ± 0.30**	**60.41 ± 1.00**
12	**6f**	**13.11 ± 0.22**	**11.28 ± 0.16**	**9.36 ± 0.28**	**18.56 ± 0.25**	**58.17 ± 0.96**
13	**8a**	**12.22 ± 0.21**	**15.18 ± 0.47**	**13.38 ± 0.25**	**15.38 ± 0.02**	**62.72 ± 0.01**
14	**8b**	**23.08 ± 0.42**	30.28 ± 0.17	**22.84 ± 0.16**	35.84 ± 0.71	ND
15	***Cis*-Platin**	4.72 ± 0.74	5.23 ± 1.00	3.81 ± 0.38	5.45 ± 0.42	ND

[a]IC_{50}: The concentration of the compound (μM) that exhibits the 50% cell growth inhibition. [b]ND-Not determined.

3A.3.2.2. Antioxidant activity

The synthesized compounds were evaluated for their *in vitro* antioxidant activity. The antioxidant activity results were depicted in table 4.

The antioxidant activity results showed that the compounds **4f** and **8a** exhibited potent antioxidant activity with the IC_{50} values 7.32 ± 0.18 μM and 4.06 ± 0.35 μM respectively. The compound **6f** exhibited significant antioxidant activity with the IC_{50} value 12.01 ± 0.26 μM. The compound **8b** exhibited moderate antioxidant activity with the IC_{50} value 17.16 ± 0.41 μM.

Table 4. The antioxidant activity of the synthesized compounds **4a-f**, **6a-f**, **8a** and **8b**.

S. No.	Entry	IC_{50} (µM) [a]
1	**4a**	31.22 ± 0.36
2	**4b**	23.41 ± 1.12
3	**4c**	32.37 ± 0.34
4	**4d**	29.06 ± 0.47
5	**4e**	25.18 ± 0.40
6	**4f**	**7.32 ± 0.18**
7	**6a**	28.13 ± 0.27
8	**6b**	37.11 ± 0.98
9	**6c**	30.31 ± 0.97
10	**6d**	36.94 ± 1.10
11	**6e**	28.46 ± 0.13
12	**6f**	**12.01 ± 0.26**
13	**8a**	**4.06 ± 0.35**
14	**8b**	**17.16 ± 0.41**
15	**Ascorbic acid**	3.45 ± 0.74

3A.3.2.3. Antibacterial activity

The *in vitro* antibacterial activity of the synthesized compounds were carried out against the selected bacterial strains such as two gram positive bacteria i.e., *Bacillus subtilis*, *Staphylococcus aureus* and two gram negative bacteria i.e., *Escherichia coli* and *Pseudomonas aeruginosa*. The results were summarized in Table 5.

The compound **8a** showed potent antibacterial influence on the four tested bacterial strains *B. subtilis*, *S. aureus*, *E. coli* and *P. aeruginosa* with MIC values 7.00 µg/mL, 10.25 µg/mL, 14.50 µg/mL and 17.00 µg/mL respectively. The compound **4a** showed potent activity on *B. subtilis* and significant activity on *S. aureus* and *E. coli* with MIC values 8.25

µg/mL, 12.50 µg/mL and 20.50 µg/mL respectively. The compound **8b** exhibited significant activity against *P. aeruginosa* and moderate activity against *B. subtilis*, *S. aureus* and *E. coli* with MIC values 20.25 µg/mL, 13.50 µg/mL, 13.50 µg/mL and 26.25 µg/mL respectively.

Table 5. The antibacterial activity of the target compounds **4a-f**, **6a-f**, **8a** and **8b**.

S. No.	Entry	Minimum Inhibitory Concentration (µg/mL)			
		B. subtilis	***S. aureus***	***E. coli***	***P. aeruginosa***
1	**4a**	**8.25**	**12.50**	**20.50**	28.25
2	**4b**	43.00	45.50	56.25	63.50
3	**4c**	39.25	39.00	34.00	37.50
4	**4d**	33.25	38.00	38.00	>100
5	**4e**	54.00	63.00	62.50	65.0
6	**4f**	50.00	58.00	>100	>100
7	**6a**	22.50	24.50	23.25	>100
8	**6b**	28.50	>100	33.50	30.00
9	**6c**	36.25	34.50	>100	34.00
10	**6d**	32.50	26.00	34.00	38.50
11	**6e**	46.00	52.00	57.00	49.25
12	**6f**	>100	>100	>100	>100
13	**8a**	**7.00**	**10.25**	**14.50**	**17.00**
14	**8b**	**13.50**	**13.50**	**26.25**	**20.25**
15	**Streptomycin**	6.25	6.25	12.5	12.5

3A.3.2.4. Antifungal activity

The *in vitro* antifungal activity of the 2-oxoquinolinyl spiropyrrolizidines was investigated on two fungal strains such as *Aspergillus niger* and *Penicillium notatum* by using the Ketoconazole as standard drug. The results were depicted in Table 6.

The compound **8a** showed potent antifungal activity against *A. niger* and *P. notatum* with MIC values 6.25 µg/mL and 8.50 µg/mL respectively. The compound **4a** showed moderate activity against *A. niger* with the MIC value 13.50 µg/mL. The compound **8b**

showed significant antifungal activity against *A. niger* and *P. notatum* with MIC values 10.25 µg/mL and 11.50 µg/mL respectively.

Table 6. The antifungal activity of the target compounds **4a-f**, **6a-f**, **8a** and **8b**.

S. No.	Entry	Minimum Inhibitory Concentration (µg/mL)	
		Aspergillus niger	***Penicillium notatum***
1	**4a**	**13.50**	16.50
2	**4b**	44.25	46.00
3	**4c**	39.50	36.25
4	**4d**	28.00	32.25
5	**4e**	41.50	38.25
6	**4f**	42.25	39.50
7	**6a**	20.00	37.50
8	**6b**	29.00	28.50
9	**6c**	32.25	30.50
10	**6d**	25.50	29.00
11	**6e**	34.50	34.50
12	**6f**	29.50	32.00
13	**8a**	**6.25**	**8.50**
14	**8b**	**10.25**	**11.50**
15	**Ketoconazole**	3.25	3.25

3A.4. Molecular docking studies

The ligand-protein complex analysis is one of the major phenomena for the structure-based modern drug design. The *in silico* molecular docking studies were carried out on the proteins HER2 (PDB ID: 3POZ) and EGFR (PDB ID: 4HJO) by using the AutoDock Tools (ADT) version 1.5.6 and the AutoDock version 4.2.5.1 docking program.

HER2, tyrosine kinase receptor, is pertained to human epidermal growth factor receptor (HER/EGFR/ERBB) family. It plays a direct role in the growth of malignancies from various origins. It is expressed on the surfaces of most of the human cells [40]. It leads to cell survival and proliferation by stimulating the mitogen-activated protein (MAP) kinase

cascades and HER3/PI3K/Akt pathway [41, 42]. HER2 signaling dependent tumorogenesis, human and other tumor cells are often considered as HER2-addicted cells [43]. The overexpression of HER2 leads to various cancers like adenocarcinoma of lungs, stomach, breast [44], ovarian [45], uterine cancers [46, 47]. The inhibition of HER2 homodimerization and HER2/HER3 heterodimerization might be responsible for their antiproliferation. It is a suitable target for the kinase inhibitors and monoclonal antibodies [40]. The epidermal growth factor receptor (EGFR) is an eminent cell-surface receptor for EGFR family [46]. It is a well known oncogenic driver [47]. The extracellular mutations of EGFR cause glioblastoma and TKD (tyrosine kinase domain) mutations cause NSCLC (non small cell lung cancer) [40-50]. Its overexpression also responsible for the anal cancer and epithelial tumors of the neck and head [51, 52].

By considering the aforementioned rationalities, we have chosen HER2 and EGFR proteins as the target protein receptors for the molecular docking studies and compared their binding energies which were depicted in Table 7. The molecular docking results for the compounds **4a-f**, **6a-f**, **8a** and **8b** against HER2 were shown in Table 8. The comparative molecular docking studies of the targeted scaffolds **4a-f**, **6a-f**, **8a** and **8b** with the target receptors HER2 and EGFR (as shown in Table 7) univocally suggests the affinity of the synthesized compounds towards the protein receptor HER2 is better than that of the protein receptor EGFR. Hence HER2 was chosen as the target receptor for the detailed discussion. Docking results revealed that the compounds **4e**, **4f** and **6f** exhibited least binding energies i.e., −10.18 kcal/mol, −10.53 kcal/mol and −10.01 kcal/mol respectively against HER2. The best docking poses of the compounds **4e**, **4f** and **6f** were shown in figures 3A.8, 3A.9 and 3A.10.

The compound **4e** exhibited four hydrogen bonds; one hydrogen bond in between the hydrogen atom of –NH- group of the oxindole ring and the amino acid residue ASP855 (1.74 Å), one hydrogen bond in between the carbonyl oxygen of the oxindole ring and the amino acid residue LYS745 (2.37 Å), two carbon-hydrogen bonds in between the methyl group of pyrrolidine ring with amino acid residues ALA743 (3.78 Å) and LEU788 (3.67 Å) respectively. The chlorine atom of the oxindole ring interacts with the amino acid residues MET766 and LEU777, the phenyl ring in the oxindole moiety interacts with the amino acid

residues LYS745 and LEU788, The phenyl ring in the quinoline moiety interacts with the amino acid residues LEU844, LEU718 and ALA743, The 2-oxo-(1*H)*pyridyl ring interacts with the amino acid residues LEU844, ALA743, LEU718 and VAL726 through hydrophobic interactions. The compound **4f** exhibited four hydrogen bonds; one hydrogen bond in between the hydrogen atom of –NH– group of the oxindole ring and the amino acid residue ASP855 (1.76 Å), one hydrogen bond in between the carbonyl oxygen of the oxindole ring and the amino acid residue LYS745 (2.41 Å), two carbon-hydrogen bonds in between the methyl group of pyrrolidine ring with amino acid residues ALA743 (3.76 Å) and LEU788 (3.73 Å) respectively. The bromine atom of the oxindole ring interacts with the amino acid residues MET766 and LEU777, the phenyl ring in the oxindole moiety interacts with the amino acid residues LYS745 and LEU788, The phenyl ring in the quinoline moiety interacts with the amino acid residues LEU844, LEU718 and ALA743, The 2-oxo-(1*H)*pyridyl ring interacts with the amino acid residues LEU844, ALA743, LEU718 and VAL726 through hydrophobic interactions.

The compound **6f** exhibited two hydrogen bonds; one hydrogen bond in between the hydrogen atom of –NH- group of the oxindole ring and the amino acid residue ASP855 (1.50 Å), one hydrogen bond in between the carbonyl oxygen of the oxindole ring and the amino acid residue LYS745 (2.32 Å). The bromine atom of the oxindole ring interacts with the amino acid residues MET766 and LEU777, the pyrrolizidine ring interacts with the amino acid residues LYS745, VAL726 and ALA743, The phenyl ring in the quinoline moiety interacts with the amino acid residues LEU844, LEU718 and ALA743, The 2-oxo-(1*H)*pyridyl ring interacts with the amino acid residues LEU844, ALA743, LEU718 and VAL726 through hydrophobic interactions.

Table 7. The molecular docking results of the target compounds with the HER2 and EGFR proteins.

S. No.	Compound	Binding energy (kcal/mol)	
		HER2 (PDB ID: 3POZ)	**EGFR (PDB ID: 4HJO)**
1	**4a**	−9.29	−8.89
2	**4b**	−8.42	−8.38
3	**4c**	−8.52	−8.45
4	**4d**	−9.57	−9.51
5	**4e**	**−10.18**	−9.75
6	**4f**	**−10.53**	−10.16
7	**6a**	−9.23	−8.57
8	**6b**	−8.83	−8.52
9	**6c**	−8.77	−8.91
10	**6d**	−9.52	−9.59
11	**6e**	−9.94	−8.87
12	**6f**	**−10.01**	−9.36
13	**8a**	−9.54	−8.85
14	**8b**	−9.32	−8.75

Table 8. The molecular docking results of the target compounds **4a-f**, **6a-f**, **8a** and **8b**.

S. No.	Compound	HER2 (PDB ID: 3POZ)			
		Binding energies (kcal/mol)	**No. of hydrogen bonds**	**Residues involved in the hydrogen bonding**	**Hydrogen bond length (Å)**
1	**4a**	−9.29	4	LYS745, ASP855, ALA743, LEU788	1.73, 2.36, 3.62, 3.79
2	**4b**	−8.42	4	LYS745, ARG841, ASN842, ASP837	1.79, 1.88, 2.14, 2.49
3	**4c**	−8.52	4	LYS745, ASP855	2.10, 2.24, 2.74, 2.92

4	**4d**	−9.57	4	LYS745, ASP837, GLY724	1.96, 2.08, 2.25, 3.76
5	**4e**	**−10.18**	4	LYS745, ASP855, ALA743, LEU788	1.74, 2.37, 3.67, 3.78
6	**4f**	**−10.53**	4	LYS745, ASP855, ALA743, LEU788	1.76, 2.41, 3.73, 3.76
7	**6a**	−9.23	3	ARG841, THR854, CYS797	2.06, 2.24, 3.86
8	**6b**	−8.83	4	LYS745, ARG841, ASN842, ASP837	1.79, 1.98, 2.02, 2.54
9	**6c**	−8.77	1	LYS745	2.18
10	**6d**	−9.52	2	LYS745, ASP855	2.23, 3.62
11	**6e**	−9.94	3	LYS745, ASP855	1.53, 2.41, 2.83
12	**6f**	**−10.01**			
13	**8a**	−9.54	3	ASP855, GLY796, CYS797	1.89, 3.53, 3.83
14	**8b**	−9.32	1	CYS797	2.18

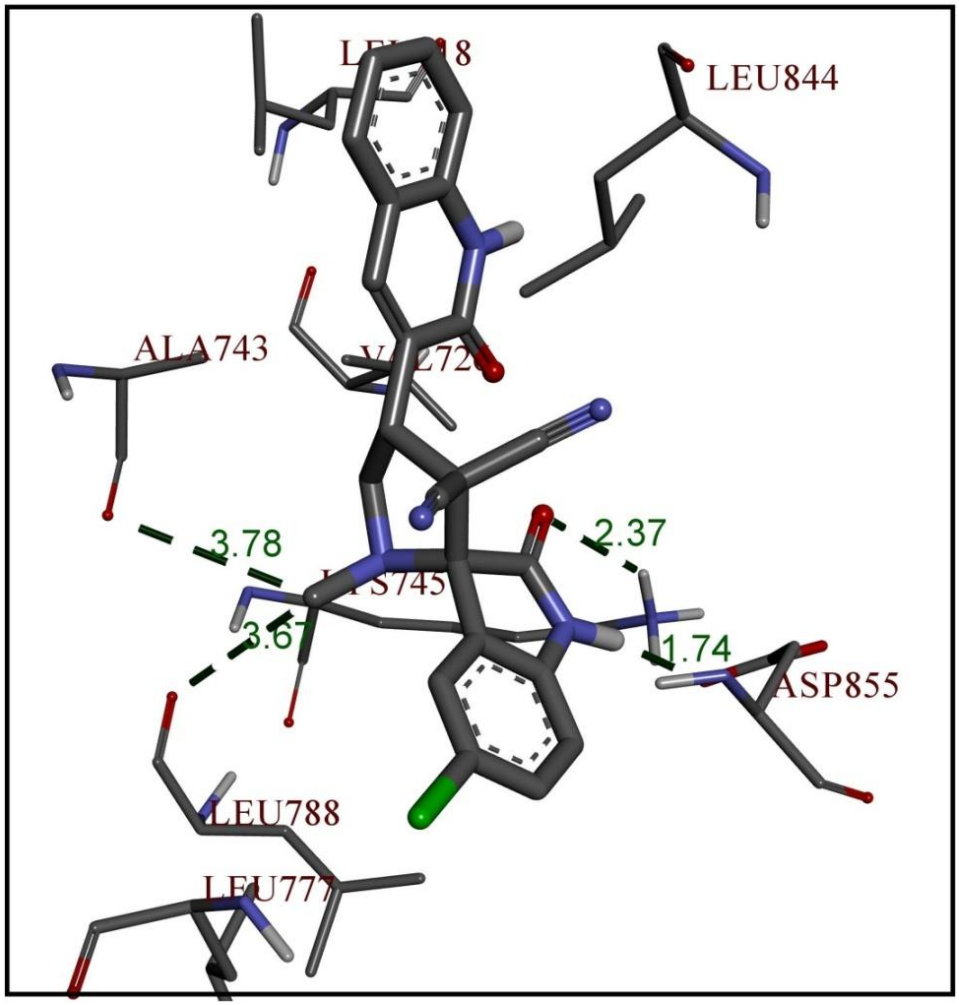

a)

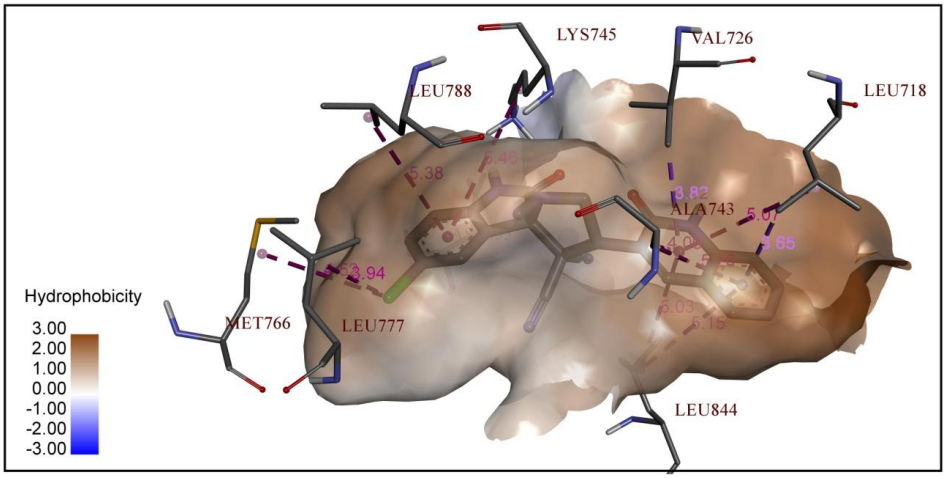

b)

Figure 3A.8. The best docking poses of **4e** with HER2. a) The hydrogen bond interactions, b) The hydrophobic interactions.

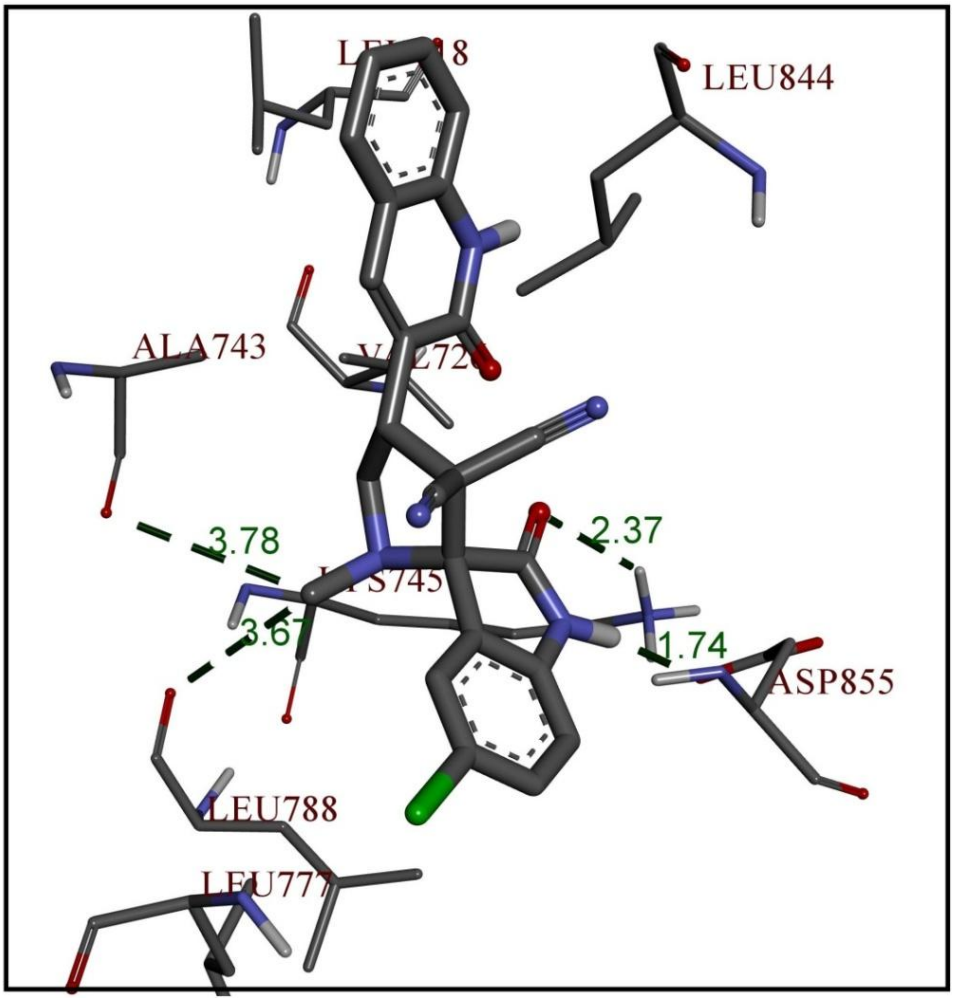

a)

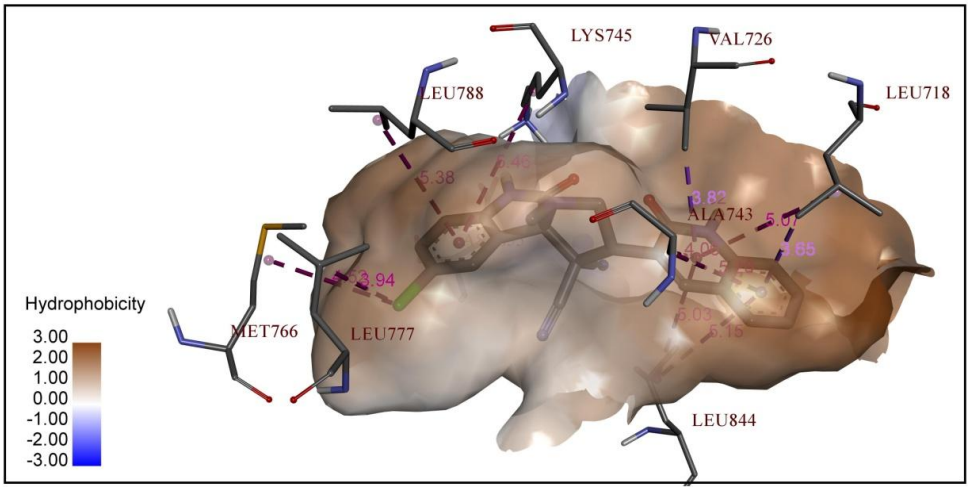

b)

Figure 3A.9. The best docking poses of **4f** with HER2. a) The hydrogen bond interactions, b) The hydrophobic interactions.

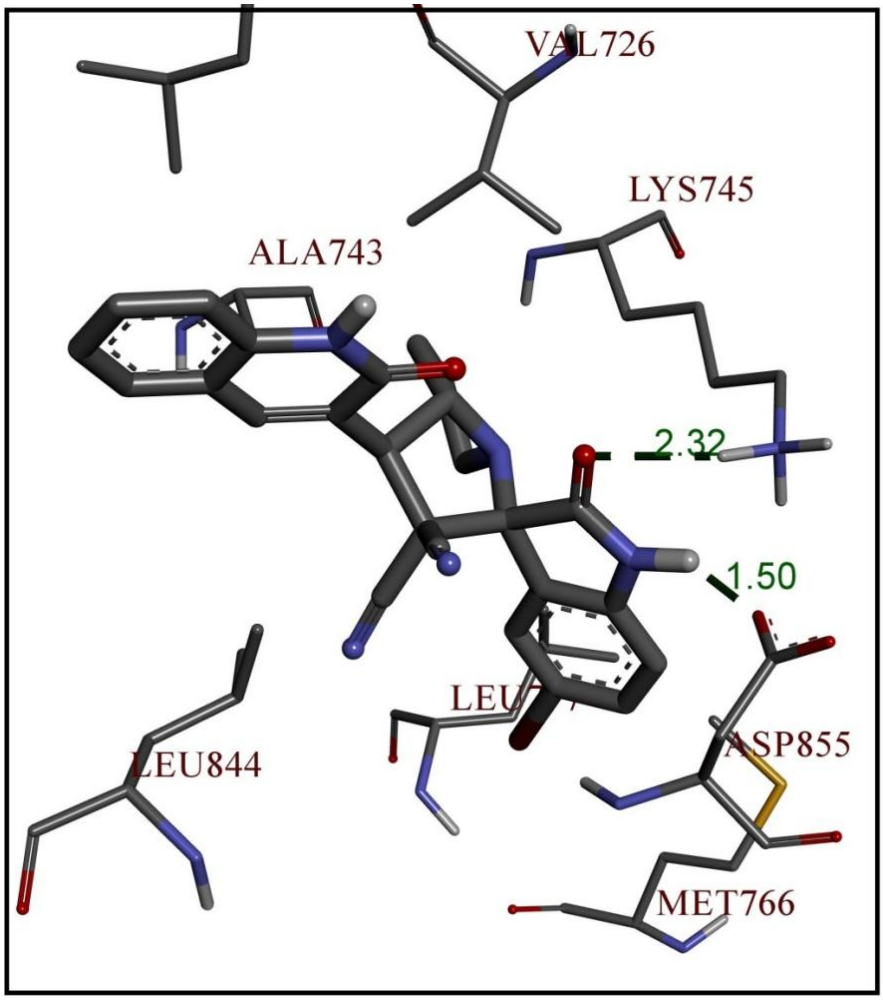

a)

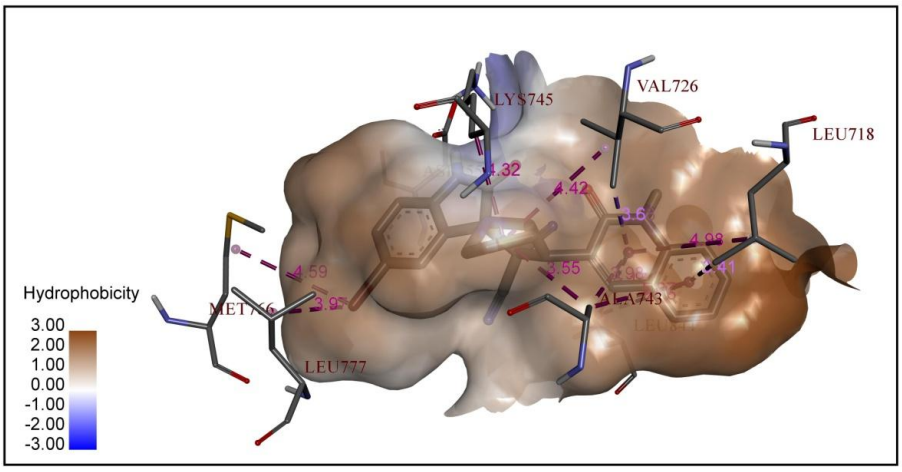

b)

Figure 3A.10. The best docking poses of **6f** with HER2. a) The hydrogen bond interactions, b) The hydrophobic interactions.

3A.5. Conclusion

A series of novel 2-oxo quinolinyl grafted spirooxindoles and spiroquinoxalines were efficiently synthesized *via* one-pot multicomponent [3+2] cycloaddition reaction in ethanol under reflux condition and characterized by various spectroscopic techniques (FTIR, NMR and Mass). Further, the synthesized compounds were evaluated for their *in vitro* anticancer, antioxidant and antimicrobial activities. The compound **4f** showed potent anticancer activity against all the tested cancer cell lines. The compounds **4e**, **6f** and **8a** were exhibited significant to moderate anticancer activity against all the four tested cancer cell lines. The *in vitro* anticancer activity was well supported by the *in silico* molecular docking studies. The compound **4f** and **8a** exhibited significant antioxidant activity. The compounds **8a** and **8b** have a significant antimicrobial influence on the tested bacterial and fungal strains.

3A.6. Spectral data

1'-Methyl-2-oxo-4'-(2-oxo-1,2-dihydroquinolin-3-yl)spiro[indoline-3,2'-pyrrolidine]-3',3'-dicarbonitrile (4a)

Colour: White. M. P. 184-186 °C. IR (KBr, cm^{-1}): 3393, 2954, 2252, 1714, 1659, 756. ^{1}H NMR (400 MHz, DMSO-*d6*) δ: 12.01 (s, 1H), 11.20 (s, 1H), 8.38 (s, 1H), 7.82 (d, 1H, *J* = 7.6 Hz), 7.57 (d, 1H, *J* = 7.6 Hz), 7.51-7.43 (m, 2H), 7.37 (d, 1H, *J* = 8.4 Hz), 7.37 (d, 1H, *J* = 8.0 Hz), 7.27-7.16 (m, 2H), 7.01-6.95 (m, 1H), 4.82 (bs, 1H), 5.17 (t, 1H, *J* = 10.0 Hz), 3.81-3.64 (m, 2H), 2.16 (s, 3H) . ^{13}C NMR (100 MHz, DMSO-*d6*) δ: 178.65, 151.20, 146.39, 141.53, 137.68, 136.96, 133.72, 133.41, 131.11, 129.57, 128.83, 128.51, 128.09, 127.94, 126.32, 111.28, 79.69, 60.28, 60.00, 40.95, 35.02. ESI mass spectrum (*m/z*): 395.15 (M+). Anal. Calcd. For $C_{23}H_{17}N_5O_2$: C, 69.86; H, 4.33; N, 17.71; found: C, 69.60.42; H, 4.27; N, 17.92.

1-Ethyl-1'-methyl-2-oxo-4'-(2-oxo-1,2-dihydroquinolin-3-yl)spiro[indoline-3,2'-pyrrolidine]-3',3'-dicarbonitrile (4b)

Colour: White. M. P. 182-184 °C. IR (KBr, cm^{-1}): 3426, 2966, 2231, 1716, 1657, 759. ^{1}H NMR (400 MHz, DMSO-*d6*) δ: 12.14 (s, 1H), 8.87 (s, 1H), 8.50 (d, 1H, *J* = 8.0 Hz), 8.24 (d, 1H, *J* = 5.6 Hz) 7.83 (d, 1H, *J* = 7.2 Hz), 7.66-7.55 (m, 3H), 7.38-7.23 (m, 2H), 4.55 (t, 1H, *J*

= 7.6 Hz), 4.17 (t, 1H, *J* = 9.2 Hz), 3.82-3.62 (m, 2H), 3.55 (t, 1H, *J* = 8.4 Hz), 2.13 (s, 3H), 1.09 (t, 3H, *J* = 6.0 Hz). ^{13}C NMR (100 MHz, DMSO-*d6*) *δ*: 179.31, 154.27, 145.32, 143.48, 143.00, 135.73, 133.94, 130.69, 129.10, 128.75, 125.81, 123.44, 111.39, 109.53, 74.89, 63.56, 52.07, 49.37, 47.04, 36.03, 13.29. ESI mass spectrum (*m/z*): 423.10 (M+). Anal. Calcd. For $C_{25}H_{21}N_5O_2$: C, 70.91; H, 5.00; N, 16.54; found: C, 71.21; H, 4.97; N, 16.76.

1'-Methyl-2-oxo-4'-(2-oxo-1,2-dihydroquinolin-3-yl)-1-propylspiro[indoline-3,2'-pyrrolidine]-3',3'-dicarbonitrile (4c)

Colour: White. M. P. 177-179 ℃. IR (KBr, cm^{-1}): 3428, 3029, 2225, 1667, 1626, 757. ^{1}H NMR (400 MHz, DMSO-*d6*) *δ*: 12.15 (s, 1H), 8.89 (s, 1H), 8.53 (d, 1H, *J* = 8.0 Hz), 8.25 (d, 1H, *J* = 5.6 Hz) 7.85 (d, 1H, *J* = 7.2 Hz), 7.69-7.53 (m, 2H), 7.40-7.25 (m, 3H), 4.57 (t, 1H, *J* = 7.6 Hz), 4.17 (t, 1H, *J* = 9.2 Hz), 3.74-3.54 (m, 3H), 2.14 (s, 3H), 1.62-1.51 (m, 2H), 0.86 (t, 3H, *J* = 6.0 Hz). ESI mass spectrum (*m/z*): 437.30 (M+). Anal. Calcd. For $C_{26}H_{23}N_5O_2$: C, 71.38; H, 5.30; N, 16.01; found: C, 71.12; H, 5.40; N, 16.26.

1-Benzyl-1'-methyl-2-oxo-4'-(2-oxo-1,2-dihydroquinolin-3-yl)spiro[indoline-3,2'-pyrrolidine]-3',3'-dicarbonitrile (4d)

Colour: White. M. P. 186-188 ℃. IR (KBr, cm^{-1}): 3427, 2951, 2225, 1722, 1659, 757. ^{1}H NMR (400 MHz, DMSO-*d6*) *δ*: 12.15 (s, 1H), 8.87 (s, 1H), 8.50 (d, 1H, *J* = 8.0 Hz), 8.27 (bs, 1H), 7.84 (d, 1H, *J* = 7.6 Hz), 7.64 (t, 2H, *J* = 8.0 Hz), 7.57 (t, 1H, *J* = 7.6 Hz), 7.46 (d, 1H, *J* = 7.6 Hz), 7.40 (t, 2H, *J* = 8.0 Hz), 7.32-7.26 (m, 3H), 7.04 (d, 1H, *J* = 7.6 Hz), 5.00 (d, 1H, *J* = 15.6 Hz), 4.85 (d, 1H, *J* = 16.0 Hz), 4.60 (t, 1H, *J* = 8.4 Hz), 4.18 (d, 1H, *J* = 9.6 Hz), 3.59 (t, 1H, *J* = 8.0 Hz), 2.15 (s, 3H). ESI mass spectrum (*m/z*): 484.10 (M+). Anal. Calcd. For $C_{30}H_{23}N_5O_2$: C, 74.21; H, 4.77; N, 14.42; found: C, 74.45.42; H, 4.69; N, 14.22.

5-Chloro-1'-methyl-2-oxo-4'-(2-oxo-1,2-dihydroquinolin-3-yl)spiro[indoline-3,2'-pyrrolidine]-3',3'-dicarbonitrile (4e)

Colour: White. M. P. 190-192 ℃. IR (KBr, cm^{-1}): 3392, 2958, 2250, 1735, 1651, 762. ^{1}H NMR (400 MHz, DMSO-*d6*) *δ*: 12.15 (s, 1H), 11.26 (s, 1H), 8.44 (s, 1H), 7.87 (d, 1H, *J* = 7.6 Hz), 7.62 (d, 1H, *J* = 7.6 Hz), 7.55 (d, 1H, *J* = 7.6 Hz), 7.53-7.48 (m, 1H), 7.43 (d, 1H, *J* = 8.4 Hz), 7.31 (d, 1H, *J* = 8.0 Hz), 7.06-7.00 (m, 1H), 5.23 (t, 1H, *J* = 10.0 Hz), 3.86-3.69

(m, 2H), 2.21 (s, 3H) . ^{13}C NMR (100 MHz, DMSO-*d6*) *δ*: 178.71, 166.20 151.26, 146.45, 141.59, 137.74, 133.78, 133.47, 131.17, 129.63, 128.89, 128.15, 127.95, 127.80, 126.31, 113.56, 111.34, 72.98, 60.34, 60.06, 41.01, 35.08. ESI mass spectrum (*m/z*): 507.25 (M+). Anal. Calcd. For $C_{23}H_{16}ClN_5O_2$: C, 64.26; H, 3.75; N, 16.29; found: C, 64.45.42; H, 3.69; N, 16.02.

5-Bromo-1'-methyl-2-oxo-4'-(2-oxo-1,2-dihydroquinolin-3-yl)spiro[indoline-3,2'-pyrrolidine]-3',3'-dicarbonitrile (4f)

Colour: White. M. P. 194-196 ℃. IR (KBr, cm^{-1}): 3392, 2847, 2250, 1716, 1652, 762. ^{1}H NMR (400 MHz, DMSO-*d6*) *δ*: 12.21 (s, 1H), 11.31 (s, 1H), 8.49 (s, 1H), 7.93 (d, 1H, *J* = 7.6 Hz), 7.68 (d, 1H, *J* = 7.6 Hz), 7.61 (d, 1H, *J* = 7.6 Hz), 7.58-7.54 (m, 1H), 7.48 (d, 1H, *J* = 8.4 Hz), 7.36 (d, 1H, *J* = 8.0 Hz), 7.12-7.06 (m, 1H), 5.28 (t, 1H, *J* = 10.0 Hz), 3.92-3.72 (m, 2H), 2.27 (s, 3H). ^{13}C NMR (100 MHz, DMSO-*d6*) *δ*: 179.06, 164.20, 151.61, 146.80, 141.94, 138.08, 137.37, 134.12, 133.82, 131.52, 129.98, 129.23, 128.50, 128.15, 126.73, 126.66, 114.56, 111.69, 73.33, 60.69, 60.41, 41.36, 35.43. ESI mass spectrum (*m/z*): 473.05 (M+). Anal. Calcd. For $C_{23}H_{16}BrN_5O_2$: C, 58.24; H, 3.40; N, 14.77; found: C, 58.45.42; H, 3.45; N, 15.02.

2-Oxo-1'-(2-oxo-1,2-dihydroquinolin-3-yl)-5',6',7',7a'-tetrahydrospiro[indoline-3,3'-pyrrolizine]-2',2'(1'*H*)-dicarbonitrile (6a)

Colour: White. M. P. 221-223 ℃. IR (KBr, cm^{-1}): 3595, 2949, 2243, 1740, 1644, 748. ^{1}H NMR (400 MHz, DMSO-*d6*) *δ*: 12.12 (s, 1H), 11.05 (s, 1H), 8.30 (s, 1H), 7.81 (d, 1H, *J* = 7.6 Hz), 7.75 (d, 1H, *J* = 7.2 Hz), 7.57 (t, 1H, *J* = 7.2 Hz), 7.46 (d, 1H, *J* = 7.6 Hz), 7.37 (d, 1H, *J* = 8.0 Hz), 7.28-7.19 (m, 2H), 6.99 (d, 1H, *J* = 7.2 Hz), 4.82 (bs, 1H), 4.43 (d, 1H, *J* = 10.0 Hz), 2.97-2.78 (m, 2H), 2.15-1.77 (m, 4H) . ^{13}C NMR (100 MHz, DMSO-*d6*) *δ*: 180.13, 164.20, 152.15, 146.85, 143.07, 138.28, 132.99, 131.71, 131.34, 130.52, 129.03, 128.44, 127.89, 125.74, 122.37, 114.56, 110.87, 73.74, 63.88, 56.60, 48.89, 48.41, 30.79, 28.12. ESI mass spectrum (*m/z*): 422.10 (M+). Anal. Calcd. For $C_{25}H_{19}N_5O_2$: C, 71.25; H, 4.54; N, 16.62; found: C, 71.42; H, 4.60; N, 16.46.

1-Ethyl-2-oxo-1'-(2-oxo-1,2-dihydroquinolin-3-yl)-5',6',7',7a'-tetrahydrospiro[indoline-3,3'-pyrrolizine]-2',2'(1'*H*)-dicarbonitrile (6b)

Colour: White. M. P. 226-228 ℃. IR (KBr, cm^{-1}): 3425, 2839, 2224, 1726, 1612, 752. ^{1}H NMR (400 MHz, DMSO-*d6*) δ: 12.20 (s, 1H), 8.93 (s, 1H), 8.56 (d, 1H, *J* = 8.0 Hz), 8.29 (bs, 1H), 7.89 (d, 1H, *J* = 7.6 Hz), 7.72-7.29 (m, 5H), 4.61 (t, 1H, *J* = 8.0 Hz), 4.22 (t, 1H, *J* = 8.80 Hz), 3.72-3.59 (m, 2H), 2.64-1.85 (m, 6H), 0.97 (t, 3H, *J* = 5.8 Hz) . ^{13}C NMR (100 MHz, DMSO-*d6*) δ: 178.65, 153.62, 144.67, 142.83, 142.35, 135.08, 133.29, 130.04, 128.45, 128.10, 125.16, 122.79, 113.52, 110.74, 74.24, 62.91, 51.41, 48.72, 46.39, 35.38, 31.41, 27.91, 12.64. ESI mass spectrum (*m/z*): 448.20 (M+). Anal. Calcd. For $C_{26}H_{21}N_5O_2$: C, 72.14; H, 5.16; N, 15.58; found: C, 72.42; H, 5.21; N, 15.36.

2-Oxo-1'-(2-oxo-1,2-dihydroquinolin-3-yl)-1-propyl-5',6',7',7a'-tetrahydrospiro[indoline-3,3'-pyrrolizine]-2',2'(1'*H*)-dicarbonitrile (6c)

Colour: White. M. P. 237-239 ℃. IR (KBr, cm^{-1}): 3413, 2963, 2249, 1715, 1609, 754. ^{1}H NMR (400 MHz, DMSO-*d6*) δ: 12.14 (s, 1H), 8.88 (s, 1H), 8.51 (d, 1H, *J* = 8.0 Hz), 8.24 (bs, 1H), 7.84 (d, 1H, *J* = 7.6 Hz), 7.69-7.52 (m, 2H), 7.39-7.24 (m, 3H), 4.55 (t, 1H, *J* = 8.0 Hz), 4.15 (t, 1H, *J* = 8.80 Hz), 3.73-3.53 (m, 2H), 1.88-2.73 (m, 6H), 1.61-1.50 (m, 2H), 0.84 (t, 3H, *J* = 5.8 Hz) . Anal. Calcd. For $C_{28}H_{25}N_5O_2$: C, 72.55; H, 5.44; N, 15.11; found: C, 72.42; H, 5.51; N, 15.36.

1-Benzyl-2-oxo-1'-(2-oxo-1,2-dihydroquinolin-3-yl)-5',6',7',7a'-tetrahydrospiro[indoline-3,3'-pyrrolizine]-2',2'(1'*H*)-dicarbonitrile (6d)

Colour: White. M. P. 242-244 ℃. ^{1}H NMR (400 MHz, DMSO-*d6*) δ: 12.10 (s, 1H), 8.80 (s, 1H), 8.44 (d, 1H, *J* = 8.0 Hz), 8.21 (bs, 1H), 7.77 (d, 1H, *J* = 7.6 Hz), 7.57 (t, 2H, *J* = 8.0 Hz), 7.50 (t, 1H, *J* = 7.6 Hz), 7.40 (d, 1H, *J* = 7.6 Hz), 7.33-7.20 (m, 5H), 7.03 (d, 1H, *J* = 7.6 Hz), 4.80 (d, 1H, *J* = 11.6 Hz), 4.70 (d, 1H, *J* = 11.6 Hz), 4.45 (d, 1H, *J* = 8.4 Hz), 4.05-3.98 (m, 1H), 2.60-1.74 (m, 6H). ^{13}C NMR (100 MHz, DMSO-*d6*) δ: 180.66, 155.63, 146.68, 144.84, 144.36, 137.09, 135.30, 132.05, 130.46, 130.11, 127.17, 124.80, 112.75, 110.89, 76.25, 64.92, 53.43, 50.73, 48.40, 37.39, 33.43, 29.92. ESI mass spectrum (*m/z*): 512.15

(M+). Anal. Calcd. For $C_{32}H_{25}N_5O_2$: C, 75.13; H, 4.93; N, 13.69; found: C, 75.31; H, 4.89; N, 13.42.

5-Chloro-2-oxo-1'-(2-oxo-1,2-dihydroquinolin-3-yl)-5',6',7',7a'-tetrahydrospiro[indoline-3,3'-pyrrolizine]-2',2'(1'*H*)-dicarbonitrile (6e)

Colour: White. M. P. 226-228 ℃. IR (KBr, cm^{-1}): 3577, 2961, 2250, 1723, 1650, 752. ^{1}H NMR (400 MHz, DMSO-*d6*) δ: 12.16 (s, 1H), 11.08 (s, 1H), 8.33 (s, 1H), 7.84 (d, 1H, *J* = 7.6 Hz), 7.78 (d, 1H, *J* = 7.2 Hz), 7.60 (t, 1H, *J* = 7.2 Hz), 7.49 (d, 1H, *J* = 7.6 Hz), 7.40 (d, 1H, *J* = 8.0 Hz), 7.29 (t, 1H, *J* = 7.6 Hz), 7.03 (d, 1H, *J* = 7.2 Hz), 4.85 (bs, 1H), 4.47 (d, 1H, *J* = 10.0 Hz), 2.99-2.81 (m, 2H), 2.19-1.80 (m, 4H) . ^{13}C NMR (100 MHz, DMSO-*d6*) δ: 180.40, 164.47, 152.42, 147.12, 143.34, 138.55, 133.26, 131.98, 131.61, 130.89, 129.30, 128.71, 128.16, 126.01, 122.64, 114.83, 111.14, 74.01, 64.15, 56.87, 49.16, 48.68, 31.06, 28.39. ESI mass spectrum (*m/z*): 507.25 (M+). Anal. Calcd. For $C_{25}H_{18}ClN_5O_2$: C, 65.86; H, 3.98; N, 15.36; found: C, 65.67; H, 3.90; N, 15.24.

5-Bromo-2-oxo-1'-(2-oxo-1,2-dihydroquinolin-3-yl)-5',6',7',7a'-tetrahydrospiro[indoline-3,3'-pyrrolizine]-2',2'(1'*H*)-dicarbonitrile (6f)

Colour: White. M. P. 232-234 ℃. ^{1}H NMR (400 MHz, DMSO-*d6*) δ: 12.08 (s, 1H), 10.99 (s, 1H), 8.25 (s, 1H), 7.77 (d, 1H, *J* = 7.6 Hz), 7.70 (d, 1H, *J* = 7.2 Hz), 7.52 (t, 1H, *J* = 7.2 Hz), 7.41 (d, 1H, *J* = 7.6 Hz), 7.30 (d, 1H, *J* = 8.0 Hz), 7.15 (t, 1H, *J* = 7.6 Hz), 6.90 (d, 1H, *J* = 7.2 Hz), 4.77 (bs, 1H), 4.37 (d, 1H, *J* = 10.0 Hz), 2.92-2.73 (m, 2H), 2.10-1.72 (m, 4H) . ^{13}C NMR (100 MHz, DMSO-*d6*) δ: 180.45, 164.51, 152.46, 147.17, 143.38, 138.59, 133.30, 132.03, 131.66, 130.84, 129.34, 128.75, 128.21, 126.06, 122.69, 114.88, 111.19, 73.87, 64.20, 56.92, 49.20, 48.73, 31.11, 28.44. Anal. Calcd. For $C_{25}H_{18}BrN_5O_2$: C, 60.01; H, 3.63; N, 14.00; found: C, 60.29; H, 3.66; N, 14.24.

1'-Methyl-4'-(2-oxo-1,2-dihydroquinolin-3-yl)spiro[indeno[1,2-b]quinoxaline-11,2'-pyrrolidine]-3',3'-dicarbonitrile (8a)

Colour: White. M. P. 243-345 ℃. IR (KBr, cm^{-1}): 3433, 2966, 2247, 1650, 757. ^{1}H NMR (400 MHz, DMSO-*d6*) δ: 12.03 (s, 1H), 8.32 (s, 1H), 7.70 (d, 1H, *J* = 7.6 Hz), 7.52-7.36 (m, 5H), 7.31 (d, 1H, *J* = 7.6 Hz), 7.21-7.09 (m, 3H), 6.95-6.88 (m, 2H), 5.12 (t, 1H, *J* = 10.0

Hz), 3.74-3.58 (m, 2H), 2.09 (s, 3H) . ^{13}C NMR (100 MHz, DMSO-*d6*) δ: 180.06, 152.61, 147.80, 142.94, 139.08, 138.37, 135.12, 134.82, 132.52, 130.98, 130.23, 129.50, 129.15, 127.73, 127.66, 114.87, 112.69, 74.33, 61.69, 61.41, 42.36, 36.43. ESI mass spectrum (*m/z*): 479.20 (M+). Anal. Calcd. For $C_{30}H_{20}N_6O$: C, 74.99; H, 4.20; N, 17.49; found: C, 75.16; H, 4.14; N, 17.71.

1'-(2-Oxo-1,2-dihydroquinolin-3-yl)-5',6',7',7a'-tetrahydrospiro[indeno[1,2-b]quinoxaline-11,3'-pyrrolizine]-2',2'(1'*H*)-dicarbonitrile (8b)

Colour: White. M. P. 184-186 °C. IR (KBr, cm^{-1}): 3444, 2978, 2250, 1649, 759. ^{1}H NMR (400 MHz, DMSO-*d6*) δ: 12.10 (s, 1H), 8.27 (s, 1H), 7.78 (d, 1H, *J* = 7.6 Hz), 7.71 (d, 1H, *J* = 7.2 Hz), 7.54 (t, 2H, *J* = 7.2 Hz), 7.43 (d, 2H, *J* = 7.6 Hz), 7.34 (d, 2H, *J* = 8.0 Hz), 7.25-7.15 (m, 3H), 6.96 (d, 1H, *J* = 7.2 Hz), 4.79 (bs, 1H), 4.39 (d, 1H, *J* = 10.0 Hz), 2.92-2.75 (m, 2H), 2.12-1.74 (m, 4H). ^{13}C NMR (100 MHz, DMSO-*d6*) δ: 166.54, 155.56, 155.03, 145.79, 145.46, 144.77, 144.12, 143.79, 139.28, 136.10, 134.03, 133.07, 131.82, 131.75, 130.97, 130.66, 130.24, 129.04, 124.14, 112.25, 111.70, 77.47, 61.40, 55.81, 49.82, 47.86, 33.34, 29.95. ESI mass spectrum (*m/z*): 507.35 (M+). Anal. Calcd. For $C_{32}H_{22}N_6O$: C, 75.87; H, 4.38; N, 16.59; found: C, 75.67; H, 4.46; N, 16.85.

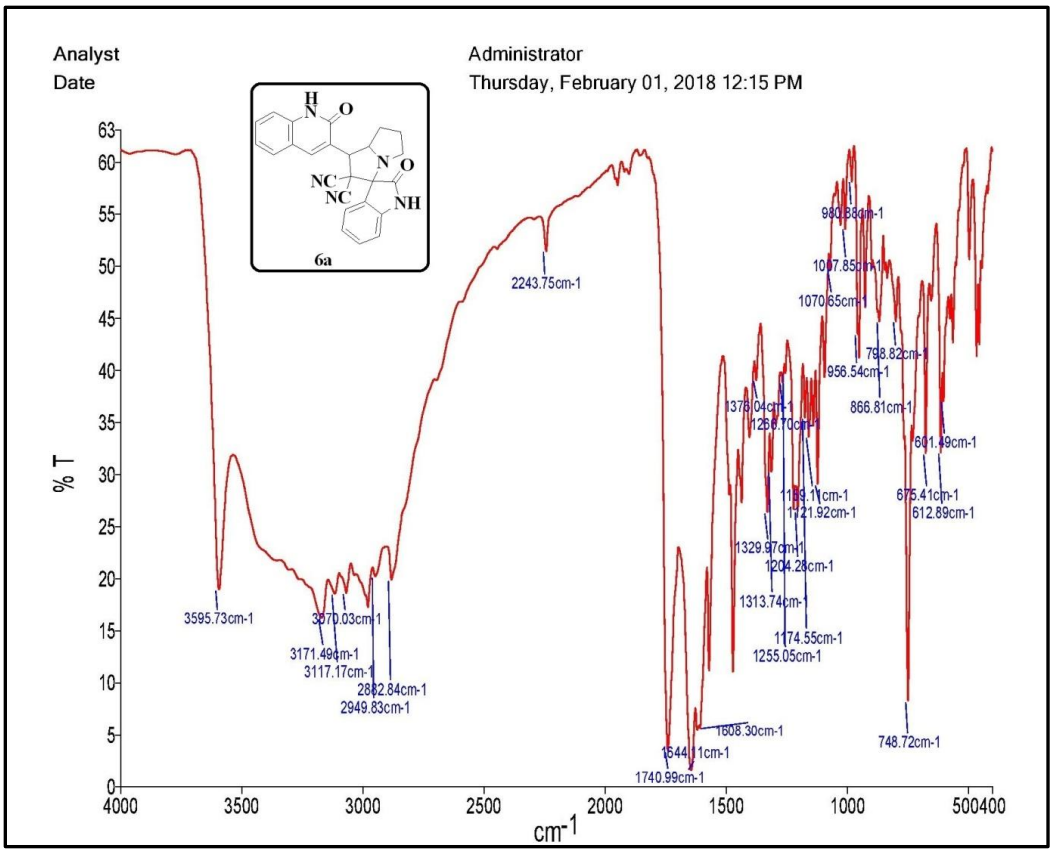

IR spectrum of the compound **6a**

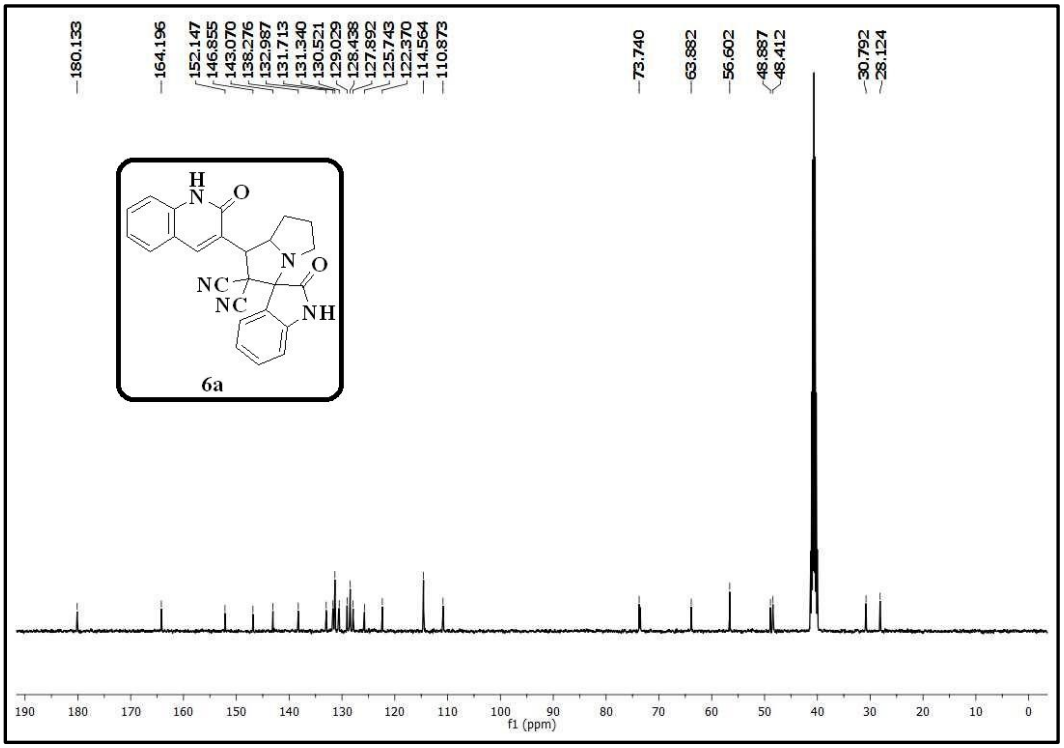

^{1}H NMR spectrum of the compound **6a**

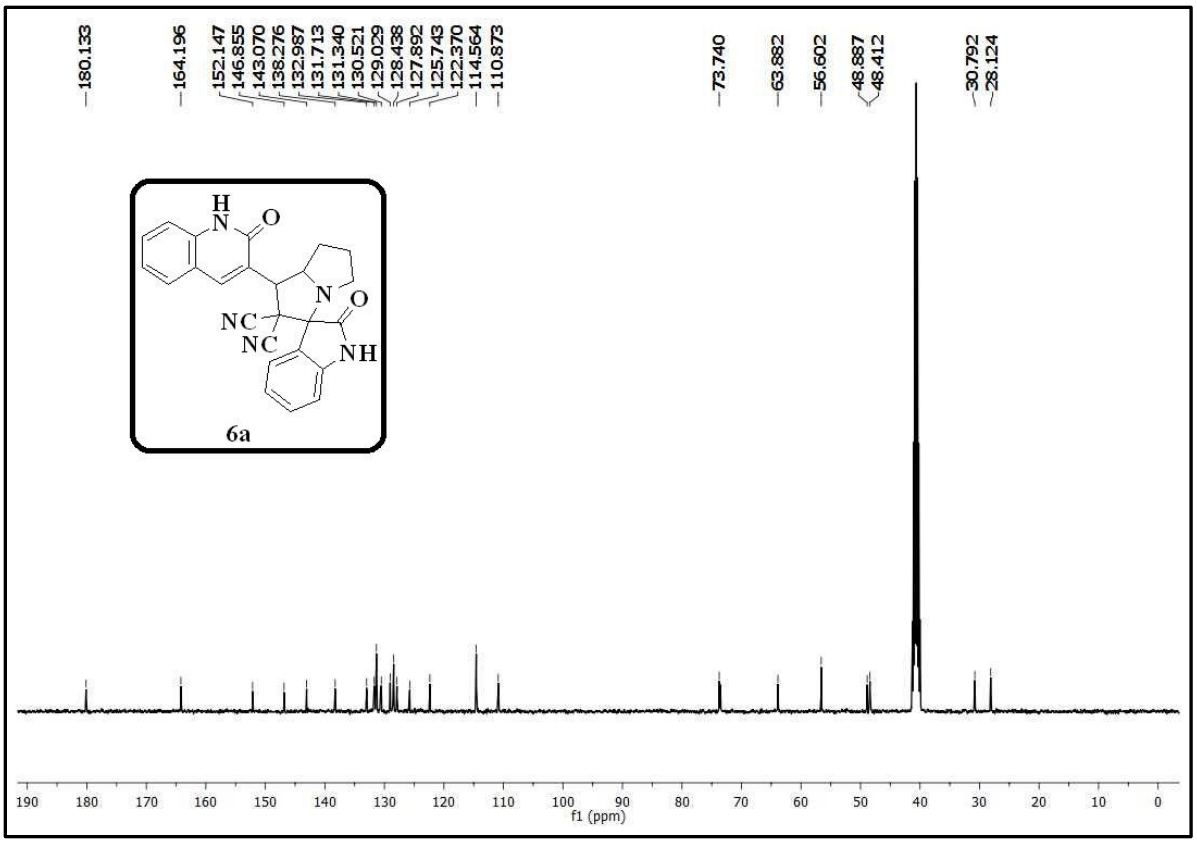

^{13}C NMR spectrum of the compound **6a**

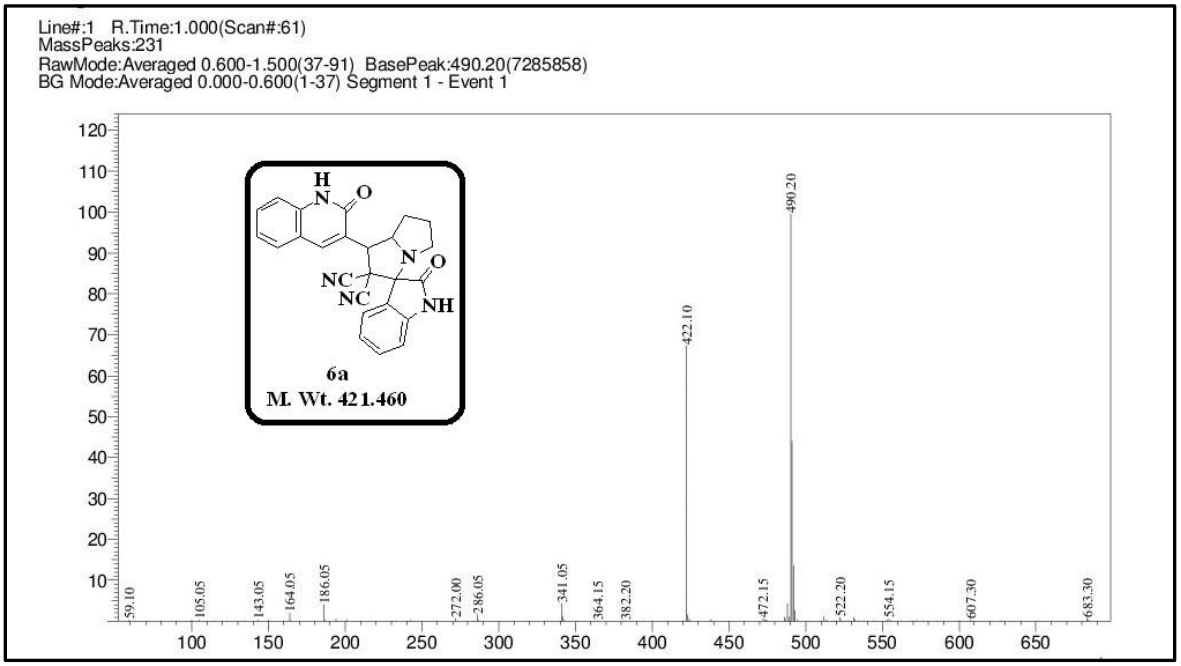

Mass spectrum of the compound **6a**

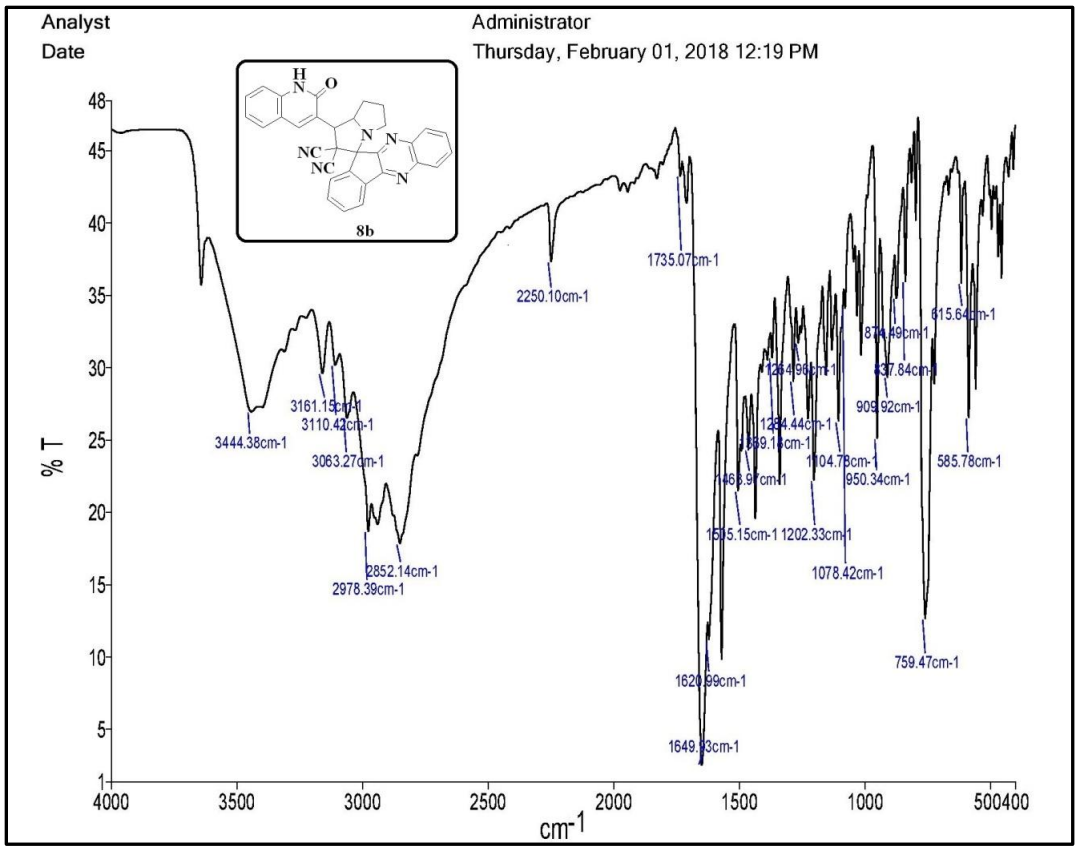

IR spectrum of the compound **8b**

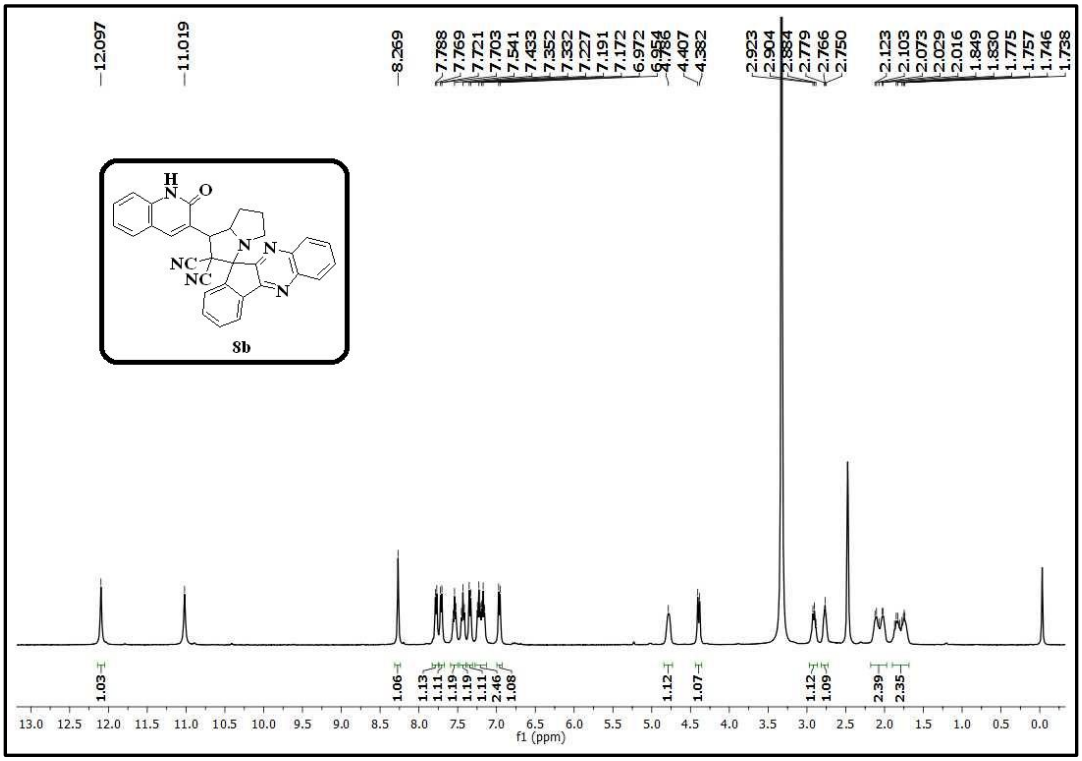

^{1}H NMR spectrum of the compound **8b**

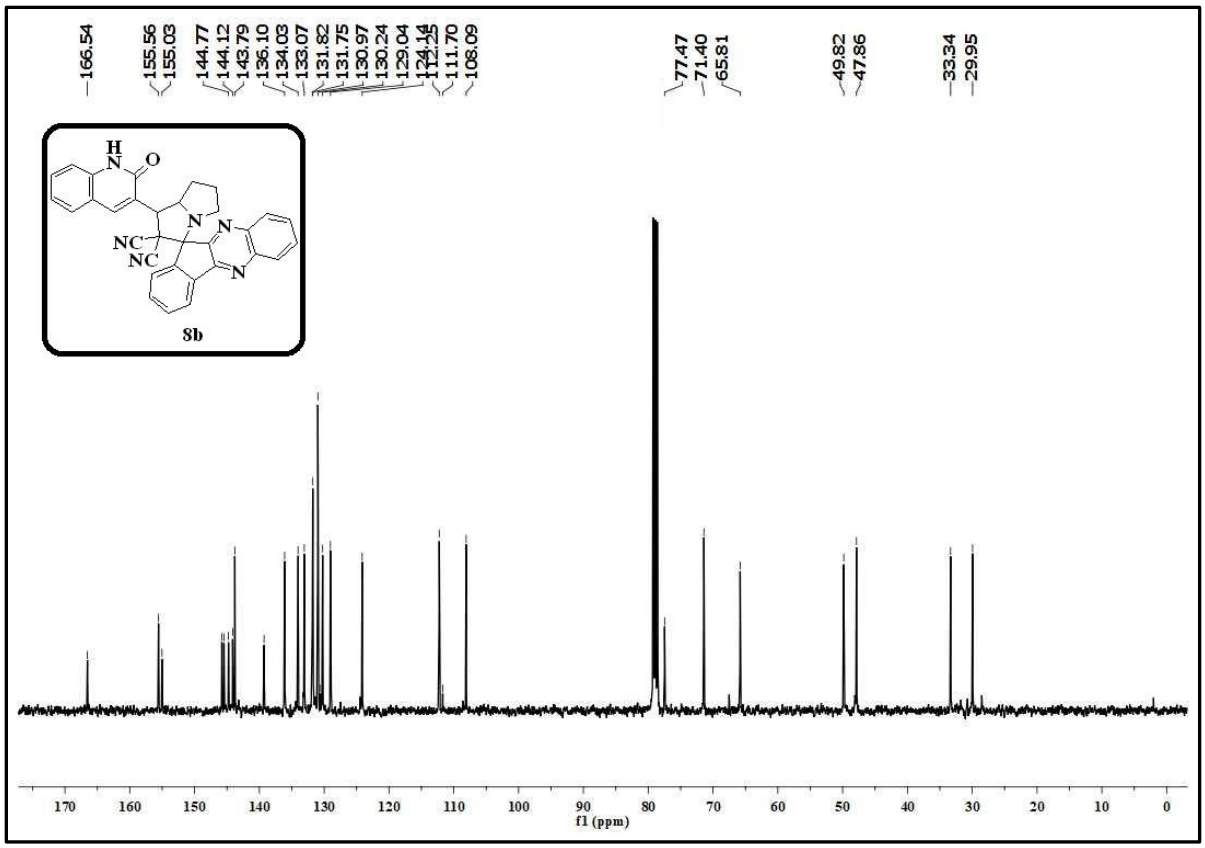

^{13}C NMR spectrum of the compound **8b**

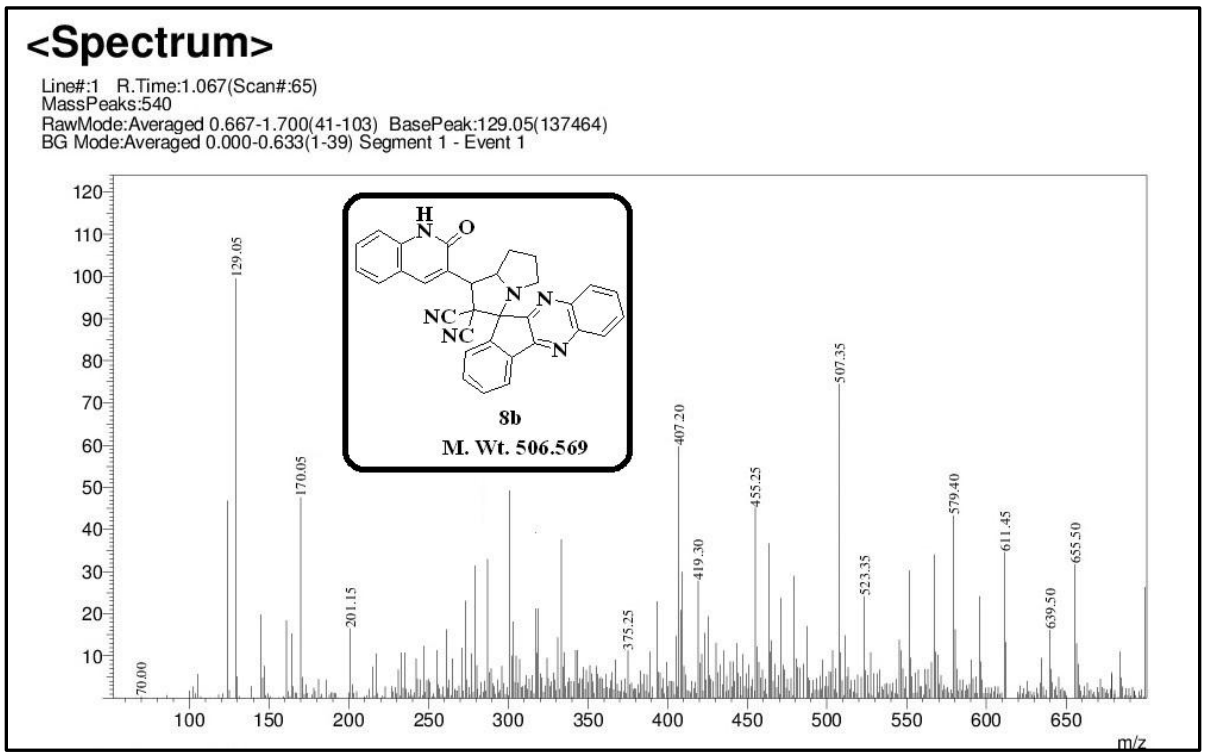

Mass spectrum of the compound **8b**

CHAPTER-III (SECTION-B)

Multicomponent 1,3-dipolar cycloaddition for the synthesis of tetrazole grafted spiropyrrolidines and pyrrolizidines and biological evaluation

3B.1. Introduction

Individually, quinolines and tetrazoles are the significant moieties that contain a broad spectrum of biological activities. The tetrazole fused quinolines were known to increase the biological activities of individual precursors [54, 55]. In particular, 4-substituted tetrazolo[1,5-*a*]quinolines are the important pharmacological molecules [56]. In modern organic chemistry, the incorporation of several chemically and biologically important compounds in a single compound is emerging as a challenging and important task for the chemists. In recent years, the multicomponent reactions (MCRs) play an efficient role in the synthesis of such hybrid molecules [57-61]. Spiro compounds are one of the important structural units in organic chemistry that contain one sp^3 carbon atom common to two rings [62, 63]. Because of the unique structural features, availability in plant and animal origins and applications in medicinal chemistry, spiro compounds occupy an eminent role in the organic synthesis. The diversified biological activities of spiro compounds are anticancer, antiviral, antiHIV, antibacterial, antifungal, anticonvulsant, local anesthetic, antiinflammatory, anticoagulant etc., [64, 65]. Among several synthetic routes to produce the spiro heterocycles, the [3+2] cycloaddition reactions occupy an eminent role in their synthesis [66-73].

MCRs are the reactions in which three or more substrates react to form diverse polyfunctional complex molecules in one-pot without isolation of the intermediate [74-77]. Waldmann et al., mentioned the MCRs as biology-oriented synthesis (BIOS) because of their efficiency to form diverse bioactive molecules [78]. The remarkable advantages of MCRs are mild conditions, high atom economy, high convergence or divergence, efficiency, library generation, decreased reaction times, easier progress of the reaction, high selectivity, etc., [79].

Marganakop et al. reported the convenient and efficient synthesis of *N*-(4-acetyl-4,5-dihydro-5-(7,8,9-substituted-tetrazolo[1,5-*a*]-quinolin-4-yl)-1,3,4-thiadiazol-2-yl)acetamides (Figure 3B.1). The target compounds were evaluated for their *in vitro* anticancer activity. These compounds were also evaluated for their DNA cleavage studies [80].

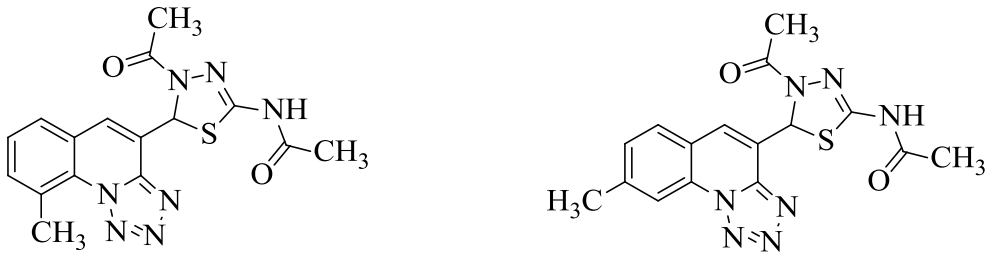

Figure 3B.1

Shingare and coworkers described the synthesis of a series of α-hydroxyphosphonates and α-acetoxyphosphonates of tetrazolo[1,5-*a*]quinoline (Figure 3B.2). The target compounds were evaluated for their *in vitro* antibacterial and antifungal activities [54].

Figure 3B.2

Subhedar et al. described the highly efficient synthesis novel tetrazoloquinoline–rhodanine conjugates *via* a multicomponent approach by using [HDBU][HSO4] as catalyst (Figure 3B.3). The target compounds were tested for their mycobacterium tuberculosis H37Ra and Mycobacterium bovis BCG activities. These compounds were also tested for their antifungal activity. The molecular docking studies were carried to support the *in vitro* mycobacaterial activity of the target compounds [81]. The authors also reported a novel approach for the synthesis of the tetrazoloquinoline–thiazolidinone scaffolds by a one-pot three-component cyclo condensation in the presence of [DBUH][OAc] as a catalyst (Figure 3B.3). These compounds were evaluated for their antimycobacterial and cytotoxic activity. The *in vitro* antimycobacterial activity was well correlated with the *in silico* molecular docking studies [82].

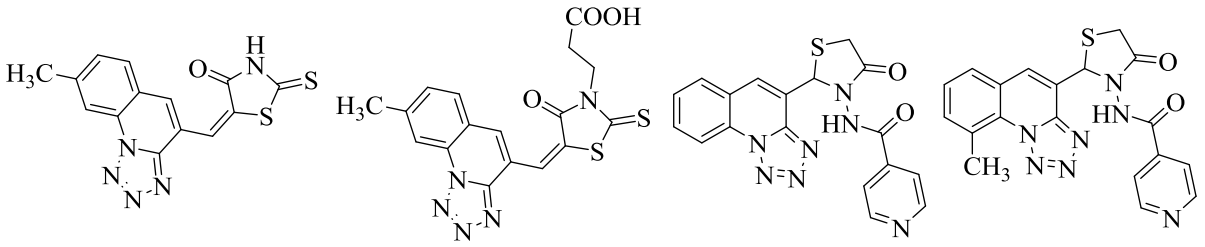

Figure 3B.3

Staniszewska et al. reported the synthesis of a series of tetrazole derivatives by using Michael-type addition reactions (Figure 3B.4). The target compounds were screened for their *in vitro* and *in vivo* studies for fungistatic potential against candida albicans, cytotoxic activity, apoptosis, antibiofilm activity and flow cytometry [83].

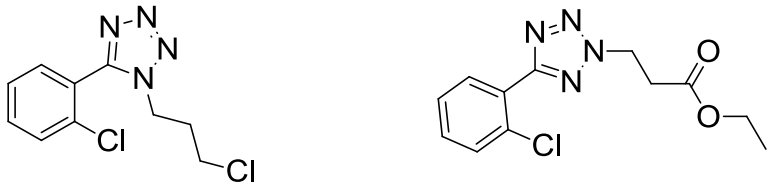

Figure 3B.4

3B.1.2. Various methods for the synthesis of the spiro compounds

Kolluri and coworkers reported the synthesis of 9-nitro-5*H*-spiro[benzo[*b*]tetrazolo[1,5-*d*][1,4]oxazepine-4,2'-oxirane] *via* an unusual ring-expansion (Scheme 3B.1) [84].

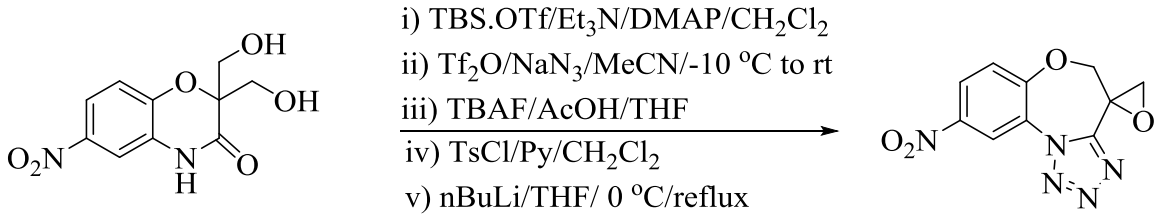

Scheme 3B.1

Rodriguez et al. described the synthesis of 1'-tetrazolylmethyl-spiro[pyrrolidine3,3'-oxindoles] *via* two coupled one-pot processes Ugi-azide/Pictet–Spengler and oxidative spiro-rearrangement (Scheme 3B.2) [85].

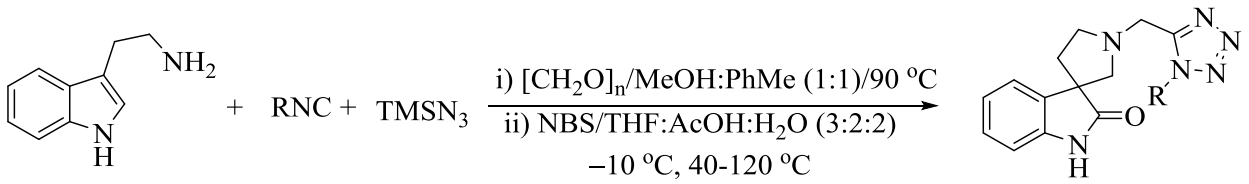

Scheme 3B.2

Kamal and coworkers reported the simple, highly efficient and environmentally benign method for the synthesis of 5'*H*-spiro[indoline-3,4'-pyrrolo[1,2-*a*]quinoxalin]-2-ones by using Amberlite IR-120H as an efficient and recyclable heterogeneous catalyst (Scheme 3B.3) [86].

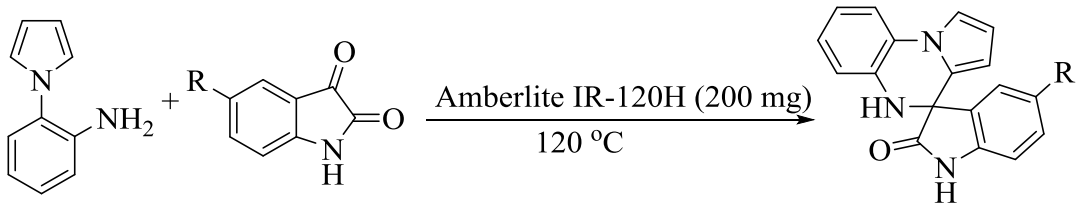

Scheme 3B.3

Preetam et al. reported an energy-efficient eco-friendly methodology for the synthesis of a series of pharmacologically important spiro[indoline-3,2'-thiazolidinones] by using a *p*-dodecylbenzene sulfonic acid (DBSA) catalyzed *via* sequential reaction approach in water at ambient temperature (Scheme 3B.4) [87].

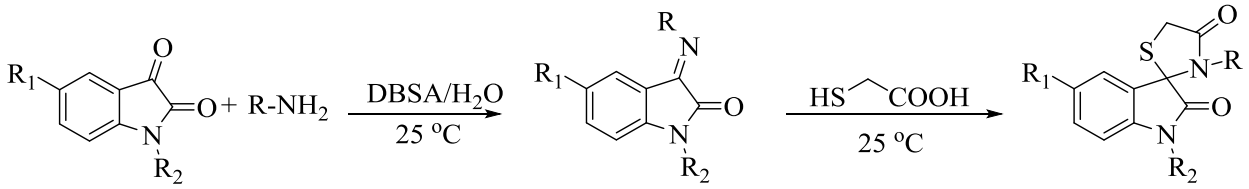

Scheme 3B.4

3B.2. Present work

By inspiring from the above mentioned significant biological applications of spiro compounds, herein, we report the synthesis of novel tetrazole fused quinolinyl spiropyrrolidines and spiropyrrolizidines *via* one-pot multicomponent [3+2] cycloaddition

reaction and evaluation of their anticancer, antioxidant, antibacterial and antifungal activities and molecular docking studies.

3B.2.1. Synthesis of the tetrazole fused quinolinyl spirooxindolopyrrolidines and pyrrolizidines 4a-f and 6a-f.

A mixture of isatin derivatives **(1a-f)**, dipolarophile **2** and sarcosine **3**/ L-proline **5** were refluxed in ethanol for 4-6h to form the target compound **4a-f** and **6a-f** (Scheme 3B.5). The progress of all the reactions was monitored by TLC. The precipitated products were filtered and purified by recrystallization in ethanol.

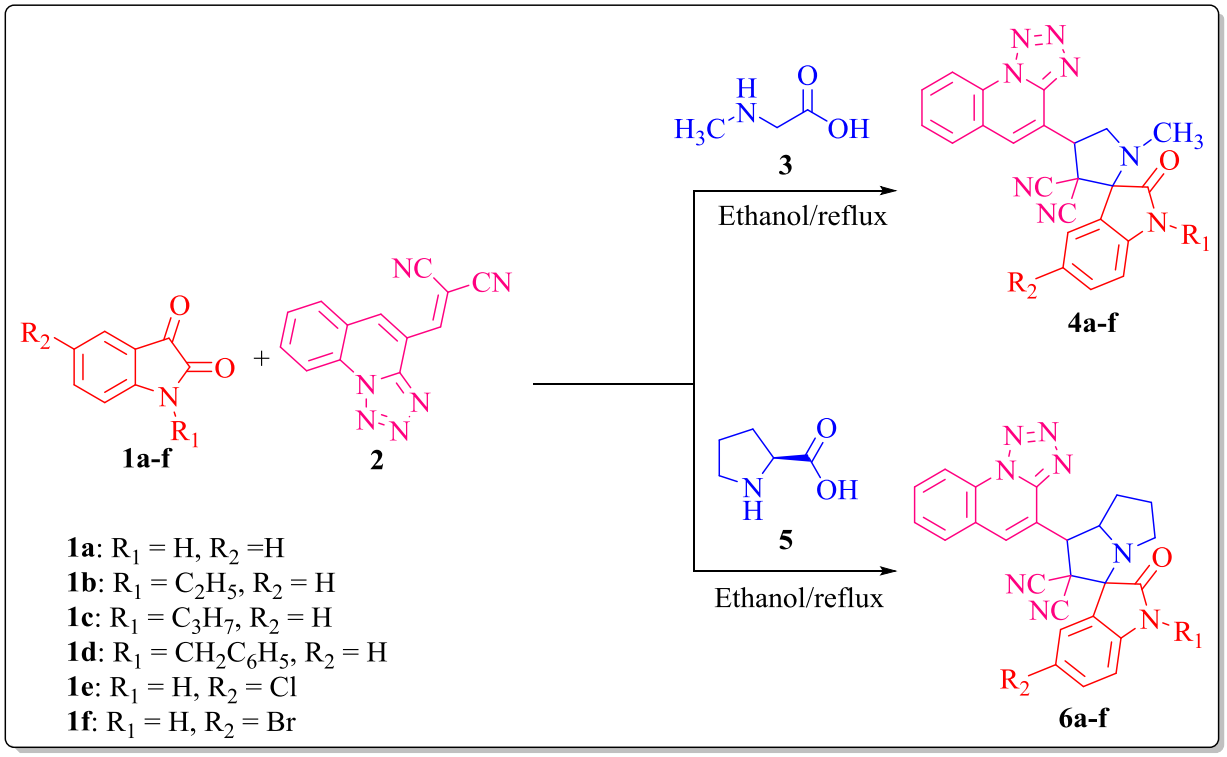

Scheme 3B.5

3B.2.2. Synthesis of the tetrazole fused quinolinyl spiroquinoxalino pyrrolizidines and pyrrolizidine 8a&b.

A mixture of 11*H*-indeno[1,2-*b*]quinoxalin-11-one **7**, dipolarophile **2** and sarcosine **3**/ L-proline **5** were refluxed in ethanol for 4-6h to form the target compound **8a** and **8b (**Scheme 3B.6). The progress of all the reactions was monitored by TLC. The precipitated products were filtered and purified by recrystallization in ethanol.

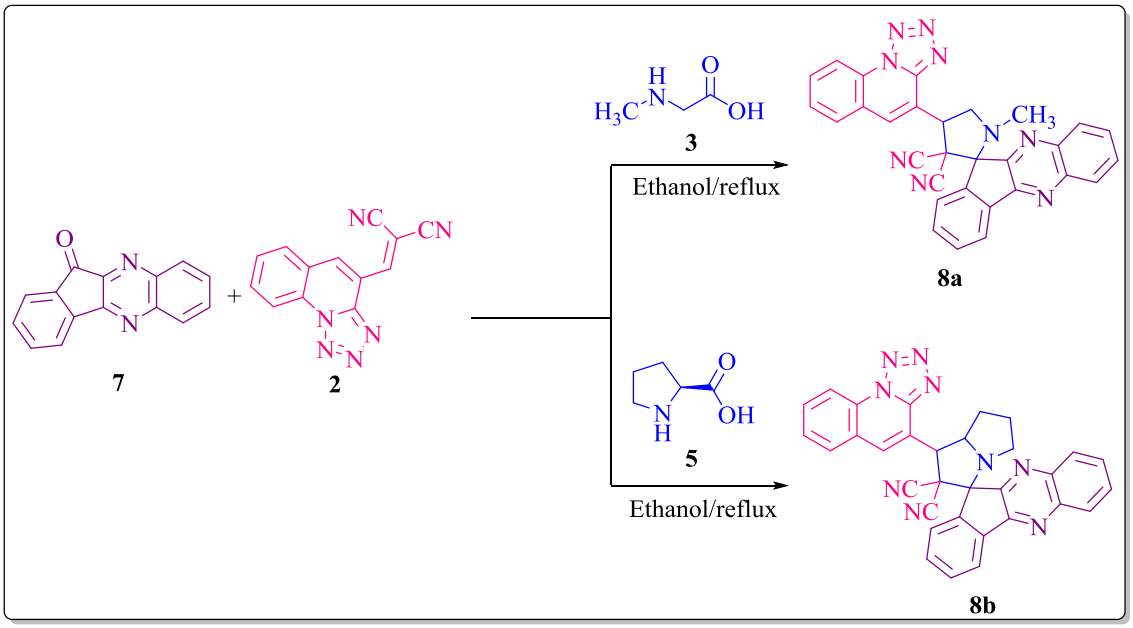

Scheme 3B.6

3B.2.3. The plausible reaction mechanism for the formation of the target compounds 4a-f, 6a-f and 8a&b (Scheme 3B.7).

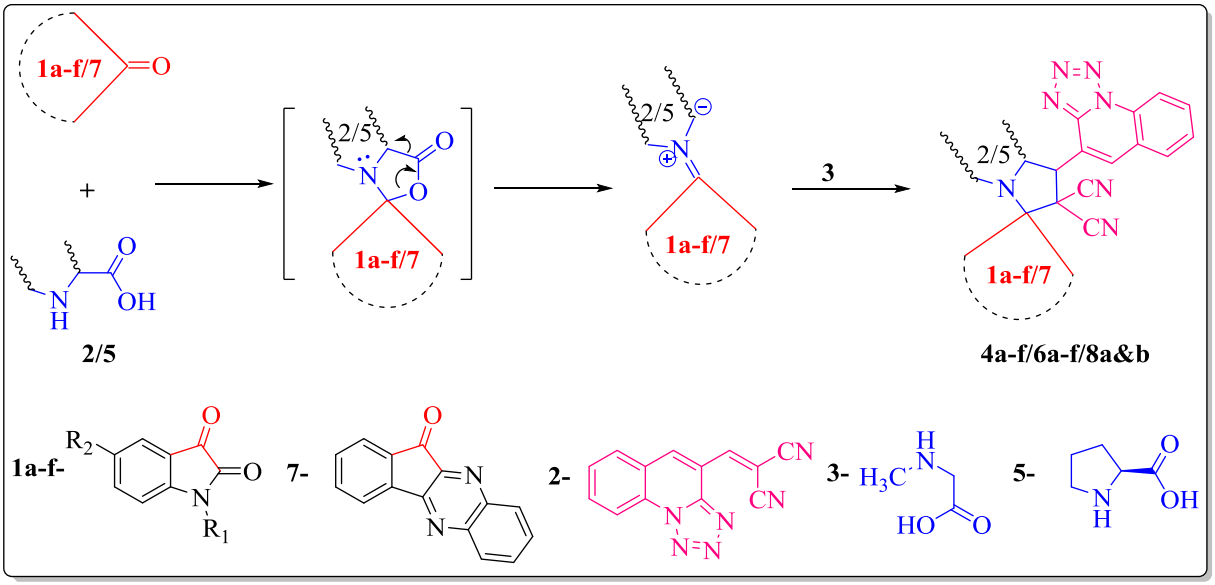

Scheme 3B.7

3B.3. Results and discussion

3B.3.1. Chemistry

Initially, the pilot experiment was carried out by taking isatin **1a**, sarcosine **3** and dipolarophile **2**, was refluxed in methanol to obtain the tetrazole fused quinolinyl spirooxindolo pyrrolidine **4a**. However, to study the effect of solvent on the reaction in the version of yields and times, the model reaction was carried out in different solvents at reflux condition. It was observed that the best yield at less time was observed in ethanol at reflux condition. Then the model reaction was carried out at different temperatures in ethanol. The screening results unveiled that the ethanol is the opted solvent for the synthesis of the tetrazole fused quinolinyl spirooxindolopyrrolidine **4a.** The screening results were tabulated in table 1.

Table 1. The optimized conditions for the synthesis of target compound **4a**[a,b,c].

S. No.	Solvent	Temperature	Time (h)	Yield (%)
1	Methanol	reflux	5	67
2	Ethanol	reflux	4	79
3	Acetonitrile	reflux	4	66
4	1,4-dioxane	reflux	6	62
5	Tetrahydrofuran	reflux	5	50
6	Ethanol	rt	24	--
7	Ethanol	60 ^{o}C	13	48

[a]A mixture of the isatin **1a** (1 mmol), sarcosine **3** (1 mmol) and dipolarophile **2** (1 mmol) were used as substrates in ethanol under reflux condition. [b]The progress of the reactions was monitored by TLC. [c]Isolated yields.

In order to explore the approach, the target compounds **4a-f** and **6a-f** were synthesized under similar optimized reaction condition by taking an equimolar mixture of isatin derivatives **1a-f,** sarcosine **3**/L-proline **5** and dipolarophile **2** as substrates (Scheme 3B.5). The azomethine ylide, generated *in situ* from isatin and secondary amino acid, reacted with the dipolarophile **2** form **4a-f** and **6a-f** in 4-6h under reflux condition *via* one-pot multicomponent 1,3-dipolar cycloaddition approach. On the other hand, the tetrazole fused

quinolinyl spiroquinoxalinopyrrolidine and pyrrolizidine **8a** and **8b** were synthesized by using an equimolar mixture of 11*H*-indeno[1,2-*b*]quinoxalin-11-one **7**, sarcosine **3**/L-proline **5** and dipolarophile **2** under reflux condition in ethanol for 3-4h (scheme 3B.6). The target compounds **4a-f**, **6a-f**, **8a** and **8b** were shown in table 2. The plausible mechanism for the formation of the target compounds **4a-f**, **6a-f**, **8a** and **8b** were shown in scheme 3B.7.

Table 2. Synthesized target compounds **4a-f**, **6a-f**, **8a** and **8b** [a,b,c].

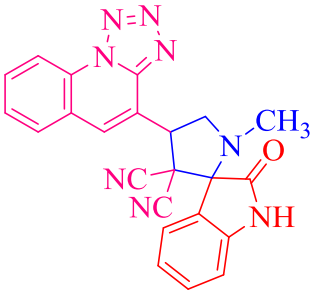

4a
(4h / 79%)

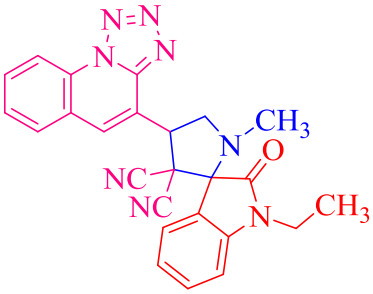

4b
(5h / 81%)

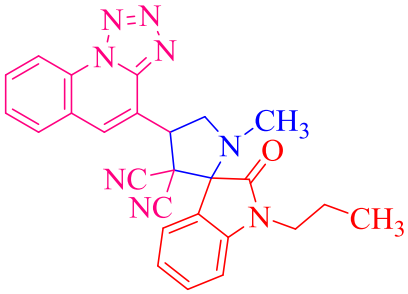

4c
(5h / 83%)

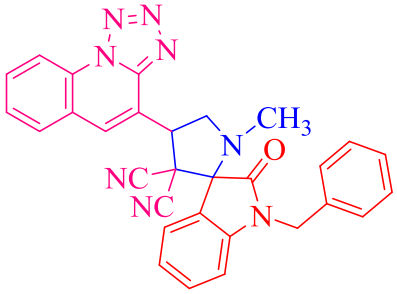

4d
(6h / 87%)

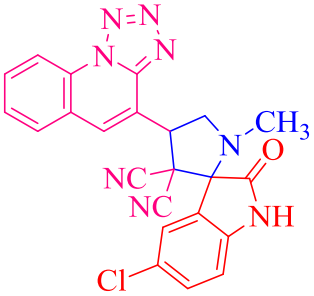

4e
(5h / 84%)

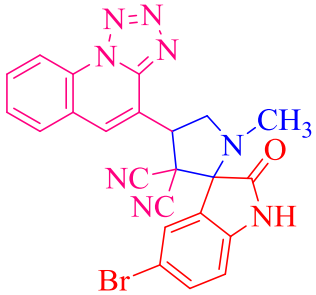

4f
(6h / 85%)

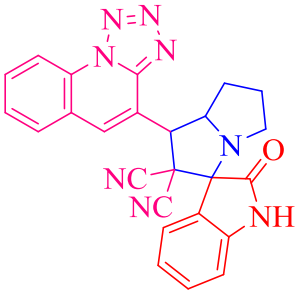

6a
(6h / 76%)

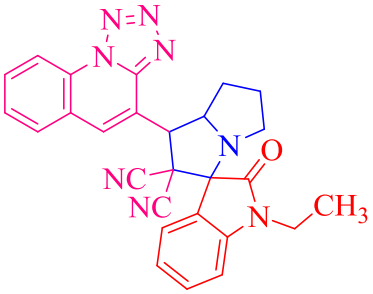

6b
(5h / 85%)

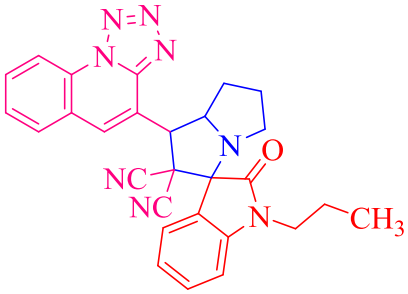

6c
(6h / 87%)

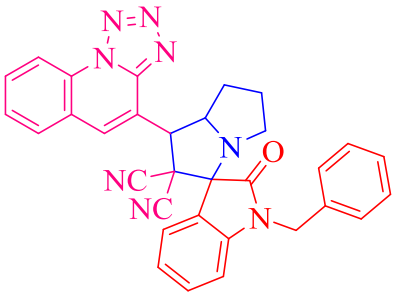

6d
(4h / 83%)

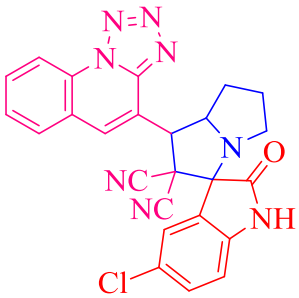

6e
(5h / 81%)

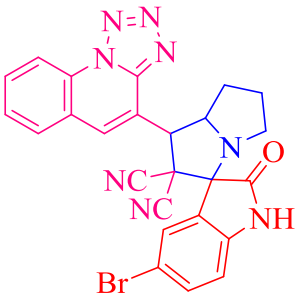

6f
(4h / 80%)

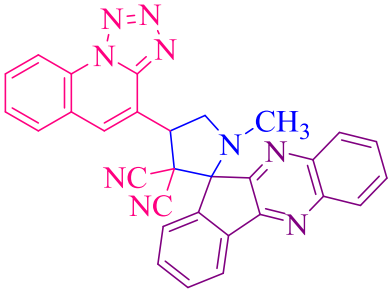

8a
(3h / 84%)

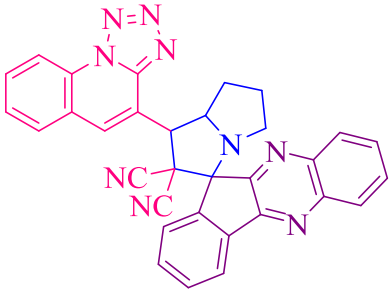

8b
(4h / 79%)

[a]All the reactions were carried out by using the equimolar mixture of isatin derivatives **1a-f**/11*H*-indeno[1,2-*b*]quinoxalin-11-one **7**, sarcosine **3**/L-proline **5**, and dipolarophile **2** under reflux condition in ethanol. [b]The progress of all the reactions was monitored by TLC. [c]Isolated yields.

3B.3.2. Biological evaluation

3B.3.2.1. Anticancer activity

The target compounds were tested for their *in vitro* anticancer activity by using MTT assay against IMR32, A549, MCF7, HeLa and HEK293T cell lines. The anticancer results were summarized in table 3.

Among all the compounds the compound **4f** exhibited the certain influence of the cytotoxic activity against four cancer liens i.e., IMR32, A549, MCF7 and HeLa with IC_{50} values 7.02 ± 0.11 µM, 9.26 ± 0.62 µM, 6.74 ± 0.97 µM and 9.74 ± 0.94 µM respectively. The compound **4a** exhibited significant activity against HeLa cell line and moderate activity against IMR32 cell line with IC_{50} values 15.88 ± 0.50 µM and 17.22 ± 0.21 µM respectively.

The compound **4e** exhibited significant activity against the four cell lines i.e., IMR32, A549, MCF7 and HeLa with IC_{50} values 9.79 ± 0.76 µM, 12.25 ± 0.29 µM, 10.48 ± 0.35 µM and 11.80 ± 0.56 µM respectively. The compound **8a** exhibited significant activity against the cell lines A549 and HeLa and moderate activity against IMR32 and MCF7 with IC_{50} values 12.18 ± 0.47 µM, 15.38 ± 0.02, 14.64 ± 0.18 µM and 13.38 ± 0.25 µM respectively. The compound **8b** exhibited moderate activity against the two cell lines IMR32 and MCF7 with IC_{50} values 18.16 ± 0.49 µM and 17.84 ± 0.37 µM respectively. Further, the compounds **4a**, **4e**, **4f** and **8a** were screened against the Human Embryonic Kidney 293 cell line and observed the IC_{50} values of 59.63 ± 0.05 µM, 78.54 ± 0.89 µM, 61.70 ± 0.32 µM and 73.54 ± 0.03 µM respectively.

Table 3. The anticancer activity of the synthesized compounds **4a-f**, **6a-f**, **8a** and **8b**.

S. No.	Entry	IC_{50} (µM) [a]				
		IMR32	**A549**	**MCF7**	**HeLa**	**HEK293T**
1	**4a**	**17.22 ± 0.21**	32.95 ± 0.15	36.38 ± 0.66	**15.88 ± 0.50**	59.63 ± 0.05
2	**4b**	37.41 ± 0.16	46.21 ± 0.26	40.72 ± 0.75	42.24 ± 0.75	ND[b]
3	**4c**	42.37 ± 0.49	34.80 ± 0.93	48.52 ± 0.15	42.21 ± 0.15	ND
4	**4d**	39.06 ± 0.75	40.43± 0.86	45.19 ± 0.29	35.11 ± 0.29	ND
5	**4e**	**9.79 ± 0.76**	**12.25 ± 0.29**	**10.48 ± 0.35**	**11.80 ± 0.56**	78.54 ± 0.89
6	**4f**	**7.02 ± 0.11**	**9.26 ± 0.62**	**6.74 ± 0.97**	**9.74 ± 0.94**	61.70 ± 0.32
7	**6a**	33.13 ± 0.93	31.41 ± 0.45	40.54 ± 0.06	40.05 ± 0.76	ND
8	**6b**	37.11 ± 0.49	48.76 ± 0.46	47.84 ± 0.36	32.42 ± 0.03	ND
9	**6c**	42.31 ± 0.37	36.35 ± 0.73	32.88 ± 0.32	48.67 ± 0.42	ND
10	**6d**	36.94 ± 0.81	40.88 ± 0.51	39.15 ± 0.75	40.55 ± 0.55	ND

11	**6e**	38.46 ± 0.04	34.14 ± 0.22	37.29 ± 0.47	31.69 ± 0.68	ND
12	**6f**	38.41 ± 0.70	49.33 ± 0.96	35.36 ± 0.28	38.36 ± 0.10	ND
13	**8a**	**14.64 ± 0.18**	**12.18 ± 0.47**	**13.38 ± 0.25**	**15.38 ± 0.02**	73.54± 0.03
14	**8b**	**18.16 ± 0.49**	30.76 ± 0.46	**17.84 ± 0.37**	25.84 ± 0.31	ND
15	***Cis*-Platin**	4.72 ± 0.74	5.23 ± 1.00	3.81 ± 0.38	5.45 ± 0.42	ND

[a]IC_{50}: The concentration of the compound (μM) that exhibits the 50% cell growth inhibition. [b]ND-Not determined.

3B.3.2.2. Antioxidant activity

The synthesized compounds were evaluated for their *in vitro* antioxidant activity. The antioxidant activity results were depicted in table 4. All the target compounds exhibited the antioxidant activity with the IC_{50} values varied from 4.42 ± 0.76 μM to 37.11 ± 0.98 μM. The compounds **4e** and **4f** exhibited potent antioxidant activity with the IC_{50} values 5.74 ± 0.15 μM and 4.42 ± 0.76 μM respectively. The compound **8a** exhibited significant antioxidant activity with IC_{50} value 8.99 ± 0.13 μM. The compound **4a** and **8b** exhibited moderate antioxidant activity with IC_{50} values 11.83 ± 0.71 μM and 11.16 ± 0.41 respectively.

Table 4. The antioxidant activity of the synthesized compounds **4a-f**, **6a-f**, **8a** and **8b**.

S. No.	Entry	IC_{50} (μM)
1	**4a**	**11.83 ± 0.71**
2	**4b**	23.41 ± 0.12
3	**4c**	32.37 ± 0.34
4	**4d**	29.06 ± 0.47
5	**4e**	**5.74 ± 0.15**
6	**4f**	**4.42 ± 0.76**
7	**6a**	28.13 ± 0.27
8	**6b**	37.11 ± 0.98

9	**6c**	30.31 ± 0.97
10	**6d**	36.94 ± 0.10
11	**6e**	28.46 ± 0.13
12	**6f**	22.41 ± 0.24
13	**8a**	**8.99 ± 0.13**
14	**8b**	**11.16 ± 0.41**
15	**Ascorbic acid**	3.45 ± 0.745

3B.3.2.3. Antibacterial activity

The *in vitro* antibacterial activity of the synthesized compounds was carried out against the selected bacterial strains such as two gram positive bacteria i.e., *Bacillus subtilis* and *Staphylococcus aureus* and two gram negative bacteria i.e., *Escherichia coli* and *Pseudomonas aeruginosa*. The results were summarized in Table 5.

Among all the synthesized compounds, the compound **8a** exhibited substantial antibacterial activity against both the tested gram positive and gram negative bacteria with MIC values 7.25 µg/mL, 9.50 µg/ml, 16.00 µg/mL and 19.50 µg/mL. The compound **4d** showed significant activity against the *E. coli* and *P. aeruginosa* and moderate activity on *B. subtilis*, *S. aureus*, with MIC values 18.00 µg/mL, 15.25 µg/mL, 19.25 µg/mL and 17.00 µg/mL respectively. The compound **8b** exhibited significant activity against *B. subtilis*, *S. aureus*, *P. aeruginosa* and moderate activity against *E. coli* with MIC values 12.50 µg/mL, 15.00 µg/mL, 22.25 µg/mL and 25.50 µg/mL respectively.

Table 5. The antibacterial activity of the target compounds **4a-f**, **6a-f**, **8a** and **8b**.

S. No.	Entry	Minimum Inhibitory Concentration (µg/mL)			
		B. subtilis	***S. aureus***	***E. coli***	***P. aeruginosa***
1	**4a**	56.25	50.50	57.50	>100
2	**4b**	43.00	45.50	56.25	63.50
3	**4c**	39.25	39.00	34.00	37.50
4	**4d**	**19.25**	**17.00**	**18.00**	**15.25**
5	**4e**	54.00	63.00	62.50	65.0

6	**4f**	50.00	58.00	>100	>100
7	**6a**	42.00	44.00	43.25	>100
8	**6b**	28.50	>100	33.50	30.00
9	**6c**	36.25	34.50	>100	34.00
10	**6d**	32.50	26.00	34.00	38.50
11	**6e**	46.00	52.00	57.00	49.25
12	**6f**	>100	>100	>100	>100
13	**8a**	**7.25**	**9.50**	**16.00**	**19.50**
14	**8b**	**12.50**	**15.00**	**25.50**	**22.25**
15	**Streptomycin**	6.25	6.25	12.5	12.5

3B.3.2.4. Antifungal activity

The *in vitro* antifungal activity of the tetrazole fused quinolinyl spiropyrrolizidines were investigated on two fungal strains such as *Aspergillus niger* and *Penicillium notatum* by using the Ketoconazole as standard drug. The antifungal results were depicted in Table 6.

The compound **8a** was exhibited potent fungal inhibition activity against *A. niger* and moderate activity against *P. notatum* with MIC values 5.25 µg/mL and 13.50 µg/mL respectively. The compound **8b** was exhibited potent inhibition activity against *A. niger* and moderate activity against *P. notatum* with MIC values 8.25 µg/mL and 11.50 µg/mL respectively. The compound **4d** showed moderate activity against the two tested fungal strains *A. niger* and *P. notatum* with MIC values 18.50 µg/mL and 20.00 µg/mL respectively.

Table 6. The antifungal activity of the target compounds **4a-f**, **6a-f**, **8a** and **8b**.

S. No.	**Entry**	**Minimum Inhibitory Concentration (µg/mL)**	
		Aspergillus niger	***Penicillium notatum***
1	**4a**	33.50	38.50
2	**4b**	44.25	46.00
3	**4c**	39.50	36.25
4	**4d**	**18.50**	**20.00**
5	**4e**	41.50	38.25

6	**4f**	42.25	39.50
7	**6a**	30.00	37.50
8	**6b**	29.00	28.50
9	**6c**	32.25	30.50
10	**6d**	25.50	29.00
11	**6e**	34.50	34.50
12	**6f**	29.50	32.00
13	**8a**	**5.25**	**13.50**
14	**8b**	**8.25**	11.50
15	**Ketoconazole**	3.25	3.25

3B.4. Molecular docking studies

The molecular docking studies were carried out against proteins HER2 (PDB ID: 3POZ) and EGFR (PDB ID: 4HJO) by using the AutoDock Tools (ADT) version 1.5.6 and the AutoDock version 4.2.5.1 docking program.

HER2 is a member of the human epidermal growth factor receptor2 (EGFR/HER/ERBB) family. It has an eminent role in the malignant growth from several origins [40]. It stimulates the mitogen-activated protein (MAP) kinase cascades and HER3/PI3K/Akt pathway, thus leads to cell survival and proliferation [41, 42]. It is expressed on most of the human cell surfaces [40]. The overexpression of HER leads to various cancers like stomach, adenocarcinoma of lungs, breast [44], uterine [46, 47], ovarian cancers [39]. It is a suitable target for the kinase inhibitors and monoclonal antibodies [40]. EGFR, an eminent cell-surface receptor, pertained to Epidermal growth factor receptor family [46]. It is a well known oncogenic driver [47]. The extracellular and TKD (tyrosine kinase domain) mutations of EGFR is causes the glioblastoma NSCLC (non small cell lung cancer) [40-50]. It plays an eminent role in the ductal system growth of mammary glands [40, 45, 88]. Its overexpression also lead the anal cancer and epithelial tumors of the neck and head [51, 52].

By considering the aforementioned reasons, we have chosen HER2 and EGFR proteins as the target receptors for the docking studies and compared their binding energies

which were summarized in Table 7. The molecular docking results for the compounds **4a-f**, **6a-f**, **8a** and **8b** against HER2 were shown in Table 8. The comparative molecular docking studies of the targeted scaffolds **4a-f**, **6a-f**, **8a** and **8b** with the target receptors HER2 and EGFR (as shown in Table 7) unambiguously indicates the affinity of the target compounds with the receptor HER2 is better than that of receptor EGFR. Hence HER2 was chosen as the target receptor for the elaborate discussion. Docking results revealed that the compounds **4a**, **4e**, **4f** and **6a** exhibited least binding energies i.e., −12.16 kcal/mol, −12.93 kcal/mol, −12.98 kcal/mol and − 12.23 kcal/mol respectively against HER2. The best docking poses of the compounds **4a**, **4e**, **4f** and **6a** were shown in figures 3B.5, 3B.6, 3B.7 and 3B.8.

The compound **4a** exhibited five hydrogen bonds; one hydrogen bond in between –NH proton of the oxindole group to the amino acid residue ASP855 (1.70 Å), one hydrogen bond in between carbonyl oxygen of oxindole group with amino acid residue LYS745 (2.39 Å), one pi-donor hydrogen bond in between the phenyl group of oxindole group with amino acid residue ASP855, two carbon-hydrogen bonds in between methyl group of pyrrolidine moiety with amino acid residues ALA743 (3.55 Å) and LEU788 (3.73 Å) respectively. The phenyl ring in the oxindole moiety interacts with amino acid residue LEU788, the phenyl ring in the quinolinyl moiety interacts with the amino acid residues VAL726 and LEU718, the pyridyl in the quinoline moiety interacts with the amino acid residues LEU844, VAL726, LEU718 and ALA743, the tetrazole ring interacts with the amino acid residues LEU844, ALA743, MET793 and LEU792 through hydrophobic interactions. The compound **4e** exhibited six hydrogen bonds; one hydrogen bond in between –NH proton of the oxindole group to the amino acid residue ASP855 (1.65 Å), one hydrogen bond in between carbonyl oxygen of oxindole group with amino acid residue LYS745 (2.36 Å), one pi-donor hydrogen bond in between the phenyl group of oxindole group with amino acid residue ASP855 (3.11 Å), one hydrogen bond in between nitrogen atom of the tetrazole moiety with amino acid residue MET793 (1.61 Å), two carbon-hydrogen bonds in between methyl group of pyrrolidine moiety with amino acid residues ALA743 (3.78 Å) and LEU788 (3.61 Å) respectively. The chlorine atom of the oxindole moiety interacts with amino acid residues MET766 and LEU777, the phenyl ring in the quinolinyl moiety interacts with the amino acid residues VAL726 and LEU718, the pyridyl in the quinoline moiety interacts with the amino acid residues LEU844, VAL726, LEU718 and ALA743, the tetrazole ring interacts with the

amino acid residues LEU844, ALA743, MET793 and LEU792 through hydrophobic interactions.

The compound **4f** exhibited six hydrogen bonds; one hydrogen bond in between –NH proton of the oxindole group to the amino acid residue ASP855 (1.65 Å), one hydrogen bond in between carbonyl oxygen of oxindole group with amino acid residue LYS745 (2.30 Å), one pi-donor hydrogen bond in between the phenyl group of oxindole group with amino acid residue ASP855 (3.06 Å), one hydrogen bond in between nitrogen atom of the tetrazole moiety with amino acid residue MET793 (1.72 Å), two carbon-hydrogen bonds in between methyl group of pyrrolidine moiety with amino acid residues ALA743 (3.76 Å) and LEU788 (3.70 Å) respectively. The bromine atom of the oxindole moiety interacts with amino acid residue LEU777, the phenyl ring in the quinolinyl moiety interacts with the amino acid residues VAL726 and LEU718, the pyridyl in the quinoline moiety interacts with the amino acid residues LEU844, VAL726, LEU718 and ALA743, the tetrazole ring interacts with the amino acid residues LEU844, ALA743, MET793 and LEU792 through hydrophobic interactions. In addition to these interactions, the bromine atom of the oxindole ring interacts with the amino acid residue LEU777 through halogen acceptor interaction in which the amino acid acts as halogen acceptor. The compound **6a** exhibited four hydrogen bonds; one hydrogen bond in between –NH proton of the oxindole group and the amino acid residue ASP855 (1.66 Å), one hydrogen bond in between carbonyl oxygen of oxindole group with amino acid residue LYS745 (2.41 Å), one pi-donor hydrogen bond in between the phenyl group of oxindole group with amino acid residue ASP855 (2.99 Å), one hydrogen bond in between nitrogen atom of the tetrazole moiety with amino acid residue MET793 (1.81 Å). The pyrrolidine ring interacts with amino acid residue LYS745, VAL726 and ALA743, the phenyl ring in the quinolinyl moiety interacts with the amino acid residues VAL726 and LEU718, the pyridyl in the quinoline moiety interacts with the amino acid residues LEU844, VAL726, LEU718 and ALA743, the tetrazole ring interacts with the amino acid residues LEU844, ALA743, MET793 and LEU792 through hydrophobic interactions.

Table 7. The molecular docking results of the target compounds with the HER2 and EGFR proteins.

S. No.	Compound	Binding energy (kcal/mol)	
		HER2 (PDB ID: 3POZ)	**EGFR (PDB ID: 4HJO)**
1	**4a**	**−12.16**	−11.32
2	**4b**	−10.27	−8.98
3	**4c**	− 9.24	−8.88
4	**4d**	−10.54	−10.18
5	**4e**	**−12.93**	−11.49
6	**4f**	**−12.98**	−11.56
7	**6a**	**−12.23**	− 9.67
8	**6b**	− 9.82	−10.25
9	**6c**	− 9.98	− 9.11
10	**6d**	−10.45	−10.45
11	**6e**	− 9.99	− 9.38
12	**6f**	−10.17	− 9.21
13	**8a**	−10.08	− 9.78
14	**8b**	−11.31	−10.05

Table 8: The docking results of the target compounds with the HER2 (PDB ID: 3POZ).

S. No.	Compound	Binding energies (kcal/mol)	HER2 (PDB ID: 3POZ)		
			No. of hydrogen bonds	**Residues involved in the hydrogen bonding**	**Hydrogen bond length (Å)**
1	**4a**	**−12.16**	5	ASP855, LYS745, ALA743, LEU788	1.70, 2.39, 3.17, 3.55, 3.73
2	**4b**	−10.27	3	LYS745, ASP855, LEU788	2.80, 3.13, 3.61
3	**4c**	− 9.24	4	ARG841, CYS797	2.22, 2.80, 3.38, 3.39

4	**4d**	−10.54	1	ASN842	3.32
5	**4e**	**−12.93**	6	ASP855, LYS745, MET793, ALA743, LEU788	1.61, 1.65, 2.36, 3.11, 3.61, 3.78
6	**4f**	**−12.98**	6	ASP855, MET793, LYS745, LEU788, ALA743	1.65, 1.72, 2.30. 3.06, 3.70. 3.76
7	**6a**	**−12.23**	4	ASP855, LYS745, MET793	1.66, 1.81, 2.41, 2.99
8	**6b**	− 9.82	2	LYS745, ASN842	1.78, 1.88
9	**6c**	− 9.98	1	LYS745	1.85
10	**6d**	−10.45	1	LYS745	1.96
11	**6e**	− 9.99	2	LYS745, ASN842	1.91, 3.79
12	**6f**	−10.17	2	LYS745, ASN842	1.86, 3.62
13	**8a**	−10.08	1	LYS745	2.18
14	**8b**	−11.31	1	ASP855	3.01

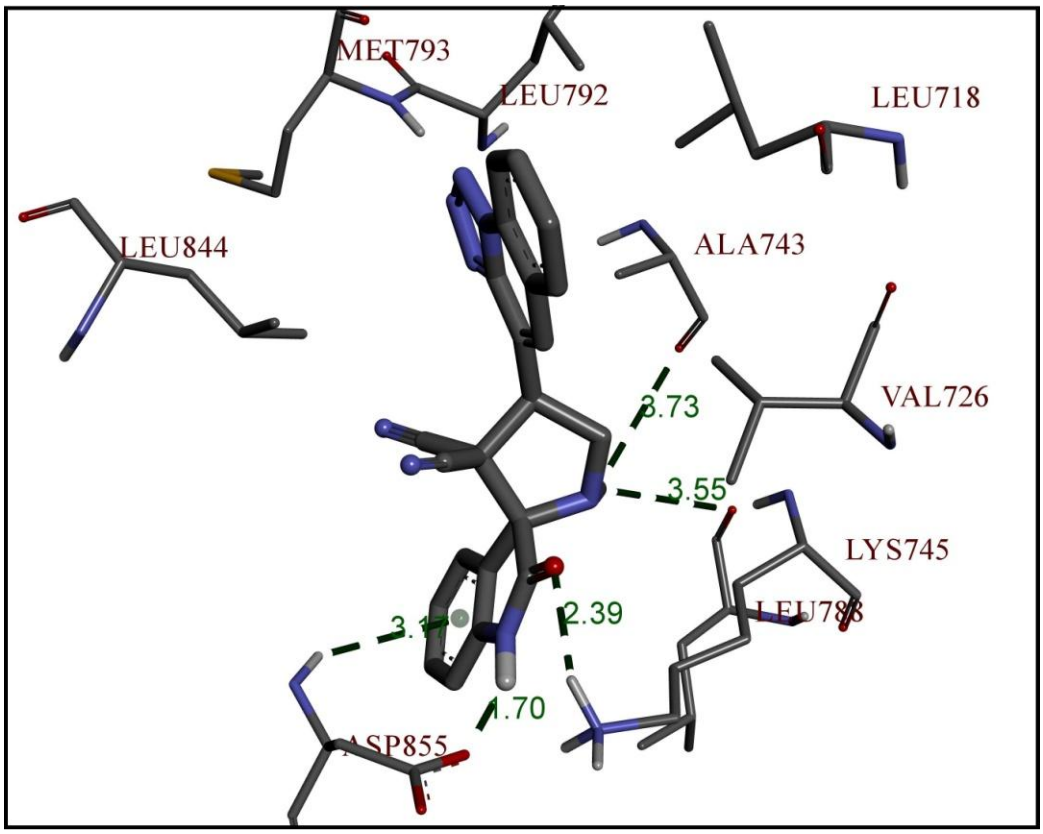

a)

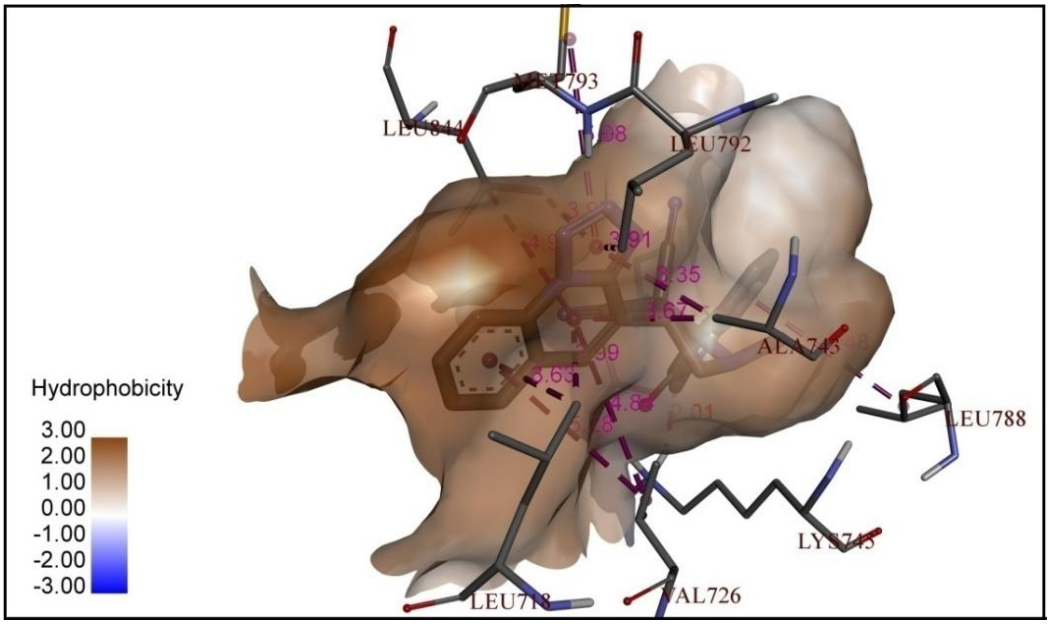

b)

Figure 3B.5. The best docking poses of **4a** with HER2. a) The hydrogen bond interactions, b) The hydrophobic interactions.

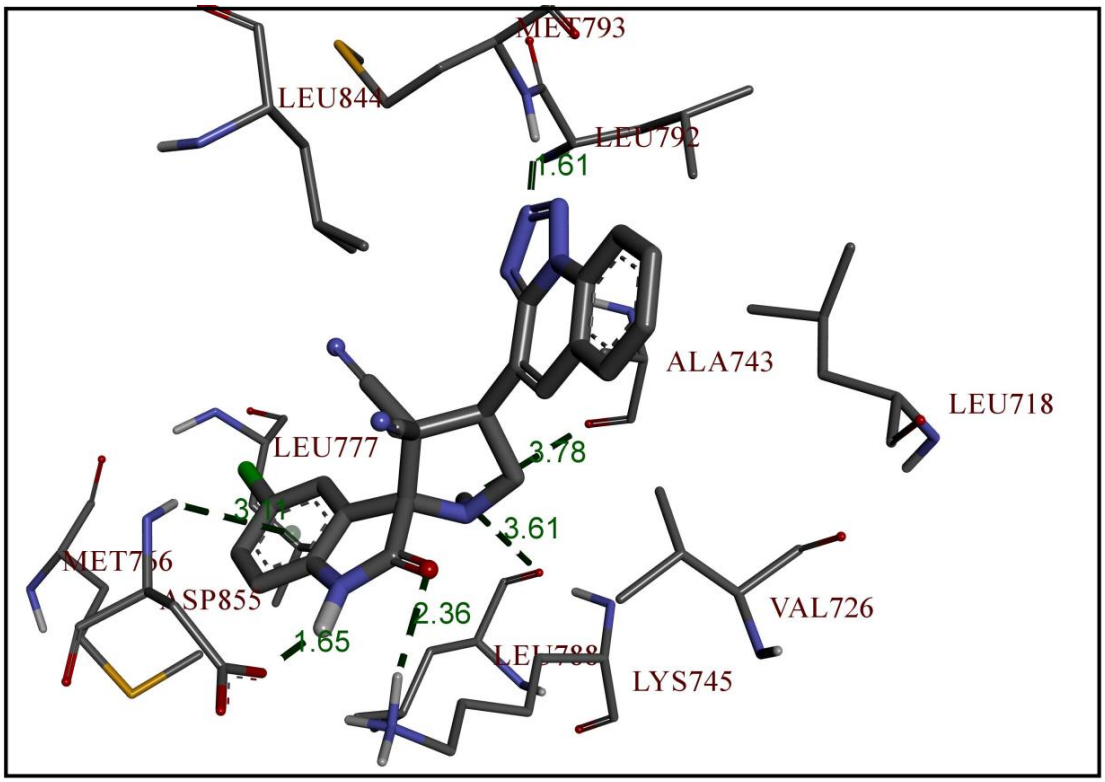

a)

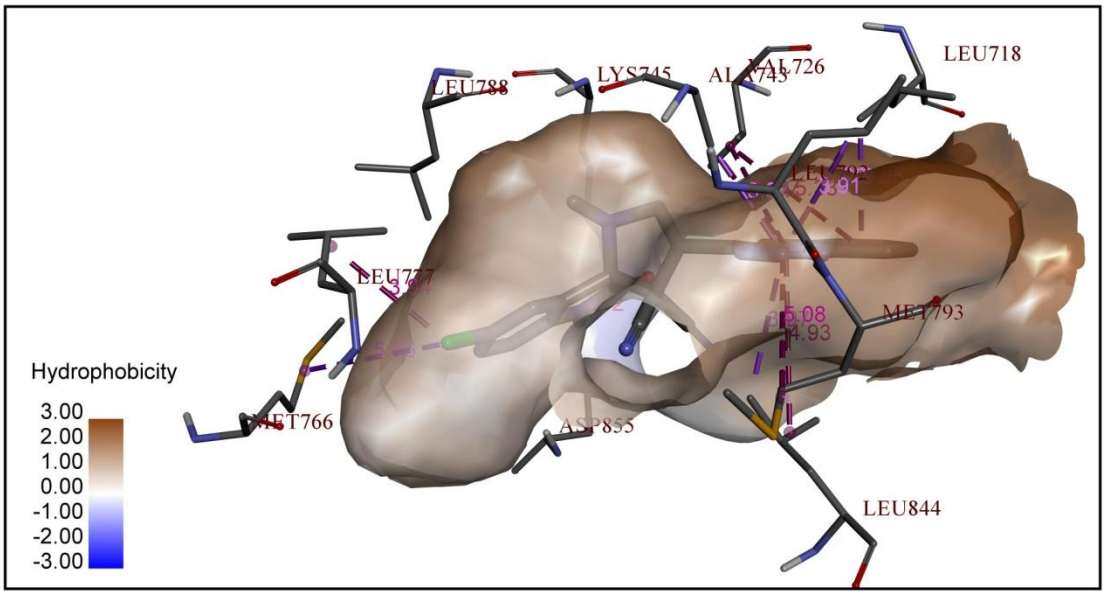

b)

Figure 3B.6. The best docking poses of **4e** with HER2. a) The hydrogen bond interactions, b) The hydrophobic interactions.

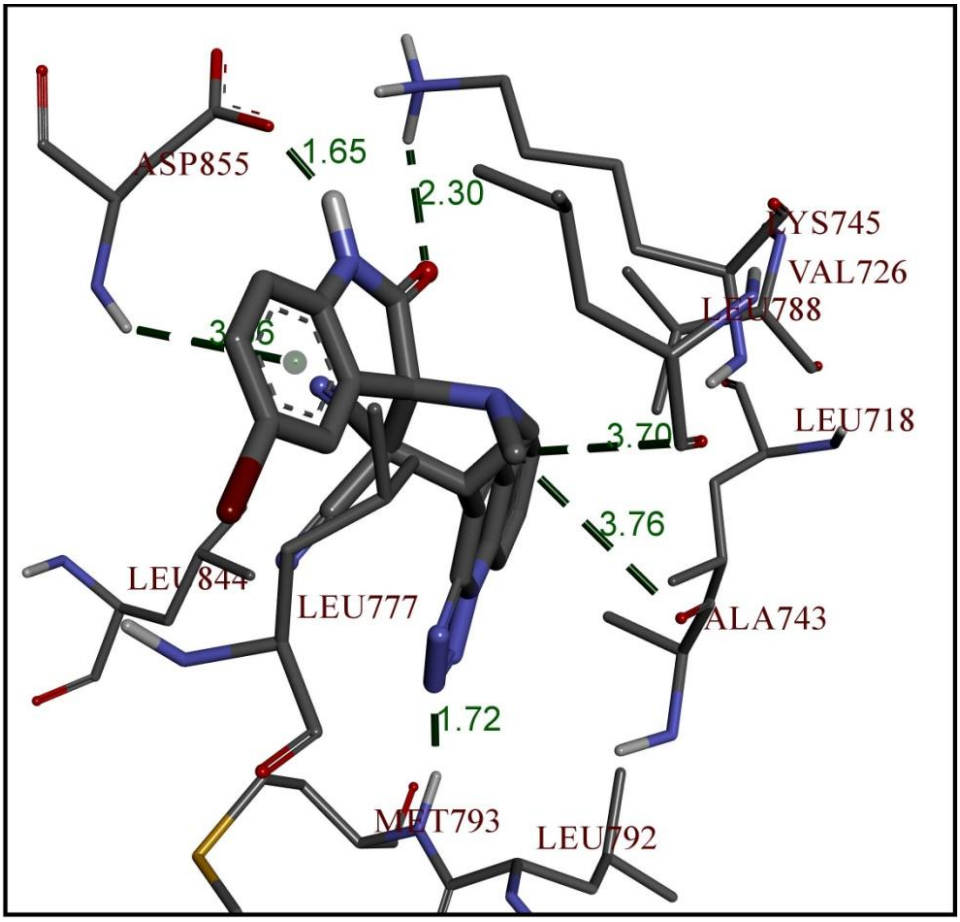

a)

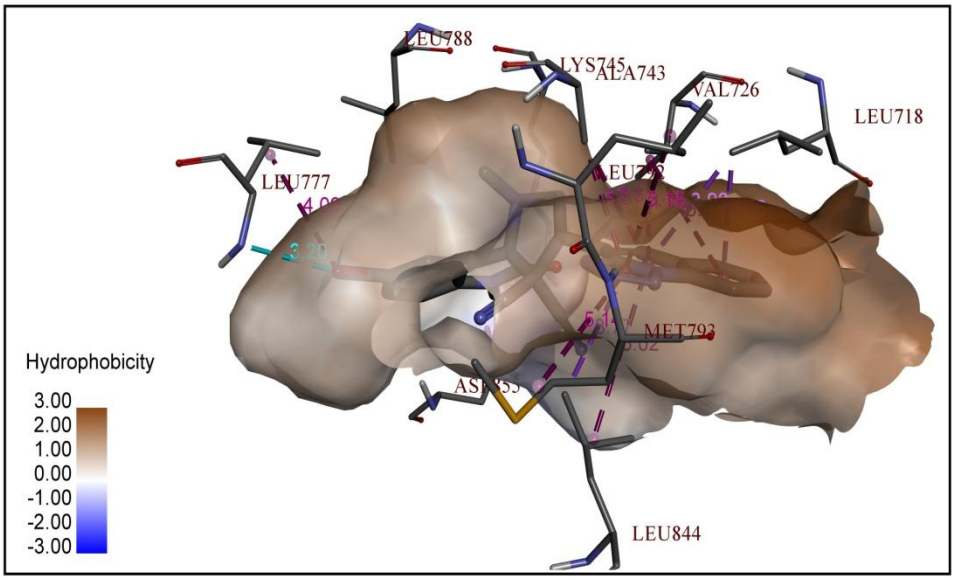

b)

Figure 3B.7. The best docking poses of **4f** with HER2. a) The hydrogen bond interactions, b) The hydrophobic interactions.

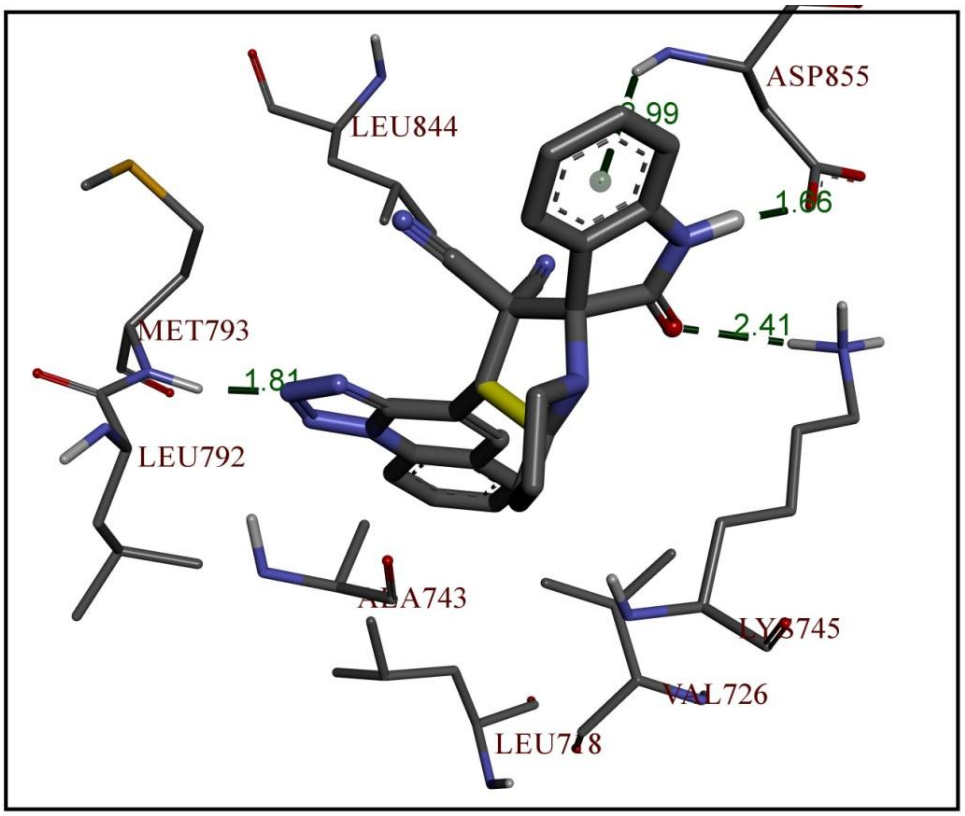

a)

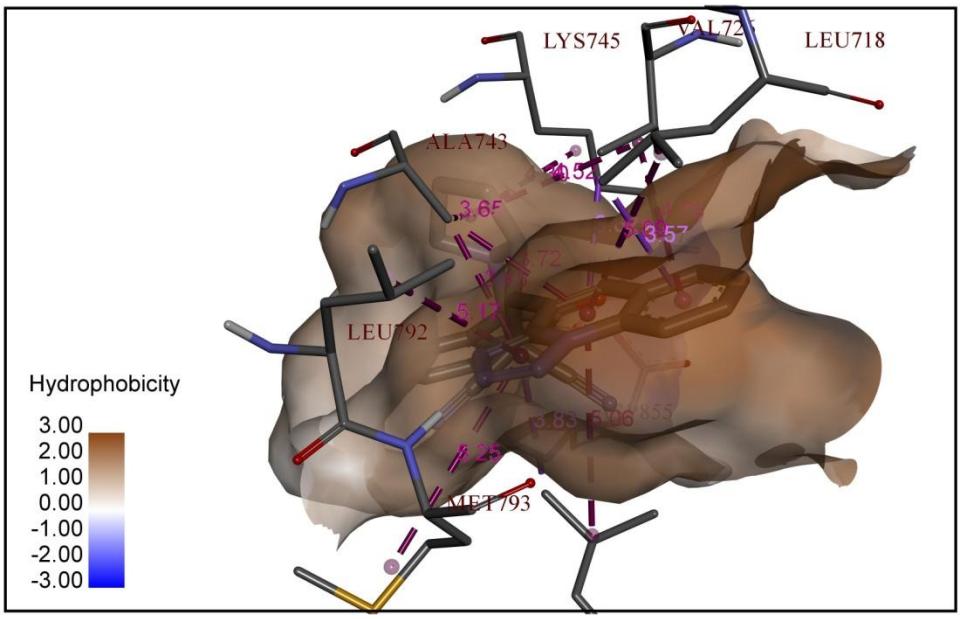

b)

Figure 3B.8. The best docking poses of **4f** with HER2. a) The hydrogen bond interactions, b) The hydrophobic interactions.

3B.5. Conclusion

A series of novel tetrazole fused quinolinyl grafted spirooxindoles and spiroquinoxalines were efficiently synthesized *via* one-pot multicomponent [3+2] cycloaddition reaction in ethanol under reflux condition and characterized by various spectroscopic techniques (FTIR, NMR and Mass). Further, the synthesized compounds were evaluated for their *in vitro* anticancer, antioxidant and antimicrobial activities. Among all the compound, the compound **4f** exhibited remarkable cytotoxic and antioxidant activities, whereas, the compounds **4a, 4e**, **8a** and **8b** were showed significant to moderate activity against all the tested cancer cell lines. The compounds **8a** and **8b** exhibited potent antibacterial and antifungal activities when compared with other synthesized compounds. The anticancer activity of all the synthesized compounds was well correlated with the molecular docking studies.

3B.6. Spectral data

1'-Methyl-2-oxo-4'-(tetrazolo[1,5-*a*]quinolin-4-yl)spiro[indoline-3,2'-pyrrolidine]-3',3'-dicarbonitrile (4a)

Colour: White. M. P. 193-195 ℃. IR (KBr, cm^{-1}): 3405, 2949, 2219, 1640. ^{1}H NMR (400 MHz, DMSO-*d6*) δ: 11.28 (s, 1H), 8.47 (s, 1H), 7.90 (d, 1H, *J* = 7.6 Hz), 7.62-7.48 (m, 3H), 7.40 (t, 1H, *J* = 8.8 Hz), 7.29 (t, 1H, *J* = 7.2 Hz), 7.25-6.98 (m, 2H), 5.25 (t, 1H, *J* = 8.8 Hz), 3.86 (t, 1H, *J* = 9.6 Hz), 3.74 (t, 1H, *J* = 10.4 Hz), 2.24 (s, 3H). ^{13}C NMR (100 MHz, DMSO-*d6*) δ: 178.65, 151.20, 146.39, 141.53, 137.68, 136.96, 133.72, 133.41, 131.11, 129.57, 128.83, 128.51, 128.09, 127.94, 126.32, 111.28, 79.69, 60.28, 60.00, 40.95, 35.02. ESI mass spectrum (*m/z*): 419.15 (M-). Anal. Calcd. For $C_{23}H_{16}N_8O$: C, 65.71; H, 3.84; N, 26.65; found: C, 65.92; H, 3.90; N, 26.46.

1-Ethyl-1'-methyl-2-oxo-4'-(tetrazolo[1,5-*a*]quinolin-4-yl)spiro[indoline-3,2'-pyrrolidine]-3',3'-dicarbonitrile (4b)

Colour: White. M. P. 201-203 ℃. IR (KBr, cm^{-1}): 2835, 2228, 1726. ^{1}H NMR (400 MHz, DMSO-*d6*) δ: 8.69 (d, 2H, *J* = 11.2 Hz), 7.32 (d, 1H, *J* = 8.0 Hz), 8.07 (t, 1H, *J* = 7.6 Hz), 7.92 (t, 1H, *J* = 7.6 Hz), 7.68 (d, 2H, *J* = 7.2 Hz), 7.58 (t, 1H, *J* = 7.2 Hz), 7.35-7.27 (m, 3H),

5.28 (d, 2H, *J* = 8.4 Hz), 4.45 (d, 1H, *J* = 9.2 Hz), 3.83-3.67 (m, 2H), 2.20 (s, 3H), 1.10 (t, 3H, *J* = 6.8 Hz). ^{13}C NMR (100 MHz, DMSO-*d6*) *δ*: 179.31, 154.27, 145.32, 143.48, 143.00, 135.73, 133.94, 130.69, 129.10, 128.75, 125.81, 123.44, 111.39, 109.53, 74.89, 63.56, 52.07, 49.37, 47.04, 36.03, 13.29. ESI mass spectrum (*m/z*): 447.15 (M-). Anal. Calcd. For $C_{25}H_{20}N_8O$: C, 66.95; H, 4.50; N, 24.99; found: C, 67.12; H, 5.60; N, 24.71.

1'-Methyl-2-oxo-1-propyl-4'-(tetrazolo[1,5-*a*]quinolin-4-yl)spiro[indoline-3,2'-pyrrolidine]-3',3'-dicarbonitrile (4c)

Colour: White. M. P. 213-215 ℃. IR (KBr, cm^{-1}): 2852, 2247, 1723. ^{1}H NMR (400 MHz, DMSO-*d6*) *δ*: 8.89 (d, 2H, *J* = 11.2 Hz), 8.52 (d, 1H, *J* = 8.0 Hz), 8.24 (bs, 8.24), 7.85 (d, 1H, *J* = 7.6), 7.69-7.53 (m, 2H), 7.40-7.24 (m, 3H), 5.56 (t, 1H, *J* = 8.0 Hz), 4.16 (t, 1H, *J* = 8.8 Hz), 3.73-3.54 (m, 3H), 2.13 (s, 3H), 1.62-1.51 (m, 2H), 0.85 (t, 3H, *J* = 6.8 Hz). ESI mass spectrum (*m/z*): 463.30 (M+). Anal. Calcd. For $C_{26}H_{22}N_8O$: C, 67.52; H, 4.79; N, 24.23; found: C, 67.27; H, 4.72; N, 24.05.

1-Benzyl-1'-methyl-2-oxo-4'-(tetrazolo[1,5-*a*]quinolin-4-yl)spiro[indoline-3,2'-pyrrolidine]-3',3'-dicarbonitrile (4d)

Colour: White. M. P. 229-231 ℃. IR (KBr, cm^{-1}): 2854, 2254, 1716. ^{1}H NMR (400 MHz, DMSO-*d6*) *δ*: 8.74-8.68 (m, 2H), 8.43-8.38 (m, 1H), 8.06 (t, 1H, *J* = 6.8 Hz), 7.90 (t, 1H, *J* = 6.0 Hz), 7.72 (d, 1H, *J* = 7.6 Hz), 7.53-7.09 (m, 7H), 5.33 (t, 1H, *J* = 8.0 Hz), 5.18-4.88 (m, 2H), 3.93-3.82 (m, 2H), 2.23 (s, 3H). ESI mass spectrum (*m/z*): 409.30 (M-). Anal. Calcd. For $C_{30}H_{22}N_8O$: C, 70.58; H, 4.34; N, 21.95; found: C, 70.72; H, 4.27; N, 22.15.

5-Chloro-1'-methyl-2-oxo-4'-(tetrazolo[1,5-*a*]quinolin-4-yl)spiro[indoline-3,2'-pyrrolidine]-3',3'-dicarbonitrile (4e)

Colour: White. M. P. 222-224 ℃. IR (KBr, cm^{-1}): 2858, 2251, 1735. ^{1}H NMR (400 MHz, DMSO-*d6*) *δ*: 11.23 (s, 1H), 8.42 (s, 1H), 7.67-7.52 (m, 2H), 7.45 (t, 1H, *J* = 8.8 Hz), 7.33 (t, 1H, *J* = 7.2 Hz), 7.29-7.02 (m, 2H), 5.21 (t, 1H, *J* = 8.0 Hz), 3.81 (t, 1H, *J* = 9.6 Hz), 3.69 (t, 1H, *J* = 10.4 Hz), 2.19 (s, 3H). ^{13}C NMR (100 MHz, DMSO-*d6*) *δ*: 179.64, 152.19, 147.38, 142.52, 138.67, 137.95, 134.71, 134.40, 132.10, 130.56, 129.98, 129.82, 129.50, 129.08, 128.88, 128.73, 127.24, 112.27, 73.91, 61.27, 60.99, 41.94, 36.01. ESI mass spectrum (*m/z*):

455.25 (M+). Anal. Calcd. For $C_{23}H_{15}ClN_8O$: C, 60.73; H, 3.32; N, 24.63; found: C, 60.99; H, 3.37; N, 24.79.

5-Bromo-1'-methyl-2-oxo-4'-(tetrazolo[1,5-*a*]quinolin-4-yl)spiro[indoline-3,2'-pyrrolidine]-3',3'-dicarbonitrile (4f)

Colour: White. M. P. 235-237 ℃. IR (KBr, cm^{-1}): 2879, 2231, 1725. ^{1}H NMR (400 MHz, DMSO-*d6*) δ: 11.19 (s, 1H), 8.37 (s, 1H), 7.84 (d, 1H, *J* = 7.6 Hz), 7.62-7.38 (m, 3H), 7.29 (t, 1H, *J* = 7.2 Hz), 7.25-6.98 (m, 2H), 5.20 (t, 1H, *J* = 6.0 Hz), 3.77 (t, 1H, *J* = 9.6 Hz), 3.65 (t, 1H, *J* = 10.4 Hz), 2.15 (s, 3H). ^{13}C NMR (100 MHz, DMSO-*d6*) δ: 179.11, 151.66, 146.84, 141.99, 138.13, 137.42, 134.17, 133.86, 131.56, 130.03, 129.28, 128.54, 128.20, 126.78, 126.70, 111.74, 73.37, 60.73, 60.45, 41.41, 35.47. Anal. Calcd. For $C_{23}H_{15}BrN_8O$: C, 55.32; H, 3.03; N, 22.44; found: C, 55.05; H, 3.07; N, 22.81.

2-Oxo-1'-(tetrazolo[1,5-*a*]quinolin-4-yl)-5',6',7',7a'-tetrahydrospiro[indoline-3,3'-pyrrolizine]-2',2'(1'*H*)-dicarbonitrile (6a)

Colour: White. M. P. 240-242 ℃. IR (KBr, cm^{-1}): 3404, 2966, 2219, 1640. ^{1}H NMR (400 MHz, DMSO-*d6*) δ: 10.95 (S, 1H), 8.20 (s, 1H), 7.71 (d, 1H, *J* = 7.6 Hz), 7.65 (d, 1H, *J* = 7.2 Hz), 7.46 (t, 1H, *J* = 7.2 Hz), 7.37 (t, 1H, *J* = 7.6 Hz), 7.28 (d, 1H, *J* = 8.0 Hz), 7.18-7.09 (m, 2H), 6.90 (d, 1H, *J* = 7.2 Hz), 4.72-7.71(m, 1H), 4.33 (d, 1H, *J* = 8.0 Hz), 2.86-2.68 (m, 2H), 2.06-1.67 (m, 4H). ^{13}C NMR (100 MHz, DMSO-*d6*) δ: 180.79, 164.85, 152.80, 147.51, 143.73, 138.93, 133.64, 132.37, 132.00, 131.18, 129.69, 129.10, 128.55, 126.40, 123.03, 115.22, 111.53, 74.21, 64.54, 57.26, 49.54, 49.07, 31.45, 28.78. ESI mass spectrum (*m/z*): 447.05 (M-). Anal. Calcd. For $C_{25}H_{18}N_8O$: C, 67.25; H, 4.06; N, 25.10; found: C, 67.05; H, 4.07; N, 24.91.

1-Ethyl-2-oxo-1'-(tetrazolo[1,5-*a*]quinolin-4-yl)-5',6',7',7a'-tetrahydrospiro[indoline-3,3'-pyrrolizine]-2',2'(1'*H*)-dicarbonitrile (6b)

Colour: White. M. P. 253-255 ℃. IR (KBr, cm^{-1}): 2854, 2255, 1735. ^{1}H NMR (400 MHz, DMSO-*d6*) δ: 8.91 (s, 1H), 8.54 (d, 1H, *J* = 8.0 Hz), 8.27 (d, 1H, *J* = 5.6 Hz), 7.87 (d, 1H, *J* = 7.2 Hz) 7.90-7.59 (m, 3H), 7.42-7.27 (m, 2H), 4.69 (d, 1H, *J* = 8.0 Hz), 4.28-4.23 (m, 1H), 3.74-3.52 (m, 2H), 2.62-1.77 (m, 6H), 1.04 (t, 3H, *J* = 7.2 Hz). ^{13}C NMR (100 MHz,

DMSO-*d6*) δ: 178.60, 153.57, 144.61, 142.78, 142.30, 135.02, 133.23, 129.98, 128.39, 128.05, 125.11, 122.73, 110.68, 108.82, 106.62, 74.18, 62.85, 51.36, 48.66, 46.34, 35.32, 31.36, 27.85, 12.58. ESI mass spectrum (*m/z*): 473.35 (M-). Anal. Calcd. For $C_{27}H_{22}N_8O$: C, 68.34; H, 4.67; N, 23.61; found: C, 68.05; H, 4.69; N, 23.87.

2-Oxo-1-propyl-1'-(tetrazolo[1,5-*a*]quinolin-4-yl)-5',6',7',7a'-tetrahydrospiro[indoline-3,3'-pyrrolizine]-2',2'(1'*H*)-dicarbonitrile (6c)

Colour: White. M. P. 249-251 °C. IR (KBr, cm^{-1}): 2849, 2255, 1737. ^1H NMR (400 MHz, DMSO-*d6*) δ: 8.78 (s, 1H), 8.41 (d, 1H, *J* = 8.0 Hz), 8.14 (bs, 1H), 7.74 (d, 1H, *J* = 7.6 Hz) 7.58-7.14 (m, 10H), 4.46 (t, 1H, *J* = 8.0 Hz), 3.63-3.43 (m, 3H), 2.49-1.40 (m, 8H), 0.75 (t, 3H, *J* = 6.8 Hz). ESI mass spectrum (*m/z*): 487.15 (M-). Anal. Calcd. For $C_{28}H_{24}N_8O$: C, 68.84; H, 4.95; N, 22.94; found: C, 69.05; H, 4.99; N, 22.78.

1-Benzyl-2-oxo-1'-(tetrazolo[1,5-*a*]quinolin-4-yl)-5',6',7',7a'-tetrahydrospiro[indoline-3,3'-pyrrolizine]-2',2'(1'*H*)-dicarbonitrile (6d)

Colour: White. M. P. 257-257 °C. IR (KBr, cm^{-1}): 2965, 2258, 1724. ^1H NMR (400 MHz, DMSO-*d6*) δ: 8.72 (s, 1H), 8.36 (d, 1H, *J* = 8.0 Hz), 8.13 (bs, 1H), 7.69 (d, 1H, *J* = 7.6 Hz) 7.51-7.12 (m, 9H), 6.90 (t, 1H, *J* = 7.6 Hz), 4.94-4.79 (m, 2H, *J* = 6.0 Hz), 4.70 (d, 1H, *J* = 8.0 Hz), 4.11-4.05 (m, 1H), 1.766-2.64 (m, 6H). ^{13}C NMR (100 MHz, DMSO-*d6*) δ: 179.73, 154.70, 145.75, 143.91, 143.43, 136.16, 134.37, 131.12, 129.53, 129.18, 126.24, 123.87, 111.82, 109.96, 75.32, 63.99, 52.49, 49.80, 47.47, 36.46, 32.50, 28.99. ESI mass spectrum (*m/z*): 536.05 (M+). Anal. Calcd. For $C_{32}H_{24}N_8O$: C, 71.63; H, 4.51; N, 20.88; found: C, 71.85; H, 4.46; N, 22.78.

5-Chloro-2-oxo-1'-(tetrazolo[1,5-*a*]quinolin-4-yl)-5',6',7',7a'-tetrahydrospiro[indoline-3,3'-pyrrolizine]-2',2'(1'*H*)-dicarbonitrile (6e)

Colour: White. M. P. 262-264 °C. IR (KBr, cm^{-1}): 2963, 2230, 1717. ^1H NMR (400 MHz, DMSO-*d6*) δ: 10.98 (S, 1H), 8.23 (s, 1H), 7.74 (d, 1H, *J* = 7.6 Hz), 7.68 (d, 1H, *J* = 7.2 Hz), 7.50 (t, 1H, *J* = 7.2 Hz), 7.39 (t, 1H, *J* = 7.6 Hz), 7.31 (d, 1H, *J* = 8.0 Hz), 7.20-7.11 (m, 2H), 6.93 (d, 1H, *J* = 7.2 Hz), 4.75-7.74(m, 1H), 4.36 (d, 1H, *J* = 8.0 Hz), 2.88-2.71 (m, 2H), 2.08-1.70 (m, 4H) . ^{13}C NMR (100 MHz, DMSO-*d6*) δ: 180.40, 164.47, 152.42, 147.12, 143.34,

138.55, 133.26, 131.98, 131.61, 130.89, 129.30, 128.71, 128.16, 126.01, 122.64, 114.83, 111.14, 74.01, 64.15, 56.87, 49.16, 48.68, 31.06, 28.39. ESI mass spectrum (*m/z*): 479.35 (M+). Anal. Calcd. For $C_{25}H_{17}ClN_8O$: C, 62.44; H, 3.56; N, 23.30; found: C, 62.65; H, 3.64; N, 23.57.

5-Bromo-2-oxo-1'-(tetrazolo[1,5-*a*]quinolin-4-yl)-5',6',7',7a'-tetrahydrospiro[indoline-3,3'-pyrrolizine]-2',2'(1'*H*)-dicarbonitrile (6f)

Colour: White. M. P. 268-270 ℃. IR (KBr, cm^{-1}): 2954, 2225, 1723. ^{1}H NMR (400 MHz, DMSO-*d6*) δ: 10.92 (S, 1H), 8.17 (s, 1H), 7.69 (d, 1H, *J* = 7.6 Hz), 7.62 (d, 1H, *J* = 7.2 Hz), 7.44 (t, 1H, *J* = 7.2 Hz), 7.33 (t, 1H, *J* = 7.6 Hz), 7.35 (d, 1H, *J* = 8.0 Hz), 7.14-7.06 (m, 2H), 6.87 (d, 1H, *J* = 7.2 Hz), 4.69-7.68(m, 1H), 4.30 (d, 1H, *J* = 8.0 Hz), 2.83-2.65 (m, 2H), 2.03-1.64 (m, 4H). ^{13}C NMR (100 MHz, DMSO-*d6*) δ: 180.10, 164.17, 152.12, 146.82, 143.04, 138.25, 132.96, 131.68, 131.31, 130.49, 129.00, 128.41, 127.86, 125.71, 122.34, 114.53, 110.84, 73.71, 63.85, 56.57, 48.86, 48.38, 30.76, 28.09.ESI mass spectrum (*m/z*): 479.35 (M+). Anal. Calcd. For $C_{25}H_{17}BrN_8O$: C, 57.15; H, 3.26; N, 21.33; found: C, 57.35; H, 3.31; N, 21.08.

1'-Methyl-4'-(tetrazolo[1,5-*a*]quinolin-4-yl)spiro[indeno[1,2-*b*]quinoxaline-11,2'-pyrrolidine]-3',3'-dicarbonitrile (8a)

Colour: White. M. P. 246-248 ℃. IR (KBr, cm^{-1}): 2924, 2251, 1712. ^{1}H NMR (400 MHz, DMSO-*d6*) δ: 8.46 (s, 1H), 8.30 (bs, 1H), 7.90 (d, 1H, *J* = 7.6 Hz), 7.65 (d, 2H, *J* = 7.6 Hz), 7.58-7.52 (m, 2H), 7.45 (t, 2H, *J* = 8.8 Hz), 7.33 (t, 1H, *J* = 7.2 Hz), 7.29-7.02 (m, 3H), 5.25 (t, 1H, *J* = 6.0 Hz), 3.88-3.71 (m, 2H), 2.24 (s, 3H). ^{13}C NMR (100 MHz, DMSO-*d6*) δ: 180.27, 152.82, 148.00, 143.15, 139.29, 138.58, 135.33, 135.02, 132.72, 131.19, 130.44, 129.70, 129.36, 127.94, 127.86, 112.90, 74.53, 61.89, 61.61, 42.57, 36.63. ESI mass spectrum (*m/z*): 506.10 (M+). Anal. Calcd. For $C_{30}H_{19}N_9$: C, 71.28; H, 3.79; N, 24.94; found: C, 71.45; H, 3.61; N, 24.75.

1'-(Tetrazolo[1,5-*a*]quinolin-4-yl)-5',6',7',7a'-tetrahydrospiro[indeno[1,2-*b*]quinoxaline-11,3'-pyrrolizine]-2',2'(1'*H*)-dicarbonitrile (8b)

Colour: White. M. P. 241-243 °C. IR (KBr, cm^{-1}): 3051, 2227, 1617. ^{1}H NMR (400 MHz, DMSO-*d6*) δ: 8.29 (s, 1H), 7.73 (d, 1H, *J* = 7.6 Hz), 7.56 (m, 3H), 7.45 (t, 1H, *J* = 8.8 Hz), 7.36 (t, 1H, *J* = 7.2 Hz), 7.27-7.18 (m, 2H), 6.99 (d, 1H, *J* = 7.2 Hz), 4.82-4.79 (m, 1H,), 4.43 (d, 1H, *J* = 8.0 Hz), 2.94-2.77 (m, 2H), 2.14-1.76 (m, 4H). ^{13}C NMR (100 MHz, DMSO-*d6*) δ: 153.51, 152.98, 143.74, 143.41, 142.72, 142.07, 141.74, 137.23, 134.05, 131.98, 131.02, 129.77, 129.70, 128.92, 128.19, 126.99, 122.09, 110.20, 109.65, 106.04, 75.42, 69.35, 63.76, 47.77, 45.81, 31.29, 27.90. Anal. Calcd. For $C_{32}H_{21}N_9$: C, 72.30; H, 3.98; N, 23.71; found: C, 72.45; H, 3.90; N, 23.92.

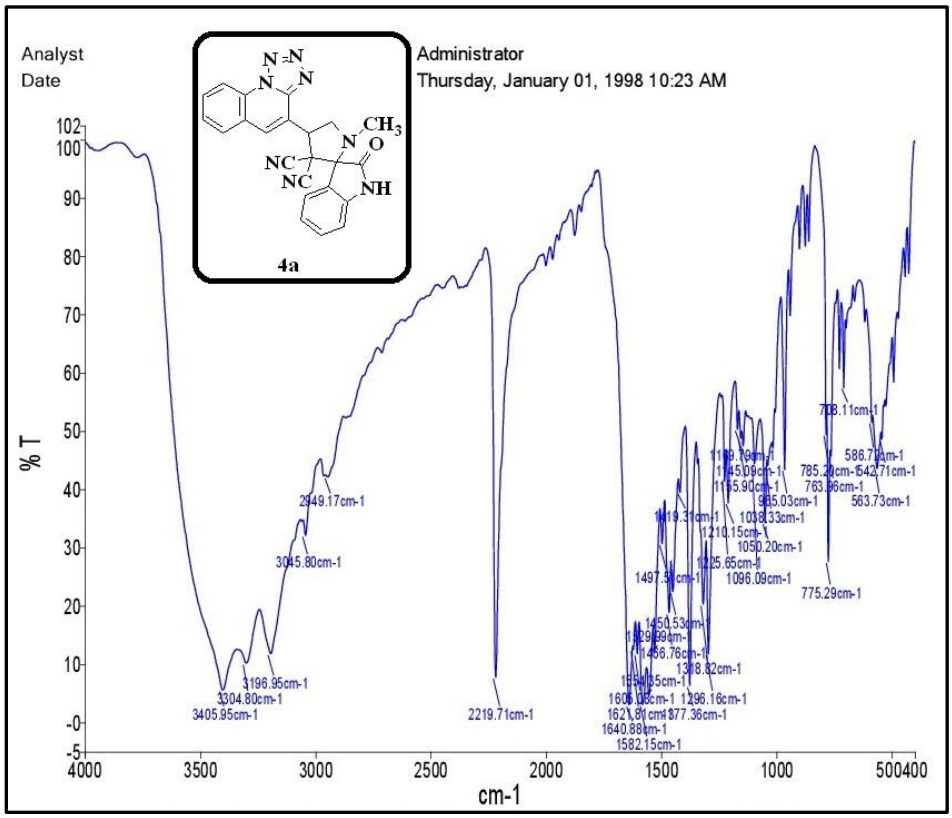

IR spectrum of the compound **4a**

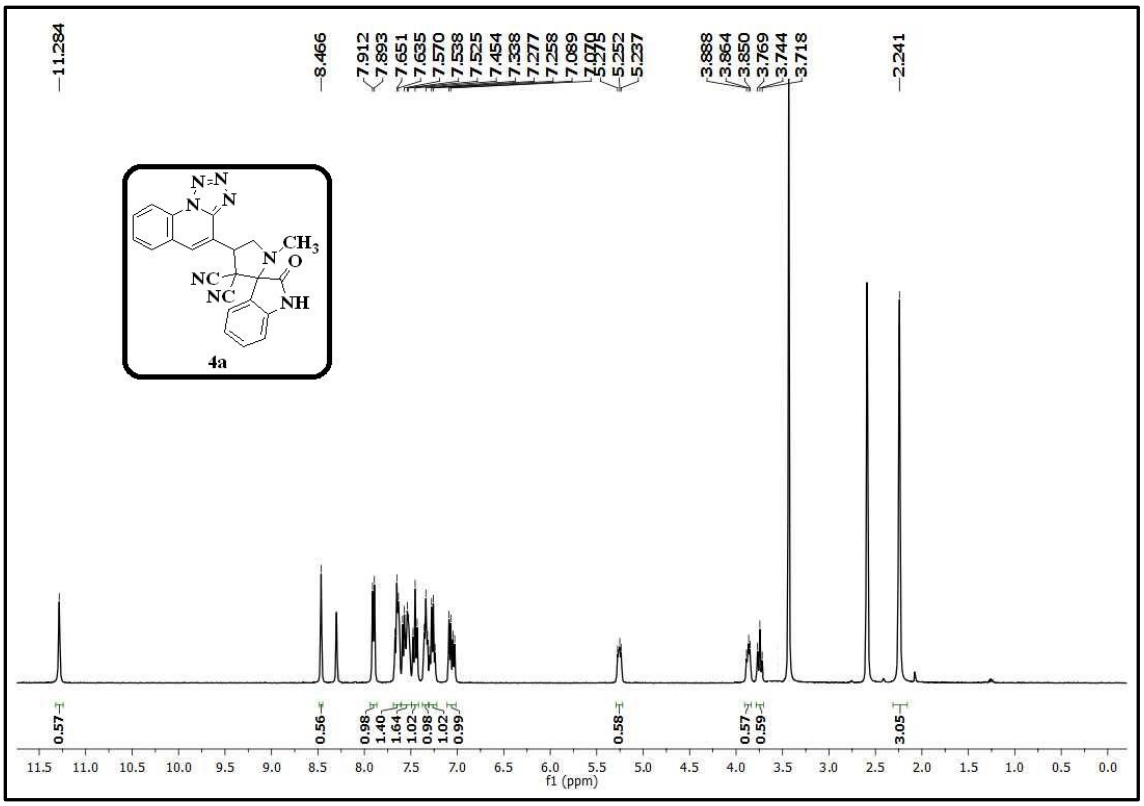

^{1}H NMR spectrum of the compound **4a**

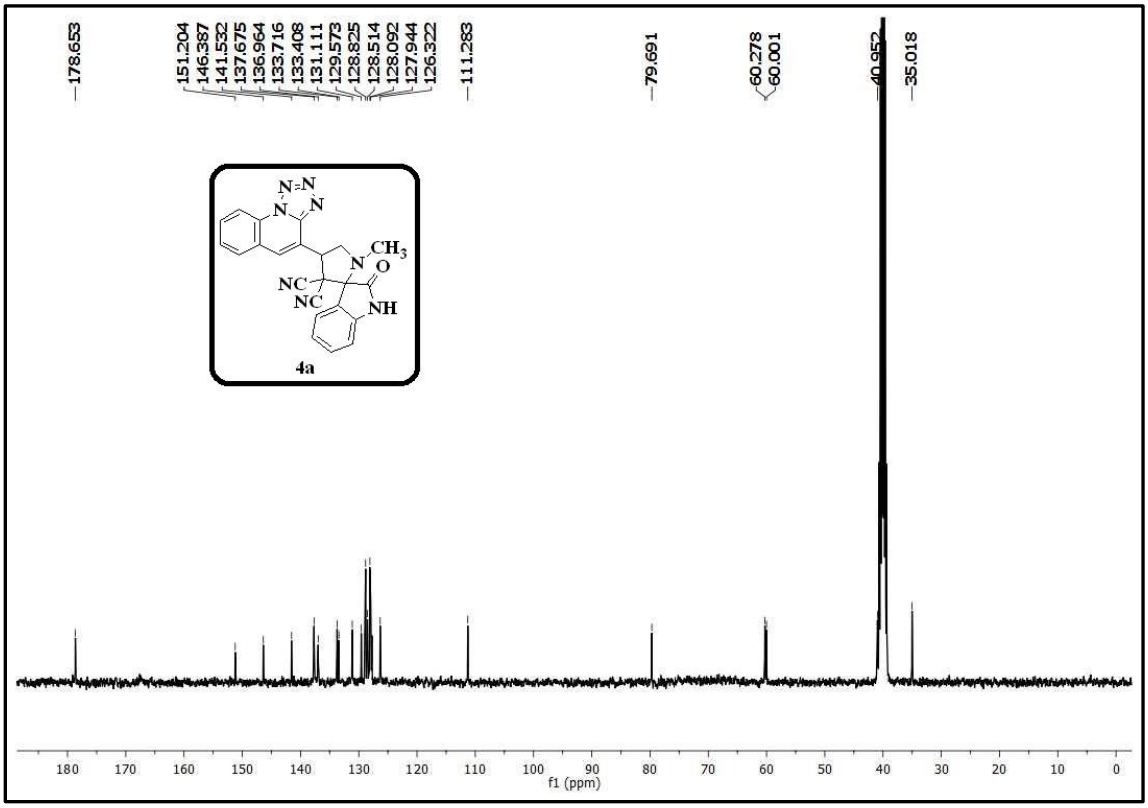

^{13}C NMR spectrum of the compound **4a**

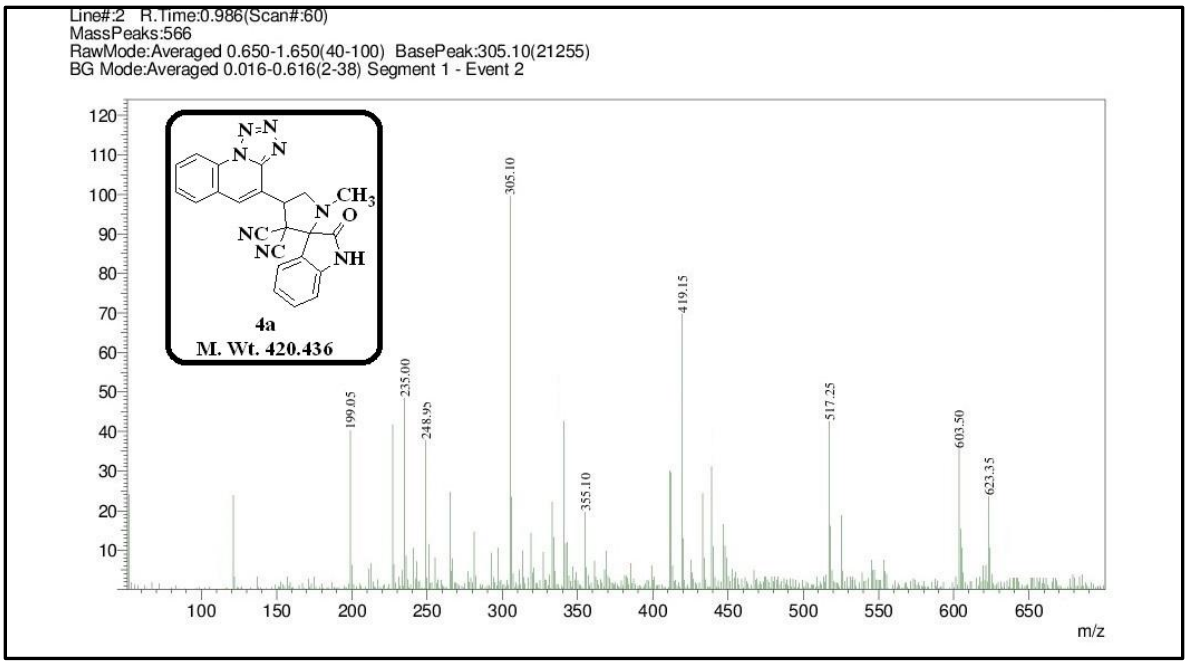

Mass spectrum of the compound **4a**

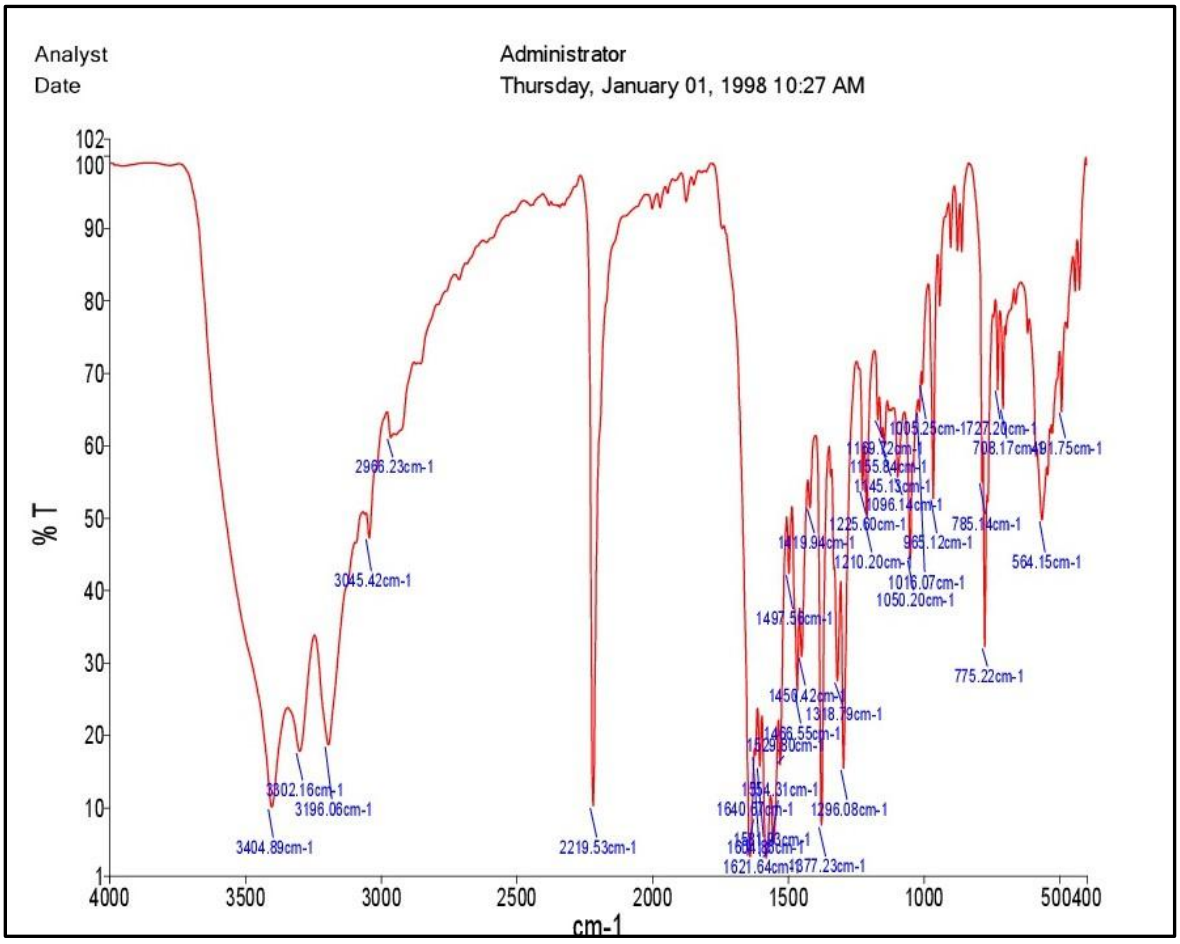

IR spectrum of the compound **6a**

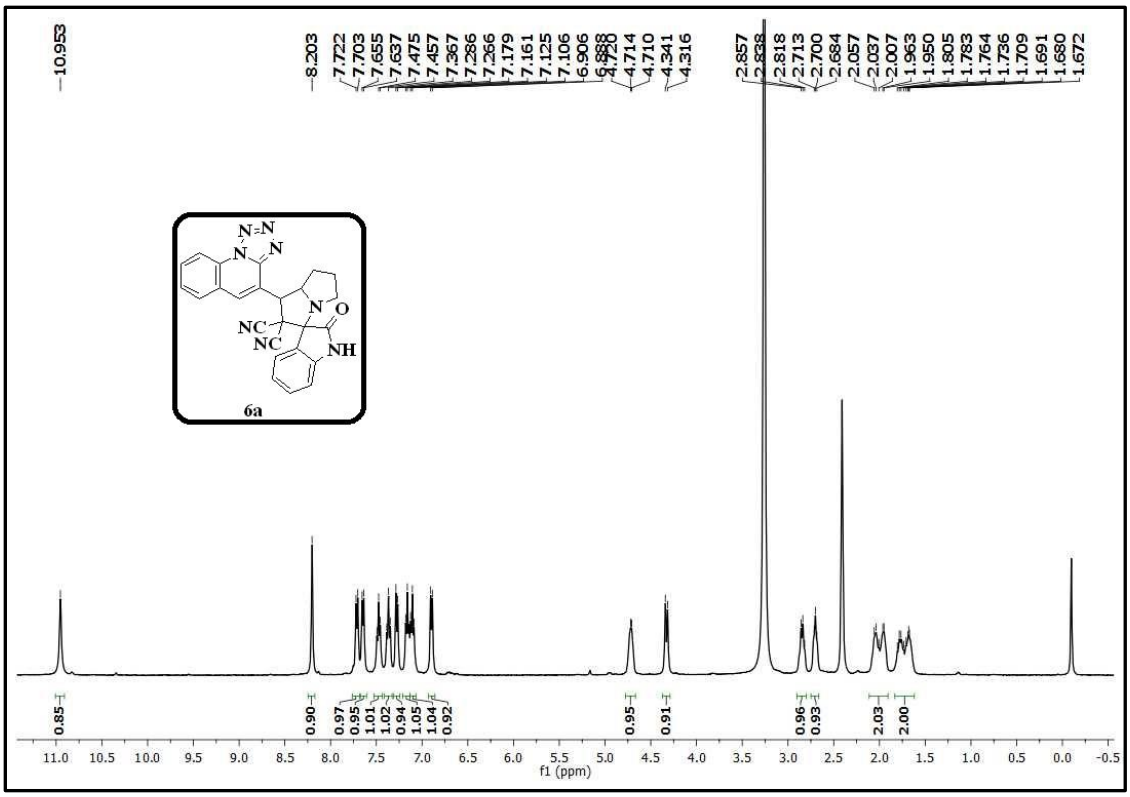

^{1}H NMR spectrum of the compound **6a**

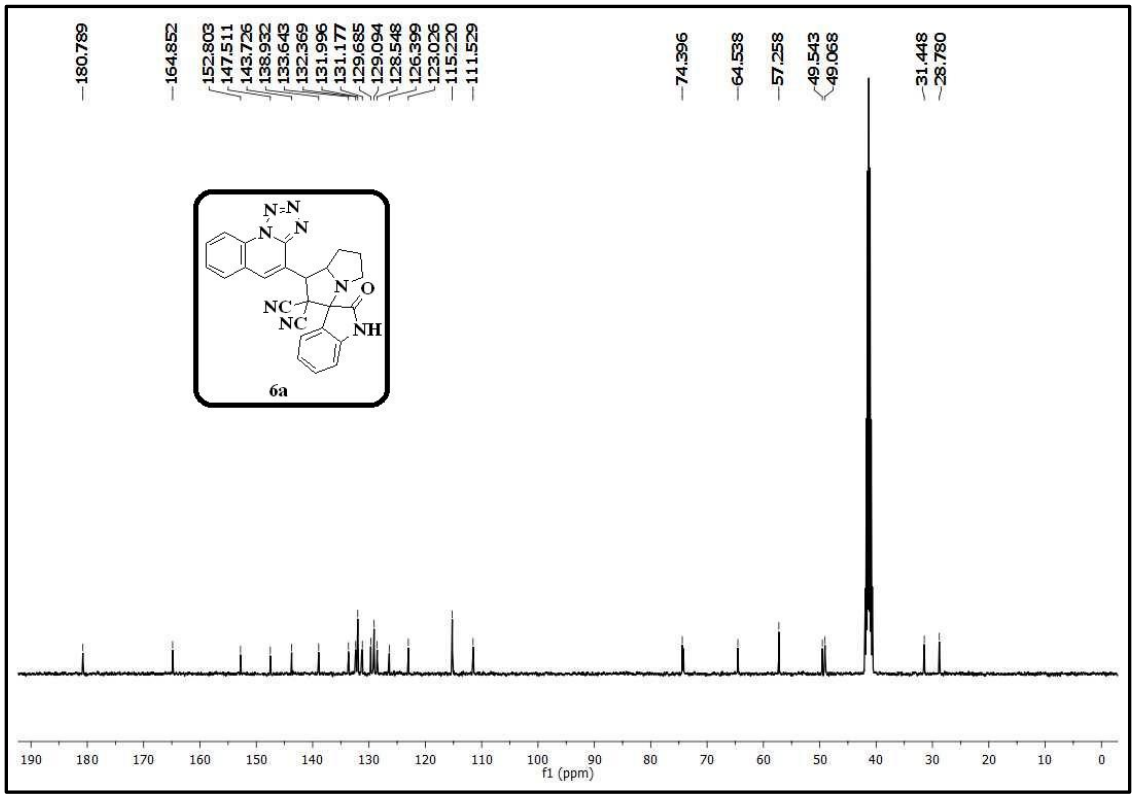

^{13}C NMR spectrum of the compound **6a**

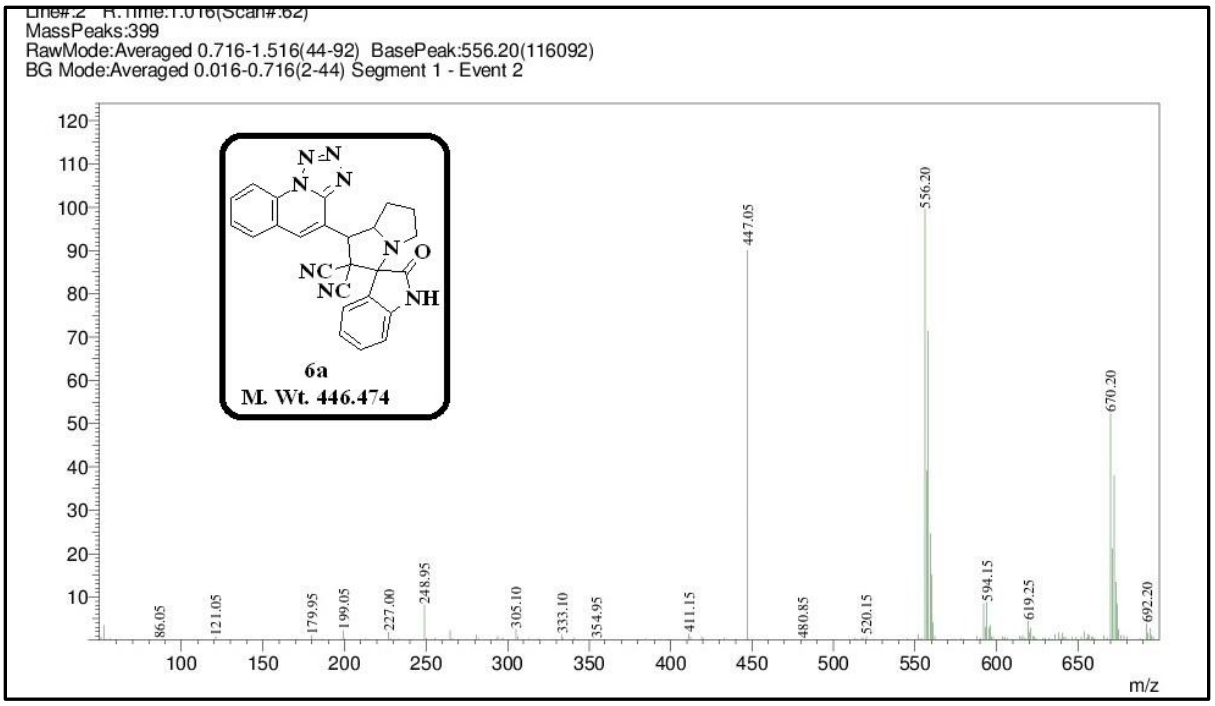

Mass spectrum of the compound **6a**

Experimental Section

Materials and methods

All the melting points were recorded by using Stuart SMP30 melting point apparatus and were uncorrected. IR spectra were recorded on Perkin-Elmer 100S series FT-IR instrument. ^{1}H NMR and ^{13}C NMR spectra were recorded in DMSO-*d*6 and $CDCl_3$ using TMS as an internal standard on a Bruker Avance III HD 400 MHz instrument and the chemical shift values were reported in ppm. Mass spectra were recorded on Joel JMSD-300 spectrometer. The column chromatography was performed on silica gel (100-120 mesh). Progress and purity of the reactions were monitored by Thin-Layer chromatography (E. Merck, Mumbai, India) and the developed chromatogram was visualized under UV light and iodine vapors. Unless otherwise stated, all the chemicals and solvents used were of high grade and purchased from Sigma-Aldrich and spectrochem. Elemental analysis was performed on an Elementar Vario EL III analytical unit and the values were ± 0.4% of theoretical values. The starting materials were prepared from the literature procedure [54-56].

Biological assay

MTT assay

The *In vitro* anticancer activity of the synthesized compounds were assayed against five different human cancer cell lines i.e., neuro blastoma cell line (IMR32), alveolar carcinoma (A549) breast cancer cell line (MCF7), cervical cancer cell line (HeLa), and human embryonic kidney 293 cell line (HEK293T). *Cis*-platin was used as standard drug. The cell viability in the presence of the test samples was measured by MTT-micro cultured tetrazolium assay [89, 90]. This assay is a quantitative colorimetric method for the determination of cell viability. The assessed parameter is the metabolic activity of viable cells. Metabolically active cells reduce pale yellow tetrazolium salt (MTT) to a dark blue water-insoluble formazan, which can be directly quantified after solubilization in DMSO. The absorbance of the formazan directly correlates with the number of viable cells. IMR32, A549, MCF7 and HEK293T cells were plated into a 96-well plate at a density 1 x 10^4 cells/well. Cells were grown overnight in the full medium and then switched to the low serum media. 1% DMSO was used as a control. After 48h of treatment with different concentrations of test compounds, the cells were incubated with MTT (2.5 mg/mL) in the CO_2 chamber for 2h. The medium was then removed and 100 mL of DMSO was added to each well to dissolve formazan crystals. After thorough mixing, the plates were read at 570 nm for optical density, which is directly correlated with cell quantity. The results were represented as a percentage of viability. All the experiments were carried out in triplicates. The relationship between surviving fraction and drug concentration was plotted to obtain the survival curves of IMR32, A549, MCF7 and HEK293T. The IC_{50} values were calculated by using linear regression analysis from the graph pad prism (5.02 version) (P values are significant <0.001). The response parameter calculated was IC_{50} value, which corresponds to the concentration required for 50% inhibition of cell viability.

Antioxidant activity

The free radical scavenging capacity of the synthesized compounds was determined by using DPPH (1,1-Diphenyl-2-picrylhydrazyl) free radical method described in the literature [91-93]. The ascorbic acid was used as a standard to measure the efficiencies of the

synthesized compounds. 0.2 mM solution of DPPH was prepared in 100% methanol. The required amount of ascorbic acid was dissolved in 100% methanol to prepare 1 mM solution and the test compounds were dissolved in 0.2% DMSO and methanol to prepare 1 mM stock solutions. From the stock solutions, different concentrations (3, 10, 30 and 100 µM) of solutions were prepared on diluting with methanol. 1 mL of each compound solution was added to the 3 mL of DPPH solution. After 30min, the absorbance of the solutions at 517 nm (A_1) was recorded using UV–Visible spectrophotometer. As a control, the absorbance of the blank solution of DPPH without test compound was also determined at 517 nm (A_0). The following equation was used for the calculation of the % of scavenging activity.

Scavenging Activity (%) = $\frac{A_0 - A_1}{A_0} \times 100$

Where A_0 is the absorbance of DPPH in the absence of antioxidant and A_1 is the absorbance of DPPH in the presence of an antioxidant. IC_{50} values were also calculated for the compounds.

Antimicrobial activity

The antibacterial and antifungal activity of the target compounds were tested against two gram-positive bacteria (*Bacillus subtilis* and *Staphylococcus aureus*) and two gram-negative bacteria, (*Escherichia coli* and *Pseudomonas aeruginosa*) and two fungal strains, (*Aspergillus niger* and *Pencillium notatum*) using disc diffusion method [94]. On using Whatmann (No. 1) paper, 6 mm diameter sterile antibiotic discs were placed over the nutrient agar medium. With the help of micropipette, 100 µg/mL concentrated compounds were transferred to each disc (Initially compounds were dissolved in DMSO); subsequently bacteria and fungi were incubated overnight at 37 °C and 25 °C, respectively. The zone of inhibition was determined in mm and distinguished using standard antibiotics. DMSO was used as a negative control, while Streptomycin 30 µg/disc (standard antibiotic) and standard antifungal drug Ketoconazole (10 µg/disc) were used as the positive controls. All the tests were carried out in triplicates and the average zone of inhibition was recorded and minimum inhibitory concentration (MIC) values for the tested compounds and standards were measured in µg/mL.

Molecular Docking protocol

In silico docking studies are useful tools to assess the binding affinity of the ligand-protein receptor. The synthesized compounds were subjected to molecular docking by using the AutoDock Tools (ADT) version 1.5.6 and AutoDock version 4.2.5.1 docking program [95]. The 3D-structures of all the synthesized compounds were prepared by using chem3D pro 12.0 software. The optimized 3D structures were saved in .pdb format. The bound ligand and water molecules in protein were removed by using Discovery Studio Visualizer version 4.0 to prepare the protein. Nonpolar hydrogens were merged and gasteiger charges were added to the protein. The grid file was saved in .gpf format. The grid box was created around the protein with spacing 0.3750 Å. The genetic algorithm was carried out with the population size and the maximum number of evaluations were 150 and 25,00,000 respectively. The docking output file was saved as Lamarckian Ga (4.2) in .dpf format. The ligand-protein complex binding sites were visualized by Discovery Studio Visualizer version 4.0.

References

1) M. Fathimunnisa, H. Manikandan, K. Neelakandan, N. R. Prasad, S. Selvanayagam, B. Sridhar, *J. Mol. Struct.* **2016**, *1122*, 205.
2) F. A. Kang, Z. Sui, *Tetrahedron Lett*. **2011**, *52*, 4204.
3) N. Sudhapriya, P. T. Perumal, C. Balachandran, S. Ignacimuthu, M. Sangeetha, M. Doble, *Eur. J. Med. Chem.* **2014**, *83*, 190.
4) K. Kenneth, D. Insuasty, R. Abonia, B. Insuasty, S. D. Bunge, *Tetrahedron Lett.* **2014**, *55*, 4395.
5) B. Yu, Z. Yu, P. P. Qi, D.Q. Yu, H.M. Liu, *Eur. J. Med. Chem.* **2015**, *95*, 35.
6) B. Yu, X. N. Sun, X. J. Shi, P. P. Qi, Y. C. Zheng, D. Q. Yu, H. M. Liu, *Steroids.* **2015**, *102*, 92.
7) G. Lotfy, M. M. Said, E. S. H. E. Ashry, E. S. H. E. Tamany, A. A. Dhfyan, Y. M. A. Aziz, A. Barakat, *Bioorg. Med. Chem.* **2017**, *25*, 1514.
8) S. T. Hilton, T. C. T. Ho, G. Pljevaljcic, K. Jones, *Org. Lett.* **2000**, *2*, 2639.
9) Y. Zhang, Y. Fang, H. Liang, H. Wang, K. Hu, X. Liu, X. Yi, Y. Peng, *Bioorg. Med. Chem. Lett.* **2013**, *23*, 107.

10) Z. C. Liu, B. D. Wang, Z. Y. Yang, Y. Li, D. D. Qin, T. R. Li, *Eur. J. Med. Chem.* **2009**, *44*, 4477.

11) P. K. Kalita, B. Baruah, P. J. Bhuyan, *Tetrahedron Lett*. **2006**, *47*, 7779.

12) P. Vincetti, A. Brianza, N. Scalacci, G. Costantino, D. Castagnolo, M. Radi, *Tetrahedron Lett*. **2016**, *57*, 1464.

13) H. Liu, G. Dou, D. Shi, *J. Comb. Chem.* **2010**, *12*, 633.

14) N, Sudhapriya, P. T. Perumal, C. Balachandran, S. Ignacimuthu, M. Sangeetha, M. Doble, *Eur. J. Med. Chem*. **2014**, *83*, 190.

15) A. S. Girli, A. Yas¸ A. Deureust, B. Kariuki, W. David, B. Knight, *Tetrahedron.* **2013**, *69*, 69.

16) F. Joao, A. A. Filho, C. Barbara, A. Lemos, S. Acacio, D. B. Souza, S. B. Pinheiro, J. Sandro, A. Greco, *Tetrahedron*. **2017**, *73*, 6977.

17) T. N. Trinh, A. McCluskey, *Tetrahedron Lett*. **2016**, *57*, 3256.

18) M. S. Reddy, L. R. Chowhan, N. S. Kumar, P. Ramesh, M. S. Babu, *Tetrahedron Lett*. **2018**, *59*,1366.

19) Y. H. He, J. F. Cao, R. Li, Y. Xiang, D.C. Yang, Z. Guan, *Tetrahedron.* **2015**, *71*, 9299.

20) M. C. Bellucci, A. Sganappa, M. Sani, A. Volonterio, *Tetrahedron.* **2015**, *71*, 7630.

21) P. Pattnaik, S. Nayak, D. R. Mishra, P. Panda, B. P. Raiguru, N. P. Mishra, S. Mohapatra, N. A. Mallampudi, C. S. Purohit. *Tetrahedron Lett.* **2018**, *59*, 2688.

22) J. D. Toker, J. P. Wentworth, Y. Hu, K. N. Houk, D. K. Janda, *J. Am. Chem. Soc.* **2000**, *122*, 3244.

23) J. Gong, Q. Wan, Q. Kang, *Org. Lett.* **2018**, *20*, 3354.

24) Z. Dong, Y. Zhu, B. Li, C. Wang, W. Yan, K. Wang, R. Wang, *J. Org. Chem.* **2017**, *82*, 3482.

25) S. Kanchithalaivan, R. V. Sumesh, R. R. Kumar, *ACS Comb. Sci*. **2014**, *16*, 566.

26) K. Karthikeyan, P. M. Sivakumar, M. Doble, P. T. Perumal, *Eur. J. Med. Chem*. **2010**, *45*, 3446.

27) S. Han, F. F. Zhang, H. Y. Qian, L. L. Chen, J. B. Pu, X. Xie, J. Z. Chen, *J. Med. Chem.* **2015**, *58*, 5751.

28) K. H. Raitio, J. R. Savinainen, J. V. lainen, J. T. Laitinen, A. Poso, T. J. rvinen, T. Nevalainen, *J. Med. Chem.* **2006**, *49*, 2022.

29) J. D. Ruiter, A. N. Brubaker, W. L. Whitmer, J. L. Stein, *J. Med. Chem.* **1986**, *29*, 2025.

30) Y. Zhang, Y. Fang, H. Liang, H. Wang, K. Hu, X. Liu, X. Yi,Y. Peng, *Bioorg. Med. Chem. Lett.* **2013**, *23*, 107.

31) Y. Huang, W. Min, Q. W. Wu, J. Sun, D. H. Shib, C. G. Yan, *New J. Chem.* **2018**, *42*, 16211.

32) A. A. Kelemena, G. Satałab, A. J. Bojarskib, G. M. Keserűa, *Bioorg. Med. Chem. Lett.* **2018**, *28*, 2418.

33) D. B. Ramachary, P. S. Reddy, K. S. Shruthi, R. Madhavachary, P. V. G. Reddy, *Eur. J. Org. Chem.* **2016**, *31*, 5220.

34) D. B. Ramachary, C. Venkaiah, P. M. Krishna, *Org. Lett.* **2013**, *15*, 714.

35) T. H. Babu, A. A. Joseph, D. Muralidharan, P. T. Perumal, *Tetrahedron Lett.* **2010**, *51*, 994.

36) K. L. Vine, L. Matesic, J. M. Locke, M. Ranson, D. Skropeta, *Anti-Cancer Agents Med Chem.* **2009,** *9*, 397.

37) P. Pakravan, S. Kashanian, M. M. Khodaei, F. J. Harding, *Pharmacol. Rep.* **2013,** *65*, 313.

38) (a) Z. Z. Ma,Y. Hano, T. Nomura, Y. J. Chen, *Heterocycles*. **1997,** *46*, 541; (b) P. G. Mandhane, R. S. Joshi, P. S. Mahajan, M. D. Nikam, D. R. Nagargoje, C. H. Gill, *Arab. J. Chem*. **2015**, *8*, 474.

39) C. Jost, J. Schilling, R. Tamaskovic, M. Schwill, A. Honegger, A. Pluckthun, *Structure*, **2013**, *21*, 1.

40) Y. Yarden, M. X. Sliwkowski, *Nat. Rev. Mol. Cell Biol.* **2001**, *2*, 127.

41) R. J. Craven, H. Lightfoot, W. G. Cancer *Surg. Oncol.* **2003**, *12*, 39.

42) M. M. Moasser, *Oncogene*. **2007**, *26*, 6469.

43) N. Buza, D. M. Roque, A. D. Santin, *Arch. Pathol. Lab. Med.* **2014**, *138*, 343.

44) A. D. Santin, S. Bellone, J. J. Roman, J. K. McKenney, S. Pecorelli, *Int. J. Gynecol. Obstet.* **2008**, *102*, 128.

45) J. Sebastian, R. G. Richards, M. P. Walker, J. F. Wiesen, Z. Werb, R. Derynck, Y. K. Hom, G. R. Cunha, R. P. Di Augustine, *Cell Growth Differ.* **1998**, *9*, 777.

46) J. H. Park, Y. Liu, M. A. Lemmon, R. Radhakrishnan, *Erlotinib binds both inactive and active conformations of the EGFR tyrosine kinase domain. Biochem. J.* **2012**, *448*, 417.

47) M. J. Frisch, G. W. Trucks, H. B. Schlegel, G. E. Scuseria, M. A. Robb, J. R. Cheeseman, G. Scalmani, V. Barone, B. Mennucci, G. A. Petersson, *Gaussian 09, Gaussian, Inc, Wallingford CT.* **2009**.

48) N. Foloppe, A. D. MacKerell, *J. Comput. Chem.* **2000**, *21*, 86.

49) C. M. Breneman, K. B. Wiberg, *J. Comput. Chem.* **1990**, *11*, 361.

50) F. Hayat, E. Moseley, A. Salahuddin, R. L. V. Zyl, A. Azam, *Eur. J. Med. Chem*. **2011**, *46*, 1897.

51) M. K. Singh, A. Chandra, B. Singh, R. M. Singh, *Tetrahedron Lett.* **2007**, *48*, 5987.

52) A. Grzelakowska, J. Kolinska, J. Sokołowska, *Society of Dyers and Colourists. Colora. Technol.* **2016**, *132*, 121.

53) F. Walker, L. Abramowitz, D. Benabderrahmane, X. Duval, D. Descatoire, D. Hénin, T. Lehy, T. Aparicio, *Hum. Pathol.* **2009**, *40*,1517.

54) A. H. Kategaonkar, R. U. Pokalwar, S. S. Sonar, V. U. Gawali, B. B. Shingate, M. S. Shingare, *Eur. J. Med. Chem*. **2010**, *45*, 1128.

55) A. A. Bekhit, O. A. El-Sayed, E. Aboulmagd, J. Park, *Eur. J. Med. Chem*. **2004**, *39*, 249.

56) S. S. Sonar, S. A. Sadaphal, R. U. Pokalwar, B. B. Shingate, M. S. Shingare, *J. Heterocyclic Chem.* **2010**, *47*, 441.

57) H. W. Han, H. Y. Qiu, C. Hu, W. X. Sun, R. W. Yang, J. L. Qi, X. M. Wang, G. H. Lu, Y. H. Yang, *Bioorg. Med. Chem. Lett*. **2016**, *26*, 3237.

58) Y. Arun, K. Saranraj, C. Balachandran, P. T. Perumal, *Eur. J. Med. Chem*. **2014**, *74*, 50.

59) A. Dömling, W. Wang, K. Wang, *Chem. Rev.* **2012**, *112*, 3083.

60) A. Hazra, Y. P. Bharitkar, D. Chakraborty, S. K. Mondal, N. Singal, S. Mondal, A. Maity, R. Paira, S. Banerjee, N. B. Mondal, *ACS Comb. Sci.* **2013**, *15*, 41.

61) W. A. Denn, *Anticancer drug development, the contribution of synthetic organic chemistry to anticancer drug development*. **2002**, Chapter *1*, 187.

62) K. Malathi, S. Kanchithalaivan, R. R. Kumar, A. I. Almansour, R. S. Kumar, N. Arumugam, *Tetrahedron Lett*. **2015**, *56*, 6132.

63) G. S. Kumar, R. Satheeshkumar, W. Kaminsky, J. Platts, K. J. R. Prasad, *Tetrahedron Lett*. **2014**, *55*, 5475.

64) P. Saraswat, G. Jeyabalan, M. Z. Hassan, M. U. Rahman, N. K. Nyola, *Synth. Commun.* **2016**, *46*, 1643.

65) Y. Sarrafi, M. Hamzehlouian, K. Alimohammadi, H. R. Khavasi, *Tetrahedron Lett*. **2010**, *51*, 4734.

66) M. A. Borad, M. N. Bhoi, N. P. Prajapati, H. D. Patel, *Synth. Commun.* **2014**, *44*, 897.

67) M. Dabiri, Z.N. Tisseh, M. Bahramnejad, A. Bazgir, *Ultrason. Sonochem.* **2011**, *18*, 1153.

68) M. Ghandi, A. Yari, S. J. T. Rezaei, A. Taheri, *Tetrahedron Lett.* **2009**, *50*, 4724.

69) E. Carlos, P. Galvis, V. V. Kouznetsov, *Org. Biomol. Chem.* **2013**, *11*, 7372.

70) V. B. Nishtala, J. B. Nanubolu, S. Basavoju, *Res Chem Intermed*. **2017**, *43*, 1365.

71) G. Periyasami, R. Raghunathan, G. Surendiran, N. Mathivanan. *Bioorg. Med. Chem. Lett*. **2008**, *18*, 2342.

72) R. R. Kumar, S. Perumal, P. Senthilkumar, P. Yogeeswari, D. Sriram. *J. Med. Chem.* **2008**, *51*, 5731.

73) P. J. Xia, Y.H. Sun, J. A. Xiao, Z. F. Zhou, S. S. Wen, Y. Xiong, G. C. Ou, X. Q. Chen, H. Yang, *J. Org. Chem.* **2015**, *80*, 11573.

74) B. H. Rotstein, S. Zaretsky, V. Rai, A. K. Yudin, *Chem. Rev.* **2014**, 114, 8323.

75) A. Dömling, *Chem. Rev.* **2006**, *106*, 17.

76) W. Chen, X. Peng, L. Zhong, Y. Li, R. Sun, *ACS Sustainable Chem. Eng.* **2015**, *3*, 1366.

77) C. Liu, M. Shen, B. Lai, A. Taheri, Y. Gu, *ACS Comb. Sci.* **2014**, *16*, 652.

78) A. N. Muller, I. R. Corre, Jr. H. Prinz, C. Rosenbaum, K. Saxena, H. J. Schwalbe, D. Vestweber, G. Cagna, S. Schunk, O. Schwarz, H. Schiewe, H. Waldmann, *Proc. Natl. Acad. Sci.* **2006**, *103*, 10607.

79) a) P. Slobbe, E. Ruijter, R. Orru, *Med. Chem. Commun.* **2012**, *3*, 1189; (b) J. Andraos, *Org. Process Res. Dev.* **2005**, *9*, 404; (c) J. Andraos, *ACS Sustainable Chem. Eng.* **2013,** *1*, 496; (d) S. Periyaraja, P. Shanmugam, A. B. Mandal, T. S. Kumar, P. Ramamurthy, *Tetrahedron.* **2013**, *69*, 2891; (e) U. Kusebauch, B. Beck, K. Messer, E. Herdtweck, A. Dömling, *Org. Lett.* **2003**, *5*, 4021; (f) S. L. Zhu, S. J. Ji, X. M. Su, C. Sun, Y. Liu, *Tetrahedron Lett.* **2008**, *49*, 1777; (g) V. Sridharan, K. Karthikeyan, Muthusubramanian, *Tetrahedron Lett.* **2006**, *47*, 4221.

80) S. B. Marganakop, R. R. Kamble, J. Hoskeri, D. J. Prasad, G. Y. Meti, *Med. Chem. Res.* **2014**, *23*, 2727.

81) D. D. Subhedar, H. M. Shaikh, N. Laxman, Y. Amar, D. Sarkar, A. Firoz, K. Khan, N. S. Jaiprakash, B. B. Shingate, *Bioorg. Med. Chem. Lett*. **2016**, *26*, 2278.

82) D. D. Subhedar, H. M. Shaikh, B. Shingate, N. Laxman, S. Dhiman, V. M. Khedkar, *Med. Chem. Commun.* **2016**, *7*, 1832.

83) M. Staniszewska,G. łgorzata, M. Ewa, A. Klaudia, K. Mirosława, L. C. Edyta, *Eur. J. Med. Chem*. **2018**, *145*, 124.

84) R. Kolluri, J. Zhang, R. Singh, M. A. J. Duncton, *Tetrahedron Lett.* **2018**, *59*, 4158.

85) N. V. A. Rodriguez, A.I. Jacome, A. R. Gomez, E. Luis, G. Cardenas, M. V. B. Unnamatla, R. G. Montano, *New J. Chem.* **2018**, *42*, 1600.

86) A. Kamal, K. S. Babu, J. Kovvuri, V. Manasa, A. Ravikumar, A. Alarifi *Tetrahedron Lett.* **2015**, *56*, 7012.

87) A. Preetam, M. Nath, *Tetrahedron Lett.* **2016**, *57*, 1502.

88) J. McBryan, J. Howlin, S. Napoletano, F. Martin, *J. Mammary Gland Biol. Neoplasia*. **2008**, *13*, 159.

89) P. Skehan, R. Storeng, D. Scudiero, A. Monks, J. McMohan, D. Vistica, J. T. Warren, H. Bokesch, S. Kenncy, M. R. Boyd, *J. Natl. Cancer Inst*. **1990**, *82*, 1107.

90) A. Monks, D. Scudiero, P. Skehan, R. Shoemaker, K. Paull, D. Vistica, C. Hose, J. Langley, P. Cromise, *J. Natl. Cancer Inst*. **1991**, *83*, 757.

91) A. Braca, N. D. Tommasi, L. D. Bari, C. Pizza, M. Politi, I. Morelli, *J. Nat. Prod*. **2001**, *64*, 892.

92) M. R. Saha, S. M. R. Hasan, R. Akter, M. M. Hossain, M. S. Alamb, M. A. Alam, M. E. H. Mazumder, *Bangl. J. Vet. Med*. **2008**, *6*, 197.

93) M. S. Blois. *Nature*. **1958**, *181*, 1199.

94) A. W. Bauer, W. M. Kirby, J. C. Sherris, M. Turck, *Am. J. Clin. Pathol.* **1966**, *45,* 493.

95) http://autodock.scripps.edu/resources/references.

CHAPTER-IV

Novel furanyl spiropyrrolizidines: Synthesis *via* 1,3-dipolar cycloaddition and biological evaluation

4.1. Introduction

Ultrasonication is a prominent technique, which is widely used in recent days in organic synthesis and it has an immense impact on the organic and parallel synthesis. The special sonochemical effects in liquids cause the chemical reactions either in homogeneous or in heterogeneous systems. The ultrasonic waves produce the microbubbles or cavities in the medium that causes the chemical reaction. These cavities produce high pressures and temperatures in their surroundings. Ultrasonic irradiation is a very effective method when compared with traditional thermal heating in the version of higher yields, less reaction time and usage of milder conditions [1].

MCR (Multicomponent reaction) approach is one the eminent strategies for the synthesis of various heterocyclic compounds in one-pot *via* the formation of several carbon-carbon and carbon-heteroatom bonds along with stereogenic centers and without the isolation of intermediates. Some of the main advantages of MCRs are high reaction rate, a high degree of atom economy, etc., [2-6]. For the last few decades, the multicomponent 1,3-dipolar cycloaddition reactions have been extensively explored because of their selectivity. The regiochemistry and stereochemistry of these reactions can be controlled by using the catalyst or suitable dipole or dipolarophile [7-11]. Several spiro compounds have been synthesized *via* multicomponent 1,3-dipolar cycloaddition under ultrasound irradiation [12-19]. Multifunctional polycyclic spiropyrrolizidines exhibit versatile bioactivities such as antibacterial, antifungal, antitumor, antimycobacterial, antiviral, etc., [20, 21]. Spiropyrrolizidines can be synthesized efficiently from azomethine ylide and electron-deficient alkenes and alkynes *via* 1,3-dipolar cycloaddition reaction [22-24]. Among various methods, one-pot three-component 1,3-dipolar cycloaddition reaction of azomethine ylide with electron-deficient olefin is a convenient route for regio- and stereo-selective synthesis of various spiropyrrolizidine derivatives [25, 26].

Raghunathan and coworkers reported the synthesis of spiropyrrolizidines through 1,3-dipolar cycloaddition reaction of azomethine ylide generated from proline and isatin with the dipolarophiles under conventional and microwave irradiation methods (Figure. 4.1). It was observed that the solvent-free solid support approach accelerated by microwave irradiation

was the prior method to obtain the target compounds. The synthesized molecules were tested for their potential as antimicrobial agents for human and plant pathogens [27].

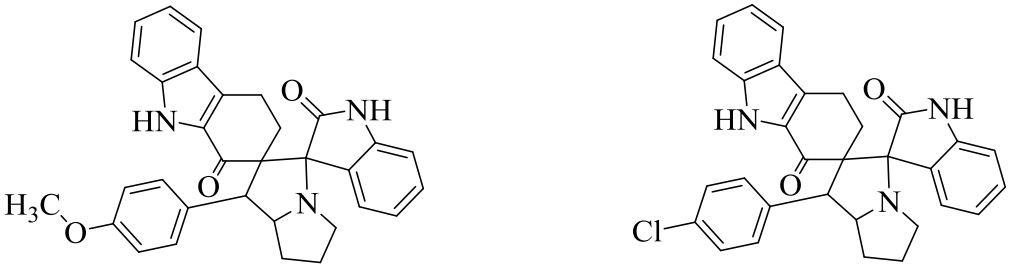

Figure 4.1

JI et al. designed and synthesized a series of spirotetrahydrothiopyran–oxindole derivatives in a multistep process (Figure. 4.2). The compounds were tested for their antitumor activity on p53-MDM2 and apoptosis. The SAR studies were explored for the obtained compounds. The antitumor activity was supported by the *in silico* molecular docking studies [28].

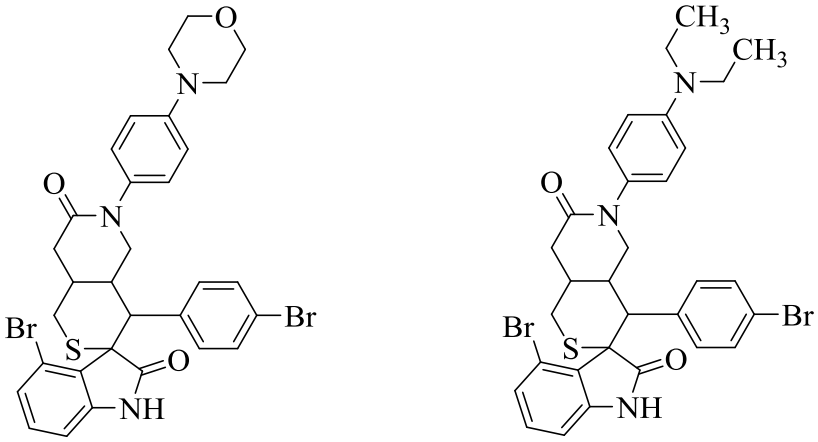

Figure 4.2

Kathirvelan et al. described the facile synthesis of highly functionalized diastereoselective 3,2'-spiropyrrolidine-oxindole derivatives *via* 1,3-dipolar cycloaddition of an azomethine ylide (Figure. 4.3). The synthesized compounds were tested for their *in vitro* antimicrobial activity and evaluated the *in silico* molecular docking studies [29].

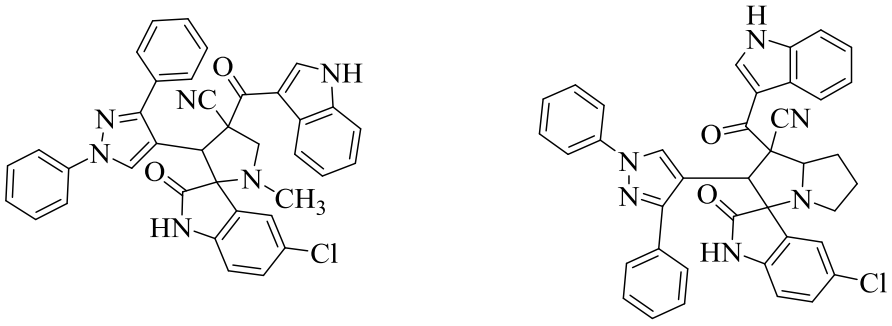

Figure 4.3

Tiwari et al. reported an efficient synthesis of a series of 2,3-dihydrooxazole-spirooxindole hybrids as antimicrobial agents (Figure. 4.4). The minimum inhibitory concentration, minimum bactericidal concentration and minimum fungicidal concentration were determined for the target compounds [30].

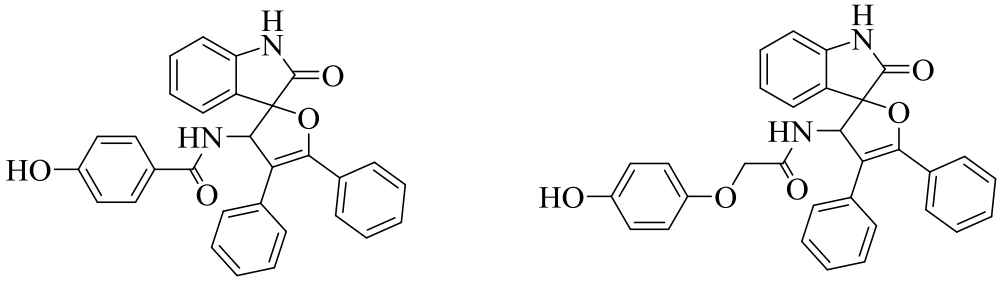

Figure 4.4

Ouyang and coworkers described the facile three-component diversity-oriented synthesis of regio- and stereo-selective oxazolones grafted spirooxindolooxazolones in one-pot (Figure. 4.5). All the synthesized compounds were evaluated for their anticancer activity. The *in vitro* anticancer activity was supported by the molecular docking studies [31].

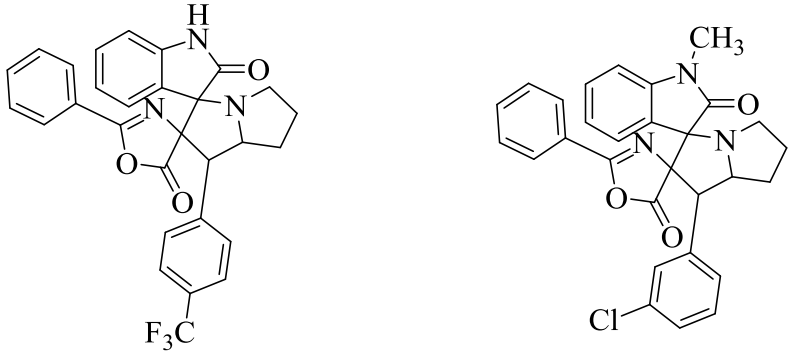

Figure 4.5

4.1.2. Different approaches for the synthesis of spirooxindoles

Kumar and coworkers reported the synthesis of piperidone grafted, mono- and bis-spirooxindole-hexahydropyrrolidine derivatives *via* one pot, three-component reaction in the ionic liquid ([Bmim]Br) medium (Scheme 4.1). Mono-spiropyrrolidines exhibited both AChE and BChE inhibition activities, whereas bis-spiropyrrolidines exhibited AChE inhibition activity. The anticholinesterase activity was well supported by the molecular docking studies [32].

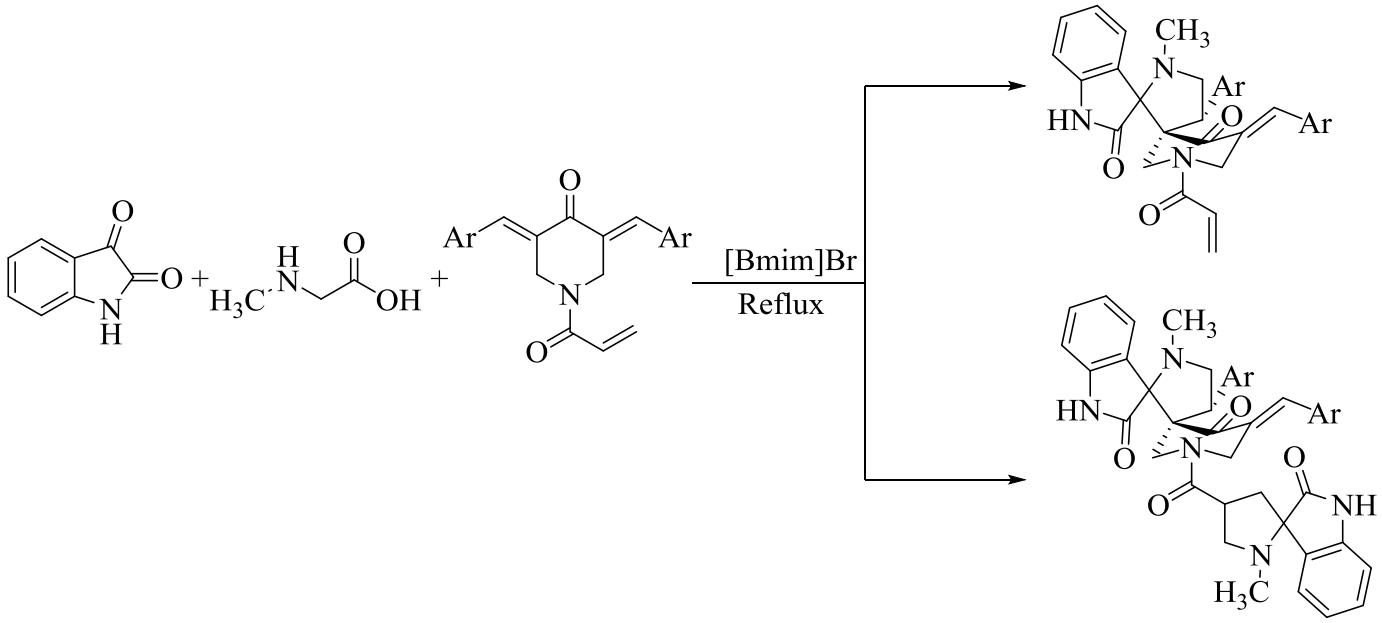

Scheme 4.1

Kamal et al. described the efficient, mild and simple method for the synthesis of pyrazolopyridine fused spirooxindoles as potential cytotoxic agents *via* one-pot multicomponent approach in an aqueous medium (Scheme 4.2). The sulphamic acid (H_2NSO_3H) was used as a green and reusable catalyst [33].

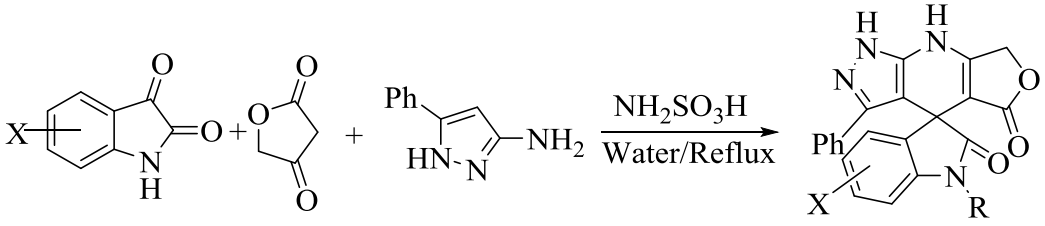

Scheme 4.2

Shaabani and coworkers reported the spiro fused heterocycles, synthesized by a pseudo four-component reaction of an aldehyde, urea and a cyclic *β*-diester or a *β*-diamide such as meldrum's acid or barbituric acid derivatives using microwave irradiation under solvent-free conditions (Scheme 4.3) [34].

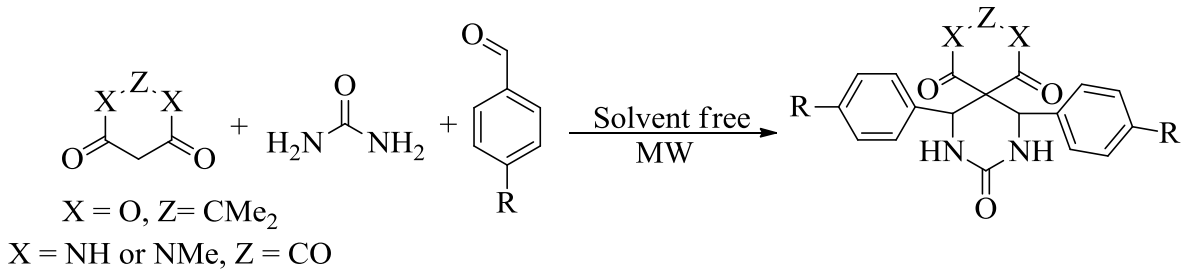

Scheme 4.3

Rezaei et al. described the facile and efficient synthesis of spiroacenaphthylene pyrazolotriazole and pyrazolophthalazine *via* one-pot three-component approach under conventional heating and ultrasonication (an environmentally benign method) methods (Scheme 4.4). A comparative study for the synthesis of target molecules under these two methods was reported [35].

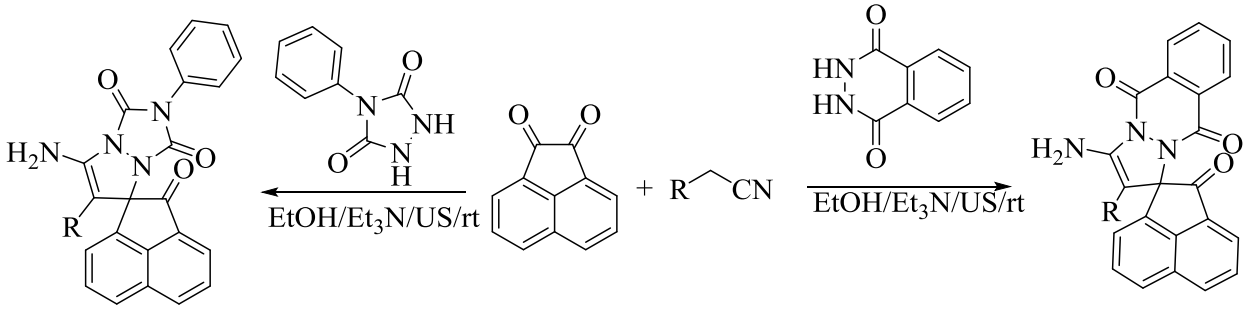

Scheme 4.4

Sarkar et al. developed an expeditious protocol for the synthesis of spiro[dihydropyridine-oxindoles] by using a reusable nano range organic catalyst (Calix[4]arene tetracarboxylic acid) *via* a Mannich type one-pot multi-component reaction in an eco-friendly solvent, water (Scheme 4.5) [36].

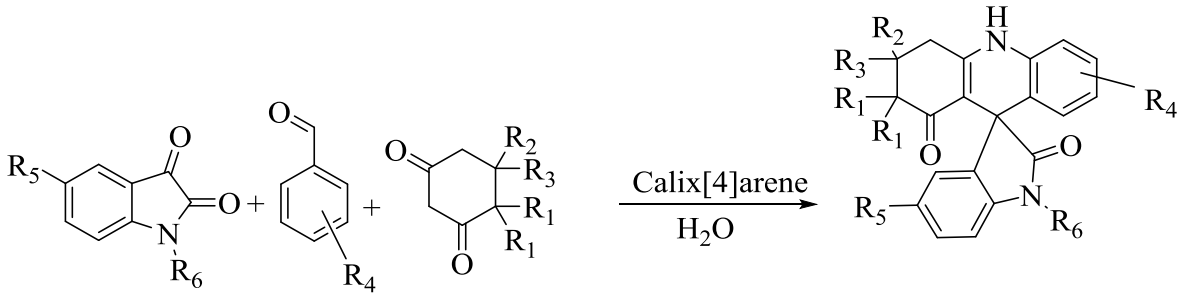

Scheme 4.5

4.2. Present work

By considering the significance of spirooxindolo pyrrolizidines herewith, we report the synthesis of the spirooxindolo and spiroquinoxalinopyrrolizidines *via* multicomponent 1,3-dipolar cycloaddition under different conditions i.e., using ultrasonication (method A), conventional heating (method B) and fusion (method C) methods. All the synthesized compounds were tested for the *in vitro* antibacterial, antifungal, antioxidant and *in silico* molecular docking studies.

4.2.1. Synthesis of furanyl spirooxindolopyrrolizidines (4a-n, 6a-c, 8a-c, 10a-c and 11)

4.2.1.1. Conventional heating

A mixture of L-proline **2** (1 mmol), isatin derivatives **1a-f**/ninhydrin **5**/11*H*-indeno[1,2-*b*]quinoxalin-11-one **7** (1 mmol) and dipolarophiles **3a-c/9** (1 mmol) in methanol was refluxed to obtain the target compounds. The progress of all the reactions was monitored by TLC. After completion of the reaction, the solvent was removed under reduced pressure and the crude product was purified by column chromatography (pet ether:ethyl acetate (1:1 v/v)) followed by recrystallization in methanol.

4.2.1.2. Ultrasound irradiation

A homogeneous mixture of L-proline **2** (1 mmol), isatin derivatives **1a-f**/ninhydrin **5**/11*H*-indeno[1,2-*b*]quinoxalin-11-one **7** (1 mmol) and dipolarophiles **3a-c/9** (1 mmol) in methanol was irradiated in an ultrasonic bath to produce the target compounds. The progress of all the reactions was monitored by TLC. To get the pure products the precipitated compounds were filtered, washed with methanol and dried.

4.2.1.3. Fusion method

A mixture of L-proline **2** (1 mmol), isatin derivatives **1a-f**/ninhydrin **5**/11*H*-indeno[1,2-*b*]quinoxalin-11-one **7** (1 mmol), dipolarophiles **3a-c/9** (1 mmol) was fused directly without solvent. Reaction progress was monitored by TLC. The products were washed with methanol (Scheme 4.6 and 4.7).

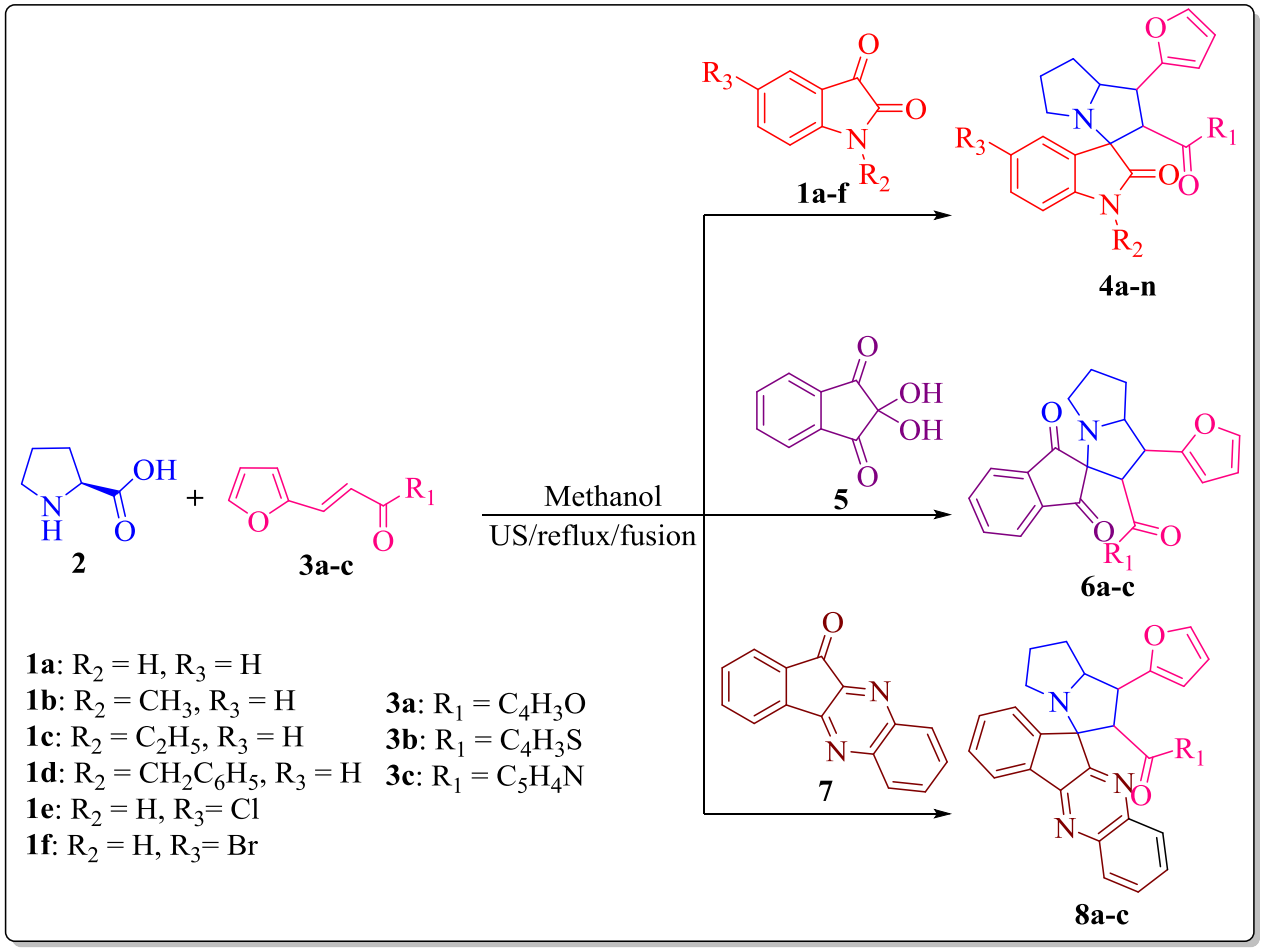

Scheme 4.6

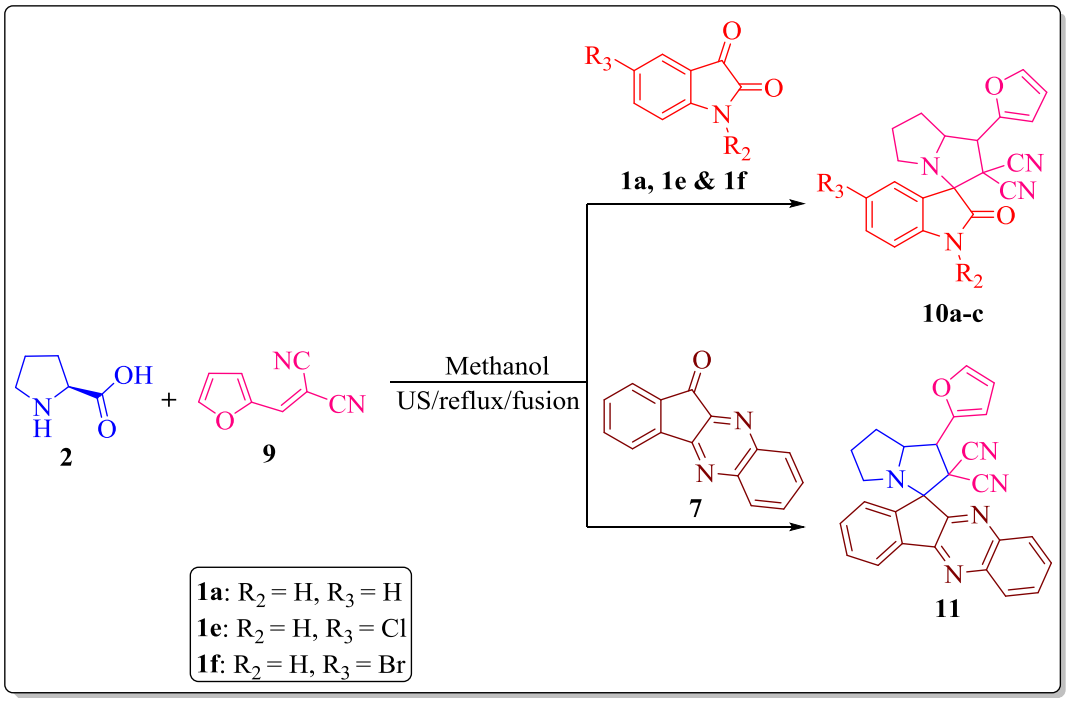

Scheme 4.7

4.2.1.4. The plausible reaction mechanism for the synthesis of the target compounds in conventional and ultrasonication methods.

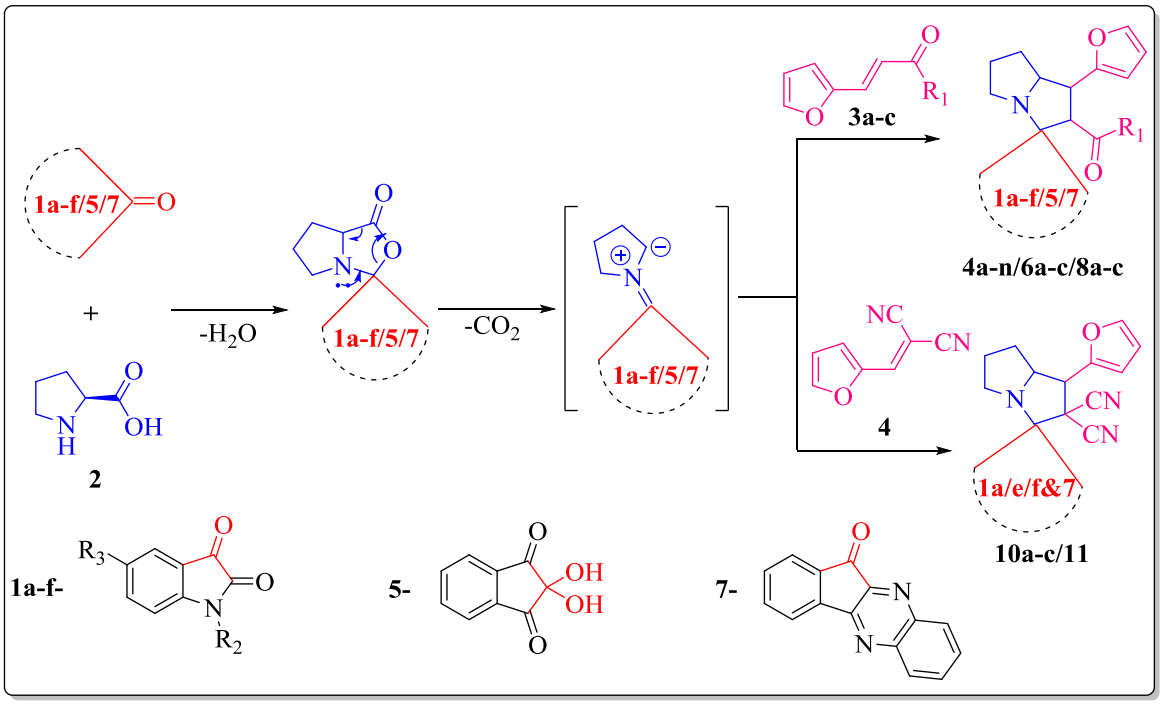

a) Under conventional method

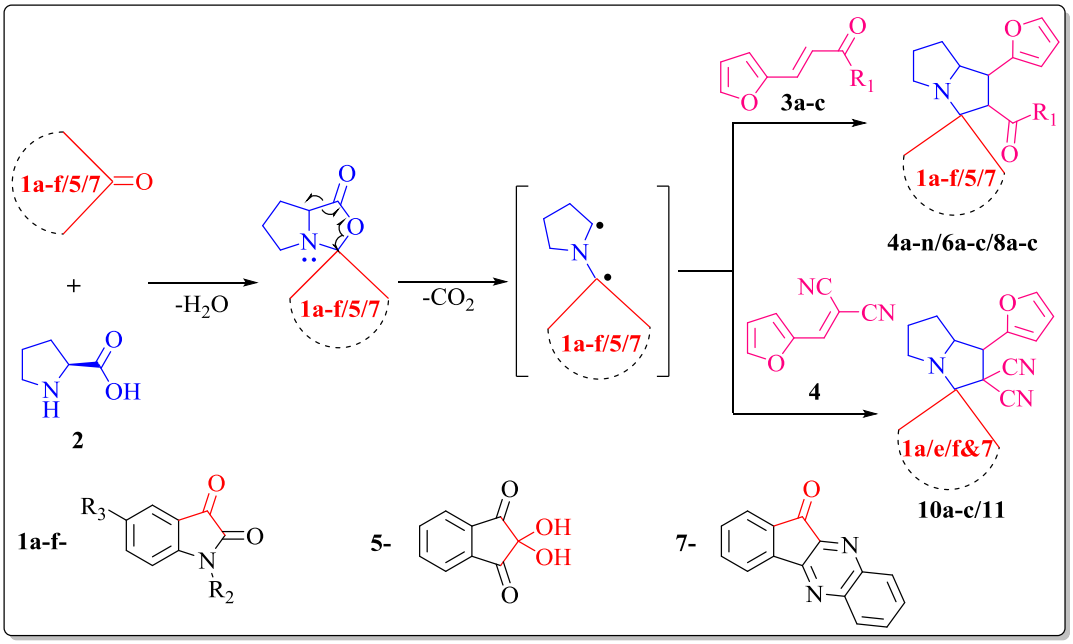

b) Under ultrasonication method

Scheme 4.8

4.2.1.5. The plausible regioselective approach of the azomethine ylide on dipolarophile

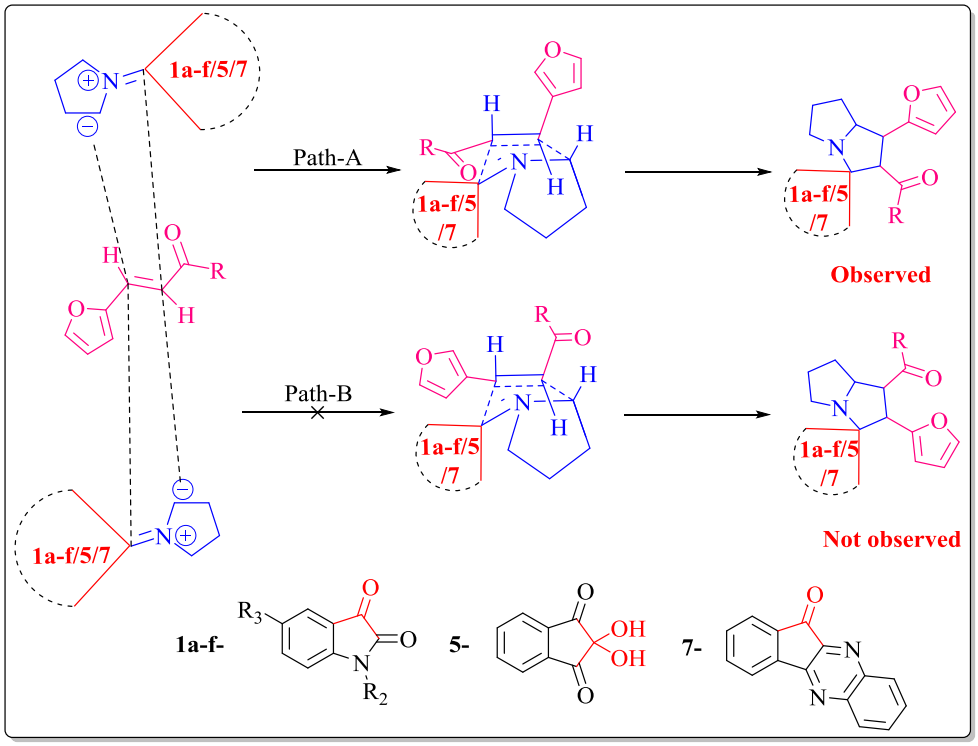

Scheme 4.9

4.3. Results and discussion

4.3.1. Chemistry

Initially, to carry out the pilot reaction, isatin **1a**, L-proline **2** and dipolarophile **3a** were chosen as starting materials under reflux condition in different solvents. The screening results showed that the methanol is the opted solvent to obtain the target compound **4a**. Then the same reaction was carried out in the ultrasonication method in methanol to obtain the target compound **4a** at room temperature. Further, the model reaction was carried out by using the fusion method (Solvent-free method). It was observed that among these three methods, ultrasonication is the best method to produce the target compound **4a.**

Table 1. The optimized reaction conditions for the synthesis of target compound **4a**[a,b,c].

S. No.	Solvent	Method	Yield (%)	Time
1	Methanol	reflux	73	1h
2	Ethanol	reflux	65	45min
3	Acetonitrile	reflux	60	45min
4	Tetrahydrofuran	reflux	55	1h
5	1,4-Dioxane	reflux	56	1h
6	Methanol	Ultrasonication	80	1min
7	Fusion	--	60	2 min

[a]All the reactions were carried out by using isatin **1a** (1 mmol), L-proline **2 (**1 mmol**)** and dipolarophile **3a** (1 mmol) as starting materials. [b]The progress of all the reactions were monitored by TLC. [c]Isolated yields.

In order to extend the reaction approach, all the reactions were carried out in these three methods to study the effect of these three methods in the version of yields and reaction times. The target compounds were synthesized by using ultrasonication method (Method-A), because the implication of ultrasound in the chemical reactions is a simple, innocuous and an excellent modification for the chemical processes. When compared to conventional method, several reactions have been reported with higher yields, better selectivity and shorter reaction times in the ultrasonic irradiation method [37, 38]. In the ultrasonication method, the starting materials were stirred for a few minutes to get the homogeneous mixture. The reaction flasks were immersed in the cleaner such that the surface of the reactants was slightly lower than

the water in the cleaner. The target compounds **4a-n**, **6a-c** and **8a-c** were synthesized by using the equimolar mixture of the isatin derivatives **1a-f**/ninhydrin **5**/11*H*-indeno[1,2-*b*]quinoxalin-11-one **7**, L-proline **2** and dipolarophiles **3a-c** in methanol under ultrasonication method (Scheme 4A.6). Whereas, the target compounds **10a-c** and **11** were synthesized from the equimolar mixture of the isatin derivatives **1a**/**1e**/**1f**/11*H*-indeno[1,2-*b*]quinoxalin-11-one **7**, L-proline **2** and dipolarophiles **9** in methanol under ultrasonication method (Scheme 4A.7). The times and yields of the reaction were shown in table 2. The plausible mechanism for the formation of the target compounds under ultrasonication method was shown in scheme 4A.8.

In reflux method (Method-B), the targeted compounds **4a-n**, **6a-c** and **8a-c** were synthesized by using the equimolar mixture of the isatin derivatives **1a-f**/ninhydrin **5**/11*H*-indeno[1,2-*b*]quinoxalin-11-one **7**, L-proline **2** and dipolarophiles **3a-c** in methanol under reflux condition (Scheme 4.6). Whereas, the target molecules **10a-c** and **11** were synthesized by refluxing the equimolar mixture of the isatin derivatives **1a/1e/1f**/11*H*-indeno[1,2-*b*]quinoxalin-11-one **7**, L-proline **2** and dipolarophile **9** in methanol (Scheme 4.7). The yields and time required for the completion of the reaction were shown in table 2. The crude products were purified by column chromatography.

In the fusion method (Method-C), the target compounds **4a-n**, **6a-c** and **8a-c** were synthesized by fusing the equimolar mixture of the isatin derivatives **1a-f**/ninhydrin **5**/11*H*-indeno[1,2-*b*]quinoxalin-11-one **7**, L-proline **2** and dipolarophiles **3a-c** (Scheme 4.6). Whereas, the target compounds **10a-c** and **11** were synthesized by fusing (method-C) the equimolar mixture of the isatin derivatives **1a/1e/1f**/11*H*-indeno[1,2-*b*]quinoxalin-11-one **7**, L-proline **2** and dipolarophile **9** (Scheme 4.7). However, the reaction was completed within 2-4min and the target compounds were obtained with moderate yields. The yields and reaction times for the completion of reaction were shown in table 2. The crude products were purified by washing the compounds with methanol.

The reason for the impact of the ultrasonication method on reaction is due to the special sonochemical effects i.e., the microbubbles or cavities formed in the reaction medium. The vigorous collapse of these acoustic cavities or micro jets produces high pressure and temperature, which accelerates the reaction rate and enhances the yield of the product. Such thermal effects that are produced from acoustic cavitations can never be gained

in the conventional method [39-42]. The target compounds obtained as a single product from ultrasound irradiation, conventional and fusion methods, which were inferred by the TLC analysis. The plausible mechanism for the synthesis of the target compounds was shown in scheme 4.11. The azomethine ylide, generated *in situ* from the nonenolizable ketones i.e., isatin derivatives **1a-f**/ninhydrin **5**/11*H*-indeno[1,2-*b*]quinoxalin-11-one **7** and secondary amino acid i.e, L-proline **2**, attacked the dipolarophiles **3a-c** and **9** at *β*-position to the carbonyl group. Because the electron density at the β-position was decreased due to the electron with drawing nature of the carbonyl group in **3a-c** and nitrile group in **9**. Hence the target compounds were formed regioselectively (Scheme 4A.9).

Table 1. The times and yields of the target compounds **4a-n**, **6a-c**, **8a-c**, **10a-c** and **11**[a,b].

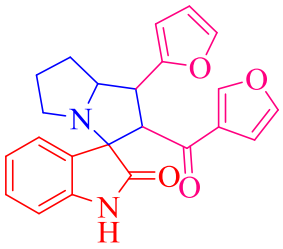	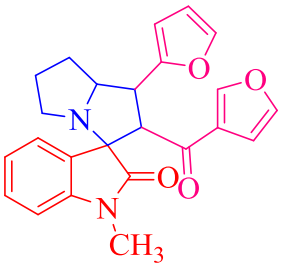	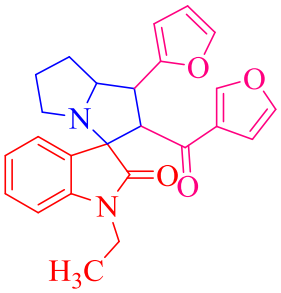
4a Method A: 60sec / 80% Method B: 1h / 73% Method C: 2min / 60%	**4b** Method A: 50sec / 82% Method B: 2h / 74% Method C: 2min / 61%	**4c** Method A: 50sec / 80% Method B: 2h / 76% Method C: 2min / 59%
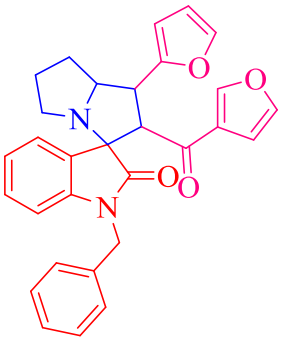	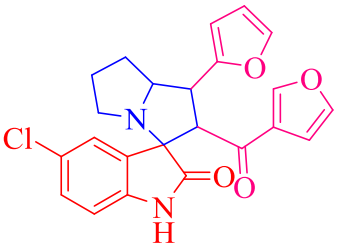	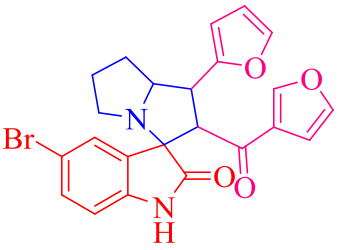
4d Method A: 50sec / 86% Method B: 2h / 70% Method C: 2min / 54%	**4e** Method A: 73sec / 78% Method B: 3h / 71% Method C: 2.5min / 57%	**4f** Method A: 70sec / 84% Method B: 3h / 69% Method C: 2min / 52%

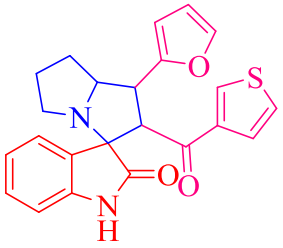

4g
Method A: 5sec / 80%
Method B: 8h / 71%
Method C: 2min / 60%

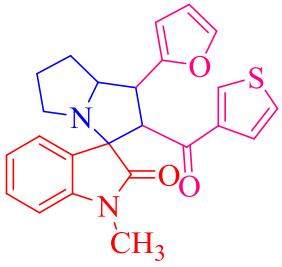

4h
Method A: 7sec / 82%
Method B: 6h / 72%
Method C: 2min / 58%

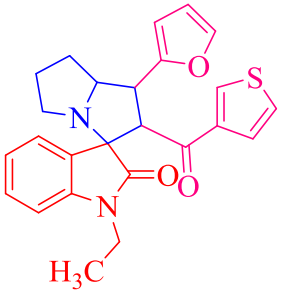

4i
Method A: 7sec / 82%
Method B: 6h / 73%
Method C: 2min / 58%

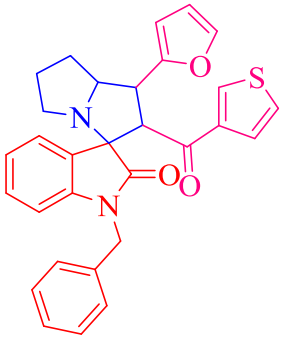

4j
Method A: 13sec / 80%
Method B: 6h / 70%
Method C: 2min / 59%

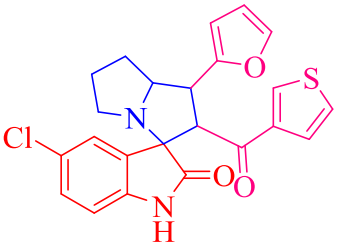

4k
Method A: 15sec / 77%
Method B: 8h / 69%
Method C: 2min / 56%

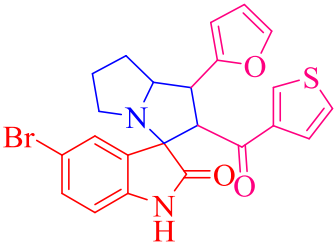

4l
Method A: 13sec / 83%
Method B: 7h / 70%
Method C: 2min / 54%

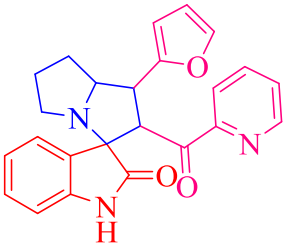

4m
Method A: 45sec / 69%
Method B: 3h / 58%
Method C: 2min / 48%

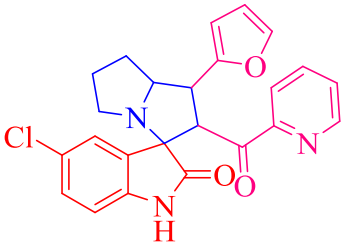

4n
Method A: 45sec / 64%
Method B: 4h / 52%
Method C: 2min / 45%

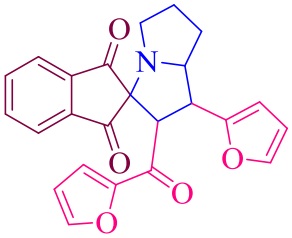

6a
Method A: 60 sec / 75%
Method B: 2h / 62%
Method C: 3min / 46%

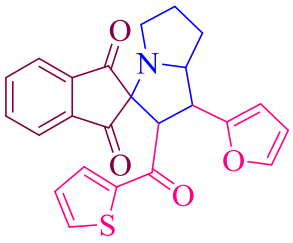

6b
Method A: 40sec / 78%
Method B: 3h / 65%
Method C: 2min / 50%

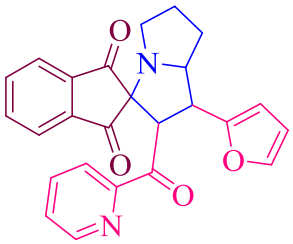

6c
Method A: 55sec / 79%
Method B: 3h / 63%
Method C: 2min / 42%

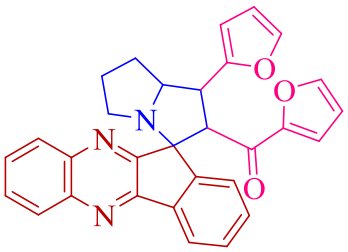

8a
Method A: 2min / 73%
Method B: 6h / 71%
Method C: 4min / 64%

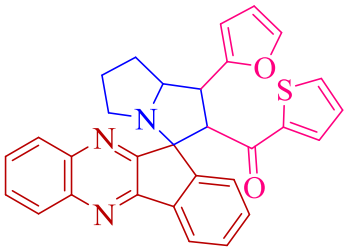

8b
Method A: 3min / 78%
Method B: 6h / 68%
Method C: 4min / 59%

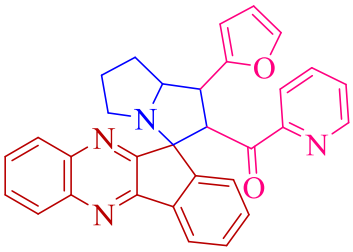

8c
Method A: 3min / 69%
Method B: 4h / 62%
Method C: 3min / 52%

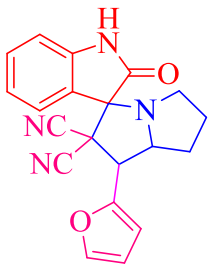

10a
Method A: 18min / 74%
Method B: 3h / 68%
Method C: 3min / 54%

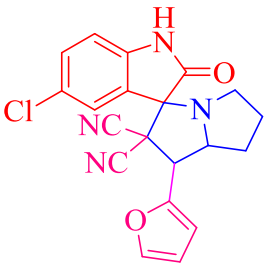

10b
Method A: 20min / 78%
Method B: 4h / 65%
Method C: 4min / 46%

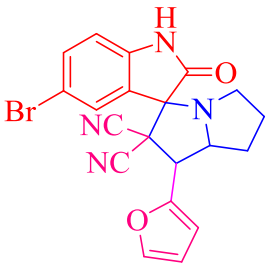

10c
Method A: 20min / 79%
Method B: 4h / 65%
Method C: 4min / 49%

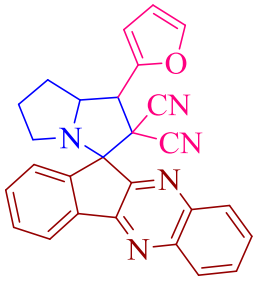

11
Method A: 25min / 80%
Method B: 3h / 63%
Method C: 4min / 48%

[a]The progress of all the reactions was monitored by TLC. [b]Isolated yields. Method A: Ultrasonication; Method B: Conventional method; Method C: Fusion method

The synthesized compounds were characterized by their IR, ^{1}H NMR, ^{13}C NMR and mass spectral analysis. For instance, the IR spectrum of the compound **4c** (Figure 4.6) showed peaks at 1720 cm^{-1} and 1667 cm^{-1} represents the carbonyl group of the oxindole ring

and carbonyl group adjacent to furan ring. In the ^{1}H NMR spectrum the peaks at δ 4.71 (d, 1H, J = 11.6 Hz), 4.30–4.25 (m, 1H) and 4.04 (t, 1H, J = 10.0 Hz) represents the protons at C11, C13 and C12 positions respectively. In ^{13}C NMR spectrum, the peaks at δ 183.77 and 178.08 correspond to the carbonyl group of the oxindole ring and carbonyl group adjacent to thiophene ring. The peak at δ 73.39 corresponds to the spiro carbon at the C2 position. Further, the formation of the compound was confirmed by the peak at *m/z* 417.20 in the mass spectrum. Finally, the structures and regiochemistry of the compounds **4c** and **4k** were confirmed by the single crystal x-ray diffraction method. The salient crystallographic data and structure refinement parameters of compounds **4c** and **4k** were shown in table 3. The crystal structure and packing diagram for the compounds **4c** and **4k** were shown in figure 4.7, 4.8, 4.9 and 4.10.

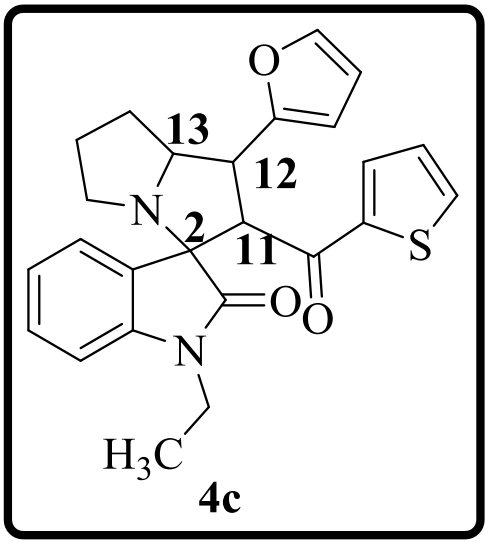

Figure 4.6

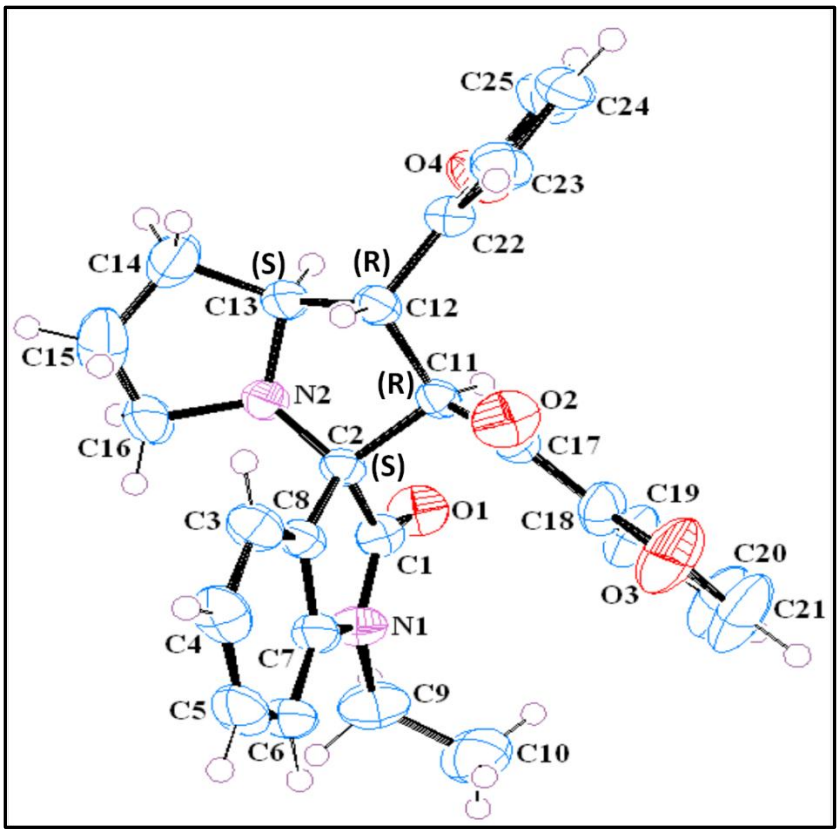

Figure 4.7. The ORTEP representation of the title compound **4c.** The thermal ellipsoids are drawn at 50% probability level. The asymmetric unit shows only one enantiomer having the configurations at the chiral centers C11 (R), C12 (R), C13 (S) and C2 (S).

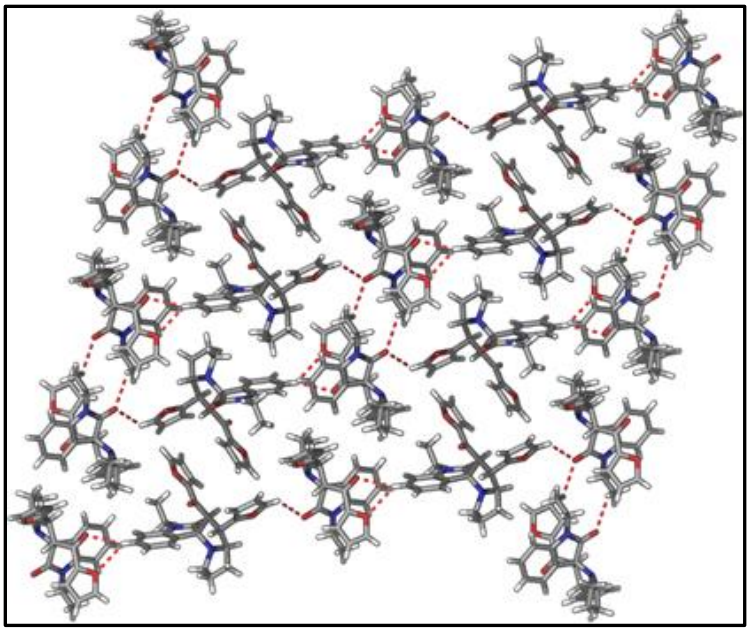

Figure 4.8. The packing diagram of the compound **4c** shows the two-dimensional layered structure with all C–H···O hydrogen bonding (view down *c*-axis).

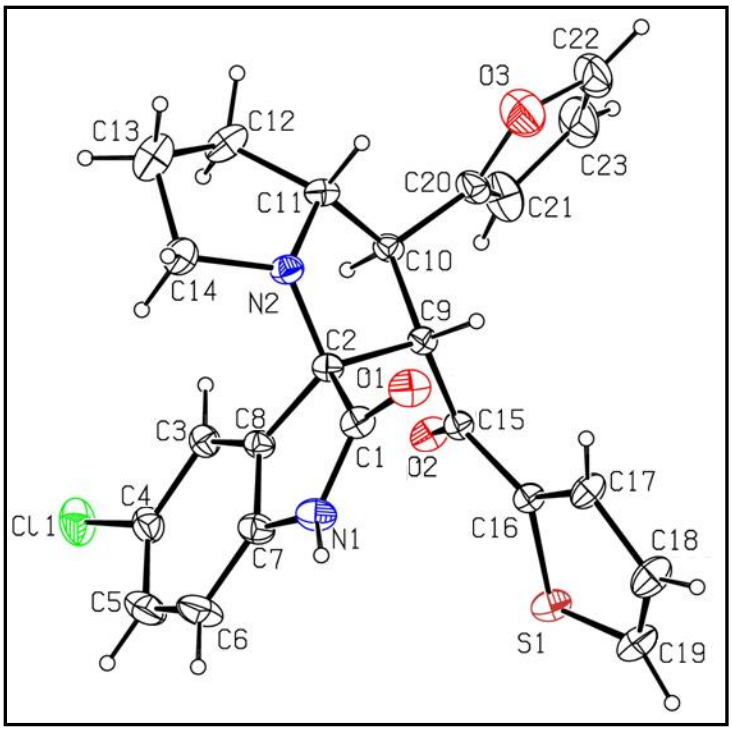

Figure 4.9. The ORTEP diagram of **4k** with the atom-numbering scheme. Displacement ellipsoids are drawn at the 20% probability level and H atoms are shown as small spheres of arbitrary radius. Only the major component of the disordered furan ring atoms is shown for clarity. The configurations at chiral centers C2, C9, C10, and C11 are R, S, S and R respectively.

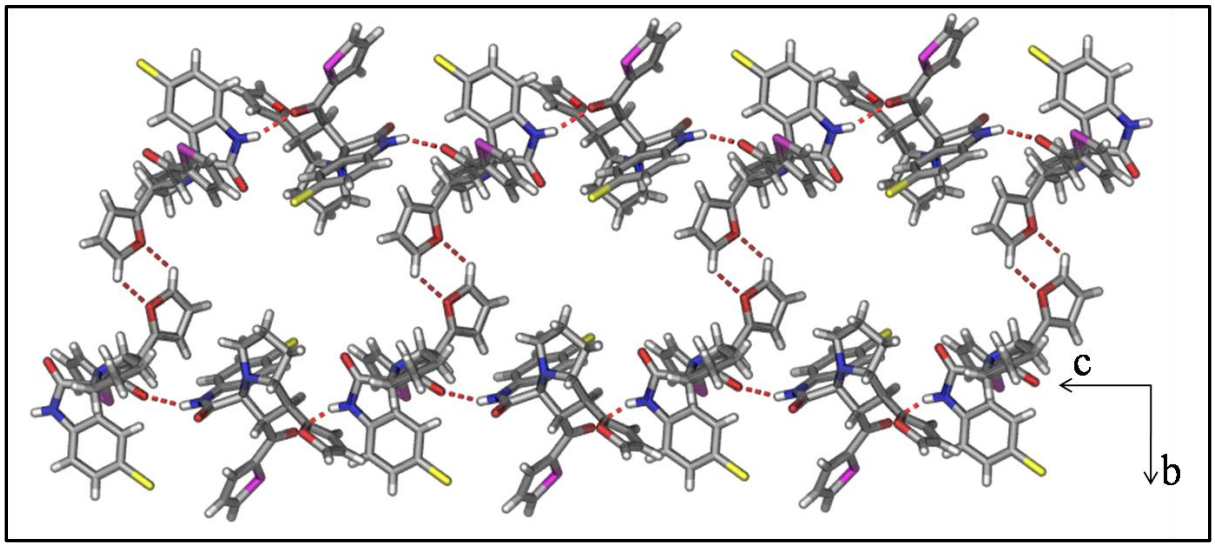

Figure 4.10. The crystal structure packing diagram of **4k**. Notice the elongated hexagonal network structures formed by N–H···O hydrogen bonds and C–H···O dimer synthons.

Table 3. The salient crystallographic data and structure refinement parameters of the compounds **4c** and **4k**.

	4c	**4k**
Empirical formula	$C_{25}H_{24}N_2O_4$	$C_{23}H_{19}ClN_2O_3S$
Formula weight	416.47	438.91
Crystal system	Monoclinic	Monoclinic
Space group	$P2_1/n$	$P2_1/c$
T/K	296(2)	293(2)
a/Å	13.9675(10)	8.2305(6)
b/Å	9.1490(6)	18.5917(13)
c/Å	16.6482(14)	13.9102(10)
α/°	90	90
β/°	104.529(4)	106.4740(10)
γ/ °	90	90
Z	4	4
V/Å^3	2059.4(3)	2041.1(3)
D_{calc}/ g/cm^3	1.333	1.428
F(000)	872	912.0
μ/mm^{-1}	0.090	0.318
θ/^{o}	1.71 to 28.39	1.879 to 25.994
Index ranges	$-18 \le h \le 18$ $-11 \le k \le 11$ $-22 \le l \le 16$	$-10 \le h \le 10$ $-22 \le k \le 22$ $-17 \le l \le 17$
N-total	16392	21054
N-independent	5067	3996
N-observed	3629	3593
Parameters	281	312
R_1 ($I > 2\sigma(I)$)	0.0677	0.0651
wR_2 (all data)	0.1979	0.1836
GOF	1.042	1.070

CCDC	1568661	1470017

4.3.2. Biological evaluation

4.3.2.1. Antibacterial activity

The *in vitro* antibacterial activity of the target compounds were carried out against selected bacterial strains such as two gram positive bacteria i.e., *Bacillus subtilis*, *Staphylococcus aureus*, and three gram negative bacteria i.e., *Escherichia coli*, *Pseudomonas aeruginosa* and *Klebsiella Pneumoniae*. The results were illustrated in Table 4.

Among all the compounds, the compound **8c** exhibited excellent antibacterial activity aginst *E. coli* with the MIC value 12.62 µg/mL and showed significant to moderate activity against *B. subtilis, S. aureus, P. aeruginosa* and *K. pneumoniae* with MIC values ranging from 13.25 µg/mL to 19.24 µg/mL. The compounds **4g**, **4m** and **6c** exhibited significant antibacterial activity against *E. coli* with MIC values 15.13 µg/mL, 14.65 µg/mL and 14.09 µg/mL. The compounds **4g** and **6c** exhibited moderate activity against the four bacterial strains *B. subtilis, S. aureus, P. aeruginosa* and *K. pneumoniae* with MIC values vary from 13.25-27.50 µg/mL. The compound **4m** exhibited moderate activity against *B. subtilis* and *S. aureus* with MIC values 17.52 µg/mL and 24.64 µg/mL respectively. The compound **4n** exhibited significant activity against *E. coli* with MIC values 20.31 µg/mL.

Table 4. Antibacterial activity of the furanyl spiropyrrolizidines**4a-n**, **6a-c**, **8a-c**, **10a-c** and **11**.

S. No.	Compound	Minimum Inhibitory Concentration (µg/mL)				
		B. subtilis	***S. aureus***	***E. coli***	***P. aeruginosa***	***K. pneumoniae***
1	**4a**	25.56	32.79	45.01	29.50	73.61
2	**4b**	24.72	28.30	58.07	85.66	36.78
3	**4c**	38.76	29.23	35.44	54.12	38.45
4	**4d**	56.34	39.15	32.43	29.89	43.51
5	**4e**	54.39	42.16	38.69	44.53	74.34
6	**4f**	63.45	71.37	47.94	73.29	78.63
7	**4g**	**17.32**	**19.56**	**15.13**	**24.22**	**20.01**

8	**4h**	29.57	27.65	36.78	53.11	51.12
9	**4i**	32.34	41.35	39.96	71.32	41.64
10	**4j**	36.23	28.65	41.14	32.37	43.42
11	**4k**	48.54	41.33	53.26	39.91	45.38
12	**4l**	54.51	75.25	49.63	61.05	50.29
13	**4m**	**17.52**	**24.64**	**14.65**	**31.63**	**35.87**
14	**4n**	23.24	28.43	20.31	41.28	33.56
15	**6a**	29.55	34.33	34.56	30.87	41.27
16	**6b**	28.60	56.72	30.85	60.39	36.60
17	**6c**	**14.56**	**18.93**	**14.09**	**27.50**	**19.34**
18	**8a**	20.03	29.81	33.72	37.54	39.57
19	**8b**	54.44	48.90	45.06	40.83	44.78
20	**8c**	**13.25**	**16.50**	**12.62**	**19.24**	**17.43**
21	**10a**	54.21	28.46	73.35	57.26	48.73
22	**10b**	43.44	50.71	39.77	35.38	37.60
23	**10c**	50.09	38.82	45.93	42.71	50.60
24	**11**	38.59	74.23	49.94	55.77	43.01
25	**Streptomycin**	6.25	6.25	12.5	12.5	12.5

[a]The values are means of triplicates with ± SD. The bacterial strains: *B. subtilis – Bacillus subtilis, S. aureus- Staphylococcus aureus, E. coli- Escherichia coli, P. aeruginosa- Pseudomonas aeruginosa, K. pneumoniae- Klebsiella pneumoniae.*

4.3.2.2. Antifungal activity

The *in vitro* antifungal activity of the furanyl spiropyrrolizidines were investigated on three fungal strains such as *Aspergillus niger*, *Penicillium notatum* and *Aspergillus parasiticus.* The results were depicted in Table 5.

The compound **8c** showed moderate activity against *A. niger* and *P. notatum* with MIC values 21.55 µg/mL and 16.22 µg/mL respectively. The compound **4n** exhibited moderate activity against *A. niger* and *A. parasiticus* with MIC values 19.12 µg/mL and 22.55 µg/mL respectively. The compound **4m** exhibited moderate activity against *P. notatum* with MIC values 19.60 µg/mL.

Table 5. The antifungal activity of the furanyl spiropyrrolizidines **4a-n**, **6a-c**, **8a-c**, **10a-c** and **11** .

S. No.	Compound	Minimum Inhibitory Concentration (µg/mL)		
		Aspergillus niger	***Penicillium notatum***	***Aspergillus parasiticus***
1	**4a**	29.63	38.62	49.04
2	**4b**	44.56	50.17	38.30
3	**4c**	39.24	46.12	49.81
4	**4d**	52.97	58.30	49.66
5	**4e**	61.16	56.73	54.21
6	**4f**	71.80	56.73	37.89
7	**4g**	27.89	34.56	32.91
8	**4h**	30.06	29.72	36.43
9	**4i**	32.33	30.76	36.41
10	**4j**	32.33	54.48	78.49
11	**4k**	72.34	59.22	58.28
12	**4l**	61.25	67.34	63.20
13	**4m**	34.65	**19.60**	33.34
14	**4n**	**19.12**	24.56	**22.55**
15	**6a**	29.90	35.50	32.11
16	**6b**	35.67	35.60	52.17
17	**6c**	39.28	72.61	48.28
18	**8a**	32.45	29.71	56.72
19	**8b**	28.26	25.68	47.09
20	**8c**	**21.55**	**16.22**	54.62
21	**10a**	39.78	33.86	51.93
22	**10b**	40.12	74.90	53.28
23	**10c**	76.21	63.50	48.65
24	**11**	35.67	40.06	38.54
25	**Ketoconazole**	3.12	3.12	4.76

[a]The values are means of triplicates with ± SD.

4.3.2.3. Antioxidant activity

All the synthesized compounds were evaluated for their *in vitro* antioxidant activity. The radical scavenging activity results were depicted in table 8.

All the compounds exhibited the radical scavenging activity with IC_{50} values ranging from 8.62 ± 0.53 µM to 46.11 ± 0.18 µM. The compounds **8c** and **6c** exhibited the potent antioxidant activity having IC_{50} values 8.62 ± 0.53 µM and 9.41 ± 0.45 µM respectively. The compounds **4e** and **4g** showed the good antioxidant activity with IC_{50} values 12.56 ± 0.33 µM and 15.07 ± 0.13 µM respectively. The compound **4m** exhibited good antioxidant activity with IC_{50} value 18.02 ± 0.22 µM.

Table 8. Antioxidant activity of the furanyl spiropyrrolizidines by DPPH scavenging assay**.**

S. No.	Compound	IC_{50} (µM)
1	**4a**	28.22 ± 0.91
2	**4b**	26.13 ± 0.83
3	**4c**	22.15 ± 0.27
4	**4d**	27.31 ± 0.42
5	**4e**	**12.56 ± 0.33**
6	**4f**	39.67 ± 0.71
7	**4g**	**15.07 ± 0.13**
8	**4h**	46.11 ± 0.18
9	**4i**	34.48 ± 0.56
10	**4j**	28.82 ± 0.93
11	**4k**	23.62 ± 0.03
12	**4l**	24.52 ± 0.18
13	**4m**	**18.02 ± 0.22**
14	**4n**	25.76 ± 0.41
15	**6a**	31.52 ± 0.64
16	**6b**	36.19 ± 0.09
17	**6c**	**9.41 ± 0.45**
18	**8a**	19.99 ± 0.75

19	**8b**	24.66 ± 0.83
20	**8c**	**8.62 ± 0.53**
21	**10a**	38.65 ± 0.61
22	**10b**	34.25 ± 0.50
23	**10c**	29.89 ± 0.05
24	**11**	28.54 ± 0.54
25	**Ascorbic acid**	6.32 ± 0.52

4.4. Molecular docking studies

The MurB is a flavoprotein, also known as UDP-*N*-acetylenolpyruvoylglucosamine reductase. It catalyzes the reduction of an enolpyruvyl uridine diphosphate-*N*-acetylglucosamine i.e., the second committed step in the biosynthesis of the peptidoglycan layer in the bacterial cell. The reduced product, UDP-*N*-acetyl muraic acid acts as a locus for peptide portion attachment of the cell wall that consequently affords the cross-links in the cell wall. These cross-links are responsible for cell rigidity. So MurB is an essential enzyme for the synthesis of bacterial cell walls. Hence it is an attractive target for the various antimicrobials [43-46]. Hence we chosen the *E. coli*: MurB (PDB ID: 1MBT) as the target protein, which was retrieved from Protein Data Bank (RCSB) (http://www.rcsb.org/pdb). *In silico* molecular docking studies were used to investigate the antibacterial mechanism and mode of interaction of the synthesized compounds with the MurB.

All the synthesized compounds **4a-n, 6a-c, 8a-c, 10a-c** and **11** exhibited good inhibition activity against the protein 1MBT. The docking results were shown in table 9. Among all the synthesized compounds, the compound **8c** showed significant inhibition activity against the protein 1MBT, which was evident by its least binding energy − 13.02 kcal/Mol. The compound **8c** form three hydrogen bonds: one in between the nitrogen atom of quinoxaline moiety and amino acid residue ILE173 with bond length 2.19 Å, two in between the two CH protons of pyrrolizine ring and amino acid residues ILE45 and PHE171 with bond lengths 3.31 Å and 3.78 Å respectively. The two phenyl rings in the quinoxaline moiety interacts with the amino acid residues ALA85, ILE45, ILE119 and ILE173, the pyrazine ring in the quinoxaline moiety interacts with the amino acid residues ILE45, ILE119 and ILE173,

pyrrolizine ring interacts with the amino acid residue ILE45 and phenyl ring in the benzoyl moiety interacts with the amino acid residues LEU46 AND VAL52 through hydrophobic interactions. The hydrophobic interactions were also responsible for the potent activitiy of the target compounds [47]. The compounds **4g** and **6c** were also exhibited good activity against the protein 1MBT with binding energy values −9.90 kcal/mol and −10.23 kcal/mol respectively. The docking poses of the compounds **4g**, **6c** and **8c** with the protein 1MBT were shown in figure 4.11, 4.12 and 4.13.

Table 9. Docking results of the furanyl spiropyrrolizidines against the protein 1MBT.

S. No.	Compound	Binding energy (Kcal/mol)	No. of hydrogen bonds	Amino acid residues involved in the hydrogen bonding	Hydrogen bond lengths (Å)
1	**4a**	− 9.67	4	GLU334, ARG327	1.69, 1.83, 2.83, 2.93
2	**4b**	− 8.70	3	ILE45, GLN168, PHE171	1.80, 3.15, 3.70
3	**4c**	− 7.74	4	ASN233, TYR125, ARG159	1.79, 1.95, 2.11, 2.84
4	**4d**	− 8.49	4	TYR125, ASN333, ARG159	1.89, 2.23, 2.28, 2.76
5	**4e**	− 8.22	4	ARG214, PRO219, GLY228, PRO111	1.90, 2.95, 2.71, 3.25
6	**4f**	− 7.47	4	GLY126, TYR125, GLY123, ALA124	2.20, 2.35, 3.04, 3.64
7	**4g**	**− 9.90**	5	ARG327, GLU334, GLN168	1.68, 2.06, 2.89, 2.97, 3.01
8	**4h**	− 7.43	6	ASN233, ARG159, TYR125, ALA124, GLN288	1.93, 2.03, 2.71, 2.94, 2.96, 3.58
9	**4i**	− 9.68	2	ILE45, PHE171	1.78, 3.51

10	**4j**	− 8.66	4	ASN233, TYR125, ARG214, ARG159	1.89, 2.07, 2.60, 2.84
11	**4k**	− 9.72	4	ILE45, ILE173, ARG327,	1.66, 2.72, 2.95, 3.62
12	**4l**	− 8.04	5	TYR125, ASN233, ARG214, ARG159	1.73, 2.00, 2.54, 2.81, 2.94
13	**4m**	− 9.01	5	GLY126, TYR125, ASN233, ALA124, GLY123	2.27, 2.37, 2.98, 3.05, 3.56
14	**4n**	− 7.62	3	ARG327, PHE163, GLN168	2.43, 2.57, 3.29
15	**6a**	− 9.22	3	ILE173, ARG 327, PHE163	2.69, 3.09, 3.54
16	**6b**	− 9.57	2	GLY47	2.54, 3.00
17	**6c**	**− 10.23**	1	ILE45	3.25
18	**8a**	− 8.76	2	SER229, ASN233	2.35, 3.44
19	**8b**	− 8.86	1	GLY47	1.71
20	**8c**	**− 13.02**	3	ILE173, PHE171, ILE45	2.19, 3.31, 3.76
21	**10a**	− 8.58	4	ARG327, SER116, GLN168	2.02, 2.29, 2.94, 3.72
22	**10b**	− 8.49	7	SER229, ARG214, PRO219, ILE110, GLY228, PRO111	1.71, 2.24, 2.31, 2.67, 3.00, 3.11, 3.56
23	**10c**	− 8.64	7	SER229, ARG214, PRO219, ILE110, GLY228, PRO111	1.71, 2.24, 2.31, 2.67, 3.02, 3.14, 3.56
24	**11**	− 8.74	4	TYR125, ASN233, SER229	2.11, 2.28, 2.62, 3.08

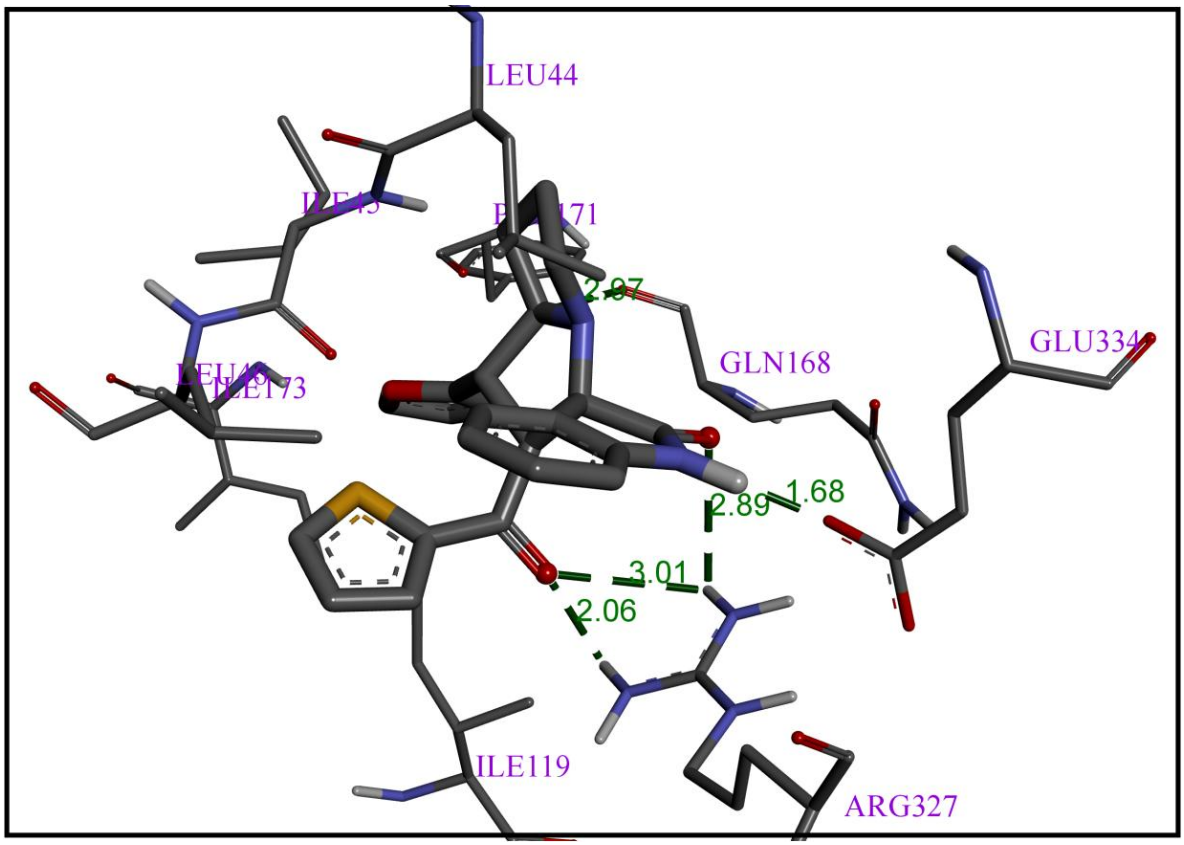

a)

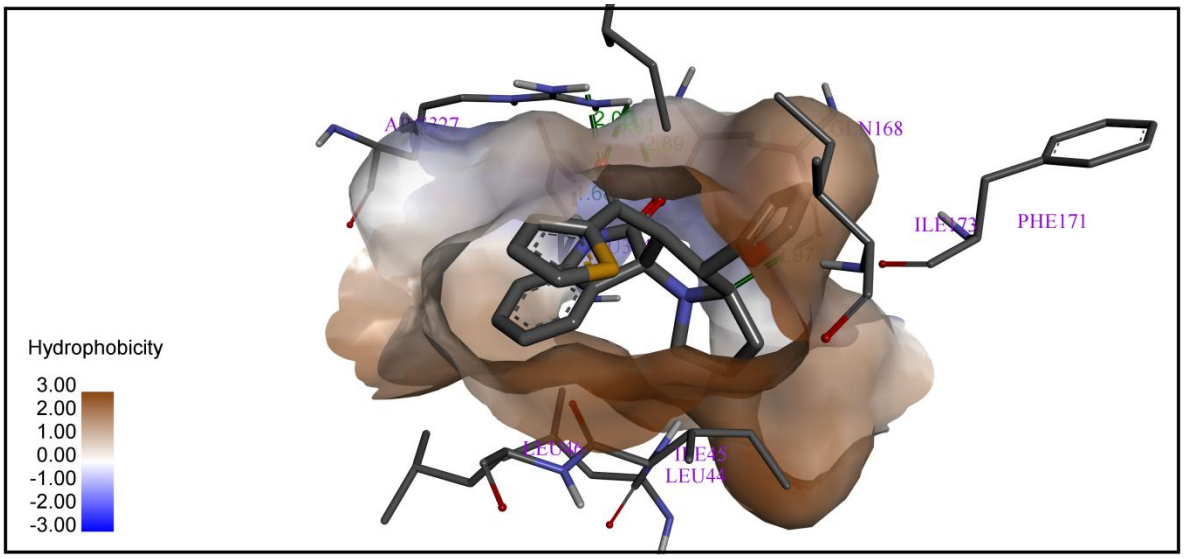

b)

Figure 4.11. The best docking pose of the compound **4g** with the protein 1MBT. a) The hydrogen bond interactions, b) The hydrophobic interactions.

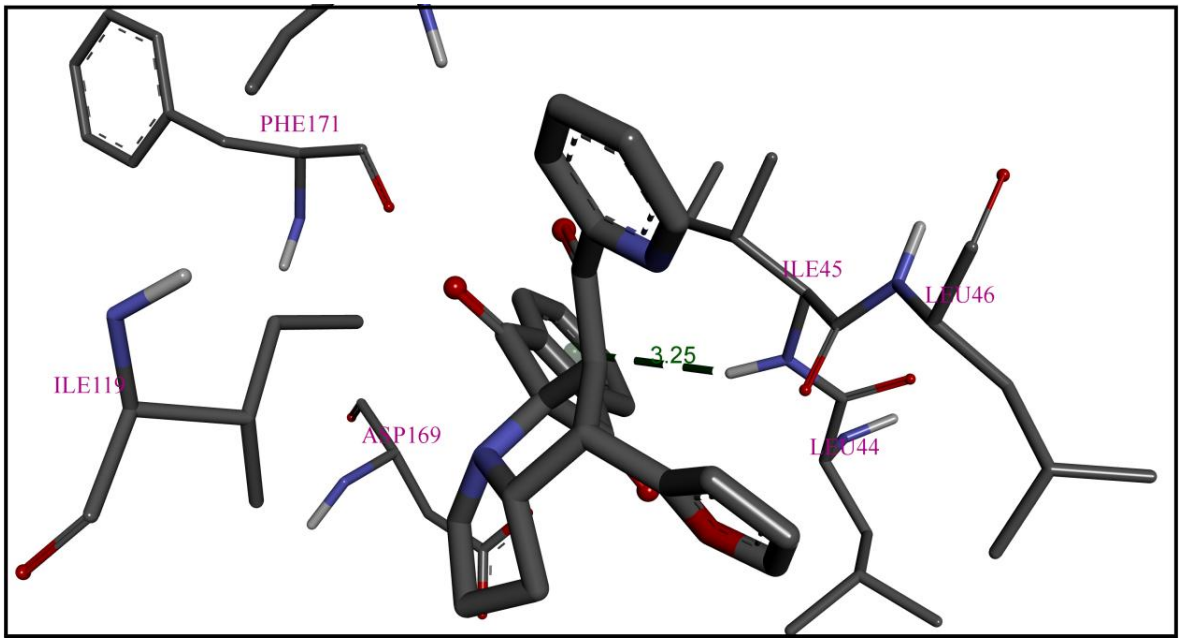

a)

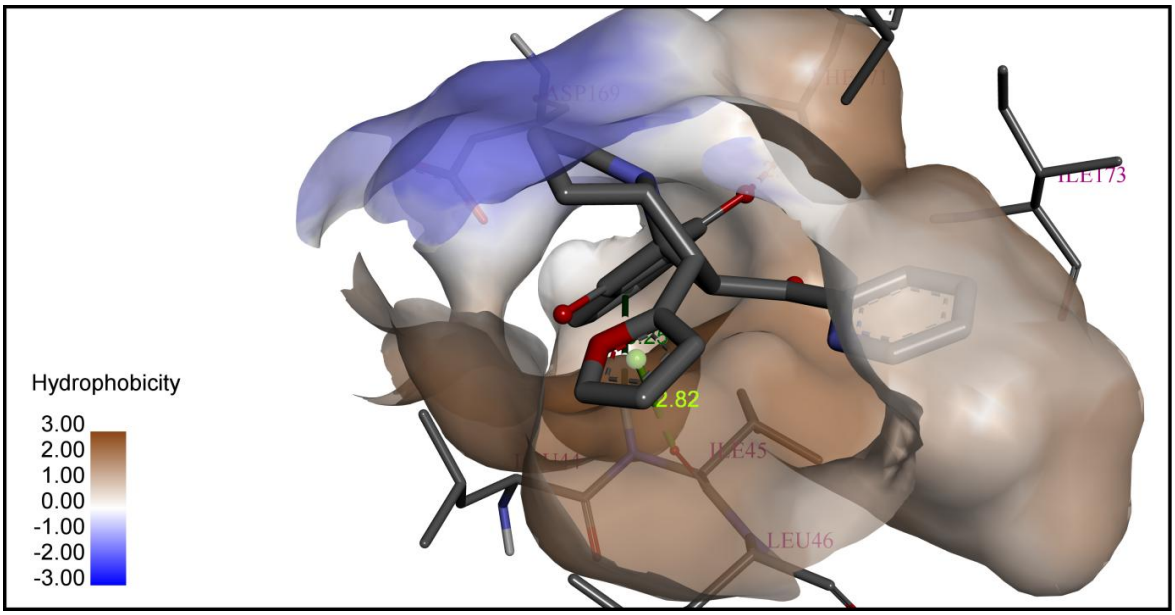

b)

Figure 4.12. The best docking pose of the compound **6c** with the protein 1MBT. a) The hydrogen bond interactions, b) The hydrophobic interactions.

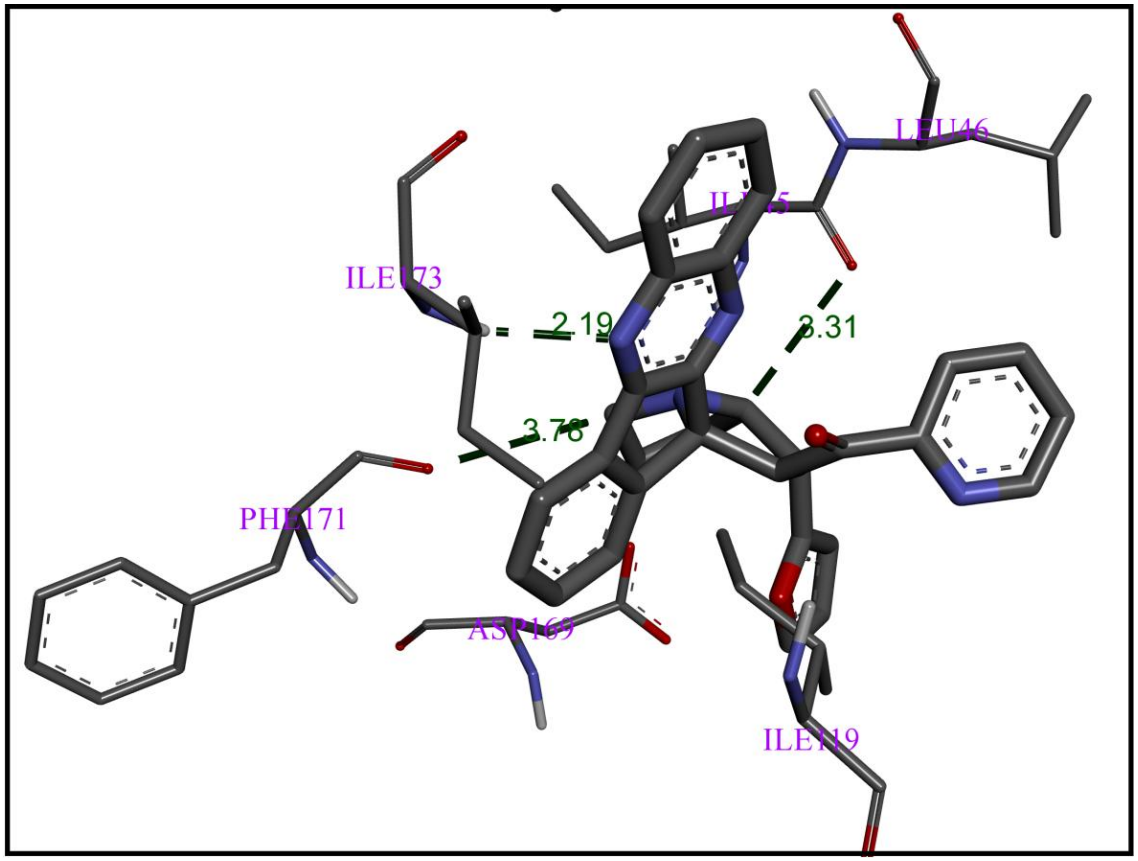

a)

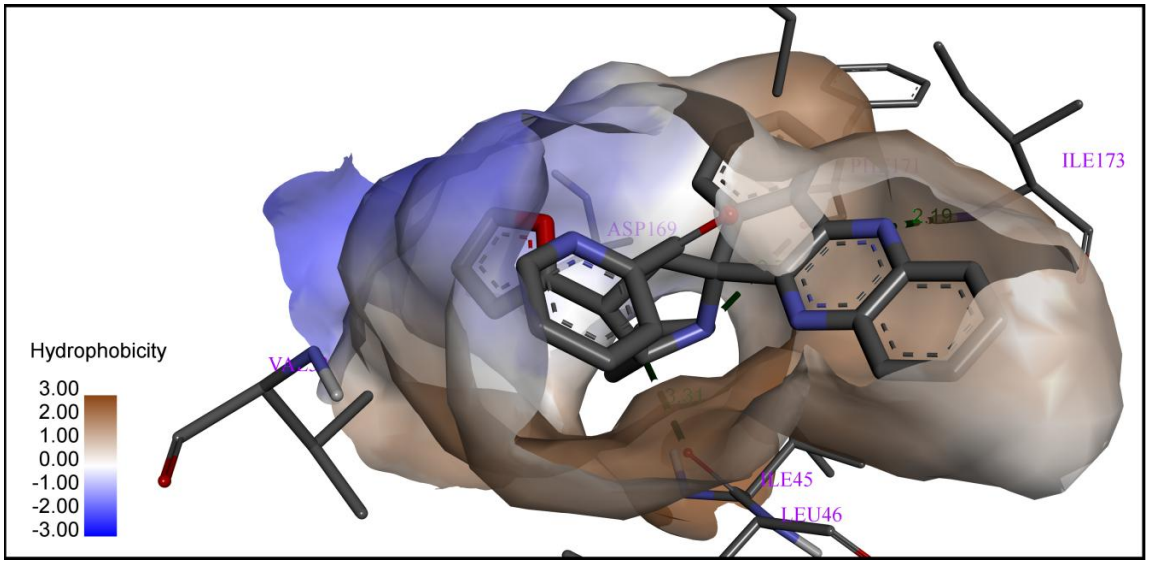

b)

Figure 4.13. The best docking pose of the compound **8c** with the protein 1MBT. a) The hydrogen bond interactions, b) The hydrophobic interactions.

4.5. Conclusion

Various spirooxindolopyrrolizidines and spiroquinoxalinopyrrolizidines were synthesized by 1,3-dipolar cycloaddition with isatin/ninhydrin/11*H*-indeno[1,2-*b*]quinoxalin-11-one with L-proline and different dipolarophiles using ultrasonication, reflux and fusion methods. The results showed that the ultrasonication method is the prior method when compared to conventional heating and fusion methods in the version of reaction times and yields. The synthesized compounds were analyzed by ^{1}H NMR, ^{13}C NMR, and mass spectrometric methods. The structures of compounds **4c** and **4k** were confirmed by single-crystal X-ray diffraction analysis. The target compounds were evaluated for their *in vitro* antimicrobial and antioxidant activities. Among all the target compounds, the compound **8c** exhibited potent antibacterial activity on *E. coli*, *P. aeruginosa* and *K. pneumoniae*. The compounds **4g**, **4m** and **6c** exhibited potent antibacterial activity on *E. coli.* The target compounds showed moderate antifungal activity against all the tested strains. The compounds **6c** and **8c** exhibited potent antioxidant activity. The least binding energy of the compound **8c** (−13.02 kcal/mol) revealed that the *in silico* molecular docking studies against the protein 1MBT were well correlated with the *in vitro* antibacterial activity

4.6. Spectral data

2'-(Furan-2-carbonyl)-1'-(furan-2-yl)-1',2',5',6',7',7a'-hexahydrospiro[indoline-3,3'-pyrrolizin]-2-one (4a)

Colour: White. M. P. 215-217 ℃. IR (KBr, cm^{-1}): 3335, 3123, 2871, 1731, 1677, 1393, 768. ^{1}H NMR (400 MHz, $CDCl_3$) δ: 7.84 (s, 1H), 7.39 (d, 1H, J = 2.4 Hz), 7.31(d, 1H, J = 2.8 Hz), 7.24 (d, 1H, J = 7.6 Hz), 7.14 (t, 1H, J = 7.6 Hz), 7.06 (d, 1H, J = 3.2 Hz), 7.00 (t, 1H, J = 7.6 Hz), 6.69 (d, 1H, J = 7.6 Hz), 6.33-6.32 (dd, 1H, $J_{1,2}$ = $J_{3,4}$ = 1.6 Hz), 6.26-6.25 (dd, 1H, $J_{1,2}$ = $J_{3,4}$ = 1.6 Hz), 6.16 (d, 1H, J = 3.6 Hz), 4.72 (d, 1H, J = 11.6 Hz), 4.29-4.23 (m, 1H), 4.04 (t, 1H, J = 10 Hz), 2.70- 2.57 (m, 2H), 2.15-1.79 (m, 4H). ^{13}C NMR (100 MHz, $CDCl_3$) δ: 207.08, 183.77, 180.50, 153.02, 147.05, 141.78, 140.38, 129.56, 127.70, 124.81, 122.42, 118.65, 112.24, 110.18, 106.17, 73.54, 68.80, 61.49, 48.13, 45.52, 30.96, 30.59, 27.15. ESI mass spectrum (*m/z*): 389.10 (M+). Anal. Calcd. for $C_{23}H_{20}N_2O_4$: C, 71.12; H, 5.19; N, 7.21; found: C, 70.94; H, 5.42; N 7.49.

2'-(Furan-2-carbonyl)-1'-(furan-2-yl)-1-methyl-1',2',5',6',7',7a'-hexahydrospiro[indoline-3,3'-pyrrolizin]-2-one (4b)

Colour: White. M. P. 184-186 ℃. IR (KBr, cm^{-1}): 3319, 3111, 2872, 1727, 1668, 1372, 757. ^{1}H NMR (400 MHz, $CDCl_3$) δ: 7.36 (d, 1H, J = 2.4 Hz), 7.30 (d, 1H, J = 2.8 Hz), 7.24-7.18 (m, 2H), 7.03-6.97 (m , 2H), 6.61 (d, 1H, J = 7.6 Hz), 6.33-6.31 (dd, 1H, $J_{1,2} = J_{3,4}$ = 2.0 Hz), 6.26-6.25 (dd, 1H, $J_{1,2} = J_{3,4}$ = 1.6 Hz), 6.15 (d, 1H, J = 3.2 Hz), 4.68 (d, 1H, J = 11.6 Hz), 4.32-4.26 (m, 1H), 4.02 (t, 1H, J = 10 Hz), 3.06 (s, 3H), 2.70-2.54 (m, 2H), 2.15-1.81 (m, 4H).^{13}C NMR (100 MHz, $CDCl_3$) δ: 188.38, 178.72, 153.02, 143.96, 143.10, 141.78, 134.46, 132.31, 129.56, 127.66, 124.37, 122.51, 110.20, 108.14, 106.18, 73.89, 69.03, 62.99, 50.82, 48.33, 45.66, 30.88, 27.34, 26.24. ESI mass spectrum (*m/z*): 403.15 (M+). Anal. Calcd. for $C_{24}H_{22}N_2O_4$: C, 71.63; H, 5.51; N, 6.96; found: C, 71.35; H, 5.79; N, 6.73.

1-Butyl-2'-(furan-2-carbonyl)-1'-(furan-2-yl)-1',2',5',6',7',7a'-hexahydrospiro[indoline-3,3'-pyrrolizin]-2-one (4c)

Colour: White. M. P. 193-195 ℃. IR (KBr, cm^{-1}): 3336, 2860, 1734, 1674, 774. ^{1}H NMR (400 MHz, $CDCl_3$) δ: 7.36 (d, 1H, J = 1.2 Hz), 7.30 (d, 1H, J = 2.0 Hz), 7.26-7.18 (m, 2H), 7.06-6.99 (m, 2H), 6.65 (d, 1H, J = 7.6 Hz), 6.33-6.32 (dd, 1H, $J_{1,2} = J_{3,4}$ = 1.6 Hz), 6.26-6.25 (dd, 1H, $J_{1,2} = J_{3,4}$ = 2.0 Hz), 6.15 (d, 1H, J = 3.2 Hz), 4.71 (d, 1H, J = 11.6 Hz), 4.30-4.25 (m, 1H), 4.04 (t, 1H, J = 10 Hz), 3.76-3.54 (m, 2H), 2.64-2.53 (m, 2H), 2.14-1.79 (m, 4H), 1.06 (t, 3H, J = 7.2 Hz).^{13}C NMR (100 MHz, $CDCl_3$) δ: 183.77, 178.08, 153.10, 152.05, 147.05, 142.40, 141.79, 129.54, 127.54, 124.59, 122.18, 119.01, 112.07, 110.17, 108.31, 106.12, 73.39, 68.84, 61.48, 48.16, 45.44, 34.84, 30.58, 27.17, 12.43. ESI mass spectrum (*m/z*): 417.20 (M+). Anal. Calcd. for $C_{25}H_{24}N_2O_4$: C, 72.10; H, 5.81; N, 6.73; found: C, 72.31; H, 5.55; N, 6.49.

1-Benzyl-1'-(furan-2-l)-2'-(furan-3-carbonyl)-1',2',5',6',7',7a'-hexahydrospiro[indoline-3,3'-pyrrolizin]-2-one (4d)

Colour: White. M. P. 197-199 ℃. IR (KBr, cm^{-1}): 2961, 1717, 1668, 759. ^{1}H NMR (400 MHz, $CDCl_3$) δ: 7.73 (s, 1H), 7.56 (d, 1H, J = 3.2 Hz), 7.30-7.22 (m, 4H), 7.16-7.12 (m, 3H), 7.08 (d, 1H, J = 3.6 Hz), 6.97 (t, 1H, J = 6.8 Hz), 6.72 (d, 1H, J = 7.6 Hz), 6.52 (d, 1H, J =

5.6 Hz), 6.37 (d, 1H, *J* = 4.8 Hz), 6.26 (d, 1H, *J* = 3.2 Hz), 4.87-4.73 (dd, 2H, $J_{1,2}$ = $J_{3,4}$ = 15.6 Hz), 4.64 (d, 1H, *J* = 11.6 Hz), 4.05-3.98 (m, 2H), 2.57-2.33 (m, 2H), 2.03-1.70 (m, 4H). ESI mass spectrum (*m/z*): 479.35 (M+). Anal. Calcd. for $C_{30}H_{26}N_2O_4$: C, 75.30; H, 5.48; N, 5.85; found: C, 75.05; H, 5.55; N, 5.67.

5-Chloro-2'-(furan-2-carbonyl)-1'-(furan-2-yl)-1',2',5',6',7',7a'-hexahydrospiro[indoline-3,3'-pyrrolizin]-2-one (4e)

Colour: White. M. P. 212-214 ℃. IR (KBr, cm^{-1}): 3280, 3107, 2863, 1729, 1651, 1393, 781. ^{1}H NMR (400 MHz, $CDCl_3$) *δ*: 7.88 (s, 1H), 7.42 (d, 1H, *J* = 2.4 Hz), 7.30 (d, 1H, *J* = 2.4 Hz), 7.22 (d, 1H, *J* = 2.0 Hz), 7.15-7.12 (dd, 1H, $J_{1,2}$ = $J_{3,4}$ = 2.0 Hz), 7.09 (d, 1H, *J* = 3.2 Hz), 6.65 (d, 1H, *J* = 8.4 Hz), 6.36-6.35 (dd, 1H, $J_{1,2}$ = $J_{3,4}$ = 1.6 Hz), 6.27-6.25 (dd, 1H, $J_{1,2}$ = $J_{3,4}$ = 2.0 Hz), 6.16 (d, 1H, *J* = 3.2 Hz), 4.72 (d, 1H, *J* = 11.6 Hz), 4.28-4.22 (m, 1H), 4.00 (t, 1H, *J* = 10 Hz), 2.64-2.61 (m, 2H), 2.16-1.75 (m, 4H). ^{13}C NMR (100 MHz, $CDCl_3$) *δ*: 188.07, 183.39, 180.51, 152.62, 152.05, 147.18, 141.89, 138.98, 129.68, 127.98, 127.82, 126.68, 118.79, 112.41, 111.08, 110.24, 106.36, 73.67, 68.85, 61.54, 48.00, 45.54, 30.65, 27.40. ESI mass spectrum (*m/z*): 423.10 (M+); Anal. Calcd. For $C_{23}H_{19}N_2O_4Cl$: C, 65.33; H, 4.53; N, 6.62; found; C, 65.61; H, 4.29; N, 6.36.

5-Bromo-2'-(furan-2-carbonyl)-1'-(furan-2-yl)-1',2',5',6',7',7a'-hexahydrospiro[indoline-3,3'-pyrrolizin]-2-one (4f)

Colour: White. M. P. 203-205 ℃. IR (KBr, cm^{-1}): 3282, 2864, 1727, 1655. ^{1}H NMR (400 MHz, $CDCl_3$) *δ*: 10.19 (s 1H), 7.56-7.04 (m, 7H), 6.53-6.07 (m, 6H) 4.57 (bs, 1H), 4.12 (bs, 1H), 3.85 (bs, 1H), 2.04-1.64 (m, 6H). Anal. Calcd. For $C_{23}H_{19}N_2O_4Br$: C, 59.11; H, 4.10; N, 5.99; found; C, 59.33; H, 4.19; N, 5.76.

1'-(Furan-2-yl)-2'-(thiophene-2-carbonyl)-1',2',5',6',7',7a'-hexahydrospiro[indoline-3,3'-pyrrolizin]-2-one (4g)

Colour: White. M. P. 231-232 ℃. IR (KBr, cm^{-1}): 3300, 3063, 2874, 1730, 1660, 1325, 751. ^{1}H NMR (400 MHz, $CDCl_3$) *δ*: 7.63 (d, 1H, *J* = 3.6 Hz), 7.48 (d, 1H, *J* = 4.0 Hz), 7.31 (d, 1H, *J* = 1.6 Hz), 7.16-6.96 (m, 4H), 6.61 (d, 1H, *J* = 7.6 Hz), 6.26-6.25 (dd, 1H, $J_{1,2}$ = $J_{3,4}$ = 1.6 Hz), 6.15 (d, 1H, *J* = 3.2 Hz), 4.83 (d, 1H, *J* = 11.6 Hz), 4.30-4.24 (m, 1H),4.02 (t, 1H, *J*

= 7.2 Hz), 2.68-2.58 (m, 2H), 2.17-1.79 (m, 4H). ^{13}C NMR (100 MHz, DMSO-*d*6) δ: 188.55, 179.74, 153.72, 143.99, 142.65, 136.38, 133.30, 129.81, 129.01, 127.99, 124.91, 121.66, 110.90, 110.11, 106.38, 73.19, 69.06, 61.84, 47.91, 45.91, 31.17, 30.27, 27.18. ESI mass spectrum (*m/z*): 405.10 (M+). Anal. Calcd. For $C_{23}H_{20}N_2O_3S$: C, 68.30; H, 4.98; N, 6.93; found: C, 68.07; H, 5.76; N, 6.69.

1'-(Furan-2-yl)-1-methyl-2'-(thiophene-2-carbonyl)-1',2',5',6',7',7a'-hexahydrospiro[indoline-3,3'-pyrrolizin]-2-one (4h)

Colour: White. M. P. 191-193 °C. IR (KBr, cm^{-1}) : 3280, 3111, 2872, 1717, 1650, 1416, 755.^{1}H NMR (400 MHz, $CDCl_3$) δ: 7.5 (d, 1H, *J* = 2.8 Hz), 7.44 (d, 1H, *J* = 4.0 Hz), 7.31 (d, 1H, *J* = 2.4 Hz), 7.24-7.17 (m, 2H), 7.04 (t, 1H, *J*= 7.6 Hz), 6.95 (t, 1H, *J*= 4.0 Hz), 6.54 (d, 1H, *J*= 7.6 Hz), 6.26-6.25 (dd, 1H, $J_{1,2} = J_{3,4}$ = 2.0 Hz), 6.16 (d, 1H, *J* = 3.2 Hz), 4.78 (d, 1H, *J* = 11.6 Hz), 4.31-4.26 (m, 1H), 4.0 (t, 1H, *J* = 11.2 Hz), 2.95 (s, 3H), 2.68-2.55 (m, 2H), 2.17-1.81(m, 4H). ^{13}C NMR (100 MHz, $CDCl_3$) δ: 183.82, 178.66, 153.09, 152.07, 146.84, 143.27, 141.76, 129.58, 127.19, 124.34, 122.41, 118.41, 112.03, 110.18, 108.10, 106.14, 73.45, 68.84, 61.92, 48.31, 45.30, 30.56, 27.11, 26.37. ESI mass spectrum (*m/z*): 419.10 (M+). Anal. Calcd. For $C_{24}H_{22}N_2O_3S$: C, 68.88; H, 5.30; N, 6.69; found: C, 68.64; H, 5.53; N, 6.93.

1-Ethyl-1'-(furan-2-yl)-2'-(thiophene-2-carbonyl)-1',2',5',6',7',7a'-hexahydrospiro[indoline-3,3'-pyrrolizin]-2-one (4i)

Colour: White. M. P. 198-200 °C. IR (KBr, cm^{-1}): 3276, 3112, 2869, 1716, 1650, 1354, 754. ^{1}H NMR (400 MHz, $CDCl_3$) δ: 7.57 (d, 1H, *J* = 3.6 Hz), 7.44 (d, 1H, *J* = 4.8 Hz), 7.31-7.18 (m, 3H), 7.04 (t, 1H, *J* = 7.6 Hz), 6.94 (t, 1H, *J* = 4.4 Hz), 6.60 (d, 1H, *J* = 8 Hz), 6.25 (s, 1H), 6.15 (d, 1H, *J* = 2.8 Hz), 4.84 (d, 1H, *J* = 11.6 Hz), 4.30-4.24 (m, 1H), 4.03 (t, 1H, *J* = 10.4 Hz), 3.67-3.45 (m, 2H), 2.64-2.54 (m, 2H), 2.15-1.78 (m, 4H), 0.95 (t, 3H, *J* = 7.2 Hz). ^{13}C NMR (100 MHz, $CDCl_3$) δ: 188.40, 178.10, 153.07, 144.12, 142.28, 141.80, 134.53, 132.74, 129.49, 127.90, 124.61, 122.23, 110.18, 108.32, 106.12, 73.69, 69.02, 62.35, 50.86, 48.17, 45.84, 34.83, 30.86, 27.36, 12.08. ESI mass spectrum (*m/z*): 433.15 (M+). Anal. Calcd. For $C_{25}H_{24}N_2O_3S$: C, 69.42; H, 5.59; N, 6.48; found: C, 69.69; H, 5.85; N, 6.19.

1-Benzyl-1'-(furan-2-l)-2'-(thiophene-3-carbonyl)-1',2',5',6',7',7a'-hexahydrospiro[indoline-3,3'-pyrrolizin]-2-one (4j)

Colour: White. M. P. 210-211 °C. IR (KBr, cm^{-1}): 2942, 1716, 1655, 749. ^{1}H NMR (400 MHz, $CDCl_3$) δ: 7.91 (d, 1H, J = 6.0 Hz), 7.57-7.56 (m, 2H), 7.32 (d, 1H, J = 6.8 Hz), 7.24-7.22 (m, 3H), 7.13 (t, 1H, J = 7.6 Hz), 7.07-7.04 (m, 3H), 7.00 (t, 1H, J = 7.6 Hz), 6.66 (d, 1H, J = 7.6 Hz), 6.37 (d, 1H, J = 5.2 Hz), 6.28 (d, 1H, J = 2.8 Hz), 4.81-4.64 (m, 3H), 4.10-4.02 (m, 2H), 2.38-1.73 (m, 6H). ESI mass spectrum (*m/z*): 493.40 (M-). Anal. Calcd. For $C_{30}H_{26}N_2O_3S$: C, 72.85; H, 5.30; N, 5.66; found: C, 72.59; H, 5.35; N, 5.92.

5-Chloro-1'-(furan-2-yl)-2'-(thiophene-2-carbonyl)-1',2',5',6',7',7a'-hexahydrospiro[indoline-3,3'-pyrrolizin]-2-one (4k)

Colour: White. M. P. 220-222 °C. IR (KBr, cm^{-1}): 3333, 2860, 1734, 1674,774. ^{1}H NMR (400 MHz, $CDCl_3$) δ: 7.62 (d, 1H, J = 4.0 Hz), 7.51 (d, 1H, J = 4.0 Hz), 7.44 (s, 1H), 7.31 (d, 1H, J = 1.2 Hz), 7.24 (dd, 1H, J = 1.0 Hz), 7.15-7.13 (dd, 1H, $J_{1,2} = J_{3,4}$ = 2.0 Hz), 6.98-6.96 (dd, 1H, $J_{1,2} = J_{3,4}$ = 4.0 Hz), 6.58 (d, 1H, J = 8.4 Hz), 6.26-6.25 (dd, 1H, $J_{1,2} = J_{3,4}$ = 2.0 Hz), 6.16 (d, 1H, J = 3.2 Hz), 4.83 (d, 1H, J = 11.6 Hz), 4.29-4.23 (m, 1H), 3.99 (t, 1H, J = 10 Hz), 2.64-2.61 (m, 2H), 2.18-1.75 (m, 4H). ^{13}C NMR (100 MHz, $CDCl_3$) δ: 207.11, 187.90, 180.16, 152.61, 144.08, 141.90, 138.82, 134.93, 132.64, 129.61, 128.06, 127.97, 126.73, 110.97, 110.23, 106.33, 73.95, 68.96, 62.38, 47.99, 46.03, 30.96, 27.55. ESI mass spectrum (*m/z*): 439.05 (M+). Anal. Calcd. For $C_{23}H_{19}N_2O_3ClS$: C, 62.94; H, 4.36; N, 6.38; found: C, 62.68; H, 4.57; N, 6.67.

5-Bromo-1'-(furan-2-yl)-2'-(thiophene-2-carbonyl)-1',2',5',6',7',7a'-hexahydrospiro[indoline-3,3'-pyrrolizin]-2-one (4l)

Colour: White. M. P. 224-226°C. IR (KBr, cm^{-1}): 3298, 2855, 1730, 1635, 737.^{1}H NMR (400 MHz, $CDCl_3$) δ: 10.53 (s, 1H), 7.91 (s, 1H), 7.59-7.13 (m, 5H), 6.59-6.26 (m, 3H), 4.66 (bs, 1H), 3.95 (bs, 2H), 2.37-1.76 (m, 6H). Anal. Calcd. For $C_{23}H_{19}N_2O_3BrS$: C, 57.15; H, 3.96; N, 5.80; found: C, 57.38; H, 3.90; N, 5.50.

1'-(Furan-2-yl)-2'-picolinoyl-1',2',5',6',7',7a'-hexahydrospiro[indoline-3,3'-pyrrolizin]-2-one (4m)

Colour: White. M. P. 212-214 ℃. IR (KBr, cm^{-1}): 3376, 3004, 2869, 1743, 1697, 1320, 760. ^{1}H NMR (400 MHz, $CDCl_3$) δ: 8.50-8.48 (m, 1H), 8.35 (s, 1H), 7.54-7.50 (m, 2H), 7.32 (d, 1H, J = 2.0 Hz), 7.22-7.24 (m, 1H), 7.03-6.94 (m, 2H), 6.80 (t, 1H, J = 7.6 Hz), 6.53 (d, 1H, J = 7.6 Hz), 6.28-6.27 (dd, 1H, $J_{1,2}$ = $J_{3,4}$ = 1.6 Hz), 6.21 (d, 1H, J = 3.2 Hz), 5.32 (d, 1H, J = 11.2 Hz), 4.35-4.29 (m, 1H), 3.98 (t, 1H, J = 10.4 Hz), 2.82-2.54 (m, 2H), 2.19-1.86 (m, 4H). ^{13}C NMR (100 MHz, $CDCl_3$) δ: 198.19, 182.03, 154.01, 152.48, 148.23, 141.59, 136.33, 129.13, 126.97, 126.90, 125.72, 121.49, 121.34, 110.15, 109.84, 105.86, 72.52, 68.59, 61.26, 48.70, 45.55, 29.79, 26.36. ESI mass spectrum (*m/z*): 399.44 (M+). Anal. Calcd. For $C_{24}H_{21}N_3O_3$: C, 72.16; H, 5.30; N, 10.52; found: C, 72.42; H, 5.49; N, 10.26.

5-Chloro-1'-(furan-2-yl)-2'-picolinoyl-1',2',5',6',7',7a'-hexahydrospiro[indoline-3,3'-pyrrolizin]-2-one (4n)

Colour: White. M. P. 209-211 ℃. ^{1}H NMR (400 MHz, $CDCl_3$) δ: 9.44 (s, 1H), 8.49 (d, 1H, J = 3.6 Hz), 7.55-7.62 (m, 3H), 7.22-7.33 (m, 2H), 7.01-6.96 (m, 2H), 6.29 (d, 1H, J = 3.2 Hz), 6.22 (d, 1H, J = 3.2 Hz), 5.31 (d, 1H, J = 11.2 Hz), 4.34-4.28 (m, 1H), 3.97 (t, 1H, J = 10.4 Hz), 2.57-2.79 (m, 2H), 2.18-1.84 (m, 4H). ^{13}C NMR (100 MHz, $CDCl_3$) δ: 197.80, 182.17, 153.66, 152.36, 148.27, 141.67, 140.37, 136.58, 129.16, 127.63, 127.17, 126.89, 121.57, 110.97, 110.20, 106.03, 72.54, 68.54, 61.31, 48.55, 45.46, 29.66, 26.50. ESI mass spectrum (*m/z*): 434.10 (M+). Anal. Calcd. For $C_{24}H_{20}N_3O_3Cl$: C, 66.44; H, 4.65; N, 9.68; found: C, 66.17; H, 4.90; N, 9.43.

2'-(Furan-2-carbonyl)-1'-(furan-2-yl)-1',2',5',6',7',7a'-hexahydrospiro[indene-2,3'-pyrrolizine]-1,3-dione (6a)

Colour: Yellow. M. P. 185-187 ℃. ^{1}H NMR (400 MHz, $CDCl_3$) δ: 7.44 (d, 1H, J = 2.4 Hz), 7.35(d, 1H, J = 2.8 Hz), 7.28 (d, 1H, J = 7.6 Hz), 7.19 (t, 1H, J = 7.6 Hz), 7.11 (d, 1H, J = 3.2 Hz), 7.43 (t, 1H, J = 7.6 Hz), 6.74 (d, 1H, J = 7.6 Hz), 6.38-6.36 (dd, 1H, $J_{1,2}$ = $J_{3,4}$ = 1.6 Hz), 6.31- 6.30 (dd, 1H, $J_{1,2}$ = $J_{3,4}$ = 1.6 Hz), 6.20 (d, 1H, J = 3.6 Hz), 4.76 (d, 1H, J = 11.6 Hz), 4.34-4.28 (m, 1H), 4.09 (t, 1H, J = 10 Hz), 2.75-2.63 (m, 2H), 2.19-1.83 (m, 4H). ^{13}C

NMR (100 MHz, DMSO) δ: 201.35, 200.94, 197.21, 151.15, 146.16, 140.43, 137.46, 138.17, 133.70, 131.35, 131.07, 128.52, 128.17, 127.77, 127.65, 123.28, 122.98, 79.61, 75.87, 73.66, 63.94, 47.61, 30.23, 28.26. ESI mass spectrum (*m/z*): 400.10 (M-). Anal. Calcd. For $C_{24}H_{19}NO_5$: C, 71.81; H, 4.77; N, 3.49; found: C, 71.61; H, 4.70; N, 3.73.

2'-(Furan-2-carbonyl)-1'-(thiophene-2-yl)-1',2',5',6',7',7a'-hexahydrospiro[indene-2,3'-pyrrolizine]-1,3-dione (6b)

Colour: Yellow. M. P. 190-192 °C. ^{1}H NMR (400 MHz, $CDCl_3$) δ: 7.62 (d, 1H, J = 3.6 Hz), 7.47 (d, 1H, J = 4.0 Hz), 7.30 (d, 1H, J = 1.6 Hz), 7.16-6.95 (m, 4H), 6.60 (d, 1H, J = 7.6 Hz), 6.26-6.24 (dd, 1H, $J_{1,2}$ = $J_{3,4}$ = 1.6 Hz), 6.15 (d, 1H, J = 3.2 Hz), 4.82 (d, 1H, J = 11.6 Hz), 4.29 - 4.23 (m, 1H), 4.02 (t, 1H , J = 7.2 Hz), 2.67-2.57 (m, 2H), 2.16-1.76 (m, 4H) . ^{13}C NMR (100 MHz, DMSO) δ. 201.42, 201.02, 197.28, 151.22, 146.24, 140.51, 138.25, 137.54, 136.74, 133.77, 131.42, 131.14, 128.60, 128.24, 127.84, 127.72, 123.36, 123.06, 79.68, 75.94, 73.73, 64.01, 47.69, 30.31, 28.33. ESI mass spectrum (*m/z*): 416.60 (M-); Anal. Calcd. For $C_{24}H_{19}NO_4S$: C, 69.05; H, 4.59; N, 3.36; found: C, 69.27; H, 4.67; N, 3.63.

1'-(Furan-2-yl)-2'-picolinoyl-1',2',5',6',7',7a'-hexahydrospiro[indene-2,3'-pyrrolizine]-1,3-dione (6c)

Colour: Yellow. M. P. 182-184 °C. ^{1}H NMR (400 MHz, $CDCl_3$) δ: 7.29(t, 2H, J = 7.2 Hz), 7.81-7.64 (m, 4H), 7.51 (t, 1H, J = 7.2 Hz), 7.34 (d, 1H, J = 4.8 Hz), 7.26 (d, 2H, J = 3.6 Hz), 6.74 (t, 1H, J = 4.0 Hz), 5.03 (d, 1H, J = 12.0 Hz), 4.84 (t, 1H, J = 10.8 Hz), 4.30-4.21 (m,1H), 2.82 (m, 2H), 2.26-1.89 (m, 4H). ^{13}C NMR (100 MHz, DMSO) δ: 201.14, 200.74, 197.00, 150.94, 145.96, 140.23, 137.97, 137.26, 136.46, 133.49, 131.14, 130.86, 128.32, 127.96, 127.56, 127.44, 123.08, 122.78, 79.40, 75.66, 73.45, 63.73, 47.41, 30.03, 28.05. ESI mass spectrum (*m/z*): 411.20 (M-). Anal. Calcd. For $C_{25}H_{20}N_2O_4$: C, 72.80; H, 4.89; N, 6.79; found: C, 72.57; H, 4.80; N, 6.53.

Furan-2-yl(1'-(furan-2-yl)-1',2',5',6',7',7a'-hexahydrospiro[indeno[1,2-b]quinoxaline-11,3'-pyrrolizin]-2'-yl)methanone (8a)

Colour: Yellow. M. P. 181-183°C. ^{1}H NMR (400 MHz, $CDCl_3$) δ: 8.37-7.16 (m, 10H), 6.61-6.22 (m, 4H), 4.87 (d, 1H, J = 11.2 Hz), 4.58-4.53 (m, 1H), 4.33 (t, 1H, J = 11.6 Hz), 2.80-

2.47 (m, 2H), 2.30-1.86 (m, 4H). ^{13}C NMR (100 MHz, $CDCl_3$) δ: 188.66, 164.54, 153.56, 153.03, 143.79, 143.46, 142.77, 142.12, 141.79, 137.28, 134.10, 132.03, 131.07, 129.82, 129.75, 128.97, 128.66, 128.24, 127.04, 122.14, 110.25, 109.70, 106.09, 75.47, 69.40, 65.50, 63.81, 47.82, 45.86, 31.34, 27.95. ESI mass spectrum (*m/z*): 473.17 (M+). Anal. Calcd. For $C_{30}H_{23}N_3O_3$: C, 76.09; H, 4.90; N, 8.87; found: C, 75.87; H, 4.65; N, 8.64.

(1'-(Furan-2-yl)-1',2',5',6',7',7a'-hexahydrospiro[indeno[1,2-b]quinoxaline-11,3'-pyrrolizin]-2'-yl)(thiopnen-2-yl)methanone (8b)

Colour: Yellow. M. P. 192-194 ℃. IR (KBr, cm^{-1}): 3103, 2942, 2853, 1657. ^{1}H NMR (400 MHz, $CDCl_3$) δ: 7.16- 8.37 (m, 10H), 6.61-6.22 (m, 4H), 4.77 (d, 1H, J = 11.2 Hz), 4.59-4.52 (m, 1H), 4.32 (t, 1H, J = 11.6 Hz), 2.70-2.49 (m, 2H), 2.28-1.91 (m, 4H). ^{13}C NMR (100 MHz, $CDCl_3$) δ: 188.66, 164.54, 153.56, 153.03, 143.79, 143.46, 142.77, 142.12, 141.79, 137.28, 134.10, 132.03, 131.07, 129.82, 129.75, 128.97, 128.66, 128.24, 127.04, 122.14, 110.25, 109.70, 106.09, 75.47, 69.40, 65.50, 63.81, 47.82, 45.86, 31.34, 27.95. ESI mass spectrum (*m/z*): 490.20 (M+). Anal. Calcd. For $C_{30}H_{23}N_3O_2S$: C, 73.60; H, 4.74; N, 8.58; found: C, 73.34; H, 4.44; N, 8.78.

(1'-(Furan-2-yl)-1',2',5',6',7',7a'-hexahydrospiro[indeno[1,2-b]quinoxaline-11,3'-pyrrolizin]-2'-yl)(pyridin-2-yl)methanone (8c)

Colour: Yellow. M. P. 193-195 ℃. IR (KBr, cm^{-1}): 3113, 2942, 2883, 1692. ^{1}H NMR (400 MHz, $CDCl_3$) δ: 8.36-8.38 (m, 1H), 8.08-8.03 (m, 1H), 7.78-7.73 (m, 3H), 7.53-7.21 (m, 7H), 6.89-6.86 (m, 1H), 6.31-6.27 (m, 2H), 5.80 (d, 1H, J = 3.6 Hz), 4.66-4.60 (m, 1H), 4.24 (t, 1H, J = 11.6 Hz), 2.78-2.48 (m, 2H), 2.27-1.93 (m, 4H). ^{13}C NMR (100 MHz, $CDCl_3$) δ: 198.27, 165.84, 154.29, 152.75, 152.32, 147.22, 144.07, 142.59, 142.42, 141.58, 137.67, 136.23, 130.64, 130.16, 129.33, 129.19, 128.70, 128.63, 127.57, 126.47, 121.85, 121.44, 110.18, 105.85, 74.30, 69.37, 62.69, 47.83, 45.27, 30.56, 27.31. ESI mass spectrum (*m/z*): 485.20 (M+). Anal. Calcd. For $C_{31}H_{24}N_4O_2$: C, 76.84; H, 4.99; N, 11.56; found: C, 76.57; H, 4.71; N, 11.76.

(1'-(Furan-2-yl)-2-oxo-5',6',7',7a'-tetrahydrospiro[indoline-3,3'-pyrrolizine]-2',2'(1'*H*)-dicarbonitrile (10a)

Colour: White. M. P. 218-220 ℃. IR (KBr, cm^{-1}): 3405, 2883, 2243, 1717, 745. ^{1}H NMR (400 MHz, $CDCl_3$) δ: 10.74 (s, 1H), 7.7 (d, 1H, J = 7.2 Hz) 7.65 (s, 1H), 7.27, (t, 1H, J = 8.0 Hz), 6.97 (t, 1H, J = 7.2 Hz), 6.82 (d, 1H, J = 7.6 Hz), 6.39 (d, 1H, J = 4.8 Hz), 6.21 (d, 1H, J = 3.2 Hz), 5.11 (s, 1H), 4.96-4.93 (m 1H), 2.66-1.69 (m, 6H). ESI mass spectrum (*m/*z): 345.25 (M+). Anal. Calcd. For $C_{20}H_{16}N_4O_2$: C, 69.76; H, 4.68; N, 16.27; found: C, 69.97; H, 4.73; N, 16. 49.

5-Chloro(1'-(furan-2-yl)-2-oxo-5',6',7',7a'-tetrahydrospiro[indoline-3,3'-pyrrolizine]-2', 2'(1'*H*)-dicarbonitrile (10b)

Colour: White. M. P. 215-217℃. IR (KBr, cm^{-1}): 3396, 2991, 2246, 1715, 760. ^{1}H NMR (400 MHz, $CDCl_3$) δ: 10.84 (s, 1H), 7.99 (s, 1H), 7.66 (d, 1H, J = 8.4 Hz), 7.22, (t, 1H, J = 8.4 Hz), 6.84 (d, 1H, J = 8.0 Hz), 6.42-6.41 (m, 1H), 6.23 (d, 1H, J = 3.6 Hz), 5.22 (s, 1H), 4.93-4.90 (m, 1H), 2.67-1.71 (m, 6H). Anal. Calcd. For $C_{20}H_{15}ClN_4O_2$: C, 63.41; H, 3.99; N, 14.79; found: C, 63. 69; H, 3.90; N, 14.50.

5-Bromo(1'-(furan-2-yl)-2-oxo-5',6',7',7a'-tetrahydrospiro[indoline-3,3'-pyrrolizine]-2', 2'(1'*H*)-dicarbonitrile (10c)

Colour: White. M. P. 227-229 ℃. ^{1}H NMR (400 MHz, $CDCl_3$) δ: 10.75(s, 1H), 7.89 (s, 1H), 7.56 (d, 1H, J = 8.4 Hz), 7.12, (t, 1H, J = 8.4 Hz), 6.74 (d, 1H, J = 8.0 Hz), 6.32-6.31 (m, 1H), 6.13 (d, 1H, J = 3.6 Hz), 5.12 (s, 1H), 4.83-4.81 (m, 1H), 2.57-1.61 (m, 6H). Anal. Calcd. For $C_{20}H_{15}BrN_4O_2$: C, 56.75; H, 3.57; N, 13.24; found: C, 57.00; H, 3.68; N, 13.01.

(1'-(Furan-2-yl)-5',6',7',7a'-tetrahydrospiro[indeno[1,2-b]quinoxaline-11,3'-pyrrolizine]-2', 2'(1'*H*)-dicabonitrile (11)

Colour: Yellow, M. P. 233-235℃. ^{1}H NMR (400 MHz, $CDCl_3$) δ: 7.98 (bs, 1H), 7.88-7.81 (m, 1H), 7.66 (d, 1H, d, 1H, J = 8.4 Hz), 7.34-7.19 (m, 1H), 6.83 (d, 1H, J = 8.0 Hz), 6.69 (d, 1H, J = 8.4 Hz), 6.44-6.35 (m, 2H), 6.22 (d, 1H, J = 3.6 Hz), 5.21 (s, 1H), 4.92-4.89 (m, 1H), 2.66-1.70 (m, 6H). Anal. Calcd. For $C_{27}H_{19}N_5O$: C, 75.51; H, 4.46; N, 16.31; found: C, 75.77; H, 4.41; N, 16.49.

4.7. Crystallographic data of compound 4c and 4k

CCDC 1568661 and CCDC 1470017 contains the supplementary crystallographic data (.cif) of the compounds **4c** and **4k** respectively. These data can be obtained free of charge from The Cambridge Crystallographic Data Centre *via* www.ccdc.cam.ac.uk/structures.

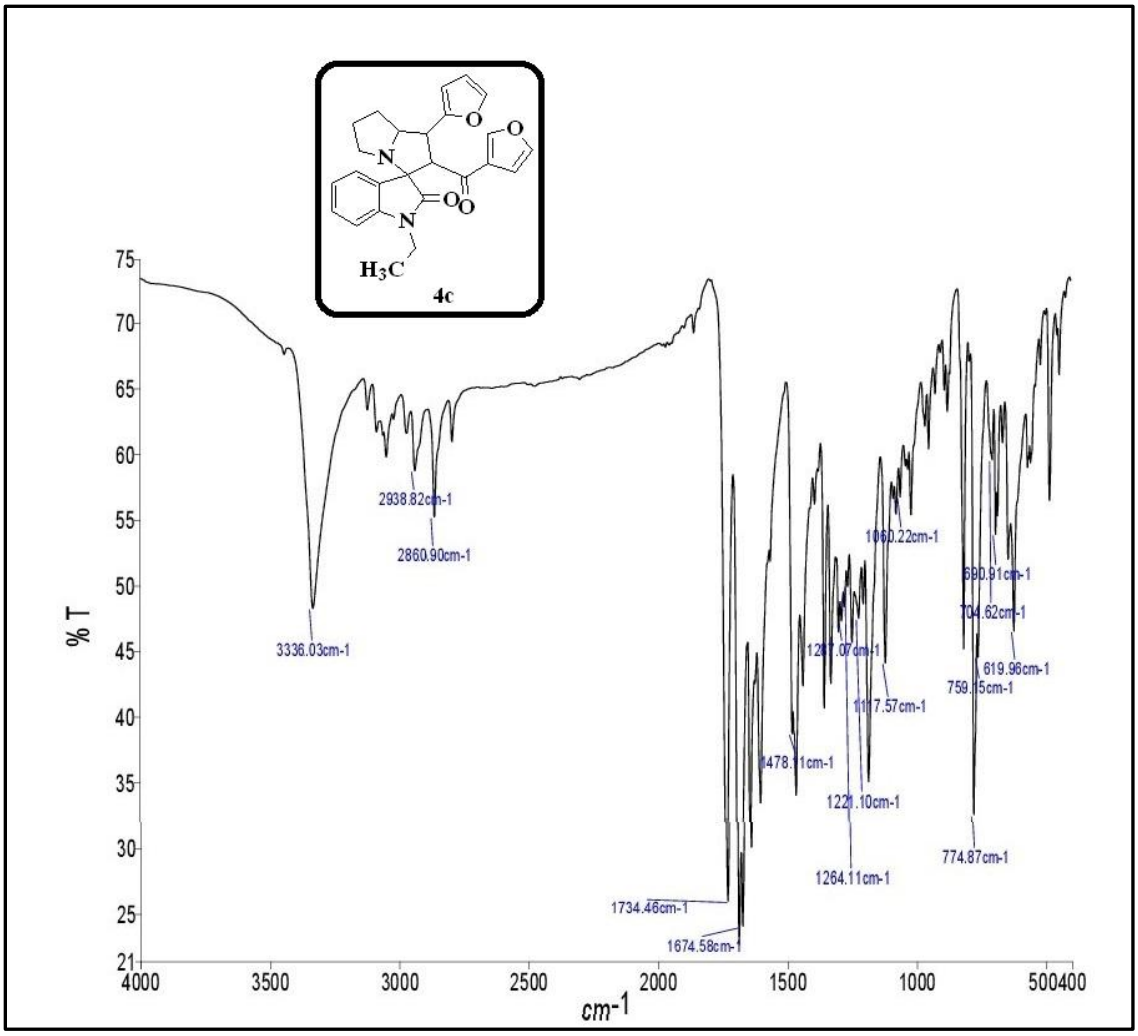

IR spectrum of the compound **4c**

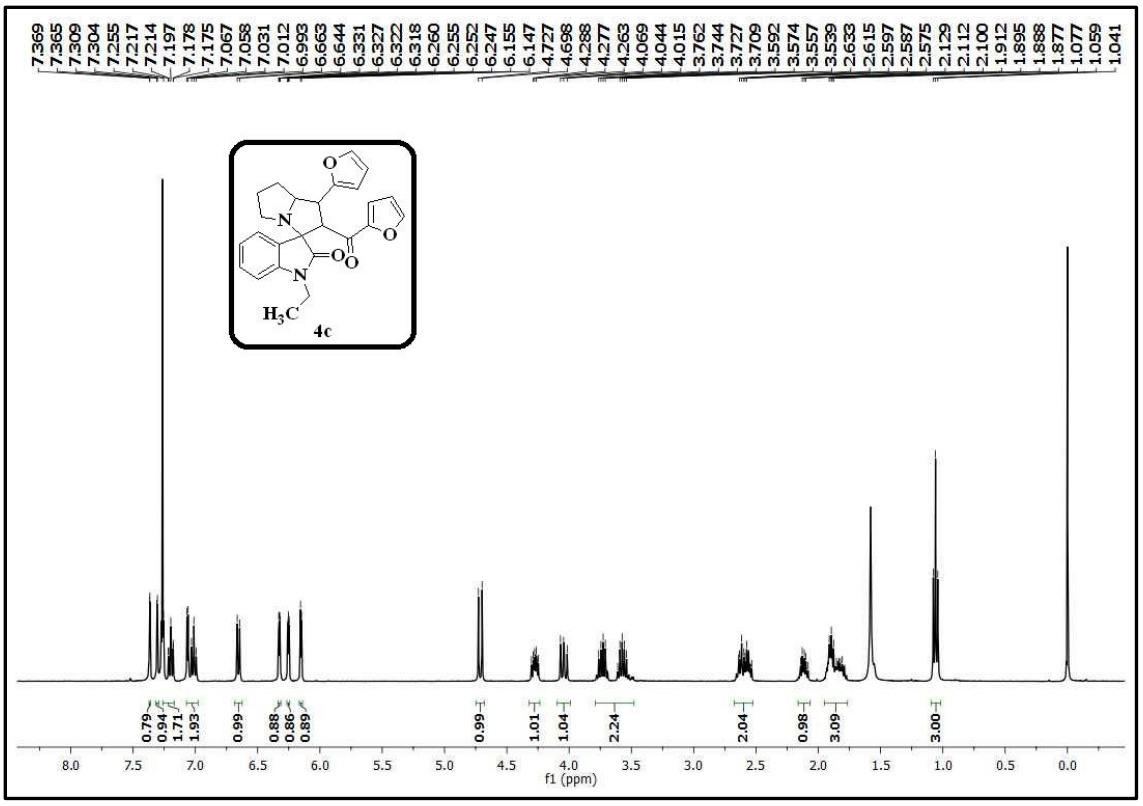

^{1}H NMR spectrum of the compound **4c**

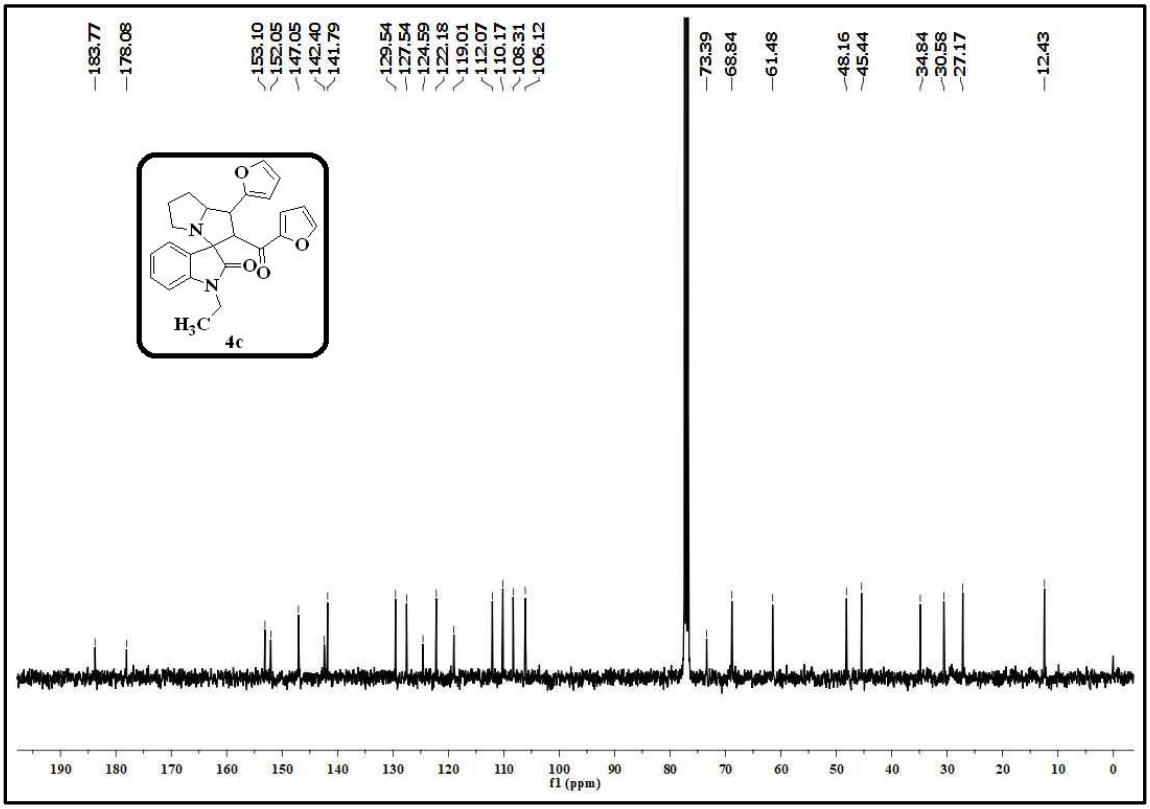

^{13}C NMR spectrum of the compound **4c**

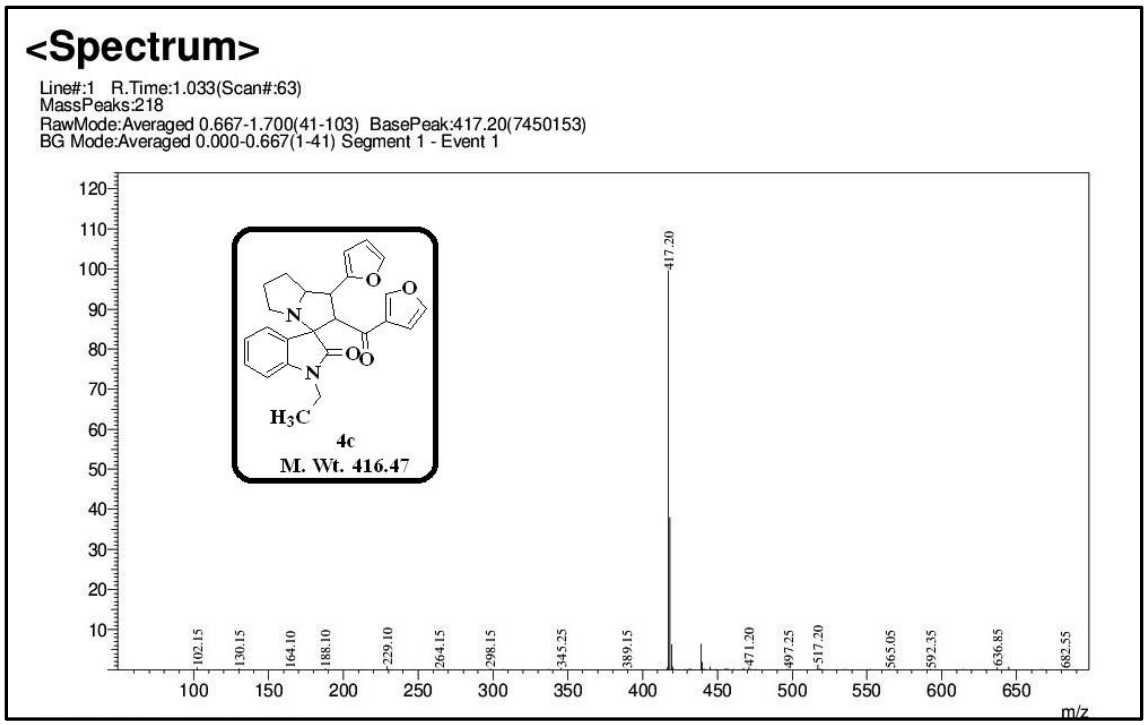

Mass spectrum of the compound **4c**

Experimental section

Materials and methods

All melting points were recorded using Stuart SMP30 melting point apparatus and are uncorrected. IR spectra were recorded on a PerkinElmer 100S series FTIR instrument. ^{1}H and ^{13}C NMR spectra were recorded in CDCl3 using tetramethylsilane (TMS) as internal standard on a Bruker Avance III HD 400 MHz instrument. Mass spectra were recorded on Joel JMSD-300 spectrometer. Elemental analyses were performed on a Carlo-Erba model EA 1108 analytical unit (Triad, NJ, USA), and the values are within ± 0.4 % of theoretical values. Column chromatography was performed on silica gel (100–120 mesh). Reaction progress and purity were monitored by thin-layer chromatography. Unless otherwise stated, all chemicals and solvents used were of high grade and purchased from Sigma Aldrich and Spectrochem. Ultrasonication was performed on PCi-Analytics-6.5L200H1DTC ultrasonic cleaner whose frequency is 25 kHz, input voltage range of 170–270 VAC at 50 Hz, and output power is 250 W (Mumbai, India). The reaction flasks were immersed throughout the cleaner such that the surface of the reactants was slightly lower than the water in the cleaner.

The dipolarophiles **3a-c**/**9** and11*H*-indeno[1,2-*b*]quinoxalin-11-one **7** were synthesized according to the literature procedure [48-50].

Single-crystal X-ray diffraction studies

X-ray data for the compound were collected at room temperature using a Bruker Smart Apex CCD diffractometer with graphite-monochromated Mo Ka radiation (k = 0.71073 Å) with x-scan method. Preliminary lattice parameters and orientation matrices were obtained from four sets of frames. Unit cell dimensions were determined using 5371 reflections. Integration and scaling of intensity data was accomplished using the SAINT program [51]. The structure was solved by direct methods using SHELXS97, and refinement was carried out by full-matrix least squares technique using SHELXL-2014/7 [52]. Anisotropic displacement parameters were included for all non-hydrogen atoms. H bound to N atom was located from the difference Fourier map. All other H atoms were positioned geometrically and treated as riding on their parent C atoms with C–H distances of 0.93–0.97 Å, and with Uiso(H) = 1.2Ueq (C) or 1.5Ueq for methyl atoms. The furan ring atoms are found to be disordered over two sites, with 0.531(4) site occupancy for C22/C23/C24/O3 atoms (representing the major component) and 0.469(4) site occupancy for C22D/C23D/C24D/O3D (minor component). PART and FVAR instructions were used for modeling the sulfur atom disorder, and DFIX instruction for restraining the C–C and C–O bond distance to their expected values. The anisotropic displacement parameters of the disordered atoms were restrained to be similar (SIMU instruction), and the direction of motion along the axis between these atoms was also restrained (DELU instruction) [53]. The software used to prepare material for publication was Mercury 2.3 (build RC4), ORTEP-3, and X-Seed [54-56].

Biological evaluation

Antimicrobial activity assay

The antibacterial and antifungal activity of all the synthesized compounds were tested against two gram-positive bacteria (Bacillus subtilis, Staphylococcus aureus) and three gram-negative bacteria (*Escherichia coli*, *Pseudomonas aeruginosa* and *Klebsiella Pneumoniae*) and three fungal strains, (*Aspergillus niger, Penicillium notatum, Aspergillus parasiticus*)

using disc diffusion method [57]. On using Whatmann (No. 1) paper, 6 mm diameter sterile antibiotic discs were placed over the nutrient agar medium. 100 μg/mL concentrated compounds were transferred to each disc with the help of micropipette (Initially compounds were dissolved in DMSO); subsequently, bacteria and fungi were incubated overnight at 37 ℃ and 25 ℃, respectively. The zone of inhibition was determined in mm and distinguished using standard antibiotics. DMSO was used as a negative control, while Streptomycin 30 μg/disc (standard antibiotic) and standard antifungal drug Ketoconazole (10 μg/disc) were used as the positive controls. All the tests were carried out in triplicates and the average zone of inhibition was recorded and minimum inhibitory concentration (MIC) values for the tested compounds and standards were measured in μg/mL and tabulated their mean values.

Antioxidant activity

The free radical scavenging capacity of all the synthesized compounds was determined by using DPPH (1,1-Diphenyl-2-picrylhydrazyl) free radical method described in the literature [58-60]. The ascorbic acid solution was used as a standard. 0.2 mM solution of DPPH was prepared in 100% methanol. The required amount of ascorbic acid was dissolved in 100% methanol to prepare 1 mM solution and the test compounds were dissolved in 0.2% DMSO and methanol to prepare 1 mM stock solutions. From the stock solutions, different concentrations (3, 10, 30 and 100 lM) of solutions were prepared on diluting with methanol. 1 mL of each compound solution was added to the 3 mL of DPPH solution. After 30min, the absorbance of the solutions at 517 nm (A1) was recorded using UV–Visible spectrophotometer. As a control, the absorbance of the blank solution of DPPH without test compound was also determined at 517 nm (A0). The following equation was used for the calculation of the percentage (%) of scavenging activity.

$$\text{Scavenging Activity (\%)} = \frac{A_0 - A_1}{A_0} \times 100$$

Where A_0 is the absorbance of DPPH in the absence of antioxidant and A_1 is the absorbance of DPPH in the presence of an antioxidant. IC_{50} values were also calculated for the compounds.

Molecular Docking protocol

The docking studies are prominent tools for the assessment of the binding affinity of the ligand-protein receptor. All the synthesized compounds were subjected to *in silico* molecular docking by using the AutoDock Tools (ADT) version 1.5.6 and AutoDock version 4.2.5.1 docking program [61]. The 3D-structures of all the synthesized compounds were prepared by using chem3Dpro 12.0 software. The optimized 3D structures were saved in .pdb format. The structure of the *E. coli* MurB (PDB ID: 1MBT) protein was extracted from the protein data bank (http://www.rcsb.org/pdb). The bound ligand and water molecules in protein were removed by using Discovery Studio Visualizer version 4.0 to prepare the protein. Nonpolar hydrogens were merged and gasteiger charges were added to the protein. The grid file was saved in .gpf format. The three dimensional grid box having dimensions 60 x 60 x 60 $Å^3$ was created around the protein with spacing 0.3750 Å. The genetic algorithm was carried out with the population size and the maximum number of evaluations were 150 and 25,00,000 respectively. The docking output file was saved as Lamarckian Ga (4.2) in .dpf format. The ligand-protein complex binding sites were visualized by Discovery Studio Visualizer version 4.0.

References

1) S. J. T. Rezaei, M. R. Nabid, A. Yari, S. W. Ng, *Ultrason. Sonochem.* **2011**, *18*, 49.
2) B. H. Rotstein, S. Zaretsky, V. Rai, A. K. Yudin, *Chem. Rev*. **2014**, *114*, 8323.
3) F. Damkaci, A. J. Szymaniak, *Chem. Educ.* **2014**, 91, 943.
4) C. M. R. Volla, I. Atodiresei, M. Rueping, *Chem. Rev.* **2014**, *114*, 2390.
5) J. Safari, Z. Zarnegar, *Ultrason. Sonochem*. **2014**, *21*, 1132.
6) E. Pelit, Z. Turgut, *Ultrason. Sonochem.* **2014**, *21*, 1600.
7) G. B. Ababsa, A. Derdour, T. Roisnel, J. A. Saez, P. Perez, E. Chamorro, L. R. Domingo, F. J. Mongin, *Org. Chem.* **2009**, *74*, 2120.
8) W. Benchouk, S. M. Mekelleche, M. J. Aurell, L. R. Domingo, *Tetrahedron.* **2009**, *65*, 4644.
9) A. K. Nacereddine, W. Yahia, S. Bouacha, A. Djerourou, *Tetrahedron Lett*. **2010**, *51*, 2617.

10) K. Alimohammadi, Y. Sarrafi, M. Tajbakhsh, S. Yeganegi, M. Hamzehloueian, *Tetrahedron.* **2011**, *67*, 1589.

11) A. Bazgir, S. Ahadi, R. Ghahremanzadeh, H. R. Khavasi, P. Mirzaei, *Ultrason. Sonochem.* **2010**, *17*, 447.

12) M. Dabiri, Z. N. Tisseh, M. Bahramnejad, A. Bazgir, *Ultrason. Sonochem*. **2011**, *18*, 1153.

13) J. Feng, K. Ablajan, A. Sali, *Tetrahedron*. **2014**, *70*, 484.

14) A. Hasaninejad, S. Firoozi, F. Mandegani, *Tetrahedron Lett*. **2013**, *54*, 2791.

15) T. Tsubogo, S. Saito, K. Seki, Y. Yamashita, S. Kobayashi, *J. Am. Chem. Soc.* **2008**, *130*, 13321.

16) W. Li, M. Shi, *J. Org. Chem*. **2008**, *73*, 4151.

17) X. X. Yan, Q. Peng, Y. Zhang, K. Zhang, W. Hong, X. L. Hou, Y. D. Wu, *Angew. Chem. Int. Ed*. **2006**, *45*, 1979.

18) M. Ghandi, A. Yari, S. J. T. Rezaei, A. Taheri, *Tetrahedron Lett*. **2009**, *50*, 4724.

19) Y. Yamashita, X. Guo, R. Takashita, *J. Am. Chem. Soc*. **2010**, *132*, 3262.

20) S. Q. Ge, Y. Y. Hua, M. Xia, *Ultrason. Sonochem.* **2009**, *16*, 232.

21) S. Haddad, S. Boudriga, F. Porzio, A. Soldera, M. Askri, M. Knorr, Y. Rousselin, M. M. Kubicki, C. Golz, C. Strohmann, *J. Org. Chem.* **2015**, *80*, 9064.

22) E. Carlos, P. Galvis, V. V. Kouznetsov, *Org. Biomol. Chem.* **2013**, *11*, 7372.

23) K. Revathy, A. Lalitha, *RSC Adv.* **2014**, *4*, 279.

24) F. Yang, J. Sun, H. Gao, C. G. Yan, *RSC Adv.* **2015**, *5*, 32786.

25) A. Thangamani, *Eur. J. Med. Chem.* **2010**, *45*, 6120.

26) R. J. Bridges, F. E. Lovering, J. M. Humphrey, M. S. Stanley, T. N. Blakely, *Bioorg. Med. Chem. Lett*. **1993**, *3*, 115.

27) G. Periyasami, R. Raghunathan, G. Surendiran, N. Mathivanan, *Bioorg. Med. Chem. Lett*. **2008**, *18*, 2342.

28) C. Ji, S. Wang, S. Chen, S. He, Y. Jiang, Z. Miao, J. Li, C. Sheng, *Bioorg. Med. Chem.* **2017**, *25*, 5268.

29) D. Kathirvelan, J. Haribabu, B. S. R. Reddy, C. Balachandran, V. Duraipandiyan, *Bioorg. Med. Chem. Lett.* **2015**, *25*, 389.

30) S. Tiwari, P. Pathak, R. Sagar, *Bioorg. Med. Chem. Lett.* **2016**, *26*, 2513.

31) H. Dong, S. Song, J. Li, C. Xu, H. Zhang, L. Ouyang, *Bioorg. Med. Chem. Lett.* **2015**, *25*, 3585.

32) Y. kia, H. Osman, R. S. Kumar, A. Basiri, V. Murugaiyah, *Bioorg. Med. Chem.* **2014**, *22*, 1318.

33) A. Kamal, K. S. Babu, M. V. P. S. V. Vardhan, S. M. A. Hussaini, R. Mahesh, S. P. Shaik, A. Alarifi, *Bioorg. Med. Chem. Lett.* **2015**, *25*, 2199.

34) A. Shaabani, A. Bazgir, *Tetrahedron Lett.* **2004**, *45*, 2575.

35) S. J. T. Rezaei, Y. Bide, M. R. Nabid, *Tetrahedron Lett.* **2012**, *53*, 5123.

36) P. Sarkar, C. Mukhopadhyay, *Tetrahedron Lett.* **2016**, *57*, 4306.

37) G. Ramesh, R. Gali, R. Velpula, B. Rajitha, *Res. Chem. Intermed.* **2016**, *42*, 3863.

38) S. Angapelly, P. V. S. Ramya, R. S. Rani, C. G. Kumar, A. Kamal, M. Arifuddin, *Tetrahedron Lett*. **2017**, *58*, 4632.

39) B. Banerjee, *Ultrason*. *Sonochem*. **2017**, *35*, 15.

40) T. J. Mason, *Chem*. *Soc*. *Rev*. **1997**, *26*, 443.

41) G. Ramesh, B. Janardhan, B. Rajitha, *Res*. *Chem*. *Intermed*. **2015**, *41*, 8099.

42) K. S. Suslick, D. A. Hammerton, R. E. Cline, *J*. *Am*. *Chem*. *Soc*. **1986**, *108*, 5641.

43) T. E. Benson, C. T. Walsh, J. M. Hogle, *Structure*. **1996**, **4**, 47.

44) T. E. Benson, J. L. Marquardt, A. C. Marquardt, F. A. Etzkorn, C. T. Walsh, *Biochemistry*. **1993**, *32*, 2024.

45) A. E. Zoeiby, F. Sanschagrin, R. C. Levesque, *Mol*. *Microbiol*. **2003**, *47*, 1.

46) R. Gondru, J. Banothu, R. K. Thatipamula, A. Sk. Hussain, R. Bavantula, *RSC Adv*. **2015**, *5*, 33562.

47) A. M. Davis, S. J. Teague, *Angew*. *Chem. Int. Ed*. **1999**, *38*, 736.

48) A. S. Amarasekara, T. B. Singh, E. Larkin, M. A. Hasan, H. Fan, *Ind. Crop. Prod*. **2015**, *65*, 546.

49) P. Gajdos, J. Miklovic, A. Krutosikova, *Chem. Heterocyclic Comp.* **2006**, *42*, 719.

50) E. Soleimani, M. Hariri, P. Saei, *C. R. Chim.* **2013**, *16*, 773.

51) SMART & SAINT. Software Reference manuals. Versions 6.28a & 5.625, Bruker Analytical X-ray Systems Inc., Madison, Wisconsin, USA. **2001**.

52) G. M. Sheldrick, SHELXS97 and SHELXL version 2014/7, http://shelx.uniac.gwdg.de/SHELX/index.php

53) P. Muller, R. H. Imer, A. L. Spek, T. R. Schneider, M. R. Sawaya, in Crystal Structure Refinement: A Crystallographer's Guide to SHELXL, ed. by P. Muller (Oxford University Press: Oxford, New York) **2006**, pp. 57; XXXV

54) C. F. Macrae, I. J. Bruno, J. A. Chisholm, P. R. Edgington, P. McCabe, E. Pidcock, L. R.Monge, R. Taylor, J. V. D. Streek, P. A. Wood, *J. Appl. Cryst.* **2008**, *41*, 466.

55) L. J. Farrugia, *J. Appl. Cryst.* **2008**, *30*, 565.

56) L. J. Barbour, *J. Supramol. Chem.* **2001**, *1*, 189.

57) Bauer, A. W.; Kirby, W. M.; Sherris, J. C.; Turck, M. *Am. J. Clin. Pathol*. **1996**, *45*, 493.

58) A. Braca, N. D. Tommasi, L. D. Bari, C. Pizza, M. Politi, I. Morelli, *J. Nat. Prod*. **2001**, *64*, 892.

59) M. R. Saha, S. M. R. Hasan, R. Akter, M. M. Hossain, M. S. Alamb, M. A. Alam, M. E. H. Mazumder, *Bangl. J. Vet. Med*. **2008**, *6*, 197.

60) M. S. Blois, *Nature.* **1958**, *181*, 1199.

61) http://autodock.scripps.edu/resources/references.

CHAPTER-V

Efficient one-pot multicomponent synthesis of novel spirooxindolo carbamates *via* Betti reaction and biological evaluation

5.1. Introduction

For the last few decades, heterocyclic chemistry occupies a significant area of research in organic chemistry. The discovery of new heterocyclic structural units still draws continued interest for the synthetic chemists, because they are the basis of many pharmaceutical, agrochemical and veterinary products. Among these heterocyclic compounds, spiro heterocyclic compounds are described as one of the important class of organic compounds, due to their unique structural features and a wide range of biological activities [1]. Several spiro heterocyclic compounds are also isolated from biological origins [2]. Among spiro compounds, spirooxindoles are versatile and pre-eminent structural units, which are most commonly present in a number of biologically active natural products like alkaloids [3, 4]. Spirooxindoles exhibited diversified pharmacological properties like antiviral, antitumor, antibiotic, anticancer, antimycobacterial, antiinflammatory etc., [5-8].

Organic carbamates plays an eminent role in various fields like agro, medicinal, polymer chemistry etc., [9-14]. Particularly, in medicinal chemistry, due to its good chemical and proteolytic stability of carbamate moieties (because of the presence of amide-ester hybrid features), the amide bonds in the drug-like molecules are altered by replacing with carbamate linkages. These linkages are introduced mainly to increase the permeability of drug-like molecules across the cell membrane and to increase the drug–target interactions [15-19]. Due to such suitable amide bond surrogates, carbamate derivatives are generally used as a potent, non-peptide antagonist of the glycoprotein IIb/IIIa receptor, anticancer agent [20-22], in the treatment of Alzheimer's dementia, Parkinson's dementia, antiretroviral therapy [23-26], chronic asthma, ascariasis, uncinariasis, oxyuriasis, trichuriasis and as HIV-1 protease inhibitor, β- and γ-secretase inhibitors, etc.,[27-31]. Even though there were several methods reported in the literature for the synthesis of organic carbamates [32-37], there are no reports to synthesize the spirooxindolocarbamates *via* a Betti reaction.

Leslie and coworkers describe the discovery of a series of novel spirocarbamates (trans-8-aminomethyl-1-oxa-3-azaspiro[4,5]decan-2-ones) *via a* multistep approach (Figure 5.1). The target compounds were found as potent NPY Y5 antagonists [41].

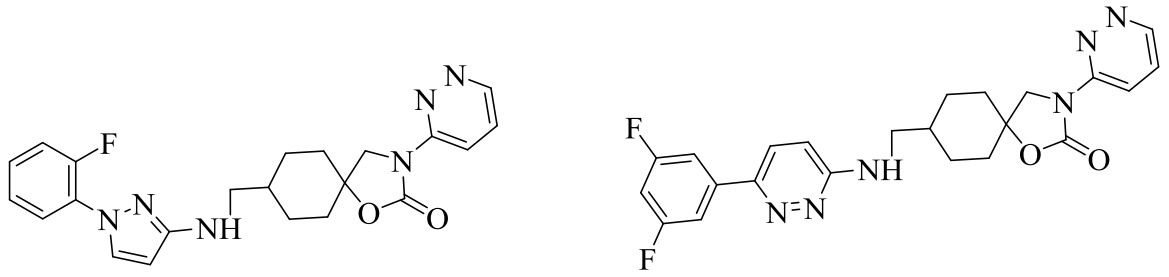

Figure 5.1

Djigoue et al. illustrated the design, chemical synthesis of 3-spiromorpholinone/3-spirocarbamate androsterone derivatives *via* a multistep process (Figure 5.2). The synthesized compounds were exhibited 17*β*-hydroxy steroid dehydrogenase type 3 inhibition activity. The target compounds were also tested for the androgenic activity on LACP-4 cell lines and inhibitory activity on intact LNCaP[17*β*-HSD3] cells [42].

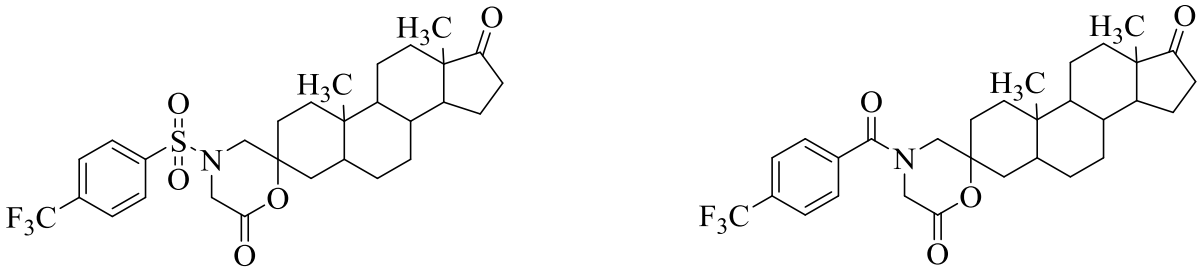

Figure 5.2

Cabedo and coworkers described the synthesis of novel differently functionalized 1-pentyl-6,7-dimethoxy-1,2,3,4-tetrahydroisoquinolines (THIQs), including dihydroisoquinolinium salts, methyl pentanoate-THIQ, 1-pentanol-THIQ, ester derivatives and carbamate derivatives *via* a multistep process by employing classic intramolecular Bischler–Napieralski cyclodehydration to generate the isoquinoline core (Figure 5.3). The bactericide, fungicide activities were evaluated and SAR were established for all the synthesized compounds [43].

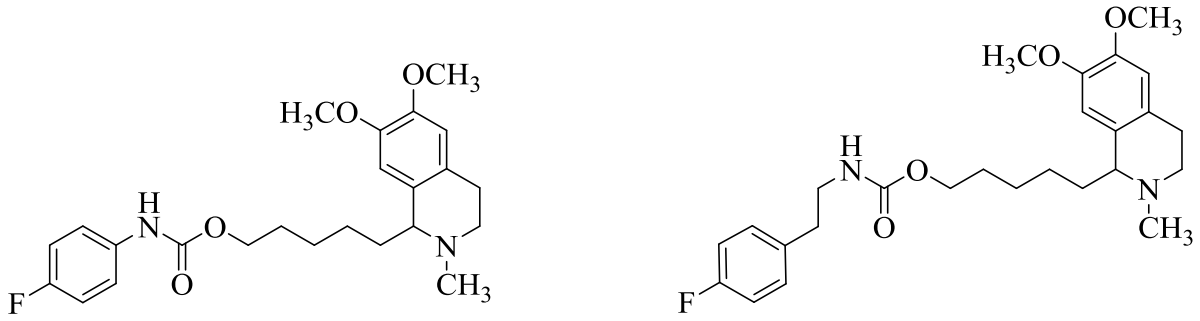

Figure 5.3

Kratky et al. reported the synthesis of novel salicylanilide N-monosubstituted carbamates and thiocarbamates (Figure 5.4). The synthesized compounds exhibited potent *in vitro* antimicrobial activity. All the target compounds were further evaluated for their *in vitro* antimycobacterial and cytotoxic activities [44].

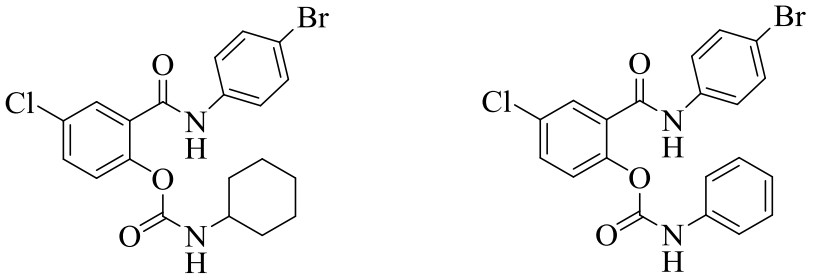

Figure 5.4

Vinsova and coworkers reported the synthesis of novel salicylanilide N-monosubstituted carbamates and thiocarbamates (Figure 5.5). The synthesized compounds were exhibited comparable or superior *in vitro* antimicrobial activity in comparison to established drugs. All the target compounds were further evaluated for their *in vitro* antimycobacterial and cytotoxic activities [45].

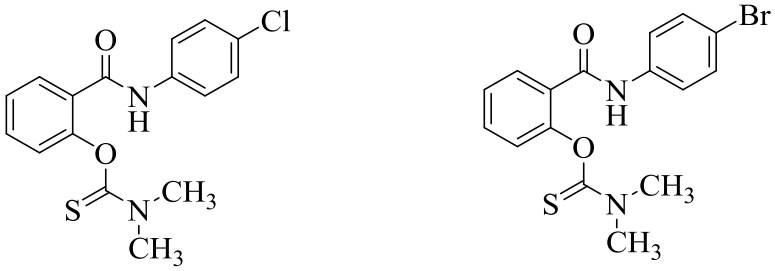

Figure 5.5

Bosze and coworkers described the synthesis of novel salicylanilide esters and carbamates. They illustrated the target compounds as combating highly resistant emerging pathogen mycobacterium abscessus and mycobacterium tuberculosis (Figure 5.6). The synthesized compounds were also tested for their *in vitro* cytotoxic activity [46].

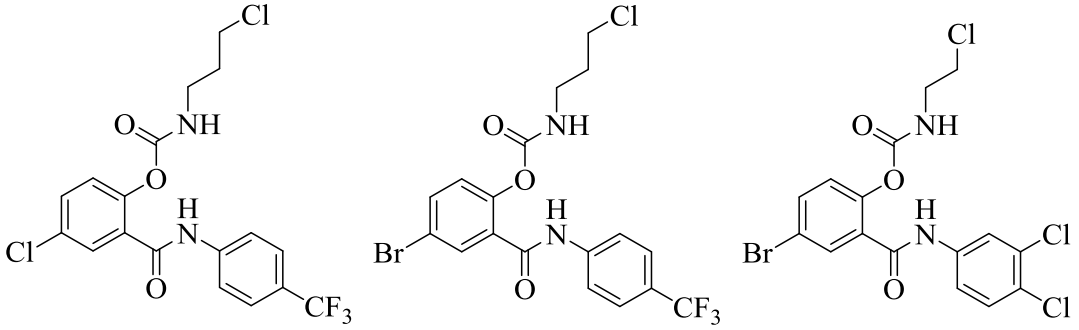

Figure 5.6

Gonec et al. reported the synthesis of a series of 1-[(2-substituted phenyl)carbamoyl]naphthalen-2-yl carbamates through the multistep process (Figure 5.7). All the target compounds were tested for their *in vitro* antimicrobial, antimycobacterial and cytotoxic studies. The SAR was discussed for the synthesized compounds [47].

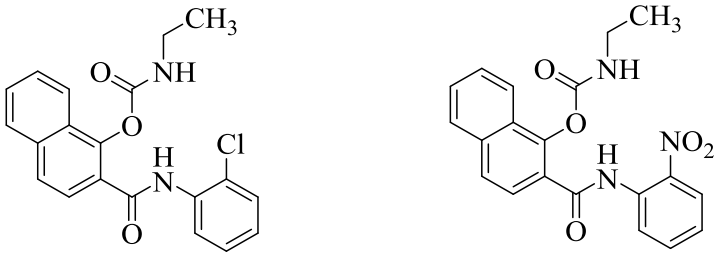

Figure 5.7

5.1.1. Diverse approaches for the synthesis of organic carbamates

Shupe et al. reported the additions of allylsilanes to N-Boc-iminooxindoles and the formation of silicon-containing spirocarbamates *via* intramolecular trapping of a *β*-silyl carbocation by using sodium tetrakis[(3,5-trifluoromethyl)phenyl]borate (NaBArF) as a catalyst (Scheme 5.1) [49].

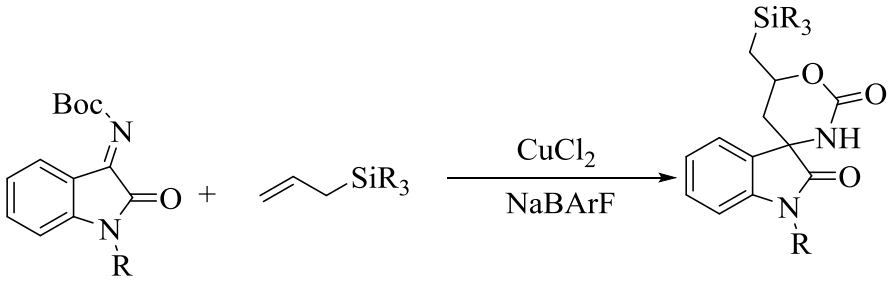

Scheme 5.1

Padwa and coworkers reported the stereochemical aspects of the iodine(III)-mediated aziridination reaction of some cyclic allylic carbamates (Scheme 5.2). The iodine(III)-mediated aziridination reaction of an indolyl-substituted carbamate requires a Rh(II) catalyst and proceeds by a metallonitrene intermediate [48].

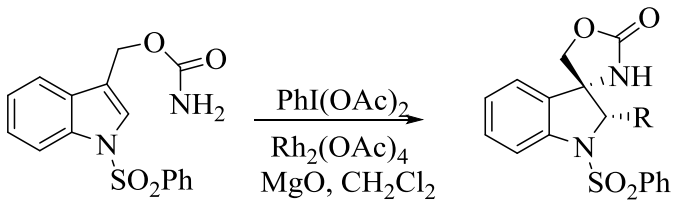

Scheme 5.2

Kumar et al. described an efficient green methodology by employing copper nanoparticles for the preparation of 2-naphthol condensed 1,3-oxazinone (cyclic carbamate) derivatives *via* a one-pot multicomponent condensation reaction in PEG-400 (Scheme 5.3). **Kapoor and coworkers** reported graphene oxide-mediated solvent-free three-component reaction for the synthesis of 1-amidoalkyl-2-naphthols and 1,2-dihydro-1-arylnaphth[1,2-*e*][1,3]oxazin-3-ones *via* one-pot multicomponent approach (Scheme 5.3). **Rao et al**. described the efficient one-pot multicomponent approach for the synthesis of the naphtha[1,2-*e*]oxazinone and 14-substituted-14*H*-dibenzo[*a,j*]xanthene derivatives promoted by zinc oxide nano particle under thermal and solvent-free conditions (Scheme 5.3). **Basavegowda et al**. demonstrates a novel green fabrication of ferromagnetic Fe_3O_4 nano particles using the leaf extract of Artemisia annua (A. annua), which is widely distributed in Asia as a medicinal plant and their novel catalytic applications for the synthesis of biologically interesting benzoxazinone and benzthioxazinone derivatives *via* multicomponent approach (Scheme 5.3) [50-53].

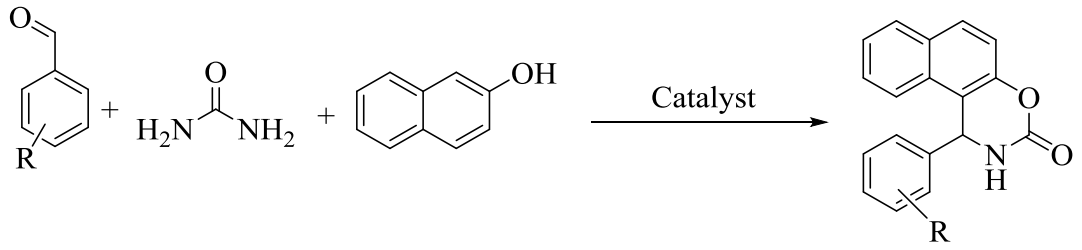

Scheme 5.3

Halimehjanib et al. reported an efficient approach for the synthesis of the alkyl-2,3-dihydro-3-oxo-1-aryl-1*H*benzo[*f*]chromen-2-yl-carbamodithioates and alkyl 3,4-dihydro-2-oxo-4-aryl-2*H*-chromen-3-yl-carbamodithioates diastereoselectively (Scheme 5.4). The reaction proceeds *via* a domino esterification/intramolecular 1,4-addition-type Friedel-Crafts alkylation reaction [54].

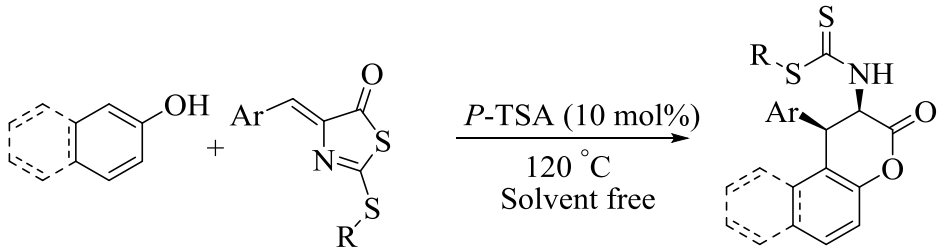

Scheme 5.4

Lei et al. described the one-pot three-component condensation reaction involving *β*-naphthol, aldehyde and urea in the presence of 10 mol% thiamine hydrochloride as a catalyst to obtain the 1,2-dihydro-1-arylnaphth[1,2-*e*][1,3]oxazine-3-ones and aryl-14*H*-dibenzo[*a*,*j*]xanthenes (Scheme 5.5) [55].

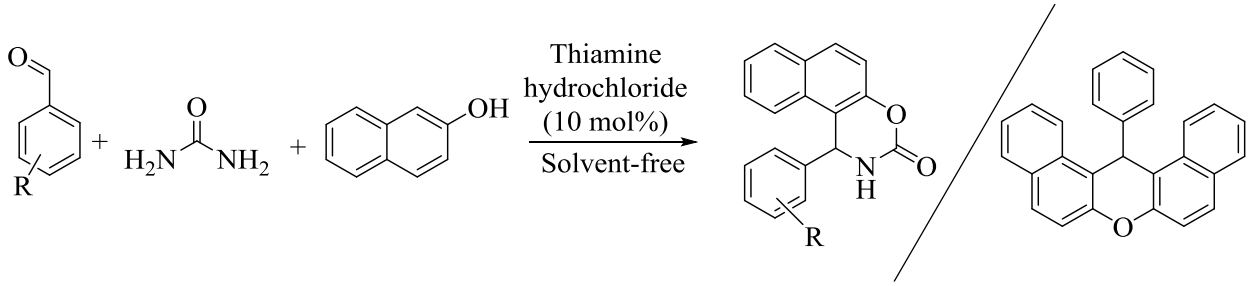

Scheme 5.5

5.2. Present work

Betti reaction is a multi-component reaction of 2-naphthol, carbonyl compounds with ammonia, amines, amides or urea [56-58]. It was assumed that the electrophilic nature of the isatin [59] and the nucleophilic nature of the 2-naphthol [57] will facilitate the Betti reaction.

Inspired by the aforementioned biological importance of carbamates, herein, we report the synthesis of spirooxindolocarbamates *via* MCR approach by employing a Betti reaction and evaluated for their *in vitro* antibacterial, antifungal and molecular docking studies.

5.2.1. Synthesis of the spirooxindolocarbamate derivatives (4a-l and 6a-d)

Isatin (1 mmol) on reaction with urea (2 mmol) and 2-naphthol (1 mmol) in acetonitrile in presence of *p*-TSA (20 mol%) at 100 °C form spirooxindolocarbamates. The crude products were purified by column chromatography (Scheme5.6).

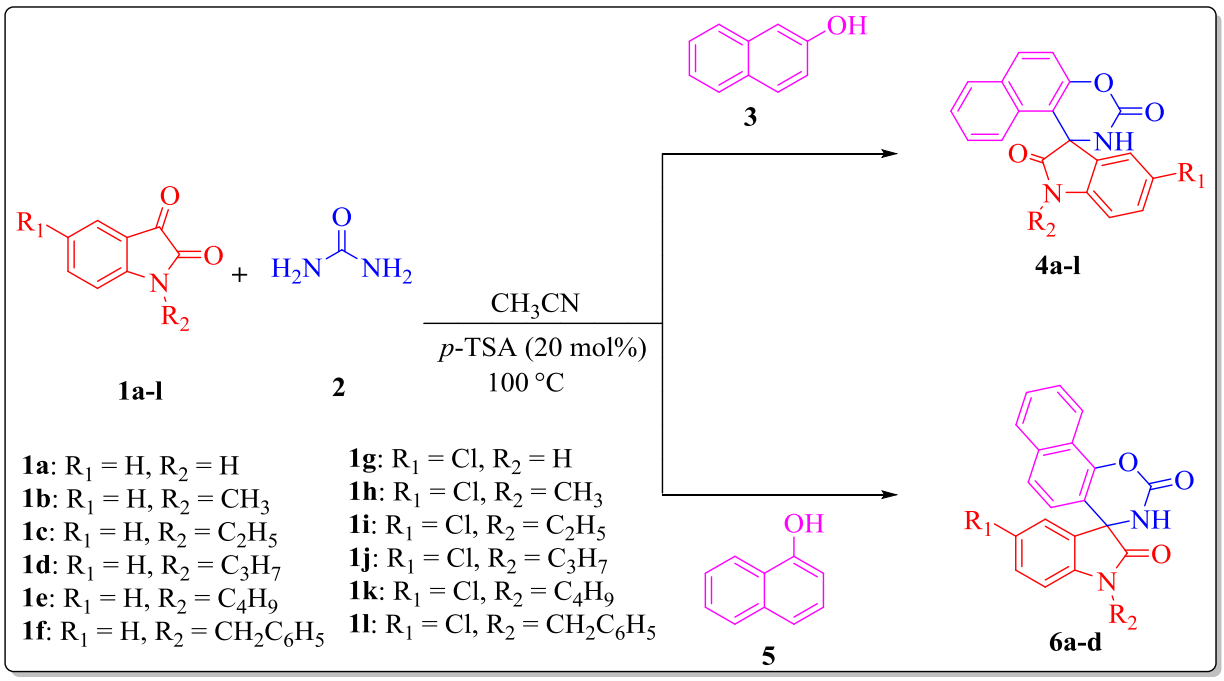

Scheme 5.6

5.2.2. The plausible reaction mechanism for the formation of the spirooxindolocarbamates 4a-l and 6a-d

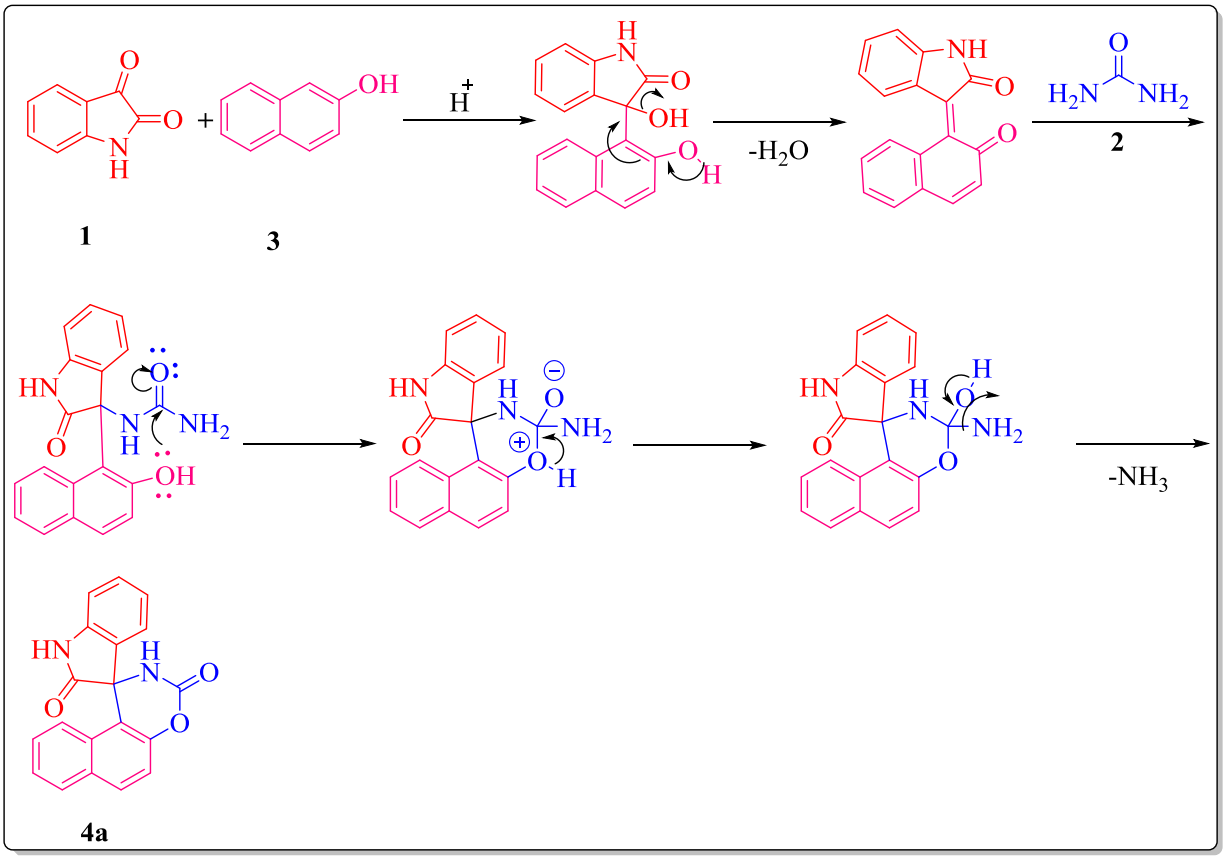

Scheme 5.7

5.3. Results and Discussion

5.3.1. Chemistry

In order to optimize the reaction (Betti reaction) condition, a pilot experiment was carried out by choosing isatin **1a**, urea **2** and 2-naphthol **3** as starting materials in different solvents like ethanol, acetonitrile and *N*,*N*-dimethylformamide to study the effect of solvents on the reaction in terms of yields and time at different temperatures in the presence and in the absence of a catalyst i.e., *p*-TSA (20 mol%). However, there was no formation of the product at room temperature even after 24h. It was observed that the product **4a** was obtained with 22% yield in acetonitrile, in the presence of *p*-TSA (20 mol%) at 80 °C. This result led to optimizing the reaction condition by carrying out the model reaction at different temperatures

in acetonitrile with 20 mol% of *p*-TSA. It was noticed that the yield of the target compound **4a** was increased to 45% when the temperature was raised to 100 °C and also there was no increase in the yield even after the temperature was raised to 110 °C. Further, the screening of the model reaction was carried out at 100 °C in acetonitrile by varying the mol% of the catalyst to study the effect of the catalyst on the reaction. The screening results showed that the 20 mol% of *p*-TSA was suitable for the reaction. These results were summarized in table 1.

Table 1. Optimized reaction conditions for the synthesis of spirooxindolocarbamates **4a**[a, b].

S. No.	Solvent	Catalyst	Temperature (°C)	Time (h)	Yield (%)[c]
1	DMF	---[d]	rt	24	0
2	C_2H_5OH	---[d]	rt	24	0
3	CH_3CN	---[d]	rt	24	0
4	DMF	*p*-TSA (20 mol%)	80	14	Trace
5	C_2H_5OH	*p*-TSA (20 mol%)	80	14	Trace
6	CH_3CN	*p*-TSA (20 mol%)	80	14	22
7	CH_3CN	*p*-TSA (20 mol%)	60	14	0
8	CH_3CN	*p*-TSA (20 mol%)	100	14	45
9	CH_3CN	*p*-TSA (20 mol%)	110	14	45
10	CH_3CN	*p*-TSA (5 mol%)	100	14	14
11	CH_3CN	*p*-TSA (10 mol%)	100	14	25
12	CH_3CN	*p*-TSA (15 mol%)	100	14	36
13	CH_3CN	*p*-TSA (30 mol%)	100	14	45
14	CH_3CN	*p*-TSA (20 mol%)	100	24	43

[a]The reaction was carried out by taking the isatin **1a** (1 mmol), urea **2** (2 mmol) and 2-naphthol **3** (1 mmol) as reactants. [b]The reaction progress was monitored by TLC. [c]Isolated yields. [d]With or without a catalyst.

The similar optimized reaction condition was executed to synthesize the remaining compounds **4b-l** and **6a-d**, the reaction was carried out with different isatin derivatives **1a-g** (1 mmol), urea **2** (2 mmol) and 2-naphthol **3**/1-naphthol **5** (1 mmol) (Scheme 5.6). The final

products were filtered and the precipitated compounds were purified by column chromatography. The target compounds **4a-l** and **6a-d** were formed with 45-69% yield in 8-26h. The reaction times and the yields of the compounds **4a-l** and **6a-d** were shown in table 2. The plausible mechanism for the synthesis of spirooxindolocarbamates was shown in scheme 5.7.

Table 2. Spirooxindolocarbamates **4a-l** and **6a-d** *via* Betti reaction[a,b.c].

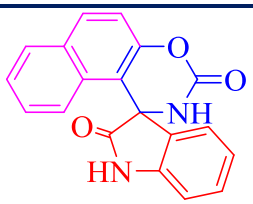 **4a** (14h / 45%)	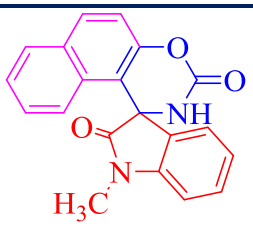 **4b** (12h / 52%)	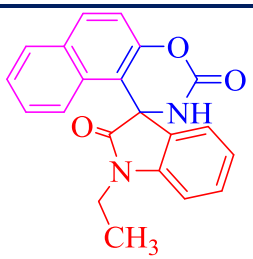 **4c** (12h / 56%)
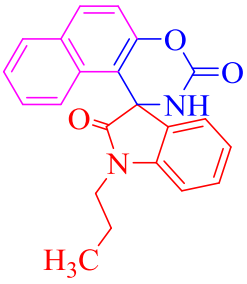 **4d** (12h / 57%)	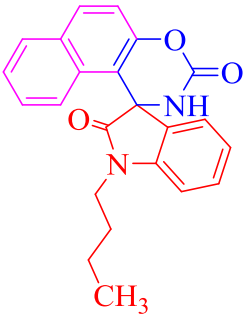 **4e** (15h / 59%)	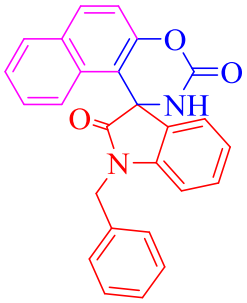 **4f** (14h / 61%)
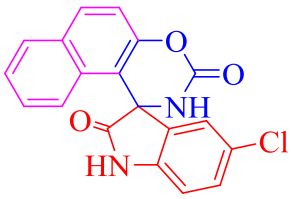 **4g** (26h / 65%)	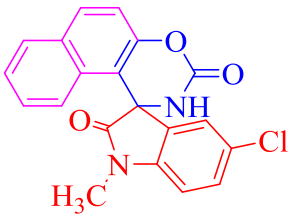 **4h** (26h / 65%)	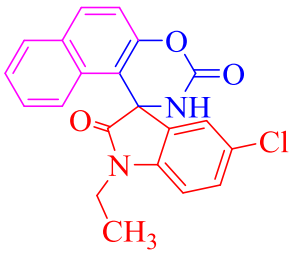 **4i** (22h / 68%)

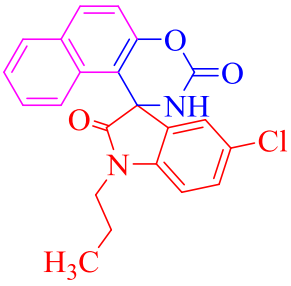

4j
(22h / 66%)

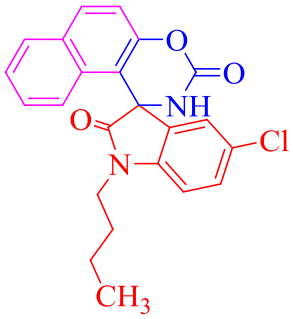

4k
(19h / 65%)

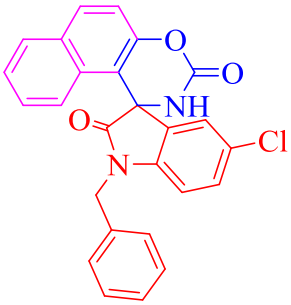

4l
(20h / 69%)

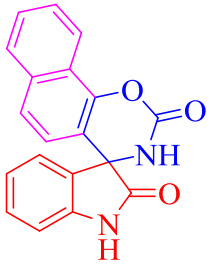

6a
(8h / 68%)

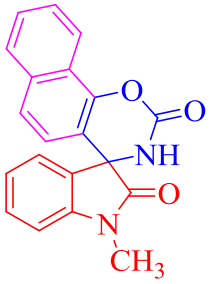

6b
(8h / 62%)

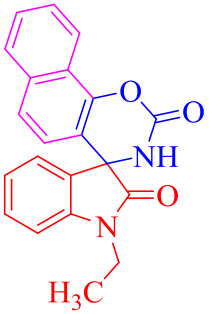

6c
(10h / 64%)

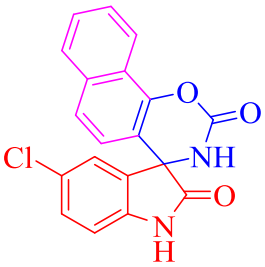

6d
(9h / 67%)

[a]Reaction conditions: Isatin derivatives **1a-l** (1 mmol), urea **2** (2 mmol), 2-naphthol **3**/1-naphthol **5** (1 mmol) in acetonitrile at 100 °C in the presence of 20 mol% of *p*-TSA. [b]The reaction progress was monitored by TLC. [c]Isolated yields.

All the synthesized compounds were characterized by IR, ^{1}H NMR, ^{13}C NMR and mass spectral data which were in good agreement with elemental analyses (CHN). For instance, the IR spectrum of the compound **4e** showed the stretching frequencies at 1741 and 1707 cm^{-1} correspond to carbonyl groups (C=O) of the oxindole ring and carbamate ring respectively. The ^{1}H NMR spectrum of the compound showed a broad singlet at δ 6.17

represents the -NH proton of the carbamate moiety. From ^{13}C NMR spectrum, the peaks at δ 174.00 and 149.53 represent the carbonyl group carbon atoms of the oxindole ring and carbamate moiety respectively. The δ value at 63.96 represents the spiro carbon atom (quaternary carbon atom). However, inorder to confirm the spiro carbon atom DEPT-90 and DEPT-135 experiments were carried out. The absence of the peak at δ 63.96 in DEPT-90 and DEPT-135 NMR spectra shows the formation of spiro carbon atom. The absence of the peaks at δ 13.80, 20.39, 29.36, 40.61 in the DEPT-90 spectrum whereas their appearance in DEPT-135 spectrum indicating the presence of the *n*-butyl group in the compound. Further, the peak at *m/z* 395.41 ($[M+Na]^+$ adduct) in mass spectrum confirms the formation of the product **4e**. For more authenticity the crystal structures of the compounds **4a** and **4e** were solved by single crystal X-ray diffraction and confirmed the formation of target compounds. The crystal structures and packing diagrams of the compounds **4a** and **4e** were shown in Figure 5.8, 5.9, 5.10 and 5.11. Crystallographic data, structure refinement parameters were shown in table 3. The geometrical parameters of hydrogen bonds of the compounds **4a** and **4e** were shown in table 4.

5.3.2. Crystal structure analysis

5.3.2.1. Crystal structure analysis of the compound 4a

The compound **4a** crystallizes in the centrosymmetric (racemate) orthorhombic *Pbca* space group with one molecule in the asymmetric unit (Figure 5.8). In this structure, both naphthaoxazinone and oxindole moieties at spiro carbon are perpendicular to each other. The crystal consists of both (R)- and (S)-enantiomers. The crystal structure analysis reveals that the molecules of **4a** form a one-dimensional tape-like structure with supramolecular tetrameric units. Four molecules [two of each (R)- and (S)-enantiomers] of **4a** interact with each other *via* N–H···O hydrogen bonds and form a supramolecular tetramer. The carbonyl (–C=O) group of oxazinone moiety of the first molecule interacts with N–H group of oxindole moiety of the second molecule with N–H···O hydrogen bonding. The carbonyl group of the second molecule of oxindole moiety interacts with the N–H group of oxazinone moiety of the third molecule. The N–H group of the oxindole moiety of the third molecule interacts with the carbonyl group of oxazinone moiety of the fourth molecule through N–H···O hydrogen bonding. The carbonyl group of oxindole moiety of the fourth molecule

interacts with the N–H group of oxindole moiety of the first molecule and forming a supramolecular tetramer. Further, the same interactions are also extended along the crystallographic *a*-axis forming a one-dimensional tape-like structure. These interactions also extend along the crystallographic *c*-axis (Figure 5.9). The perpendicularity is existed in between the naphtha-oxazinone and oxindole moieties. The driving force for this perpendicularity is the presence of C–H···π interactions i.e., the C–H bond of naphthalene moiety interacts with the oxindole ring (π-centroid) through C–H···π interactions.

5.3.2.2 Crystal structure analysis of the compound 4e

The compound **4e** crystallizes in the centrosymmetric (racemate) triclinic *P*-1 space group with two molecules in the asymmetric unit (Figure 5.10). The crystal consists of both (R)- and (S)-enantiomers. In this structure, both naphthaoxazinone and oxindole moieties at spiro carbon are perpendicular to each other. The crystal structure analysis reveals that the molecules of **4e** form a ‘’parquet floor’’ network structure in the crystal with N–H···O and C–H···O hydrogen bonds. The two inversion related molecules [(R)- and (S)-enantiomers] of **4e** form a homodimer synthon *via* N–H···O hydrogen bonds. These dimers are connected with translation related other homodimers *via* two molecules of **4e** forming a supramolecular hexamer with C–H···O hydrogen bonds. These hexamers are propagating along the crystallographic *a*- and *c*-axes forming a parquet floor network structure (Figure 5.11). Further, the crystal structure was stabilized by weak C–H···O and π··· π interactions.

Table 3. The salient crystallographic data and structure refinement parameters of the compounds **4a** and **4e**.

	4a	**4e**
Empirical formula	$C_{19}H_{12}N_2O_3$	$C_{23}H_{20}N_2O_3$
Formula weight	316	358.38
Crystal system	Orthorhombic	Triclinic
Space group	*Pbca*	*P*-1
T/K	293(2)	293(2)
a/Å	8.1136(4)	8.7911(4)
b/Å	15.3166(5)	11.7906(6)

c/Å	23.9691(11)	18.4608(10)
α/°	90	100.258(2)
β/°	90	91.539(2)
γ/ °	90	90.285(2)
Z	8	4
V/Å^3	2978.7(2)	1882.15(16)
D_{calc}/ g/cm^3	1.343	1.265
F(000)	1232	752
μ/mm^{-1}	1.067	0.085
θ/º	3.668 to 71.796	1.121 to 25.997
Index ranges	$-9 \leq h \leq 9$	$-10 \leq h \leq 10$
	$-11 \leq k \leq 18$	$-14 \leq k \leq 14$
	$-29 \leq l \leq 28$	$-21 \leq l \leq 22$
N-total	7270	35576
N-independent	2863	7296
N-observed	2002	6546
Parameters	265	665
R_1 ($I > 2\sigma(I)$)	0.0495	0.0392
wR_2 (all data)	0.1122	0.0999
GOF	1.036	1.113
CCDC	1558759	1558760

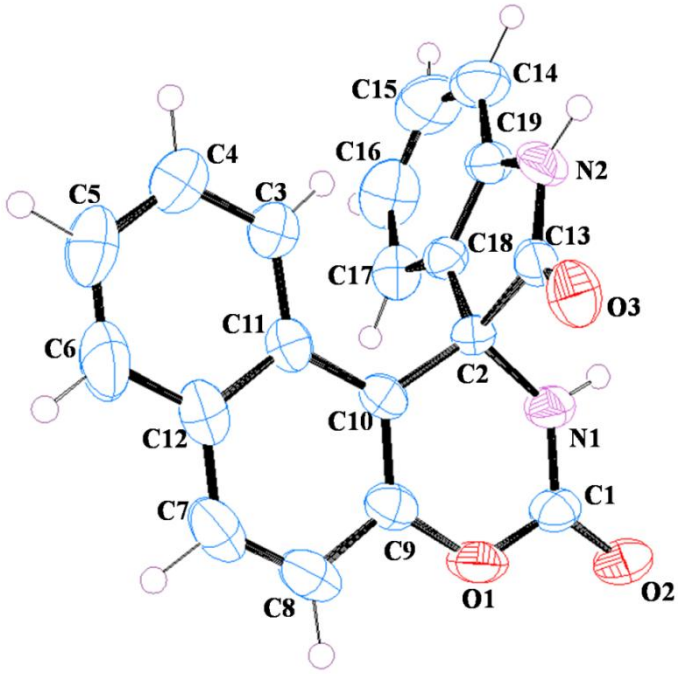

Figure 5.8. The ORTEP representation of the compound **4a**. The thermal ellipsoids are drawn at 50% probability level. The represented **4a** molecule has (S)-configuration at the chiral spiro carbon atom.

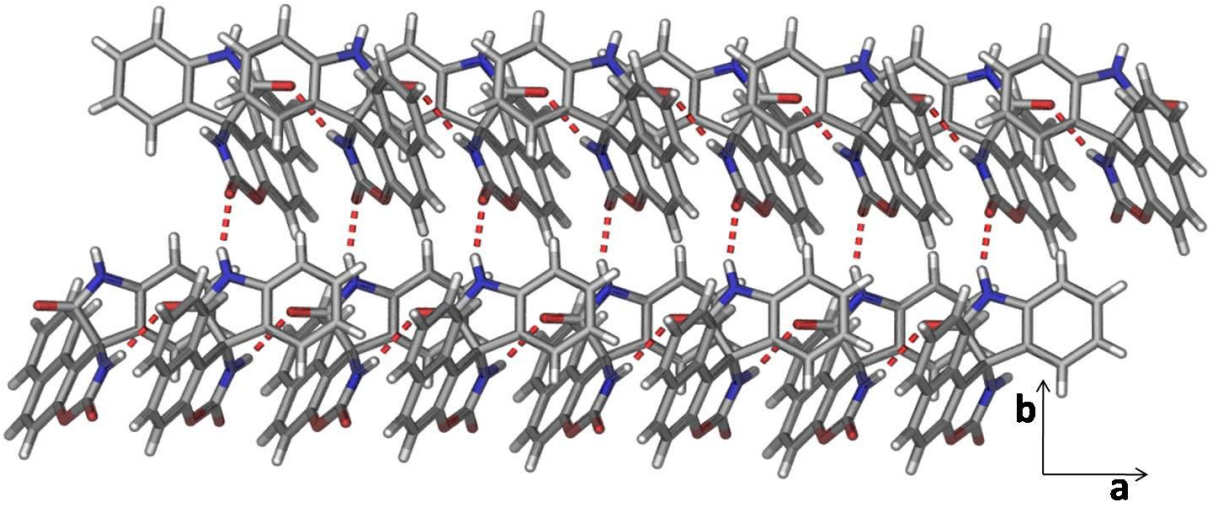

Figure 5.9. The packing diagram of crystal structure **4a** shows a one-dimensional tape-like structure along the crystallographic *a*-axis

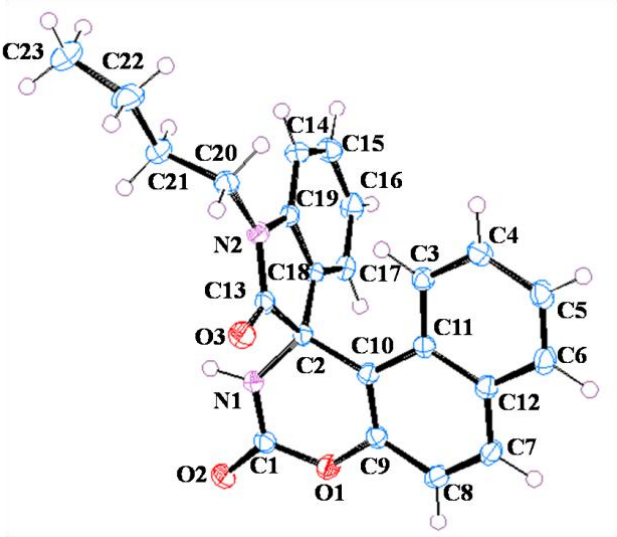

Figure 5.10. The ORTEP representation of the compound **4e**. The thermal ellipsoids are drawn at 50% probability level. The asymmetric unit contains two molecules, but only one molecule has shown for clarity. The represented **4e** molecule has (R)-configuration at the chiral spiro carbon atom.

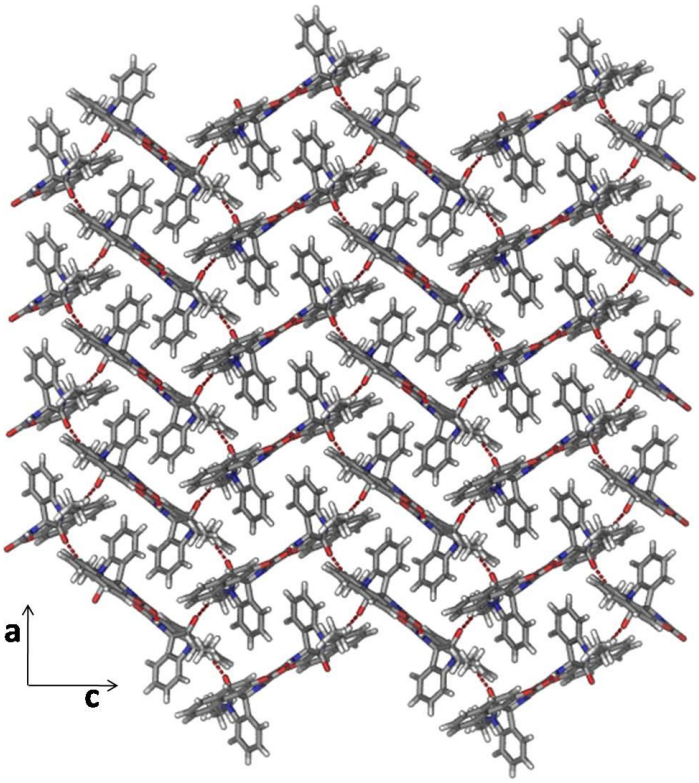

Figure 5.11. The packing diagram of the crystal structure **4e** shows a parquet floor structure in the crystal with N–H···O and C–H···O hydrogen bonds.

Table 4. Geometrical parameters of the hydrogen bonds in compounds **4a** and **4e**.

Compound	D–H···A[a]	D···A (Å)	H···A (Å)	D–H···A (º)	Symmetry code
	N(1)–H(1A)···O(3)	3.121(3)	2.19	153'	1/2+x,y,1/2-z
	N(2)–H(2A)···O(2)	2.851(2)	1.90	156'	-x,1/2+y,1/2-z
4a	Intra C(3)–H(3)···N(2)	3.502(3)	2.68	133	---
	C(8)–H(8)···N(2)	3.784(3)	2.82	148'	-1/2-x,-1/2+y,z
	C(14)–H(14)···O(2)	3.584(4)	2.84	126'	-x,1/2+y,1/2-z
	C(17)–H(17)···O(2)	3.386(3)	2.80	114	1/2+x,y,1/2-z
	N(3)–H(29)···O(5)	2.8247(17)	1.82	173'	-x,-y,-z
	N(4)–H(30)···O(6)	2.8774(17)	1.89	166'	1-x,1-y,1-z
	Intra C(21)–H(5)···N(1)	3.351(2)	2.37	150	---
	Intra C(4)–H(11)···O(3)	2.910(2)	2.47	103	---
	C(4)–H(12)···O(1)	3.236(2)	2.24	152	1+x,y,z
	C(40)–H(13)···O(3)	3.2341(19)	2.57	119	---
	Intra C(40)–H(13)···N(2)	3.354(2)	2.36	152'	---
4e	C(27)–H(16)···O(3)	3.208(2)	2.27	143	---
	Intra C(27)–H(17)···O(1)	2.903(2)	2.43	105	---
	C(9)–H(22)···O(6)	3.275(2)	2.36	142	1+x,y,z
	C(41)–H(24)···O(3)	3.203(2)	2.49	122	---
	C(41)–H(24)···O(6)	3.368(2)	2.47	140'	1-x,1-y,1-z
	C(34)–H(33)···O(5)	3.519(2)	2.51	155	1+x,y,z
	C(20)–H(36)···O(1)	3.594(2)	2.82	128	1+x,y,z

[a]All of the C–H and N–H distances are neutron normalized to 1.083 and 1.009 Å respectively.

5.3.4. Biological evaluation

5.3.4.1. Antibacterial activity

The *in vitro* antibacterial activity of the target molecules were carried out against five different bacterial strains such as *B. subtilis* and *S. aureus* (gram-positive bacteria); *E. coli, P. aeruginosa* and *K. pneumoniae* (gram-negative bacteria) respectively. The results were depicted in Table 5.

Among all the target compounds, the compound **4f** with *N*-benzyl group was more active (MIC value 7.5 µg/mL) than the standard drug ciprofloxacin (9.25 µg/mL) against *E. coli*. The compound **4d**, **4l** and **6c** exhibits significant antibacterial activity against *E. coli.* with MIC values 10.5 µg/mL, 10.5 µg/mL and 9.5 µg/mL respectively. The compounds **4c** and **4e** showed significant antibacterial activity against *S. aureus* with MIC value 10.5 µg/mL.

Table 5. Antibacterial activity of the spirooxindolocarbamates **4a-l** and **6a-d (**MIC, µg/mL**)**.

S. No.	Compound	Minimum Inhibitory Concentration (µg/mL)				
		B. subtilis	***S. aureus***	***E. coli***	***P. aeruginosa***	***K. pneumoniae***
1	**4a**	>50.0	13.0	14.5	15.5	16.5
2	**4b**	30.5	11.5	12.0	11.5	15.5
3	**4c**	17.5	**10.5**	11.5	14.5	10.5
4	**4d**	14.5	12.0	**10.5**	13.5	32.5
5	**4e**	>50.0	**10.5**	12.5	15.5	10.5
6	**4f**	12.5	13.5	**7.5**	11.5	>50.0
7	**4g**	12.5	17.5	12.5	13.5	14.0
8	**4h**	22.0	>50.0	15.5	23.5	24.5
9	**4i**	19.5	19.0	17.5	20.0	22.0
10	**4j**	15.0	31.5	16.0	17.5	19.0
11	**4k**	19.5	17.0	23.0	34.0	>50.0
12	**4l**	14.5	16.0	**10.5**	15.5	24.5
13	**6a**	25.5	34.5	18.5	>50.0	>50
14	**6b**	22.0	27.5	14.5	16.5	12.5
15	**6c**	13.5	15.0	**9.5**	13.5	>50.0

16	**6d**	28.0	36.5	19.5	45.0	>50.0
17	**Ciprofloxacin**	8.3	9.25	9.25	8.08	4.5

[a] The values are means of triplicates with ± SD. The bacterial strains: *B. Subtilis – Bacillus subtilis, S. aureus- Staphylococcus aureus, E. coli- Escherichia Coli, P. aeruginosa- Pseudomonas aeruginosa, K. pneumoniae- Klebsiella Pneumoniae.*

5.3.4.2. Antifungal activity

The *in vitro* antifungal activity of the target compounds were investigated on two fungal strains such as *Aspergillus niger* and *Penicillium notatum.* The results were summarized in Table 6. Among all the synthesized compounds, the compounds **4a** and **4f e**xhibited the moderate activity against *Aspergillus niger* with MIC values 17.5 µg/mL and 18.0 µg/mL respectively.

Table 6. Antifungal activity of the spirooxindolocarbamates **4a-l** and **6a-d (**MIC, µg/mL**).**

S. No.	Compound	Minimum Inhibitory Concentration (µg/mL)	
		Aspergillus niger	***Penicillium notatum***
1	**4a**	**17.5**	>50.0
2	**4b**	>50.0	>50.0
3	**4c**	47.0	43.5
4	**4d**	33.5	43.5
5	**4e**	28.5	48.0
6	**4f**	**18.0**	39.0
7	**4g**	>50.0	42.5
8	**4h**	23.5	34.0
9	**4i**	35.5	38.0
10	**4j**	34.0	41.0
11	**4k**	22.0	31.5
12	**4l**	33.5	45.0
13	**6a**	>50.0	>50.0
14	**6b**	45.0	>50.0
15	**6c**	26.5	>50.0

16	**6d**	37.5	39.0
17	**Ketoconazole**	3.5	3.5

[a]The values are means of triplicates with ± SD.

5.3.4.3. Antioxidant activity

All the synthesized compounds **4a-l** and **6a-d** were evaluated for their *in vitro* radical scavenging activity. The radical scavenging activity results were shown in table 7.

All the compounds exhibited the radical scavenging activity with IC_{50} values ranging from 7.06 ± 0.78 µM to 32.55 ± 0.15 µM. Among all the compounds, the compound **4f** and **4l** exhibiting potent antioxidant activity with IC_{50} values 9.12 ± 0.01 µM and 7.06 ± 0.78 µM respectively. The compounds **4k (**14.56 ± 0.27 µM**)** and **6c (**17.35 ± 0.05 µM**)** were exhibited significant antioxidant activity.

Table 7. The antioxidant activity of the target compounds **4a-l** and **6a-d** by DPPH method.

S. No.	Compound	IC_{50} (µM)
1	**4a**	31.80 ± 0.82
2	**4b**	27.17 ± 0.90
3	**4c**	24.12 ± 0.04
4	**4d**	22.33 ± 1.06
5	**4e**	19.53 ± 0.27
6	**4f**	**9.12 ± 0.01**
7	**4g**	28.07 ± 0.51
8	**4h**	32.55 ± 0.15
9	**4i**	25.60 ± 0.10
10	**4j**	24.54 ± 0.11
11	**4k**	**14.56 ± 0.27**
12	**4l**	**7.06 ± 0.78**
13	**6a**	28.40 ± 0.70
14	**6b**	24.01 ± 0.17
15	**6c**	**17.35 ± 0.05**
16	**6d**	24.10 ± 0.08
17	**Ascorbic acid**	6.63 ± 0.68

5.4. Molecular docking studies

DNA gyrase protein belongs to type II topoisomerase family, is one of the major bacterial proteins. The negative supercoiling of bacterial circular DNA was catalyzed by this protein with the help of free energy involved in the ATP hydrolysis. Because of its properties like DNA replication and transcription, it becomes a preferred target for the antibacterial agents [60]. The assessment of ligand-protein complexes is one of the important criteria for modern structural based drug design. The docking studies were carried out against the DNA gyrase protein (PDB ID: 1KZN) [60] by using AutoDock Tools (ADT) version 1.5.6 and AutoDock version 4.2.5.1 docking program. The *in vitro* antibacterial activity of the synthesized compounds was well correlated with their *in silico* calculated binding energies. When compared with the other compounds, the compounds **4f**, **6c**, **6b**, **6a**, **4d** and **4c** were exhibited good binding energies i.e., −8.51, −7.92, −7.64, −7.61, −7.51, −7.46 kcal/mol respectively. Among all these compounds, compound **4f** exhibited the highest binding energy (− 8.51 Kcal/mol) than the other compounds. The number of hydrogen bonds, residues involved in the hydrogen bonds and their bond lengths were shown in table 7. The compounds **4a**, **4b**, **4c**, **4d, 4g** and **6a** form hydrogen bonds with amino acid residues of the protein 1KZN. Even though there are no hydrogen bonds in the ligand-protein complexes formed from the compounds **4e**, **4f, 6b** and **6c,** they exhibited good binding energies than the other molecules. This information suggested that several pi-type interactions formed in between the ligand and protein were responsible for their high binding energies. The docking poses of the target compounds with the protein 1KZN were shown in figure 5.12.

Table 7. Docking results of the synthesized compounds against the protein DNA protein gyrase (PDB ID: 1KZN).

S. No.	Compound	Binding Energy (kcal/mol)	No. of hydrogen bonds	Residues involved in the Hydrogen bonds	Hydrogen Bond lengths (Å)
1	**4a**	−7.10	5	HIS95, ALA96, VAL120, SER121, ILE90	1.83, 2.12, 2.95, 3.07, 3.09
2	**4b**	−7.29	4	ALA96, HIS95, VAL120, ILE90	1.83, 2.09, 2.99, 3.09

3	**4c**	−7.46	4	HIS95, ALA96, VAL120, ILE90	1.84, 2.10, 2.99, 3.07
4	**4d**	−7.51	4	HIS95, ALA96, VAL120, ILE90	1.75, 2.32, 2.86, 3.07
5	**4e**	−7.44	--	--	--
6	**4f**	**−8.51**	--	--	--
7	**4g**	−7.20	5	HIS95, ALA96, VAL120, SER121, ILE90	1.84, 2.12, 2.94, 3.07, 3.10
8	**4h**	−7.40	5	ILE90, VAL120, ALA96, HIS95, SER121	1.87, 2.18, 2.95, 2.98, 3.01
9	**4i**	−7.55	4	ALA96, HIS95, VAL120, ILE90	1.84, 2.09, 2.99, 3.07
10	**4j**	−7.68	5	VAL120, ALA96, ILE90, SER121, HIS95	1.88,2.17, 2.95, 2.98, 3.02
11	**4k**	−7.44	4	VAL120, ALA96, HIS95, ILE90	1.86, 2.10, 2.99, 3.08
12	**4l**	−7.88	1	ASN46	2.15
13	**6a**	−7.61	1	HIS116	1.97
14	**6b**	−7.64	--	--	--
15	**6c**	**−7.92**	--	--	--
16	**6d**	−7.07	2	GLY77, GLU50	2.17, 3.06

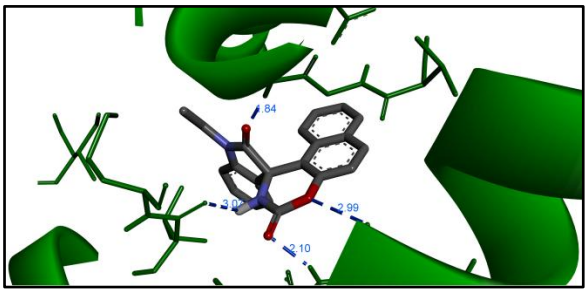

a)

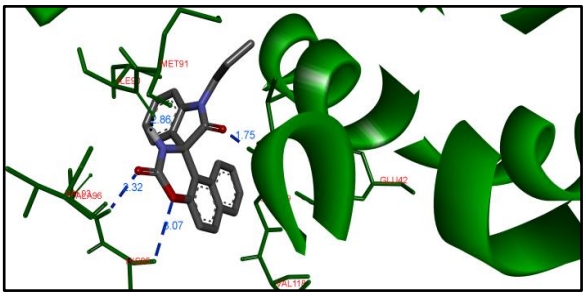

b)

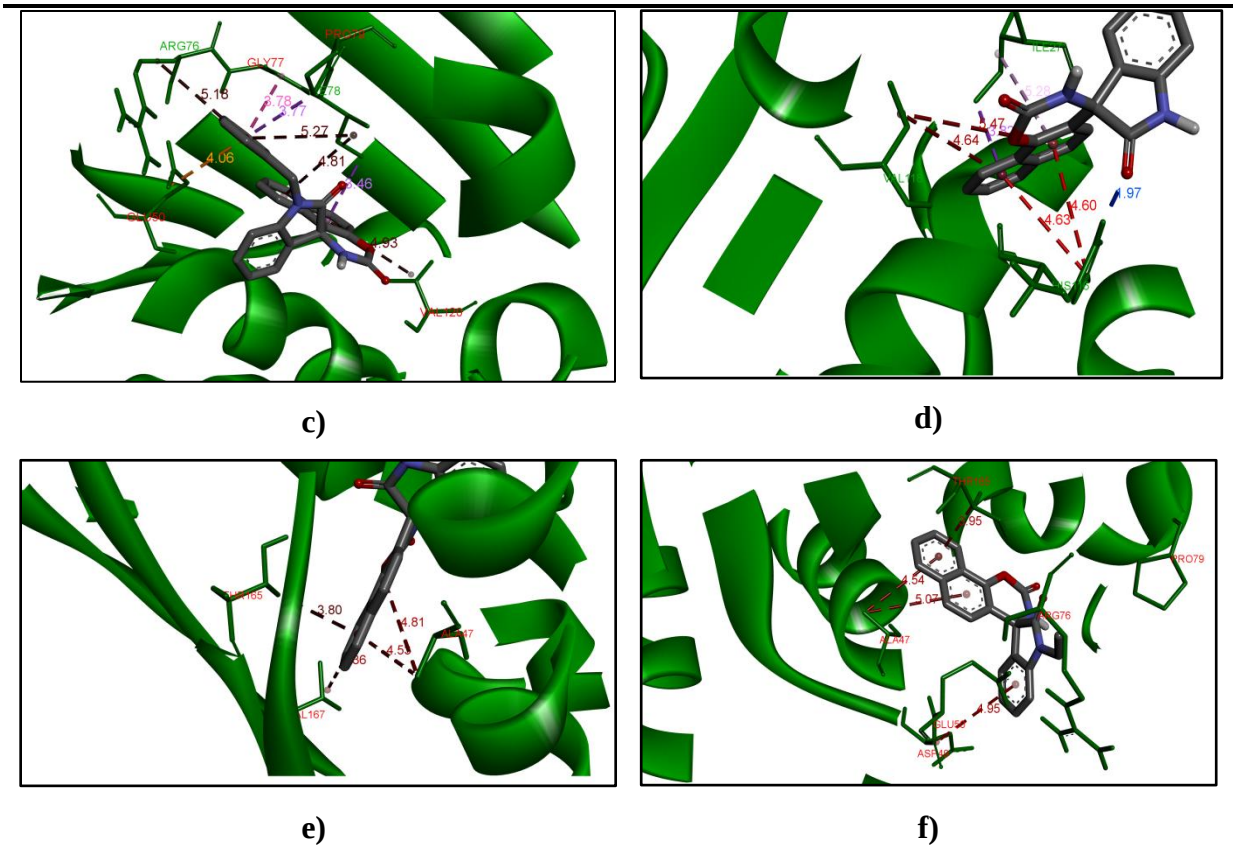

c) **d)**

e) **f)**

Figure 5.12. The best docking poses of the compounds a) **4c**, b) **4d**, c) **4f**, d) **6a**, e) **6b** and f) **6c** with the DNA gyrase protein (PDB ID: 1KZN).

5.5. Conclusion

Various spirooxindolocarbamates were synthesized *via* a one-pot multi-component approach by using a Betti reaction and characterized by spectral methods. Further, the structures of the compounds **4a** and **4e** were confirmed by SXRD method. The compounds were tested for their *in vitro* antibacterial activity and found that majority of the compounds exhibit good to moderate activity towards *B. subtilis*, *S. aureus*, *E. Coli*, *P. aeruginosa* and *K. pneumoniae*. Particularly, the compounds **4f**, **4l** and **6c** were recognized as lead molecules, exhibiting the promising activity against *E. Coli* and showing the MIC values 7.5 µg/mL, 10.5 µg/mL and 9.5 µg/mL respectively. Docking results of the synthesized molecules were well correlated *in vitro* antibacterial activity. The compounds **4a** and **4f** showed moderate activity against the fungal strain *A. niger*. The compound **4f** and **4l** exhibited potent antioxidant activity with IC_{50} values 9.12 ± 0.01 µM and 7.06 ± 0.78 µM respectively.

5.6. Spectral data

Spiro[indoline-3,1'-naphtho[1,2-*e*][1,3]oxazine]-2,3'(2'*H*)-dione (4a)

Colour: White. M. P. 294-295 ^{o}C. IR (KBr, cm^{-1}): 3427, 1741, 1707. ^{1}H NMR (400 MHz, DMSO-*d6*) δ: 6.88 (s, 1H, *J* = 10.0 Hz), 6.98 (t, 1H, *J* = 10.8 Hz), 7.05 (d, 2H, *J* = 9.2 Hz), 7.18-7.33 (m, 4H), 7.87 (d, 1H, *J* = 10.4 Hz), 7.96 (d, 1H, *J* = 12.0 Hz), 11.04 (s, 1H). ^{13}C NMR (100 MHz, DMSO-*d6*) δ: 181.00, 154.35, 153.03, 146.82, 137.01, 136.94, 135.97, 135.79, 134.55, 133.96, 132.92, 130.20, 128.34, 127.16, 122.45, 116.14, 114.82, 68.87. ESI mass spectrum (*m/z*): 339.2 ([M+Na]$^{+}$). Anal. Calcd. For $C_{19}H_{12}N_2O_3$: C, 72.15; H, 3.82; N, 8.86; found: C, 71.94; H, 3.72; N, 7.68.

1-Methyl spiro[indoline-3,1'-naphtho[1,2-*e*][1,3]oxazine]-2,3'(2'*H*)-dione (4b)

Colour: White. M. P. 293-295 °C. IR (KBr, cm^{-1}): 3425, 2871, 1739, 1702. ^{1}H NMR (400 MHz, $CDCl_3$) δ: 3.38 (s, 3H), 6.12 (s, 1H), 6.81 (d, 1H, *J* = 8.4 Hz), 7.07 (t, 2H, *J* = 8.0 Hz), 7.16-7.2 (m, 2H), 7.31-7.35 (m, 2H), 7.46 (t, 1H, *J* = 8.0 Hz), 7.79 (d, 1H, *J* = 8.0 Hz), 7.87 (s, 1H, *J* = 9.2 Hz). ^{13}C NMR (100 MHz, $CDCl_3$) δ: 174.14, 149.56, 148.94, 142.85, 132.02, 131.40, 131.19, 130.51, 129.33, 129.06, 127.80, 125.39, 125.10, 124.45, 122.22, 117.55, 109.46, 109.11, 63.98, 27.00. ESI mass spectrum (*m/z*): 353.12 ([M+Na]$^{+}$). Anal. Calcd. for $C_{20}H_{14}N_2O_3$: C, 72.72; H, 4.27; N, 8.48; found: C, 72.94; H, 5.42; N, 8.24.

1-Ethyl spiro[indoline-3,1'-naphtho[1,2-*e*][1,3]oxazine]-2,3'(2'*H*)-dione (4c)

Colour: White. M. P. 281-283 °C. IR (KBr, cm^{-1}): 3531, 2937, 1706, 1671. ^{1}H NMR (400 MHz, $CDCl_3$) δ: 1.4 (t, 3H, *J* = 6.0 Hz), 3.8-4.04 (m, 2H) , 5.85 (s, 1H), 6.89 (d, 1H, *J* = 8.0 Hz), 7.04-7.47 (m, 7H), 7.78-7.88 (m, 2H). ESI mass spectrum (*m/z*): 367.15 ([M+Na]$^{+}$). Anal. Calcd. for $C_{21}H_{16}N_2O_3$: C, 73.24; H, 4.68; N, 8.13; found: C, 72.00; H, 4.57; N, 8.29.

1-Propyl spiro[indoline-3,1'-naphtho[1,2-*e*][1,3]oxazine]-2,3'-(2'*H*)-dione (4d)

Colour: White. M. P. 248-250 °C. IR (KBr, cm^{-1}): 3428, 2866, 1742, 1706. ^{1}H NMR (400 MHz, $CDCl_3$) δ: 1.04 (t, 3H, *J* = 6.0 Hz), 1.8-1.89 (m, 2H), 3.71-3.90 (m, 2H), 5.93 (s, 1H), 6.89 (d, 1H, *J* = 8.0 Hz), 7.06 (t, 2H, *J* = 6.4 Hz), 7.15-7.20 (m, 2H), 7.31-7.34 (m, 2H), 7.44 (t, 1H, *J* = 6.4 Hz), 7.79 (d, 1H, *J* = 6.8 Hz), 7.87 (d, 1H, *J* = 7.2 Hz). ^{13}C NMR (100 MHz,

$CDCl_3$) δ: 174.05, 149.55, 148.98, 142.45, 131.94, 131.39, 131.08, 130.67, 129.31, 129.09, 127.55, 125.56, 125.09, 124.16, 122.46, 117.56, 109.67, 109.21, 63.96, 42.44, 20.68, 11.60. ESI mass spectrum (*m/z):* 381.14 ($[M+Na]^+$). Anal. Calcd. for $C_{22}H_{18}N_2O_3$: C, 73.73; H, 5.06; N, 7.82; found: C, 73.94; H, 5.18; N, 7.69.

1-Butyl spiro[indoline-3,1'-naphtho[1,2-*e*][1,3]oxazine]-2,3'(2'*H*)-dione (4e)

Colour: White. M. P. 237-239 ℃. IR (KBr, cm^{-1}): 3428, 2841, 1710, 1674. ^1H NMR (400 MHz, $CDCl_3$) δ: 0.99 (t, 3H, *J* = 6.0 Hz), 1.44-1.50 (sextet, 2H, *J* = 6.0 Hz), 1.75-1.82 (m, 2H), 3.74-3.94 (m, 2H), 6.17 (s, 1H), 6.88 (d, 1H, *J* = 6.8 Hz), 7.03-7.07 (m, 2H), 7.14-7.19 (m, 2H), 7.30-7.34 (m, 2H), 7.43 (t, 1H, *J* = 6.4 Hz), 7.78 (d, 1H, *J* = 6.4 Hz), 7.86 (d, 1H, *J* = 7.2 Hz). ^{13}C NMR (100 MHz, $CDCl_3$) δ: 174.00, 149.53, 142.41, 131.94, 131.40, 131.08, 130.69, 129.31, 129.09, 127.51, 125.56, 125.10, 124.16, 122.47, 117.55, 109.67, 109.20, 63.96, 40.61, 29.36, 20.39, 13.80. ESI mass spectrum (*m/z*): 395.18 ($[M+Na]^+$). Anal. Calcd. for $C_{23}H_{20}N_2O_3$: C, 74.18; H, 5.41; N, 7.52; found: C, 73.92; H, 5.49; N, 7.27.

1-Benzyl spiro[indoline-3,1'-naphtho[1,2-e][1,3]oxazine]-2,3'(2'*H*)-dione (4f)

Colour: White. M. P. 263-265 ℃. IR (KBr, cm^{-1}): 3419, 2875, 1730, 1707. ^1H NMR (400 MHz, $CDCl_3$) δ: 4.85 (d, 1H, *J* = 15.2), 5.23 (d, 1H, *J* = 14.8 Hz), 5.55 (s, 1H), 6.75 (d, 1H, *J* = 8.8 Hz), 6.96-7.06 (m, 2H), 7.2 (d, 1H, *J* = 8.0 Hz), 7.30-7.45 (m, 6H), 7.8 (d, 1H, *J* = 8.0 Hz), 7.89 (d, 1H, *J* = 8.8 Hz). ESI mass spectrum (*m/z*): 446.25 ($[M+K]^+$). Anal. Calcd. for $C_{26}H_{18}N_2O_3$: C, 76.83; H, 4.46; N, 6.89; found: C, 76.94; H, 4.36; N, 7.19.

5-Chlorospiro[indoline-3,1'-naphthol[1,2-*e*][1,3]oxazine-2,3'(2'*H*)-dione (4g)

Colour: White. M. P. 283-284 ℃. IR (KBr, cm^{-1}): 3446, 2967, 1743, 1718. ^1H NMR (400 MHz, DMSO-*d6*) δ: 5.69 (s, 1H), 6.74 (d, 1H, *J* = 10.0 Hz), 6.83 (d, 1H, *J* = 11.2 Hz), 7.11 (d, 1H, *J* = 10.4 Hz), 7.18 (d, 1H, *J* = 9.2 Hz), 7.45 (d, 1H, *J* = 10.0 Hz), 7.60 (t, 1H, *J* = 8.4 Hz), 7.70 (t, 1H, *J* = 9.2 Hz), 8.32 (d, 1H, *J* = 12.0 Hz), 9.32 (d, 1H, *J* = 11.2 Hz), 10.52 (s, 1H). Anal. Calcd. for $C_{19}H_{11}ClN_2O_3$: C, 65.06; H, 3.16; N, 7.99; found: C, 65.30; H, 3.07; N, 7.77.

5-Chloro-1-methylspiro[indoline-3,1'-naphtho[1,2-*e*][1,3]oxazine]-2,3'(2'*H*)-dione (4h)

Colour: White. M. P. 275-278 ºC. ^{1}H NMR (400 MHz, $CDCl_3$) δ: 3.37 (s, 3H), 6.11 (s, 1H), 6.80 (d, 1H, J = 8.4 Hz), 7.06 (t, 1H, J = 8.0 Hz), 7.14-7.18 (m, 2H), 7.30-7.33 (m, 2H), 7.44 (t, 1H, J = 8.0 Hz), 7.78 (d, 1H, J = 8.0 Hz), 7.86 (s, 1H, J = 9.2 Hz). ^{13}C NMR (100 MHz, $CDCl_3$) δ: 174.19, 149.61, 148.99, 142.90, 132.07, 131.44, 131.24, 130.56, 129.38, 129.11, 127.85, 125.44, 125.15, 124.50, 122.27, 117.60, 109.50, 109.16, 64.03, 27.05. Anal. Calcd. for $C_{20}H_{14}N_2O_3$: C, 65.85; H, 3.59; N, 7.68; found: C, 65.59; H, 3.62; N, 7.90.

5-Chloro-1-ethyl spiro[indoline-3,1'-naphtho[1,2-*e*][1,3]oxazine]-2,3'(2'*H*)-dione (4i)

Colour: White. M. P. 265-267 ºC. ^{1}H NMR (400 MHz, $CDCl_3$) δ: 1.55 (t, 3H, J = 6.0 Hz), 3.90-4.07 (m, 2H), 5.83 (s, 1H), 6.92 (d, 1H, J = 8.0 Hz), 7.04-7.47 (m, 6H), 7.78-7.89 (m, 2H). Anal. Calcd. for $C_{21}H_{16}N_2O_3$: C, 66.58; H, 3.99; N, 7.40; found: C, 66.72; H, 3.95; N, 7.66.

5-Chloro-1-propyl spiro[indoline-3,1'-naphtho[1,2-e][1,3]oxazine]-2,3'(2'H)-dione (4j)

Colour: White. M. P. 240-242 ºC. ^{1}H NMR (400 MHz, $CDCl_3$) δ: 1.05 (t, 3H, J = 6.0 Hz), 1.80-1.89 (m, 2H), 3.72-3.91 (m, 2H), 5.94 (s, 1H), 6.90 (d, 1H, J = 8.0 Hz), 7.06 (t, 2H, J = 6.4 Hz), 7.16-7.21 (m, 2H), 7.31-7.35 (m, 1H), 7.45 (t, 1H, J = 6.4 Hz), 7.79 (d, 1H, J = 6.8 Hz), 7.88 (d, 1H, J = 7.2 Hz). ^{13}C NMR (100 MHz, $CDCl_3$) δ: 174.04, 149.53, 148.97, 142.44, 131.93, 131.38, 131.07, 130.66, 129.29, 129.07, 127.54, 125.55, 125.08, 124.15, 122.45, 117.55, 109.66, 109.20, 63.95, 42.43, 20.67, 11.59. Anal. Calcd. for $C_{22}H_{18}N_2O_3$: C, 67.26; H, 4.36; N, 7.13; found: C, 67.52; H, 4.30; N, 7.30.

1-Butyl-5-chlorospiro[indoline-3,1'-naphtho[1,2-*e*][1,3]oxazine]-2,3'(2'*H*)-dione (4k)

Colour: White. M. P. 228-230 ºC. ^{1}H NMR (400 MHz, $CDCl_3$) δ: 1.05 (t, 3H, J = 6.0 Hz), 1.50-1.56 (m, 2H), 1.81-1.88 (m, 2H), 3.80-3.99 (m, 2H), 6.23 (s, 1H), 6.95 (d, 1H, J = 6.8 Hz), 7.09-7.13 (m, 2H), 7.20-7.25 (m, 2H), 7.36-7.40 (m, 1H), 7.49 (t, 1H, J = 6.4 Hz), 7.85 (d, 1H, J = 6.4 Hz), 7.92 (d, 1H, J = 7.2 Hz). ^{13}C NMR (100 MHz, $CDCl_3$) δ: 173.55, 149.08, 141.96, 131.49, 130.94, 130.63, 130.24, 128.85, 128.63, 127.05, 125.11, 124.65, 123.71,

122.02, 117.10, 109.22, 108.75, 63.51, 40.16, 28.91, 19.94, 13.35. Anal. Calcd. for $C_{23}H_{20}N_2O_3$: C, 67.90; H, 4.71; N, 6.89; found: C, 67.68; H, 4.79; N, 6.97.

1-Benzyl-5-chlorospiro[indoline-3,1'-naphtho[1,2-*e*][1,3]oxazine]-2,3'(2'*H*)-dione (4l)

Colour: White. M. P. 268-270 °C. ^{1}H NMR (400 MHz, $CDCl_3$) δ: 4.86 (d, 1H, J = 15.2), 5.25 (d, 1H, J = 14.8 Hz), 5.56 (s, 1H), 6.77 (d, 1H, J = 8.8 Hz), 6.97-7.07 (m, 2H), 7.21 (d, 1H, J = 8.0 Hz), 7.31-7.46 (m, 5H), 7.81 (d, 1H, J = 8.0 Hz), 7.91 (d, 1H, J = 8.8 Hz). Anal. Calcd. for $C_{26}H_{18}N_2O_3$: C, 70.83; H, 3.89; N, 6.35; found: C, 70.67; H, 3.66; N, 6.51.

Spiro[indoline-3,4'-naphtho[1,2-e][1,3]oxazine]-2,2'(3'H)-dione (6a)

Colour: White. M. P. 286-287 °C. IR (KBr, cm^{-1}) : 3428, 2866, 1740, 1707. ^{1}H NMR (400 MHz, $CDCl_3$+DMSO-*d6*) δ: 5.59 (s, 1H), 6.64 (d, 1H, J = 11.2 Hz), 6.73-6.81 (m, 2H), 6.98 (t, 1H, J = 10.0 Hz), 7.2 (t, 2H, J = 8.0 Hz), 7.53 (m, 2H), 8.19 (d, 1H, J = 8.0 Hz), 9.18 (d, 1H, J = 11.2 Hz) 10.13 (s, 1H). ^{13}C NMR (100 MHz, $CDCl_3$+DMSO-*d6*) δ: 181.00, 154.35, 153.03, 146.82, 137.01, 136.94, 135.97, 135.79, 134.55, 133.96, 132.92, 130.20, 128.34, 127.16, 122.45, 116.14, 114.82, 68.87. ESI mass spectrum (*m/z*): 339.1 ($[M+Na]^+$). Anal. Calcd. for $C_{19}H_{12}N_2O_3$: C, 72.15; H, 3.82; N, 8.86; found: C, 71.97; H, 3.88; N, 8.56.

1-Methyl spiro[indoline-3,4'-naphtho[1,2-*e*][1,3]oxazine]-2,2'(3'*H*)-dione (6b)

Colour: White. M. P. 255-257 °C. IR (KBr, cm^{-1}): 3431, 2868, 1710, 1692. ^{1}H NMR (400 MHz, $CDCl_3$+DMSO-*d6*) δ: 3.17 (s, 3H), 5.69 (s, 1H), 6.73 (d, 1H, J = 10.8 Hz), 6.82 (d, 1H, J = 11.2 Hz), 7.11 (d, 1H, J = 10.4 Hz), 7.18 (d, 1H, J = 10.0 Hz), 7.36-7.5 (m, 2H), 7.602 (t, 1H, J = 9.2 Hz), 7.69 (t, 1H, J = 9.2 Hz), 8.31 (d, 1H, J = 12.0 Hz), 9.32 (d, 1H, J = 11.2 Hz). ^{13}C NMR (100 MHz, $CDCl_3$+DMSO-*d6*) δ: 181.48, 162.06, 159.17, 148.85, 137.88, 137.41, 133.71, 133.53, 131.69, 131.11, 130.54, 129.69, 128.96, 127.52, 127.18, 113.41, 111.66, 71.04, 31.56. ESI mass spectrum (*m/z*): 370.17 ($[M+K]^+$). Anal. Calcd. for $C_{20}H_{14}N_2O_3$: C, 72.72; H, 4.27; N, 8.48; found: C, 72.48; H, 4.36; N, 8.63.

2-Ethyl spiro[indoline-3,4'-naphtho[1,2-*e*][1,3]oxazine]-2,2'(3'*H*)-dione (6c)

Colour: White. M. P. 210-212 °C. IR (KBr, cm^{-1}): 3532, 2844, 1706, 1672. ^{1}H NMR (400 MHz, $CDCl_3$) δ: 1.41 (t, 3H, J = 6.0 Hz), 3.8-4.05 (m, 2H), 5.86 (s, 1H), 6.89 (d, 1H, J = 8.0

Hz), 7.04-7.47 (m, 7H), 7.89 (m, 2H). ESI mass spectrum (*m/z*): 384.21 ($[M+K]^+$). Anal. Calcd. for $C_{21}H_{16}N_2O_3$: C, 73.24; H, 4.68; N, 8.13; found: C, 72.46; H, 4.91; N, 8.39.

5-Chlorospiro[indoline-3,4'-naphtho[2,1-e][1,3]oxazine]-2,2'(3'H)-dione (6d)

Colour: White. M. P. 292-294 ^oC. ^1H NMR (400 MHz, DMSO-*d6*) δ: 6.97 (s, 1H, J = 10.0 Hz), 7.07 (t, 1H, J = 10.8 Hz), 7.10 (d, 2H, J = 9.2 Hz), 7.27-7.42 (m, 3H), 7.90 (d, 1H, J = 10.4 Hz), 8.00 (d, 1H, J = 12.0 Hz), 8.94 (s, 1H), 11.13 (s, 1H). Anal. Calcd. For $C_{19}H_{12}N_2O_3$: C, 65.06; H, 3.16; N, 7.99; found: C, 65.24; H, 3.22; N, 7.71.

5.7. Crystallographic data of compound 4a and 4e

CCDC 1558759 and CCDC 1558760 contains the supplementary crystallographic data (.cif) of the compounds **4a** and **4e** respectively. These data can be obtained free of charge from The Cambridge Crystallographic Data Centre *via* www.ccdc.cam.ac.uk/structures.

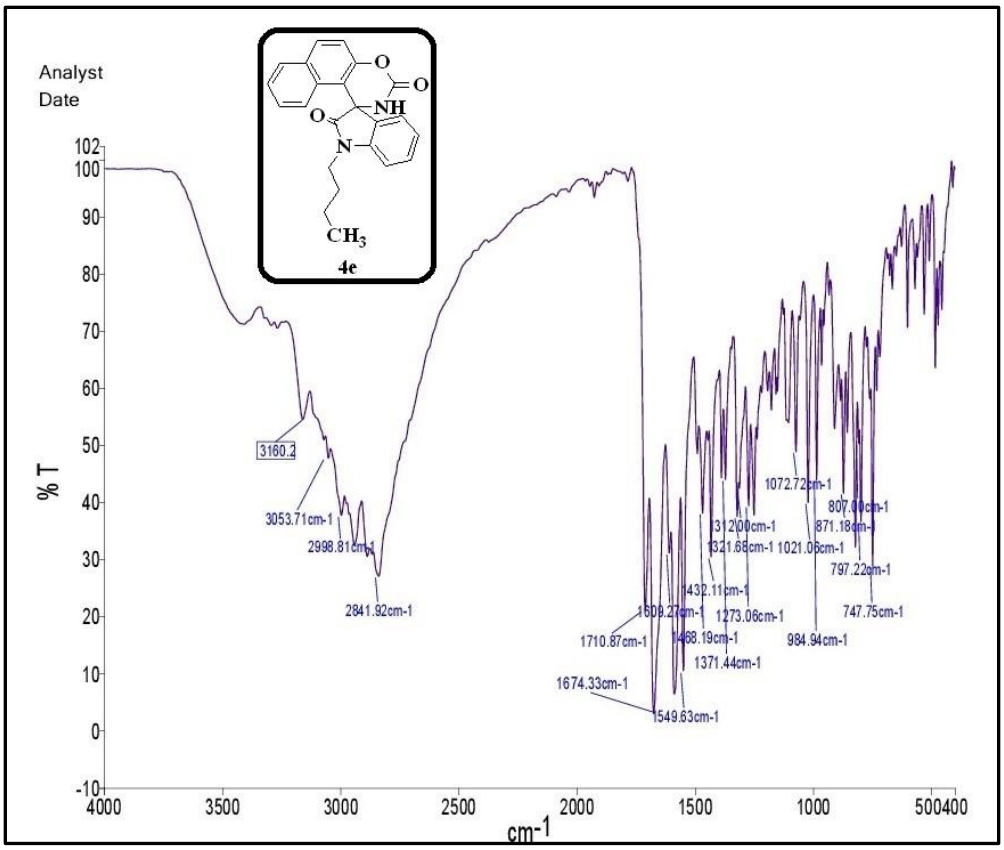

IR spectrum of the compound **4e**

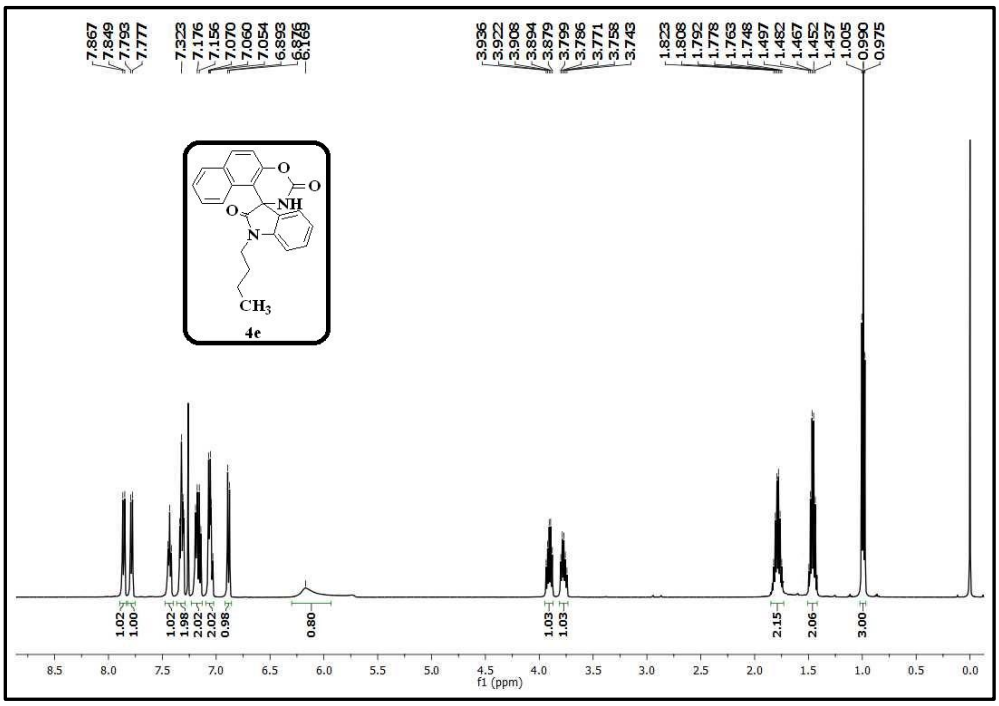

^{1}H NMR spectrum of the compound **4e**

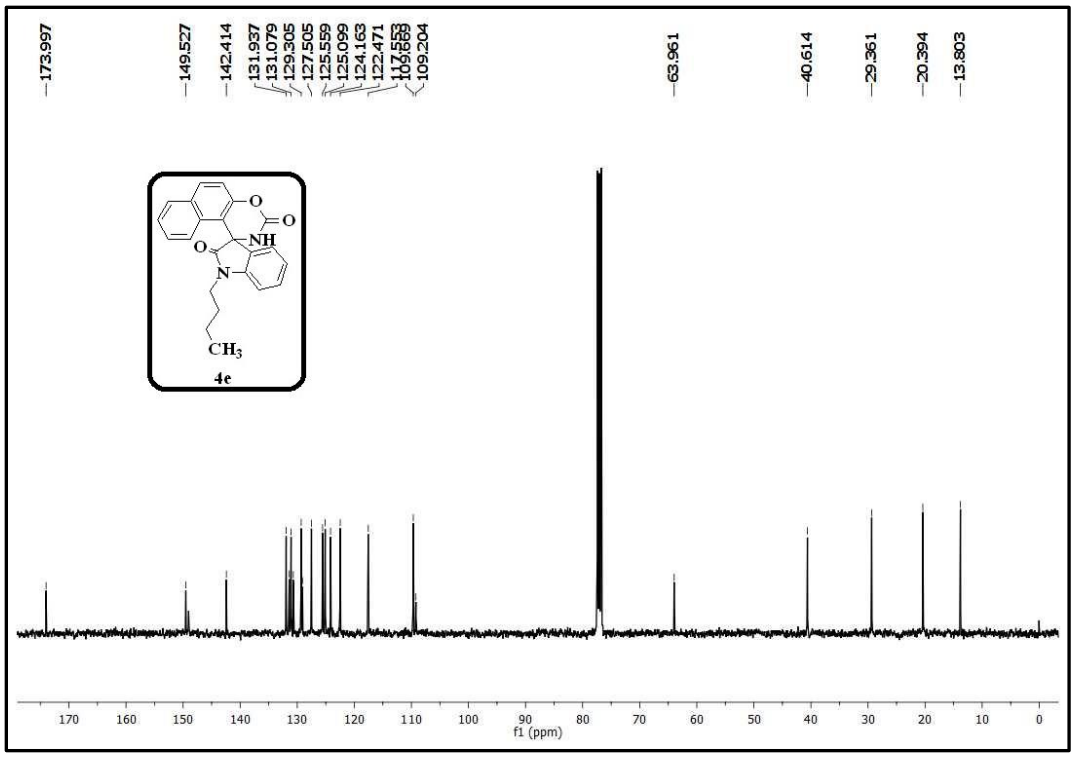

^{13}C NMR spectrum of the compound **4e**

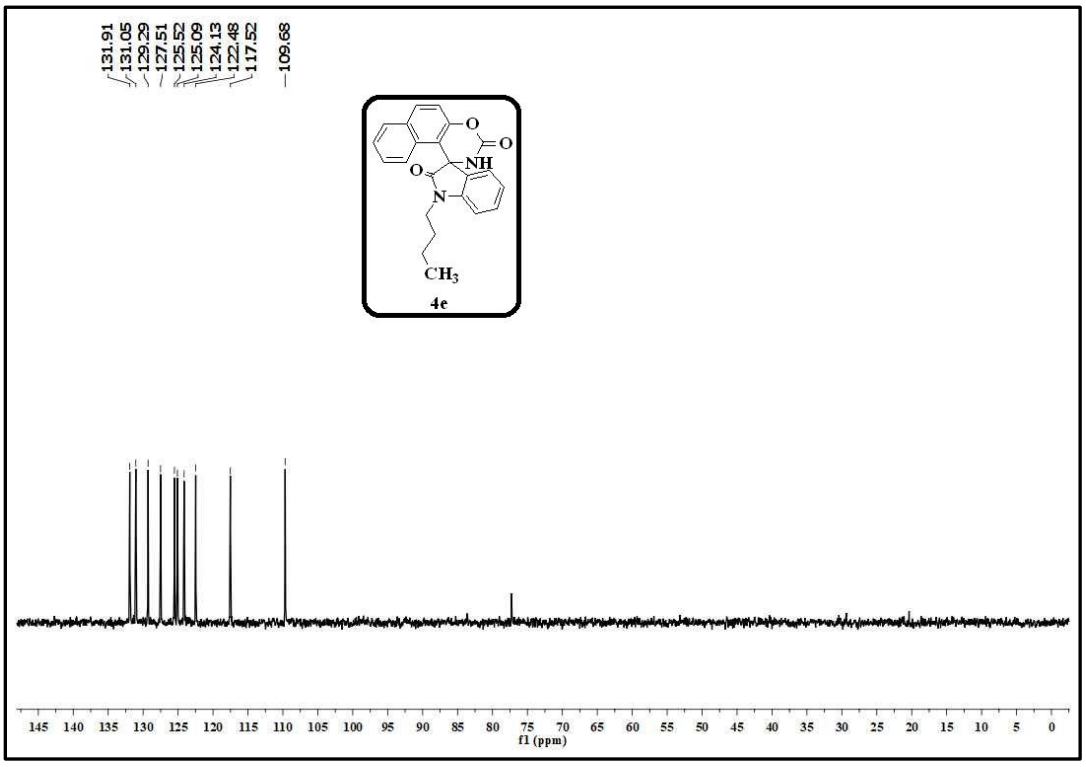

DEPT-90 spectrum of the compound **4e**

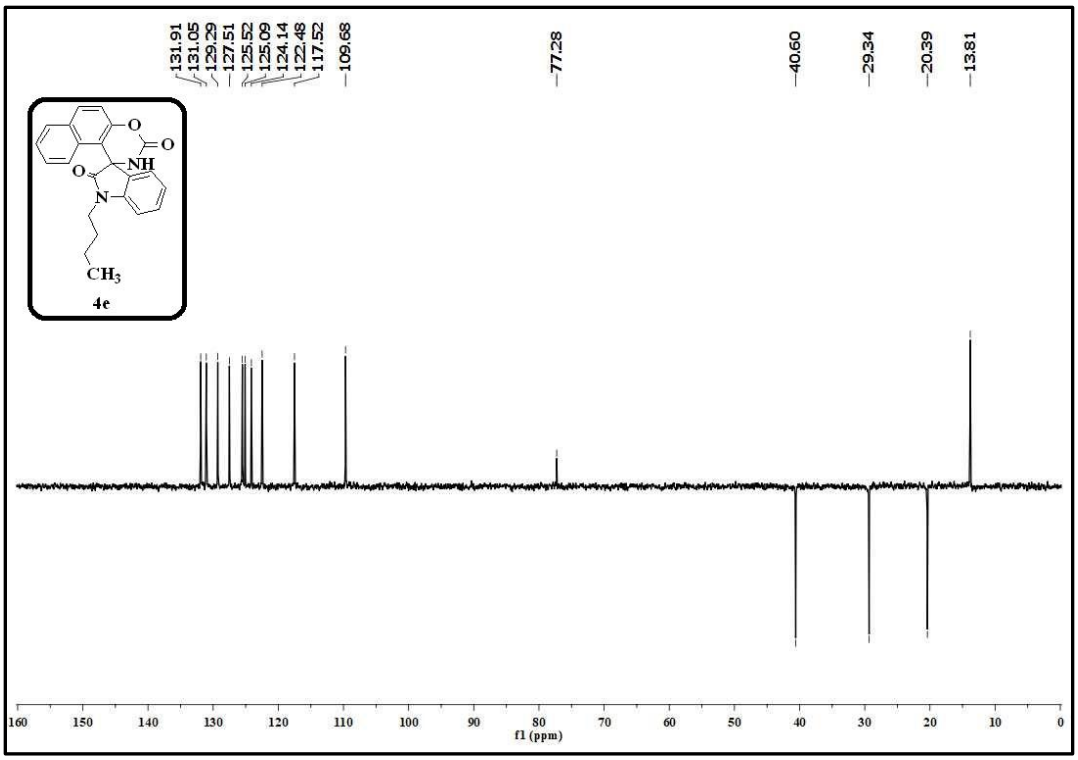

DEPT-135 spectrum of the compound **4e**

Experimental section

Materials and methods

All the melting points were recorded by using Stuart SMP30 melting point apparatus and were uncorrected. IR spectra were recorded on Perkin-Elmer 100S series FT-IR instrument. ^{1}H NMR and ^{13}C NMR spectra were recorded in DMSO-*d*6 and $CDCl_3$ using TMS as an internal standard on a Bruker Avance III HD 400 MHz instrument and the chemical shift values were reported in ppm. Mass spectra were recorded on Joel JMSD-300 spectrometer. Progress and purity of the reactions were monitored by Thin-Layer chromatography (E. Merck, Mumbai, India) and the developed chromatogram was visualized under UV light and iodine vapors. Column chromatography was performed on silica gel (100–120 mesh). Unless otherwise stated, all the chemicals and solvents used were of high grade and purchased from Sigma-Aldrich and spectrochem. Elemental analysis was performed on an Elementar Vario EL III analytical unit and the values were ± 0.4% of theoretical values.

Crystal structure determination of compounds 4a and 4e

The single crystal X-ray data of the compounds were collected on a Bruker Kappa APEX-II CCD DUO X-Ray diffractometer at 296(2)K using graphite-monochromated Mo K_α radiation (λ = 0.71073 Å). No absorption correction was carried out. The unit cell dimensions are determined by least-squares analysis and the reflection data is integrated using the SHELXTL program [61]. The crystal structures are solved by direct methods using SHELXS-97, and refinement is carried out by full-matrix least-squares technique (F^2) using SHELXL-97 [62]. Anisotropic displacement parameters are included for other than H-atoms. The N−H hydrogen atoms were located from difference Fourier maps. All the aromatic and aliphatic C−H hydrogens are positioned geometrically and treated as riding on their parent C-atoms with C−H distances of 0.93-0.97 Å. The software Mercury 2.3 (Build RC4), ORTEP-3 and X-Seed are used to prepare material for publication [63].

Biological evaluation

Antibacterial and antifungal activity

The antibacterial and antifungal activity of the target molecules spirooxindolocarbamates were carried out against different bacterial strains by using well diffusion method [64]. The bacterial strains were procured from the Microbial Type Culture Collection and Gene Bank (MTCC), CSIR-Institute of Microbial Technology, Chandigarh, India. The microbial cultures were preserved at –20 °C in microcentrifuge tube having 40% sterile glycerol. The reference strains were seeded on the surface of the Petri plates, which contains the Muller-Hinton agar with 0.1 mL o previously prepared microbial suspensions individually containing 1.5×10^8 *cfu* mL^{-1} (equal to 0.5 McFarland standard). Wells of 6.0 mm diameter were prepared in the medium plates using a cork borer and the synthesized compounds dissolved in 10% DMSO at a dose range of 50–0.97 µg/mL were added in each well under sterile conditions in a laminar air flow chamber. Standard antibiotic solutions of Ciprofloxacin at a dose range of 50-0.97 µg $well^{-1}$, served as positive control, while the well containing DMSO served as negative control. The plates were incubated for antibacterial activity at 37 °C for 24h and for antifungal activity 24 °C at 48h. The well containing the least concentration showing the inhibition zone is considered as the minimum inhibitory

concentration (MIC). All the experiments were carried out in triplicates and mean values are represented.

Antioxidant activity

The free radical scavenging capacity of the synthesized compounds was determined by using DPPH (1,1-Diphenyl-2-picrylhydrazyl) free radical method described in the literature [65-67]. Ascorbic acid was used as a standard to measure the efficiencies of the synthesized compounds. 0.2 mM solution of DPPH was prepared in 100% methanol. The required amount of ascorbic acid was dissolved in 100% methanol to prepare 1 mM solution and the test compounds were dissolved in 0.2% DMSO and methanol to prepare 1 mM stock solutions. From the stock solutions, different concentrations (3, 10, 30 and 100 µM) of solutions were prepared by diluting with methanol. 1 mL of each compound solution was added to the 3 mL of DPPH solution. After 30min, the absorbance of the solutions at 517 nm (A_1) was recorded using UV–Visible spectrophotometer. As a control, the absorbance of the blank solution of DPPH without test compound was also determined at 517 nm (A_0). The following equation was used for the calculation of the percentage (%) of scavenging activity.

Scavenging Activity (%) = $\frac{A_0 - A_1}{A_0} \times 100$

Where A_0 is the absorbance of DPPH in the absence of antioxidant and A_1 is the absorbance of DPPH in the presence of an antioxidant. IC_{50} values were also calculated for the compounds.

Molecular Docking protocol

Docking methods are useful tools to estimate the binding affinity of the ligand-protein receptor computationally. The synthesized compounds were subjected to molecular docking by using the AutoDock Tools (ADT) version 1.5.6 and AutoDock version 4.2.5.1 docking program [68]. The 3D-structures of all the synthesized compounds were prepared by using chem3D pro 12.0 software. The energy minimization of these 3D structures was carried out by using Discovery Studio Visualizer version 4.0 and saved in .pdb format. The structure of the bacterial DNA gyrase enzyme (PDB ID: 1KZN) was extracted from the protein data bank (http://www.rcsb.org/pdb). Then the protein was prepared by removing the bound ligand and water molecules by using Discovery Studio Visualizer version 4.0. Nonpolar hydrogens were

merged and gasteiger charges were added to the protein. The grid file was saved in .gpf format. A genetic algorithm was carried out with the population size and the maximum number of evaluations were 150 and 25,00,000 respectively. The docking output file was saved as Lamarckian Ga (4.2) in .dpf format. The binding sites of the ligand-protein receptor complex were visualized by Discovery Studio Visualizer version 4.0.

References

1) R. Rios, *Chem. Soc. Rev.* **2012**, *41*, 1060.
2) P. Saraswata, G. Jeyabalana, Md. Z. Hassana, M. U. Rahmana, N. K. Nyolaa, *Syn. Commun.* **2016**, *46*, 1643.
3) P. Yuvaraj, B. S. R. Reddy, *Tetrahedron Lett.* **2014**, *565*, 806.
4) A. Dandia, S. Khan, P. Soni, A. Indora, D. K. Mahawar, P. Pandya, C. S. Chauhan, *Bioorg. Med. Chem. Lett.* **2017**, *27*, 2873.
5) S. Pal, Md. N. Khan, S. Karamthulla, L. H. Choudhury, *Tetrahedron Lett*. **2015**, *56*, 359.
6) Y. Arun, G. Bhaskar, C. Balachandran, S. Ignacimuthu, P. T. Perumal, *Bioorg. Med. Chem. Lett.* **2013**, *23*, 1839.
7) P. K. Warghude, P. D. Dharpure, R. G. Bhat, *Tetrahedron Lett.* **2018**, *59*, 4076.
8) S. M. Rajesh, S. Perumal, J. C. Menendez, P. Yogeeswari, D. Sriram, *Med. Chem. Comm.* **2011**, *2*, 626.
9) E. Chandralekha, A. Thangamani, R. Valliappan, *Res. Chem. Intermed*. **2013**, *39*, 961.
10) G. Chen, J. Yang, S. Gao, Y. Zhang, X. Hao, *Res. Chem. Intermed*. **2015**, *41*, 4987.
11) B. Testa, J. M. Mayer, *Hydrolysis in Drug and Prodrug Metabolism-Chemistry, Biochemistry, and Enzymology*; Wiley-VCH: Weinheim, Germany, **2003**.
12) A. Dibenedetto, M. Aresta, C. Fragale, M. Narracci, *Green Chem*. **2002**, *4*, 439.
13) S. P. Gupte, A. B. Shivarkar, P. V. Chaudhari, *Chem. Commun*. **2001**, *24*, 2620.
14) L. L. Martin, L. Davis, J. T. Klein, P. Nemoto, G. E. Olsen, G. M. Bores, F. Camacho, W. W. Petko, D. K. Rush, D. Selk, C. P. Smith, H. M. Vargas, J. T. Winslow, R. C. effland, D. M. Fink, *Bioorg. Med. Chem. Lett*. **1997**, *7*, 157.
15) J. Vagner, H. Qu, V. J. Hruby, *Curr. Opin. Chem. Biol*. **2008**, *12*, 292.

16) J. S. Nowick, *Org. Biomol. Chem*. **2006**, *4*, 3869.

17) R. M. Liskamp, D. T. Rijkers, J. A. Kruijtzer, J. Kemmink, *Chem. Bio. Chem*. **2011**, *12*, 1626.

18) C. Y. Cho, E. J. Moran, S. R. Cherry, J. C. Stephans, S. P. Fodor, C. L. Adama, A. Sumdaram, J. W. Jacobs, P. G. Schultz, *Science.* **1993**, *261*, 1303.

19) A. K. Ghosh, M. Brindisi, *J. Med. Chem.* **2015**, *58*, 2895.

20) S. A. Mousa, W. F. DeGrado, D. X. Mu, R. P. Kapil, B. R. Lucchesi, T. M. Reilly, *Circulation.* **1996**, *93*, 537.

21) C. B. Xue, J. Wityak, T. M. Sielecki, et al. *J. Med. Chem*. **1997**, *40*, 2064.

22) A. Saito, T. Yamashita, Y. Mariko, Y. Nosaka, K. Tsuchiya, T. Ando, T. Suzuki, T. Tsuruo, O. Nakanishi, *Proc. Natl. Acad. Sci. U.S.A.* **1999**, *96*, 4592.

23) B. R. Williams, A. Nazarians, M. A. Gill, *Clin. Ther*. **2003**, *25*, 1634.

24) M. Emre, D. Aarsland, A. Albanese, E. J. Byrne, G. Deuschl, P. P. De Deyn, F. Durif, J. Kulisevsky, T. Van Laar, A. Lees, W. Poewe, A. Robillard, M. M. Rosa, E. Wolters, P. Quarg, S. Tekin, R. Lane, *N. Engl. J. Med*. **2004**, *351*, 2509.

25) B. M. Best, M. Goicoechea, *Expert Opin. Drug. Metab. Toxicol*. **2008**, *4*, 965.

26) J. S. Madero, A. V. Keever, P. Mendez, J. L. M. Gomez, I. T. Escobar, F. G. Escolano, I. J. Kasusky, M. M. Aquino, C. R. Santos, L. P. Saleme, S. R. Frausto, B. A. Puente, L. E. S. Ramirez, V. Lima, F. B. Zamudio, B. C. Ramirez, J. Montaner, *J. Acquired Immune Defic. Syndr*. **2010**, *53*, 582.

27) W. Phipatanakul, P. A. Eggleston, C. M. K. Walker, J. Kesavanathan, D. Sweitzer, R. A. Wood, *J. Allergy Clin. Immunol*. **2000**, *105*, 704.

28) P. J. Luder, B. Siffert, F. Witassek, F. Meister, J. Bircher, *Eur. J. Clin. Pharmacol*., **1986**, *31*, 443.

29) A. K. Ghosh, R. P. Sridhar, N. Kumaragurubaran, Y. Koh, I. T. Weber, H. Mitsuya, *Chem. Med. Chem.* **2006**, *1*, 939.

30) A. K. Ghosh, D. D. Anderson, I. T. Weber, H. Mitsuya, *Angew. Chem. Int. Ed.* **2012**, *51*, 1778.

31) J. U. Peters, G. Galley, H. Jacobsen, C. Czech, D. P. Pierson, E. A. Kitas, L. Ozmen, *Bioorg. Med. Chem. Lett.* **2007**, *17*, 5918.

32) E. F. V. Scriven, K. Turnbull, *Chem. Rev*. **1988**, *88*, 297.

33) M. Yoshida, N. Hara, S. Okuyama, *Chem. Commun*. **2000**, *2*, 151.

34) R. N. Salvatore, F. X. Chu, A. S. Nagle, E. A. Kapxhiu, R. M. Cross, K. W. Jung, *Tetrahedron*. **2002**, *58*, 3329.

35) R. N. Salvatore, J. A. Ledger, K. W. Jung, *Tetrahedron Lett.* **2001**, *42*, 6023.

36) P. Gogoi, D. Konwar, *Tetrahedron Lett*. **2007**, *48*, 531.

37) S. Cenini, C. Crotti, M. Pizzotti, F. Porta, *J. Org. Chem*. **1988**, *53*, 1243.

38) (a) B. L. Gadilohar, H. S. Kumbhar, G. S. Shankarling, *New J. Chem*. **2015**, *39*, 4647; (b) J. Mou, G. Gao, C. Chen, J. Liu, J. Gao, Y. Liu, D. Pei, *RSC Adv*. **2017**, *7*, 13868.

39) H. Gao, J. Sun, C. G. Yan, *Chin*. *Chem*. *Lett*. **2015**, *26*, 353.

40) M. Kidwai, R. Chauhan, *Asian J. Org. Chem*. **2013**, *2*, 395.

41) C. P. Leslie, J. Bentley, M. Biagetti, S. Contini, R. D. Fabio, D. Donati, T. Genski, S. Guery, A. Mazzali, G. Merlo, D. A. Pizzi, F. Sacco, C. Seri, M. Tessari, L. Zonzini, L. Caberlotto, *Bioorg. Med. Chem. Lett.* **2010**, *20*, 6103.

42) G. B. Djigoué, L. C. Kenmogne, J. Roy, R. Maltais, D. Poirier, *Bioorg. Med. Chem.* **2015**, *23*, 5433.

43) A. Galán, L. Moreno, J. Párraga, Á. Serrano, M. J. Sanz, D. Cortes, N. Cabedo, *Bioorg. Med. Chem.* **2013**, *21*, 3221.

44) M. Krátky, J. Vinšová, *Bioorg. Med. Chem*. **2016**, *24*, 1322.

45) M. Kratky, M. Volkova, E. Novotna, F. Trejtnar, J. Stolarikova, J. Vinšova, *Bioorg. Med. Chem.* **2014**, *22*, 4073.

46) Z. Baranyai, M. Kratký, J. Vinsova, N. Szabo, Z. Senoner, K. Horvati, J. Stolaríkova, S. David, S. Bosze, *Eur. J. Med. Chem.* **2015**, *101*, 692.

47) T. Gonec, S. Pospisilova, L. Holanova, J. Stranik, A. Cernikova, V. Pudelkova, J. Kos, M. Oravec, P. Kollar, A. Cizek, J. Jampilek, *Molecules.* **2016**, *21*, 1189.

48) B. H. Shupe, E. E. Allen, J. P. MacDonald, S. O. Wilson, A. K. Franz, *Org. Lett*. **2013**, *15*, 3218.

49) A. Padwa, T. Stengel, *Org. Lett.* **2002**, *4*, 2137.

50) A. Kumar, A. Saxena, M. Dewan, A. De, S. Mozumdar, *Tetrahedron Lett.* **2011**, *52*, 4835.

51) A. Gupta, D. Kour, V. K. Gupta, K. K. Kapoor, *Tetrahedron Lett.* **2016**, *57*, 4869.

52) G. B. D. Rao, M. P. Kaushik, A. K. Halve, *Tetrahedron Lett.* **2012**, *53*, 2741.

53) N. Basavegowda, K. B. S. Magar, K. Mishra, Y. R. Lee, *New J. Chem.* **2014**, *38*, 5415.

54) A. Z. Halimehjani, M. Khoshdoun, *J. Org. Chem.* **2016**, *81*, 5699.

55) M. Lei, L. Ma, L. Hu, *Synth. Commun.* **2011**, *41*: 3424.

56) (a) B. L. Gadilohar, H. S. Kumbhar and G. S. Shankarling, *New J. Chem.* **2015**, *39*, 4647; (b) J. Mou, G. Gao, C. Chen, J. Liu, J. Gao, Y. Liu and D. Pei, *RSC Adv*. **2017**, *7*, 13868.

57) H. Gao, J. Sun, C. G. Yan, *Chin*. *Chem*. *Lett*. **2015**, *26*, 353.

58) M. Kidwai, R. Chauhan, *Asian J. Org. Chem*. **2013**, *2*, 395.

59) (a) G. S. Singh, Z. Y. Desta, *Chem*. *Rev*. **2012**, *112*, 6104; (b) M. B. Teimouri, F. Zolfaghari, S. Naderi, *Tetrahedron*. **2017**, *73*, 262.

60) (a) D. Lafitte, V. Lamour, P. O. Tsvetkov, A. A. Makarov, M. Klich, P. Deprez, D. Moras, C. Briand, R. Gilli, *Biochemistry.* **2002**, *41*, 7217; (b) D. B. Janakiramudu, D. S. Rao, C. Srikanth, S. Madhusudhana, P. S. Murthy, M. Nagalakshmidevamma, P. V. Chalapathi, C. N. Raju, *Res. Chem. Intermed*. **2018**, *44*, 469.

61) SHELXTL. *Program for the Solution and Refinement of Crystal Structures*, (version 6.14); Bruker AXS Wisconsin USA, **2000**.

62) G. M. Sheldrick, SHELX-97: *Program for the Solution and refinement of Crystal Structures*, University of Göttingen, Germany, **1997**.

63) (a) C. F. Macrae, I. J. Bruno, J. A. Chisholm,P. R. Edgington, P. McCabe, E. Pidcock, L. R. Monge, R. Taylo, J. V. D. Streek , P. A. Wood, *J. Appl. Cryst.* **2008**, *41*, 466; (b) M. N. Burnett, C. K. Johnson, ORTEPIII, Report ORNL-6895, Oak Ridge National Laboratory, Tennessee, USA. **1996**; (c) L. J. Farrugia, *J. Appl. Cryst*. **1997**, *30*, 565. (d) L. J. Barbour, *J. Supramol. Chem.* **2001**, *1*, 189.

64) D. Amsterdam, Susceptibility Testing of Antimicrobials in Liquid Media. In Antibiotics in Laboratory Medicine; Loman, V., Ed., 4th ed.; Williams and Wilkins: Baltimore, MD, **1996**, 52.

65) A. Braca, N. D. Tommasi, L. D. Bari, C. Pizza, M. Politi, I. Morelli, *J. Nat. Prod.* **2001**, *64*, 892.

66) M. R. Saha, S. M. R. Hasan, R. Akter, M. M. Hossain, M. S. Alamb, M. A. Alam, M. E. H. Mazumder, *Bangl. J. Vet. Med.* **2008**, *6*, 197.

67) M. S. Blois, *Nature*. **1958**, *181*, 1199.

68) http://autodock.scripps.edu/resources/references.

CHAPTER-VI (SECTION-A)

Deep eutectic solvent $ZnCl_2$+Urea promoted synthesis of spirooxindoles

6A.1. Introduction

For the past few decades, several green protocols are designed and developed to minimize environmental pollution. In this regard, deep eutectic solvents (DESs) and Multicomponent reactions (MCRs) play a vital role [1-3]. DESs are treated as ionic liquid analogs because they are using as promising renewable green media [1, 2]. The rational selection of the hydrogen bond donor and the acceptor in proper proportions produce the new eutectic phase characterized by a melting point i.e., below 100 °C [4, 5]. Along with hydrogen bond interactions the electrostatic forces and Van Der Waals interactions are also sometimes formed [5]. The important features of the DESs are low transition temperature, low volatility, nonflammability, nontoxicity, water compatibility, etc. In general, the mixture of metal halides and urea is able to form DES by decreasing the lattice energy and consequently the freezing point of the system [6].

Spiro compounds are important core structures in several pharmacophoric moieties. Especially, spirooxindoles exhibit remarkable biological activities like anticancer [7], antimicrobial, antimycobacterial etc [8]. Xanthenes and 4*H*-pyrans were also had a broad range of biological activities [9, 10].

Ashok and coworkers reported a simple, efficient and eco-friendly synthetic protocol for the synthesis of the pyranoxanthenes *via* one-pot three-component reaction under microwave irradiation. All the target compounds were evaluated for their antimicrobial, antioxidant and molecular docking studies (Figure 6A.1) [11].

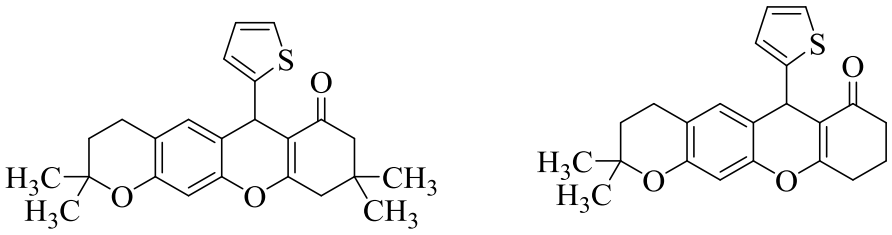

Figure 6A.1

Parthasarathy et al. have reported the microwave assisted synthesis of spirooxindoles *via* tandem double condensation of spirooxindoles in the presence of a gold catalyst (NaAuCl4.2H2O). The target compounds were evaluated for their in vitro antibacterial,

antifungal and cytotoxic activity. The cytotoxic studies were well supported by the molecular docking studies (Figure 6A.2) [12].

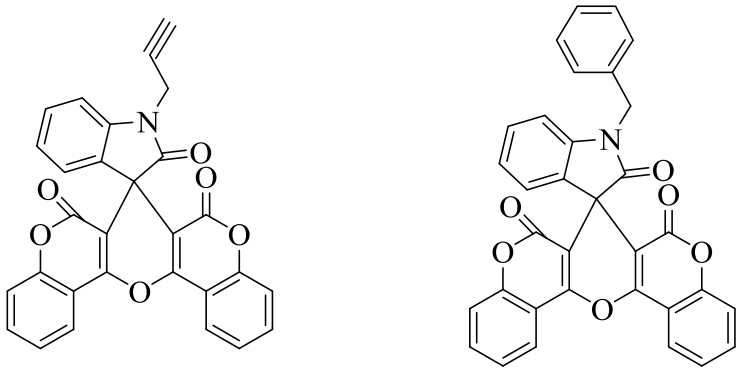

Figure 6A.2

Yousefi et al. described an improved, forthright and highly efficient one-pot synthesis of a wide range of pharmaceutically exciting diverse kind of functionalized 2-amino-3-cyano-4*H*-pyrans by using piperazine as a catalyst in an aqueous medium. Antibacterial activity was evaluated for selected compounds (Figure 6A.3) [13].

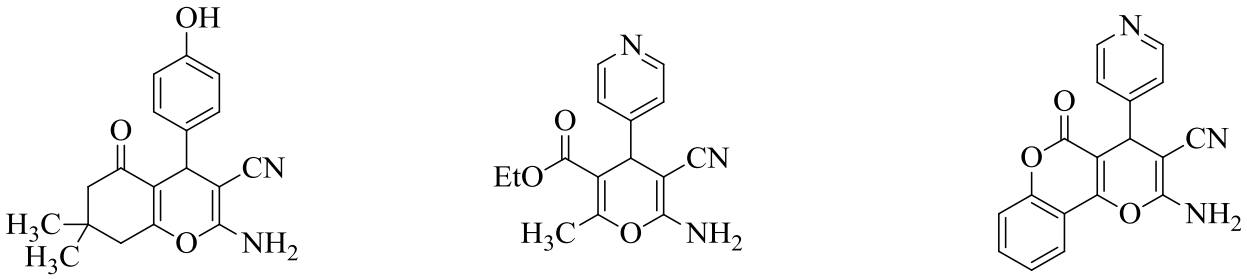

Figure 6A.3

6A.1.1. Various methodologies for the synthesis of spirooxindolopyrans and xanthenes

Shen and coworkers reported a simple and efficient method for the synthesis of spiro[indoline-3,9'-xanthene]trione derivatives (Scheme 6A.1). The reaction was promoted by the catalytic amount of magnesium perchlorate, $Mg(ClO_4)_2$ [9]. **Ghasemzadeh et al**. described the synthesis of spiro[indoline-3,9'-xanthene]trione derivatives in aqueous media by using a magnetic recyclable nano catalyst γ-Fe_2O_3@SiO_2-EC-Zn^{II} i.e., Zn^{II} immobilized on creatinated epibromohydrin functionalized γ-Fe_2O_3@SiO_2 nano particles (Scheme 6A.1)

[13]. **Chandam and coworkers** described a simple, proficient and an elegant synthetic route for the synthesis of spiroxanthene derivatives by using Low melting oxalic acid dihydrate: proline mixture (LTTM) as dual solvent/catalyst under the umbrella of green chemistry (Scheme 6A.1) [14]. **Niknam et al**. reported an eco-friendly method for the synthesis of hydroxyspiro[indoline-3,9'-xanthene]triones as new spiro[indoline-3,9'-xanthene]trione derivatives *via* pseudo three component condensation reaction in the presence of silica-bonded *n*-propyl triethylenetetramine sulfamic acid in refluxing ethanol (Scheme 6A.1) [15].

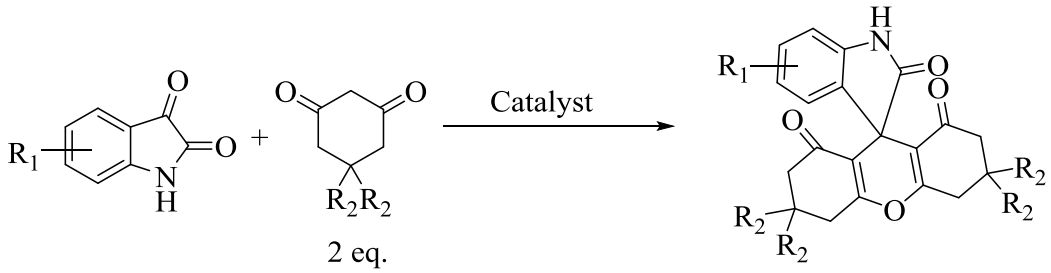

Scheme 6A.1

Rong and coworkers described a facile and efficient three-component procedure for the synthesis of substituted spiro[indoline-3,7'-pyrano[3,2-*c*:5,6-*c*']dichromene]-2,6',8'-trione derivatives by using Iodine (I_2) as catalyst (Scheme 6A.2) [16].

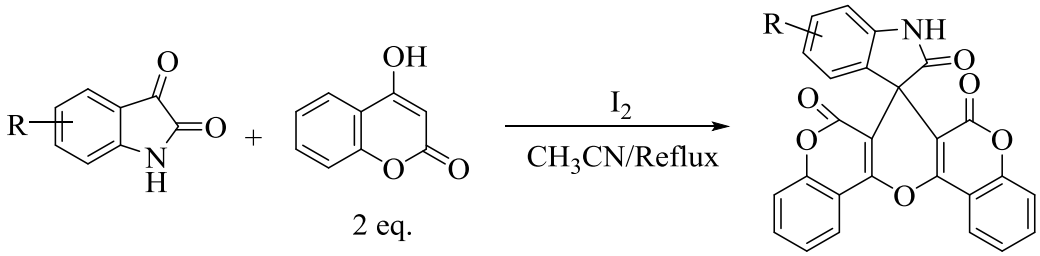

Scheme 6A.2

Salek et al. reported the convenient synthesis of spiropyran derivatives by using sulfonic acid functionalized 1,4-diazabicyclo[2.2.2]octane (DABCO)-based magnetic nano particle Fe_3O_4 $[Fe_3O_4@SiO_2@Pr\text{-}DABCO\text{-}SO_3H]Cl_2$ as catalyst (Scheme 6A.3) [17]. **Joshi et al**. described a simple, clean and efficient method for the synthesis of spirooxindole derivatives in water at 100 °C by using cerium ammonium nitrate (CAN) as catalyst (Scheme 6A.3) [18].

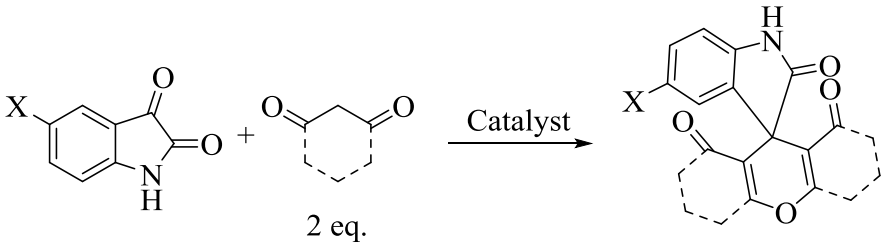

Scheme 6A.3

6A.2. Present work

Because of their broad spectrum of biological activities of these compounds, the synthesis of spirooxindolopyrans and xanthenes are still of interest. The synthesis of spirooxindolo pyrans and xanthenes in presence of DES was less investigated. Herein, we report the efficient synthesis of spirooxindolo pyrans and xanthenes *via* pseudo three-component reaction by using $ZnCl_2$+Urea as a deep eutectic solvent.

6A.2.1. General procedure for the synthesis of spirooxindolopyrans and xanthenes 6a-c, 7a-c, 8a-c and 9a-c

A mixture of isatin derivatives **1a-c** (1 mmol) and pyrimidine-2,4,6(1*H*,3*H*,5*H*)-trione **2**/4-hydroxy-2*H*-chromen-2-one **3**/1*H*-indene-1,3(2*H*)-dione **4**/5,5-dimethylcyclohexane-1,3-dione **5** (2 mmol) in $ZnCl_2$+Urea at 80 ºC produce the target compounds **6a-c, 7a-c, 8a-c** and **9a-c**. The progress of all the reactions was monitored by TLC. The reaction mixture was poured into ice cold water. The obtained precipitate was filtered and washed twice with ice cold water and dried. The pure products were obtained by washing the obtained precipitates with ethyl acetate (Scheme 6A.8).

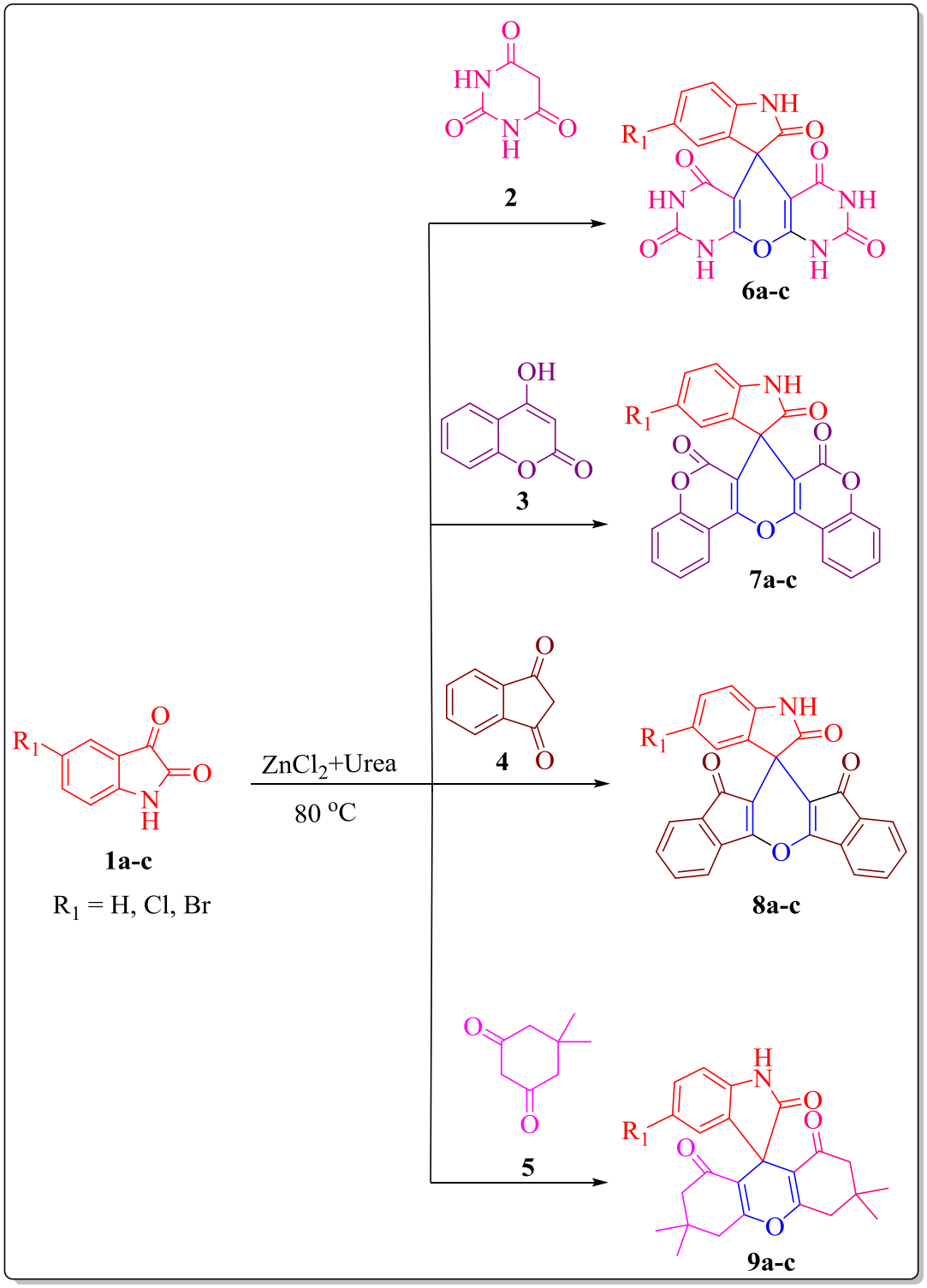

Scheme 6A.8

6A.2.2. The plausible mechanism for the synthesis of spirooxindolopyrans (6a-c, 7a-c and 8a-c) and xanthenes (9a-c)

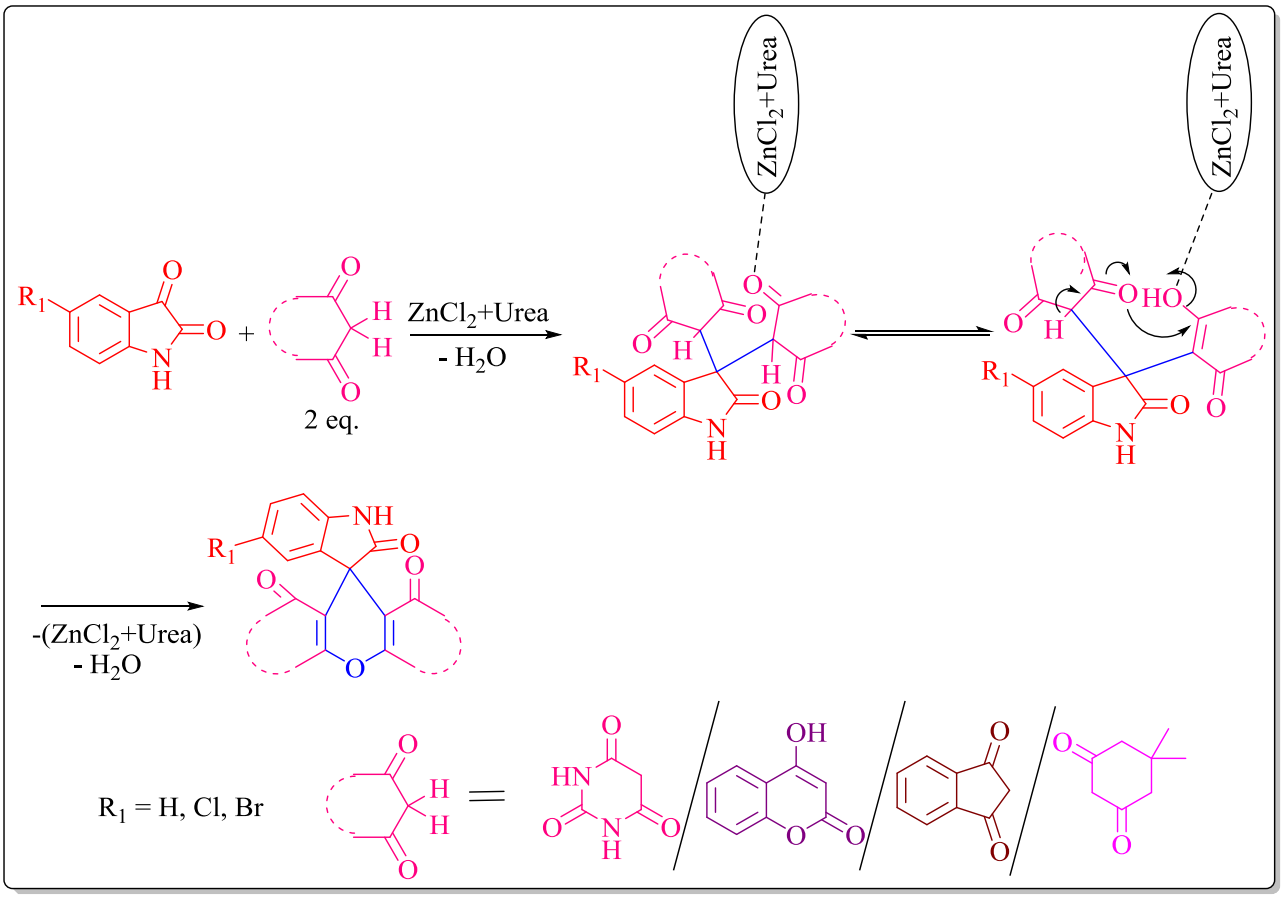

Scheme6A.9

6A.3. Results and discussion

Initially, a model reaction was carried out by choosing isatin **1a** (1 mmol) and 5,5-dimethylcyclohexane-1,3-dione **5** (2 mmol) to optimize the reaction condition in different solvents like water, ethylene glycol and $ZnCl_2$+Urea. From the results, it was observed that the deep eutectic solvent $ZnCl_2$+Urea is the opted solvent for the synthesis of the target compound **9a**. Then the model reaction was screened at different temperatures in the solvent $ZnCl_2$+Urea. The optimized reaction conditions were shown in table 1.

Table 1. Optimized reaction conditions[a].

S. No.	Solvent	Temperature (°C)	Time (min)	Yield (%)[b]
1	Water	100	120	22
2	Ethylene glycol	100	120	48
3	$ZnCl_2$+Urea	80	30	86
4	$ZnCl_2$+Urea	70	50	80
5	$ZnCl_2$+Urea	90	30	86

[a]All the reactions were carried out by using isatin **1a** (1 mmol) and dimethylcyclohexane-1,3-dione **5** (2 mmol) as starting materials. [b]Isolated yield.

In order to extend this approach the target compounds, i.e., spirooxindolopyrans (**6a-c**, **7a-c** and **8a-c**) and xanthenes (**9a-c**) were prepared by employing the above optimized reaction condition (Scheme 6A.8). The target compounds were obtained in 28-50min with 82-95% of yields. The time and yields of the reaction were shown in table 2. The progress of all the reactions was monitored by TLC. After completion of the reaction, the reaction mixture was poured in ice cold water. The obtained precipitate was filtered and washed twice with ice-cold water and dried. The pure products were obtained by washing the obtained precipitate with ethyl acetate. The plausible reaction mechanism was shown in scheme 6A.9.

Table 2. Times and Yields of the target compounds[a,b,c].

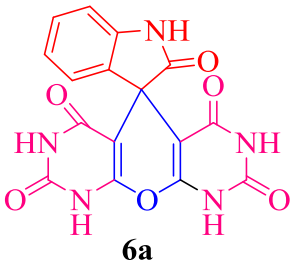 **6a**	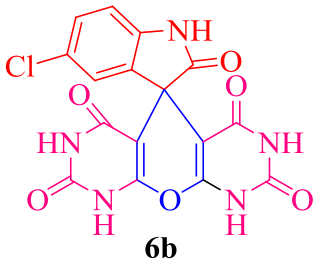 **6b**	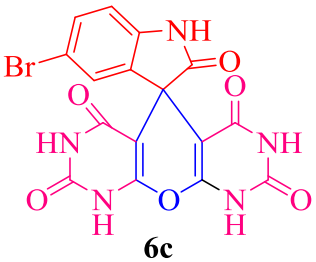 **6c**
(35min / 92%)	(48min / 86%)	(50min / 82%)

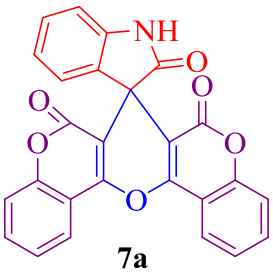

7a

(38min / 93%)

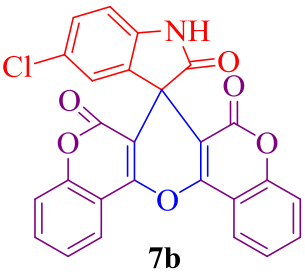

7b

(38min / 87%)

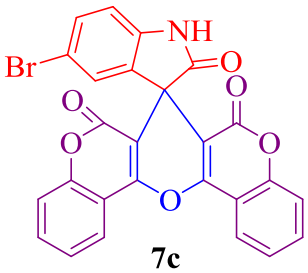

7c

(45min / 85%)

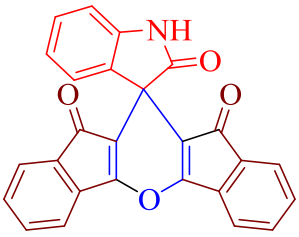

8a

(28min / 95%)

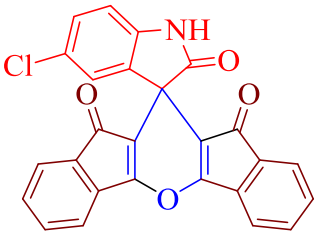

8b

(35min / 90%)

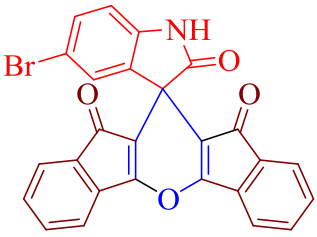

8c

(40min / 88%)

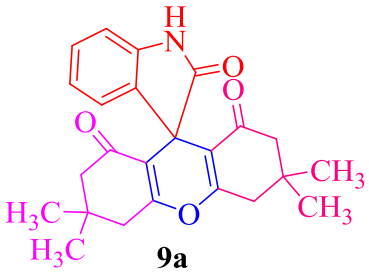

9a

(30min / 86%)

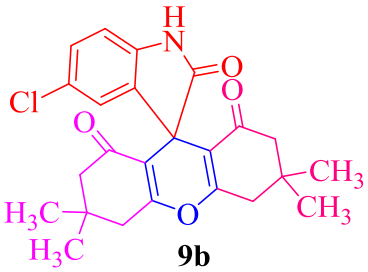

9b

(37min / 89%)

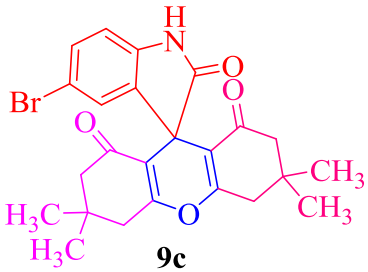

9c

(35min / 85%)

[a]All the reactions were carried out by using isatin **1a** (1 mmol) and pyrimidine-2,4,6(1*H*,3*H*,5*H*)-trione **2**/4-hydroxy-2*H*-chromen-2-one **3**/1*H*-indene-1,3(2*H*)-dione **4**/5,5-dimethylcyclohexane-1,3-dione **5** (2 mmol) as starting materials. [b]The progress of all the reactions was monitored by TLC. [c]Isolated yield.

The structures of all the target compounds were characterized by ^{1}H NMR and ^{13}C NMR spectroscopy. For instance, the ^{1}H NMR of the compound **9a** shows a peak at δ 10.33 (s, 1H) correspond to the –NH proton of oxindole ring. The peaks at δ 2.67-2.03 (m, 8H) correspond to the eight –CH_2 protons and peaks at δ 1.04 (s, 6H), 0.95 (s, 6H) correspond to the twelve –CH_3 protons. In ^{13}C NMR spectrum, the peaks at δ 195.75 and 179.07 correspond to the carbonyl groups of xanthene rings and oxindole ring respectively. The peak at δ 50.44 corresponds to the spiro carbon atom.

6A.4. Conclusion

The spirooxindolopyrans and xanthenes were synthesized using the deep eutectic solvent $ZnCl_2$+Urea efficiently *via* pseudo three-component approach. The advantages of this method are the usage of green solvent (DES), mild reaction conditions, lower reaction times and higher yields.

6A.5. Spectral data

Spiro[indoline-3,5'-pyrano[2,3-*d*:6,5-*d*']dipyrimidine]-2,2',4',6',8'(1'*H*,3'*H*,7'*H*,9'*H*)-pentaone (6a)

Colour: White. M. P. >300 ℃. ^{1}H NMR (400 MHz, DMSO-*d*6) δ: 11.20 (s, 4H), 10.58 (s, 1H), 7.48 (d, 1H, *J* = 8.0 Hz), 6.90 (t, 2H, *J* = 7.6 Hz), 6.68 (d, 1H, *J* = 7.6 Hz). ^{13}C NMR (100 MHz, DMSO-*d6*) δ: 175.82, 167.40, 150.22, 142.81, 129.13, 127.64, 124.07, 121.78, 109.80, 50.57 Anal. Calcd. For $C_{16}H_9N_5O_6$: C, 52.32; H, 2.47; N, 19.07; found: C, 52.50; H, 2.52; N, 19.29.

5-Chlorospiro[indoline-3,5'-pyrano[2,3-*d*:6,5-*d*']dipyrimidine]-2,2',4',6',8'(1'*H*,3'*H*,7'*H*,9'*H*)-pentaone (6b)

Colour: White. M. P. >300 ℃. ^{1}H NMR (400 MHz, DMSO-*d*6) δ: 11.21 (s, 4H), 10.59 (s, 1H), 7.23 (s, 1H), 6.91 (t, 2H, *J* = 7.6 Hz), 6.70 (d, 1H, *J* = 7.6 Hz). ^{13}C NMR (100 MHz, DMSO-*d6*) δ: 178.48, 163.75, 161.47, 153.17, 149.16, 143.25, 133.31, 128.09, 122.72, 121.38, 112.69, 108.88, 50.27 Anal. Calcd. For $C_{16}H_8ClN_5O_6$: C, 47.84; H, 2.01; N, 17.43; found: C, 47.57; H, 2.09; N, 17.67.

5-Bromospiro[indoline-3,5'-pyrano[2,3-*d*:6,5-*d*']dipyrimidine]-2,2',4',6',8'(1'*H*,3'*H*,7'*H*,9'*H*)-pentaone (6c)

Colour: White. M. P. >300 ℃. ^{1}H NMR (400 MHz, DMSO-*d*6) δ: 11.42 (s, 4H), 10.81 (s, 1H), 7.45 (s, 1H), 7.13 (t, 2H, *J* = 7.6 Hz), 6.92 (d, 1H, *J* = 7.6 Hz). ^{13}C NMR (100 MHz, DMSO-*d6*) δ: 178.54, 163.80, 161.42, 153.27, 149.13, 143.26, 133.33, 127.99, 122.78, 121.42, 112.71, 53.50 Anal. Calcd. For $C_{16}H_8BrN_5O_6$: C, 43.07; H, 1.81; N, 15.70; found: C, 43.32; H, 1.89; N, 15.67.

Spiro[indoline-3,7'-pyrano[3,2-*c*:5,6-*c*']dichromene]-2,6',8'-trione (7a)

Colour: White. M. P. 178-180 ℃. ^{1}H NMR (400 MHz, DMSO-*d*6) *δ*: 10.70 (s, 1H), 8.00 (d, 1H, *J* = 10.4 Hz), 7.79 (t, 1H, *J* = 11.2 Hz), 7.55 (t, 2H, *J* = 10.4 Hz), 7.47 (d, 1H, *J* = 11.2 Hz), 7.25-7.17 (m, 4H), 6.98-1.88 (m, 3H). ^{13}C NMR (100 MHz, DMSO-*d6*) *δ*: 177.47, 161.36, 158.02, 153.05, 151.67, 149.11, 133.96, 132.15, 128.78, 125.16, 123.59, 121.73, 116.41, 111.92, 109.10, 103.35, 45.80. Anal. Calcd. For $C_{30}H_{24}ClN_3O_2$: C, 71.72; H, 3.01; N, 3.22; found: C, 71.58; H, 2.98; N, 3.45.

5-Chlorospiro[indoline-3,7'-pyrano[3,2-*c*:5,6-*c*']dichromene]-2,6',8'-trione (7b)

Colour: White. M. P. 164-166 ℃. ^{1}H NMR (400 MHz, DMSO-*d*6) *δ*: 10.43 (s, 1H), 8.07 (d, 2H, *J* = 8.0 Hz), 7.92 (d, 1H, *J* = 8.4 Hz), 7.78 (t, 1H, *J* = 7.2 Hz), 7.64 (t, 1H, *J* = 7.2 Hz), 7.41 (d, 2H, *J* = 8.0 Hz), 7.23-7.19 (m, 2H), 7.12 (d, 1H, *J* = 8.0 Hz), 6.58 (d, 1H, *J* = 8.4 Hz). ^{13}C NMR (100 MHz, DMSO-*d6*) *δ*: 177.96, 161.51, 157.92, 153.35, 151.97, 149.08, 134.06, 132.12, 128.59, 124.96, 123.73, 121.93, 116.47, 112.02, 109.10, 103.28, 46.16. Anal. Calcd. For $C_{30}H_{24}ClN_3O_2$: C, 66.47; H, 2.57; N, 2.98; found: C, 66.66; H, 2.68; N, 2.79.

5-Bromospiro[indoline-3,7'-pyrano[3,2-*c*:5,6-*c*']dichromene]-2,6',8'-trione (7c)

Colour: White. M. P. 187-189 ℃. ^{1}H NMR (400 MHz, DMSO-*d*6) *δ*: 10.73 (s, 1H), 8.37 (d, 2H, *J* = 8.0 Hz), 8.22 (d, 1H, *J* = 8.4 Hz), 7.08 (t, 1H, *J* = 7.2 Hz), 7.93 (t, 1H, *J* = 7.2 Hz), 7.71 (d, 2H, *J* = 8.0 Hz), 7.54-7.39 (m, 2H), 7.42 (d, 1H, *J* = 8.0 Hz), 6.88 (d, 1H, *J* = 8.4 Hz). ^{13}C NMR (100 MHz, DMSO-*d6*) *δ*: 177.79, 161.53, 158.01, 153.15, 152.02, 147.98, 133.96, 132.52, 128.47, 125.02, 123.77, 122.05, 116.48, 111.92, 108.97, 103.48, 45.88. Anal. Calcd. For $C_{30}H_{24}ClN_3O_2$: C, 60.72; H, 2.35; N, 2.72; found: C, 60.95; H, 2.29; N, 2.97.

10*H*,12*H*-spiro[diindeno[1,2-*b*:2',1'-*e*]pyran-11,3'-indoline]-2',10,12-trione (8a)

Colour: White. M. P.239-241 ℃. ^{1}H NMR (400 MHz, DMSO-*d*6) *δ*: 10.48 (s, 1H), 7.96 (d, 1H, *J* = 10.8 Hz), 7.69 (t, 1H, *J* = 9.6 Hz), 7.44 (t, 2H, *J* = 10.0 Hz), 7.37-7.22 (m, 5H), 7.00-6.92 (m, 3H). ^{13}C NMR (100 MHz, DMSO-*d6*) *δ*: 176.00, 165.38, 159.90, 152.02, 142.45, 133.00, 130.53, 130.02, 124.46, 123.63, 123.16, 122.06, 116.04, 115.56, 109.97, 100.35,

45.80. Anal. Calcd. For $C_{26}H_{13}NO_4$: C, 77.41; H, 3.25; N, 3.47; found: C, 77.68; H, 3.20; N, 3.62.

5-Chloro-10*H*,12*H*-spiro[diindeno[1,2-b:2',1'-e]pyran-11,3'-indoline]-2',10,12-trione (8b)

Colour: White. M. P. 230-232 ℃. ^{1}H NMR (400 MHz, DMSO-*d*6) δ: 10.54 (s, 1H), 7.96 (d, 1H, J = 10.8 Hz), 7.69(t, 1H, J = 9.6 Hz), 7.44 (t, 1H, J = 10.0 Hz), 7.37-7.22 (m, 5H), 7.00-6.92 (m, 3H). ^{13}C NMR (100 MHz, DMSO-*d6*) δ: 176.32, 164.90, 160.02, 151.97, 142.45, 133.03, 130.46, 129.92, 124.66, 123.46, 122.04, 115.97, 115.35, 110.04, 100.46, 47.10. Anal. Calcd. For $C_{26}H_{12}ClNO_4$: C, 71.32; H, 2.76; N, 3.20; found: C, 71.58; H, 2.83; N, 3.51.

5-Bromo-10*H*,12*H*-spiro[diindeno[1,2-b:2',1'-*e*]pyran-11,3'-indoline]-2',10,12-trione (8c)

Colour: White. M. P. 224-226 ℃. ^{1}H NMR (400 MHz, DMSO-*d*6) δ: 10.43 (s, 1H), 8.33 (s, 1H), 8.07 (d, 1H, J = 8.0 Hz), 7.95 (d, 1H, J = 7.6 Hz), 7.79 (t, 1H, J = 8.4 Hz), 7.66 (t, 1H, J = 7.6 Hz), 7.47-7.39 (m, 4H), 7.25 (d, 1H, J = 8.4 Hz), 6.59 (d, 1H, J = 7.6 Hz). ^{13}C NMR (100 MHz, DMSO-*d6*) δ: 177.01, 165.45, 160.10, 152.05, 142.00, 133.53, 130.56, 130.04, 124.64, 123.43, 123.16, 121.97, 116.03, 115.36, 109.95, 100.38, 50.27. Anal. Calcd. For $C_{26}H_{12}BrNO_4$: C, 64.75; H, 2.51; N, 2.90; found: C, 64.95; H, 4.58; N, 2.79.

3',3',6',6'-Tetramethyl-3',4',6',7'-tetrahydrospiro[indoline-3,9'-xanthene]-1',2,8'(2'*H*,5'*H*)-trione (9a)

Colour: White. M. P. > 300 ℃. ^{1}H NMR (400 MHz, DMSO-*d*6) δ: 10.33 (s, 1H), 7.11 (bs, 1H), 6.86-6.79 (m, 3H), 2.66-2.50 (m, 4H), 2.23-2.01 (m, 4H), 1.04 (s, 6H), 0.95 (s, 6H). ^{13}C NMR (100 MHz, DMSO-*d6*) δ: 195.75, 179.07, 164.02, 143.26, 133.90, 127.89, 122.19, 121.16, 112.60, 108.76, 50.44, 45.25, 40.07, 31.48, 27.84, 26.39. Anal. Calcd. For $C_{24}H_{25}ClNO_4$: C, 73.64; H, 6.44; N, 3.58; found: C, 74.45; H, 6.50; N, 3.79.

5-Chloro-3',3',6',6'-tetramethyl-3',4',6',7'-tetrahydrospiro[indoline-3,9'-xanthene]-1',2,8'(2'*H*,5'*H*)-trione (9b)

Colour: White. M. P. >300 °C. ^{1}H NMR (400 MHz, DMSO-*d*6) δ: 10.52 (s, 1H), 7.40-7.19 (m, 3H), 2.67-2.51 (m, 4H), 2.30-2.03 (m, 4H), 1.52 (s, 6H), 0.96 (s, 6H). ^{13}C NMR (100 MHz, DMSO-*d6*) δ: 195.90, 178.97, 163.92, 143.16, 133.96, 127.75, 122.26, 121.19, 112.76, 108.75, 50.60, 45.20, 31.49, 27.89, 26.49. Anal. Calcd. For $C_{24}H_{24}ClNO_4$: C, 67.68; H, 5.68; N, 3.29; found: C, 67.94; H, 5.58; N, 3.01.

5-Bromo-3',3',6',6'-tetramethyl-3',4',6',7'-tetrahydrospiro[indoline-3,9'-xanthene]-1',2,8'(2'*H*,5'*H*)-trione (9c)

Colour: White. M. P. >300 °C. ^{1}H NMR (400 MHz, DMSO-*d*6) δ: 10.54 (s, 1H), 7.55-7.19 (m, 3H), 2.66-2.51 (m, 4H), 2.23-2.02 (m, 4H), 1.03 (s, 6H), 0.95 (s, 6H). ^{13}C NMR (100 MHz, DMSO-*d6*) δ: 196.00, 179.01, 164.02, 143.15, 134.00, 127.79, 122.26, 121.19, 112.68, 108.75, 50.67, 45.23, 31.46, 27.76, 26.50. Anal. Calcd. For $C_{24}H_{24}BrNO_4$: C, 61.28; H, 5.14; N, 2.98; found: C, 61.48; H, 5.18; N, 2.79.

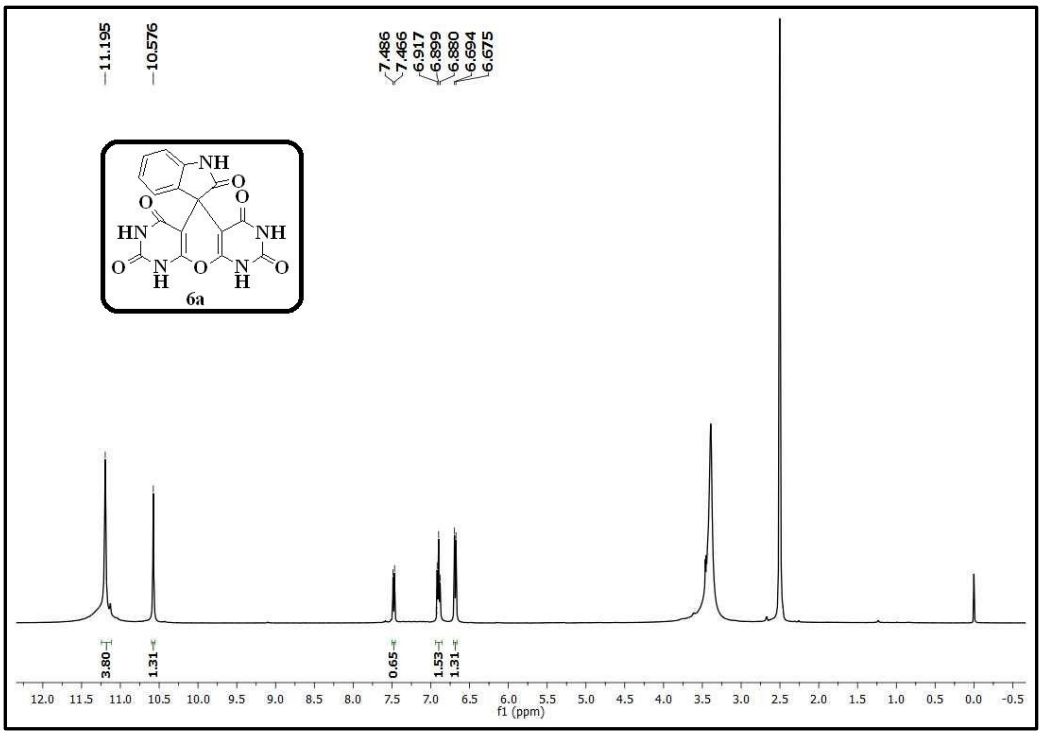

^{1}H NMR spectrum of the compound **6a**

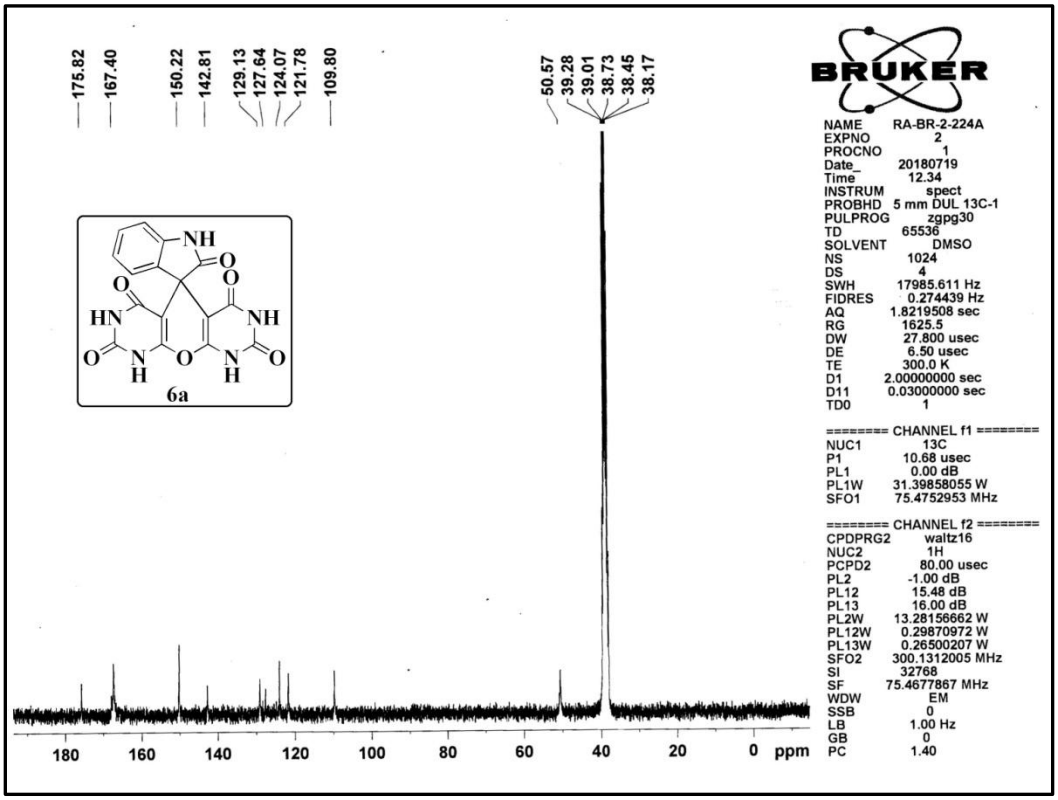

^{13}C NMR spectrum of the compound **6a**

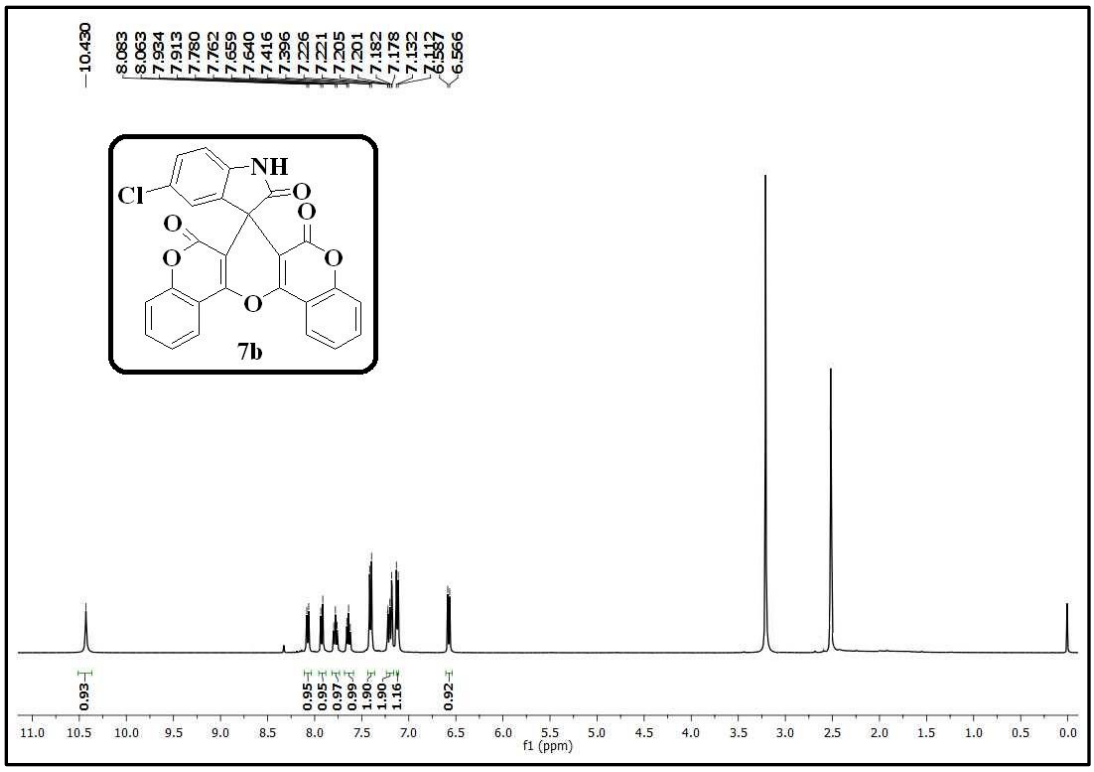

^{1}HNMR spectrum of the compound **7b**

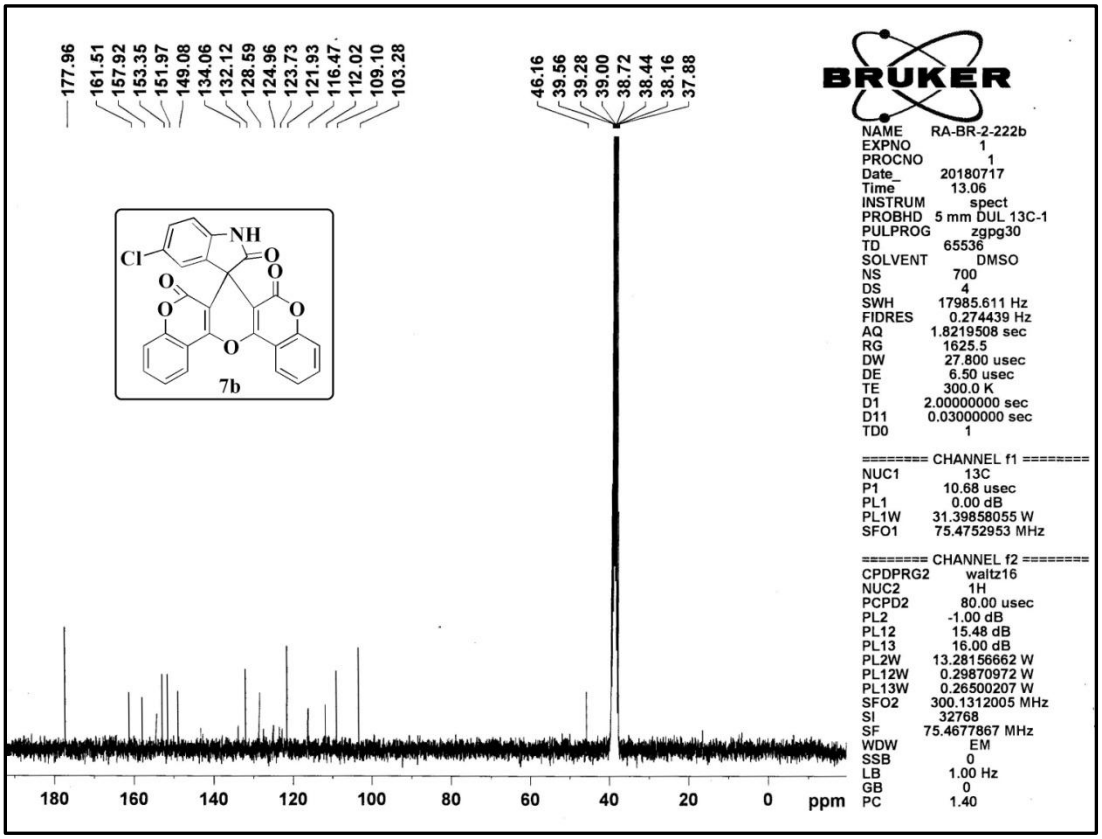

^{13}C NMR spectrum of the compound **7b**

CHAPTER-VI (SECTION-B)

Deep eutectic solvent $ZnCl_2$+Urea assisted synthesis of novel morpholine containing spirooxindoles and biological evaluation

6B.1. Introduction

Nowadays, deep eutectic solvents (DESs) are treated as a new class of ionic liquid (IL) analogs because they contain many characteristics and properties with ILs [19]. DESs are defined as system composed of a mixture of at least two components i.e., a hydrogen bond acceptor (HBA) and a hydrogen bond donor (HBD), which are able to self-associate to form a new eutectic phase characterized by a melting point below 100 °C, which is lower than that of each individual component [5]. The main constituents of these solvents are high melting temperature solids that show strong hydrogen bonding interactions. The resultant combinations often provide wide liquid range and unusual low transition temperatures [2]. They often show low volatility, water-compatibility, nontoxicity, non-flammability, wide liquid range, biocompatibility, biodegradability, etc. Furthermore, they show the ability to characterize their physical properties by choosing the right DES constituents in terms of chemical nature, relative compositions or water content [20]. DESs have been applied in various fields like organic reactions [21-24], extractions [25], electrochemistry [26-28] and enzyme reactions [29].

Spirooxindoles are important structural motifs present in several natural alkaloids and biologically relevant synthetic compounds [30]. Furthermore, spirooxindole derivatives have been reported to possess antimicrobial, AChE inhibitory activities, antimycobacterial activity, MDM2-p53 inhibitors, analgesic and anticancer [30-32].

Sakhuja et al. reported the synthesis of a series of spiro[indole-thiazolidine] and spiro[indole-pyran] derivatives (Figure 6B.1). The synthesized compounds were evaluated for their antimicrobial activity [32].

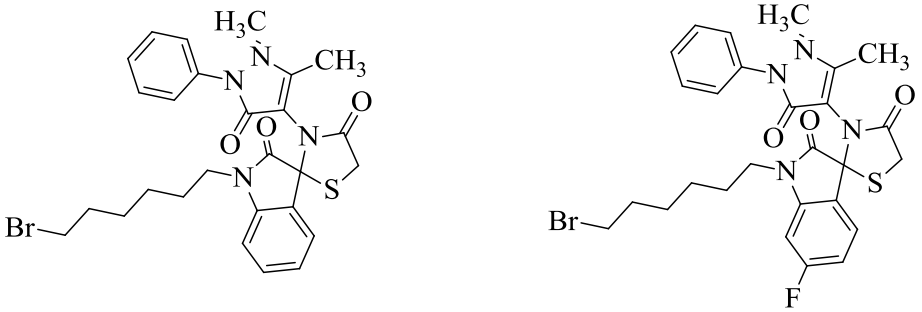

Figure 6B.1

Kim et al. described the synthesis of a series of oxazolidinones having spiro[2,4]heptane moieties (Figure 6B.2). Their *in vitro* antibacterial activity against both gram positive and gram negative bacteria were tested and the effect of substituents on the oxazolidinone ring was investigated [33].

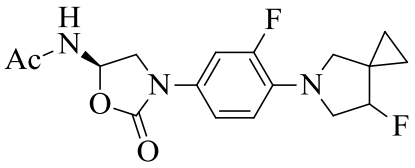

Figure 6B.2

Rapposelli and coworkers reported the synthesis and biological evaluation of 5-membered spiro heterocycle-benzopyran derivatives against myocardial ischemia (Figure 6B.3) [34].

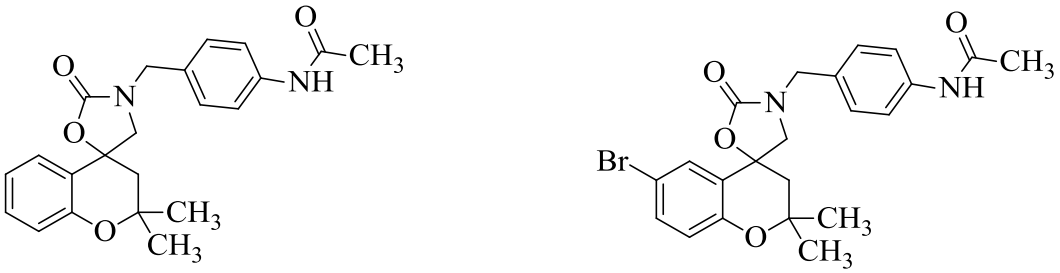

Figure 6B.3

Ye et al. reported the design, synthesis and molecular docking studies of spiro[indoline-3,4'-piperidine]-2-ones as potential c-Met inhibitors (Figure 6B.4) [35].

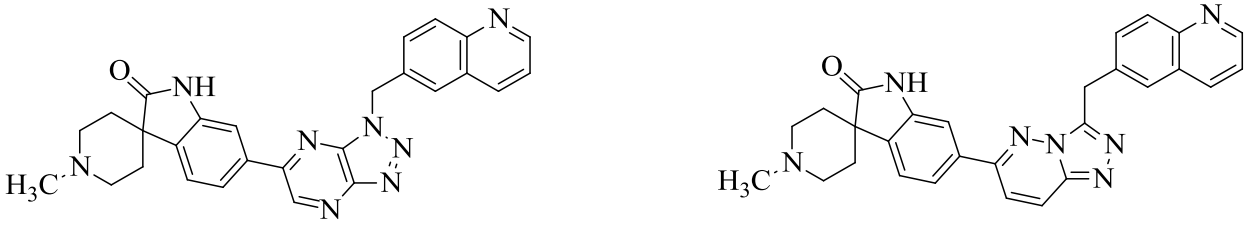

Figure 6B.4

6B.1.1. Various methods for the synthesis of the spirooxindoles

De et al. reported an expeditious and efficient synthesis of spiro-pyrazolo[3,4-*b*]pyridines catalyzed by recyclable mesoporous aluminosilicate nanoparticles in aqueous ethanol (Scheme 6B.1) [36].

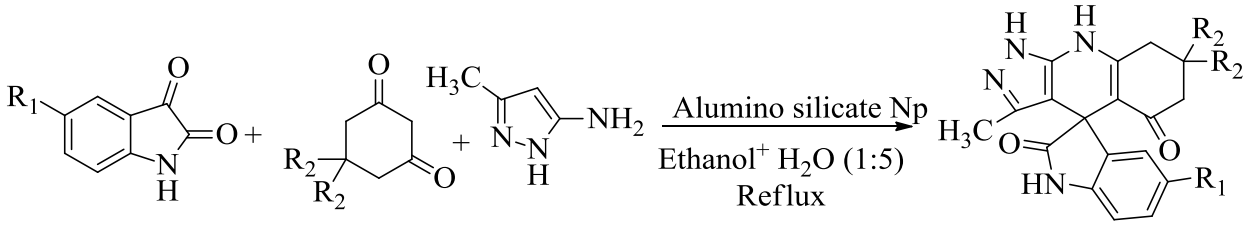

Scheme 6B.1

Elinson and coworkers described cascade assembly of *N*,*N*'-dialkyl barbituric acids and aldehydes *via* a simple and efficient one-pot approach to obtain the substituted 1,5-dihydro-2*H*,2'*H*-spiro-(furo[2,3-*d*]pyrimidine-6,5'-pyrimidine)-2,2',4,4',6'(1'*H*,3*H*,3'*H*)-pentone framework (Scheme 6B.2**)** [37].

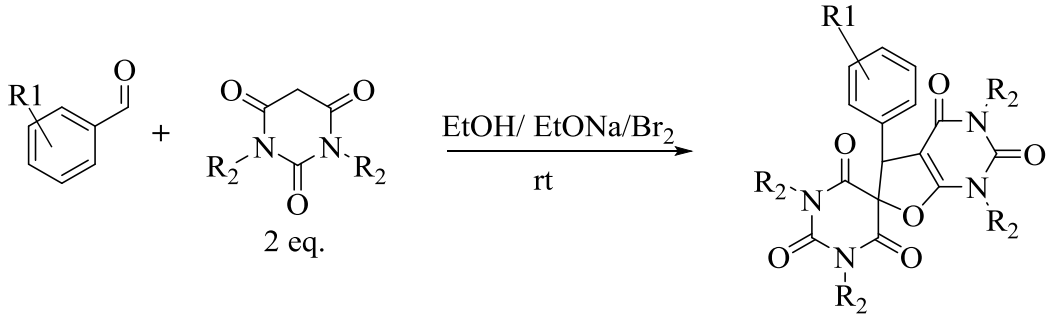

Scheme 6B.2

Bayat and coworkers described an efficient one-pot four-component condensation reaction for the chemoselective synthesis of spiro[acenaphthylene-1,4'-pyrano[2,3-*c*]pyrazol]-2-ones and spiro[acenaphthylene-1,5'-pyrano[2,3-*d*]pyrimidine]-triones (Scheme 6B.3) [38].

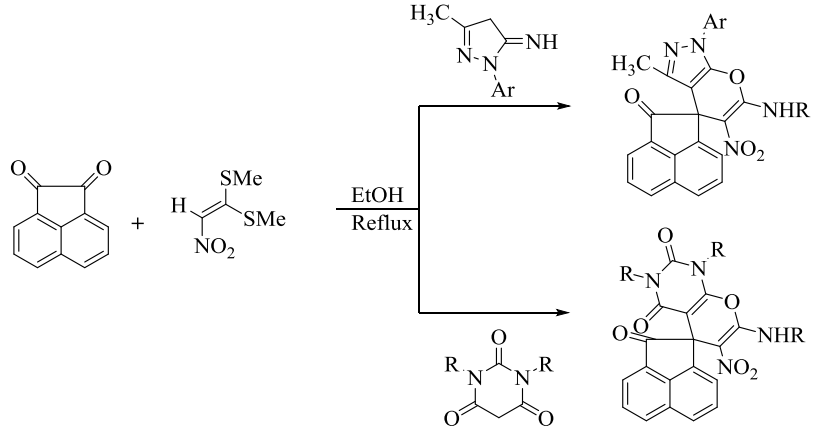

Scheme 6B.3

Haung et al. reported the construction of functionalized spiro 1,4-benzoxazine oxindole derivatives *via* domino Mannich-alkylation of *α*-halocarbonyl compounds with imines (Scheme 6B.4) [39].

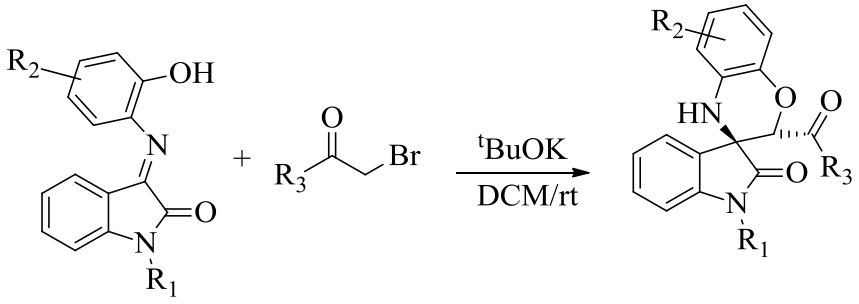

Scheme 6B.4

6B.2. Present work

Based on the aforementioned view of DES and biological importance of spirooxindoles herewith, we report the green approach for the synthesis of various spirooxindoles by using the DES, $ZnCl_2$+Urea.

6B.2.1. General procedure for the synthesis of the spirooxindoles 7a-c, 8a-c, 9a-c and 10a-c

A mixture of isatin derivatives **1a-c** (1 mmol), 3-fluoro-4-morpholinoaniline **2** (1 mmol) and pyrimidine-2,4,6(1*H*,3*H*,5*H*)-trione **3**/4-hydroxy-2*H*-chromen-2-one **4**/1*H*-indene-1,3(2*H*)-Dione **5**/5,5-dimethylcyclohexane-1,3-dione **6** (2 mmol) were reacted in deep eutectic solvent $ZnCl_2$+Urea at 80 °C. The progress of all the reactions was monitored by TLC. After completion of the reaction, the crude products were transferred into crushed ice and the obtained precipitate was filtered and dried. These products were washed with ethanol to get pure compounds (Scheme 6B.5).

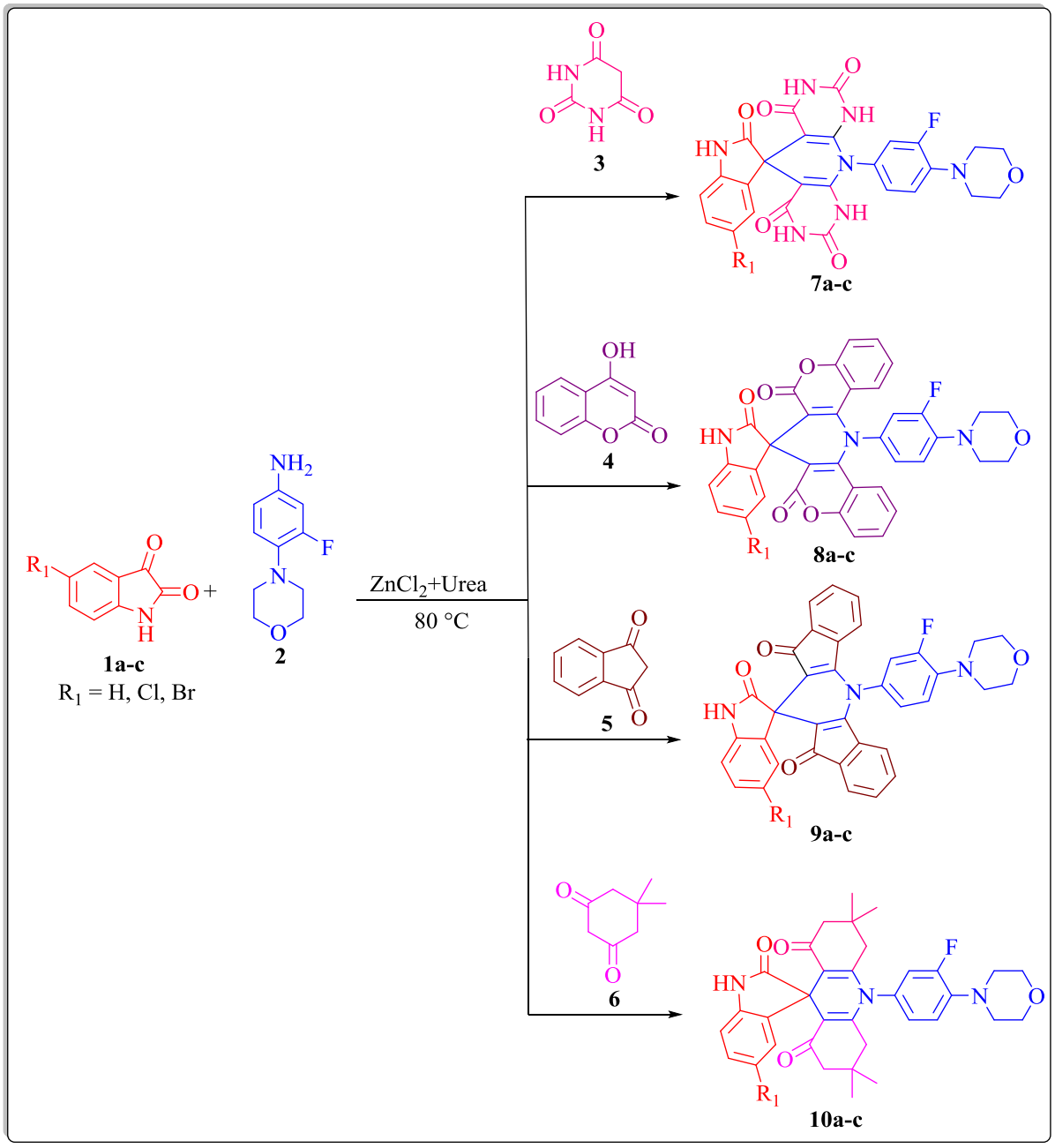

Scheme 6B.5

6B.2.2. The plausible reaction mechanism for the formation of target compounds 7a-c, 8a-c, 9a-c and 10a-c

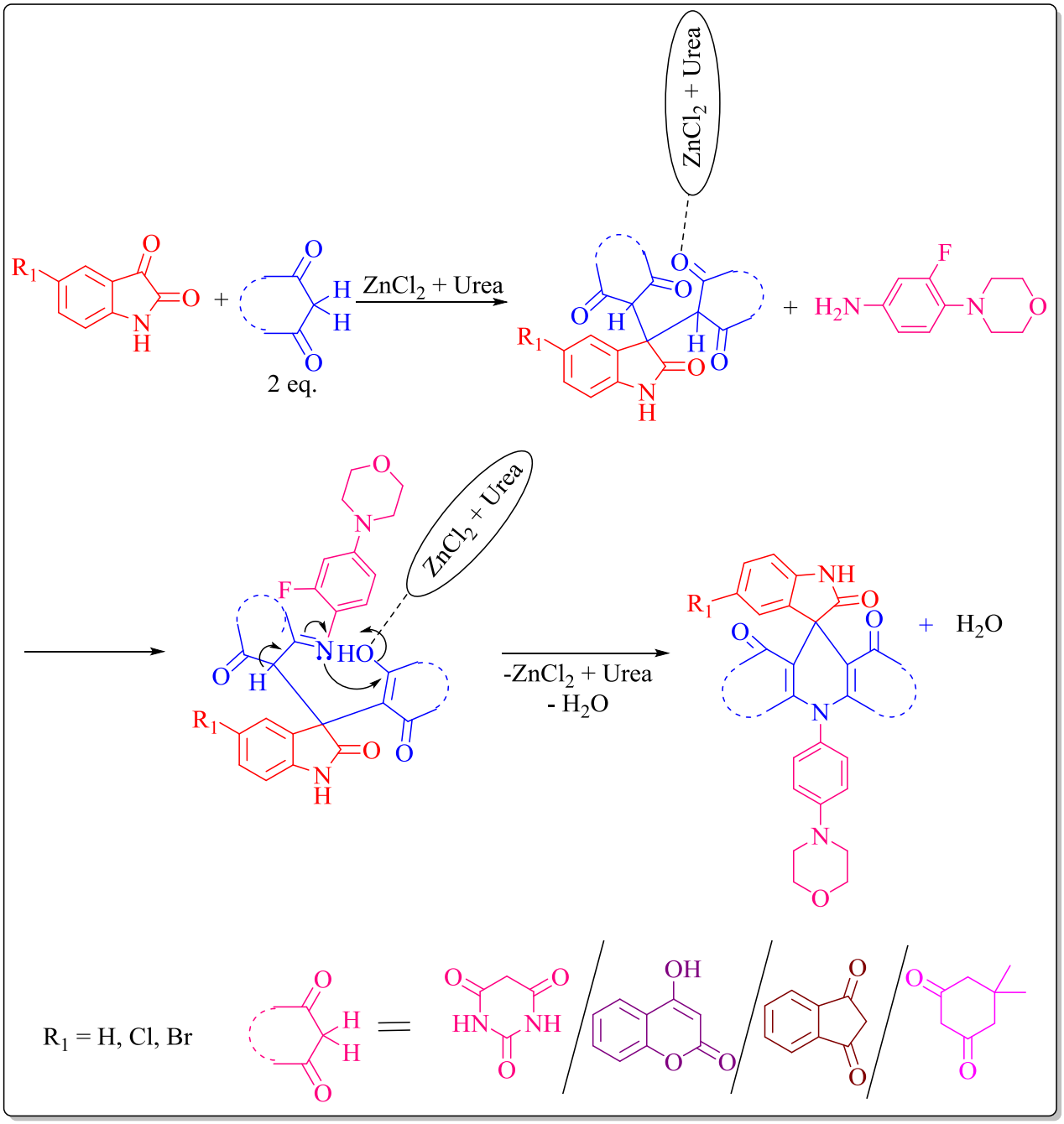

Scheme 6B.6

6B.3. Results and discussion

6B.3.1. Chemistry

Initially, isatin **1a**, 2-fluoro-4-morpholinoaniline **2** and pyrimidine-2,4,6(1*H*,3*H*,5*H*)-trione **3** were taken as a starting material in order to optimize the reaction conditions in different solvents water, ethylene glycol and DES ($ZnCl_2$+Urea). *p*-TSA (20 mol%) was used as a catalyst for the model reaction in water and ethylene glycol at 100 °C. However, the target compound **7a** was formed with moderate yield. Then, the model reaction was carried out in the deep eutectic solvent $ZnCl_2$+Urea with out any catalyst at 80 °C. In this case, the target compound **7a** was formed with good yield. Further, the model reaction was carried out in $ZnCl_2$+Urea at different temperatures. The optimized reaction conditions were shown in table 1.

Table 1. The optimized reaction conditions[a.b].

S. No.	Solvent	Catalyst	Temperature (ºC)	Time (min)	Yield (%)
1	Water	*p*-TSA (20 mol%)	100	120	58
2	Ethylene glycol	*p*-TSA (20 mol%)	100	120	52
3	$ZnCl_2$+Urea	--	80	30	82
4	$ZnCl_2$+Urea	--	70	50	75
5	$ZnCl_2$+Urea	--	90	30	82

[a]All the reactions were carried out by using isatin **1a** (1 mmol), 3-fluoro-4-morpholinoaniline **2** and pyrimidine-2,4,6(1*H*,3*H*,5*H*)-trione **3** as starting materials. [b]Isolated yield.

In order to explore the reaction approach the target compounds **7a-c, 8a-c, 9a-c** and **10a-c** were synthesized from the isatin derivatives **1a-c** (1 mmol), 3-fluoro-4-morpholinoaniline **2** (1 mmol) and pyrimidine-2,4,6(1*H*,3*H*,5*H*)-trione **3**/4-hydroxy-2*H*-chromen-2-one **4**/1*H*-indene-1,3(2*H*)-Dione **5**/5,5-dimethylcyclohexane-1,3-dione **6** (2 mmol) in deep eutectic solvent $ZnCl_2$+Urea at 80 °C (Scheme 6B.5). The target compounds were formed in 60-80min with 80-89% of yield. The progress of all the reactions was monitored by TLC. After completion of the reaction, the crude products were transferred into crushed ice and the obtained precipitate was filtered and dried. These products were washed with ethanol to get pure compounds. The time and yield for the formation of target

compounds were shown in table 2. The plausible reaction mechanism was shown in scheme 6B.6.

Table 2. Time and yields of the target compounds **7a-c**, **8a-c**, **9a-c** and **10a-c**[a,b,c].

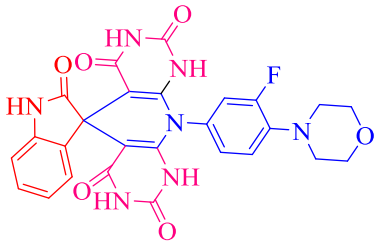 **7a** (65min / 82%)	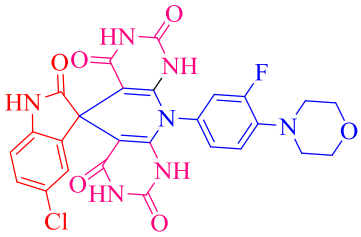 **7b** (75min / 85%)	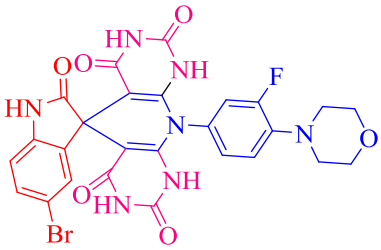 **7c** (75min / 85%)
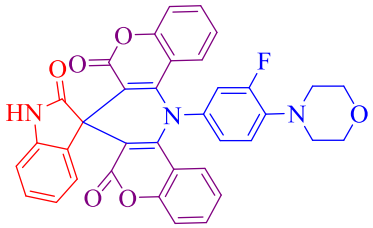 **8a** (60min / 80%)	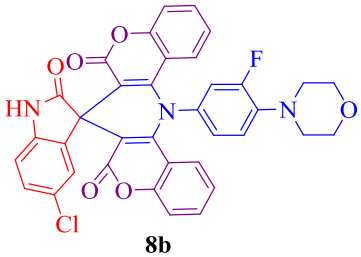 **8b** (65min / 89%)	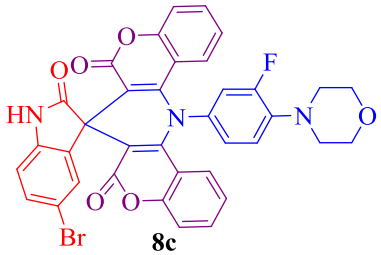 **8c** (80min / 86%)
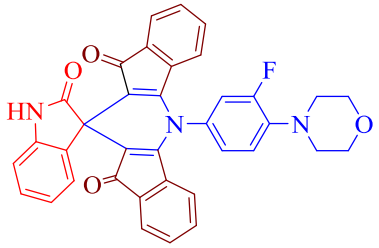 **9a** (67min / 84%)	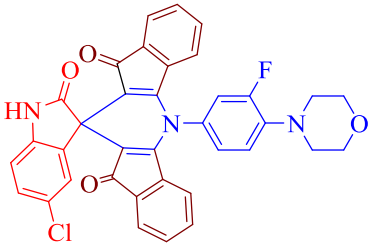 **9b** (72min / 84%)	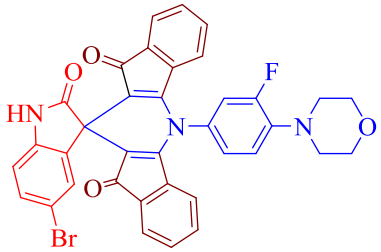 **9c** (70min / 82%)
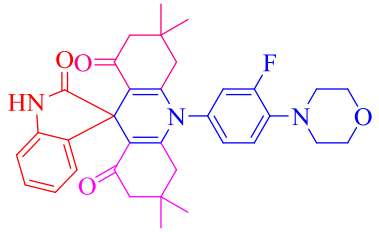 **10a** (80min / 87%)	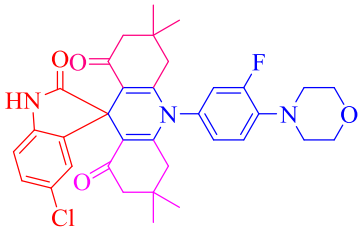 **10b** (70min / 89%)	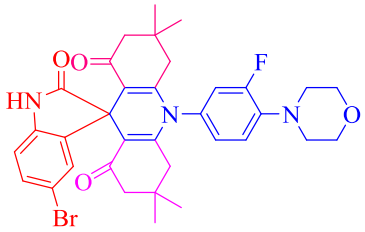 **10c** (80min / 83%)

[a]All the reactions were carried out by using isatin derivatives **1a-c** (1 mmol), 3-fluoro-4-morpholinoaniline **2** (1 mmol) and pyrimidine-2,4,6(1*H*,3*H*,5*H*)-trione **3**/4-hydroxy-2*H*-chromen-2-one **4**/1*H*-indene-1,3(2*H*)-Dione **5**/5,5-dimethylcyclohexane-1,3-dione **6** (2 mmol) in deep eutectic solvent $ZnCl_2$+Urea at 80 °C. [b]The progress of all the reactions was monitored by TLC.[c]Isolated yield.

6B.3.2. Biological evaluation

6B.3.2.1. Anticancer activity

The target compounds were tested for their *in vitro* anticancer activity by using MTT assay against A549, MCF7, HeLa and HEK293T cell lines. The MTT assay results were summarized in table 3**.**

Among all the compounds, the compound **9a** exhibited the potent influence of the cytotoxic activity against MCF7 and HeLa cell lines with IC_{50} values 6.47 ± 0.01µM and 9.14 ± 0.32 µM respectively. The compound **7c** exhibit the potent activity against HeLa cell line with IC_{50} value 6.81 ± 0.01 µM. The compound **8c** exhibit the potent activity against MCF7 cell line with IC_{50} value 9.56 ± 0.12 µM. Further, the compounds **7c**, **8c** and **9a** were screened against the Human Embryonic Kidney 293 (HEK293T) cell line and observed that the IC_{50} values 64.36 ± 0.08 µM, 75.47 ± 0.51 µM and 67.12 ± 0.03 µM respectively.

Table 3. The *in vitro* anticancer activity of the synthesized compounds **7a-c**, **8a-c**, **9a-c** and **10a-c**.

S. No.	Entry	IC_{50} (µM) [a]			
		A549	**MCF7**	**HeLa**	**HEK293T**
1	**7a**	35.12 ± 0.81	44.56 ± 0.23	43.21 ± 0.31	ND[b]
2	**7b**	43.64 ± 0.56	39.78 ± 1.02	36.76 ± 0.44	ND
3	**7c**	25.63 ± 0.08	23.01 ± 1.02	**6.81 ± 0.01**	64.36 ± 0.08
4	**8a**	41.16 ± 0.11	28.20 ± 0.18	42.90 ± 0.81	ND
5	**8b**	47.92 ± 0.17	39.29 ± 0.95	44.61 ± 0.02	ND
6	**8c**	22.25 ± 0.21	**9.56 ± 0.12**	18.12 ± 0.81	75.47 ± 0.51
7	**9a**	17.84 ± 0.05	**6.47 ± 0.01**	**9.14 ± 0.32**	67.12 ± 0.03
8	**9b**	29.18 ± 0.41	34.56 ± 0.14	32.02 ± 0.43	ND
9	**9c**	36.10 ± 0.01	43.06 ± 0.54	37.43 ± 0.40	ND
10	**10a**	35.36 ± 0.90	31.33 ± 0.65	39.24 ± 0.21	ND
11	**10b**	37.23 ± 0.24	27.60 ± 0.49	38.31 ± 0.72	ND
12	**10c**	38.43 ± 0.12	31.17 ± 0.89	26.09 ± 0.74	ND

13	***Cis*-Platin**	5.23 ± 1.00	3.81 ± 0.38	5.45 ± 0.42	ND

[a]IC_{50}: The concentration of the compound (μM) that exhibits the 50% cell growth inhibition. [b]ND-Not determined.

6B.3.2.2. Antioxidant activity

The synthesized compounds were evaluated for their *in vitro* antioxidant activity. The antioxidant activity results were depicted in table 4. All the target compounds exhibited the antioxidant activity with the IC_{50} values varied from 7.34 ± 0.17 μM to 38.17 ± 0.18 μM. The compound **9a** exhibit the potent antioxidant activity with the IC_{50} value 7.34 ± 0.17 μM. The compounds **7c** and **8c** exhibited significant antioxidant activity with IC_{50} values 10.84 ± 0.05 μM and 10.06 ± 0.23 μM respectively.

Table 4. The antioxidant activity of the synthesized compounds **7a-c**, **8a-c**, **9a-c** and **10a-c**.

S. No.	Entry	IC_{50} (μM)
1	**7a**	31.83 ± 0.71
2	**7b**	24.31 ± 0.42
3	**7c**	**10.84 ± 0.05**
4	**8a**	27.09 ± 0.64
5	**8b**	24.57 ± 0.11
6	**8c**	**10.06 ± 0.23**
7	**9a**	**7.34 ± 0.17**
8	**9b**	38.17 ± 0.18
9	**9c**	37.01 ± 0.93
10	**10a**	31.60 ± 0.04
11	**10b**	32.84 ± 0.61
12	**10c**	24.41 ± 0.22
13	**Ascorbic acid**	3.45 ± 0.745

6B.3.2.3. Antibacterial activity

The *in vitro* antibacterial activity of the synthesized compounds were carried out against the selected bacterial strains such as two gram positive bacteria i.e., *Bacillus subtilis*

and *Staphylococcus aureus* and two gram negative bacteria i.e., *Escherichia coli and Pseudomonas aeruginosa*. The results were summarized in Table 5.

Among all the synthesized compounds, the compound **8c** exhibited potent antibacterial activity against *E. coli* and *P. aeruginosa* with MIC values 13.50 µg/mL and 15.50 µg/mL respectively. The compound **7c** showed potent activity against *B. subtilis* and *E. coli* with MIC values 7.50 µg/mL and 17.50 µg/mL respectively.

Table 5. The antibacterial activity of the target compounds **7a-c**, **8a-c**, **9a-c** and **10a-c**.

S. No.	Entry	Minimum Inhibitory Concentration (µg/mL)			
		B. subtilis	***S. aureus***	***E. coli***	***P. aeruginosa***
1	**7a**	27.50	30.50	27.50	32.50
2	**7b**	23.00	>100	36.25	32.50
3	**7c**	**7.50**	18.50	**17.50**	27.50
4	**8a**	28.00	16.34	26.50	>100
5	**8b**	>100	43.00	42.50	45.00
6	**8c**	14.50	16.00	**13.50**	**15.50**
7	**9a**	>100	44.00	43.25	>100
8	**9b**	28.50	23.00	33.50	30.00
9	**9c**	36.25	34.50	>100	34.00
10	**10a**	32.50	26.00	>100	>100
11	**10b**	46.00	52.00	57.00	49.50
12	**10c**	>100	>100	>100	>100
15	**Streptomycin**	6.25	6.25	12.5	12.5

6B.3.2.4. Antifungal activity

The *in vitro* antifungal activity of the target compounds were investigated on two fungal strains such as *Aspergillus niger* and *Penicillium notatum.* The obtained results were depicted in Table 6.

The compound **7c** was exhibited potent fungal inhibition activity against *A. niger* with MIC values 8.00 µg/mL. The remaining compounds exhibited moderate antifungal activity.

Table 6. The antifungal activity of the target compounds **7a-c**, **8a-c**, **9a-c** and **10a-c**.

S. No.	Entry	Minimum Inhibitory Concentration (µg/mL)	
		Aspergillus niger	***Penicillium notatum***
1	**7a**	35.00	14.00
2	**7b**	38.50	44.00
3	**7c**	**8.00**	19.00
4	**8a**	28.00	46.25
5	**8b**	21.50	42.25
6	**8c**	23.50	25.00
7	**9a**	27.50	34.50
8	**9b**	27.25	28.00
9	**9c**	38.25	34.00
10	**10a**	24.25	28.50
11	**10b**	39.50	31.50
12	**10c**	29.50	33.00
13	**Ketoconazole**	3.25	3.25

6B.4. Molecular docking studies

The molecular docking studies were carried out against proteins HER2 (PDB ID: 3POZ) and EGFR (PDB ID: 4HJO) by using the AutoDock Tools (ADT) version 1.5.6 and the AutoDock version 4.2.5.1 docking program.

EGFR, a prominent cell-surface receptor, related to the epidermal growth factor receptor family [40]. It is a well known oncogenic driver [41]. The extracellular and tyrosine kinase domain mutations of EGFR are responsible for glioblastoma NSCLC (non small cell lung cancer) [42-45]. It plays a vital role in the ductal system growth of mammary glands [41, 46, 47]. It's over expression also leads the anal cancer and epithelial tumors of the neck and head [48, 49]. HER2 is a member of the human epidermal growth factor receptor2

(EGFR/HER/ERBB) family, plays an eminent role in the malignant growth from several origins [48]. It stimulates the mitogen-activated protein kinase cascades and HER3/PI3K/Akt pathway. These pathways lead the cell survival and proliferation [49, 50]. It is expressed on the most of the human cell surfaces [48]. The overexpression of HER leads to various cancers like stomach, adenocarcinoma of the lungs, breast [51], uterine [51, 52], ovarian cancers [52]. It is a suitable target for the kinase inhibitors and monoclonal antibodies [53].

By examining the aforementioned reasons, EGFR and HER2 proteins have chosen as the target receptors for the docking studies. The binding energies of the target compounds with these proteins were compared and summarized in Table 7. The molecular docking studies of the targeted scaffolds with the target receptors EGFR and HER2 were compared (as shown in Table 7) and the results certainly confirm the affinity of all the synthesized compounds with the receptor EGFR is better than that of receptor HER2. Hence the protein receptor EGFR was preferred as the target receptor for the elaborate discussion. The hydrogen bonding profile of the target compounds with the protein EGFR was shown in Table 8.

Among all the compounds, the compound **9a** exhibited least binding energy −10.72 kcal/mol. It forms five hydrogen bonds with amino acid residues LYS721 (1.84 Å), PRO853 (2.66 Å), PHE669 (2.68 Å), VAL852 (2.83 Å) and LEU838 (3.03 Å). The phenyl ring in the isatin moiety interacts with the amino acid residues LYS851 and PRO853, the oxindole ring interacts with the amino acid residue PRO853, the phenyl ring in the indanone moiety interacts with the amino acid residues ARG817, LEU834 and ALA835, the phenyl ring in the 3-fluoro phenyl moiety interacts with amino acid residues LEU838 and PRO853, the morpholine ring interacts with the amino acid residues ALA840, ALA847 and VAL852 through hydrophobic interactions. Along with these hydrophobic interactions, there were electrostatic interactions with amino acid residues LYS721, ARG817 and ASP813. The best docking poses of the compound **9a** were shown in figure 6B.5.

Table 7. The molecular docking results of the target compounds with the EGFR and HER2 proteins.

S. No.	Compound	Binding energy (kcal/mol)	
		EGFR (PDB ID: 4HJO)	**HER2 (PDB ID: 3POZ)**
1	**7a**	−7.30	−6.78
2	**7b**	−7.19	−6.74
3	**7c**	−7.39	− 7.35
4	**8a**	−7.36	−6.98
5	**8b**	−7.57	−6.87
6	**8c**	−7.56	−6.19
7	**9a**	**−10.72**	−9.89
8	**9b**	−9.78	− 9.19
9	**9c**	−9.59	− 9.23
10	**10a**	−8.53	−7.45
11	**10b**	−6.96	− 6.59
12	**10c**	−6.74	−6.57

Table 8. The docking results of the target compounds with the EGFR (PDB ID: 4HJO).

S. No	Compound	Binding energy (kcal/mol)	No. of hydrogen bonds	Residues involved in the hydrogen bonding	Hydrogen bond length (Å)
1	**7a**	−7.30	3	CYS773, ARG817, LEU694	2.18, 2.73, 3.42
2	**7b**	−7.19	3	CYS773, ARG817, LEU694	2.78, 2.96, 3.11
3	**7c**	−7.39	3	CYS773, ARG817, LEU694	2.24, 2.48, 3.09
4	**8a**	−7.36	2	GLY697, PHE699	2.56, 2.65
5	**8b**	−7.57	2	GLY697, PHE699	2.62, 2.72
6	**8c**	−7.56	2	GLY697, PHE699	2.53, 2.59
7	**9a**	**−10.72**	5	LYS721, PRO853,	1.84, 2.66,

				PHE669, VAL852, LEU838	2.68, 2.83, 3.03
8	**9b**	−9.78	4	PRO853, PHE669, VAL852, LEU838	2.45, 2.51, 2.88, 3.07
9	**9c**	−9.59	4	PRO853, VAL852, LEU838, LEU838	2.34, 2.71, 2.93, 3.18
10	**10a**	−8.53	2	GLY695, THR766	2.05, 3.04
11	**10b**	−6.96	2	GLY695, THR766	2.66, 3.20
12	**10c**	−6.74	2	GLY695, THR766	2.84, 3.23

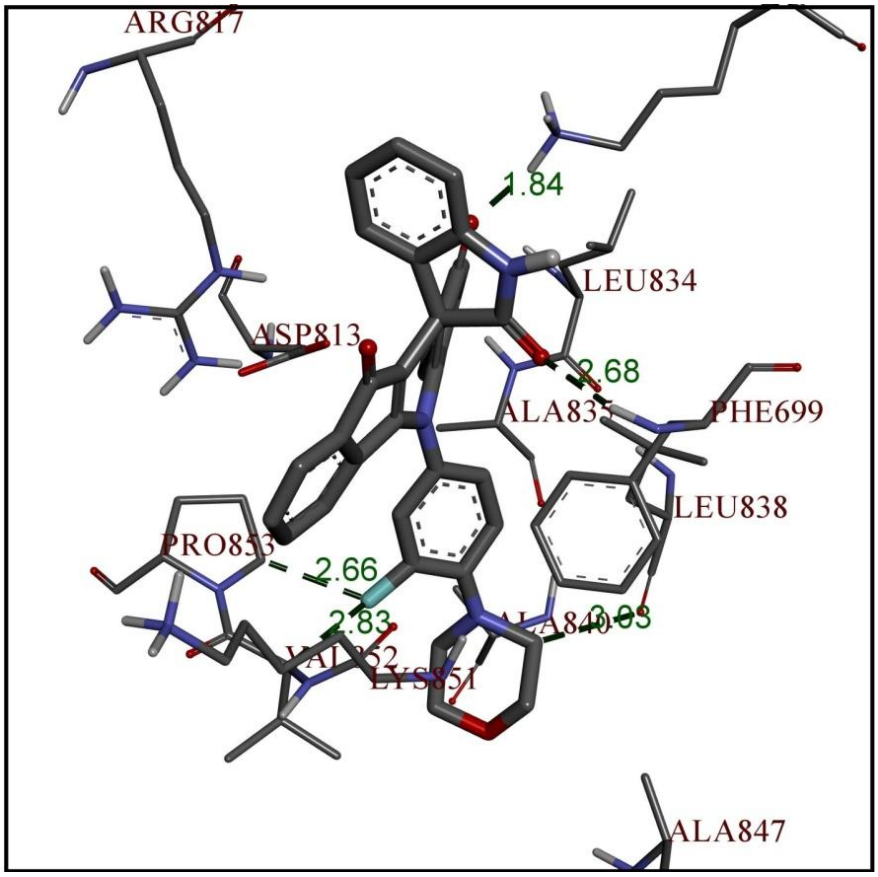

a)

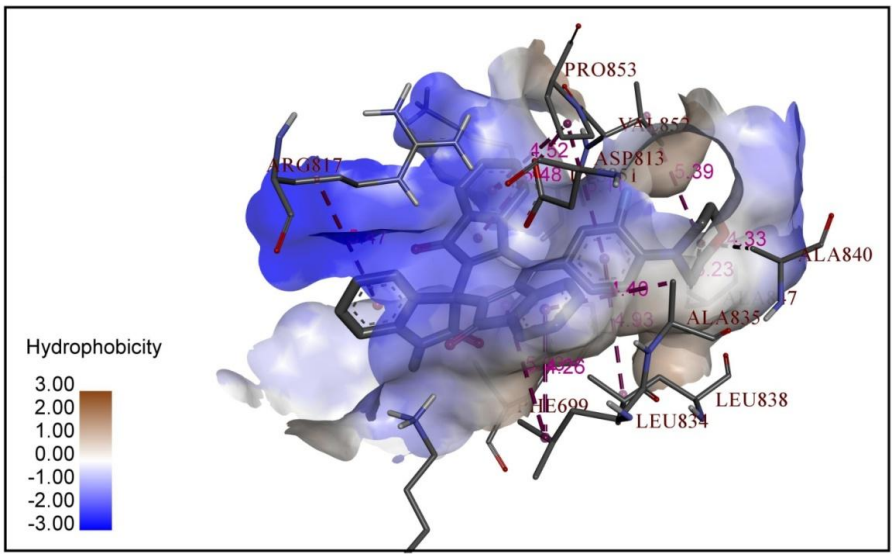

b)

Figure 6B.5. The best docking poses of the compound **9a** with the EGFR protein. a) The hydrogen bond interactions, b) The hydrophobic interactions.

6B.5. Conclusion

A series of morpholine containing spirooxindoles were synthesized efficiently by using deep eutectic solvent $ZnCl_2$+Urea. The target compounds were evaluated for their *in vitro* anticancer, antioxidant, antimicrobial activities. Among all the compounds, the compound **9a** exhibited potent anticancer activity against MCF7 and HeLa cell lines. The compound **9a** exhibited potent antioxidant activity. The compounds **8c** exhibited potent antibacterial activity against *E. coli* and *P. aeruginosa*. The compound **7c** showed potent anti bacterial activity on *B. subtilis* and potent antifungal activity on *A. niger*. The *in silico* molecular docking studies EGFR protein (PDB ID: 4HJO) were well correlated with the *in vitro* anticancer activity of the target compounds.

6B.6. Spectral data

10'-(3-Fluoro-4-morpholinophenyl)-1'*H*-spiro[indoline-3,5'-pyrido[2,3-*d*:6,5-*d*']dipyrimidine]-2,2',4',6',8'(3'*H*,7'*H*,9'*H*,10'*H*)-pentaone (7a)

Colour: White. M. P. 284-286 °C. IR (KBr, cm^{-1}): 3319, 1735, 1693, 1665. ^{1}H NMR (400 MHz, DMSO-*d6*) δ: 11.20 (s, 4H), 10.58 (s, 1H), 7.48 (d, 1H, J = 8.0 Hz), 7.17-7.09 (m, 4H),

6.90 (t, 1H, *J* = 7.6 Hz), 6.69 (d, 1H, *J* = 7.6 Hz), 4.65 (s, 4H), 3.88 (s, 4H,). ^{13}C NMR (100 MHz, DMSO-*d6*) *δ*: 190.01, 178.15, 156.77, 142.69, 141.29, 136.55, 136.29, 132.84, 132.59, 130.27, 128.57, 121.88, 121.73, 111.31, 110.72, 66.57, 50.46, 46.40. Anal. Calcd. For $C_{26}H_{20}FN_7O_6$: C, 57.25; H, 3.70; N, 17.97; found: C, 57.52; H, 3.78; N, 18.14.

5-Chloro-10'-(3-fluoro-4-morpholinophenyl)-1'*H*-spiro[indoline-3,5'-pyrido[2,3-*d*:6,5-*d*']dipyrimidine]-2,2',4',6',8'(3'*H*,7'*H*,9'*H*,10'*H*)-pentaone (7b)

Colour: white. M. P. 289-291 ℃. IR (KBr, cm^{-1}): 3309, 1737, 16963, 1671. ^{1}H NMR (400 MHz, DMSO-*d6*) *δ*: 11.15 (s, 4H), 10.54 (s, 1H), 7.44 (d, 1H, *J* = 8.0 Hz), 7.18 (s, 1H), 7.13-7.05 (m, 2H), 6.86 (t, 1H, *J* = 7.2 Hz), 6.65 (d, 1H, *J* = 7.6 Hz), 4.78 (s, 4H), 3.81 (s, 4H,). ^{13}C NMR (100 MHz, DMSO- *d6*) *δ*: 191.56, 179.70, 158.32, 144.24, 142.84, 138.10, 137.84, 134.39, 134.14, 131.82, 130.12, 128.16, 123.43, 112.86, 112.27, 68.12, 52.01, 47.95. Anal. Calcd. For $C_{26}H_{19}ClFN_7O_6$: C, 53.85; H, 3.30; N, 16.91; found: C, 53.62; H, 3.21; N, 16.75.

5-Bromo-10'-(3-fluoro-4-morpholinophenyl)-1'*H*-spiro[indoline-3,5'-pyrido[2,3-*d*:6,5-*d*']dipyrimidine]-2,2',4',6',8'(3'*H*,7'*H*,9'*H*,10'*H*)-pentaone (7c)

Colour: White. M. P. 295-297 ℃. IR (KBr, cm^{-1}): 3313, 1731, 1692, 1661. ^{1}H NMR (400 MHz, DMSO-*d6*) *δ*: 11.42 (s, 4H), 10.80 (s, 1H), 7.69 (d, 1H, *J* = 8.0 Hz), 7.44 (s, 1H), 7.39-7.32 (m, 2H), 7.13 (t, 1H, *J* = 7.2 Hz), 6.91 (d, 1H, *J* = 7.6 Hz), 4.64 (s, 4H), 3.74 (s, 4H,). ^{13}C NMR (100 MHz, DMSO-*d6*) *δ*: 191.48, 179.62, 158.24, 144.16, 142.76, 138.02, 137.76, 134.31, 134.06, 131.74, 130.04, 128.08, 123.35, 112.78, 112.19, 68.04, 51.93, 47.87. Anal. Calcd. For $C_{26}H_{19}BrFN_7O_6$: C, 50.02; H, 3.07; N, 15.70; found: C, 50.23; H, 3.12; N, 15.52.

14-(3-Fluoro-4-morpholinophenyl)-6*H*-spiro[dichromeno[4,3-*b*:3',4'-*e*]pyridine-7,3'-indoline]-2',6,8(14*H*)-trione (8a)

Colour: White. M. P. 198-200 ℃. IR (KBr, cm^{-1}): 3338, 1728, 1685. ^{1}H NMR (400 MHz, DMSO-*d6*) *δ*: 10.42 (s, 1H), 8.06 (d, 1H, *J* = 8.0 Hz), 7.92 (d, 2H, *J* = 8.4 Hz), 7.78 (d, 1H, *J* = 7.2 Hz), 7.64 (t, 2H, *J* = 7.2 Hz), 7.44-7.33 (m, 7H), 7.26 (s, 1H), 6.52 (d, 1H, *J* = 8.0 Hz), 4.71 (s, 4H), 3.78 (s, 4H). ^{13}C NMR (100 MHz, DMSO-*d6*) *δ*: 188.64, 164.52, 158.36, 153.55, 153.01, 143.78, 143.45, 142.76, 142.11, 141.78, 137.26, 134.09, 132.02, 131.06, 129.80, 129.74, 128.96, 128.65, 128.23, 127.03, 122.12, 110.24, 109.69, 106.08, 69.39,

63.80, 47.81. Anal. Calcd. For $C_{36}H_{24}FN_3O_6$: C, 70.47; H, 3.94; N, 6.85; found: C, 70.68; H, 3.86; N, 6.74.

5'-Chloro-14-(3-fluoro-4-morpholinophenyl)-6*H*-spiro[dichromeno[4,3-*b*:3',4'-*e*]pyridine-7,3'-indoline]-2',6,8(14*H*)-trione (8b)

Colour: White. M. P. 205-207 °C. IR (KBr, cm^{-1}): 3305, 1732, 1688. ^{1}H NMR (400 MHz, DMSO-*d6*) δ: 10.73 (s, 1H), 8.38 (d, 1H, , *J* = 8.0 Hz), 8.23 (d, 1H, *J* = 8.4 Hz), 8.08 (t, 1H, *J* = 7.2 Hz), 7.94 (t, 2H, *J* = 7.2 Hz), 7.71 (d, 3H, *J* = 8.0 Hz), 7.53-7.41 (m, 5H), 6.89 (d, 2H, *J* = 8.4 Hz), 4.76 (s, 4H), 3.65 (s, 4H). ^{13}C NMR (100 MHz, DMSO-*d6*) δ: 187.83, 163.71, 152.74, 152.20, 142.97, 142.64, 141.94, 141.29, 140.96, 136.45, 133.28, 131.21, 130.25, 128.99, 128.93, 128.15, 127.84, 127.41, 126.21, 121.31, 109.42, 108.88, 105.27, 68.58, 62.99, 46.99. Anal. Calcd. For $C_{36}H_{23}ClFN_3O_6$: C, 66.72; H, 3.58; N, 6.48; found: C, 66.56; H, 3.67; N, 6.67.

5'-Bromo-14-(3-fluoro-4-morpholinophenyl)-6*H*-spiro[dichromeno[4,3-*b*:3',4'-*e*]pyridine-7,3'-indoline]-2',6,8(14*H*)-trione (8c)

Colour: White. M. P. 183-185 °C. IR (KBr, cm^{-1}): 3301, 1734, 1666. ^{1}H NMR (400 MHz, DMSO-*d6*) δ: 10.44 (s, 1H), 8.06 (d, 1H, *J* = 8.0 Hz), 7.94 (d, 1H, *J* = 8.4 Hz), 7.79 (d, 1H, *J* = 7.2 Hz), 7.66 (t, 2H, *J* = 7.2 Hz), 7.46-7.35 (m, 7H), 7.27 (s, 1H), 6.54 (d, 1H, *J* = 8.0 Hz), 4.47 (s, 4H), 3.97 (s, 4H). ^{13}C NMR (100 MHz, DMSO-*d6*) δ: 187.71, 163.59, 152.61, 152.08, 142.84, 142.51, 141.82, 141.17, 140.84, 136.33, 133.15, 131.08, 130.12, 128.87, 128.80, 128.02, 127.72, 127.29, 126.09, 121.19, 109.30, 108.76, 105.15, 68.46, 62.86, 46.87. $C_{36}H_{23}BrFN_3O_6$: C, 62.44; H, 3.35; N, 6.07; found: C, 62.68; H, 3.27; N, 6.34.

5-(3-Fluoro-4-morpholinophenyl)-10*H*-spiro[diindeno[1,2-*b*:2',1'-*e*]pyridine-11,3'-indoline]-2',10,12(5*H*)-trione (9a)

Colour: White. M. P. 173-175 °C. IR (KBr, cm^{-1}): 3348, 2907, 1681. ^{1}H NMR (400 MHz, DMSO-*d6*) δ: 10.31 (s, 1H), 7.94 (d, 1H, *J* = 8.0 Hz), 7.81 (d, 2H, *J* = 8.4 Hz), 7.67 (d, 1H, *J* = 7.2 Hz), 7.53 (t, 2H, *J* = 7.2 Hz), 7.33-7.25 (m, 5H), 7.24 (d, 2H, *J* = 8.4 Hz), 7.15 (s, 1H), 6.41 (d, 1H, *J* = 8.0 Hz), 4.32 (s, 4H), 3.84 (s, 4H). ^{13}C NMR (100 MHz, DMSO-*d6*) δ: 182.05, 157.93, 146.96, 146.42, 137.19, 136.86, 136.16, 135.51, 135.18, 130.67, 127.50,

125.43, 124.46, 123.21, 123.15, 122.37, 122.06, 121.63, 120.43, 115.53, 103.64, 103.10, 99.49, 62.80, 57.21, 41.21. Anal. Calcd. For $C_{36}H_{24}FN_3O_4$: C, 74.35; H, 4.16; N, 7.23; found: C, 74.58; H, 4.24; N, 7.34.

5'-Chloro-5-(3-fluoro-4-morpholinophenyl)-10*H*-spiro[diindeno[1,2-*b*:2',1'-*e*]pyridine-11,3'-indoline]-2',10,12(5*H*)-trione (9b)

Colour: White. M. P. 180-182 ℃. IR (KBr, cm^{-1}): 3319, 1739, 1697. ^{1}H NMR (400 MHz, DMSO-*d6*) δ: 10.22 (s, 1H), 7.86 (d, 1H, , *J* = 8.0 Hz), 7.72 (d, 1H, *J* = 8.4 Hz), 7.57 (t, 1H, *J* = 7.2 Hz), 7.43 (t, 2H, *J* = 7.2 Hz), 7.20 (d, 3H, *J* = 8.0 Hz), 7.01-6.90 (m, 5H), 6.37 (d, 2H, *J* = 8.4 Hz), 4.25 (s, 4H), 3.79 (s, 4H). ^{13}C NMR (100 MHz, DMSO-*d6*) δ: 182.90, 158.78, 147.81, 147.27, 138.04, 137.71, 137.01, 136.36, 136.03, 131.52, 128.35, 126.28, 125.31, 124.06, 124.00, 123.22, 122.91, 122.48, 121.28, 116.38, 104.49, 103.95, 100.34, 63.65, 58.06, 42.06. Anal. Calcd. For $C_{36}H_{23}ClFN_3O_4$: C, 70.19; H, 3.76; N, 6.82; found: C, 70.35; H, 3.72; N, 6.57.

5'-Bromo-5-(3-fluoro-4-morpholinophenyl)-10*H*-spiro[diindeno[1,2-*b*:2',1'-*e*]pyridine-11,3'-indoline]-2',10,12(5*H*)-trione (9c)

Colour: White. M. P. 189-191 ℃. IR (KBr, cm^{-1}): 3336, 1733, 1673. ^{1}H NMR (400 MHz DMSO-*d6*) δ: 10.35 (s, 1H), 7.98 (d, 1H, *J* = 8.0 Hz), 7.85 (d, 1H, *J* = 8.4 Hz), 7.70 (d, 1H, *J* = 7.2 Hz), 7.57 (t, 2H, *J* = 7.2 Hz), 7.37-7.26 (m, 7H), 7.19 (s, 1H), 6.45 (d, 1H, *J* = 8.0 Hz), 4.38 (s, 4H), 3.88 (s, 4H). ^{13}C NMR (100 MHz, DMSO-*d6*) δ: 182.69, 158.57, 147.59, 147.06, 137.82, 137.49, 136.80, 136.15, 135.82, 131.31, 128.13, 126.06, 125.10, 123.85, 123.78, 123.00, 122.70, 122.27, 121.07, 116.17, 104.28, 103.74, 100.13, 63.44, 57.84, 41.85. Anal. Calcd. For $C_{36}H_{23}BrFN_3O_4$: C, 65.47; H, 3.51; N, 6.36; found: C, 65.62; H, 3.59; N, 6.50.

10-(3-Fluoro-4-morpholinophenyl)-3,3,6,6-tetramethyl-3,4,6,7-tetrahydro-2*H*-spiro[acridine-9,3'-indoline]-1,2',8(5*H*,10*H*)-trione (10a)

Colour: White. M. P. 290-292 ℃. IR (KBr, cm^{-1}): 3264, 2864, 1717, 1683. ^{1}H NMR (400 MHz, DMSO-*d6*) δ: 10.00 (s, 1H), 7.64 (d, 1H, *J* = 8.0 Hz), 7.50 (d, 1H, *J* = 7.6 Hz), 7.35 (t, 1H, *J* = 7.2 Hz), 7.21 (t, 1H, *J* = 7.2 Hz), 6.98 (d, 2H, *J* = 8.0 Hz), 6.70 (d, 1H, *J* = 8.0 Hz),

4.90 (s, 4H), 3.57 (s, 4H), 2.74-2.39 (m, 8H), 0.97 (s, 6H), 0.90 (s, 6H). Anal. Calcd. For $C_{34}H_{36}FN_3O_4$: C, 71.69; H, 6.37; N, 7.38; found: C, 71.96; H, 6.43; N, 7.67.

5'-Chloro-10-(3-fluoro-4-morpholinophenyl)-3,3,6,6-tetramethyl-3,4,6,7-tetrahydro-2*H*-spiro[acridine-9,3'-indoline]-1,2',8(5*H*,10*H*)-trione (10b)

Colour: White. M. P. 282-285 °C. IR (KBr, cm^{-1}): 3366, 2907, 1719, 1682. ^1H NMR (400 MHz, DMSO-*d6*) δ: 10.09 (s, 1H), 7.73 (d, 1H, *J* = 8.0 Hz), 7.50 (d, 1H, *J* = 7.6 Hz), 7.44 (t, 1H, *J* = 7.2 Hz), 7.30 (t, 1H, *J* = 7.2 Hz), 7.00 (d, 1H, *J* = 8.0 Hz), 6.79 (d, 1H, *J* = 8.0 Hz), 4.99 (s, 4H), 3.66 (s, 4H), 2.73-2.38 (m, 8H), 1.02 (s, 6H), 0.95 (s, 6H). Anal. Calcd. For $C_{34}H_{35}ClFN_3O_4$: C, 67.60; H, 5.84; N, 6.96; found: C, 67.47; H, 5.75; N, 6.78.

5'-Bromo-10-(3-fluoro-4-morpholinophenyl)-3,3,6,6-tetramethyl-3,4,6,7-tetrahydro-2*H*-spiro[acridine-9,3'-indoline]-1,2',8(5*H*,10*H*)-trione (10c)

Colour: White. M. P. 275-277 °C. IR (KBr, cm^{-1}): 3355, 2865, 1739, 1685. ^1H NMR (400 MHz, DMSO-*d6*) δ: 10.05 (s, 1H), 7.70 (d, 1H, *J* = 8.0 Hz), 7.55 (d, 1H, *J* = 7.6 Hz), 7.40 (t, 1H, *J* = 7.2 Hz), 7.26 (t, H, *J* = 7.2 Hz), 7.03 (d, 1H, *J* = 8.0 Hz), 6.75 (d, 1H, *J* = 8.0 Hz), 4.95 (s, 4H), 3.62 (s, 4H), 2.80-2.41 (m, 8H), 1.06 (s, 6H), 1.01 (s, 6H). Anal. Calcd. For $C_{34}H_{35}BrFN_3O_4$: C, 62.96; H, 5.44; N, 6.48; found: C, 62.64; H, 5.51; N, 6.40.

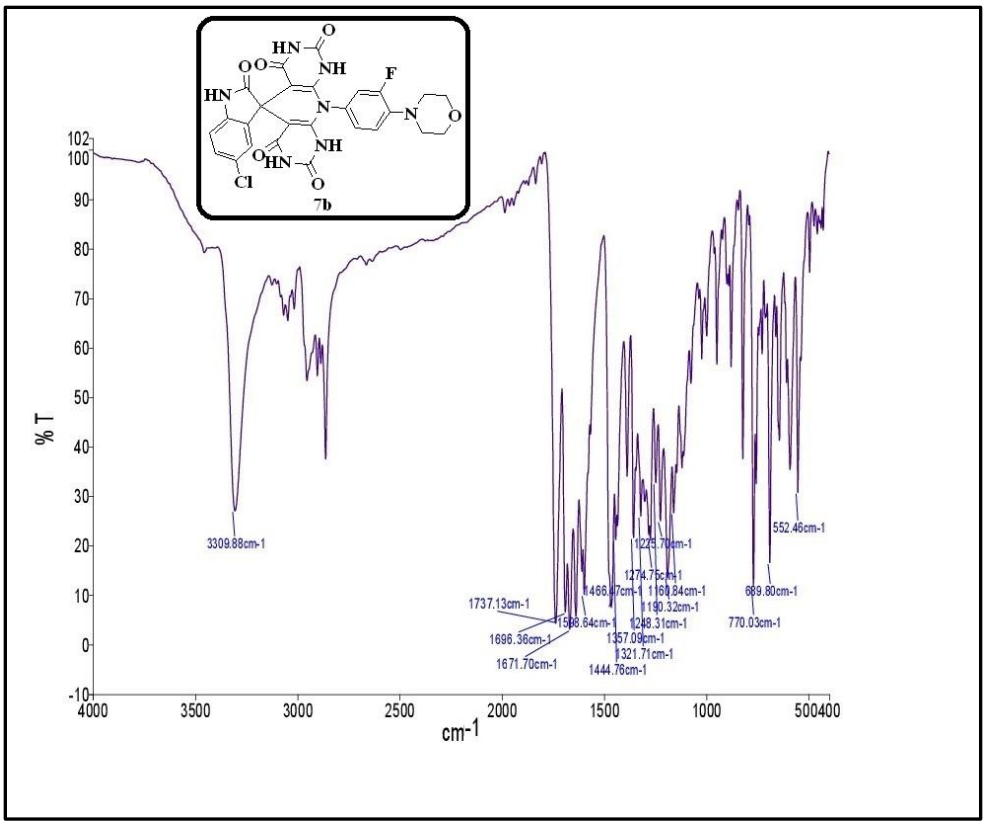

IR spectrum of the compound **7b**

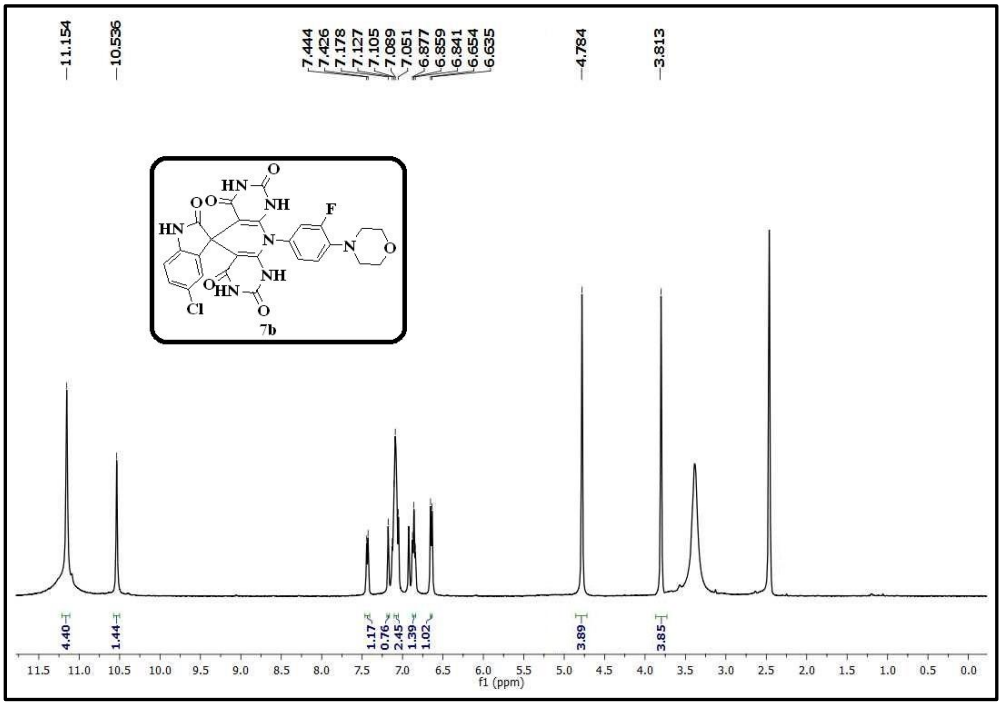

^{1}H NMR spectrum of the compound **7b**

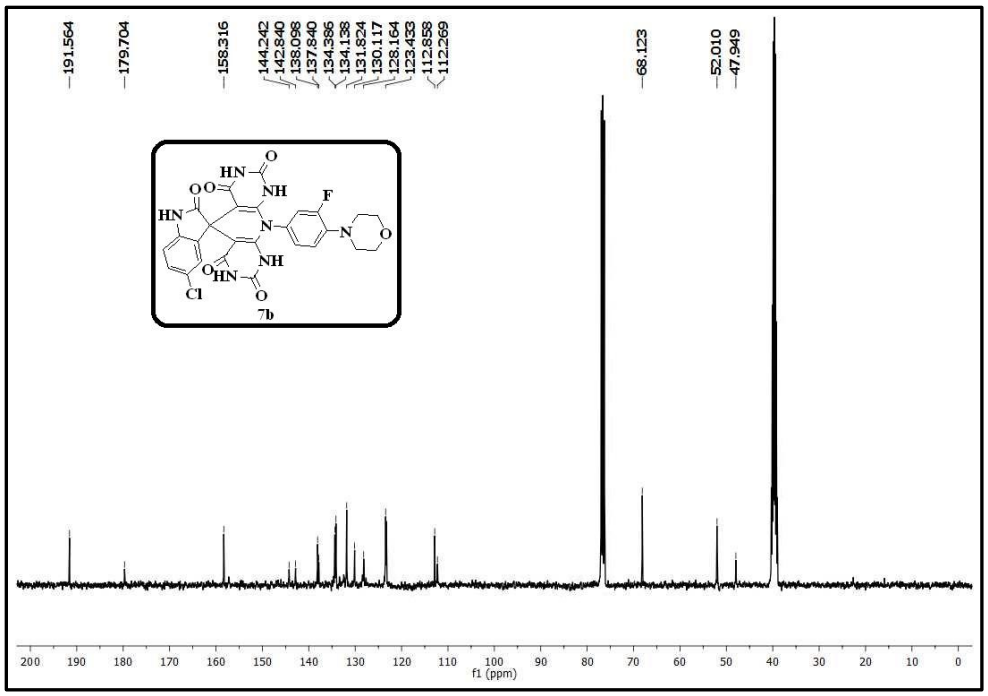

^{13}C NMR spectrum of the compound **7b**

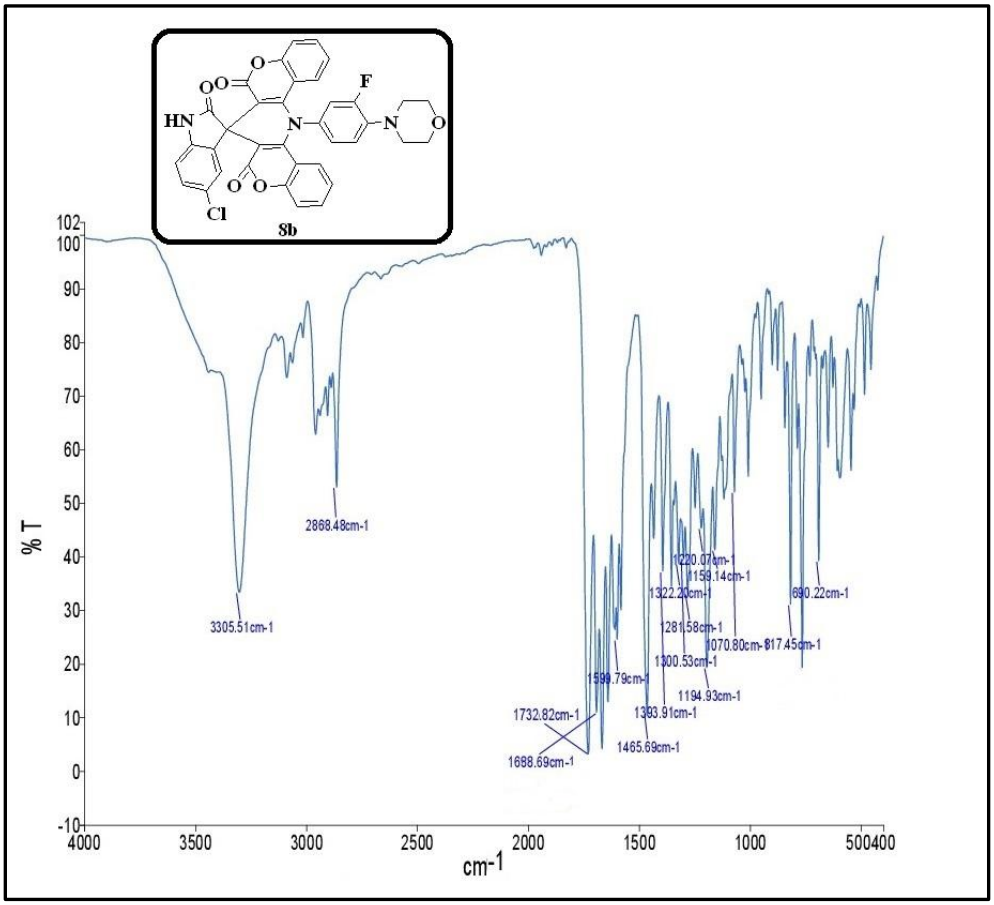

IR spectrum of the compound **8b**

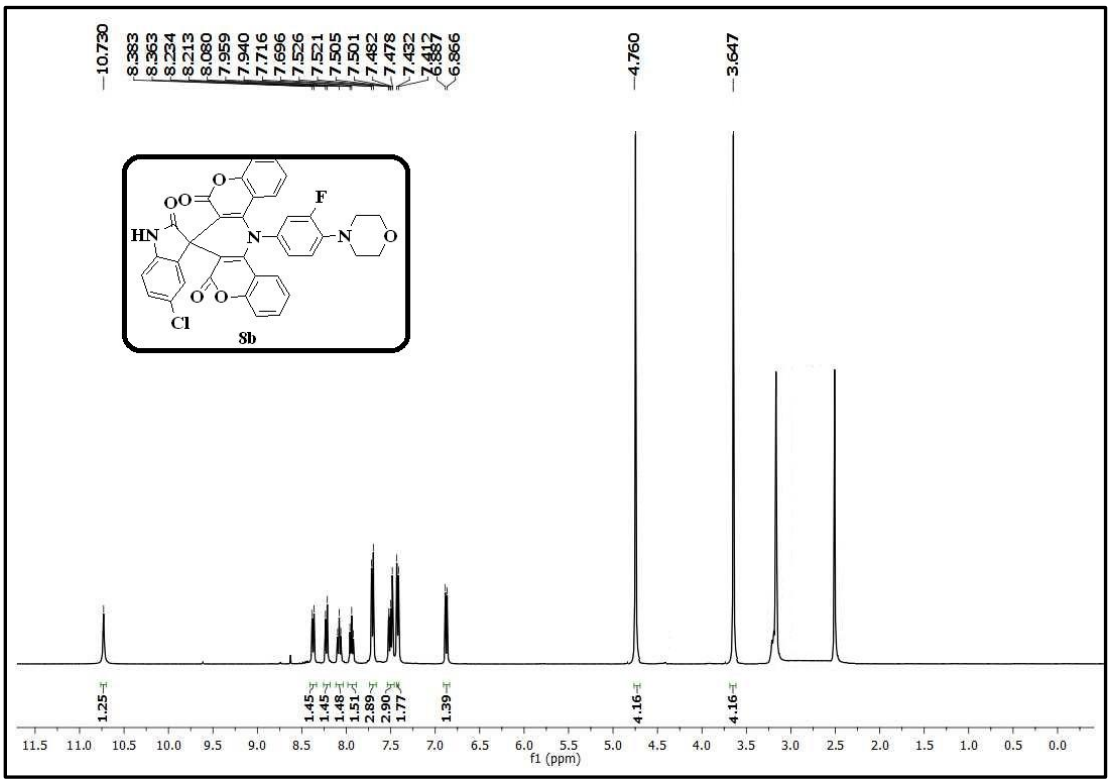

^{1}H NMR spectrum of the compound **8b**

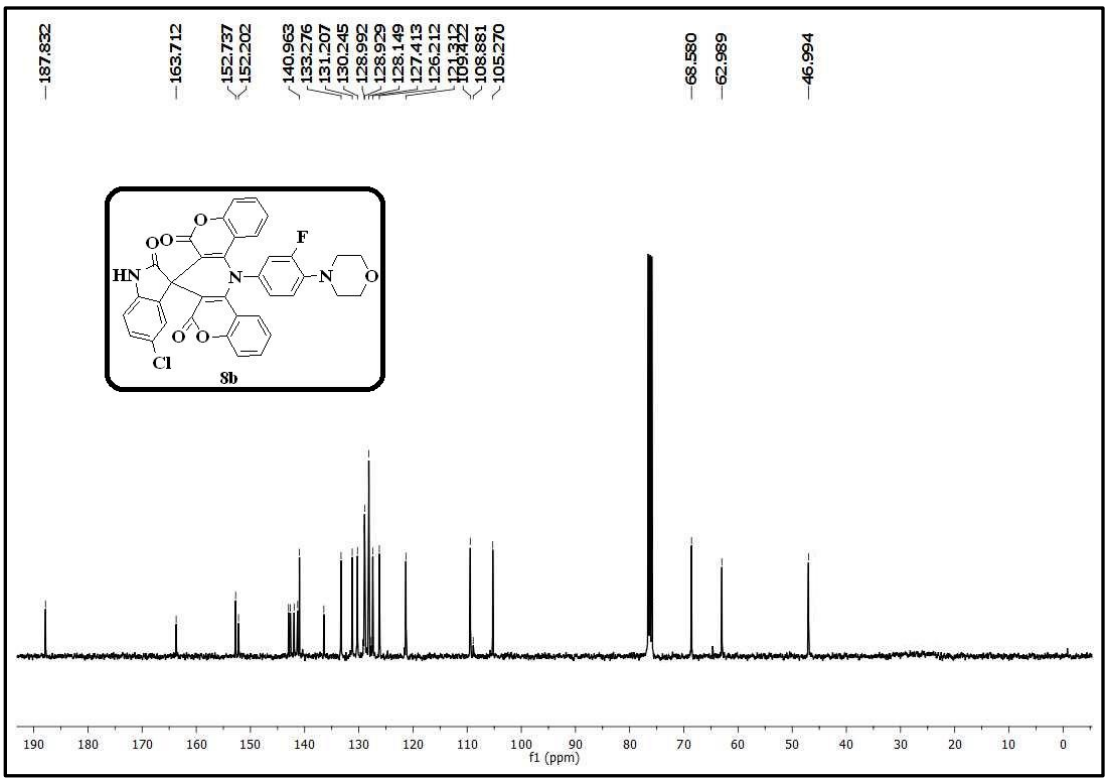

^{13}C NMR spectrum of the compound **8b**

Experimental Section

Materials and methods

All the melting points were recorded by using Stuart SMP30 melting point apparatus and were uncorrected. ^{1}H NMR and ^{13}C NMR spectra were recorded in DMSO-*d*6 and $CDCl_3$ using TMS as an internal standard on a Bruker Avance III HD 400 MHz instrument and the chemical shift values were reported in ppm. Mass spectra were recorded on Joel JMSD-300 spectrometer. Progress and purity of the reactions were monitored by Thin-Layer chromatography (E. Merck, Mumbai, India) and the developed chromatogram was visualized under UV light and iodine vapors. Unless otherwise stated, all the chemicals and solvents used were of high grade and purchased from Sigma-Aldrich and spectrochem. Elemental analysis was performed on an Elementar Vario EL III analytical unit and the values were ± 0.4% of theoretical values. The deep eutectic solvent $ZnCl_2$+Urea was prepared using a literature procedure [54].

Biological assay

MTT assay

The *in vitro* anticancer activity of the synthesized compounds were assayed against four different human cancer cell lines i.e., alveolar carcinoma (A549), breast cancer cell line (MCF7), cervical cancer line (HeLa) and human embryonic kidney 293 cell line (HEK293T). *Cis*-platin was used as standard drug. The cell viability in the presence of the test samples was measured by MTT-micro cultured tetrazolium assay [55, 56]. This assay is a quantitative colorimetric method for the determination of cell viability. The assessed parameter is the metabolic activity of viable cells. Metabolically active cells reduce pale yellow tetrazolium salt (MTT) to a dark blue water-insoluble formazan, which can be directly quantified after solubilization in DMSO. The absorbance of the formazan directly correlates with the number of viable cells. The A549, MCF-7 and HEK293T cells were plated into a 96-well plate at a density 1 x 10^4 cells/well. The Cells were grown overnight in the full medium and then switched to the low serum media. The 1% DMSO was used as a control. After 48h of the treatment with different concentrations of the test compounds, the cells were incubated with MTT (2.5 mg/mL) in the CO_2 chamber for 2h. The medium was then removed and 100 mL

of DMSO was added to each well to dissolve formazan crystals. After thorough mixing, the plates were read at 570 nm for optical density, which is directly correlated with the cell quantity. The results were represented as a percentage of viability. All the experiments were carried out in triplicates. The relationship between surviving fraction and drug concentration was plotted to obtain the survival curves of IMR32, A549, MCF7 and HEK293T. The IC_{50} values were calculated by using linear regression analysis from the graph pad prism (5.02 version) (P values are significant <0.001). The response parameter calculated was IC_{50} value, which corresponds to the concentration required for the 50% inhibition of the cell viability.

Antioxidant activity

The free radical scavenging capacity of the synthesized compounds was determined by using DPPH (1,1-Diphenyl-2-picrylhydrazyl) free radical method described in the literature [57-59]. Ascorbic acid was used as a standard to measure the efficiencies of the synthesized compounds. 0.2 mM solution of DPPH was prepared in 100% methanol. The required amount of ascorbic acid was dissolved in 100% methanol to prepare 1 mM solution and the test compounds were dissolved in 0.2% DMSO and methanol to prepare 1 mM stock solutions. From the stock solutions, different concentrations (3, 10, 30 and 100 µM) of solutions were prepared by diluting with methanol. 1 mL of each compound solution was added to the 3 mL of DPPH solution. After 30min, the absorbance of the solutions at 517 nm (A_1) was recorded using UV–Visible spectrophotometer. As a control, the absorbance of the blank solution of DPPH without test compound was also determined at 517 nm (A_0). The following equation was used for the calculation of the percentage (%) of scavenging activity.

$$\text{Scavenging Activity (\%)} = \frac{A_0 - A_1}{A_0} \times 100$$

Where A_0 is the absorbance of DPPH in the absence of antioxidant and A_1 is the absorbance of DPPH in the presence of an antioxidant. IC_{50} values were also calculated for the compounds.

Antimicrobial activity assay

The antibacterial and antifungal activity of all the synthesized compounds, were tested against two gram-positive bacteria (*Bacillus subtilis* and *Staphylococcus aureus*) and two gram-negative bacteria (*Escherichia coli* and *Pseudomonas aeruginosa*) and two fungal

strains, (*Aspergillus niger* and *Penicillium notatum*) using disc diffusion method [60]. On using Whatmann (No. 1) paper, 6 mm diameter sterile antibiotic discs were placed over the nutrient agar medium. 100 μg/mL concentrated compounds were transferred to each disc with the help of micropipette (Initially compounds were dissolved in DMSO); subsequently bacteria and fungi were incubated overnight at 37 ℃ and 25 ℃, respectively. The zone of inhibition was determined in mm and distinguished by using standard antibiotics. The DMSO was used as a negative control, while streptomycin 30 μg/disc (standard antibiotic) and standard antifungal drug Ketoconazole (10 μg/disc) were used as the positive controls. All the tests were carried out in triplicates and the average zone of inhibition was recorded and minimum inhibitory concentration (MIC) values for the tested compounds and standards were measured in μg/mL and tabulated their mean values.

Molecular Docking protocol

In silico docking studies are useful tools to assess the binding affinity of the ligand-protein receptor. The synthesized compounds were subjected to molecular docking by using the AutoDock Tools (ADT) version 1.5.6 and AutoDock version 4.2.5.1 docking program [61]. The 3D-structures of all the synthesized compounds were prepared by using chem3D pro 12.0 software. The optimized 3D structures were saved in .pdb format. The structures of the proteins were extracted from the protein data bank (http://www.rcsb.org/pdb). The bound ligand and water molecules in protein were removed by using Discovery Studio Visualizer version 4.0 to prepare the protein. Nonpolar hydrogens were merged and gasteiger charges were added to the protein. The grid file was saved in .gpf format. The three dimensional grid box having dimensions 60 x 60 x 60 $Å^3$ was created around the protein with spacing 0.3750 Å. The genetic algorithm was carried out with the population size and the maximum number of evaluations were 150 and 25,00,000, respectively. The docking output file was saved as Lamarckian Ga (4.2) in .dpf format. The ligand-protein complex binding sites were visualized by Discovery Studio Visualizer version 4.0.

References

1) F. Cardellini, M. Tiecco, R. Germani, G. Cardinali, L. Corte, L. Roscini, N. Spreti, *RSC Adv*. **2014**, *4*, 55990.

2) M. Francisco, A. V. D. Bruinhorst, M. C. Kroon, *Green Chem.* **2012**, *14*, 2153.

3) A. M. Zonouz, I. Eskandari, H. R. Khavasi, *Tetrahedron Lett*. **2012**, *53*, 5519.

4) T. Welton, *Chem. Rev.* **1999**, *99*, 2071.

5) L. I. N. Tomé, V. Baião, W. D. Silva, C. M. A. Brett, *Applied Mater. Today.* **2018**, *10*, 30.

6) M. Francisco, A. V. D. Bruinhorst, M. C. Kroon, *Angew. Chem. Int. Ed.* **2013**, *52*, 3074.

7) B. Yu, D. Q. Yu, H. M. Liu, *Eur. J. Med. Chem.* **2015**, *97*, 673.

8) Y. Arun, K. Saranraj, C. Balachandran, P. T. Perumal, *Eur. J. Med. Chem.* **2014**, *74*, 50.

9) C. Chen, C. Lv, J. Liang, J. Jin, L. Wang, C. Wu, R. Shen, *Molecules.* **2017**, *22*, 1295.

10) M. S. Ghasemzadeh, B. Akhlaghinia, *Chemistry Select*. **2018**, *3*, 3161.

11) D. Ashok, M. G. Devulapally, V. K. Aamate, S. Gundu, S. Adam, S. D. S. Murthy, S. Balasubramanian, B. Naveen, T. Parthasarathy, *J. Mol. Struct.* **2019**, *1177*, 215.

12) K. Parthasarathy, C. Praveen, J. C. Jeyaveeran, A. A. M. Prince, *Bioorg. Med. Chem. Lett.* **2016**, *26*, 4310.

13) M. R. Yousefi, O. G. Jolodar, F. Shirini, *Bioorg. Chem.* **2018**, *81*, 326.

14) D. R. Chandam, A. A. Patravale, S. D. Jadhav, M. B. Deshmukh, *J. Mol. Liq.* **2017**, *240*, 98.

15) K. Niknam, A. Ebrahimpour, A. Barmak, G. Mohebbi. *Montasch. Chem.* **2018**, *149*, 73.

16) L. Gao, Y. Zha, S. Tao, Y. Gao, M. Chen, L. Jiang, L. Rong, *Res. Chem. Intermed.* **2015**, *41*, 5627.

17) M. R. Salek, M. A. Zolfigol, M. Zarei, *Res. Chem. Intermed.* **2018**, *44*, 5255.

18) R. Joshi, A. Kumawat, S. Singh, T. K. Roy, T.T. Pardasanic, *J. Heterocyclic Chem.* **2018**, *55*, 1783.

19) E. L. Smith, A. P. Abbott, K. S. Ryder, *Chem. Rev*. **2014**, *114*, 11060.

20) A. Abbott, R. C. Harris, K. S. Ryder, C. D. Agostino, L. F. Gladden, M. D. Mantle, *Green Chem*. **2011**, *13*, 82.

21) G. Imperato, E. Eibler, J. Niedermaier, B. König, *Chem. Commun.* **2005**, *36*, 1170.

22) S. Gore, S. Baskaran, B. König, *Green Chem.* **2011**, *13*, 1009.

23) F. Ilgen, B. König, *Green Chem.* **2009**, *11*, 848.

24) A. P. Abbott, J. Collins, I. Dalrymple, R. C. Harris, R. Mistry, F. Qiu, J. Scheirer, W. R. Wise, *Australian J. Chem.* **2009**, *62*, 341.

25) C. A. Nkuku, R. J. LeSuer, *J. Physic. Chem. B.* **2007**, *111*, 13271.

26) M. Figueiredo, C. Gomes, R. Costa, A. Martins, C. M. Pereira, F. Silva, *Electrochim. Acta*. **2009**, *54*, 2630.

27) H. R. Jhong, D. S. H. Wong, C. C. Wan, Y. Y. Wang, T. C. Wei, *Electrochem. Commun.* **2009**, *11*, 209.

28) J. T. Gorke, F. Srienc, R. J. Kazlauskas, *Chem. Commun.* **2008**, *10*, 1235.

29) R. V. Sumesh, A. Shylaja, R. R. Kumar, A. I. Almansour, R. S. Kumar, *Tetrahedron Lett*. **2018**, *59*, 4086.

30) (a) M. A. Alil, R. Ismail, T. S. Choon, R. S. Kumar, H. Osman, N. Arumugam, A. I. Almansour, K. Elumalai, A. Singh, *Bioorg. Med. Chem. Lett.* **2012**, *22*, 508; (b) P. Prasanna, K. Balamurugan, S. Perumal, P. Yogeeswari, D. Sriram, *Eur. J. Med. Chem.* **2010**, *45*, 5653; (c) A. Dandia, S. Khan, P. Soni, A. Indora, D. K. Mahawar, P. Pandya, C. S. Chauhan, *Bioorg. Med. Chem. Lett.* **2017**, *27*, 2873.

31) H. Shao, X. W. Huang, L. Song, W. T. Zhou, G. P. Tang, L. Ye, *Tetrahedron Lett*. **2018**, *59*, 3088.

32) R. Sakhuja, S. S. Panda, L. Khanna, S. Khurana, S. C. Jain, *Bioorg. Med. Chem. Lett.* **2011**, *21*, 5465.

33) S. Y. Kim, H. B. Park, J. H. Cho, K. H. Yoo, C. H. Oh, *Bioorg. Med. Chem. Lett.* **2009**, *19*, 2558.

34) S. Rapposelli, M. C. Breschi, V. Calderone, M. Digiacomo, A. Martelli, L. Testai, M. Vanni, A. Balsamo, *Eur. J. Med. Chem.* **2011**, *46*, 966.

35) L. Ye, T. Tian, Z. H. Li, H. Jin, Z. G. Zhu, S. Wan, J. Zhang, P. Yu, J. Zhang, S. Wu, *Eur. J. Med. Chem.* **2012**, *50*, 370.

36) K. De, A. Bhaumik, B. Banerjee, C. Mukhopadhyay, *Tetrahedron Lett*. **2015**, *56*, 1614.

37) M. N. Elinson, A. N. Vereshchagin, N. O. Stepanov, P. A. Belyakov, G. I. Nikishin, *Tetrahedron Lett.* **2010**, *51*, 6598.

38) M. Bayat, Z. Amiri, *Tetrahedron Lett*. **2017**, *58*, 4260.

39) X. Huang, Y. R. Zhang, X. S. Li, D. C. Xu, J. W. Xie, *Tetrahedron Lett.* **2013**, *54*, 5857.

40) J. Sebastian, R. G. Richards, M. P. Walker, J. F. Wiesen, Z. Werb, R. Derynck, Y. K. Hom, G. R. Cunha, R. P. Di Augustine, *Cell Growth Differ.* **1998**, *9*, 777.

41) J. H. Park, Y. Liu, M. A. Lemmon, R. Radhakrishnan, *Biochem. J.* **2012**, *448*, 417.

42) M. J. Frisch, G. W. Trucks, H. B. Schlegel, G. E. Scuseria, M. A. Robb, J. R. Cheeseman, G. Scalmani, V. Barone, B. Mennucci, G. A. Petersson, *Gaussian 09, Gaussian, Inc, Wallingford CT.* **2009**.

43) N. Foloppe, A. D. MacKerell, *J. Comput. Chem.* **2000**, *21*, 86.

44) C. M. Breneman, K. B. Wiberg, *J. Comput. Chem.***1990**, *11*, 361.

45) J. McBryan, J. Howlin, S. Napoletano, F. Martin, *J. Mammary Gland Biol. Neoplasia*, **2008**, *13*, 159.

46) M. D. Sternlicht, S. W. Sunnarborg, *J. Mammary Gland Biol. Neoplasia.* **2008**, *13*, 181.

47) F. Walker, L. Abramowitz, D. Benabderrahmane, X. Duval, D. Descatoire, D. Hénin, T. Lehy, T. Aparicio, *Hum. Pathol.* **2009**, *40*,1517.

48) T. J. Lynch, D. W. Bell, R. Sordella, S. Gurubhagavatula, R. A. Okimoto, B. W. Brannigan, P. L. Harris, S. M. Haserlat, J. G. Supko, F. G. Haluska, D. N. Louis, D. C. Christiani, J. Settleman, D. A. Haber, *N. Engl. J. Med.* **2004**, *350*, 2129.

49) C. Jost, J. Schilling, R. Tamaskovic, M. Schwill, A. Honegger, A. Pluckthun, *Structure.* **2013**, *21*, 1.

50) Y. Yarden, M. X. Sliwkowski, *Nat. Rev. Mol. Cell Biol.* **2001**, *2*, 127.

51) R. J. Craven, H. Lightfoot, W. G. Cance, *Surg. Oncol.* **2003**, *12*, 39.

52) N. Buza, D. M. Roque, A. D. Santin, *Arch. Pathol. Lab. Med.* **2014**, *138*, 343.

53) A. D. Santin, S. Bellone, J. J. Roman, J. K. McKenney, S. Pecorelli, *Int. J. Gynecol. Obstet.* **2008**, *102*, 128.

54) N. Seyedi, H. Khabazzadeh, S. Saeednia, *Synth. React. Inorg. Metal-Org. Nano-Metal Chem.* 2015, *45*, 1501.

55) P. Skehan, R. Storeng, D. Scudiero, A. Monks, J. McMohan, D. Vistica, J. T. Warren, H. Bokesch, S. Kenncy, M. R. Boyd, *J. Natl. Cancer Inst*. **1990**, *82*, 1107.

56) A. Monks, D. Scudiero, P. Skehan, R. Shoemaker, K. Paull, D. Vistica, C. Hose, J. Langley, P. Cromise, *J. Natl. Cancer Inst*. **1991**, *83*, 757.

57) A. Braca, N. D. Tommasi, L. D. Bari, C. Pizza, M. Politi, I. Morelli, *J. Nat. Prod*. **2001**, *64*, 892.

58) M. R. Saha, S. M. R. Hasan, R. Akter, M. M. Hossain, M. S. Alamb, M. A. Alam, M. E. H. Mazumder, *Bangl. J. Vet. Med*. **2008**, *6*, 197.

59) M. S. Blois, *Nature*. **1958**, *181*, 1199.

60) A. W. Bauer, W. M. Kirby, J. C. Sherris, M. Turck, *Am. J. Clin. Pathol.* **1966**, *45*, 493.

61) http://autodock.scripps.edu/resources/references.

SUMMARY

CHAPTER-I

Introduction

In this chapter, a brief introduction and the biological importance of various spiro heterocyclic compounds is discussed. For the last afew decades, heterocyclic chemistry occupied a major area in organic chemistry. Among the heterocyclic compounds, spiro heterocyclic compounds are described as one of the important class of organic compounds, due to their unique structural features and a wide range of biological activities [1]. Initially, these compounds were isolated from biological origins [2]. Spiro compounds exhibit diversified pharmacological properties like antiviral, antitumor, antibiotic, anticancer, antimycobacterial, antiinflammatory, etc., [3-5]. These wide range of applications of the spiro heterocyclic scaffolds prompted us to synthesize the new spiro heterocyclic scaffolds by amalgamating with one or more pharmacophore units by employing solvent-free conditions, conventional and non-conventional methods.

The literature survey of the present study are presented in the chaptaer I. The chapters II-VI deal with the synthesis of the compounds using multicomponent approach. The biological activities, namely anticancer, antioxidant, antimicrobial, molecular docking studies have also been studied. The chapters II-IV comprised with the 1,3-dipolar cycloaddition reaction. The synthesis of the compounds presented in chapter V was based on the Betti-reaction. The chapter VI describes the synthesis of various spirooxindoles using deep eutectic solvent $ZnCl_2$+Urea. The majority of the spiro compounds described in the thesis were synthesized under the conventional method. However, spiro compounds included in the chapter IV were synthesized by employing the ultrasonication method.

The structures of the synthesized compounds were characterized by FTIR, NMR and Mass spectral methods and also single crystal X-ray diffraction (Chapters II, IV, and V). The MTT assay was carried out for the evaluation of anticancer activity of the target compounds presented in the chapters II-III and VIB by using *cis*-platin as a standard drug. The antioxidant activity of the target compounds in the chapters II-V and VIB were carried out by using DPPH (1,1-diphenyl-2-picrylhydrazyl free radical) method with ascorbic acid as a standard drug. The disc diffusion method was used for the antimicrobial evaluation of the target compounds discussed in chapters III-V and VIB. Streptomycin (Chapters III-IV and

VIB) and ciprofloxacin (Chapter-V) were used as standard drugs for antibacterial activity. Ketoconazole was used as a standard drug for antifungal activity. The molecular docking studies were carried out by using AutoDock Tools (ADT) version 1.5.6 and AutoDock version 4.2.5.1 docking program.

CHAPTER-II (SECTION-A)

Multicomponent regioselective synthesis of quinolinyl spiropyrrolizidines *via* 1,3-dipolar cycloaddition and biological evaluation

Quinoline moiety based scaffolds play a vital role in medicinal chemistry because of their wide occurrence in natural products and a broad spectrum of biological activities [6].

An equimolar mixture of ninhydrin **1**, L-proline **2** and dipolarophiles **3a-g** in methanol at room temperature for 30-90min, produce the target compounds **4a-g** (Scheme 2A.1). Similarly, 11*H*-indeno[1,2-*b*]quinoxalin-11-one **5,** L-proline **2** and dipolarophiles **3a-g** in methanol under reflux condition for 3-5h to produce the target compounds **6a-g** (Scheme 2A.1). The crystal structures of the compounds **4e** and **6a** were shown in figure 2A.1.

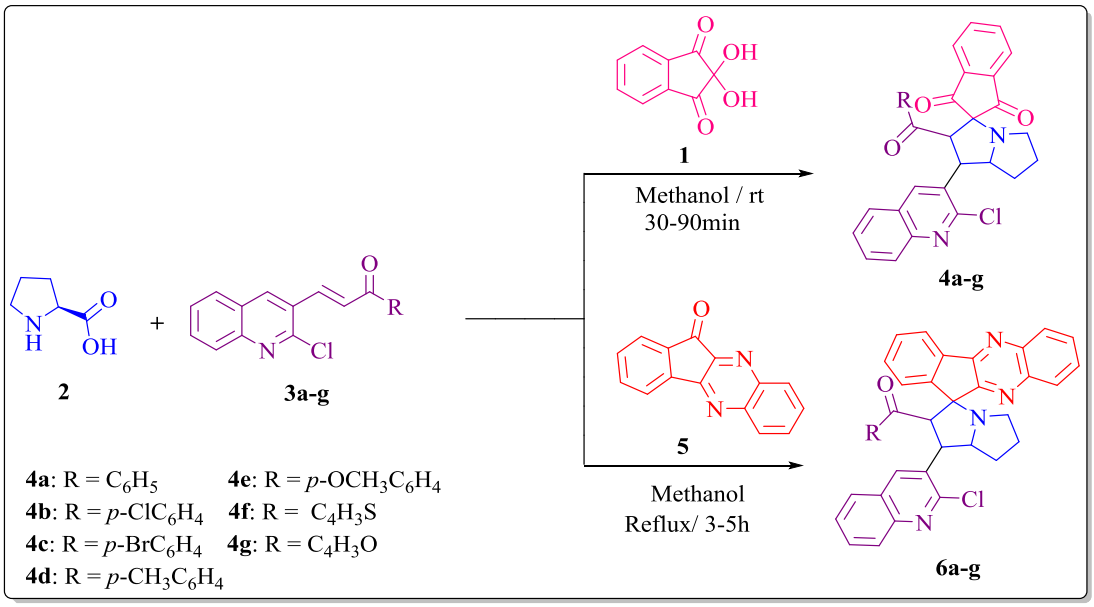

Scheme 2A.1. Synthesis of the spirooxindolopyrrolizidines **4a-g** and **6a-g**.

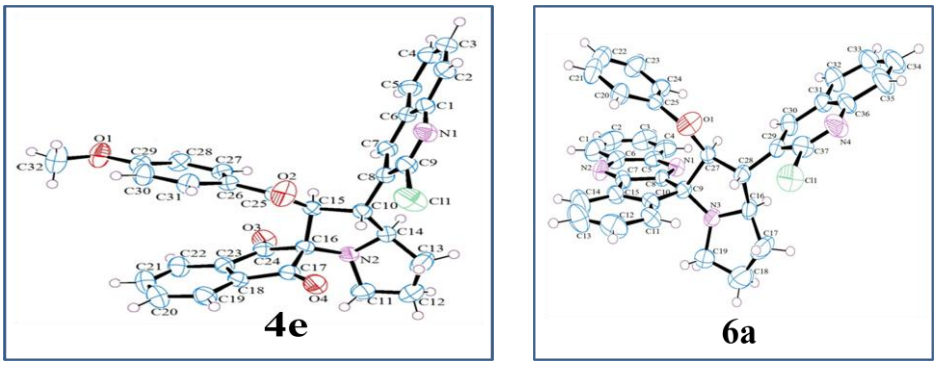

Figure 2A.1. The ORTEP representation of the compounds **4e** and **6a**. The asymmetric units of the compound **4e** shows only one enantiomer having the configurations at the chiral centers C10 (R), C14 (R) and C15 (S). The Asymmetric units of compound **6a** shows only one enantiomer having the configurations at the chiral centers C9 (R), C16 (R), C27 (S) and C28 (R).

Anticancer activity

Among the target compounds **4a-g** and **6a-g**, the compound **6f** showed significant activity against A549 cell line with IC_{50} value 12.18 ± 0.44 µM.

Antioxidant activity

Among all the synthesized compounds, the compound **6f** exhibited potent antioxidant activity with IC_{50} value 8.64 ± 0.43 µM. The compound **6e (**12.33 ± 0.72 µM**)** exhibited significant antioxidant activity.

Molecular docking studies

The comparative molecular docking studies with target scaffolds **4a-g** and **6a-g** unambiguously confirm that the receptor IDO1 (PDB ID: 2D0U) is better than that of the receptors ALK (PDB ID: 2XP2) and EGFR (PDB ID: 4HJO). Among all the synthesized compounds, the compound **6f** exhibited the least binding energy −11.83 kcal/mol and form one hydrogen bond with the receptor IDO1. Its best docking poses were shown in figure 2A.2.

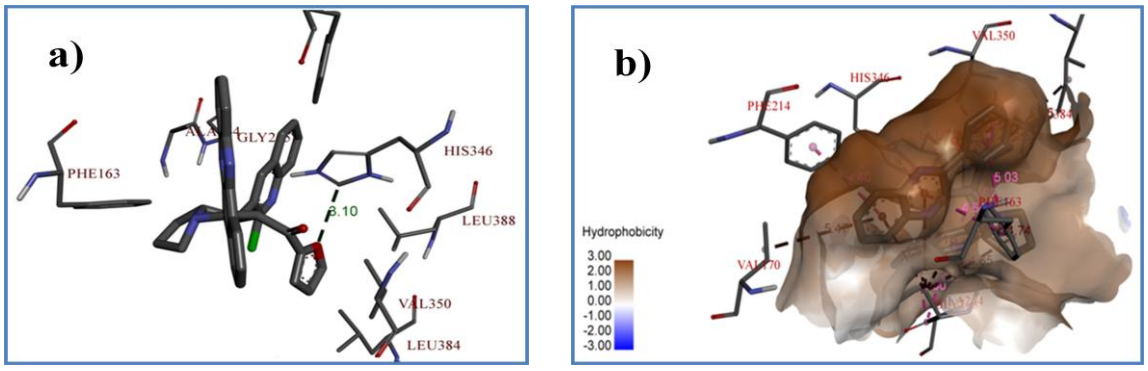

Figure 2A.2. The best docking poses of the compound **6f** with protein IDO1. a) The hydrogen bonding interaction, b) The hydrophobic interaction.

CHAPTER-II (SECTION-B)

Facile and efficient synthesis of 2-oxoquinolinyl spiropyrrolidines and pyrrolizidines *via* 1,3-dipolar cycloaddition reaction and biological evaluation

The combination of the quinoline or its derivatives with other compounds may increase their biological activity or create a new medicinal property like antitumor activity, cytotoxic towards leukemia P388 cells, etc., [7].

An equimolar mixture of isatin derivatives **1a-c**, L-proline **2** and quinolinyl chalcones **3a-g** were refluxed in ethanol for 2-5h and produce the target compounds **4a-u** (Scheme 2B.1). The crystal structure of the compound **4d** was shown in figure 2B.1.

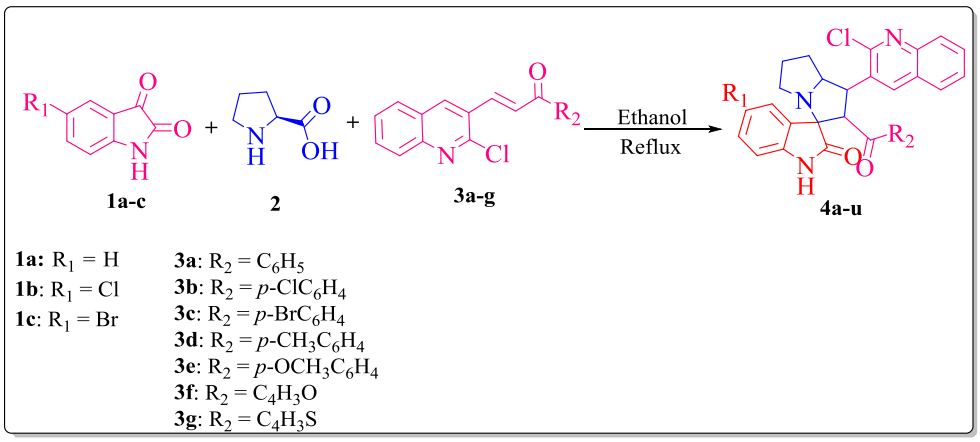

Scheme 2B.1. Synthesis of the spirooxindolopyrrolizidines **4a-u**.

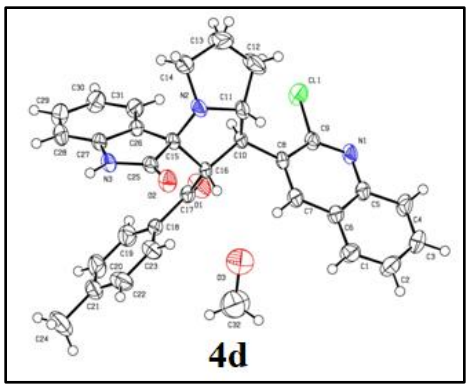

Figure 2B.1. The ORTEP representation of the compound **4d** (methanol solvate). The asymmetric units of compound **4d** shows only one enantiomer having the configurations at the chiral centers C10 (R), C11 (R), C15 (R) and C16 (S).

Anticancer activity

Among all the synthesized compounds, the compound **4q** exhibited excellent activity against IMR32, A549 and MCF7 cell lines with IC_{50} values 9.60 ± 0.101 µM, 11.01 ± 0.445 µM and 10.49 ± 0.411 µM respectively.

Antioxidant activity

Among all the compounds, compound **4p** and **4q** exhibited potent antioxidant activity with the IC_{50} values 9.02 ± 0.42 µM and 7.53 ± 0.37 µM respectively. The compounds **4j (**11.52 ± 0.63 µM**)**, **4k (**12.89 ± 0.07 µM) and **4l (**10.29 ± 0.21 µM**)** exhibited significant antioxidant activity.

Molecular docking studies

The comparative molecular docking studies unveiled that the receptor IDO1 (PDB ID: 2D0U) is better than that of receptors ALK (PDB ID: 4HJO) and EGFR (PDB ID: 2XP2). Among all the synthesized compounds, the compound **4q** exhibited the least binding energy −11.32 kcal/mol and form one hydrogen bond with the receptor IDO1. Its best docking poses were shown in figure 2B.2.

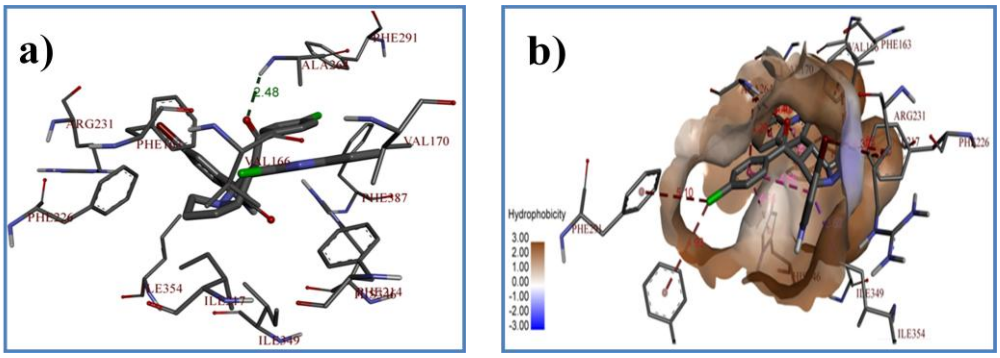

Figure 2B.2. The docking poses of the compound **4q** with the protein IDO1. a) The hydrogen bonding interaction, b) The hydrophobic interaction.

CHAPTER-III (SECTION-A)

Facile and efficient synthesis of 2-oxoquinolinyl spiropyrrolidines and pyrrolizidines *via* 1,3-dipolar cycloaddition and biological evaluation

Spirooxindoles are one of the important classes of the heterocyclic compounds have gained much importance because of their unique structural features, their wide occurrence in several natural/synthetic products and various medicinal properties [1]. Indenoquinoxalines and 2-oxoquinoline have also possessed a wide range of biological applications [8-9].

The target compounds **4a-f** and **6a-f** were synthesized by taking an equimolar mixture of isatin derivatives **1a-f,** sarcosine **3**/L-proline **5** and dipolarophile **2** as substrates (Scheme 3A.1) in 3-5h under reflux condition. On the other hand, the target compounds **8a** and **8b** were synthesized by using an equimolar mixture of 11*H*-indeno[1,2-*b*]quinoxalin-11-one **7**, sarcosine **3**/L-proline **5** and dipolarophile **2** under reflux condition in ethanol for 2-3h (Scheme 3A.2).

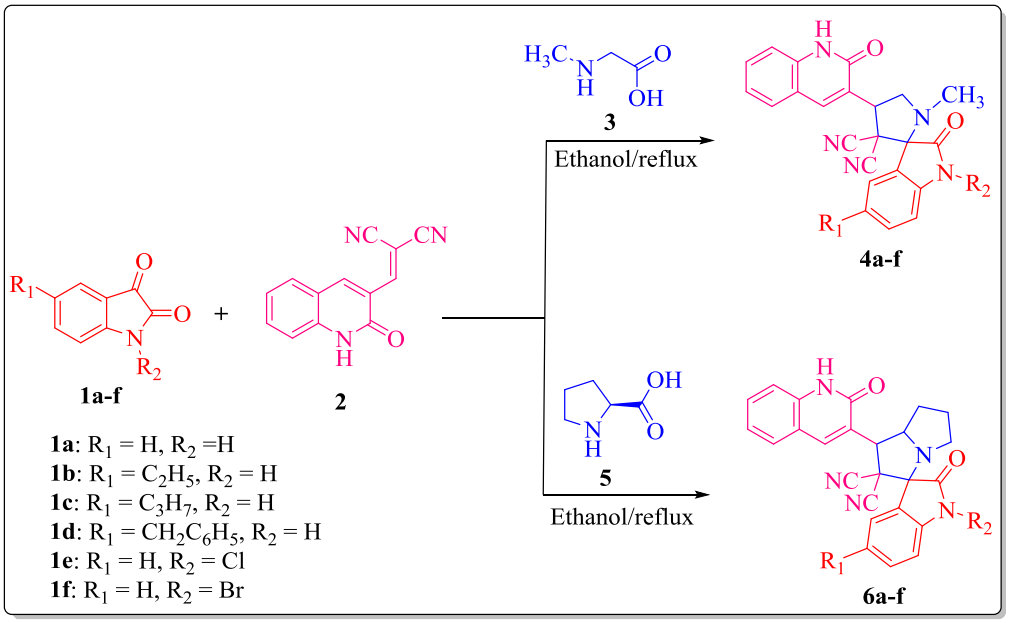

Scheme 3A.1. Synthesis of the spirooxindolopyrrolidines and pyrrolizidines **4a-f** and **6a-f**.

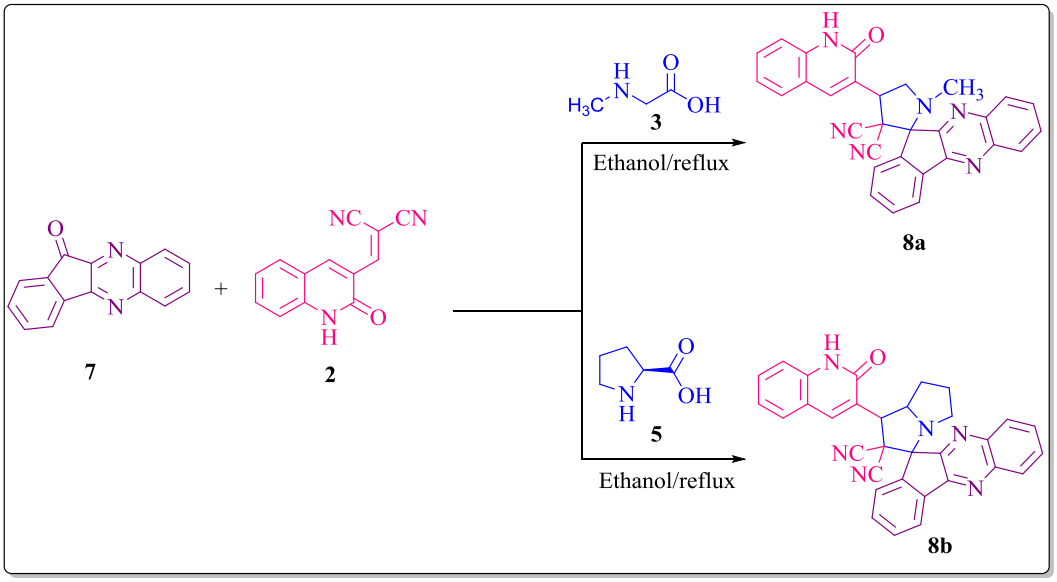

Scheme 3A.2. Synthesis of the spiroquinoxalinopyrrolidines and pyrrolizidines **8a** and **8b**.

Antioxidant activity

The compounds **4f** and **8a** exhibited potent antioxidant activity with the IC_{50} values 7.32 ± 0.18 µM and 4.06 ± 0.35 µM respectively.

Antimicrobial activity

The compound **8a** showed potent antibacterial influence against *B. subtilis*, *S. aureus*, *E. coli* and *P. aeruginosa* with MIC values 7.00 µg/mL, 10.25 µg/mL, 14.50 µg/mL and 17.00 µg/mL respectively and potent antifungal activity against *A. niger* and *P. notatum* with MIC values of 6.25 µg/mL and 8.50 µg/mL respectively. The compound **4a** showed potent activity against *B. subtilis* with MIC value 8.25 µg/mL.

Molecular docking studies

The molecular docking studies univocally suggest that protein HER2 (PDB ID: 3POZ) is better than that of the protein EGFR (PDB ID: 4HJO). Among all the compounds, the compound **4f** exhibited the least binding energy (− 10.53 kcal/mol) and form four hydrogen bonds with the protein HER2. The best docking poses of the compound **4f** was shown in figure 3A.1.

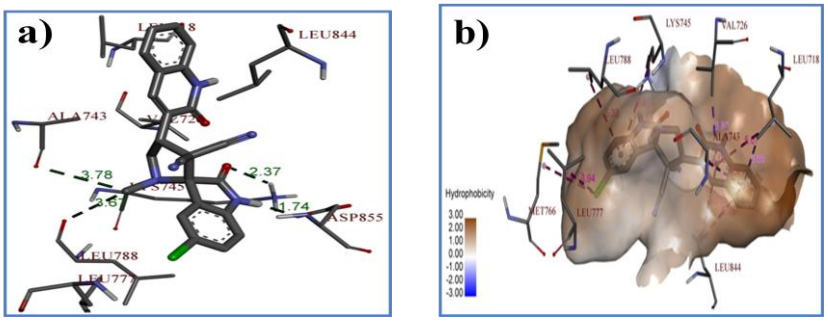

Figure 3A.1. The best docking poses of **4f** with HER2. a) The hydrogen bonding interactions, b) The hydrophobic interactions.

CHAPTER-III (SECTION-B)

One-pot multicomponent 1,3-dipolar cycloaddition approach for the synthesis of tetrazole grafted spiropyrrolidines and pyrrolizidines and biological evaluation

Quinolines and tetrazoles are the important moieties that contain a broad spectrum of biological activities. The tetrazole fused quinolines were known to increase the biological activities of individual precursors [10].

The target compounds **4a-f** and **6a-f** were synthesized from an equimolar mixture of isatin derivatives **1a-f,** sarcosine **3**/L-proline **5** and dipolarophile **2** as substrates (Scheme 3B.1) in 4-6h under reflux condition. On the other hand, the target compounds **8a** and **8b** were synthesized by using an equimolar mixture of 11*H*-indeno[1,2-*b*]quinoxalin-11-one **7**, sarcosine **3**/L-proline **5** and dipolarophile **2** under reflux condition in ethanol for 3-4h (Scheme 3B.2).

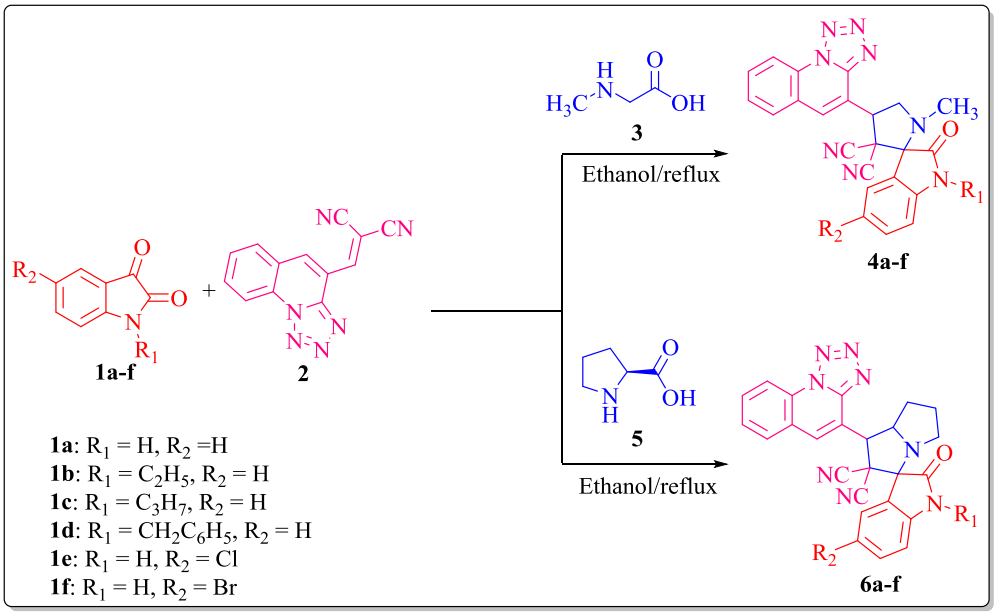

Scheme 3B.1. Synthesis of the spirooxindolopyrrolidines and pyrrolizidines **4a-f** and **6a-f**.

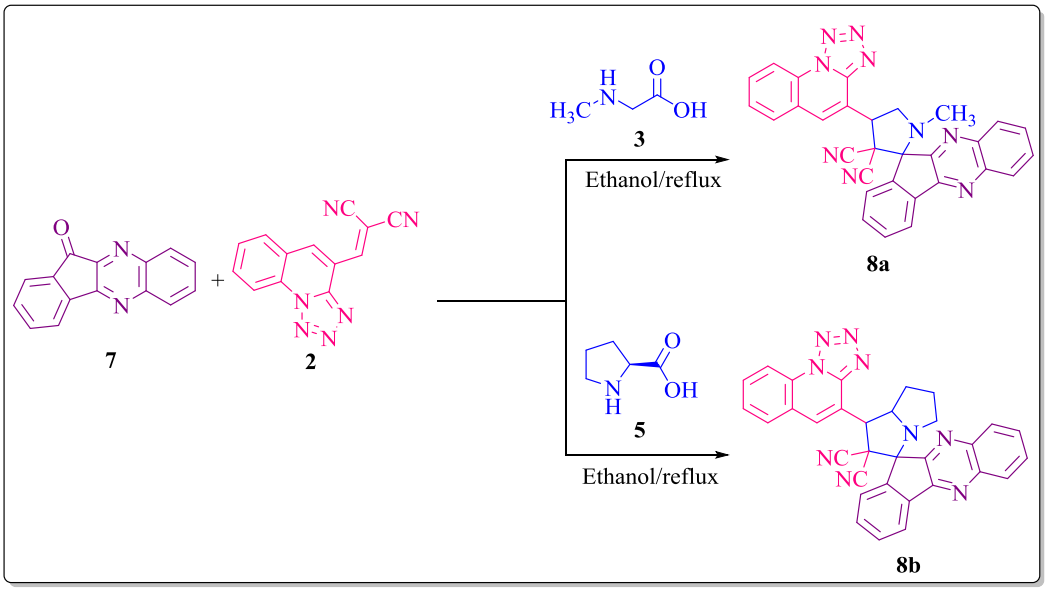

Scheme 3B.2. Synthesis of the spiroquinoxalinopyrrolidines and pyrrolizidines **8a** and **8b**.

Anticancer activity

Among all the target compounds, the compound **4f** exhibited certain influence of the cytotoxic activity against four cancer cell lines i.e., IMR32, A549, MCF7 and HeLa with IC_{50} values 7.02 ± 0.112 µM, 9.26 ± 0.623 µM, 6.74 ± 0.973 µM and 9.74 ± 0.948 µM respectively. The compounds **4a** and **8a** exhibited significant activity against HeLa cell line with IC_{50} values 15.88 ± 0.504 µM and 15.38 ± 0.020 µM respectively. The compound **4e** exhibited significant activity against the four cell lines i.e., IMR32, A549, MCF7 and HeLa with IC_{50} values 9.79 ± 0.764 µM, 12.25 ± 0.294 µM, 10.48 ± 0.356 µM and 11.80 ± 0.565 µM respectively.

Antioxidant activity

Among all the target compounds, the compounds **4e** and **4f** exhibited potent antioxidant activity with the IC_{50} values 5.74 ± 0.15 µM and 4.42 ± 0.76 µM respectively. The compound **8a** exhibited significant antioxidant activity with IC_{50} values 8.99 ± 0.13 µM.

Antimicrobial activity

Among all the synthesized compounds, the compound **8a** exhibited substantial antibacterial activity against both the tested gram positive and gram negative bacteria with MIC values 7.25 µg/mL, 9.50 µg/mL, 16.00 µg/mL and 19.50 µg/mL respectively. The compounds **8a** and **8b** have exhibited potent fungal inhibition activity against *A. niger* with MIC values of 5.25 µg/mL and 8.25 µg/mL respectively.

Molecular docking studies

The comparative molecular docking studies revealed that the receptor HER2 (PDB ID: 3POZ) is better than that of receptor EGFR (PDB ID: 4HJO). The compound **4f** exhibited the least binding energy i.e., −12.98 kcal/mol and form six hydrogen bonds with protein HER2. Its best docking poses were shown in figure 3B.1.

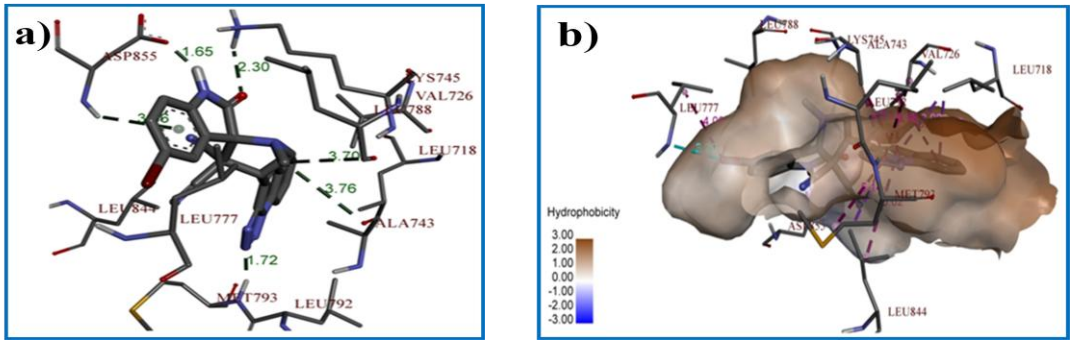

Figure 3B.1. The best docking poses of **4f** with HER2. a) The hydrogen bonding interactions, b) The hydrophobic interactions.

CHAPTER-IV

Novel furanyl spiropyrrolizidines: Synthesis *via* 1,3-dipolar cycloaddition approach, antimicrobial, antioxidant activity and molecular docking studies

Multifunctional polycyclic spiropyrrolizidines that are efficiently synthesized *via* 1,3-dipolar cycloaddition reaction, exhibit versatile bioactivities [11].

The furanyl spiropyrrolizidines were synthesized by using an equimolar mixture of isatin derivatives **1a-f**/ninhydrin **5**/11*H*-indeno[1,2-*b*]quinoxalin-11-one **7** (1 mmol), L-proline **2** (1 mmol), dipolarophiles **3a-c/9** (1 mmol) in methanol under ultrasonication (Method A), conventional (Method B) and fusion (Method C) (Scheme 4.1 & 4.2). The results showed that ultrasonication method is the prior method when compared with the reflux and fusion methods. The crystal structures for the compounds **4c** and **4k** were given in figure 4.1.

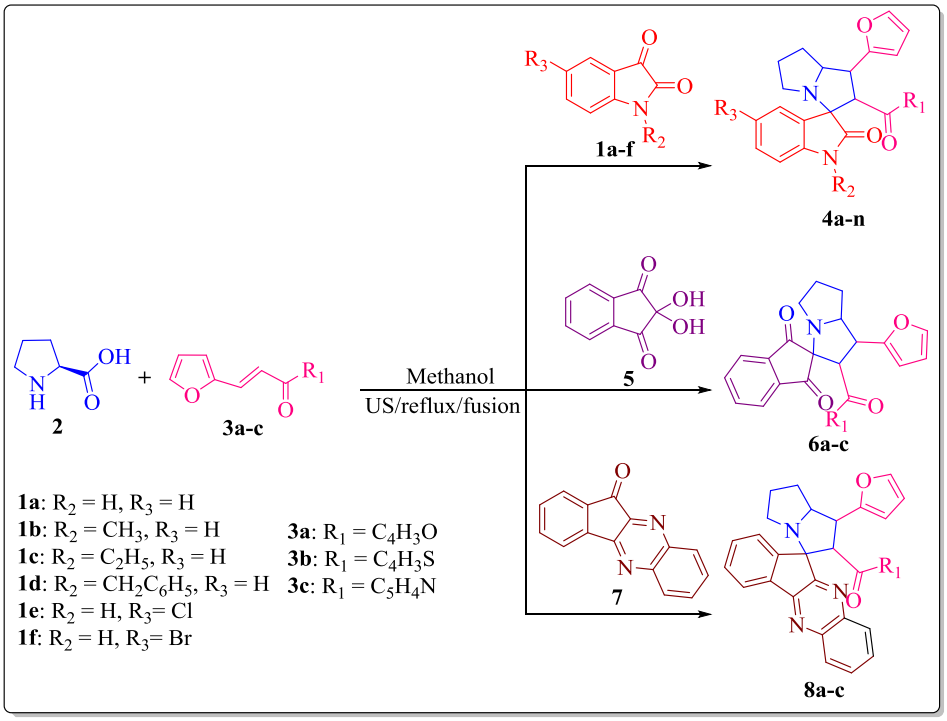

Scheme 4.1. Synthesis of the spiropyrrolizidines **4a-n**, **6a-c** and **8a-c**.

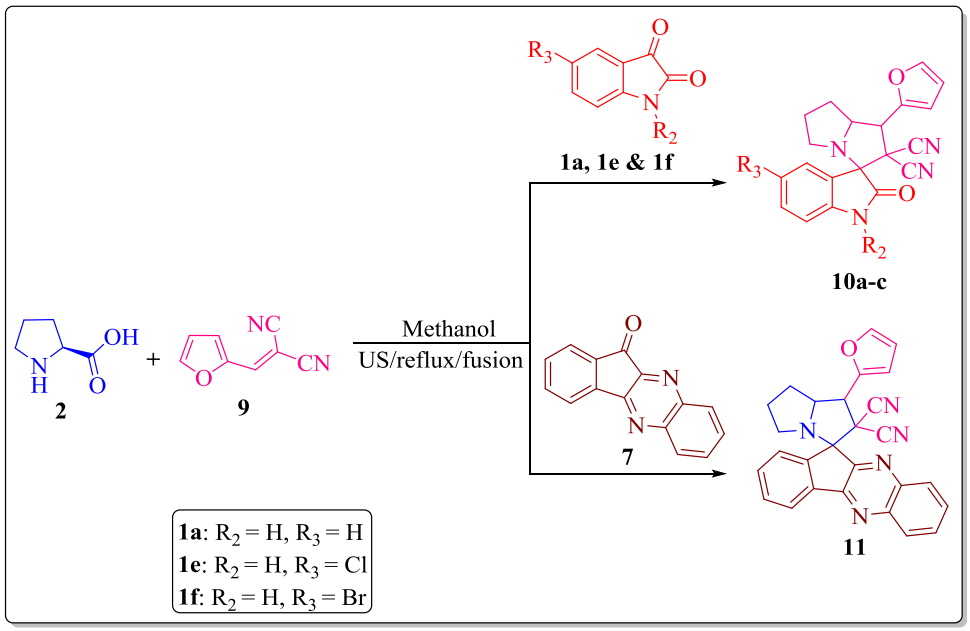

Scheme 4.2. Synthesis of spiropyrrolizidines **10a-c** and **11**.

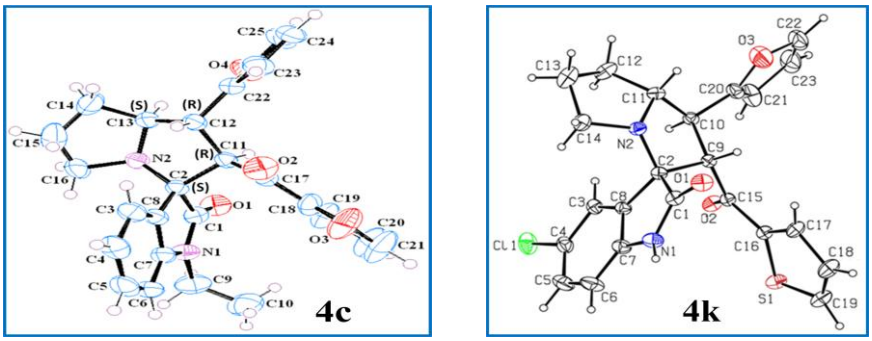

Figure 4.1. The ORTEP representation of the compounds **4c** and **4k**. The asymmetric unit of the compound **4c** shows only one enantiomer having the configurations at the chiral centers C11 (R), C12 (R), C13 (S) and C2 (S). The configurations of the compound **4k** at chiral centers C2 (R), C9 (S), C10 (S), and C11 (R).

Antimicrobial activity

Among all the compounds, the compound **8c** exhibited excellent antibacterial activity against *E. coli* with the MIC value 12.62 µg/mL.

Antioxidant activity

The compounds **8c** and **7c** exhibited the potent antioxidant activity with IC_{50} values of 8.62 ± 0.53 µM and 9.41 ± 0.45 µM respectively.

Molecular docking studies

Among all the synthesized compounds, the compound **8c** exhibit good inhibition activity by exhibiting least binding energy (−13.02 kcal/mol) and form three hydrogen bonds with the protein MurB (1MBT) and its best docking poses were shown in figure 4.2.

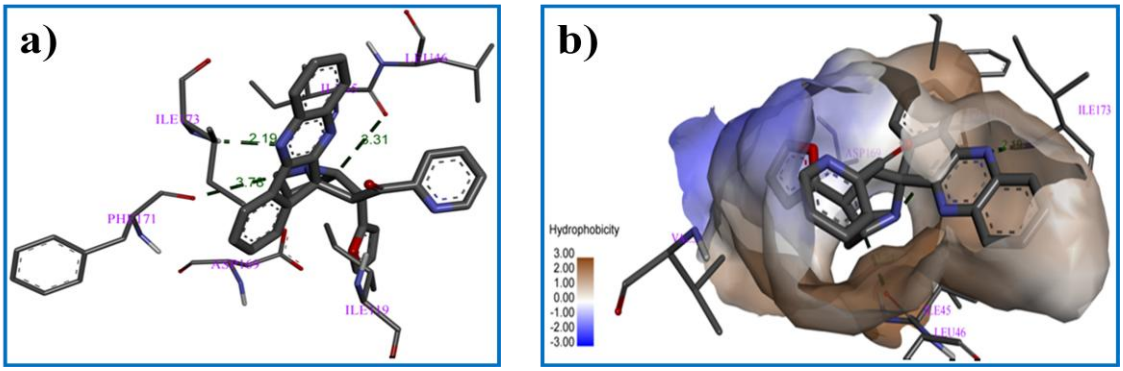

Figure 4.2. The best docking pose of the compound **8c** with the protein 1MBT. a) The hydrogen bonding interactions, b) The hydrophobic interactions.

CHAPTER-V

Efficient one-pot multicomponent synthesis of novel spirooxindolo carbamates *via* Betti reaction: Antimicrobial, antioxidant and molecular docking studies

Organic carbamates have gained much attention from the chemists, because of their vital role in various fields like medicinal, agro, polymer chemistry and their several pharmacological properties etc., [12-13].

The target compounds **4a-l** and **6a-d** were synthesized by using different isatin derivatives **1a-l** (1 mmol), urea **2** (2 mmol) and 2-naphthol **3**/1-naphthol **5** (1 mmol) for 8-26h (Scheme 5.1). The crystal structures of the compounds **4a** and **4e** were shown in figure 5.1.

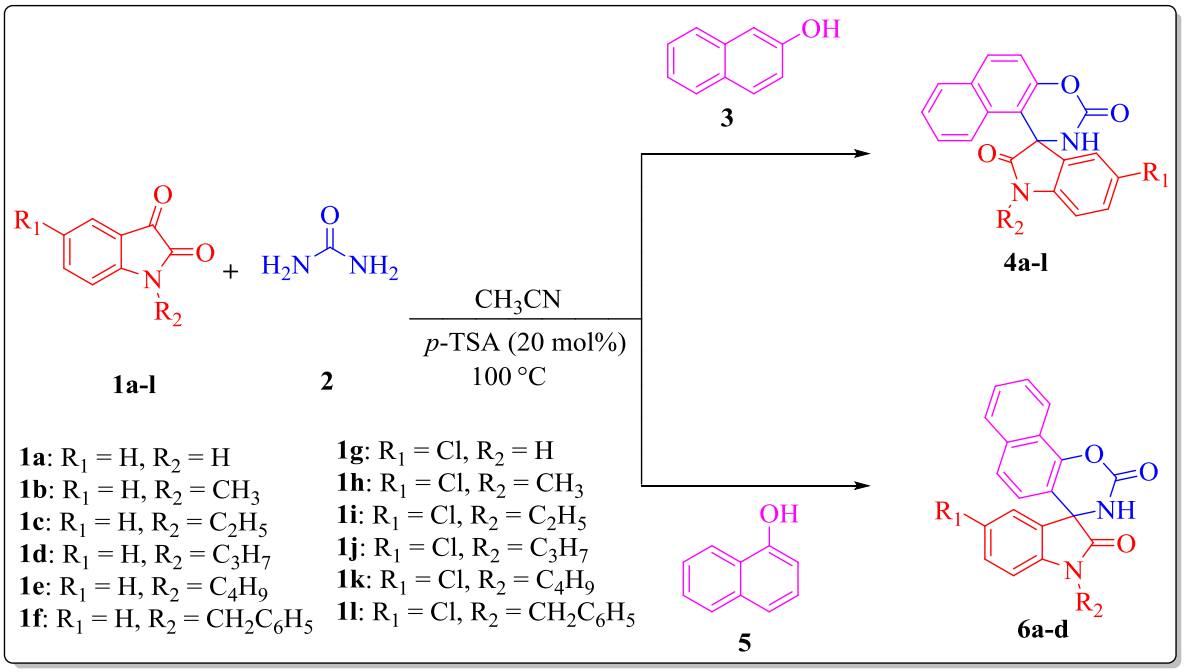

Scheme 5.1. Synthesis of spirooxindolo carbamates **4a-l** and **6a-d**.

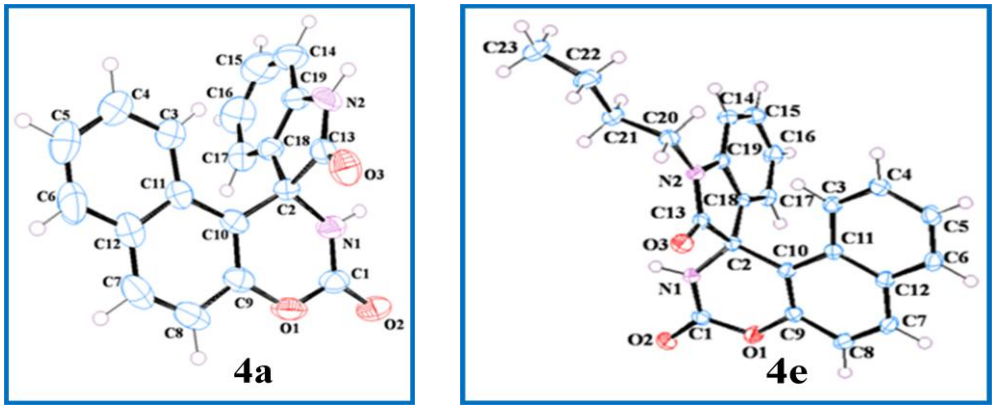

Figure 5.1. The ORTEP representation of the compounds **4a** and **4e**. The represented **4a** molecule has (S)-configuration at the chiral spiro carbon atom. The represented **4e** molecule has (R)-configuration at the chiral spiro carbon atom.

Antimicrobial activity

The compound **4f** (7.5 µg/mL) was more active against *E. coli*. The compound **4l** and **6c** exhibited significant antibacterial activity against *E. coli.* with MIC values 10.5 µg/mL and 9.5 µg/mL respectively.

Antioxidant activity

Among all the compounds, the compound **4f** and **4l** exhibiting potent antioxidant activity with IC_{50} values 9.12 ± 0.01 µM and 7.06 ± 0.78 µM respectively.

Molecular docking studies

Among all the synthesized compounds, the compounds **4f** and **6c** were exhibited good binding energies i.e., −8.51 and −7.92 kcal/mol respectively with DNA gyrase protein (PDB ID:1KZN) and their best docking poses were shown in figure 5.2.

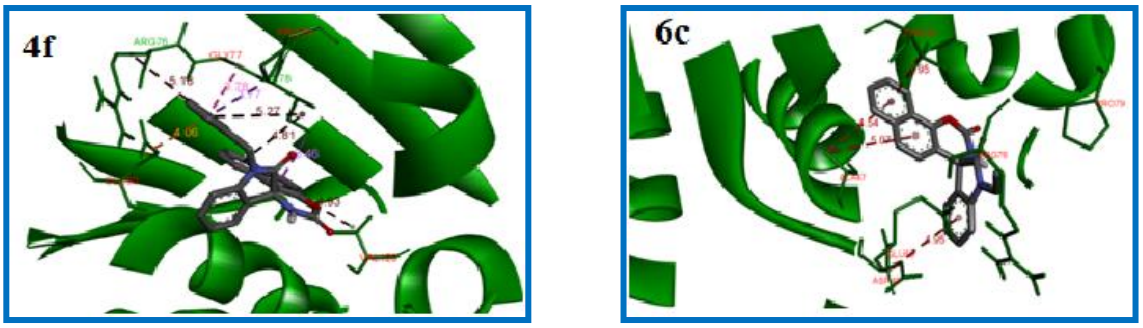

Figure 5.2. The best docking poses of the compounds **4f** and **6c** with the DNA gyrase protein.

CHAPTER-VI (SECTION-A)

Deep eutectic solvent $ZnCl_2$+Urea promoted synthesis of spirooxindoles

DESs (deep eutectic solvents) are a new class of solvents formed from the eutectic mixture of hydrogen bond donor and acceptor. They are used as alternative to the ionic liquids. They are characterized by a melting point (below 100 °C) lower than that of each individual component. These constituting components should additionally possess safe characteristics, low toxicity, renewability and biodegradability as well as low cost [14].

The target compounds **5a-c**, **6a-c** and **7a-c** were synthesized by treating isatin derivatives **1a-c** (1 mmol) and pyrimidine-2,4,6(1*H*,3*H*,5*H*)-trione **2**/4-hydroxy-2*H*-chromen-2-one **3**/1*H*-indene-1,3(2*H*)-dione **4**/dimethylcyclohexane-1,3-dione **5** (2 mmol) in the deep eutectic solvent, $ZnCl_2$+Urea at 80 °C for 30-60min (Scheme 6A.1).

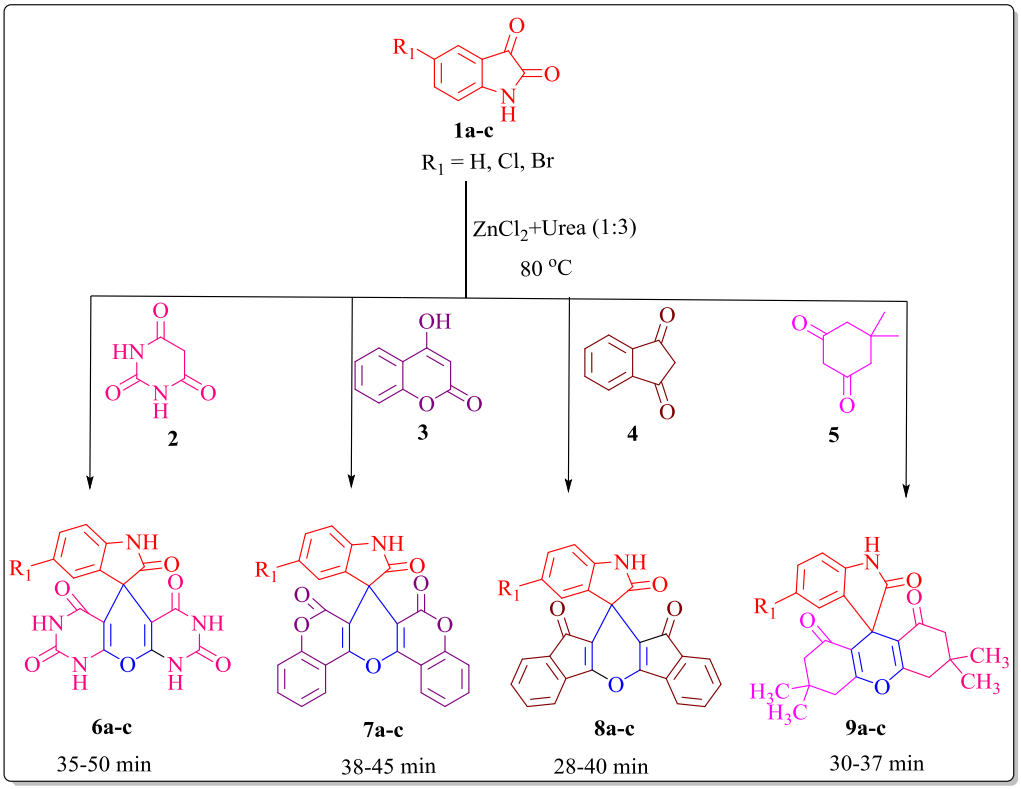

Scheme 6A.1. Synthesis of the spirooxindoles **6a-c**, **7a-c**, **8a-c** and **9a-c**.

CHAPTER-VI (SECTION-B)

Deep eutectic solvent $ZnCl_2$+Urea assisted synthesis of morpholine containing spirooxindoles and biological evaluation

Spiro compounds are a group of generally less investigated compounds. Many spiro compounds possess very promising biological activities as anticancer agents, antibacterial agents, anticonvulsant agents, antituberculosis agents, anti-Alzheimer's agents, etc., [1-5]. Morpholines are privileged backbones and are abundantly used as substituents or scaffolds in drugs and medicinal chemistry. They can improve pharmacokinetic (PK) properties of molecules, such as water solubility and metabolic stability, while not being essential for direct receptor binding [15].

The target compounds **6a-c**, **7a-c**, **8a-c**, **9a-c** and **10a-c**, were synthesized from the mixture of isatin derivatives **1a-c** (1 mmol), 3-fluoro-4-morpholinoaniline **2** and pyrimidine-2,4,6(1*H*,3*H*,5*H*)-trione **3**/4-hydroxy-2*H*-chromen-2-one **4**/1*H*-indene-1,3(2*H*)-dione **5**/dimethylcyclohexane-1,3-dione **6** (2 mmol) in the deep eutectic solvent ($ZnCl_2$+Urea) for 60-80min (Scheme 6B.1).

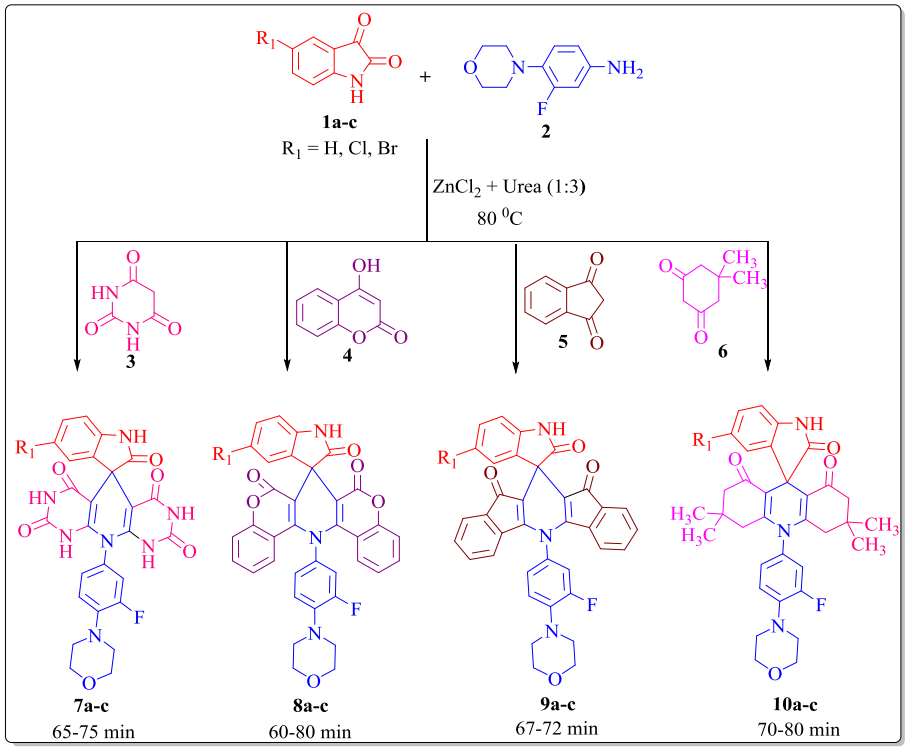

Scheme 6B.1. Synthesis of the spirooxindoles **7a-c**, **8a-c**, **9a-c** and **10a-c**.

Anticancer activity

The anticancer activity results showed that the compound **9a** exhibited potent activity against the MCF7 cell line and moderate activity against HeLa cell line with IC_{50} values 6.47 ± 0.007 µM and 9.14 ± 0.318 µM respectively.

Antioxidant activity

The compound **9a** (7.34 ± 0.17 µM) exhibited potent antioxidant activity.

Antimicrobial activity

The compound **7c** showed potent antibacterial activity against the *B. subtilis* with MIC value 7.50 µg/mL. The compound **8c** showed potent antibacterial activity against *E. coli* with MIC values 13.50 µg/mL.

Molecular docking studies

The molecular docking studies revealed that the protein receptor EGFR (PDB ID: 4HJO) is better than that of the protein receptor HER2 (PDB ID: 3POZ). Among all the compounds, the compounds **9a** exhibit the least binding energy i.e., −10.72 kcal/mol and form five hydrogen bonds with cancer protein EGFR. Its best docking poses were shown in figure 6B.1.

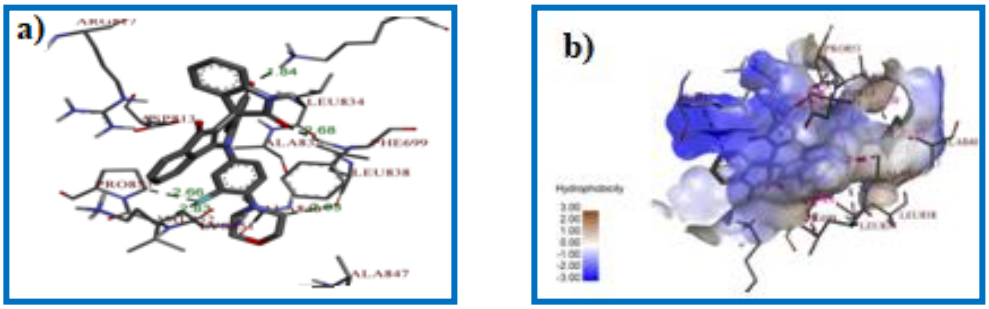

Figure 6B.1. The best docking poses of **9a** with EGFR. a) The hydrogen bonding interactions, b) The hydrophobic interactions.

References

1) (a) K. N. Reddy, U. Subhadhra, B. Sridhar, B. V. S. Reddy, *Org. Biomol. Chem.* **2018**, *16*, 2522; (b) R. Rios, *Chem. Soc. Rev*. **2012**, *41*, 1060.
2) P. Saraswata, G. Jeyabalan, Md. Z. Hassana, M. U. Rahmana, N. K. Nyolaa, *Synth. Commun*. **2016**, *46*, 1643.
3) S. Haddad, S. Boudriga, F. Porzio, A. Soldera, M. Askri, M. Knorr, Y. Rousselin, M.M. Kubicki, C. Golz, C. Strohmann, *J. Org. Chem*. **2015**, *80*, 9064.
4) Y. Arun, G. Bhaskar, C. Balachandran, S. Ignacimuthu, P. T. Perumal, *Bioorg. Med. Chem. Lett.* **2013**, *23*, 1839.
5) S. Timmarayaperumal, S. Sivakumar, *New J. Chem*. **2018**, *42*, 4061

6) W. S. Hamama, M. E. Ibraham, A. A. Gooda, H. H. Zoorob, *RSC Adv.* **2018**, *8*, 8484.

7) (a) Z. Z. Ma, Y. Hano, T. Nomura, Y. J. Chen, *Heterocycles*. **1997**, *46*, 541; (b) P. G. Mandhane, R. S. Joshi, P. S. Mahajan, M. D. Nikam, D. R. Nagargoje, C. H. Gill. *Arab. J. Chem.* **2015**, *8*, 474; (c) F. Hayat, E. Moseley, A. Salahuddin, R. L. V. Zyl, A. Azam, *Eur. J. Med. Chem.* **2011**, *46*, 1897.

8) (a) C. H. Tseng, Y. R. Chen, C. C. Tzeng, W. Liu, C. K. Chou, C. C. Chiu, Y. L. Chen, *Eur. J. Med. Chem*. **2016**, *108*, 258; (b) K. S. Mani, B. Murugesapandian, w. Kaminsky, S. P. Rajendran, *Tetrahedron Lett.* **2018**, *59*, 2921; (c) Y. C. Yu, W. B. Kuang, R. Z. Huang, Y. L. Fang, Y. Zhang, Z. F. Chen, X. L. Ma, *Med. Chem. Commun*. **2017**, *8*, 1158.

9) B. Yu, Z. Yu, P. P. Qi, D. Q. Yu, H. M. Liu, *Eur. J. Med. Chem*. **2015**, *95*, 35.

10) A. H. Kategaonkar, R. U. Pokalwar, S. S. Sonar, V. U. Gawali, Bapurao B. Shingate, Murlidhar S. Shingare, *Eur. J. Med. Chem*. **2010**, *45*, 1128.

11) (a) P. Shanmugam, B. Viswambharan, S. Madhavan, *Org. Lett*. **2007**, *9*, 4095; (b) J. Li, J. Wang, Z. Xu, S. Zhu. *ACS Comb. Sci*. **2014**, *16*, 506; (c) S. Q. Ge, Y. Y. Hua, M. Xia, *Ultrason. Sonochem*. **2009**, *16*, 232; (d) Y. Yong, L. W. Ya, W. Z. Hua, C. Y. Zheng, X. X. Ying, Z. X. Mei, Y. W. Cheng, *Org. Lett*. **2018**, *20*, 4453.

12) (a) E. Chandralekha, A. Thangamani, R. Valliappan, *Res. Chem. Intermed*. **2013**, *39*, 961; (b) G. Chen, J. Yang, S. Gao, Y. Zhang, X. Hao, *Res. Chem. Intermed*. **2015**, *41*, 4987.

13) S. A. Mousa, W. F. DeGrado, D. X. Mu, R. P. Kapil, B. R. Lucchesi, T. M. Reilly, *Circulation.* **1996**, *93*, 537.

14) (a) E. L. Smith, A. P. Abbott, K. S. Ryder, *Chem. Rev*. **2014**, *114*, 11060; (b) F. Sebest, L. Kasarrubios, H. S. Rzepa, A. J. P. White, S. D. Gonzalez, *Green Chem*. **2018**, doi: 10.1039/c8gc01797b.

15) P. Patil, R. Madhavachary, K. Kurpiewska, J. K. Tłuscik, A. Dömling, *Org. Lett.* **2017**, *19*, 642.

LIST OF PUBLICATIONS

List of Publications

Published

1. Ultrasound-assisted rapid and efficient one-pot synthesis of furanyl spirooxindolo and spiroquinoxalinopyrrolizidines by 1,3-dipolar cycloaddition: a green protocol.
   Venkata Bharat Nishtala, Jagadeesh Babu Nanubolu and Srinivas Basavoju.
   Research on Chemical Intermediates, **2017**, *43*, 1365-1381.

2. Crystal structure and Molecular docking studies of 1-ethyl-2'-(furan-2-carbonyl)-1'-(furan-2-yl)-1',2',5',6',7',7a'-hexahydrospiro[indoline-3,3'-pyrrolizin]-2-one.
   Venkata Bharat Nishtala and Srinivas Basavoju.
   Journal of Chemical Crystallography, **2018**, *48*, 78–90.

Manuscripts under preparation

1. Synthesis of spirooxindolocarbamates based on Betti reaction: Antibacterial, antifungal, antioxidant and molecular docking studies.
   Venkata Bharat Nishtala and Srinivas Basavoju.

2. Facile and regioselective synthesis of quinolinyl spiroindene and spiroquinoxolinopyrrolizidines *via* 1,3-dipolar cycloaddition reaction: Antioxidant, Cytotoxic and IDO1 targeting molecular docking studies.
   Venkata Bharat Nishtala and Srinivas Basavoju.

3. Novel 2-oxoquinolinyl spiropyrrolizidines: Synthesis, anticancer activity, antioxidant activity, antimicrobial activity and molecular docking studies.
   Venkata Bharat Nishtala and Srinivas Basavoju.

4. $ZnCl_2$+Urea, the deep eutectic solvent promoted synthesis of the spirooxindolopyrans and xanthenes *via* a pseudo three-component approach.

   Venkata Bharat Nishtala and Srinivas Basavoju.

PAPERS PRESENTED IN INTERNATIONAL AND NATIONAL CONFERENCES

International

1. **International workshop and symposium on "Green Chemistry and Technology (IWSGCT-18)**" in Dungar Govt. College, Bikaner, Rajasthan, India, in association with RSC-London during 15-18, October 2018.

2. **International conference on "Advanced Functional Materials (ICFAM-2017)**" in RGUKT, Basar, Telangana state, India, during 18-20, December 2017.

3. **6th International Symposium on "Current Trends in Drug Discovery and Research, (CTDDR-2016)"** organized by Central Drug Research Institute (CDRI), Lucknow, UP, India during 25th-28th February, 2016.

National

1. **National symposium on "Recent Advances in Chemical and Material Sciences"** held on 20-21st August 2016 organized by Rajiv Gandhi University of Knowledge Technologies Basar.

2. **National seminar on "Recent Advances in Chemistry (RAC-2015)",** at Department of Chemistry, Kakatiya University, Warangal during 30-31, March, 2015.

3. **UGC sponsored Two Day National Seminar on "Recent Trends and Challenges in Chemical Sciences (RTCCS)"** organized by Kakatiya University, Warangal during 24-25th March 2017.

4. **National Conference on ""Recent Development in Chemical Sciences and Allied Technologies"** organized by National Institute of Technology Warangal, Warangal during 29-30th June,2017.

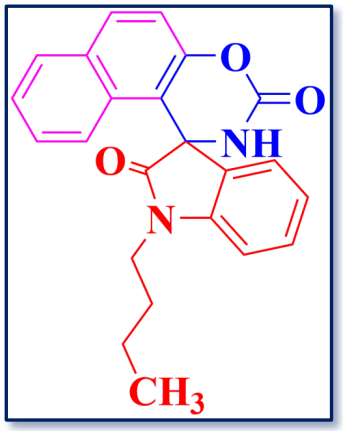

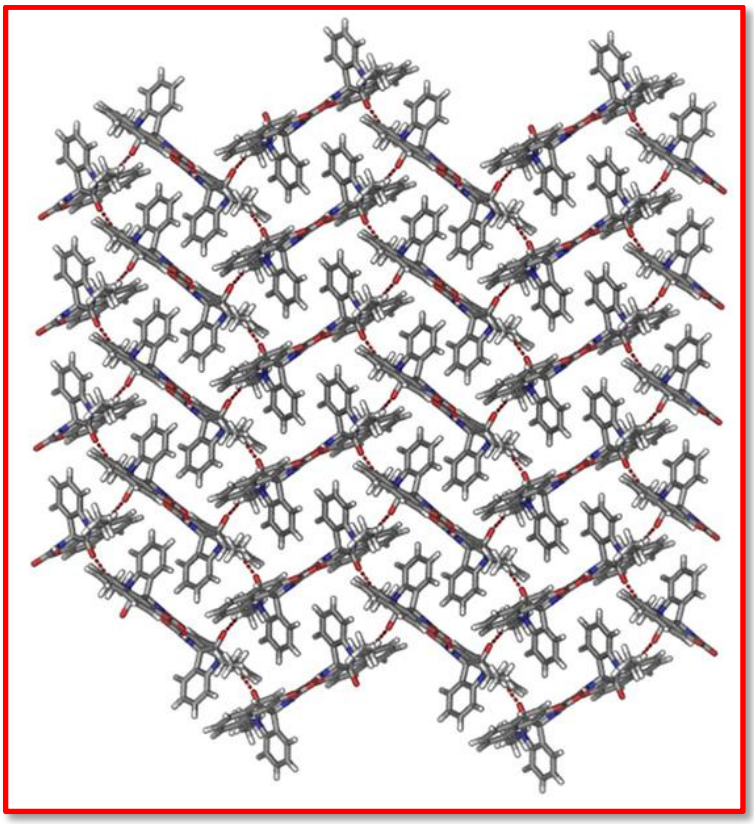

*One of the synthesized compounds in this thesis showed **parquet floor** structure in its crystal.*